Synthese substituierter Acene und Untersuchung ihrer Struktur-Eigenschaftsbeziehungen

Dissertation
der Mathematisch-Naturwissenschaftlichen Fakultät
der Eberhard Karls Universität Tübingen
zur Erlangung des Grades eines
Doktors der Naturwissenschaften
(Dr. rer. nat.)

vorgelegt von
Thomas Geiger
aus Böblingen

Tübingen
2020

Gedruckt mit Genehmigung der Mathematisch-Naturwissenschaftlichen Fakultät der Eberhard Karls Universität Tübingen.

Tag der mündlichen Qualifikation:	27.05.2020
Dekan:	Prof. Dr. Wolfgang Rosenstiel
1. Berichterstatter:	Prof. Dr. Holger F. Bettinger
2. Berichterstatter:	Prof. Dr. Bernd Speiser
3. Berichterstatter:	Prof. Dr. Milan Kivala

“ *Daß ich erkenne, was die Welt im Innersten zusammenhält.* ”

Johann Wolfgang von Goethe, *Faust I*

Danksagung

Meinem Doktorvater Prof. Dr. Holger F. Bettinger gilt mein expliziter Dank für die Bereitstellung der herausfordernden Themen, die Betreuung der Arbeit, den intensiven fachlichen Diskurs und die Bereitschaft, seinen Erfahrungsschatz mit mir zu teilen.

Ich bedanke mich bei allen momentanen und ehemaligen Mitgliedern das Arbeitskreises Bettinger, insbesondere Constanze Keck, Klara Edel, John Bauer und Ralf Einholz für die gemeinsame Zeit, gegenseitige Motivation und die Gespräche jenseits aller fachlichen Diskussionen. Zusätzlicher Dank gilt allen Bachelorand(en)/-innen und Modulpraktikant(en)/-innen, die durch ihre Synthesen zum Gelingen dieser Arbeit beigetragen haben.

Bei den Mitgliedern der NMR-Abteilung, Dr. Markus Kramer, Paul Schuler, Dominik Brzecki, Priska Kolb sowie Dr. Norbert Grzegorzek möchte ich mich für die Durchführung von Messungen, die Einführung ins Hochfeld-NMR, Unterstützung bei Messproblemen und die angenehme Atmosphäre bedanken. Besonderer Dank gilt Paul Schuler, der mir bei jedem einzelnen Gespräch Neues bezüglich NMR-Technik beibringen konnte.

Großer Dank gilt des Weiteren den Mitarbeitern der Analytikabteilung, Dr. Dorothee Wistuba, Dr. Peter Haiss und Claudia Krause für die Durchführung der massenspektrometrischen Untersuchungen, Hilfestellung bei der Auswertung und die Motivation, auch die schwierigen Fälle mit großem Engagement zu bearbeiten.

Bei Thorsten Hummel möchte ich mich für die Hilfe bei der Durchführung von Sublimationsexperimenten sowie die Geduld, sämtliche Fragen zur Röntgendiffraktometrie zu beantworten bedanken. Weiterhin gilt mein Dank Dr. Cäcilia Maichle-Mössmer, Elke Niquet, Dr. Hartmut Schubert, Dr. Claudio Schrenk sowie den Mitarbeitern von Rigaku Europe SE für die Durchführung von Röntgenbeugungsexperimenten und das Lösen der Strukturen.

Zusätzlich möchte ich allen Kooperationspartnern, die durch ihre Untersuchungen und Expertise zu Veröffentlichungen beigetragen haben, meinen tiefen Dank aussprechen.

Ich danke meinen Eltern, dass sie mir dieses Studium ermöglicht und mich immer unterstützt haben, ohne sie wäre diese Arbeit nicht möglich gewesen.

All meinen Freunden danke ich für die gemeinsam verbrachte Zeit und Unterstützung, die auch in den schwierigen Phasen dieser Arbeit nie nachgelassen hat und freue mich auf weitere schöne Jahre.

Inhaltsverzeichnis

Abbildungsverzeichnis **III**

Tabellenverzeichnis **V**

Abkürzungsverzeichnis **VII**

Zusammenfassung **XI**

Abstract **XIII**

Publikationsliste und Eigenanteile **XV**

1 Untersuchung zum Einfluss der London-Dispersion auf die Anthracenphotodimerisierung **1**

1.1 Fundamentale Wechselwirkungen 1

1.2 Photochemie des Anthracens 5

1.2.1 Bekannte Photodimere substituierter Anthracene . . 7

1.3 Zielsetzung 7

1.4 Zusammenfassung der Ergebnisse 8

1.4.1 Synthese substituierter Anthracene durch Suzuki-Miyaura-Reaktion 8

1.4.2 Synthese substituierter Anthracene über die korrespondierenden Chinone 10

1.4.3 Photodimerisierung 2,3-dialkylsubstituierter Anthracene 14

2 Synthese und Charakterisierung neuartiger, tetrafluorsubstituierter Pentacene **19**

2.1 Eigenschaften der Acene 19

2.1.1 Synthese von Pentacen und dessen Derivaten 22

2.2 Zielsetzung 23

2.3 Zusammenfassung der Ergebnisse 24

2.3.1 Thermische Tetrafluorpentacensynthese 26

2.3.2 NMR-spektroskopische Untersuchungen 27

2.3.3 Festkörperstrukturen 30

2.3.4 UV/Vis-Spektroskopie der Neutralverbindungen . . 31

2.3.5 Radikalkationen 33

2.3.6 Dikationen 35

Literaturverzeichnis **39**

Lebenslauf **51**

Anhang **53**

Abbildungsverzeichnis

1.1 Dimerisierung des Tritylradikals. 3
1.2 Synthese des diadamantylsubstituierten Naphthalins **8**. 5
1.3 Reaktion des Anthracengerüstes mit $^1O_2$. 6
1.4 Photodimerisierung 9-,10-substituierter Anthracene. 7
1.5 Synthese der 2,3-disubstituierten Anthracene **16**–**18** über 2,3-Dibromanthracen (**15**) ausgehend von Phthalid (**11**) 9
1.6 Chinonroute zur Synthese der 2,3-disubstituierten Anthracene. 11
1.7 Molekülstruktur von 2,2',3,3'-Tetra-*iso*-butyldianthracen (**26**) im Einkristall. 15
1.8 Auftragung der natürlich Logarithmen der Isomerenverhältnisse *anti*:*syn* gegen Chartons ν-Parameter. 16

2.1 Allgemeine Strukturformel der Acene. 19
2.2 Methoden zur Synthese des 2,3,9,10-Tetrafluorpentacens (**27**). . 23
2.3 Synthese der Arinvorstufe **33**. 25
2.4 Synthese der Acenvorstufen **35** und **38** für die thermische Pentacensynthese, ausgehend von Bisdien **28**. 26
2.5 Thermische Reaktion der Ethenopentacene **35**, **38** und **39** mit Tetrazin **40**. 27
2.6 Vergleich der ^{1}H- und ^{19}F-NMR-Spektren vor und nach Erhitzen von 1,4,8,11-Tetrafluorpentacen (**29**) in TCE-d_2 auf 120 °C. . . 29
2.7 Vergleich der Kristallstrukturen von **29** und **30**. 30
2.8 UV/Vis-, Fluoreszenz- und Anregungspektren von 1,4,8,11-Tetrafluorpentacen (**29**) und 1,4,9,10-Tetrafluorpentacen (**30**). . . 32

2.9 UV/Vis/NIR-Spektren der Radikalkationen der Tetrafluorpentacene in einer 2 M Lösung von MSS in Nitrobenzol. 34
2.10 ESR-Spektren von $\mathbf{29}^{+\cdot}$ und $\mathbf{30}^{+\cdot}$. 35
2.11 UV/Vis-Spektren der Tetrafluorpentacen-Dikationen. 36
2.12 Vollständige Zuordnung der NMR-Signale der Tetrafluorpentacen-Dikationen. 38

Tabellenverzeichnis

1.1 Vergleich der Untergruppen von Interaktionsmöglichkeiten innerhalb der Van-der-Waals-Wechselwirkungen. 2
1.2 Isolierte Ausbeuten für die einzelnen Syntheseschritte der Chinonroute. 13

2.1 Vergleich chemischer Verschiebungen verschiedener Acenderivate in Lösung. 28
2.2 Auf B3LYP/6-311+G**-Theorieniveau berechnete Energien für HOMO und LUMO sowie daraus resultierende HOMO-LUMO-Abstände. 33
2.3 Vergleich der experimentell ermittelten, langwelligsten Absorptionsbanden der Tetrafluorpentacen-Dikationen mit berechneten Werten. 37

Abkürzungsverzeichnis

ACN	Acetonitril
Äq	Äquivalent(e)
akt.	aktiviert
DCM	Dichlormethan
DDQ	2,3-Dichlor-5,6-dicyano-1,4-benzochinon
DED	Dispersionsenergiedonor
DFT	Dichtefunktionaltheorie
DIPA	Diisopropylamin
EI	Elektronenstoßionisation
ESI	Elektrosprayionisation
ESR	Elektronenspinresonanz
HMDS	Hexamethyldisilazan
HOMO	Highest occupied molecular orbital/höchstes besetztes Molekülorbital
ISC	Intersystem Crossing
kat.	katalytisch

LUMO	Lowest unoccupied molecular orbital/niedrigstes unbesetztes Molekülorbital
M	Molarität
MSS	Methansulfonsäure
n-BuLi	*n*-Butyllithium
NIR	Nahinfrarot
NMO	*N*-Methylmorpholin-*N*-oxid
NMR	Nuclear Magnetic Resonanz/Kernspinresonanz
NOE	Nuclear Overhauser effect/Kern-Overhauser-Effekt
OFET	Organischer Feldeffekttransistor
PAK	Polyzyklischer aromatischer Kohlenwasserstoff
PcEP	Pentacenendoperoxid
perm.	permanent
ppm	Chemische Verschiebung im NMR-Experiment
RT	Raumtemperatur
sec	sekundär
TCE	1,1,2,2-Tetrachlorethan
TD	Time-dependent/zeitabhängig
temp.	temporär
TEMPO	2,2,6,6-Tetramethylpiperidinyloxyl
tert	tertiär

TfO	Triflatgruppe
THF	Tetrahydrofuran
TIPS	Triisopropylsilylgruppe
TMS	Trimethylsilylgruppe
Ts	Tosylgruppe
UDEFT	Uniform Driven Equilibrium Fourier Transform
UV	Ultravioletter Teil des elektromagnetischen Spektrums
VdW	Van-der-Waals
Vis	Sichtbarer Teil des elektromagnetischen Spektrums
ZnPc	Zinkphthalocyanin

Zusammenfassung

Untersuchung zum Einfluss der London-Dispersion auf die Anthracenphotodimerisierung

In diesem Projekt wurde eine Reihe 2,3-dialkylsubstituierter Anthracenderivate synthetisiert. Die Synthesen wurden zum einen über Suzuki-Miyaura-Kreuzkupplungschemie an 2,3-Dibromanthracen, zum anderen über die Reduktion der entsprechenden Anthrachinone realisiert. Die so synthetisierten Monomere wurden durch UV-Bestrahlung in einer photochemisch erlaubten $[4 + 4]$-Cycloaddition, einer Reaktion, die bereits seit dem 19. Jahrhundert bekannt ist, in die entsprechenden Dimere überführt. Die erhaltenen Dimergemische wurden aufgetrennt, und die Produktverhältnisse mit substituentenspezifischen sterischen Parametern korreliert. Es wurde eine lineare Abhängigkeit der Daten gefunden, die auf eine nahezu ausschließlich sterische Reaktionskontrolle hindeutet. Nur einer der untersuchten Substituenten weicht von dieser linearen Abhängigkeit ab und zeigt Hinweise eines Einflusses von Dispersionswechselwirkungen auf den Übergangszustand der Reaktion und damit das Produktverhältnis.

Synthese und Charakterisierung neuartiger, tetrafluorsubstituierter Pentacene

Pentacen ($C_{22}H_{14}$) findet häufig als p-Typ (Löcherleitung) Halbleitermaterial in beispielsweise organischen Feldeffekttransistoren (OFETs) Verwendung. Mittels Substitution mit elektronenziehenden Gruppen, zum Beispiel Fluoratomen, lässt sich der Halbleitungstyp zu n-Typ (Elektronenleitung)

konvertieren, was neue Anwendungsmöglichkeiten eröffnet. Im Rahmen dieser Arbeit wurde zum einen die im Arbeitskreis entwickelte Methode zur thermischen Synthese von Pentacenen über einen Diels-Alder-retro-Diels-Alder-Mechanismus im Hinblick auf die Ausbeute eines bereits bekannten Tetrafluoropentacenderivates optimiert. Zum anderen erfolgte die Synthese zweier neuer Tetrafluorpentacenderivate. Diese wurden im Festkörper, in Lösung sowie in silico untersucht. Neben der Abhängigkeit des HOMO-LUMO-Abstands vom Substitutionsmuster konnte durch Röntgenstrukturanalyse zusätzlich eine Abhängigkeit des Kristallpackungsmotivs (Fischgrätmuster versus pi-Stapelung) nachgewiesen werden. Für zwei Derivate wurde n-Typ Halbleitung im OFET gefunden. Die Verbindungen wurden durch Ein- beziehungsweise Zwei-Elektronen-Oxidation in Lösung in ihre Radikal- bzw. Dikationen überführt, welche ebenfalls eingehend charakterisiert wurden.

Abstract

Investigation on the influence of London dispersion on the anthracene photodimerization

In this project, a number of novel, 2,3-dialkylsubstituted anthracene derivatives were synthesized. The syntheses were realized by performing either Suzuki-Miyaura cross-coupling reactions on 2,3-dibromoanthracene or by reduction of the corresponding anthraquinones. The monomers synthesized in these ways were converted into their dimers by UV-radiation in a photochemically allowed [4 + 4]-cycloaddition reaction. This reaction is known since the 19^{th} century. The obtained dimers were separated and the product ratios were correlated with substituent specific steric parameters. A linear dependency was found, which suggests an almost exclusive reaction control by steric influence. Only one of the investigated substituents deviates from this behaviour, being an indication for the influence of dispersion interactions on the transition state of the reaction and therefore the product ratios.

Synthesis and charaterization of novel, tetrafluorosubstituted pentacenes

Pentacene ($C_{22}H_{14}$) is a commonly used p-type (hole conduction) semiconductor material for example in organic field-effect transistors (OFETs). By substitution with electron-withdrawing groups, e.g. fluorine atoms, the conduction mode can be converted to n-type (electron conduction). This allows for new applications. In this work, the synthesis of pentacenes by a Diels-Alder-retro-Diels-Alder reaction sequence developed in this research group

was optimized in regard to the yield of an already known tetrafluoropentacene derivative. Additionally, two new tetrafluoropentacene derivatives were synthesized. These were investigated in the solid state, in solution and in silico. Besides an alteration of the optical band gap which was found to be dependant on the substitution pattern, an additional dependance of the crystal packing motifs (herringbone versus pi-stacking) was observed by X-ray crystallography. For two derivatives, n-type semiconduction was found in OFET measurements. The compounds were converted into their radicalcations and dications by one- or two-electron oxidation in solution and these were characterized in detail as well.

Publikationsliste und Eigenanteile

[1] Shen, B.; Geiger, T.; Einholz, R.; Reicherter, F.; Schundelmeier, S.; Maichle-Mössmer, C.; Speiser, B.; Bettinger, H. F., *J. Org. Chem.* **2018**, *83*, 3149–3158.

Synthese der in der Publikation untersuchten Hauptverbindung **5c** durch thermische Umsetzung der Vorstufe mit 1,2,4,5-Tetrazindicarbonsäuredimethylester. Züchtung eines Einkristalles der Verbindung, der die Aufklärung der Kristallstruktur ermöglichte. Generierung und vollständige, zur Publikation geeignete spektroskopische Charakterisierung des Radikalkations und Dikations der Verbindung mittels ESR- (Radikalkation), UV/Vis/NIR- und NMR-Spektroskopie (Dikation). Die zum Erhalt stabiler NMR-Spektren geeignete Methode der Probenpräparation wurde im Zuge dieser Veröffentlichung entwickelt und es konnte gezeigt werden, dass die Oxidation nicht unter Entwicklung molekularen H_2- oder HD-Gases verläuft.

Bin Shen führte die photochemische Synthese der Verbindung sowie die computerchemischen Rechnungen durch und verfasste den Großteil des Manuskripts. Ralf Einholz führte die initialen Oxidationsexperimente durch und Florian Reicherter wirkte bei der Kristallisation der Verbindung aus heißer Lösung mit. Simon Schundelmeier sowie Prof. Dr. Bernd Speiser zeichnen sich für die Durchführung der Cyclovoltammetrieexperimente und die Analyse der daraus erhaltenen Daten verantwortlich. Dr. Cäcilia Maichle-Mössmer führte die Röntgenbeugungsexperimente an Einkristallen durch und löste die Strukturen. Die

Projektidee stammt von Prof. Dr. Holger F. Bettinger, er betreute das Projekt wissenschaftlich in allen Phasen.

[2] Breuer, T.; Geiger, T.; Bettinger, H. F.; Witte, G., *J. Phys.: Condens. Matter* **2018**, *31*, 034003.

Synthese von 2,3,9,10-Tetrafluorpentacen in einer ausreichenden Menge und Reinheit für XPS-Messungen von Molekülmischungen mit Buckminsterfulleren C_{60}. Die weiteren Projektschritte wurde von Dr. Tobias Breuer sowie Prof. Dr. Gregor Witte durchgeführt.

[3] Geiger, T.; Haupt, A.; Maichle-Mössmer, C.; Schrenk, C.; Schnepf, A.; Bettinger, H. F., *J. Org. Chem.* **2019**, *84*, 10120–10135.

Synthese und Charakterisierung der für die Untersuchungen verwendeten substituierten Anthracene sowie vorhergehender Zwischenstufen. Etablierung einer Methode zur Photodimerisierung der synthetisierten Anthracene sowie Auftrennung der Isomerengemische mittels Säulenchromatographie oder fraktionierter Kristallisation. Züchtung aller Einkristalle, die zur Aufnahme von Röntgenbeugungsexperimenten geeignet waren und deren Kristallstrukturen in der Publikation enthalten sind. Durchführung quantenchemischer Rechnungen, zur Struktur *tert*-butylsubstituierter Dianthracene sowie zu den Grundzuständen und angeregten Zuständen der untersuchten Anthracene. Diskussion und Erklärung der erhaltenen Produktverhältnisse mittels des von Charton entwickelten Parameters v.
Die Projektidee stammt von Prof. Dr. Holger F. Bettinger, Anne Haupt synthetisierte und photodimerisierte unter meiner Anleitung das Neopentylderivat. Prof. Dr. Andreas Schnepf stellte Messzeit am Synchrotron (ANKA) zur Verfügung, Dr. Claudio Schrenk führte dort die Röntgenbeugungsmessungen an Verbindung **37a** durch und zeichnet sich für die Strukturlösung der Verbindung verantwortlich. Dr. Cäcilia Maichle-Mössmer trug durch alle übrigen Röntgenbeugungsmessungen sowie Strukturlösungen zur Veröffentlichung bei.

[4] Geiger, T.; Schundelmeier, S.; Hummel, T.; Ströbele, M.; Leis, W.; Seitz, M.; Zeiser, C.; Moretti, L.; Maiuri, M.; Cerullo, G.; Broch, K.; Vahland, J.; Leo, K.; Maichle-Mössmer, C.; Speiser, B.; Bettinger, H. F., *Chem. Eur. J.* **2020**, *26*, 3420–3434.

Synthese zweier neuer Isomere des Tetrafluoropentacens (Verbindung **10** sowie **11**), für die eine neuartige Synthesestrategie über eine Kobayashi-Arinvorstufe entwickelt wurde. Charakterisierung der Substanzen im Festkörper und in Lösung. Durchführung aller quantenchemischer Rechnungen sowie Korrelation der daraus erhaltenen Daten mit experimentellen Werten. Oxidation der neu synthetisierten Verbindungen zu den Radikal- und Dikationen in Lösung und Vollcharakterisierung dieser Ionen. Koordination der im Projekt beteiligten Arbeitsgruppen sowie Hauptautor des Manuskripts. Dies schließt Korrektur, Formatierung und Zusammenführung der von den Kooperationspartnern übersandten Manuskriptteile mit ein.

Die Projektidee stammt von Prof. Dr. Holger F. Bettinger, die Kooperationspartner zeigen sich für die Cyclovoltammetriemessungen und deren Auswertung (Simon Schundelmeier, Prof. Dr. Bernd Speiser), den Bau von OFETs und Performancemessungen (Jörn Vahland, Prof. Dr. Karl Leo) und die Untersuchung der Singlet Fission (Clemens Zeiser, Dr. Luca Moretti, Dr. Margherita Maiuri, Prof. Dr. Giulio Cerullo, JProf. Dr. Katharina Broch) verantwortlich. Thorsten Hummel half mit seiner Expertise bei der Einkristallzüchtung der neu synthetisierten Tetrafluorpentacenderivate, Dr. Markus Ströbele löste eine dieser Strukturen und Dr. Cäcilia Maichle-Mössmer zeigte sich für die Röntgenbeugungsmessungen an Einkristallen von Verbindung **1**, **5** und **8** sowie deren Strukturlösungen verantwortlich. Die Lumineszenzmessungen bei tiefen Temperaturen wurden im Labor von Prof. Dr. Michael Seitz unter Mithilfe von Dr. Wolfgang Leis durchgeführt.

Die in der vorliegenden Dissertationsschrift diskutierten Ergebnisse sind in den Publikationen Nummer 1, 3 und 4 der Publikationsliste veröffentlicht worden, die entsprechenden Publikationen finden sich im Anhang.

Die Zustimmung der jeweiligen Verlage zur Reproduktion bzw. Vervielfältigung wurde eingeholt. Aus den Publikationen entnommene Abbildungen wurden in ihrer Größe verändert und Verbindungsnummern angepasst, beziehungsweise die enthaltenen Beschriftungen ins Deutsche übersetzt. Die innerhalb dieser Dissertationsschrift verwendete Nummerierung der Verbindungen weicht von den innerhalb der Publikationen verwendeten Nummerierungen ab.

1 Untersuchung zum Einfluss der London-Dispersion auf die Anthracenphotodimerisierung

1.1 Fundamentale Wechselwirkungen

Die moderne Physik unterscheidet im Wesentlichen vier sogenannte Fundamentalkräfte, durch die alle Arten von Interaktionen von Teilchen untereinander – seien sie massebehaftet oder nicht – beschrieben werden können.[1] Neben den starken und schwachen Wechselwirkungen sowie der Gravitation existiert hierbei die Klasse der elektromagnetischen Wechselwirkungen. Hierzu zählen klassische Beispiele wie die Coulombwechselwirkungen zwischen geladenen Teilchen wie sie aus dem Alltag bekannt sind, aber auch schwächere, nicht-kovalente Wechselwirkungen (Van-der-Waals-Kräfte). Die Van-der-Waals-Kräfte können ihrerseits in weitere Untergruppen, entsprechend der miteinander interagierenden Partner unterteilt werden (s. Tabelle 1.1). Neben den sogenannten Keesom-Kräften, also der Wechselwirkung permanenter Dipole miteinander, existiert die Gruppe der Debye-Wechselwirkungen, welche die Interaktion von permanenten Dipolen mit polarisierbaren Partnern, wobei diese Partner selbst zu einem kurzlebigen induzierten Dipol werden, beschreibt. Die letzte Interaktionsmöglichkeit besteht in der Wechselwirkung von zwei ungeladenen, jedoch polarisierbaren Teilchen durch temporäre Fluktuation ihrer Elektronenhüllen. Hierbei kann sich durch eine kurzzeitig asymmetrische Ladungsverteilung ein kurzlebiger Dipol bilden, der seinerseits in der Lage ist, induzierte Dipole in einem polarisierbaren

Partner zu erzeugen. Dieser Interaktionstyp wird nach seinem Entdecker London-Dispersion genannt.[2–4]

Tabelle 1.1: Vergleich der verschiedenen Untergruppen von Interaktionsmöglichkeiten innerhalb der Van-der-Waals-Wechselwirkungen zwischen permanenten Dipolen, permanenten Dipolen und polarisierbaren Partnern ($\hat{=}$ induzierten Dipolen) sowie temporären, durch Fluktuation der Elektronenhülle entstandenen Dipolen und polarisierbaren Partnern.

Wechselwirkungstyp	beobachtete Wechselwirkung
Keesom	perm. Dipol $\longleftrightarrow$ perm. Dipol
Debye	perm. Dipol $\longleftrightarrow$ polarisierbarer Partner
London	temp. Dipol $\longleftrightarrow$ polarisierbarer Partner

Die London-Dispersion ist stark entfernungsabhängig ($\propto R^{-6}$, vgl. Gleichung 1.1, gezeigt für ein Teilchenpaar AB) und kann klassischerweise durch ein Lennard-Jones-Potential angenähert werden.[3, 4]

$$\mathrm{E}_{\mathrm{AB}}^{\mathrm{disp}} = -\frac{3}{2}\frac{I_{\mathrm{A}} I_{\mathrm{B}}}{I_{\mathrm{A}} + I_{\mathrm{B}}}\frac{\alpha_{\mathrm{A}}\alpha_{\mathrm{B}}}{R^6} \tag{1.1}$$

Obwohl die London-Dispersion damit im Vergleich zu anderen in der Natur existenten Wechselwirkungen auf den ersten Blick nur geringe Auswirkung zu haben scheint, kann sie dennoch einen signifikanten Beitrag zu Teilchenwechselwirkungen ausmachen. Das nicht kovalent gebundene Benzol-Dimer beispielsweise wird durch Dispersionswechselwirkungen stabilisiert.[5, 6] Erweitert man die Betrachtung desweiteren auch auf kovalent gebundene Moleküle, so lassen sich hier ebenfalls sowohl durch physikalisch-chemische Methoden als auch durch die Methoden der Computerchemie Stabilitätsbeiträge nachweisen, die über intuitiv erwartete Werte hinausgehen können. Ein prominentes Beispiel hierfür ist das sogenannten „*hexaphenylethane riddle*“ (s. Abbildung 1.1).

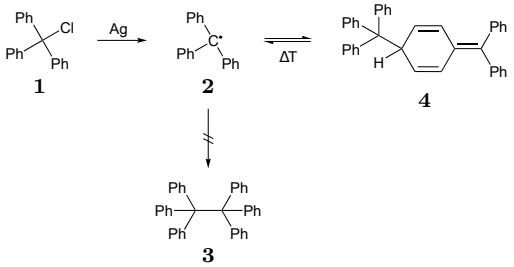

Abbildung 1.1: Dimerisierung des durch Einwirkung elementaren Silbers auf Triphenylchlormethan **1** entstehenden Tritylradikals **2**.[7] Statt Hexaphenylethan **3** entsteht die chinoide Spezies **4**,[8] welche durch Erhitzen wieder in Radikal **2** überführt werden kann.

Das aus Triphenylchlormethan (**1**) durch Einwirkung von elementarem Silber enstehende Triphenylmethylradikal (**2**)[7] dimerisiert nicht durch Bildung einer C-C Einfachbindung der zwei stabilisierten Radikalzentren, sondern durch *para*-Angriff eines der Radikalzentren an einem der Phenylreste des Dimerisierungspartners unter Auflösung von dessen Aromatizität zur chinoiden Spezies (**4**). Die Struktur des Reaktionsproduktes konnte mittels NMR-Spektroskopie aufgeklärt werden.[8] Diese Beobachtung wurde aufgrund der zu dieser Zeit verfügbaren Erklärungsmöglichkeiten als sterische Repulsion der im antizipierten Produkt räumlich nahestehenden Phenylreste erklärt. Dass eine Erklärung des Experiments über rein sterische Überlegungen nicht ausreichend ist, konnte bei Durchführung derselben Reaktion, diesmal jedoch unter Verwendung des Tri-(3,5-di-*tert*-butylphenyl)chlormethans gezeigt werden, wobei hier das direkte Dimerisierungsprodukt Hexa-(3,5-di-*tert*-butyl)ethan isoliert werden konnte.[9] Räumlich anspruchsvolle, polarisierbare Substituenten werden in diesem Zusammenhang auch als Dispersionsenergiedonoren (DEDs) bezeichnet.[10] Quantenchemische Rechnungen zeigen, dass im Falle der *tert*-Butylsubstitution die London-Dispersion zwischen den *tert*-Butylgruppen aufgrund ihrer additiven Wirkung über die

Molekülоberflächen maßgeblich zur Stabilisierung des Moleküls beiträgt.[11] Durch Neutronenbeugungsexperimente konnte gezeigt werden, dass im ungebundenen Molekülpaar, in dem beide Radikalpositionen durch Wasserstoffatome terminiert wurden, die beiden Wasserstoffatome direkt aufeinander zu zeigen und ihr Abstand 1.57 Å beträgt. Dieser Wert liegt unterhalb der kombinierten Van-der-Waals-Radien und wird über die zwischen den Molekülen wirkenden Dispersionswechselwirkungen erklärt.[12] Für eine Adamantylsubstitution gleichen Musters wurde eine im Vergleich, trotz noch ungünstigerer sterischer Parameter, noch stärkere Stabilisierung berechnet.[11] Die verwendeten quantchechemischen Methoden wurden durch Grimme et al.[13] für Dispersionswechselwirkungen korrigiert, wobei entweder das B3LYP-D3 Funktional oder dessen für kurze Abstände mit den von Becke und Johnson eingeführten Dämpfungsfunktionen[14–16] korrigierte Version B3LYP-D3(BJ) verwendet wird. Zusätzlich existieren Post-Hartree-Fock-Methoden, die Dispersionskorrekturen bereits implizit enthalten, beispielsweise Møller-Plesset-Störungstheorie zweiter Ordnung (MP2).[17, 18]

Im Zuge der Diskussion attraktiver Dispersionswechselwirkungen[10] wird eine Arbeit von Yamaguchi et al.[19] zitiert. Diese beschreibt, ausgehend von der Arinvorstufe **5**, die intermediäre Bildung des entsprechenden Arins (**6**), welches anschließend mit 2-Adamantylfuran zu Epoxynaphthalin **7** als Hauptprodukt reagiert (s. Abbildung 1.2). **7** wurde in einer nachfolgenden siebenstufigen Synthese zu Naphthalin **8** umgesetzt. In diesem Produkt stehen beide Adamantylsubstituenten auf derselben Seite des Rings. Die räumliche Struktur der Verbindung konnte durch röntgenkristallographische Analyse des finalen Reaktionsprodukts **8** aufgeklärt werden.

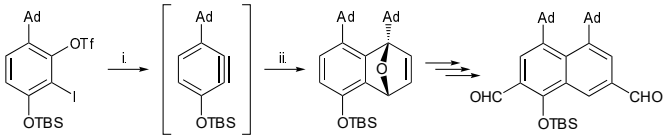

5 **6** **7** **8**

Abbildung 1.2: Synthese des diadamantylsubstituierten Naphthalins **8**. i. MeLi, Et_2O, 40 °C, ii. 2-Adamantylfuran, 10 min, 67 %.

Ausgehend von dieser präparativen Arbeit erwuchs die Idee, als Projektbeitrag zum Schwerpunktprogramm SPP1807 „Control of London dispersion interactions in molecular chemistry“ der Deutschen Forschungsgemeinschaft (DFG) die photochemisch erlaubte [$\pi_{4s} + \pi_{4s}$]-Cycloaddition des Anthracens zu untersuchen. Dieses Schwerpunktprogramm widmet sich der Untersuchung der London-Dispersion mithilfe von sowohl computer- und physikochemischen Methoden als auch klassisch präparativer (an-)organischer Chemie.

1.2 Photochemie des Anthracens

Neben klassischen Aromatenreaktionen wie nukleophiler oder elektrophiler Aromatensubstitution geht Anthracen eine von Fritzsche[20, 21] im 19. Jahrhundert entdeckte Photoreaktion ein, bei der durch Bestrahlung einer gesättigten Lösung von Anthracen in Toluol durch Sonnenlicht Kristalle einer farblosen Verbindung erhalten wurden, die einen anderen Schmelzpunkt als das Edukt besaßen. Die von Hengstenberg und Palacios vorgeschlagene Struktur dieses Produktes, des sogenannten Dianthracens,[22] wurde durch Ehrenberg mittels Röntgenstrukturanalyse bestätigt,[23] eine weitere Verfeinerung der Struktur wurde von Abboud et al.[24] vorgenommen. Die Bildung des Dianthracens erfolgt hierbei aus einem angeregten Komplex (engl. excited complex/exciplex) heraus,[25–30] der sich aus einem Anthracenmolekül im S_1-Zustand (durch Absorption im UV-Bereich des Spektrums) und

einem Anthracenmolekül im Grundzustand zusammensetzt. Aus dem Exciplex wird entweder das Dianthracenmolekül gebildet oder der Exciplex wird strahlungslos (Intersystem Crossing, ISC) bzw. über Photolumineszenz desaktiviert. Die Dimerisierung erfolgt über eine photochemisch erlaubte $[\pi_{4s} + \pi_{4s}]$-Cycloaddition. Je nach verwendeten Reaktionsparametern kann es zur Bildung unterschiedlicher Produkte oder von Produktgemischen kommen (s. Abschnitt 1.2.1). Wird die Photoreaktion beispielsweise in mit Sauerstoff gesättigten Lösemitteln durchgeführt, so bildet sich durch Reaktion des Anthracens mit angeregtem Singulettsauerstoff das Anthracenendoperoxid **9** (s. Abbildung 1.3), das thermisch oder katalysiert durch Säure oder Base unter Oxidation zum Anthrachinon (**10**) umlagern kann.[31]

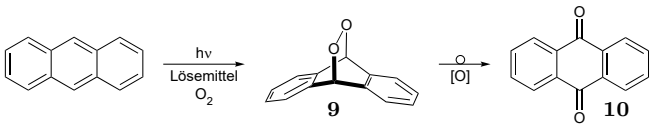

Abbildung 1.3: Reaktion des Anthracengerüstes mit $^1O_2$. Das gebildete Peroxid **9** kann durch Heizen oder Zugabe von Säure bzw. Base und Oxidation ins Anthrachinon **10** umgewandelt werden.

Zusätzlich handelt es sich bei der Photodimerisierung um eine Gleichgewichtsreaktion. Zwar kann Dianthracen prinzipiell auch durch Bestrahlung im kurzwelligen Bereich des Spektrums ($\approx$ 254 nm) gewonnen werden, jedoch kann Absorption bei derselben Wellenlänge auch zur Cycloreversion in die entsprechenden Monomere führen. Aufgrund der genannten Nebenreaktionen wurden die in dieser Arbeit beschriebenen Anthracendimerisierungen in entgastem Lösemittel und durch Bestrahlung im Wellenlängenbereich 305–400 nm durchgeführt (s. Abschnitt 1.4.3).

1.2.1 Bekannte Photodimere substituierter Anthracene

Basierend auf Fritzsches Entdeckung hat sich eine Vielzahl von Arbeitsgruppen der Untersuchung der Photochemie von Anthracenderivaten gewidmet. Bei der Reaktion von 9- beziehungsweise 9,10-substituierten Anthracenen sind zwei Isomere des Dianthracens möglich (s. Abbildung 1.4), in denen die Substituenten entweder auf den entgegengesetzten Seiten des Moleküls stehen (*head-tail*/*ht*, *anti*) oder in dieselbe Richtung orientiert sind (*head-head*/*hh*, *syn*).[25, 26, 32–34]

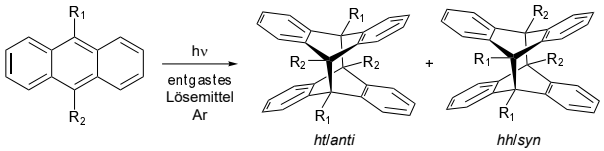

Abbildung 1.4: Photodimerisierung 9-,10-substituierter Anthracene. Je nach gewähltem Substituenten ist die Bildung von zwei Photoprodukten zu beobachten.

Die beiden Isomere können in der Regel aufgrund ihres unterschiedlichen Dipolmoments voneinander getrennt werden. Wird Anthracen jedoch in 9-Position mit der sterisch anspruchsvollen *tert*-Butylgruppe substituiert, so kann keine Bildung des entsprechenden Dianthracens nachgewiesen werden. Stattdessen wird die dem Dewarbenzol[35, 36] strukturell ähnliche Verbindung Dewaranthracen erhalten.[37, 38]

1.3 Zielsetzung

Im Hinblick auf Yamaguchis Diels-Alder Experiment und Fritzsches Photodimerisierung von Anthracen sollte im Rahmen der vorliegenden Arbeit die Anthracendimerisierung von mit Dispersionsenergiedonoren (DEDs) substituierten Anthracenen untersucht werden. Da wie jedoch gezeigt die Substitution mit DEDs in der 9-Position die Dimerisierung unterdrückt, wurden Mo-

dellsysteme synthetisiert und charakterisiert, die die entsprechenden DEDs in den 2,3-Positionen tragen. In dieser Produktklasse sind bis heute nur die Dimere des 2,3-Di-*n*-undecylanthracens bekannt, die durch Hopf et al. im Hinblick auf selbstassemblierende Systeme untersucht wurden.[39] Durch Bestimmung der Produktverhältnisse sowie durch quantenchemische Rechnungen sollten im Rahmen der vorliegenden Arbeit hierüber Rückschlüsse auf das Vorhandensein von Dispersionswechselwirkungen im Exciplex und gegebenenfalls deren Größe im Vergleich zu den klassischen repulsiven Wechselwirkungen gewonnen werden.

1.4 Zusammenfassung der Ergebnisse

1.4.1 Synthese substituierter Anthracene durch Suzuki-Miyaura-Reaktion

Die anfänglichen Versuche zur Synthese eines *tert*-butylsubstituierten Anthrachinons über Umsetzung von Naphthochinon mit 2,3-Di-*tert*-butylthiophendioxid[40–46] waren nicht erfolgreich, da kein Umsatz, auch bei Änderung der Reaktionsparameter wie beispielsweise Lösemittel, Temperatur oder Katalysator, beobachtet werden konnte. Daher wurde, um eine möglichst effiziente Synthese zum Aufbau einer Datenbank von Anthracenderivaten zu entwickeln, die Synthese des literaturbekannten 2,3-Dibromanthracens[47] mit anschließender Derivatisierung durch Suzuki-Miyaura-Kreuzkupplung mit Alkylboronsäuren angestrebt.[48]

Durch Umsetzung von Phthalid **11** mit $[Et_3O]BF_4$ nach Vorschrift von Meerwein,[49] anschließende Reduktion des stark hygroskopischen Oxoniumsalzes **12** mittels $LiAlH_2(OEt)_2$[50] und baseninduzierte 1,4-Eliminierung kann aus dem cyclischen Acetal **13** Isobenzofuran erzeugt werden,[51, 52] welches mit 1,2,4,5-Tetrabrombenzol unter Zugabe von MeLi, in diesem Fall jedoch unter eher untypisch hohen Temperaturen, zum Epoxyanthracen **14** umgesetzt werden kann (s. Abbildung 1.5). Durch anschließende Deoxygenie-

rung mit niedervalentem Titan, welches durch Umsetzung von $TiCl_4 \cdot 2\,THF$ mit aktiviertem Zinkpulver in THF als Lösemittel generiert wurde, kann 2,3-Dibromanthracen (**15**) in reiner Form erhalten werden, welches jedoch zumindest bei Raumtemperatur unlöslich in herkömmlichen organischen Lösemitteln ist.

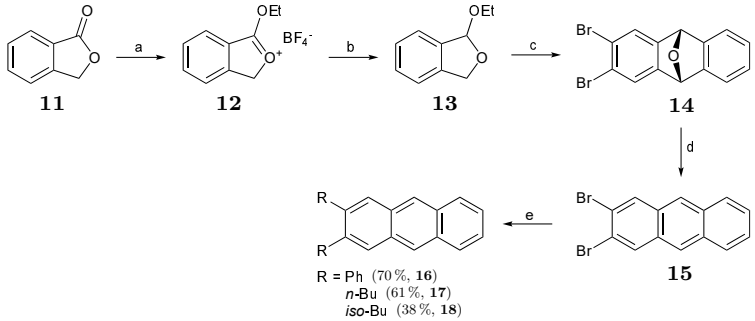

11 **12** **13** **14** **15**

Abbildung 1.5: Synthese der 2,3-disubstituierten Anthracene **16**–**18** über 2,3-Dibromanthracen (**15**) ausgehend von Phthalid (**11**). a) $[Et_3O]BF_4$, 1,2-Dichlorethan, RT, 72 h, 83 %, b) $LiAlH_4$, THF/EtOH, RT, 2 h, 81 %, c) i. MeLi/kat. DIPA, Et_2O, RT, 3 h, ii. 1,2,4,5-Tetrabrombenzol, MeLi, Rückfluss über Nacht, 45 %, d) $TiCl_4 \cdot 2\,THF$, akt. Zn, THF, 0 °C, Rückfluss über Nacht, 59 %, e) $RB(OH)_2$, Na_2CO_3, 12–22 mol % $Pd(PPh_3)_4$, Toluol/H_2O, 110 °C, 5–7 d.

Das ^{13}C-Spektrum von Verbindung **15** kann aufgrund ihrer Schwerlöslichkeit nur bei höheren Temperaturen, in diesem Fall 120 °C in DMSO-d_6, aufgenommen werden. Das Spektrum gleicht dem nahezu zeitgleich von Bunz et al.[53] publizierten Spektrum, welches bei 100 °C in Pyridin-d_5 erhalten wurde. Da **15** jedoch unter den Bedingungen der Suzuki-Miyaura-Reaktion (Toluol/H_2O, 110 °C) komplett gelöst vorliegt, stellt dies kein Hindernis für die Reaktion dar. Für eine erste Reaktionsoptimierung wurde die Synthese des 2,3-Diphenylanthracens (**16**) angestrebt, da die spektroskopischen Daten

dieser Verbindung bereits durch eine Publikation von Bailey und Williams bekannt sind, die die Verbindung durch Reduktion des entsprechenden Chinons erhalten haben.[54, 55] Nach fünf Tagen bei 110 °C und einer Gesamtmenge von 12 mol % Katalysator konnte 2,3-Diphenylanthracen (**16**) in einer Ausbeute von 70 % isoliert werden. Da diese Testreaktion, wenn auch unter Verwendung einer vergleichsweise großen Menge an Katalysator und langen Reaktionszeiten dennoch gute Ausbeuten lieferte, wurde die Reaktion auf die Umsetzung mit *n*-Butyl-, *iso*-Butyl- und *sec*-Butylboronsäure ausgeweitet, wodurch 2,3-Di-*n*-butyl- (**17**) und 2,3-Di-*iso*-butylanthracen (**18**) in Ausbeuten von 61 bzw. 38 % erhalten werden konnten. Im Falle der Umsetzung mit *sec*-Butylboronsäure konnte reines Anthracen, vermutlich gebildet aufgrund einer doppelten Hydrodehalogenierung durch β-H-Eliminierung an der Boronsäure,[56–58] isoliert werden. Die erwarteten Kupplungsprodukte konnten nicht nachgewiesen werden.[48] Zusätzlich zeigten sich, neben den langen Reaktionszeiten, dem hohen Verbrauch an Katalysator sowie der Unvereinbarkeit der Reaktion mit Boronsäuren, die eine β-H-Eliminierung eingehen können, noch Probleme beim Versuch, die entsprechenden Reaktionen in größerem Maßstab durchzuführen, da vermehrt Nebenprodukte auftraten. Daher war die Etablierung einer zweiten Syntheseroute notwendig.

1.4.2 Synthese substituierter Anthracene über die korrespondierenden Chinone

Neben der bereits erwähnten Synthese substituierter Anthrachinone durch Umsetzung von Naphthochinon mit substituierten Thiophendioxiden[40–46] können diese auch durch eine Umsetzung mit 2,3-disubstituierten Buta-1,3-dienen erhalten werden (s. Abbildung 1.6). Werden methoxysubstituierte Butadiene verwendet, sind alkoxy- bzw. hydroxysubstituierte Anthracene zugänglich.[59] Die zur Synthese verwendeten Butadiene konnten prinzipiell über zwei verschiedene Syntheserouten erzeugt werden.[48]

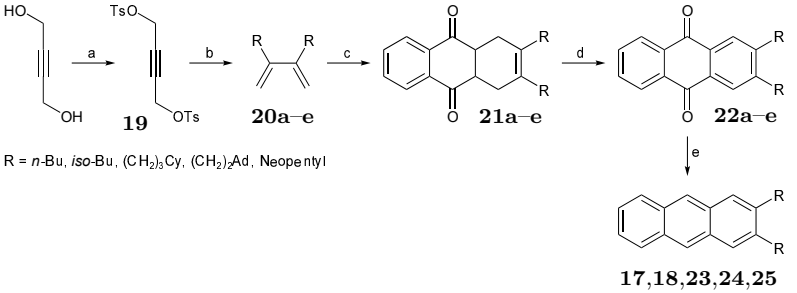

Abbildung 1.6: Chinonroute zur Synthese der 2,3-disubstituierten Anthracene **17**, **18**, **23**, **24** und **25**. a) TsCl, THF/Natronlauge, 0 °C, 2 h, 91 %, b) RMgBr/CuBr · LiBr oder RZnCl/CuCN · 2 LiCl, THF, −50 °C über Nacht, c) 1,4-Naphthochinon, EtOH, 80 °C über Nacht, d) 5 % ethanolische KOH, O_2, 45 min RT, 1 h 65 °C, e) Al, $HgCl_2$, CBr_4, Cyclohexanol, 140 °C über Nacht.

Die Umsetzung von 2,3-Dimethylbutadien mit Lochmann-Schlosser-Base in *n*-Pentan liefert das Butadiendianion, welches in einer C1-Kettenverlängerung mit einem Alkylbromid durch S_N2-Reaktion zum entsprechenden Butadien reagiert (nicht in Abbildung 1.6 gezeigt).[60,61] Da die Isolierung und Aufreinigung des pyrophoren Dianions aufwendig ist und selbst nach Versuchen zur Reaktionsoptimierung nur geringe Ausbeuten erhalten wurden, wurde dieser Syntheseweg wieder verworfen. Stattdessen wurde das Ditosylat **19**[62] mit den aus den entsprechenden Grignardverbindungen unter Zugabe von CuBr/LiBr erzeugten weichen Cupraten umgesetzt,[63] die eine S_N2'-Reaktion an der Dreifachbindung ermöglichen. Hierdurch konnten die Butadiene **20a–e** gewonnen werden. Durch Verwendung frisch hergestellter Grignardlösungen konnten zusätzliche Ausbeutesteigerungen erreicht werden. Ausgenommen hiervon war allerdings die Reaktion zur Synthese des ethyladamantylsubstituierten Systems **20d**, bei der in initialen Versuchen nur geringe Mengen des Butadiens unter gleichzeitiger Isolierung nicht abreagierten Ethyladamantylbromids, vermutlich durch dessen Reaktionsträg-

heit mit Magnesium, erhalten wurden. Diese ließen sich auch nicht weiter aufreinigen, da sowohl das Bromid als auch das disubstituierte Butadien ähnliche physikalische Eigenschaften aufweisen. Eine zusätzliche Problematik ergab sich durch eine inkonsistente Reproduzierbarkeit der Ergebnisse, da bei nicht allen der daraufhin durchgeführten Wiederholungsreaktionen überhaupt Produkt isoliert werden konnte. Eine Reihe von Methoden zur Erhöhung der Reaktivität von in Grignardreaktionen reaktionsträgen Bromiden sind bekannt, darunter unter anderem die klassischen Aktivierungen mittels Anätzen mit Iod oder 1,2-Dibromethan, gegenbenenfalls unter Kombination mit TMSCl oder Zugabe von Turbogrinardverbindungen.[64]

Eine Reaktionsoptimierung unter Verwendung aller genannter Methoden führte jedoch zu keiner Ausbeutesteigerung. Letztlich konnte die Reaktion dennoch mittels einer Vorschrift von Knochel et al.[65] erfolgreich durchgeführt werden, indem eine LiCl-vermittelte Mg-Insertion mit anschließender Ummetallierung zum korrespondierenden Zinkorganyl vorgenommen wurde, welches anschließend mit $CuCN \cdot 2\,LiCl$ und gemäß der allgemeinen Vorschrift mit Ditosylat **19** umgesetzt wurde. Insgesamt konnten somit Mengen größer als 1 g des Butadiens **20d** isoliert werden, die jedoch immer noch mit dem nicht abreagierten Bromid verunreinigt waren. Daher kann keine Angabe über die isolierte Ausbeute gemacht werden (Ausbeuten für alle anderen Derivate s. Tabelle 1.2).[48]

Tabelle 1.2: Isolierte Ausbeuten für die einzelnen Syntheseschritte der Chinonroute.

	Ausbeute / %			
R	S_N2'	Diels-Alder	Oxidation	MPV-Reduktion
n-Bu (**a**)	41	54	96	65
iso-Bu (**b**)	26	60	90	67
$(CH_2)_3$Cy (**c**)	90	73	96	81
$(CH_2)_2$Ad (**d**)	–[a]	–[a]	46	74
Neopentyl (**e**)	67	31[b]	97	63

[a] Aufgrund von Verunreinigung mit nicht abreagiertem Bromid kann keine Ausbeute angegeben werden. [b] Katalysiert mittels $[AlCl_3 \cdot 2\,THF]$.

Die synthetisierten Butadiene **20a**–**e** wurden anschließend in Übernachtreaktionen bei 80 °C in Ethanol mit 1,4-Naphthochinon zu den korrespondierenden Diels-Alder-Addukten **21a**–**e** umgesetzt, welche durch Kühlen des Reaktionsgemisches auf −10 °C und anschließendes Auswaschen der nicht abreagierten Edukte mittels eiskaltem Ethanol in Form farbloser bis rotbrauner Feststoffe in sehr guten Ausbeuten isoliert werden konnten. Für Butadien **20e** war aufgrund seiner ungünstigen Konformation[61] Lewis-Säure-Katalyse mittels des $[AlCl_3 \cdot 2\,THF]$-Komplexes[66] vonnöten. Die Produkte konnten in der Regel direkt für die nachfolgende Reaktion eingesetzt werden. In Fällen in denen Waschen mit Ethanol nicht ausreichte um alle Verureinigungen zu entfernen war eine Aufreinigung mittels Säulenchromatographie erfolgreich. Im Falle der Umsetzung des 2,3-Di(ethyladamantyl)-butadiens **20d** konnten neben dem Diels-Alder-Addukt zusätzlich die einfach bzw. zweifach oxidierten Spezies isoliert werden.[48] Dies kann dadurch erklärt werden, dass durch die Verunreinigung des eingesetzten Butadiens mit nicht abreagiertem Bromid die exakte Stöchiometrie zwischen den Reaktionspartnern nicht eingestellt werden konnte, das Naphthochinon also ggf. im Überschuss vorlag. Dieses fungiert in diesem Fall vermutlich als Oxidationsmittel. Die

oxidative Wirkung von Chinonen ist literaturbekannt.[67] Da der nachfolgende Reaktionsschritt jedoch ohnehin eine Oxidationsreaktion ist, konnte das isolierte Dreikomponentengemisch ohne weitere Aufreinigung eingesetzt werden. Die Oxidation der Diels-Alder-Addukte **21a**–**e** mittels O_2 in 5 % ethanolischer KOH führte in allen Fällen zur Bildung der gewünschten Produkte (**22a**–**e**) in hohen Ausbeuten. Durch die anschließende Reduktion der erhaltenen Chinone unter den Bedingungen der Meerwein-Ponndorf-Verley-Reduktion (MPV-Reduktion) mittels $Al(OCy)_3$ in entgastem Cyclohexanol wurden die entsprechenden Anthracene in sehr guten Ausbeuten erhalten. Die spektralen Daten der durch Suzuki-Miyaura-Reaktion und mittels dieses Synthesewegs synthetisierten 2,3-Di-*n*-butyl- (**17**) sowie 2,3-Di-*iso*-butylanthracene (**18**) stimmen überein.

1.4.3 Photodimerisierung 2,3-dialkylsubstituierter Anthracene

Die entsprechenden Photoexperimente wurden, um die Reaktion von Anthracen mit Singulettsauerstoff zum Anthracenendoperoxid zu unterdrücken, in entgastem Lösemittel durchgeführt, wobei der Wellenlängenbereich 305–400 nm verwendet wurde, um die ebenfalls unter Absorption kurzwelligerer UV-Strahlung einsetzende Cycloreversion zu unterdrücken.[48] Als geeignetstes Lösemittel stellte sich hierbei Toluol heraus, da es sich gegenüber der verwendeten UV-Strahlung inert verhält und die für die Untersuchungen verwendeten Monomere in Toluol, im Gegensatz zu polareren Lösemitteln wie beispielsweise Aceton oder Acetonitril, eine höhere Löslichkeit besitzen. Zudem bildet Toluol selbst keine starken Wechselwirkungen mit den Monomeren aus, was für eine Untersuchung der relativ schwachen London-Dispersion von Vorteil ist. Neben den synthetisierten disubstituierten Anthracenderivaten **17**, **18**, **23**, **24** und **25** wurden 2,3-Dimethyl-, 2-*Tert*-butyl- sowie das über eine Stufe aus 9,10-Dihydroanthracen synthetisierbare 2,6-Di-*tert*-butylanthracen[68] unter den angegebenen Bedingungen dimerisiert. Für den kleinsten Substituenten (Me) konnte gezeigt werden, dass kein Einfluss der

Sterik auf das Produktverhältnis besteht, da beide Produkte gemäß NMR-Integration im Verhältnis 1:1 gebildet wurden. Die *tert*-butylsubstituierten Anthracene hingegen zeigen eine klare Präferenz zur Bildung der Produkte mit *anti*-Symmetrie, was eindeutig durch Röntgendiffraktometrie an Einkristallen der erhaltenen Verbindungen belegt ist. Neben Kristallstrukturen für eine Reihe von *anti*-Dimeren wurde die Kristallstruktur des *syn*-Dimers (**26**) des 2,3-Di-*iso*-butylanthracens erhalten (s. Abbildung 1.7), welche die erste bekannte Struktur dieser Art darstellt.[48]

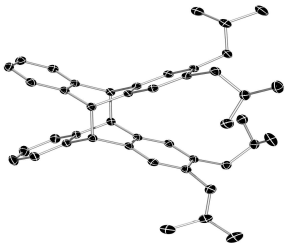

Abbildung 1.7: Molekülstruktur von 2,2',3,3'-Tetra-*iso*-butyldianthracen (**26**) im Einkristall. Für die Darstellung werden U_{ij}-Tensoren mit 50 % Wahrscheinlichkeit verwendet, Wasserstoffatome werden zur besseren Übersichtlichkeit nicht dargestellt.

Selbst in Fällen, in denen keine Einkristalle der Verbindungen vorliegen, konnte dennoch die Konnektivität der Produkte über NOE-Spektroskopie ermittelt und damit das Produktverhältnis bestimmt werden. Die erhaltenen Produktverhältnisse (*anti*:*syn*), beziehungsweise deren natürliche Logarithmen wurden mit dem von Charton enwickelten, auf Van-der-Waals-Radien beruhenden Parameter ν korreliert, der einen Ausdruck für den sterischen Anspruch eines Substituenten darstellt.[69]

Die Auftragung (s. Abbildung 1.8) mit Ausnahme des ^{t}Bu-Substituenten, da dieser wie anhand der Produktverhältnisse verdeutlicht von vornherein klare Präferenz der *anti*-Produkte zeigt, liefert eine nahezu lineare Beziehung für den Großteil der aufgetragenen Substituenten ($R^2 = 0.98$). Einzig der ^{i}Bu-Substituent zeigt eine beträchtliche Abweichung zum gemäß der Regressionsgeraden zu erwartenden Wert, es bildet sich also mehr *syn*-Produkt als theoretisch vorhergesagt. Ein möglicher Einfluss von Dipol-Dipol-Wechselwirkungen wurde anhand der auf ωB97XD/6-31G*-Theorieniveau berechneten Dipolmomente der S_0- und S_1-Zustände der Anthracenmonomere untersucht. Wenn solche Wechselwirkungen die Energien der beiden betrachteten Übergangszustände beeinflussen würden, so wäre die antiparalelle Anordnung stets energiegünstiger und die Bildung der *anti*-Dimere immer stark bevorzugt. Aufgrund der Tatsache, dass 2,3-Dimethylanthracen jedoch ein relativ großes Dipolmoment, im Speziellen im S_1-Zustand besitzt, jedoch keinerlei Selektivität für die Bildung eines der beiden Isomere aufweist, kann ein solcher Einfluss ausgeschlossen werden.[48]

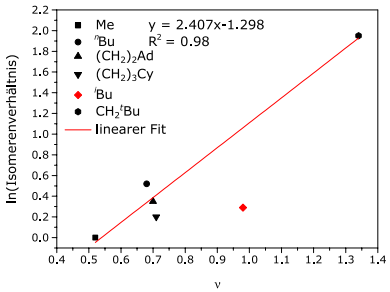

Abbildung 1.8: Auftragung der natürlich Logarithmen der Isomerenverhältnisse *anti*:*syn* gegen Chartons ν-Parameter. Die lineare Regression durch fünf der sechs Datenpunkte zeigt eine lineare Korrelation mit $R^2 = 0.98$. Der ^{i}Bu-Substituent wurde aufgrund starker Abweichung nicht bei der linearen Regression berücksichtigt.

Die gezeigten Ergebnisse deuten darauf hin, dass die Photodimerisierung von Anthracen weitestgehend (gezeigt anhand der Korrelation mit Charton-Parametern) durch die Sterik der Substituenten beeinflusst wird. Einzig der ^{i}Bu-Substituent weicht von diesem Verhalten ab und zeigt ein Produktverhältnis, anhand dessen ein Einfluss von London-Dispersion auf die Selektivität der Reaktion diskutiert werden kann. Eine Untersuchung der Reaktion mittels in silico Methoden unter expliziter Einbeziehung von Dispersionswechselwirkungen durch die GD3-Korrektur, die einen energetischen Einblick in die bei der Photodimerisierung wirkenden Kräfte eröffnen würde, scheitert jedoch an der Tatsache, dass bis dato kein passendes Modell gefunden werden konnte, mit dem der Reaktionsverlauf und dessen Produkte ohne Konvergenzprobleme abgebildet werden können. Hierfür wäre die Anwendung anspruchsvollerer Methoden von Nöten, die uns jedoch derzeit nicht zur Verfügung stehen.

2 Synthese und Charakterisierung neuartiger, tetrafluorsubstituierter Pentacene

2.1 Eigenschaften der Acene

Die Stoffgruppe der Acene ist eine Untergruppe von polyzyklischen aromatischen Kohlenwasserstoffen (PAKs), die aus linear annelierten Benzolringen besteht (s. Abbildung 2.1). Als kleinster Vertreter der Gruppe wird laut IUPAC Anthracen angesehen.[70] Eine wesentliche Eigenschaft der homologen Reihe der Acene ist die nahezu inverse lineare Abhängigkeit ihres HOMO-LUMO-Abstands von der Anzahl der Ringe.[71]

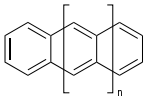

Abbildung 2.1: Allgemeine Strukturformel der Acene.

Während kleinere Homologe wie zum Beispiel Anthracen aufgrund eines relativ großen HOMO-LUMO-Abstands stabil gegenüber beispielsweise der Reaktion mit Sauerstoff unter Normalbedingungen sind, nimmt die Reaktivität innerhalb der homologen Reihe mit kleiner werdendem energetischem Abstand der beiden Orbitale zu. Penta-, Hexa-[72] und Heptacen weisen im Festkörper eine relativ hohe Stabilität im Vergleich zur Lösung auf,[73] wohingegen die unsubstituierten, höheren Homologen, beispielsweise Nona-,[74, 75] Deca-,[76] Undeca-[77, 78] sowie Dodecacen[79] nur durch on-surface Experimente oder mittels Matrixisolation unter kryogenen Bedingungen in Edel-

gasmatrix erzeugt und nachgewiesen werden können. Die Synthese einer Reihe kinetisch stabilisierter Derivate des Nonacens wurde von Miller et al.[80] sowie Anthony et al.[81] realisiert. Aufgrund ihrer Halbleitereigenschaften sind Acene besonders für den Bau elektronischer Bauteile, beispielsweise organischer Feldeffektransistoren (OFETs) interessant.[82–84] Diese können in Form dünner Schichten, auf Folien als Substrat aufgebracht, als flexible Bauteile verwendet werden.[85,86] Insbesondere auf Pentacen liegt hier aufgrund seiner guten Verfügbarkeit bei noch hinreichender Stabilität gegenüber Sauerstoff und UV-Licht ein Augenmerk der Materialwissenschaften. Unsubstituiertes Pentacen zeigt aufgrund der Lage seines HOMOs[1] p-Typ Halbleitungseigenschaften[87,88] mit einer von der Wahl des Substrats abhängigen Ladungsträgerbeweglichkeit im Device[89] von bis zu $35\,\mathrm{cm}^2/\mathrm{Vs}$ im Einkristall bei Raumtemperatur.[90] Es konnte experimentell gezeigt werden, dass sich der Leitungstyp von p- in n-Typ Halbleitung konvertieren lässt, wenn das Pentacengerüst mit elektronenziehenden Gruppen, wie beispielsweise Fluoratomen oder Nitrilgruppen substituiert wird, die das LUMO energetisch absenken.[87,91–93] Für 1,2,3,4-Tetrafluorpentacen wurde durch Chien et al.[94] experimentell gezeigt, dass diese Verbindung abhängig vom gewählten Elektrodenmaterial entweder p- oder n-Typ-Halbleitung aufweist.

Die Einführung von Fluoratomen hat sich als nützliche Möglichkeit erwiesen, die elektronischen Eigenschaften von Molekülen beziehungsweise Molekülmischungen zu steuern. Die Arbeitsgruppe um Leo[95] konnte zeigen, dass sich der HOMO-LUMO-Abstand in Mischungen von ZnPc mit partiell fluorierten Zinkphthalocyaninen (F_nZnPcs) in Abhängigkeit des Dotierungsgrades verändern lässt, was auf Coulomb-Wechselwirkungen zurückgeführt wird.[96] Eine Reihe computerchemischer Untersuchungen von partiell fluorierten Pentacenen und deren Wechselwirkung mit beispielsweise der Cu(111)-Oberfläche zeigt ein klare Abhängigkeit des Molekül-Substrat-Abstands vom Fluorierungsgrad, welche durch eine zunehmende Repulsion

[1] $E_{HOMO} = -4.94\,\mathrm{eV}$ berechnet auf B3LYP/6-311+G**-Theorieniveau.

der F_{2p}-Orbitale begründet wird.[97,98] Aufgrund dieser Beobachtungen wird die Möglichkeit diskutiert, die Effizienz der Ladungsträgerinjektion über den Fluorgehalt des zum Devicebau verwendeten Pentacens zu steuern. Um vielversprechende Kandidaten innerhalb der Gruppe der Fluorpentacene zu finden, wurden die elektronischen Eigenschaften von 15 symmetrisch substituierten Fluorpentacenen von Lukeš et al.[99] berechnet. Es konnte gezeigt werden, dass die anhand von Dimerpaaren berechneten Ladungsträgerbeweglichkeiten für Perfluorpentacen am geringsten sind und ihr Maximum für das 1,4,8,11-Tetrafluorpentacen ($\mu = 7.3\,\mathrm{cm}^2/\mathrm{Vs}$) in Abhängigkeit von der gewählten Dimerkonfiguration erreichen.[99] Im Vergleich zu rein fluorsubstituierten Pentacenen, von denen bis dato nur wenige Vertreter synthetisiert und charakterisiert wurden, ist die Gruppe fluorsubstituierter Pentacene, die zusätzlich TIPS-Acetylengruppen tragen, größer. Wasikiewicz et al.[100] waren in der Lage zu zeigen, dass die gemessenen Leitfähigkeiten durch Variation des Substitutionsmusters und der Anzahl der Fluoratome beeinflusst werden können.

Neben der Anpassung elektronischer Strukturen auf molekularer Ebene kann die Einführung von Fluorsubstituenten auch im Sinne des sogenannten „*crystal engineering*“ genutzt werden.[101–105] Der Einfluss des Fluorsubstitutionsmusters auf die Packungsmotive von partiell fluorsubstituierten Rubrenen wurde eindrucksvoll von Ogden et al. unter Beweis gestellt.[106] Der Ladungsträgerübertritt im Festkörper und damit die Leitfähigkeit sowie daraus folgend die Deviceperformance ist außerdem maßgeblich vom Packungsmotiv abhängig, was durch eine Veränderung der Kopplung der nächsten Nachbarn in einer Kristallpackung erklärt werden kann. Eine computerchemische Untersuchung von unter anderem Pentacen durch Rui et al.[107] kam zu dem Schluss, dass die Effizienz des Ladungsübertritts für den Fall von π-π-Stapelung maximiert werden kann. Die angesprochenen Entdeckungen zeigten sich vielversprechend genug, um die Synthese der zu 2,3,9,10-Tetrafluorpentacen[108] regioisomeren Verbindungen 1,4,8,11- sowie 1,4,9,10-Te-

trafluorpentacen anzustreben, insbesondere unter dem Gesichtspunkt, dass das 1,4,8,11-Isomer aufgrund der von Lukeš et al. durchgeführten computerchemischen Rechnungen[99] Interesse von Materialwissenschaftlern geweckt hat. Die ermittelten Stoffeigenschaften können weiterhin zum tieferen Verständnis und damit auch zur Entwicklung neuer Strukturmotive mit verbesserten Eigenschaften herangezogen werden.

2.1.1 Synthese von Pentacen und dessen Derivaten

Die erste Synthese des Pentacens gelang Clar ausgehend von *o*-Xylol und Benzoylchlorid.[109, 110] Nach Friedel-Crafts-Acylierung, Pyrolyse des Reaktionsproduktes in Anwesenheit von Kupfer und Transferdehydrogenierung konnte Pentacen isoliert werden. Desweiteren kann Pentacen auch aus seinem korrespondierenden Chinon mittels klassischer MPV-Reduktion gewonnen werden.[111, 112] Das Chinon als Startmaterial bietet zudem den Vorteil, dass die Einführung von Substituenten in den Positionen 6 und 13 durch Umsetzung mit C-Nukleophilen und anschließender reduktiver Aromatisierung mittels Zugabe von Säure/$SnCl_2$ möglich ist.[113, 114] Die im Arbeitskreis etablierten Methoden der Synthese des 2,3,9,10-Tetrafluorpentacens (**27**, s. Abbildung 2.2) gehen von der ethenoverbrückten Pentacenvorstufe aus.[108, 115] Diese kann durch Diels-Alder-Reaktion von Bisdien **28** mit dem aus 1,2-Dibrom-4,5-difluorbenzol unter Li-Halogen-Austausch gebildeten 1,2-Didehydro-4,5-difluorbenzol und anschließende Aromatisierung des Diels-Alder-Adduktes generiert werden.[108] Das erhaltene Ethenopentacen wird entweder thermisch durch die Umsetzung mit 1,2,4,5-Tetrazin-3,6-dicarbonsäuredimethylester oder durch Dihydroxylierung, Oxidation zum verbrückten α-Diketon und photochemische Abspaltung von Kohlenmonoxid mittels der sogenannten Strating-Zwanenburg-Reaktion in das Pentacen überführt.[116, 117] Diese Reaktionssequenz ist prinzipiell auch für die Darstellung der Photovorstufen der längeren, unsubstituierten Acene geeignet, liefert jedoch durch den um zwei Schritte längeren Reaktionsweg schlechtere Ausbeuten bzw. geringere Mengen an Vorstufe.[108, 115]

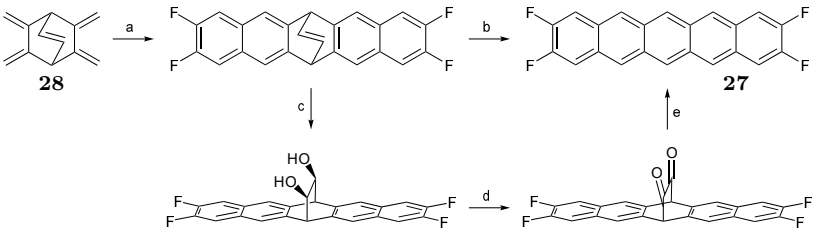

Abbildung 2.2: Methoden zur Synthese des 2,3,9,10-Tetrafluorpentacens (**27**). a) (i.) 1,2-Dibrom-4,5-difluorbenzol, *n*-BuLi, Toluol, −50 °C auf RT über Nacht, (ii.) Chloranil, Toluol, Reflux über Nacht oder DDQ, $CHCl_3$, RT über Nacht, b) 1,2,4,5-Tetrazindicarbonsäuredimethylester, *n*-Pentylether, 1.5 min 180 °C, anschließend 0 °C, c) OsO_4 (kat.)/NMO, Aceton/H_2O, 48 h RT, d) TEMPO/NaOCl, KBr, $NaHCO_3$ DCM, 48 h, e) hν, Toluol, 20 min.

2.2 Zielsetzung

Im Zuge dieses Projekts sollte die Synthese zweier weiterer, zu 2,3,9,10-Tetrafluorpentacen (**27**)[108, 115] komplementärer Isomere erfolgen, von denen das Isomer mit 1,4,8,11-Substitutionsmuster im Hinblick auf erste theoretische Rechnungen vielversprechende Halbleitereigenschaften zeigt.[99] Eine Synthesestrategie für geeignete, ethenoverbrückte Pentacenvorstufen mittels klassischer organischer Synthese sollte etabliert, und diese Verbindungen anschließend mittels der literaturbekannten Synthese auf thermischem Weg in die Pentacene überführt werden. Neben der Charakterisierung und Untersuchung der (physiko-)chemischen Eigenschaften der Neutralverbindungen in Lösung sowie im Festkörper sollten zusätzlich Untersuchungen zu Stabilität und Eigenschaften der prinzipiell aus den Neutralverbindungen durch Einbeziehungsweise Zwei-Elektronen-Oxidation gebildeten Radikal- und Dikationen durchgeführt werden.

2.3 Zusammenfassung der Ergebnisse

Ausgehend von der von Bettinger et al.[108] publizierten Synthese des 2,3,9,10-Tetrafluorpentacens (**27**) wurde der Versuch unternommen, 1,4,8,11-Tetrafluorpentacen (**29**) sowie 1,4,9,10-Tetrafluorpentacen (**30**) auf analogem Wege zu generieren. Die Umsetzung des nach Gabioud und Vogel[118, 119] synthetisierten Bisdiens (**28**)[2] mit 1,2-Dibrom-3,6-difluorbenzol unter den Bedingungen des Li-Halogen-Austausches mittels Zugabe von *n*-BuLi bei −50 °C führte jedoch nach NMR-spektroskopischer Analyse der Rohprodukte nicht zur Bildung des entsprechenden Diels-Alder-Addukts. Dieses sollte sich durch das charakteristische Signal der aliphatischen Protonen auch in etwaigen Produktgemischen gut nachweisen lassen, im entsprechenden Verschiebungsbereich ließ sich jedoch, auch nach mehrmaliger Durchführung der Reaktion mit veränderten Parametern, kein Produktsignal nachweisen.

Als alternative Methode zur Generierung des 1,2-Didehydro-3,6-difluorbenzols wurde auf eine auf Arbeiten von Kobayashi basierende Methode zurückgegriffen.[120] Hierbei kann durch Zugabe einer Fluoridionenquelle (Kaliumfluorid/18-Krone-6 oder Cäsiumfluorid) zu einem *o*-Trimethylsilyltriflat das entsprechende Arin generiert werden. Insbesondere für die Naturstoffsynthese bietet diese Methode Vorteile, da im Gegensatz zum Lithium-Halogen-Austausch sehr milde Bedingungen vorherrschen.

Ausgehend von 2-Brom-3,6-difluorphenol (**31**) erfolgte die Umsetzung mit Hexamethyldisilazan (HMDS) in THF (s. Abbildung 2.3). Aus dem TMS-geschützten Phenol (nicht in der Abbildung gezeigt) konnte durch Umlagerung mittels Zugabe von *n*-BuLi *o*-TMS-Phenol **32** erhalten werden. Anschließend wurde daraus mit Tf_2O unter Verwendung von Pyridin als nukleophilem Katalysator Verbindung **33** generiert. Im Vergleich zur ersten literaturbekannten Synthese der Zielverbindung durch Osakada et al.[121]

[2] Die Kristallstruktur der Verbindung konnte durch langsames Abdampfen einer Lösung in *n*-Hexan erhalten werden.

konnte durch die vorhergehende Isolierung von **32** die erhaltene Ausbeute an Arinvorstufe **33** zwar nicht gesteigert, jedoch die Reinheit des Produktes signifikant verbessert werden.[122]

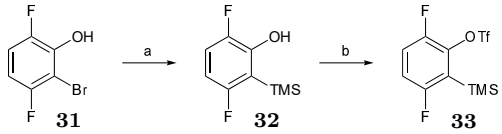

Abbildung 2.3: Synthese der Arinvorstufe **33**.[120, 123] a) HMDS, THF, Reflux über Nacht, anschließend −78 °C, *n*-BuLi, 36 %, b) Tf_2O, Pyridin, DCM, 0 °C, über Nacht, 85 %.

Nach Reaktion von Bisdien **28** mit 2.2 Äq **33** unter Verwendung von CsF als Fluoridionenquelle in ACN/DCM (1:1) konnte das Bisaddukt **34** isoliert und durch DDQ-Oxidation in Chloroform bei Raumtemperatur ins verbrückte Pentacen **35** überführt werden (s. Abbildung 2.4). Zur Synthese des Pentacenprecursors mit 1,4,9,10-Substitutionsmotiv wurden Verbindung **28** und **33** im Verhältnis 1:1 bei ansonsten unveränderten Reaktionsbedingungen umgesetzt. Das aus der Reaktion erhaltene Monoaddukt **36** wurde anschließend, unter den bereits bei der Synthese von 2,3,9,10-Tetrafluorpentacen (**27**) verwendeten Bedingungen,[108] mit 1,2-Dibrom-4,5-difluorbenzol zu Diels-Alder-Addukt **37** umgesetzt, welches ebenfalls in sehr guten Ausbeuten mittels Oxidation mit DDQ ins Ethenopentacen **38** überführt werden konnte. Für die Röntgendiffraktometrie geeignete Einkristalle von Verbindung **35** sowie **38** konnten durch langsame Kristallisation aus Dichlormethan erhalten werden.[122]

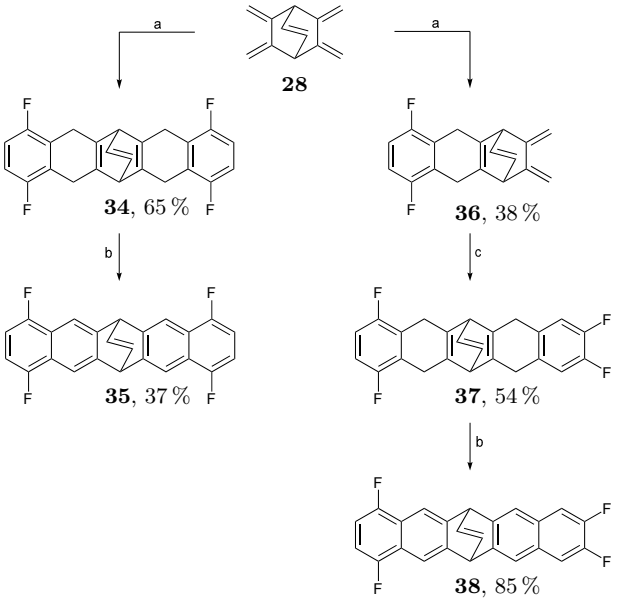

Abbildung 2.4: Synthese der Acenvorstufen **35** und **38** für die thermische Pentacensynthese, ausgehend von Bisdien **28**.[122] a) 1 Äq Arinvorstufe **33** für Monoaddukt **36** oder 2.2 Äq **33** für Bisaddukt **34**, CsF, ACN/DCM, 45 °C, über Nacht, b) DDQ, $CHCl_3$, RT über Nacht, c) 1,2-Dibrom-4,5-difluorbenzol, *n*-BuLi, Toluol, −50 °C auf RT über Nacht.

2.3.1 Thermische Tetrafluorpentacensynthese

Die über die beschriebenen Reaktionen synthetisierten Vorstufen (s. Abschnitt 2.3) sowie 2,3,9,10-Tetrafluor-Ethenopentacen (**39**)[108] wurden der thermischen Sequenz von Diels-Alder-Reaktion und doppelter retro-Diels-Alder-Reaktion mit 1,2,4,5-Tetrazindicarbonsäuredimethylester (**40**)[124, 125] unterworfen (s. Abbildung 2.5). Unter Freisetzung von N_2 und 1,2-Pyridazin-3,6-dicarbonsäuredimethylester (**41**) können die tetrafluorierten Pentacene **27**, **29** und **30** erhalten werden.

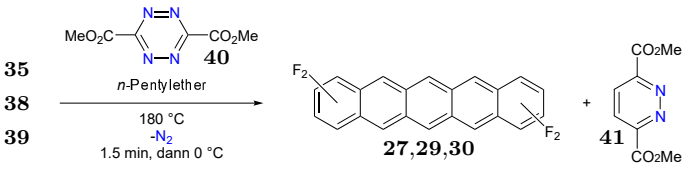

Abbildung 2.5: Thermische Reaktion der Ethenopentacene **35**, **38** und **39** mit Tetrazin **40**. Ausbeuten nach Syntheseoptimierung: 2,3,9,10-Tetrafluorpentacen (**27**, 36 %), 1,4,8,11-Tetrafluorpentacen (**29**, 30 %), 1,4,9,10-Tetrafluorpentacen (**30**, 43 %).

Durch Senkung der Reaktionstemperatur um 5 °C, mehrmaliges Wiederholen der Reaktion, sowie kombinierte Aufreinigung der aus den Einzelreaktionen erhaltenen Feststoffe konnte die Ausbeute im Vergleich zur Erstsynthese von 2,3,9,10-Tetrafluorpentacen (**27**)[108] auf das Dreifache erhöht werden. Die anderen Derivate wurden in Ausbeuten von 30 (**29**) bzw. 43 % (**30**) erhalten. Die erhaltenen Substanzmengen reichten aus, um neben den Komplettcharakterisierungen der Neutralverbindungen auch die Charakterisierung der entsprechenden Radikal- und Dikationen vorzunehmen sowie Kooperationspartnern ausreichend Material für Singlet Fission Messungen sowie den OFET-Devicebau zur Verfügung zu stellen.

2.3.2 NMR-spektroskopische Untersuchungen

Da die NMR-Spektren (^{1}H, ^{19}F) von Verbindung **27** aufgrund von Schwerlöslichkeit erst bei erhöhter Temperatur erhalten werden konnten,[108] wurden die anfänglichen NMR-Experimente zur Charakterisierung der neu synthetisierten Pentacene ebenfalls bei 120 °C durchgeführt. Für 1,4,8,11-Tetrafluorpentacen (**29**) zeigte sich, dass sich noch während der Spektrenaquisition neue Signale unter Verschwinden der zum Pentacen gehörenden Signale bildeten (s. Abbildung 2.6). Das nach längerem Erhitzen erhaltene Spektrum wies aufgrund der Signalzahl und des Integrationsverhältnisses (8:8:4) auf ein Produkt mit gleicher Symmetrie wie der des Edukts hin. Durch Vergleich der Si-

gnallagen mit Daten für Pentacenendoperoxid (PcEP)[126] kann die Bildung des entsprechenden Endoperoxids jedoch ausgeschlossen werden (s. Tabelle 2.1). Der weitere Vergleich mit Daten für das thermisch gebildete Dimer von 1,2,3,4-Tetrafluorpentacen[94] und Diheptacen[73] sowie für Dianthracen und die Photodimere der 2,3-dialkylsubstituierten Anthracenderivate[48] lässt die Bildung des entsprechenden kovalenten Dimers **42** (s. Abbildung 2.6) in Lösung vermuten.

Tabelle 2.1: Vergleich chemischer Verschiebungen verschiedener Acenderivate in Lösung, δ-Werte in ppm.

	$\delta(^1\mathrm{H})$	$\delta(^{13}\mathrm{C}\{^1\mathrm{H}\})$
42	5.30	53.6
PcEP[126]	6.28	–[b]
Dianthracen[a]	4.54	53.8
1,2,3,4-Tetrafluorpentacen-Dimer[94]	5.00	–[b]
Diheptacen[73]	5.30	54.0

[a] Gewonnen durch Photodimerisierung von Anthracen in Lösung mittels UV-Bestrahlung (305–400 nm) in Toluol. [b] Keine experimentellen Daten verfügbar.

Aufgrund der Labilität der Verbindung unter EI-Bedingungen, ähnlich zu den in [48] synthetisierten Dianthracenen und gleichzeitiger Schwerlöslichkeit (ESI-Messung nicht möglich) konnten keine Massenspektren der unzersetzten Substanz erhalten werden. Stattdessen wurde ein mit dem Monomer identisches Massenspektrum gleichen Fragmentierungsmusters erhalten. Zwar liegt weder eine Kristallstruktur, noch ein hochauflösendes Massenspektrum vor, jedoch bieten die anderen Charakterisierungsmethoden genügend Anhaltspunkte, die die postulierte Struktur bestätigen. Mittels 2 D-NMR-Messungen konnte eine vollständige Signalzuordnung vorgenommen werden.[122]

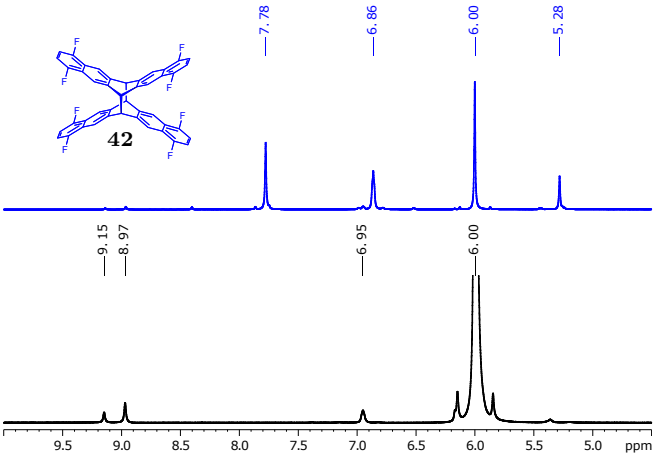

(a) ^{1}H-NMR Spektrum in TCE-d_2 vor (schwarz) und nach (blau) Erhitzen auf 120 °C.

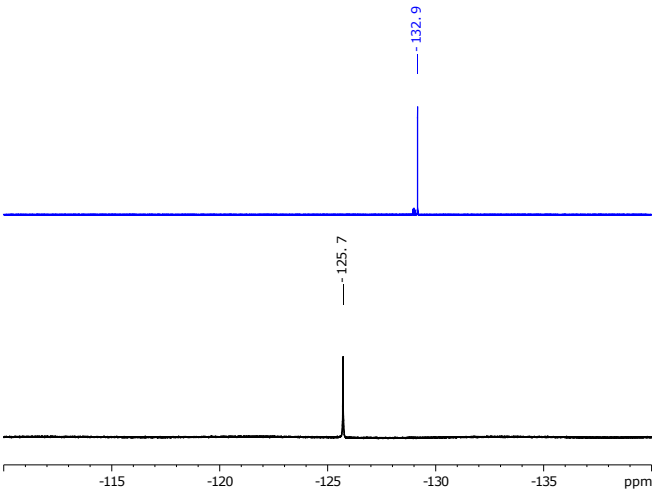

(b) ^{19}F-NMR Spektrum in TCE-d_2 vor (schwarz) und nach (blau) Erhitzen auf 120 °C.

Abbildung 2.6: Vergleich der ^{1}H- und ^{19}F-NMR-Spektren vor und nach Erhitzen einer Probe von 1,4,8,11-Tetrafluorpentacen (**29**) in TCE-d_2 auf 120 °C.

Durch NMR-Messungen bei Zimmertemperatur konnte die Dimerisierung von **29** und die im Vergleich dazu langsame Dimerisierung von **30** unterdrückt werden. Die entsprechenden Verbindungen waren aufgrund ihrer im Vergleich zu **27** besseren Löslichkeit bei Raumtemperatur jedoch ausreichend löslich, um NMR-Spektren (^{1}H, ^{19}F) zu erhalten, die eine komplette Signalzuordnung möglich machten. Die ^{13}C-Spektren konnten jedoch auch durch Verwendung der UDEFT-Pulssequenz[127] nicht erhalten werden. Für die Zuordnung der ^{19}F-Signale von **30** wurde das Spektrum mit den Spektren der beiden anderen Derivate korreliert, da **30** eine Superposition der Spektren der anderen beiden Verbindungen darstellt.

2.3.3 Festkörperstrukturen

Da 1,4,8,11-Tetrafluorpentacen (**29**), wie in Abschnitt 2.3.2 gezeigt, bei höheren Temperaturen zum Dimer reagiert, konnte die zur Züchtung von Einkristallen von 2,3,9,10-Tetrafluorpentacen (**27**) verwendete Methode der langsamen Kristallisation aus heißer Lösung[115] nicht angewendet werden. Sowohl **29** als auch 1,4,9,10-Tetrafluorpentacen (**30**) wurden im Vakuum sublimiert, wodurch für die Röntgenstrukturanalyse geeignete Einkristalle erhalten wurden.[122]

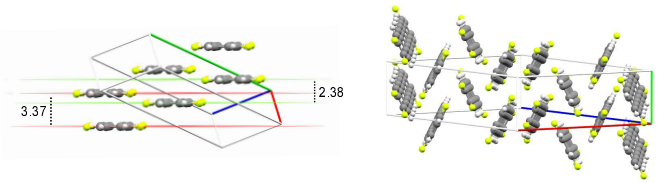

(a) Kristallstruktur von **29**. **(b)** Kristallstruktur von **30**.

Abbildung 2.7: Vergleich der Kristallstrukturen von **29** (a) und **30** (b). Zur Darstellung werden U_{ij}-Tensoren mit 50 % Wahrscheinlichkeit verwendet. Wasserstoffatome wurden in mittels ShelXTL[128] optimierten Positionen platziert. Abstände sind in Å angegeben.

Das Pentacengerüst von **29** zeigt eine alternierende C-C-Bindungslänge zwischen 1.33–1.44 Å, die C-F-Bindungen sind zwischen 1.36–1.37 Å lang.[122] Die kürzesten intermolekularen F-F-Abstände betragen 3.34 Å. Im Gegensatz zu **27** kristallisiert **29** allerdings nicht in der für Pentacen typischen herringbone-Struktur, sondern weist um circa 2.47 Å treppenartig gegeneinander verschobene Schichten auf (s. Abbildung 2.7a). Direkt übereinander gestapelte Moleküle besitzen einen Abstand von 3.37 Å und zeigen ein π-π-Stapelmotiv. Entlang der kristallographischen *b*-Achse ist jede zweite Lage um 24.6° gekippt.[122] Die im Kristall gefundenen VdW-Dimerpaare sind strukturell zu den von Bendikov et al.[129] bei der computerchemischen Untersuchung der thermischen Pentacendimerisierung erhaltenen VdW-Dimeren des Pentacens nahezu identisch. Die Vororientierung der Moleküle in der Festkörperpackung kann als Erklärung für die beobachtete, schnelle thermische Dimerisierung von **29** herangezogen werden.[122] Im Vergleich zu **29** zeigt Verbindung **30** C-C- und C-F-Bindungslängen im gleichen Bereich, jedoch sind die intermolekularen F-F-Abstände mit circa 2.91 Å deutlich kürzer als in **29**. **30** kristallisiert wie **27** in einem herringbone-Motiv (s. Abbildung 2.7b), was durch die stärkere strukturelle Ähnlichkeit beider Verbindungen begründet werden kann.

2.3.4 UV/Vis-Spektroskopie der Neutralverbindungen

Die UV/Vis-Spektren der neu synthetisierten Tetrafluorpentacene **29** sowie **30** in entgastem Dichlormethan (s. Abbildung 2.8) zeigen eine acentypische Schwingungsprogression ($\approx 1400\,\mathrm{cm}^{-1}$)[130] der p-Banden. Die Spektren beider Verbindungen sind symmetrisch im Bezug auf den 0-0-Übergang und entsprechen den Erwartungen gemäß des Franck-Condon-Prinzips. Ein Vergleich mit dem UV/Vis-Spektrum von 2,3,9,10-Tetrafluorpentacen (**27**)[115] zeigt einen bathochromen Shift der p-Banden der Spektren in der Reihe **27** $\rightarrow$ **30** $\rightarrow$ **29**. Für die α-Banden ist ebenfalls ein bathochromer Shift zu erkennen, der jedoch im Vergleich zur Verschiebung der p-Banden sehr viel kleiner ausfällt. Zusätzlich zur Messung der Fluoreszenzspektren wur-

den die Fluoreszenzlebensdauern τ bei 77 K sowie die Triplettenergien aller drei Verbindungen bestimmt. Für alle drei Spezies liegen die Lebensdauern im Nanosekundenbereich.[122]

Die Triplettzustände, ermittelt aus NIR-Emissisionsspektren in CD_2Cl_2 bei 77 K unterscheiden sich nur um wenige Nanometer und liegen alle zwischen 0.93–0.94 eV. Diese Energien sind in guter Übereinstimmung mit den durchgeführten computerchemischen Untersuchungen sowie der experimentell im Rubrenkristall gemessenen Triplettenenergie von Pentacen (0.86 eV).[131] Die relative energetische Lage der S_1- und T_1-Zustände aller drei Fluorpentacene erfüllt die Singlet Fission Bedingung $E(S_1) \geq 2\ E(T_1)$.[132] Singlet Fission konnte experimentell durch die Arbeitsgruppe Broch (Universität Tübingen) nachgewiesen werden.[122]

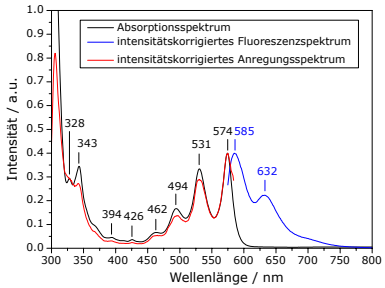

(a) 1,4,8,11-Tetrafluorpentacen (**29**).

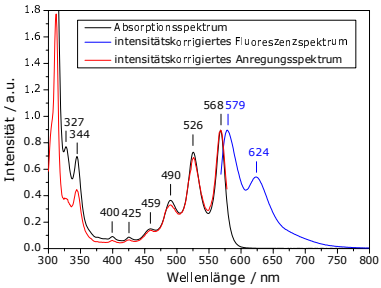

(b) 1,4,9,10-Tetrafluorpentacen (**30**).

Abbildung 2.8: UV/Vis-, Fluoreszenz- und Anregungspektren von (a) 1,4,8,11-Tetrafluorpentacen (**29**, $\lambda_{Ex} = 574$ nm), (b) 1,4,9,10-Tetrafluorpentacen (**30**, $\lambda_{Ex} = 568$ nm).

Ein Vergleich mit berechneten HOMO- und LUMO-Energien sowie den daraus erhaltenen HOMO-LUMO-Abständen (s. Tabelle 2.2) zeigt, dass sich die HOMO-Energien um maximal 0.03 eV unterscheiden und damit nahezu unabhängig vom Substitutionsmuster sind. Dagegen unterscheiden sich die

LUMO-Energien um bis zu 0.08 eV, die Veränderung des HOMO-LUMO-Abstandes und damit auch der Lage der langwelligsten Absorptionsbande ist damit stark von der energetischen Stabilisierung des LUMO abhängig.

Tabelle 2.2: Auf B3LYP/6-311+G**-Theorieniveau berechnete Energien (in eV) für HOMO, LUMO und den HOMO-LUMO-Abstand (ΔE).

	Pentacen	**29**	**30**	**27**
E_{HOMO}	−4.94	−5.39	−5.38	−5.36
E_{LUMO}	−2.75	−3.21	−3.17	−3.13
ΔE	2.19	2.18	2.21	2.23

2.3.5 Radikalkationen

Durch Lösen der Acene in einer 2 M Lösung von Methansulfonsäure (MSS) in Nitrobenzol lassen sich die Radikalkationen der Verbindungen durch Ein-Elektronen-Oxidation erzeugen, wie für 2,3,9,10-Tetrafluorpentacen (**27**) und eine Reihe anderer Acene gezeigt werden konnte.[115, 133] Die Spektren der Radikalkationen weisen ausgeprägte Absorptionsbanden im NIR-Bereich und vergleichsweise schwache Absorptionsbanden im sichtbaren Bereich des Spektrums auf (s. Abbildung 2.9). Im Vergleich zu den Spektren der Neutralverbindungen ist zwischen $\mathbf{27}^{+\cdot} \rightarrow \mathbf{30}^{+\cdot} \rightarrow \mathbf{29}^{+\cdot}$ ein stärkerer Shift innerhalb der Reihe erkennbar. Mittels TD-DFT-Rechnung auf UB3LYP/6-311+G**-Theorieniveau wurden die angeregten Zustände der Radikalkationen untersucht. Die Rechnungen zeigen ebenfalls eine bathochrome Verschiebung der Banden, wie sie auch schon für die Neutralverbindungen beobachtet wurde, allerdings ist dieser Shift sehr viel stärker ausgeprägt. Die UV/Vis/NIR-Spektren wurden durch zeitabhängige Messungen über einen Zeitraum von 6 h beobachtet und nehmen an Intensität ab, etwaige Zersetzungsprodukte wurden nicht weiter charakterisiert.

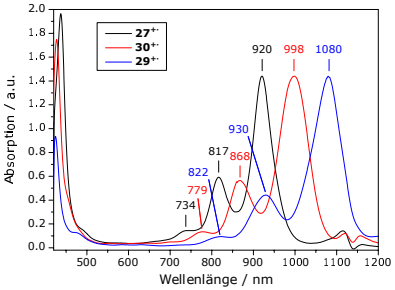

Abbildung 2.9: UV/Vis/NIR-Spektren der Radikalkationen der Tetrafluorpentacene in einer 2 M Lösung von MSS in Nitrobenzol.

Die ESR-Spektren der Radikalkationen (s. Abbildung 2.10) wurden in abgeschmolzenen ESR-Röhrchen gemessen. Im Vergleich zu den UV/Vis-Spektren zeigen diese nur einen geringfügigen Verlust an Intensität im selben Zeitfenster, jedoch nimmt ihre Auflösung ab. Für die ESR-Simulationen wurden als Startparameter die auf UB3LYP/EPR-III-Theorieniveau[134] berechneten Werte verwendet. Für $\mathbf{29}^{+\cdot}$ wurden für die Hyperfeinkopplungen $a_{\mathrm{H6/13}} = 4.86\,\mathrm{G}$, $a_{\mathrm{H5/7/12/14}} = 3.16\,\mathrm{G}$, $a_{\mathrm{F1/4/8/11}} = 2.21\,\mathrm{G}$ und $a_{\mathrm{H2/3/9/10}} = 1.18\,\mathrm{G}$ erhalten.[122] Das Spektrum kann durch die Simulation mit ausreichender Genauigkeit beschrieben werden, die nach außen hin kleiner werdenden Kopplungen zeigen eine starke Lokalisierung des Elektrons am zentralen Ring an. Die Simulation des ESR-Spektrums von $\mathbf{30}^{+\cdot}$ lieferte $a_{\mathrm{H6/13}} = 4.34\,\mathrm{G}$, $a_{\mathrm{H7/12}} = 3.56\,\mathrm{G}$, $a_{\mathrm{H5/14}} = 2.65\,\mathrm{G}$, $a_{\mathrm{F1/4}} = 2.34\,\mathrm{G}$, $a_{\mathrm{H8/11}} = 1.49\,\mathrm{G}$, $a_{\mathrm{H2/3}} = 1.04\,\mathrm{G}$ sowie $a_{\mathrm{F9/10}} = 0.61\,\mathrm{G}$.[122] Das sich zwischen beiden Naphthalin-Untereinheiten unterscheidende Substitutionsmuster zeigt einen erkennbaren Effekt auf die erhaltenen Kopplungskonstanten. Während der allgemeine Trend der Verkleinerung der Kopplungen nach außen hin immer noch vorhanden ist, zeigt sich, dass die Kopplungskonstanten in Summe innerhalb der 1,4-fluorsubstituierten Naphthalineinheit größer als in der 9,10-fluorierten Einheit sind. Diese stärkere Kopplung kann tendenziell durch eine räumliche Annäherung des Elektrons zu seinen Kopplungspartnern hin erklärt werden,

wodurch gezeigt werden kann, dass sich das Substitutionsmuster direkt auf die Aufenthaltswahrscheinlichkeit des Elektrons auswirkt. Eine Analyse der berechneten Orbitalformen sowie Spindichten zeigt eine stärkere Lokalisierung des HOMOs beziehungsweise höhere Spindichten am 1,4-substituierten Napthalinsystem[122] und bestätigt damit diese Vermutung.

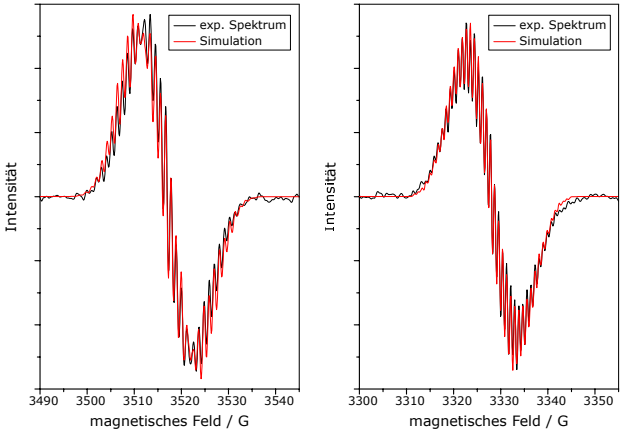

(a) 1,4,8,11-Tetrafluorpentacen-Radikalkation (**29**$^{+\cdot}$). **(b)** 1,4,9,10-Tetrafluorpentacen-Radikalkation (**30**$^{+\cdot}$).

Abbildung 2.10: ESR-Spektren von **29**$^{+\cdot}$ (a) sowie **30**$^{+\cdot}$ (b), die experimentellen und mittels Simulation erhaltenen Spektren sind überlagert dargestellt.

2.3.6 Dikationen

Die optischen Spektren der 2,3,9,10- (**27**$^{2+}$), 1,4,8,11- (**29**$^{2+}$) und 1,4,9,10-Tetrafluorpentacen-Dikationen (**30**$^{2+}$), die durch Lösen der Neutralverbindungen in Oleum (20–30 % freies SO_3) erzeugt werden können,[115, 122, 133] sind im Vergleich zu den Spektren der Radikalkationen blauverschoben, die Lösung besitzen eine tiefgrüne bis braunviolette Farbe. Die Oxidation verläuft vermutlich nicht, wie von Einholz als möglicher Mechanismus

vorgeschlagen,[133] unter Bildung von molekularem Wasserstoff, da dieser nicht im NMR-Experiment nachgewiesen werden konnte. Im Gegensatz zu den Spektren der Radikalkationen fällt der bathochrome Shift innerhalb der Reihe der drei Derivate geringer aus. Das Dikation des 2,3,9,10-Tetrafluorpentacens ($\mathbf{27}^{2+}$)[115] absorbiert, wie auch bereits bei den Neutralverbindungen und Radikalkationen beobachtet, am kurzwelligsten und besitzt als einzige Verbindung in dieser Reihe ein invertiertes Intensitätsprofil der Banden. Der Grund für diese Inversion konnte nicht geklärt werden. Alle drei Spezies sind unter den stark oxidativen Bedingungen über Monate hinweg stabil.

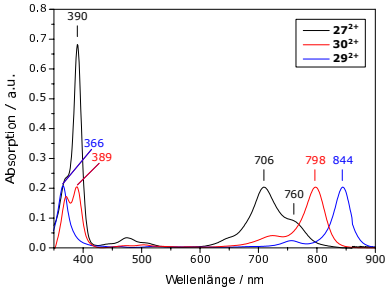

Abbildung 2.11: UV/Vis-Spektren von 2,3,9,10- ($\mathbf{27}^{2+}$), 1,4,8,11- ($\mathbf{29}^{2+}$) sowie 1,4,9,10-Tetrafluorpentacen-Dikation ($\mathbf{30}^{2+}$) in Oleum.

Zusätzlich wurden die ersten zehn elektronisch angeregten Zustände der Dikationen mittels zeitabhängiger DFT-Rechnung berechnet (s. Tabelle 2.3). Hierbei konnte gezeigt werden, dass sich die langwelligsten Absorptionsbanden insbesondere für $\mathbf{29}^{2+}$ und $\mathbf{30}^{2+}$ mit guter Genauigkeit berechnen lassen.

Tabelle 2.3: Vergleich der experimentell ermittelten, langwelligsten Absorptionsbanden (ganzzahlige Werte in nm, Werte in Klammern in eV) und der mittels TD-DFT auf B3LYP/6-311+G**-Theorieniveau berechneten Werte.

	experimentell	berechnet
$\mathbf{27}^{2+}$	760 (1.63)	667 (1.86)
$\mathbf{29}^{2+}$	844 (1.47)	722 (1.72)
$\mathbf{30}^{2+}$	798 (1.55)	695 (1.78)

Neben den optischen Spektren war es zusätzlich möglich die NMR-Spektren der Verbindungen zu erhalten. Für die NMR-Messungen können die Neutralverbindungen jedoch nicht einfach in deuterierter Schwefelsäure gelöst werden, da abhängig vom verwendeten Substanz-/Schwefelsäureverhältnis entweder keine Signale erhalten werden, oder diese innerhalb kurzer Zeit an Intensität verlieren und verschwinden.[115] Als Erklärung für dieses Phänomen wurde ein schneller H/D-Austausch innerhalb der Lösung angenommen. Als Kontrollexperiment wurde **27** in nicht deuterierter, rauchender Schwefelsäure gelöst und D_2SO_4 als externer Standard zum Locken und Shimmen das Magnetfelds verwendet. Mithilfe dieses Experiments wurden wie auch im UV/Vis-Experiment langzeitstabile (leichte Signalverbreiterung nach mehreren Monaten) NMR-Spektren von $\mathbf{27}^{2+}$ erhalten, die eine vollständige Signalzuordnung mittels 2 D-Methoden möglich machten. Auf gleichem Wege konnten auch die NMR-Spektren von $\mathbf{29}^{2+}$ und $\mathbf{30}^{2+}$ erhalten werden. Für $\mathbf{30}^{2+}$ konnte die Signalzuordnung, analog zu den Neutralverbindungen, über die Korrelation mit den Spektren der beiden anderen Dikationen vorgenommen werden.

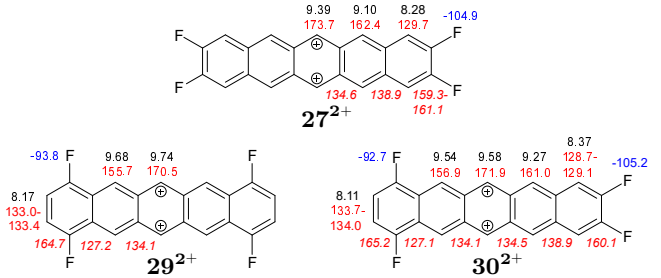

Abbildung 2.12: Vollständige Zuordnung der NMR-Signale der Dikationen $\mathbf{27}^{2+}$, $\mathbf{29}^{2+}$ sowie $\mathbf{30}^{2+}$. Chemische Verschiebungen (in ppm) für ^{1}H in schwarz, ^{13}C{^{1}H} in rot und ^{19}F in blau dargestellt. Kursive Werte geben die Verschiebungen für quartäre Kohlenstoffatome an.

Eine Analyse der chemischen Verschiebung zeigt ausgehend vom innersten Ring jeweils für jedes zweite Kohlenstoffatom eine besonders starke Entschirmung, die fluortragenden Kohlenstoffatome sind des Weiteren durch den -I-Effekt der Substituenten entschirmt. Berechnete isotrope NMR-Abschirmungskonstanten zeigen ein ähnlich alternierendes Muster, weshalb davon ausgegangen werden kann, dass die positiven Ladungen primär an diesen Kohlenstoffatomen lokalisiert sind. Dies erscheint im Sinne der mesomeren Grenzstrukturen, die für die Dikationen formuliert werden können, sinnvoll.

Literaturverzeichnis

[1] Bleck-Neuhaus, J., *Elementare Teilchen: Von den Atomen über das Standard-Modell bis zum Higgs-Boson*, Springer-Verlag, **2012**.

[2] Eisenschitz, R.; London, F., *Z. Phys.* **1930**, *60*, 491–527.

[3] London, F., *Z. Phys. Chem.* **1930**, *B11*, 222–251.

[4] London, F., *Z. Phys.* **1930**, *63*, 245–279.

[5] Podeszwa, R.; Bukowski, R.; Szalewicz, K., *J. Phys. Chem. A* **2006**, *110*, 10345–10354.

[6] Pitoňák, M.; Neogrády, P.; Řezáč, J.; Jurečka, P.; Urban, M.; Hobza, P., *J. Chem. Theory Comput.* **2008**, *4*, 1829–1834.

[7] Gomberg, M., *J. Am. Chem. Soc.* **1900**, *22*, 757–771.

[8] Lankamp, H.; Nauta, W. T.; MacLean, C., *Tetrahedron Lett.* **1968**, *9*, 249–254.

[9] Rösel, S.; Balestrieri, C.; Schreiner, P. R., *Chem. Sci.* **2017**, *8*, 405–410.

[10] Wagner, J. P.; Schreiner, P. R., *Angew. Chem. Int. Ed.* **2015**, *54*, 12274–12296.

[11] Rösel, S.; Becker, J.; Allen, W. D.; Schreiner, P. R., *J. Am. Chem. Soc.* **2018**, *140*, 14421–14432.

[12] Rösel, S.; Quanz, H.; Logemann, C.; Becker, J.; Mossou, E.; Cañadillas-Delgado, L.; Caldeweyher, E.; Grimme, S.; Schreiner, P. R., *J. Am. Chem. Soc.* **2017**, *139*, 7428–7431.

[13] Grimme, S.; Antony, J.; Ehrlich, S.; Krieg, H., *J. Chem. Phys.* **2010**, *132*, 154104.

[14] Johnson, E. R.; Becke, A. D., *J. Chem. Phys.* **2005**, *123*, 024101.

[15] Becke, A. D.; Johnson, E. R., *J. Chem. Phys.* **2005**, *123*, 154101.

[16] Johnson, E. R.; Becke, A. D., *J. Chem. Phys.* **2006**, *124*, 174104.

[17] Møller, C.; Plesset, M. S., *Phys. Rev.* **1934**, *46*, 618–622.

[18] Tkatchenko, A.; DiStasio, Jr., R. A.; Head-Gordon, M.; Scheffler, M., *J. Chem. Phys.* **2009**, *131*, 094106.

[19] Aikawa, H.; Takahira, Y.; Yamaguchi, M., *Chem. Commun.* **2011**, *47*, 1479–1481.

[20] Fritzsche, J., *Z. Angew. Chem.* **1867**, *10*, 290.

[21] Fritzsche, J., *J. Prakt. Chem.* **1867**, *101*, 333–343.

[22] Hengstenberg, J.; Palacios, J., *Strukturber. II* **1932**, 916.

[23] Ehrenberg, M., *Acta Cryst.* **1966**, *20*, 177–182.

[24] Abboud, K. A.; Simonsen, S. H.; Roberts, R. M., *Acta Crystallogr. C* **1990**, *46*, 2494–2496.

[25] Bouas-Laurent, H.; Castellan, A.; Desvergne, J.-P.; Lapouyade, R., *Chem. Soc. Rev.* **2000**, *29*, 43–55.

[26] Bouas-Laurent, H.; Castellan, A.; Desvergne, J.-P.; Lapouyade, R., *Chem. Soc. Rev.* **2001**, *30*, 248–263.

[27] Bowen, E. J., *Trans. Faraday Soc.* **1954**, *50*, 97–102.

[28] Bowen, E. J.; Tanner, D. W., *Trans. Faraday Soc.* **1955**, *51*, 475–481.

[29] Birks, J. B.; Aladekomo, J. B., *Photochem. Photobiol.* **1963**, *2*, 415–418.

[30] Yang, N. C.; Shold, D. M.; Kim, B., *J. Am. Chem. Soc.* **1976**, *98*, 6587–6596.

[31] Klaper, M.; Wessig, P.; Linker, T., *Chem. Commun.* **2016**, *52*, 1210–1213.

[32] Becker, H. D., *Chem. Rev.* **1993**, *93*, 145–172.

[33] Becker, H. D.; Langer, V., *J. Org. Chem.* **1993**, *58*, 4703–4708.

[34] Bouas-Laurent, H.; Castellan, A.; Desvergne, J.-P., *Pure Appl. Chem.* **1980**, *52*, 2633–2648.

[35] van Tamelen, E. E.; Pappas, S. P., *J. Am. Chem. Soc.* **1963**, *85*, 3297–3298.

[36] van Tamelen, E. E.; Pappas, S. P.; Kirk, K. L., *J. Am. Chem. Soc.* **1971**, *93*, 6092–6101.

[37] Guesten, H.; Mintas, M.; Klasinc, L., *J. Am. Chem. Soc.* **1980**, *102*, 7936–7937.

[38] Dreeskamp, H.; Jahn, B.; Pabst, J., *Z. Naturforsch. A* **1981**, *36*, 665–668.

[39] Hopf, H.; Greiving, H.; Bouas-Laurent, H.; Desvergne, J.-P., *Eur. J. Org. Chem.* **2009**, *2009*, 1868–1870.

[40] Nakayama, J.; Machida, H.; Saito, R.; Hoshino, M., *Tetrahedron Lett.* **1985**, *26*, 1983–1984.

[41] Nakayama, J.; Yamaoka, S.; Hoshino, M., *Tetrahedron Lett.* **1987**, *28*, 1799–1802.

[42] Nakayama, J.; Yamaoka, S.; Hoshino, M., *Tetrahedron Lett.* **1988**, *29*, 1161–1164.

[43] Nakayama, J.; Yamaoka, S.; Nakanishi, T.; Hoshino, M., *J. Am. Chem. Soc.* **1988**, *110*, 6598–6599.

[44] Nakayama, J.; Konishi, T.; Ishii, A.; Hoshino, M., *Bull. Chem. Soc. Jpn.* **1989**, *62*, 2608–2612.

[45] Nakayama, J.; Yu, T.; Sugihara, Y.; Ishii, A., *Chem. Lett.* **1997**, *26*, 499–500.

[46] Nakayama, J.; Hasemi, R.; Yoshimura, K.; Sugihara, Y.; Yamaoka, S., *J. Org. Chem.* **1998**, *63*, 4912–4924.

[47] Akula, M. R., *Org. Prep. Proced. Int.* **1990**, *22*, 102–104.

[48] Geiger, T.; Haupt, A.; Maichle-Mössmer, C.; Schrenk, C.; Schnepf, A.; Bettinger, H. F., *J. Org. Chem.* **2019**, *84*, 10120–10135.

[49] Meerwein, H.; Borner, P.; Fuchs, O.; Sasse, H. J.; Schrodt, H.; Spille, J., *Chem. Ber.* **1956**, *89*, 2060–2079.

[50] Moss, R. J.; Rickborn, B., *J. Org. Chem.* **1982**, *47*, 5391–5393.

[51] Crump, S. L.; Rickborn, B., *J. Org. Chem.* **1984**, *49*, 304–310.

[52] Crump, S. L.; Netka, J.; Rickborn, B., *J. Org. Chem.* **1985**, *50*, 2746–2750.

[53] Hoffmann, H.; Mukanov, D.; Ganschow, M.; Rominger, F.; Freudenberg, J.; Bunz, U. H. F., *J. Org. Chem.* **2019**, *84*, 9826–9834.

[54] Bailey, D.; Williams, V. E., *Tetrahedron Lett.* **2004**, *45*, 2511–2513.

[55] Bailey, D.; Williams, V. E., *J. Org. Chem.* **2006**, *71*, 5778–5780.

[56] Navarro, O.; Kaur, H.; Mahjoor, P.; Nolan, S. P., *J. Org. Chem.* **2004**, *69*, 3173–3180.

[57] Li, L.; Zhao, S.; Joshi-Pangu, A.; Diane, M.; Biscoe, M. R., *J. Am. Chem. Soc.* **2014**, *136*, 14027–14030.

[58] Li, C.; Chen, T.; Li, B.; Xiao, G.; Tang, W., *Angew. Chem. Int. Ed.* **2015**, *54*, 3792–3796.

[59] Pozzo, J.-L.; Clavier, G. M.; Colomes, M.; Bouas-Laurent, H., *Tetrahedron* **1997**, *53*, 6377–6390.

[60] Bahl, J. J.; Bates, R. B.; Gordon, B., *J. Org. Chem.* **1979**, *44*, 2290–2291.

[61] Bates, R. B.; Gordon, B.; Highsmith, T. K.; White, J. J., *J. Org. Chem.* **1984**, *49*, 2981–2987.

[62] Hudiono, Y. C.; Miller, A. L.; Gibson, P. W.; LaFrate, A. L.; Noble, R. D.; Gin, D. L., *Ind. Eng. Chem. Res.* **2012**, *51*, 7453–7456.

[63] Kleijn, H.; Westmijze, H.; Meijer, J.; Vermeer, P., *Recl. Trav. Chim. Pays-Bas* **1980**, *99*, 340–343.

[64] Krasovskiy, A.; Knochel, P., *Angew. Chem. Int. Ed.* **2004**, *43*, 3333–3336.

[65] Sämann, C.; Dhayalan, V.; Schreiner, P. R.; Knochel, P., *Org. Lett.* **2014**, *16*, 2418–2421.

[66] Fringuelli, F.; Girotti, R.; Pizzo, F.; Vaccaro, L., *Org. Lett.* **2006**, *8*, 2487–2489.

[67] Wendlandt, A. E.; Stahl, S. S., *Angew. Chem. Int. Ed.* **2015**, *54*, 14638–14658.

[68] Whitton, A. J.; Kumberger, O.; Müller, G.; Schmidbaur, H., *Chem. Ber.* **1990**, *123*, 1931–1939.

[69] Charton, M., *J. Am. Chem. Soc.* **1975**, *97*, 1552–1556.

[70] Moss, G. P.; Smith, P. A. S.; Tavernier, D., *Pure Appl. Chem.* **1995**, *67*, 1307.

[71] Houk, K. N.; Lee, P. S.; Nendel, M., *J. Org. Chem.* **2001**, *66*, 5517–5521.

[72] Watanabe, M.; Chang, Y. J.; Liu, S.-W.; Chao, T.-H.; Goto, K.; Islam, M. M.; Yuan, C.-H.; Tao, Y.-T.; Shinmyozu, T.; Chow, T. J., *Nat. Chem.* **2012**, *4*, 574–578.

[73] Einholz, R.; Fang, T.; Berger, R.; Grüninger, P.; Früh, A.; Chassé, T.; Fink, R. F.; Bettinger, H. F., *J. Am. Chem. Soc.* **2017**, *139*, 4435–4442.

[74] Tönshoff, C.; Bettinger, H., *Angew. Chem. Int. Ed.* **2010**, *49*, 4125–4128.

[75] Zuzak, R.; Dorel, R.; Krawiec, M.; Such, B.; Kolmer, M.; Szymonski, M.; Echavarren, A. M.; Godlewski, S., *ACS Nano* **2017**, *11*, 9321–9329.

[76] Krüger, J.; García, F.; Eisenhut, F.; Skidin, D.; Alonso, J. M.; Guitián, E.; Pérez, D.; Cuniberti, G.; Moresco, F.; Peña, D., *Angew. Chem. Int. Ed.* **2017**, *56*, 11945–11948.

[77] Shen, B.; Tatchen, J.; Sanchez-Garcia, E.; Bettinger, H. F., *Angew. Chem. Int. Ed.* **2018**, *57*, 10506–10509.

[78] Zuzak, R.; Dorel, R.; Kolmer, M.; Szymonski, M.; Godlewski, S.; Echavarren, A. M., *Angew. Chem. Int. Ed.* **2018**, *57*, 10500–10505.

[79] Eisenhut, F.; Kühne, T.; García, F.; Fernández, S.; Guitián, E.; Pérez, D.; Trinquier, G.; Cuniberti, G.; Joachim, C.; Peña, D.; Moresco, F., *ACS Nano* **2020**, *14*, 1011–1017.

[80] Kaur, I.; Jazdzyk, M.; Stein, N. N.; Prusevich, P.; Miller, G. P., *J. Am. Chem. Soc.* **2010**, *132*, 1261–1263.

[81] Purushothaman, B.; Bruzek, M.; Parkin, S. R.; Miller, A.-F.; Anthony, J. E., *Angew. Chem.* **2011**, *123*, 7151–7155.

[82] Di, C.-a.; Zhang, F.; Zhu, D., *Adv. Mater.* **2013**, *25*, 313–330.

[83] Anthony, J. E., *Chem. Rev.* **2006**, *106*, 5028–5048.

[84] Anthony, J. E., *Angew. Chem. Int. Ed.* **2008**, *47*, 452–483.

[85] Yi, H. T.; Payne, M. M.; Anthony, J. E.; Podzorov, V., *Nat. Commun.* **2012**, *3*, 1259.

[86] Yi, M.; Guo, J.; Li, W.; Xie, L.; Fan, Q.; Huang, W., *RSC Adv.* **2015**, *5*, 95273–95279.

[87] Yamashita, Y., *Sci. Technol. Adv. Mater.* **2009**, *10*, 024313–024313.

[88] Kaushik, B. K.; Kumar, B.; Prajapati, S.; Mittal, P., *Organic Thin-Film Transistor Applications: Materials to Circuits*, CRC Press, **2016**.

[89] Klauk, H.; Halik, M.; Zschieschang, U.; Eder, F.; Schmid, G.; Dehm, C., *Appl. Phys. Lett.* **2003**, *82*, 4175–4177.

[90] Jurchescu, O. D.; Baas, J.; Palstra, T. T. M., *Appl. Phys. Lett.* **2004**, *84*, 3061–3063.

[91] Sakamoto, Y.; Suzuki, T.; Kobayashi, M.; Gao, Y.; Fukai, Y.; Inoue, Y.; Sato, F.; Tokito, S., *J. Am. Chem. Soc.* **2004**, *126*, 8138–8140.

[92] Swartz, C. R.; Parkin, S. R.; Bullock, J. E.; Anthony, J. E.; Mayer, A. C.; Malliaras, G. G., *Org. Lett.* **2005**, *7*, 3163–3166.

[93] Quinn, J. T. E.; Zhu, J.; Li, X.; Wang, J.; Li, Y., *J. Mater. Chem. C* **2017**, *5*, 8654–8681.

[94] Chien, C.-T.; Chiang, T.-C.; Watanabe, M.; Chao, T.-H.; Chang, Y. J.; Lin, Y.-D.; Lee, H.-K.; Liu, C.-Y.; Tu, C.-H.; Sun, C.-H.; Chow, T. J., *Tetrahedron Lett.* **2013**, *54*, 903–906.

[95] Schwarze, M.; Tress, W.; Beyer, B.; Gao, F.; Scholz, R.; Poelking, C.; Ortstein, K.; Günther, A. A.; Kasemann, D.; Andrienko, D.; Leo, K., *Science* **2016**, *352*, 1446–1449.

[96] Ueno, N., *Science* **2016**, *352*, 1395–1396.

[97] Toyoda, K.; Hamada, I.; Lee, K.; Yanagisawa, S.; Morikawa, Y., *J. Phys. Chem. C* **2011**, *115*, 5767–5772.

[98] Toyoda, K.; Hamada, I.; Yanagisawa, S.; Morikawa, Y., *Org. Electron.* **2011**, *12*, 295–299.

[99] Lukeš, V.; Cagardová, D.; Michalík, M.; Poliak, P., *Synth. Met.* **2018**, *240*, 67–76.

[100] Wasikiewicz, J. M.; Abu-Sen, L.; Horn, A. B.; Koelewijn, J. M.; Parry, A. V. S.; Morrison, J. J.; Yeates, S. G., *J. Mater. Chem. C* **2016**, *4*, 7309–7315.

[101] Reichenbächer, K.; Süss, H. I.; Hulliger, J., *Chem. Soc. Rev.* **2005**, *34*, 22–30.

[102] Berger, R.; Resnati, G.; Metrangolo, P.; Weber, E.; Hulliger, J., *Chem. Soc. Rev.* **2011**, *40*, 3496–3508.

[103] Chopra, D.; Row, T. N. G., *CrystEngComm* **2011**, *13*, 2175–2186.

[104] Dou, J.-H.; Zheng, Y.-Q.; Yao, Z.-F.; Yu, Z.-A.; Lei, T.; Shen, X.; Luo, X.-Y.; Sun, J.; Zhang, S.-D.; Ding, Y.-F.; Han, G.; Yi, Y.; Wang, J.-Y.; Pei, J., *J. Am. Chem. Soc.* **2015**, *137*, 15947–15956.

[105] Yao, Z.-F.; Wang, J.-Y.; Pei, J., *Cryst. Growth Des.* **2018**, *18*, 7–15.

[106] Ogden, W. A.; Ghosh, S.; Bruzek, M. J.; McGarry, K. A.; Balhorn, L.; Young, V.; Purvis, L. J.; Wegwerth, S. E.; Zhang, Z.; Serratore, N. A.; Cramer, C. J.; Gagliardi, L.; Douglas, C. J., *Cryst. Growth Des.* **2017**, *17*, 643–658.

[107] Ya-Rui, S.; Hui-Ling, W.; Ya-Ting, S.; Yu-Fang, L., *CrystEngComm* **2017**, *19*, 6008–6019.

[108] Bula, R. P.; Oppel, I. M.; Bettinger, H. F., *J. Org. Chem.* **2012**, *77*, 3538–3542.

[109] Clar, E.; John, F., *Ber. dtsch. Chem. Ges.* **1929**, *62*, 3021–3029.

[110] Clar, E.; John, F., *Ber. dtsch. Chem. Ges.* **1930**, *63*, 2967–2977.

[111] Bruckner, V.; Karczag, A.; Körmendy, K.; Meszaros, M.; Tomasz, J., *Tetrahedron Lett.* **1960**, *1*, 5–6.

[112] Goodings, E. P.; Mitchard, D. A.; Owen, G., *J. Chem. Soc., Perkin Trans. 1* **1972**, 1310–1314.

[113] Anthony, J. E.; Brooks, J. S.; Eaton, D. L.; Parkin, S. R., *J. Am. Chem. Soc.* **2001**, *123*, 9482–9483.

[114] Marshall, J. L.; Lehnherr, D.; Lindner, B. D.; Tykwinski, R. R., *ChemPlusChem* **2017**, *82*, 967–1001.

[115] Shen, B.; Geiger, T.; Einholz, R.; Reicherter, F.; Schundelmeier, S.; Maichle-Mössmer, C.; Speiser, B.; Bettinger, H. F., *J. Org. Chem.* **2018**, *83*, 3149–3158.

[116] Strating, J.; Zwanenburg, B.; Wagenaar, A.; Udding, A. C., *Tetrahedron Lett.* **1969**, *10*, 125–128.

[117] Yamada, H.; Yamashita, Y.; Kikuchi, M.; Watanabe, H.; Okujima, T.; Uno, H.; Ogawa, T.; Ohara, K.; Ono, N., *Chem. Eur. J.* **2005**, *11*, 6212–6220.

[118] Gabioud, R.; Vogel, P., *Tetrahedron* **1980**, *36*, 149–154.

[119] Gabioud, R.; Vogel, P., *Helv. Chim. Acta* **1983**, *66*, 1134–1147.

[120] Himeshima, Y.; Sonoda, T.; Kobayashi, H., *Chem. Lett.* **1983**, *12*, 1211–1214.

[121] Tsuchido, Y.; Ide, T.; Suzaki, Y.; Osakada, K., *Bull. Chem. Soc. Jpn.* **2015**, *88*, 821–823.

[122] Geiger, T.; Schundelmeier, S.; Hummel, T.; Ströbele, M.; Leis, W.; Seitz, M.; Zeiser, C.; Moretti, L.; Maiuri, M.; Cerullo, G.; Broch, K.; Vahland, J.; Leo, K.; Maichle-Mössmer, C.; Speiser, B.; Bettinger, H. F., *Chem. Eur. J.* **2020**, *26*, 3420–3434.

[123] Medina, J. M.; Mackey, J. L.; Garg, N. K.; Houk, K. N., *J. Am. Chem. Soc.* **2014**, *136*, 15798–15805.

[124] Boger, D. L.; Coleman, R. S.; Panek, J. S.; Huber, F. X.; Sauer, J., *J. Org. Chem.* **1985**, *50*, 5377–5379.

[125] Boger, D. L.; Panek, J. S.; Patel, M., *Org. Synth.* **1992**, 79–88.

[126] Sparfel, D.; Gobert, F.; Rigaudy, J., *Tetrahedron* **1980**, *36*, 2225–2235.

[127] Piotto, M.; Bourdonneau, M.; Elbayed, K.; Wieruszeski, J.-M.; Lippens, G., *Magn. Reson. Chem.* **2006**, *44*, 943–947.

[128] Sheldrick, G., *Acta Cryst. A* **2015**, *71*, 3–8.

[129] Zade, S. S.; Zamoshchik, N.; Reddy, A. R.; Fridman-Marueli, G.; Sheberla, D.; Bendikov, M., *J. Am. Chem. Soc.* **2011**, *133*, 10803–10816.

[130] Clark, P. A.; Brogli, F.; Heilbronner, E., *Helv. Chim. Acta* **1972**, *55*, 1415–1428.

[131] Burgos, J.; Pope, M.; Swenberg, C. E.; Alfano, R. R., *Phys. Status Solidi B* **1977**, *83*, 249–256.

[132] Smith, M. B.; Michl, J., *Chem. Rev.* **2010**, *110*, 6891–6936.

[133] Einholz, R., *Über die Reaktivität Großer Acene - In Lösung, in Matrix und unter sauer-oxidativen Bedingungen*, Dissertation, Universität Tübingen, **2016**.

[134] Barone, V., Structure, Magnetic Properties and Reactivities of Open-Shell Species From Density Functional and Self-Consistent Hybrid Methods, In: *Recent Advances in Density Functional Methods*, Chong, D. P., Ed., World Scientific, **1995**, 287–334.

Lebenslauf

Name:	Thomas Geiger
Geburtsdatum:	27. Juni 1991
Geburtsort:	Böblingen

Akademische Ausbildung

10/2015–04/2020	Promotion an der Eberhard Karls Universität Tübingen über die *Synthese substituierter Acene und Untersuchung ihrer Struktur-Eigenschaftsbeziehungen* bei Prof. Dr. Holger F. Bettinger
07/2015	Master of Science Chemie an der Eberhard Karls Universität Tübingen bei Prof. Dr. Holger F. Bettinger zu *Untersuchungen zur Synthese von Pentacencarbonitrilen*
11/2012	Bachelor of Science Chemie an der Eberhard Karls Universität Tübingen bei Prof. Dr. Stephanie Grond, Titel: *Chemische Naturstoffderivatisierung zur Aufklärung der absoluten Konfiguration der Spirotetronat-Glykoside aus Streptomyces sp. JP90*
10/2009–07/2015	Studium der Chemie an der Eberhard Karls Universität Tübingen

Schulische Ausbildung

06/2009	Abitur
2001–2009	Stiftsgymnasium Sindelfingen
1997–2001	Grundschule Königsknoll, Sindelfingen

Anhang

Geiger, T.; Haupt, A.; Maichle-Mössmer, C.; Schrenk, C.; Schnepf, A.; Bettinger, H. F., *J. Org. Chem.* **2019**, *84*, 10120–10135.

Shen, B.; Geiger, T.; Einholz, R.; Reicherter, F.; Schundelmeier, S.; Maichle-Mössmer, C.; Speiser, B.; Bettinger, H. F., *J. Org. Chem.* **2018**, *83*, 3149–3158.

Geiger, T.; Schundelmeier, S.; Hummel, T.; Ströbele, M.; Leis, W.; Seitz, M.; Zeiser, C.; Moretti, L.; Maiuri, M.; Cerullo, G.; Broch, K.; Vahland, J.; Leo, K.; Maichle-Mössmer, C.; Speiser, B.; Bettinger, H. F., *Chem. Eur. J.* **2020**, *26*, 3420–3434.

Die aufgeführten Publikationen sind nicht analog zur Publikationsliste in chronologischer Reihenfolge, sondern nach thematischer Zugehörigkeit geordnet.

JOC The Journal of Organic Chemistry
Cite This: J. Org. Chem. 2019, 84, 10120−10135
Article
pubs.acs.org/joc

Synthesis and Photodimerization of 2- and 2,3-Disubstituted Anthracenes: Influence of Steric Interactions and London Dispersion on Diastereoselectivity

Thomas Geiger,[†] Anne Haupt,[†] Cäcilia Maichle-Mössmer,[‡] Claudio Schrenk,[‡] Andreas Schnepf,[‡] and Holger F. Bettinger*[,†]

[†]Institut für Organische Chemie and [‡]Institut für Anorganische Chemie, Eberhard-Karls-Universität Tübingen, Auf der Morgenstelle 18, 72076 Tübingen, Germany

Supporting Information

ABSTRACT: There is increased evidence that the effect of bulky groups in organic, organometallic, and inorganic chemistry is not only repulsive but can be attractive because of London dispersion interactions. The influence of the size of primary alkyl substituents in 2- and 2,3-positions of anthracenes on the diastereoselectivity (anti vs syn dimer) of the $[\pi_{4s} + \pi_{4s}]$ photoinduced dimerization is investigated. The synthesis of the anthracene derivatives was achieved by Suzuki−Miyaura reaction of 2,3-dibromoanthracene with alkylboronic acids as well as by reduction of anthraquinones that were obtained from 2,3-disubstituted 1,3-butadienes and naphthoquinone followed by dehydrogenation. The mixtures of dianthracene isomers were analyzed with respect to the anti/syn-ratio of the products by X-ray crystallography and nuclear Overhauser effect spectroscopy. While for the 2,3-dimethylanthracene the anti and syn isomers were formed in equal amounts, the anti dimers are the major products in all other cases. A linear correlation (R^2 = 0.98) between the steric size (Charton parameter) and the isomeric ratio suggests that the selectivity is dominated by classical repulsive steric effects. An exception is the iso-butyl substituent that produces an increased amount of the syn isomer. It is suggested that this is due to an exalted effect of London dispersion interactions.

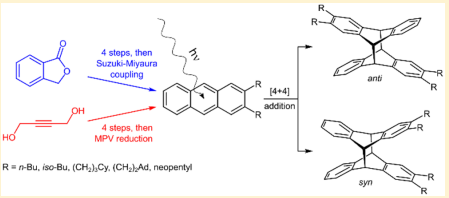

1. INTRODUCTION

Fritzsche's 1867 photoexperiment, the irradiation of anthracene (**1**) in solution by sunlight, is a milestone for organic photochemistry (Scheme 1).[1] The proposed structure of the product,[2] the so called dianthracene (**2**) was confirmed through X-ray analysis by Ehrenberg one century later.[3] The most remarkable structural feature of dianthracene is the rather long C−C bond of 1.62 Å between the bridgehead carbon atoms.[3−5]

Scheme 1. Possible Photoreactions of Anthracene in Solution[a]

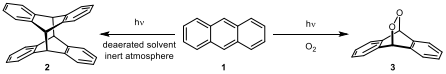

[a]When oxygen is present the formation of endoperoxides can be observed.

Mechanistic investigation of this bimolecular, photochemically allowed $[\pi_{4s} + \pi_{4s}]$ cycloaddition leading to **2** suggested that the photodimerization can proceed through an excited complex (eq 1)[6−9] and the nature of this excited species was reviewed by Bouas-Laurent et al.[10] In solutions containing oxygen, an alternative reaction pathway is possible giving anthracene endoperoxide (**3**) through reaction of the anthracene core with singlet oxygen (Scheme 1).[11,12]

$$\begin{aligned} A &\underset{k_{-1}}{\overset{k_1}{\rightleftharpoons}} A^* \\ A + A^* &\underset{k_{-2}}{\overset{k_2}{\rightleftharpoons}} [AA]^* \overset{k_{ISC}}{\underset{k_{PL}}{<}} \\ [AA]^* &\xrightarrow{k_3} D \end{aligned} \qquad (1)$$

ISC = intersystem crossing, PL = photoluminescence

In the past, several groups have investigated the photochemical behavior of anthracene and its derivatives, preferably substituted in the 9- and 10-positions.[13−16] In these cases in principle two products, the so called head−head (hh/syn, **4a**) and head−tail (ht/anti, **4b**) isomers can possibly be formed (Scheme 2). The selectivities observed in the reaction (Table 1) were attributed to steric and electrostatic effects.[17] This reasoning is supported by results obtained from the photodimerization of monomers carrying bulky substituents in the 9-position, where the formation of some unusual structural

Received: May 17, 2019
Published: August 7, 2019

DOI: 10.1021/acs.joc.9b01317
J. Org. Chem. 2019, 84, 10120−10135

Scheme 2. Examples for the Formation of the hh/syn (4a) and ht/anti (4b) Homodimers in Solution of Anthracene Derivatives Substituted in the 9 and 10 Positions[a]

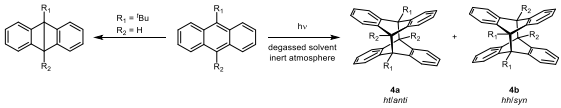

[a]Bulky substituents suppress the dimerization.[13,14,18,19]

Table 1. Yields for the Photodimerization of Anthracenes Substituted in 9- and 10-Positions[13,14]

		yield/%	
R_1	R_2	**4a**	**4b**
Me	H	66	34
OMe	H	55	38
OMe	Me	50	–
Br	H	43	–

motifs, for example, the Dewar form of anthracene is promoted and dimerization is suppressed.[18,19] These experiments can be interpreted as evidence for the operation of steric effects as governing factor for the selectivity in photochemical $[\pi_{4s} + \pi_{4s}]$ cycloadditions. Moreover, steric strain was also identified to have a bathochromic shift effect on absorption spectra of anthracenes.[20,21]

The closely related thermal $[\pi_{4s} + \pi_{2s}]$ Diels–Alder reaction between sterically demanding reagents was reported by Yamaguchi et al.[22] The reaction of 2-(1-adamantyl)furan with the aryne produced from precursor **5** (Scheme 3) gives

Scheme 3. Yamaguchi's Experiment Giving the Syn Isomer as the Major Product[22]

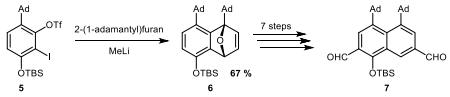

epoxynaphthalene **6** as shown by X-ray crystallographic analysis of the final product **7**. Obviously, the Diels–Alder reaction had produced the isomer with adamantyl substituents in adjacent positions as the major product (67%) while the allegedly less crowded product only formed to minor extent (12%). This result appears to be in contrast to the expectation based on steric arguments and it was suggested[23] that attractive, noncovalent dispersion forces[24] arising from large, polarizable substituents (dispersion energy donors, DEDs) could be important for the formation of **6**.[23,25]

There is currently considerable interest in elucidating the effect of London dispersion on the structural, energetic, and chemical properties of organic, organometallic, and inorganic compounds.[23,26,27] While the influence of attractive dispersive interactions can be substantial, in particular in the gas phase, there is evidence that the effect can be attenuated by solvents.[28] A study of the chemoselectivity of the reaction between secondary alcohols of variable size with carboxylic acid chlorides catalyzed by 9-azajulolidine reported by Zipse et al.[29−31] observed that the more sizeable aryl-substituted alcohols show higher selectivities due to $\pi-\pi$ and dispersion interactions. The lengths of alkyl chains only had minor influence on the selectivities.[29]

Yamaguchi's observation (Scheme 3) may be indicative of the importance of dispersion interactions on the diastereoselectivity of a Diels–Alder cycloaddition reaction. We considered it worthwhile to study another cycloaddition reaction and chose the photochemical $[\pi_{4s} + \pi_{4s}]$ cycloaddition between two anthracene moieties. In our study, we investigated the dimerization of anthracene monomers bearing alkyl substituents in the 2-, 2,3-, or 2,6-positions using toluene as solvent because strong intermolecular interactions should be attenuated in this solvent. The influence of short range ($\propto r^{-6}$), noncovalent interactions (London dispersion forces) on the relative amounts of possible photoproducts was investigated. Currently, there is only one known example of the photodimerization of an anthracene substituted with a DED (*n*-undecyl) in the 2,3-positions, which has been investigated under the aspect of self-assembling systems.[32] Steric effects on the formation of homo- and heterodimers of 9,10-di- or 2,9,10-trimethylanthracene and phenyl-substituted anthracenes have been investigated by Williams et al.[33] Herein, we report the synthesis of the anthracene monomers employed in the photoreactions by two different synthetic approaches and the selectivities of their photodimerization. Single-crystal X-ray crystallography as well as nuclear Overhauser effect (NOE) spectroscopy experiments are used for structure elucidation.

2. RESULTS AND DISCUSSION

2.1. Syntheses. *2.1.1. General Considerations.* 2,3-Dimethylanthracene (**8**) as well as 2-*tert*-butylanthracene (**9**) were obtained directly from chemical suppliers and were used as received, all the other monomers used in this study were synthesized via one step or in cases of the newly prepared compounds, multistep syntheses. The disubstituted 2,6-di-*tert*-butylanthracene (**11**) was synthesized in 18% yield using a slightly modified version of the one-step reaction reported by Schmidbaur et al.[34] A Friedel–Crafts alkylation protocol converts 9,10-dihydroanthracene (**10**) followed by immediate oxidation to the target molecule **11** (Scheme 4).

2.1.2. Suzuki–Miyaura Route. To streamline the synthesis of 2,3-disubstituted monomers, we decided on a linear five-step reaction sequence synthesizing 2,3-dibromoanthracene (**18**) by

Scheme 4. Synthesis of 2,6-Di-*tert*-butylanthracene (11) from 9,10-Dihydroanthracene (10)[a]

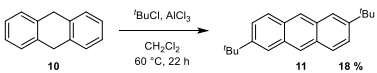

[a]The byproduct of the reaction, 2,7-di-*tert*-butylanthracene could not be isolated with sufficient purity for the irradiation experiments.

DOI: 10.1021/acs.joc.9b01317
J. Org. Chem. 2019, 84, 10120−10135

Scheme 5. Synthesis of 2,3-Dibromoanthracene (18) from Phthalide (12) as Starting Material

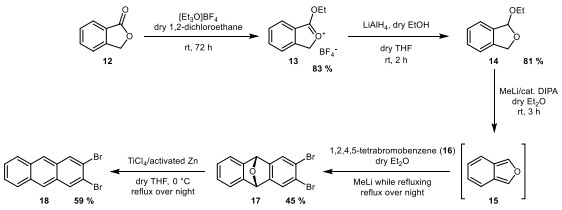

Akula's[35] method (Scheme 5) and employing a Suzuki–Miyaura reaction in the final step. We converted phthalide **12** using Meerwein's salt and a modified version of Meerwein's reaction protocol[36] into the highly hygroscopic oxonium salt (**13**) in 84% yield. For the conversion of **13** to ethyl acetal **14** Rickborn's reduction protocol using $LiAlH_2(OEt)_2$ was applied.[37] Acetal **14** was purified by distillation in oil pump vacuum avoiding elevated temperatures as the material undergoes rapid polymerization.[38]

Compound **14** can be converted into the intermediate isobenzofuran (**15**) by base-induced 1,4-elimination.[39,40] This intermediate is fairly stable at room temperature[41] and can be detected by NMR spectroscopy.[42] Complete conversion of the starting material was verified by NMR spectroscopy of an aliquot of the reaction mixture. Isobenzofuran **15** then reacts with 1,2-dibromo-4,5-benzyne prepared in situ from 1,2,4,5-tetrabromobenzene (**16**) to give the epoxyanthracene **17**.[35] We obtained the highest yields for **17** when the Diels–Alder reaction between **15** and **16** was carried out under refluxing conditions using 0.9 equiv of **16**. Overall, the reaction gives, even under our optimized conditions, only poor yields of compound **17**, as the reaction is highly unselective indicated by the formation of an abundance of byproducts. Our findings regarding the yield of this reaction step are in agreement with a report by Mack and Miller who investigated the formation of the analogues *N*-methyl-bridged derivative.[43] Epoxyanthracene **17** was deoxygenated using a low-valent titanium complex generated from $TiCl_4(THF)_2$ which was prepared in situ by addition of $TiCl_4$ to dry and degassed tetrahydrofuran (THF) and reduced through addition of activated zinc dust at 0 °C. After addition of **17**, the reaction was carried out overnight at 60 °C. This procedure was advantageous compared to other deoxygenation methods, for example, $Fe_2(CO)_9$ in benzene[35] or $HClO_4$ in EtOH[44] as no product formation was observed in our hands here. Purification of the crude material proved difficult as **18** shows only low solubility in common organic solvents at room temperature. The parent 2,3-dibromoanthracene (**18**) was isolated in 59% yield after recrystallization from toluene. Because of its low solubility, NMR spectra were recorded in DMSO-d_6 at 120 °C.

Next, we investigated the cross-coupling capabilities of **18** in Suzuki–Miyaura reactions as these can be run under fairly convenient conditions and the starting material is soluble at the reaction temperature (Scheme 6). The reaction of **18** with phenylboronic acid was used as a benchmarking system to improve the reaction conditions as 2,3-diphenylanthracene (**19**) was already synthesized by Williams and Bailey through reduction of the corresponding anthraquinone.[45,46] Under optimized conditions using 12 mol % of $Pd(PPh_3)_4$ and 4 equiv of phenylboronic acid a maximum yield of 70% of **19** was

Scheme 6. Suzuki–Miyaura Coupling Reaction of 18 and Boronic Acids

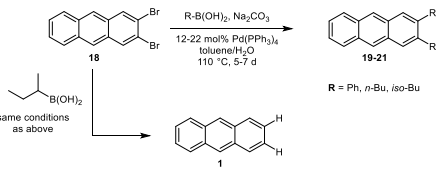

achieved after reacting for five days at 110 °C. The spectra of the product were in agreement with published data.[46] The optimized reaction conditions were applied to the reaction of **18** with *n*-butyl, iso-butyl, and *sec*-butyl boronic acid. Thin-layer chromatography (TLC) analysis in intervals of 24 h showed that in all three cases, the conversion of the starting material was incomplete after five days; therefore, another 10 mol % of the catalyst was added to the reaction mixtures. After additional two days, TLC analysis indicated complete consumption of **18** and the formation of products (**19**–**21**) with bright blue fluorescence. These were isolated in acceptable yields (Table 2) by flash column chromatography on silica gel and subsequently purified on reverse phase silica gel.

Table 2. Yields for the Suzuki–Miyaura Coupling Reaction of 18 and Boronic Acids

	yield/%	
R =	coupling product	anthracene
phenyl (**19**)	70	–
n-Bu (**20**)	61	–
iso-Bu (**21**)	38	–
sec-Bu	–	30

2,3-Di-*n*-butylanthracene (**20**) and 2,3-di-iso-butylanthracene (**21**) were obtained in yields of 61 and 38%, respectively. The compounds could be fully characterized using two-dimensional NMR spectroscopy. Interestingly, in case of the reaction with *sec*-butyl boronic acid neither the mono- nor the dicoupling products could be identified in the spectra. Instead, anthracene (**1**) was isolated in 30% yield and in high purity. The hydrodehalogenation in Suzuki reactions of aromatic halides with secondary alkyl boronic acids via β-hydride elimination is an extensively discussed problem and it is attempted to be avoided by application of novel catalyst systems.[47−49] Here, we are able to report the first example of a double hydrodehalogenation of an aromatic dihalide. After the reaction proved to give the unbranched coupling products in

DOI: 10.1021/acs.joc.9b01317
J. Org. Chem. 2019, 84, 10120−10135

Scheme 7. Multistep Route Used for the Synthesis of Anthracene Monomers 20, 21, 32, 35, and 36

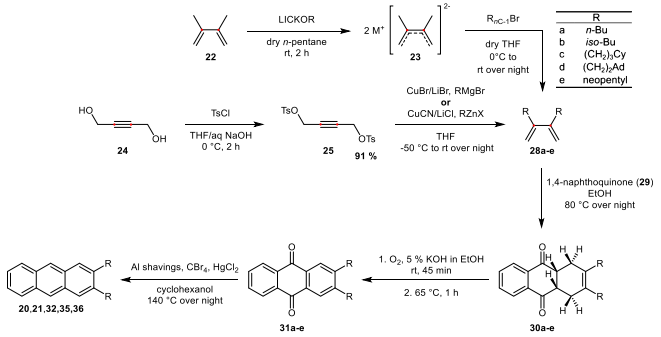

acceptable yields, the reactions were run in larger scale, but in these cases the yields drastically decreased while the number and amount of byproducts formed in the reaction increased.

2.1.3. Quinone Route. As the results of the upscaling experiments turned out to be unsatisfying, a second approach for the synthesis of the target monomers was used (Scheme 7).[50−53] In the same manner, using dimethoxy- or diethoxybuta-1,3-diene, the synthesis of alkoxy- or hydroxy-substituted anthracenes has been achieved by Pozzo et al.[54]

This strategy involves the individual synthesis of disubstituted buta-1,3-dienes, which can be accomplished by conversion of 2,3-dimethylbuta-1,3-diene (**22**) into its corresponding dianion **23** by reaction with LICKOR (Lochmann−Schlosser base) in dry *n*-pentane and subsequent reaction with an alkyl halide via an S_N2 pathway to give butadienes **28a−e**.[55,56] An alternative method leading to the same products converts 2-butyne-1,4-diol (**24**) into the ditosylate **25**[57] which then can be converted into **28a−e** by reaction with cuprates[58] or lithium heterocuprates[59] formed by the addition of Grignard reagents to a mixture of CuBr and LiBr in dry THF. The yields for this reaction step could be maximized when freshly prepared Grignard reagent and stoichiometric amounts of CuBr and LiBr were used. 3-Cyclohexylpropylmagnesium bromide was prepared in the usual manner from 1-bromo-3-cyclohexylpropane **26**. Bromide **26** was prepared by a slightly modified version of Rebek's original synthesis.[60]

Introduction of the ethyl(1-adamantyl) substituent was achieved by synthesis of the corresponding bromide (**27**) obtained from the reaction of 1-adamantaneethanol with $ZnBr_2$ in aqueous HBr[61] and converting the bromide to the organozinc compound by an established method.[62] The synthesis of the organozinc compound was made necessary as the classical preparation of the Grignard reagent gave only low yields of the impure product. Nevertheless, the yield for this reaction step could not be determined as the product spectra were indicative of unreacted bromide (**27**) which could not be removed entirely. In comparison, the ditosylate route gave better yields overall compared to the LICKOR method (Table 3) as the synthesis and handling of the dianionic butadiene species **23** is less convenient. The butadienes (**28a−e**) prepared underwent rapid reaction with 1,4-naphthoquinone (**29**) in boiling EtOH to give the corresponding Diels−Alder adducts (**30a−e**) in good yields and high purity even

Table 3. Summarized Yields for the Reaction Sequences Leading to Anthracene Monomers 20, 21, 32, 35, and 36

	yield/%			
R =	S_N2	Diels−Alder step	oxidation	MPV reduction
n-Bu (**a**)	41	54	96	65
iso-Bu (**b**)	26	60	90	67
$(CH_2)_3Cy$ (**c**)	90[a]	73	96	81
$(CH_2)_2Ad$ (**d**)	−[b]	−[b]	46	74
neopentyl (**e**)	67	31[c]	97	63

[a]Using freshly prepared Grignard reagent. [b]Yield could not be determined. [c]Catalyzed by [$AlCl_3$ + 2 THF] complex.

without further purification. In the NMR spectra of the isobutyl derivative (**30b**), two distinct signals in the ^1H as well as the ^{13}C spectra for the endo and exo methyl groups could be detected. A definitive signal assignment was not possible because of a lack of NOE correlation in the spectra. Regarding the reaction of diene **28d** with 1,4-naphthoquinone (**29**), an exact stoichiometric ratio could not be used because of the aforementioned impurities. Because an excess of **29** was used in this synthesis, not only the Diels−Alder adduct **30d** but also the oxidation products **30d-2H** and **31d** could be isolated (Scheme 8) because excess of **29** works as an oxidizing agent here.

Diene **28e** gave only 10% yield of product using this method. The reason for this observation is presumably that the required s-cis conformation of the diene is very unfavorable for steric reasons.[56] Catalyzing the reaction using the [$AlCl_3$ + 2 THF] complex[63] in dichloromethane results in an increased yield of 31%.

The tetrahydroquinones **30a−e** and compound **30d-2H** could further be oxidized by O_2 in 5% ethanolic KOH to give single products as confirmed by TLC analysis. The quinones obtained (**31a−e**) were of sufficient purity for the next reaction step without further purification. After reduction of the quinones under MPV conditions using $Al(OCy)_3$ prepared in situ in degassed cyclohexanol as reducing agent, 2,3-di-*n*-butylanthracene (**20**, 65%), 2,3-di-iso-butylanthracene (**21**, 67%), 2,3-di-(3-cyclohexyl)propylanthracene (**32**, 81%), 2,3-di-(ethyl-2-(1-adamantyl))anthracene (**35**, 74%), and 2,3-dineopentylanthracene (**36**, 63%) could be isolated. The spectra of **20** and **21** prepared in this way were in agreement with the data obtained from the Suzuki−Miyaura coupling

DOI: 10.1021/acs.joc.9b01317
J. Org. Chem. 2019, 84, 10120−10135

Scheme 8. Reaction of Diene 28d with an Excess of 1,4-Naphthoquinone (29)[a]

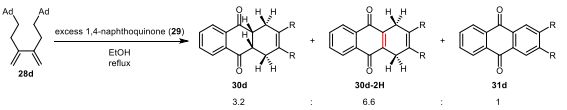

[a]Relative yields of products are given.

Scheme 9. Proposed Mechanism for the Formation of Spirocyclic Compound 33 under MPV Reaction Conditions

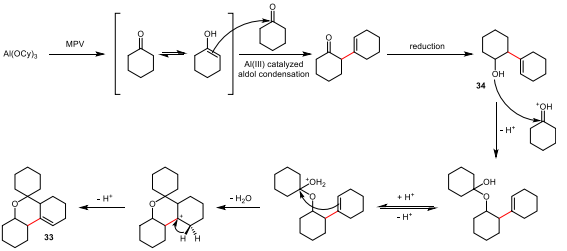

Scheme 10. Photodimerization Products of 9 and the Disubstituted Derivative 11 as well as of the 2,3-Disubstituted Anthracenes 8, 20, 21, 32, 35, and 36[a]

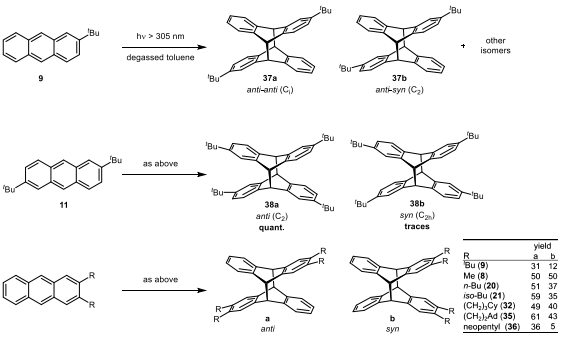

[a]Isolated yields of single experiments (in percent) are given.

reactions. The UV spectra as well as fluorescence data of the newly prepared compounds show the typical absorption and emission bands of the anthracene system (see Supporting Information, Figures S98−S102). The influence of the substituents on the spectra in comparison to unsubstituted anthracene is almost negligible which can be ascribed to only minor modifications of the frontier orbital energy gaps arising from inductive substituent effects.

An unexpected observation was made during the removal of cyclohexanol from compound **32** in an oil pump vacuum at 90 °C. To our surprise, single crystals formed within minutes in the upper part of the flask which were subjected to X-ray crystallography. Contrary to our expectations, the crystals were not monomeric anthracene **32**, but the more complex spirocyclic structure **33** (Scheme 9) which formed in 0.2% yield based on the amount of cyclohexanol used in the synthesis. As only a ^{1}H spectrum of this compound was published by Chauzov and Parchinskii,[64] we have fully characterized it. As the earlier report[64] described the formation of **33** starting from 2-(1′-cyclohexenyl)cyclohexanol (**34**), we suggest a mechanism for the formation of **33** via the intermediate product **34** in solution under the MPV reaction conditions (Scheme 9). In this mechanism, cyclohexanone formed during the MPV reduction process of the anthraquinone presumably undergoes an Al(III) catalyzed homo aldol condensation to give the β-γ unsaturated condensation product. Similar findings were reported for In(III)- and Ru(III)-catalyzed condensations of cyclohexanone.[65,66]

The length of the double bond in **33**, 1.33(5) Å, is the same as the one reported by Bauer and Chang for the structure of cyclohexene in the vapor phase.[67] All the other bond lengths and angles in this ring are within 2% and 3%, respectively, compared to the values reported for cyclohexene (selected values are listed in Table S1 in the Supporting Information).

DOI: 10.1021/acs.joc.9b01317
J. Org. Chem. 2019, 84, 10120−10135

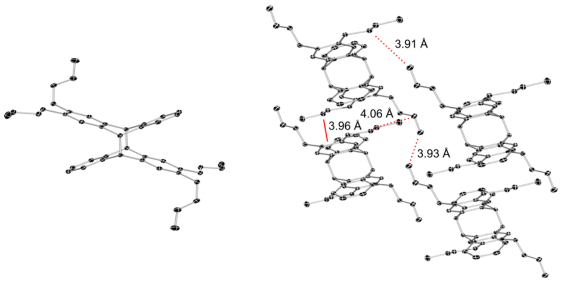

Figure 1. Molecular structure of dianthracene **40a** (left) and packing within the crystal viewed along the *a* axis (right). Hydrogen atoms are omitted for clarity and ellipsoid probability was set to 50%. The closest intermolecular C−C contacts between carbon atoms marked by dotted lines are given; the distance between the molecular planes is indicated by a solid line.

From the single-crystal structure, the relative configuration of the stereocenters was determined to be cis.

2.2. Photodimerization. All anthracene monomers were subjected to irradiation in solution under an Ar atmosphere using a 500 W high-pressure mercury lamp in combination with a dichroic mirror and additional optical cutoff filters. The wavelength region between 305 and 400 nm was selected as shorter wavelengths cause cycloreversion of the forming dimers. Almost all dimers prepared in this study could be separated into the individual isomers by means of column chromatography or fractional crystallization. The individual isomers were characterized by NMR spectroscopy, including NOE spectroscopy, mass spectrometry (MS), and X-ray crystallography. The absence of NOE signals between the substituent hydrogen atoms and both the aromatic doublets of doublets in the spectra of the monomer as well as one of the regioisomers was a sufficient proof for unambiguous assignment of the structures in cases where no X-ray data were obtained. We were able to obtain single crystals of the anti compounds because of their lower solubility in almost all the cases. X-ray crystallography proved our initial structural assignments that were based on NOE spectroscopy. MS using EI and GC/EI-MS methods showed only the radical cations of the monomeric species as the dimers are not stable under these conditions. Electrospray ionization MS (ESI-MS) conditions proved suitable as the dimers could be detected directly in the form of ion adducts, thus enabling also high-resolution mass analysis. Interestingly, a screening of the dimer ion affinities against Li^+, Na^+, K^+, and NH_4^+ by comparison of the strength of the respective ESI signals shows a tendency toward increased binding of cations with larger radii. This is in contrast to electrostatic considerations for cation−π interactions,[68−70] but could arise from a better fit of the larger ions between the wings of the dimers.

The dimerization of 2-*tert*-butylanthracene (**9**) led to complete conversion of the starting material. One of the four possible photodimers directly precipitated from the solution and could be isolated by filtration. X-ray analysis of single crystals obtained by the diffusion method at 8 °C shows that this compound is the C_i symmetrical dimer **37a**, forming in 31% yield (Scheme 10). From the mother liquor we were able to crystallize a second isomer in 12% yield which proved to be the C_2 symmetrical dimer **37b** based on X-ray diffraction. The ^{1}H NMR spectrum as well as ESI-MS investigation of the remaining mother liquor showed evidence for the existence of the other two photoisomers, but their separation was unsuccessful because of their low tendency to crystallize.

We investigated the doubly substituted anthracene derivative **11** to force the substituents into closer proximity in the photoproducts. In this case a single product was obtained in essentially quantitative yield which was shown by X-ray crystallography to consist of the C_2 symmetrical anti dimer (**38a**), suggesting a strong influence of steric hindrance between the substituents upon dimerization. The syn dimer (**38b**) was only detected in trace amounts in an analytical high-performance liquid chromatography (HPLC) run as a peak with the same mass as **38a**, but it could not be isolated.

2,3-Dimethylanthracene (**8**) converted cleanly and quantitatively after 16 h of irradiation into the corresponding dimers (**39a**/**b**) in a 1:1 ratio as indicated by NMR spectroscopy. Separation of both isomers by chromatographic methods failed because of their identical retention factors on a silica gel column. However, the anti dimer **39a**, as proven by X-ray analysis, could be crystallized selectively from this mixture by diffusion of toluene into a $CHCl_3$ solution of the isomer mixture, forming clear cubic crystals within a night. These single crystals turned opaque quickly when removed from the mother liquor indicating the co-crystallization of solvent. Indeed, the data obtained showed that the unit cell contains two molecules of $CHCl_3$. Because of poor *R*-value bond lengths and angles are not discussed here. After several months of crystallization, the mother liquor contained the syn dimer **39b** together with still about 10% of **39a**.

Dimerization of the other species that we investigated showed incomplete conversion of the starting material as indicated by TLC analysis. As we changed the substituent from methyl to the higher homologue *n*-butyl and the branched systems, we observed an overall slower reaction shown by time-dependent UV/vis spectroscopy experiments.

2.3. X-ray Crystallography. We were able to obtain single crystals suitable for X-ray diffraction of compounds **31c**, **31d**, **33**, **37a**, **37b**, **38a**, **39a**, **40a**, and **41a** (methods used for crystal growth are described in the Experimental Section, for detailed crystallographic data see Supporting Information, Section 3). Only the most interesting structural motifs are discussed here. Anti dimer **40a** crystallizes in a staircase motif, the individual molecules are shifted laterally with a distance of the molecular planes of about 4 Å (Figure 1). The structure is stabilized by intermolecular intertwining of the *n*-butyl substituents with C−C contacts of about 4 Å, which is well within the regime of

DOI: 10.1021/acs.joc.9b01317
J. Org. Chem. 2019, 84, 10120−10135

attractive dispersion forces.[71−73] The packing resembles a laterally displaced staircase motif. The distance between the bridgehead carbon atoms is 1.609(2) Å.

An exception to the preferred crystallization of the anti dimers is the dimer pair **41a**/**b**. There, we were able to crystallize the syn dimer (Figure 2). This is the first example of a single-crystal structure of a syn dianthracene with a 2,3-substitution pattern. The values found are within the range of attractive dispersion interactions considering the possible H−H contacts. The distance between the bridgehead carbon atoms is 1.615(7) Å.

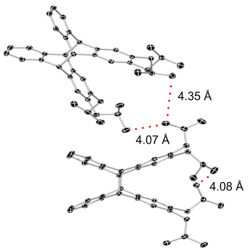

Figure 2. Molecular structure of antidimer **41b**, hydrogen atoms are omitted for clarity, ellipsoid probability was set to 50%. The closest intra- and intermolecular C−C contacts between the carbon atoms marked with dotted lines are given.

The bond lengths between the bridgehead carbon atoms of the compounds prepared herein only show minor variations because of the substitution pattern and are similar to the experimental values reported for dianthracene (**2**) (Scheme 11)[4,5] as well as values calculated by Grimme et al.[74] The connecting bonds between the anthracene core and the substituents are slightly longer compared to the toluene molecule,[75] but shorter in comparison to the structure of 1,3,5-tri-*tert*-butylbenzene.[76] Structure optimization at the B3LYP-D3/def2TZVP level of theory reproduces the experimental C−C bond lengths in a satisfactory manner considering the possible deviations between individual molecule and solid phase data.

2.4. Selectivity of Photodimerization. The isomeric ratios were determined by NMR integration of the isomeric mixtures and additionally from the isolated yields after separation. Both yield the same results and reveal that formation of the anti products is preferred for all anthracene derivatives except for the 2,3-dimethyl system where the anti (**39a**) and syn (**39b**) isomers are formed in equal amounts (Table 4). The linear *n*-butyl substituent favors the formation of the antidimer **40a** by about 14 percentage points (pp), while the iso-butyl substituent gives 24 pp excess of anti dimer (**41a**). For substitution with $(CH_2)_2$Ad, we find an 18 pp excess of the anticompound. This excess is reduced to 9 pp with the $(CH_2)_3$Cy substituent, but it increases to 31 pp with the neopentyl substituent. The isomeric ratios reflect the energetic relationships of transition states that may be approximated by reactive intermediates in the sense of the Hammond postulate, and in photoreactions these correspond to conical intersections and excimers, respectively. The energetic preference may be associated with steric and electronic effects. An important contribution to the latter may involve dipole−dipole interactions, as all 2,3-dialkylanthracenes have a permanent dipole moment, as well as attractive dispersion interactions between the substituents (Scheme 12). The dipole moments of the ground and excited states computed at the ωB97XD/6-31G* level of theory (Table 4) show that the dipole moment vector of the excited state has the same orientation as that of the ground state, but its value is always larger. This would indicate that based on dipole−dipole interactions, the anti isomer should always be favored, as indeed observed. However, the methyl derivative is among those compounds with largest

Table 4. Isomeric Ratio and Dipole Moments (μ in Debye) for the Ground States (S_0) and First Excited Singlet (S_1) States of Monomers Calculated at the ωB97XD/6-31G* Level of Theory for 2,3-Dialkyl-Substituted Anthracenes[a]

		$\mu_{monomer}$		
R	*a*/*b* ratio	S_0	S_1	$\Delta\mu(S_1 - S_0)$
Me (**8**)	1	0.93	1.41	0.48
n-Bu (**20**)	1.38	1.13	1.41	0.28
iso-Bu (**21**)	1.68	0.63	0.95	0.32
$(CH_2)_3$Cy (**32**)	1.22	1.15	1.43	0.28
$(CH_2)_2$Ad (**35**)	1.42	1.47	2.17	0.7
neopentyl (**36**)	7.2	0.67	1.04	0.37

[a] *a*/*b* ratios are based on the isolated yields from single photoexperiments.

Scheme 11. Comparison of the Bond Length between the Bridgehead Atoms of Dianthracene (2), Refined by Abboud et al.,[5] the Bond Length between the Ring and the Substituent in Toluene[75] as well as 1,3,5-Tri-*tert*-butylbenzene[76] and the Substituted Dianthracene Derivatives 37a, 37b, 38a, and 40a Prepared in This Investigation[a]

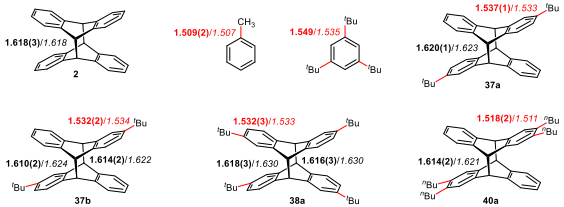

[a] Experimental values for the bond length between bridgehead carbons (black) as well as the bond lengths for the connecting bonds between the aromatic rings and the substituents (red) are given in bold letters. Values in italics were calculated at the B3LYP-D3/def2TZVP level of theory.

DOI: 10.1021/acs.joc.9b01317
J. Org. Chem. 2019, 84, 10120−10135

Scheme 12. Relative Orientation of Two Anthracene Molecules in the Exciplex/TS in Respect to Their Dipole Vectors (Red Arrows) as well as Steric Repulsion between the Substituents (Blue Sphere) is Shown

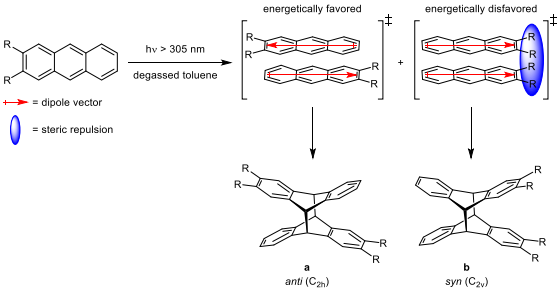

excited state dipole moment, while the neopentyl derivative has a smaller dipole moment. As the methyl compound shows no, and the much bulkier neopentyl group shows a significant anti selectivity, the influence of dipole−dipole interactions on the selectivity is at most minor.

This suggests that steric effects may play an important role for the regioselectivity of the photodimerization. In order to quantify steric effects, Taft has introduced substituent parameters,[77] and his approach, though criticized,[78,79] has received attention and refinement, for example, by Dubois et al.[80] Additionally, Charton has developed a set of ν parameters based on van der Waals radii.[81] Using Charton's ν parameters, we obtain a linear relationship for the isomeric ratio of photodimers. If the branched iso-Bu group is excluded from the correlation, the quality of the correlation is excellent ($R^2 = 0.98$, see Figure 3). The positive correlation indicates that the result of the photodimerization can be described with classical steric parameters. Although these parameters may implicitly take into account both repulsive and attractive interaction forces,[82] it appears that an exalted influence of dispersion effects is not required for explaining the isomeric ratios for most of the substituents that we have investigated.

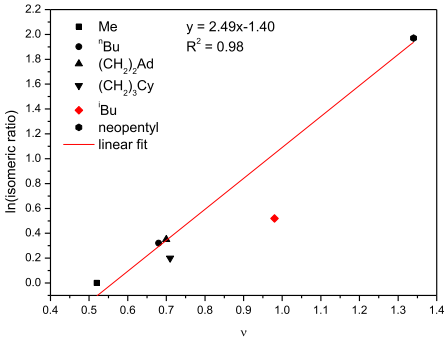

Figure 3. Plot of selected values of ln(isomeric ratio) vs ν for the corresponding substituent.[81] The linear correlation found shows the influence of steric interactions on the reaction outcome. The ^{t}Bu substituent is only depicted but not taken into consideration for the linear regression.

The iso-butyl substituent is exceptional. The isomeric ratio is smaller, that is, the amount of the syn isomer obtained is much larger than expected based on the linear correlation. The reason for this observation is unclear. We note that the difference of the dipole moments of the ground and first excited states is similar to those computed for other substituents. This suggests that dipole−dipole or dipole−induced dipole interactions are most likely not responsible for the reduced importance of steric interactions. In addition, and as stated above, the orientation of the dipole moments would favor the formation of the anti isomer anyways. Hence, the relative increase of the syn isomer amount is most likely associated with another effect. All the substituents that we investigated are connected to the anthracene moiety by primary carbon atoms, but only the iso-butyl and the neopentyl groups branch. One explanation is that the branching at the β carbon atom of iso-butyl allows for a sufficient amount of attractive London dispersion interaction in the product forming complex so that the syn isomer is formed in greater amount than expected based on steric arguments. The additional β branch of the neopentyl group would then result in severe steric strain. In this picture, there exists a subtle balance between steric strain and attractive London dispersion interaction in the product forming complex that is only detectable in the case of the iso-butyl group. It is not clear if this is the correct interpretation of the observations, and hence we call for a detailed computational investigation with methods that are able to account for London dispersion interaction between molecules in the electronically excited state.

3. CONCLUSIONS

We have described the synthesis of a new family of anthracene derivatives bearing primary alkyl groups of varying size in their respective 2- and 3-positions by Suzuki−Miyaura reaction of 2,3-dibromoanthracene (**18**) as well as by a classical quinone chemistry approach. The anthracene monomers obtained were investigated with regards to the selectivity of dimerization in photoinduced [$\pi_{4s} + \pi_{4s}$] cycloadditions; furthermore, their spectral properties were investigated by UV/vis and fluorescence spectroscopy. We have shown a convenient way to synthesize and separate the obtained isomers and have fully characterized the structures by all available spectroscopic methods as well as X-ray analysis of several anti dimers (**37a**, **37b**, **38a**, **39a**, and **40a**) and syn dimer **41b**. The anti dimers

DOI: 10.1021/acs.joc.9b01317
J. Org. Chem. 2019, 84, 10120−10135

show lower solubility and better crystallization behavior than their syn counterparts as a result of their dipole moments being small because of their symmetry. Even when no single crystals of either of the isomers were obtained, the structures could still be assigned using the NOE spectroscopy technique. There is a linear correlation with good R^2 of the isomeric ratios found for four of the investigated substituents with Charton's ν parameter. Hence, we conclude that the diastereoselectivity of the $[\pi_{4s} + \pi_{4s}]$ cycloaddition of substituted anthracenes is mainly influenced by steric effects arising from the substituents introduced to the anthracene backbone while London dispersion plays only a comparatively minor role in this context. Photodimerization of 2,3-di-iso-butylanthracene produces more of the syn isomer than expected based on the linear correlation. While the origin of this behavior is unclear, it is suggested to result from the London dispersion interaction between the iso-butyl groups in the transition state of photodimerization. This should be substantiated by computational investigations in the future.

4. EXPERIMENTAL SECTION

4.1. General. Reagents were used as purchased from Acros Organics, Sigma-Aldrich or TCI Europe. Oxygen 5.0 was obtained from Westfalen AG. Anhydrous solvents were either obtained from Acros Organics, or, in the cases of CH_2Cl_2, THF, and toluene taken from a MBRAUN SPS 800 solvent purification system. Solvents were degassed by passing through a stream of Ar gas or the freeze−pump−thaw method. MPLC chromatography was performed on an Interchim PuriFlash 430 system using prepacked silica gel columns of appropriate lengths (particle size: 20 μm), solvent mixtures (HPLC grade) are reported in v/v ratios. NMR spectra were recorded on either a Bruker AVANCE III HD 400 MHz, Bruker AVANCE III HDX 400 MHz (high temperature spectra), Bruker Avance III HDX 600 MHz equipped with a 5 mm Prodigy BBO-CryoProbe (NOE spectra), or Bruker AVANCE III HDX 700 MHz spectrometer equipped with a 5 mm Prodigy BBO-CryoProbe using $CDCl_3$ or C_6D_6 as solvent. High-temperature NMR experiments were carried out in DMSO-d_6. GC/EI-MS experiments were performed on a HP 6890 gas chromatograph with an HP MSD 5793 mass detector. A 30 m × 0.25 mm column with a 95% dimethylpolysiloxane/5% diphenylpolysiloxane coating and a film thickness of 0.25 μm was used. Low-resolution EI data were obtained from a Finnigan TSQ 70 with quadrupole mass analyzer, high-resolution data were obtained using a Finnigan MAT 95 spectrometer with sector field mass analyzer. HRESI spectra were measured on a Bruker maXis 4G mass spectrometer with UHR-TOF mass analyzer. Melting points were recorded on a BÜCHI Melting-Point 540 and are reported uncorrected. For elemental analysis, a HEKAtech Euro 3000 CHN analyzer system was used. Absorption spectra of the anthracene monomers were measured on a PerkinElmer LAMBDA 1050, the respective fluorescence and excitation spectra were obtained from an Agilent Cary Eclipse fluorescence spectrometer.

4.2. Procedures. *4.2.1. 2,6-Di-tert-butyl-anthracene (11).*[34] To a suspension of 9,10-dihydroanthracene (5 g, 27.7 mmol) in a mixture of *tert*-butyl chloride (16.5 mL, 152 mmol, 5.5 equiv) and CH_2Cl_2 (17 mL), $AlCl_3$ (0.2 g, 1.15 mmol, 0.05 equiv) was added carefully. The reaction mixture was stirred for 22 h at 60 °C in an oil bath. After cooling down to rt, the solid was triturated with CH_2Cl_2 (25 mL) in an ultrasonic bath for 5 min. The residue was recrystallized from either *n*-hexane (thin plates) or toluene (chunky crystals) to give the title compound; yield: 0.52 g (1.80 mmol, 18%). ^{1}H NMR ($CDCl_3$, 400 MHz): δ 8.33 (s, 2 H), 7.93 (d, J = 8.9 Hz, 2 H), 7.87 (d, J = 1.7 Hz, 2 H), 7.55 (dd, J_1 = 8.9 Hz, J_2 = 2.0 Hz, 2 H), 1.45 (s, 18 H). ^{13}C{^{1}H} NMR ($CDCl_3$, 101 MHz): δ 147.4, 131.1, 130.6, 127.9, 125.5, 124.9, 122.4, 35.1, 31.1.

4.2.2. O-Ethylphthalide Tetrafluoroborate (13).[36] To a solution of phthalide (16.3 g, 121.6 mmol) in dry 1,2-dichloroethane $[Et_3O]BF_4$ (23.1 g, 121.6 mmol, 1 equiv) was added in one portion. After stirring for 3 d at rt the precipitate was filtered, washed subsequently with dry 1,2-dichloroethane (100 mL) and dry Et_2O (100 mL), and dried in vacuo to give compound **13** as colorless, highly hygroscopic crystals; yield: 25.2 g (100.9 mmol, 83%). mp 121 °C. ^{1}H NMR ($CDCl_3$, 400 MHz): δ 8.15−8.11 (m, 1 H), 8.08−8.02 (m, 1 H), 7.89−7.85 (m, 1 H), 7.80−7.73 (br t, J = 7.6 Hz, 1 H), 6.32 (br s, 2 H), 5.31 (q, J = 7.2 Hz, 2 H), 1.74 (t, J = 7.2 Hz, 3 H). Anal. Calcd for $C_{10}H_{11}BF_4O_2$: C, 48.04; H, 4.44. Found: C, 47.89; H, 4.51.

4.2.3. 1-Ethoxy-1,3-dihydroisobenzofuran (14).[37] Dry EtOH (21.3 mL, 365.2 mmol, 4.4 equiv) was added dropwise to a suspension of lithium aluminum hydride (7.56 g, 199.2 mmol, 2.4 equiv) in anhydrous THF (300 mL) at 0 °C. After 15 min, **13** (20.75 g, 83 mmol) was added rapidly and the reaction mixture was stirred at rt for 2 h. The reaction was quenched by dropwise addition of 10% aq NaOH (120 mL) and the solids were filtered off. The filtrate was concentrated under reduced pressure, extracted with Et_2O (2 × 50 mL), and the combined organic phases were dried over anhydrous K_2CO_3. After removing the volatiles, the oily residue was distilled under reduced pressure using an oil bath as heat source to give a colorless oil; yield: 8.0 g (48.8 mmol, 81%). bp 80 °C/2 mbar. Higher temperatures should be avoided as the material is prone to polymerization at elevated temperatures. ^{1}H NMR ($CDCl_3$, 400 MHz): δ 7.43−7.25 (m, 4 H), 6.26 (d, J = 2.2 Hz, 1 H), 5.23 (dd, J_1 = 12.6 Hz, J_2 = 1.7 Hz, 1 H), 5.03 (d, J = 12.6 Hz, 1 H), 3.83−3.61 (m, 2 H), 1.26 (t, J = 7.1 Hz, 3 H). ^{13}C{^{1}H} NMR ($CDCl_3$, 101 MHz): δ 140.1, 137.8, 129.2, 127.8, 123.1, 121.2, 106.9, 72.3, 63.1, 15.6. MS (EI) m/z (%): 163.1 (80) $[M]^{+\bullet}$, 135.1 (65), 119.0 (100), 105.1 (36), 91.0 (34), 77.1 (20).

4.2.4. 1,2,4,5-Tetrabromobenzene (16). Iron dust (2.2 g, 39.4 mmol, 0.18 equiv) was suspended in Br_2 (40 mL, 780 mmol, 3.7 equiv) at rt and stirred for 15 min. To this mixture, a solution of 1,4-dibromobenzene (50 g, 212 mmol) in $CHCl_3$ (200 mL) was added dropwise. The resulting solution was stirred for 3 d at 60 °C in an oil bath. After cooling to rt, 10% aq Na_2SO_3 (200 mL) was added dropwise followed by dilution with sat. Na_2SO_3 solution (1 L). The solid was removed by filtration and washed with water and methanol (100 mL each). The organic phase was separated, washed with brine (3 × 100 mL), and dried over anhydrous Na_2SO_4. After removing the solvent under reduced pressure, both the solid and the residue from the initial filtration were combined and washed with CH_2Cl_2 (2.5 L). Evaporation to dryness afforded a colorless solid; yield: 72.4 g (184 mmol, 87%). ^{1}H NMR ($CDCl_3$, 400 MHz): δ 7.86 (s, 2 H). ^{13}C{^{1}H} NMR ($CDCl_3$, 101 MHz): δ 137.3, 124.5.

4.2.5. 2,3-Dibromo-9,10-dihydro-9,10-epoxyanthracene (17).[35] To a solution of **14** (0.5 mL, 3.65 mmol) in anhydrous Et_2O (20 mL), DIPA (40 μL, cat.) was added followed by the dropwise addition of MeLi (2.3 mL of a 1.6 M solution in Et_2O, 3.7 mmol, 1 equiv) over 20 min at rt. The resulting yellow solution was stirred for 3 h at rt after which complete conversion of the starting material was confirmed by NMR spectroscopy. 1,2,4,5-Tetrabromobenzene (1.28 g, 3.25 mmol, 0.9 equiv) was added in one portion and the solution was heated to reflux in an oil bath. MeLi (2 mL of a 1.6 M solution in Et_2O, 3.2 mmol, 0.9 equiv) was added dropwise and the mixture was refluxed overnight. After cooling to rt, water and Et_2O (200 mL each) were added. The organic phase was washed with water (3 × 100 mL) and brine (3 × 100 mL), dried over anhydrous Na_2SO_4, and evaporated. The resulting solid was purified by flash chromatography (silica gel, *n*-hexane/EtOAc 6:1) to give **17** as colorless solid; yield: 0.51 g (1.45 mmol, 45%). R_f (silica gel, *n*-hexane/EtOAc 6:1): 0.43. mp 201−202 °C. ^{1}H NMR ($CDCl_3$, 400 MHz): δ 7.56 (s, 2 H), 7.33 (dd, J_1 = 5.3 Hz, J_2 = 3.0 Hz, 2 H), 7.06 (dd, J_1 = 5.3 Hz, J_2 = 3.0 Hz, 2 H), 6.02 (s, 2 H). ^{13}C{^{1}H} NMR ($CDCl_3$, 101 MHz): δ 149.4, 147.0, 126.7, 125.8, 121.8, 120.9, 82.2. MS (EI) m/z (%): 351.9 (31) $[M]^{+\bullet}$, 322.9 (13), 271.0 (31), 243.0 (45), 163.1 (100), 81.5 (16).

4.2.6. 2,3-Dibromoanthracene (18).[35] Zinc was activated by vigorously stirring a suspension of zinc dust (16 g) in 4% aq HCl (100 mL) for 10 min at rt. The aqueous phase was decanted and the solid was washed with water (4 × 200 mL). After filtration, the solid was washed with EtOH (50 mL), acetone (100 mL), and dry Et_2O (100

DOI: 10.1021/acs.joc.9b01317
J. Org. Chem. 2019, 84, 10120−10135

mL). After drying in vacuo overnight at 80 °C in an oil bath, the activated zinc was transferred to an oven-dried Schlenk flask and stored under Ar. A three-neck round-bottom flask was charged with dry, degassed THF (40 mL) and cooled to 0 °C. $TiCl_4$ (2 mL, 31 mmol, 5.5 equiv) was added dropwise cautiously and the resulting bright yellow suspension was stirred for 20 min. Activated zinc dust (2 g, 31 mmol, 9.2 equiv) was added in one portion and the resulting dark green suspension was stirred for an additional 15 min. The reaction mixture was heated to 70 °C for 45 min in an oil bath and then cooled to 0 °C again. A solution of 2,3-dibromo-9,10-dihydro-9,10-epoxyanthracene (**17**) (1.16 g, 3.3 mmol) in THF (15 mL) was added slowly and the reaction mixture was heated to 65 °C overnight in an oil bath. After cooling to rt the organic phase was poured into 10% aq HCl (100 mL) and stirred until the formed solid turned colorless. After filtration, the liquid phase was extracted with CH_2Cl_2 (3 × 200 mL) and the combined organic phases were washed with water (3 × 150 mL), dried over anhydrous Na_2SO_4, and removed in vacuo. The remaining yellow solid was recrystallized from toluene to give pale yellow flakes; yield: 0.65 g (1.93 mmol, 59%). mp 238−240 °C. ^{1}H NMR (DMSO-d_6, 400 MHz, 120 °C): δ 8.56 (s, 2 H), 8.55 (s, 2 H), 8.08 (dd, J_1 = 6.5 Hz, J_2 = 3.3 Hz, 2 H), 7.57 (dd, J_1 = 6.6 Hz, J_2 = 3.2 Hz, 2 H). ^{13}C{^{1}H} NMR (DMSO-d_6, 101 MHz, 120 °C): δ 131.8, 131.5, 129.9, 127.5, 125.8, 125.0, 119.8. MS (EI) m/z (%): 336.0 (6) $[M]^{+\bullet}$, 256.1 (16), 176.1 (16), 134.1 (11), 119.1 (9), 91.1 (85), 71.2 (89), 55.2 (100), 43.2 (30), 31.1 (16).

*4.2.7. 2-Butyne-1,4-diol Ditosylate (**25**).*[57] 2-Butyne-1,4-diol (4.30 g, 50 mmol) was dissolved in a mixture of THF (100 mL) and 10% aq NaOH (100 mL). After cooling to 0 °C a solution of tosylchloride (20.97 g, 110 mmol, 2.2 equiv) in THF (150 mL) was added dropwise. After complete addition, the mixture was stirred for 2 h at this temperature and the aqueous phase was extracted with EtOAc (2 × 250 mL). The combined organic phases were washed with brine (100 mL). After drying over anhydrous $MgSO_4$, the solvent was removed under reduced pressure leaving a light grey powder; yield: 18.0 g (45.6 mmol, 91%). mp 93 °C. ^{1}H NMR ($CDCl_3$, 400 MHz): δ 7.76 (d, J = 8.2 Hz, 4 H), 7.35 (d, J = 8.2 Hz, 4 H), 4.58 (s, 4 H), 2.45 (s, 6 H). ^{13}C{^{1}H} NMR ($CDCl_3$, 101 MHz): δ 145.6, 132.9, 130.0, 128.2, 81.1, 57.2, 21.8. MS (ESI) m/z: 395.0 $[M + H]^+$, 417.0 $[M + Na]^+$, 433.0 $[M + K]^+$.

*4.2.8. 1-Bromo-3-cyclohexylpropane (**26**).*[60] Under an atmosphere of nitrogen, 3-cyclohexylpropan-1-ol (5 mL, 32 mmol) was cooled to 0 °C and PBr_3 (1.6 mL, 17.2 mmol, 0.55 equiv) was added dropwise via syringe. After complete addition, the solution was stirred for 15 min at 0 °C, allowed to warm to rt and stirred for additional 2 h. The mixture was heated to 100 °C in an oil bath overnight and then poured on a mixture of ice and water (100 mL). Brine (50 mL) was added and the aqueous phase was separated and extracted with Et_2O (3 × 50 mL). The combined organic phases were dried over anhydrous Na_2SO_4 and removed in vacuo to give a colorless oil; yield: 5.80 g (28.3 mmol, 88%). ^{1}H NMR ($CDCl_3$, 400 MHz): δ 3.39 (t, J = 7.0 Hz, 2 H), 1.91−1.82 (m, 2 H), 1.74−1.60 (m, 5 H), 1.34−1.07 (m, 6 H), 0.97−0.81 (m, 2 H). ^{13}C{^{1}H} NMR ($CDCl_3$, 101 MHz): δ 37.2, 36.1, 34.6, 33.4, 30.5, 26.7, 26.5. MS (EI) m/z (%): 203.9 (35) $[M]^{+\bullet}$, 125.0 (4), 83.0 (100), 67.0 (7), 55.0 (28), 41.0 (12).

*4.2.9. 1-(2-Bromoethyl)adamantane (**27**).* A mixture of 1-adamantaneethanol (10.33 g, 57.3 mmol) and $ZnBr_2$ (33.55 g, 149 mmol, 2.6 equiv) in 48% aq HBr (210 mL) was stirred at 125 °C in an oil bath overnight. After cooling down to rt, the solution was diluted with water (100 mL) and extracted with EtOAc (3 × 100 mL). The combined organic phases were washed with sat. aq $NaHCO_3$ (3 × 100 mL), water (3 × 100 mL), and brine (100 mL), and dried over Na_2SO_4 and removed under reduced pressure to give colorless crystals; yield: 11.13 g (45.8 mmol, 80%). mp 65 °C. ^{1}H NMR ($CDCl_3$, 400 MHz): δ 3.44−3.37 (m, 2 H), 1.95 (s, 3 H), 1.75−1.67 (m, 5 H), 1.66−1.59 (m, 3 H), 1.51 (d, J = 2.5 Hz, 6 H). ^{13}C{^{1}H} NMR ($CDCl_3$, 101 MHz): δ 48.3, 42.3, 37.1, 34.1, 29.3, 28.7. MS (EI) m/z (%): 242.1 (9) $[M]^{+\bullet}$, 135.2 (100), 107.1 (29), 93.1 (47), 79.1 (50), 67.2 (17), 55.2 (9), 41.2 (17).

4.3. General Procedure for Suzuki−Miyaura reaction of 2,3-Dibromoanthracene (18). Compound **18** (0.45 g, 1.34 mmol), the boronic acid derivative (5.35 mmol, 4 equiv) and Na_2CO_3 (0.62 g, 5.90 mmol, 4.4 equiv) were added to a mixture of toluene (40 mL) and water (15 mL). The suspension was purged for 1 h with nitrogen and $Pd(PPh_3)_4$ (0.185 g, 0.16 mmol, 12 mol %) was added followed by an additional hour of purging with nitrogen. After 5 d at 110 °C using an oil bath as heat source the reaction mixture was allowed to cool to rt, water (30 mL) was added and the aqueous phase was extracted with a 1:1 mixture of toluene/EtOAc (3 × 30 mL). The combined organic phases were subsequently washed with water (3 × 30 mL) and brine (30 mL), dried over anhydrous Na_2SO_4, and removed under reduced pressure. The remaining black solid was purified by flash chromatography (silica gel, *n*-hexane). In the cases of compound **20** and **21**, a second chromatographic step with reverse-phase silica gel (RP-18) using acetonitrile/MeOH/H_2O 5:5:3 as eluent was performed.

*4.3.1. 2,3-Diphenylanthracene (**19**).* The general procedure was applied on 50 mg (0.15 mmol) of 2,3-dibromoanthracene. Colorless crystalline solid; yield: 34.7 mg (0,11 mmol, 73%). ^{1}H NMR ($CDCl_3$, 400 MHz): δ 8.47 (s, 2 H), 8.06 (s, 2 H), 8.03 (dd, J_1 = 6.4 Hz, J_2 = 3.2 Hz, 2 H), 7.48 (dd, J_1 = 6.5 Hz, J_2 = 3.1 Hz, 2 H), 7.29−7.25 (m, 10 H). ^{13}C{^{1}H} NMR ($CDCl_3$, 101 MHz): δ 141.5, 139.1, 132.2, 130.1, 129.7, 128.4, 128.0, 126.8, 126.3, 125.6. The spectra are in agreement with published data.[46]

*4.3.2. 2,3-Di-n-butylanthracene (**20**).* Colorless crystalline solid; yield: 0.26 g (0.90 mmol, 67%) mp 104−106 °C. ^{1}H NMR (C_6D_6, 400 MHz): δ 8.22 (s, 2 H), 7.88 (dd, J_1 = 6.5 Hz, J_2 = 3.2 Hz, 2 H), 7.72 (s, 2 H), 7.28 (dd, J_1 = 6.5 Hz, J_2 = 3.3 Hz, 2 H), 2.74 (t, J = 7.7 Hz, 4 H), 1.71−1.61 (m, 4 H), 1.40 (sext, J = 7.3 Hz, 4 H), 0.95 (t, J = 7.3 Hz, 6 H). ^{13}C{^{1}H} NMR (C_6D_6, 101 MHz): δ 139.6, 132.1, 131.8, 128.6, 127.2, 125.6, 125.2, 33.4, 33.1, 23.2, 14.3. HRMS (EI) m/z: $[M]^{+\bullet}$ calcd for $C_{22}H_{26}$, 290.2029; found, 290.2022. UV/vis (*n*-hexane) λ_{max} (log ε): 312 (3.07), 327 (3.40), 342 (3.63), 359 (3.75), 378 (3.63).

*4.3.3. 2,3-Di-iso-butylanthracene (**21**).* The general procedure was applied on 50 mg (0.15 mmol) of 2,3-dibromoanthracene. Colorless crystalline solid; yield: 20.7 mg (0.071 mmol, 48%). mp 126 °C. ^{1}H NMR ($CDCl_3$, 400 MHz): δ 8.31 (s, 2 H), 7.96 (dd, J_1 = 6.4 Hz, J_2 = 3.2 Hz, 2 H), 7.72 (s, 2 H), 7.40 (dd, J_1 = 6.6 Hz, J_2 = 3.4 Hz, 2 H), 2.68 (d, J = 6.6 Hz, 4 H), 1.99 (sept, J = 6.7 Hz, 2 H), 1.00 (d, J = 6.6 Hz, 12 H). ^{13}C{^{1}H} NMR ($CDCl_3$, 101 MHz): δ 138.8, 131.5, 131.0, 128.2, 127.9, 125.1, 124.9, 42.7, 29.7, 22.9. HRMS (EI) m/z: $[M]^{+\bullet}$ calcd for $C_{22}H_{26}$, 290.2029; found, 290.2021. UV/vis (*n*-hexane) λ_{max} (log ε): 314 (3.38), 328 (3.70), 344 (3.93), 360 (4.04), 379 (3.93).

4.4. General Procedure for the Synthesis of 2,3-Disubstituted Buta-1,3-dienes (28a−e). A suspension of CuBr (4.01 g, 28 mmol, 2.1 equiv) and LiBr (2.43 g, 28 mmol, 2.1 equiv) in dry THF (50 mL) was cooled to −50 °C and the Grignard reagent (28 mmol, 1.6 M solution in THF, 2.1 equiv) was added dropwise. After stirring for 20 min, a solution of **25** (5.26 g, 13.3 mmol) in THF (40 mL) was added dropwise and the mixture was allowed to warm to rt overnight. Sat. aq NH_4Cl (200 mL) was added in small portions and the aqueous phase was extracted with *n*-pentane (100 mL). The organic phase was washed with water (3 × 50 mL), dried over anhydrous Na_2SO_4, and evaporated. The oily light orange residue was distilled under reduced pressure using an oil bath as heat source to give a colorless oil.

*4.4.1. 2,3-Di-n-butyl-buta-1,3-diene (**28a**).* The reaction was conducted following the general procedure using 6 g (16.75 mmol) of ditosylate **25**. Colorless oil; yield: 1.13 g (6.81 mmol, 41%). bp 70 °C/25 mbar. ^{1}H NMR ($CDCl_3$, 400 MHz): δ 5.05 (br s, 2 H), 4.91 (br s, 2 H), 2.23 (t, J = 7.4 Hz, 4 H), 1.47−1.24 (m, 8 H), 0.91 (t, J = 7.2 Hz, 6 H). ^{13}C{^{1}H} NMR ($CDCl_3$, 101 MHz): δ 148.2, 111.4, 34.1, 31.0, 22.7, 14.1. MS (EI) m/z (%): 166.1 (12) $[M]^{+\bullet}$, 124.0 (15), 109.0 (36), 95.0 (22), 82.0 (100), 67.0 (27), 55.0 (13), 41.0 (20). The ^{1}H data are in agreement with published data.[58]

*4.4.2. 2,3-Di-iso-butyl-buta-1,3-diene (**28b**).* The reaction was conducted following the general procedure using 7.55 g (20.15 mmol) of ditosylate **25**. Colorless oil; yield: 0.87 g (5.24 mmol, 26%). bp 60 °C/20 mbar ^{1}H NMR ($CDCl_3$, 400 MHz): δ 5.04 (d, J = 2.3 Hz, 2 H), 4.86 (br s, 2 H), 2.09 (d, J = 7.1 Hz, 4 H), 1.74 (sept, J = 6.6 Hz, 2 H), 0.87 (d, J = 6.6 Hz, 12 H). ^{13}C{^{1}H} NMR ($CDCl_3$, 101 MHz): δ

DOI: 10.1021/acs.joc.9b01317
J. Org. Chem. 2019, 84, 10120−10135

147.2, 113.1, 44.3, 26.8, 22.7. MS (EI) m/z (%): 166.1 (33) $[M]^{+\bullet}$, 151.0 (10), 123.0 (100), 109.0 (43), 95.0 (76), 81.0 (33), 68.0 (28), 55.0 (15), 43.0 (29). The ^{1}H data are in agreement with published data.[56]

4.4.3. 2,3-Di-(3-cyclohexylpropyl)-buta-1,3-diene (28c). 3-Cyclohexylpropylmagnesium bromide in THF was prepared from 1-bromo-3-cyclohexylpropane (**26**) and Mg turnings in the usual manner. Colorless oil; yield: 2.18 g (7.22 mmol, 54%). bp 122 °C/6 × 10^{-2} mbar. ^{1}H NMR ($CDCl_3$, 400 MHz): δ 5.03 (br s, 2 H), 4.90 (br s, 2 H), 2.19 (t, J = 7.6 Hz, 4 H), 1.74−1.59 (m, 12 H), 1.48−1.38 (m, 4 H), 1.22−1.16 (m, 10 H), 0.91−0.83 (m, 4 H). $^{13}C\{^1H\}$ NMR ($CDCl_3$, 101 MHz): δ 148.3, 111.4, 37.8, 37.5, 34.8, 33.6, 26.9, 26.6, 26.1. HRMS (EI) m/z: $[M]^{+\bullet}$ calcd for $C_{22}H_{38}$, 302.2968; found, 302.2961.

4.4.4. 2,3-Di-(ethyl-2-(1-adamantyl))buta-1,3-diene (28d). 1 M $ZnCl_2$ and 1 M CuCN·2 LiCl solutions were prepared according to published procedure using anhydrous THF which was degassed prior to use.[62] Mg turnings ground under an atmosphere of Ar (0.4 g, 16.4 mmol, 2 equiv) were suspended in THF (15 mL) and 1,2-dibromoethane (0.82 mmol, 70 mL, 5 mol %) followed by TMSCl (0.82 mmol, 0.1 mL, 5 mol %) was added. To this solution, $ZnCl_2$ in THF (18.1 mL, 18.1 mmol, 1.1 equiv) was added dropwise. After complete addition, 1-(2-bromoethyl)adamantane (4 g, 16.5 mmol) was added in portions and the reaction was stirred overnight at 70 °C in an oil bath. After cooling to rt, the solution of the zinc reagent was added dropwise to a CuCN·2 LiCl solution in THF (16.5 mL, 16.5 mmol, 1 equiv) at −50 °C and stirred for 20 min, followed by addition of **25** (2.6 g, 6.6 mmol, 0.4 equiv) in THF (20 mL). The solution was allowed to warm to rt overnight, sat. aq NH_4Cl (100 mL) was added and the aqueous phase was extracted with *n*-pentane (100 mL). The organic phase was washed with water (3 × 50 mL), dried over Na_2SO_4, and evaporated, leaving a colorless oil; yield: 3.12 g. As the material is contaminated with unreacted bromide evident by the EI mass spectra only the characteristic signals for the double bonds are given. Additionally, the HR-EI mass spectrum confirms the proposed sum formula of the product. ^{1}H NMR ($CDCl_3$, 400 MHz): δ 5.03 (br s, 2 H), 4.91 (br s, 2 H). $^{13}C\{^1H\}$ NMR ($CDCl_3$, 101 MHz): δ 149.1, 111.2. HRMS (EI) m/z: $[M]^{+\bullet}$ calcd for $C_{28}H_{42}$, 378.3281; found, 378.3289.

4.4.5. 2,3-Di-neopentyl-buta-1,3-diene (28e). Neopentylmagnesium bromide was prepared from neopentylbromide and Mg turnings in the usual manner. The reaction was conducted following the general procedure using 5.9 g (15 mmol) of ditosylate **25**. Colorless oil; yield: 1.94 g (10 mmol, 67%). bp 92 °C/30 mbar. ^{1}H NMR ($CDCl_3$, 400 MHz): δ 5.14 (d, J = 2.6 Hz, 2 H), 4.73 (d, J = 2.6 Hz, 2 H), 2.15 (s, 4 H), 0.90 (s, 18 H). $^{13}C\{^1H\}$ NMR ($CDCl_3$, 101 MHz): δ 150.0, 115.9, 47.3, 31.8, 30.0. MS (EI) m/z (%): 194.1 (3) $[M]^{+\bullet}$, 123.0 (16), 71.0 (7), 57.0 (100). The spectra are in agreement with published data.[56]

4.5. General Procedure for the Synthesis of 2,3-Disubstituted 1,4,4a,9a-Tetrahydro-9,10-anthraquinone Derivates (30a−e). A solution of 1,4-naphthoquinone (1.08 g, 6.83 mmol) and the corresponding butadiene (6.92 mmol, 1.01 equiv) in EtOH (15 mL) was refluxed overnight in an oil bath. After cooling to rt, the flask was kept at −10 °C overnight. The solid was filtered off, washed with ice cold EtOH (20 mL), and dried in oil pump vacuum to give a light grey to brown solid. The products are of sufficient purity for the next reaction step but can be further purified by flash chromatography (silica gel, *n*-hexane/CH_2Cl_2 2:1) if necessary.

4.5.1. 2,3-Di-n-butyl-1,4,4a,9a-tetrahydro-9,10-anthraquinone (30a). 2,3-Di-*n*-butyl-buta-1,3-diene (**28a**) (2.28 g, 13.69 mmol) was used for this synthesis. Colorless solid; yield: 2.79 g (8.6 mmol, 64%). R_f (silica gel, *n*-hexane/CH_2Cl_2 2:1): 0.24. mp 81−84 °C. ^{1}H NMR ($CDCl_3$, 400 MHz): δ 8.04 (dd, J_1 = 5.8 Hz, J_2 = 3.3 Hz, 2 H), 7.73 (dd, J_1 = 5.8 Hz, J_2 = 3.3 Hz, 2 H), 3.38−3.31 (m, 2 H), 2.52−2.41 (m, 2 H), 2.22−2.12 (m, 2 H), 2.00 (t, J = 7.9 Hz, 4 H), 1.41−1.23 (m, 8 H), 0.90 (t, J = 7.1 Hz, 6 H). $^{13}C\{^1H\}$ NMR ($CDCl_3$, 101 MHz): δ 198.6, 134.3, 134.2, 128.2, 126.9, 47.4, 32.6, 30.7, 28.8, 22.9, 14.2. HRMS (EI) m/z: $[M]^{+\bullet}$ calcd for $C_{22}H_{28}O_2$, 324.2084; found, 324.2073.

4.5.2. 2,3-Di-iso-butyl-1,4,4a,9a-tetrahydro-9,10-anthraquinone (30b). 2,3-Diisobutyl-buta-1,3-diene (**28b**) (1.55 g, 9.35 mmol) was used for the synthesis. Colorless solid; yield: 1.69 g (5 mmol, 54%). R_f (silica gel, *n*-hexane/CH_2Cl_2 2:1): 0.35. mp 105−106 °C. ^{1}H NMR ($CDCl_3$, 400 MHz): δ 8.04 (dd, J_1 = 5.8 Hz, J_2 = 3.3 Hz, 2 H), 7.73 (dd, J_1 = 5.8 Hz, J_2 = 3.3 Hz, 2 H), 3.38−3.31 (m, 2 H), 2.52−2.42 (m, 2 H), 2.21−2.12 (m, 2 H), 1.97−1.90 (m, 4 H), 1.78 (sept, J = 6.7 Hz, 2 H), 0.86−0.84 (two d; not resolved, J = 6.7 Hz, 12 H). $^{13}C\{^1H\}$ NMR ($CDCl_3$, 101 MHz): δ 198.6, 134.3, 134.2, 128.4, 126.9, 47.4, 42.0, 29.1, 27.1, 22.7, 22.6. HRMS (EI) m/z: $[M]^{+\bullet}$ calcd for $C_{22}H_{28}O_2$, 324.2084; found, 324.2092.

4.5.3. 2,3-Di-(3-cyclohexylpropyl)-1,4,4a,9a-tetrahydro-9,10-anthraquinone (30c). Colorless crystalline solid; yield: 3.04 g (6.60 mmol, 73%). R_f (silica gel, *n*-hexane/CH_2Cl_2 2:1): 0.22. mp 122−124 °C. ^{1}H NMR ($CDCl_3$, 400 MHz): δ 8.04 (dd, J_1 = 5.5 Hz, J_2 = 3.3 Hz, 2 H), 7.73 (dd, J_1 = 5.6 Hz, J_2 = 3.3 Hz, 2 H), 3.33 (br t, J = 4.2 Hz, 2 H), 2.52−2.38 (m, 2 H), 2.22−2.11 (m, 2 H), 1.96 (t, J = 7.8 Hz, 4 H), 1.76−1.61 (m, 12 H), 1.40−1.30 (m, 4 H), 1.18−1.05 (m, 9 H), 0.94−0.76 (m, 5 H). $^{13}C\{^1H\}$ NMR ($CDCl_3$, 101 MHz): δ 198.6, 134.3, 134.2, 128.3, 127.0, 47.4, 37.7, 33.6, 33.5, 33.2, 28.8, 26.9, 26.6, 25.7. HRMS (EI) m/z: $[M]^{+\bullet}$ calcd for $C_{32}H_{44}O_2$, 460.3336; found, 460.3346.

4.5.4. 2,3-Di-(ethyl-2-(1-adamantyl))-1,4,4a,9a-tetrahydro-9,10-anthraquinone (30d). This compound was synthesized by reaction of impure diene **28d** with an excess of 1,4-naphthoquinone using the general procedure. Colorless crystalline solid; yield: 0.16 g (0.3 mmol). R_f (silica gel, *n*-hexane/CH_2Cl_2 2:1): 0.38. mp 113−118 °C. ^{1}H NMR ($CDCl_3$, 400 MHz): δ 8.04 (dd, J_1 = 5.8 Hz, J_2 = 3.3 Hz, 2 H), 7.73 (dd, J_1 = 5.8 Hz, J_2 = 3.3 Hz, 2 H), 3.33 (br t, 4.8 Hz, 2 H), 2.50−2.38 (m, 2 H), 2.19−2.09 (m, 2 H), 1.99−1.85 (m, 10 H), 1.70 (br d, J = 12.0 Hz, 6 H), 1.62 (br d, J = 12.0 Hz, 6 H), 1.48 (d, J = 2.3 Hz, 12 H), 1.17−1.04 (m, 4 H). $^{13}C\{^1H\}$ NMR ($CDCl_3$, 101 MHz): δ 198.7, 134.3, 134.2, 128.4, 127.0, 47.5, 43.1, 42.5, 37.4, 32.5, 29.0, 28.9, 25.8. MS (EI) m/z (%): 536.4 (100) $[M]^{+\bullet}$, 518.4 (5), 373.2 (74), 355.2 (9), 210.0 (10), 135.1 (45), 93.1 (8). Alongside Diels−Alder adduct **30d** the oxidation products **30d-2H** and **31d** could be isolated.

4.5.5. 2,3-Di-(ethyl-2-(1-adamantyl))-1,4-dihydro-9,10-anthraquinone (30d-2H). Orange solid; yield: 0.33 g (0.61 mmol). R_f (silica gel, *n*-hexane/CH_2Cl_2 2:1): 0.52. mp 256−262 °C. ^{1}H NMR ($CDCl_3$, 400 MHz): δ 8.09 (dd, J_1 = 5.8 Hz, J_2 = 3.3 Hz, 2 H), 7.70 (dd, J_1 = 5.8 Hz, J_2 = 3.3 Hz, 2 H), 3.19 (s, 4 H), 2.10−2.02 (m, 4 H), 1.98 (br s, 6 H), 1.73 (br d, J = 12.0 Hz, 6 H), 1.65 (br d, J = 11.8 Hz, 6 H), 1.53 (d, J = 2.2 Hz, 12 H), 1.21−1.12 (m, 4 H). $^{13}C\{^1H\}$ NMR ($CDCl_3$, 101 MHz): δ 184.7, 142.4, 133.6, 132.3, 127.0, 126.3, 43.1, 42.5, 37.4, 32.6, 29.5, 28.9, 25.3. MS (EI) m/z (%): 534.2 (2), 518.4 (2), 369.2 (76), 135.1 (100), 93.0 (21).

4.5.6. 2,3-Di-(ethyl-2-(1-adamantyl))-9,10-anthraquinone (31d). Orange solid; yield: 0.049 g (0.092 mmol). R_f (silica gel, *n*-hexane/CH_2Cl_2 2:1): 0.42. mp 261−264 °C. ^{1}H NMR ($CDCl_3$, 400 MHz): δ 8.29 (dd, J_1 = 5.8 Hz, J_2 = 3.3 Hz, 2 H), 8.03 (s, 2 H), 7.77 (dd, J_1 = 5.8 Hz, J_2 = 3.3 Hz, 2 H), 2.73−2.66 (m, 4 H), 2.02 (br s, 6 H), 1.76 (br d, J = 12.2 Hz, 6 H), 1.68 (br d, J = 12.0 Hz, 6 H), 1.60 (d, J = 2.2 Hz, 12 H), 1.40−1.33 (m, 4 H). $^{13}C\{^1H\}$ NMR ($CDCl_3$, 101 MHz): δ 183.5, 149.2, 134.0, 133.9, 131.5, 128.3, 127.2, 46.3, 42.6, 37.3, 32.9, 28.9, 26.5. HRMS (EI) m/z: $[M]^{+\bullet}$ calcd for $C_{38}H_{44}O_2$, 532.3336; found, 532.3359.

4.5.7. 2,3-Di-neopentyl-1,4,4a,9a-tetrahydro-9,10-anthraquinone (30e). To a mixture of anhydrous CH_2Cl_2 (110 mL) and anhydrous THF (0.12 mL, 1.49 mmol), $AlCl_3$ (0.1 g, 0.74 mmol) was added all at once and the mixture was stirred for 15 min. 1,4-Naphthoquinone (2.63 g, 15 mmol, 1.08 eq) was added and the mixture was stirred for another 15 min, followed by addition of the diene **28e** (2.79 g, 14 mmol) in one portion. The resulting mixture was stirred at reflux overnight using an oil bath as heat source. After cooling, the solvent was removed under reduced pressure and the black residue was purified by flash chromatography (silica gel, *n*-hexane/CH_2Cl_2 2:1). Yellow solid; yield: 1.59 g (4.51 mmol, 31%). R_f (silica gel, *n*-hexane/CH_2Cl_2 2:1): 0.38. mp 91−94 °C. ^{1}H NMR ($CDCl_3$, 400 MHz): δ 8.04 (dd, J_1 = 5.8 Hz, J_2 = 3.3 Hz, 2 H), 7.73

DOI: 10.1021/acs.joc.9b01317
J. Org. Chem. 2019, 84, 10120−10135

(dd, J_1 = 5.8 Hz, J_2 = 3.3 Hz, 2 H), 3.37−3.30 (m, 2 H), 2.64−2.54 (m, 2 H), 2.33−2.23 (m, 2 H), 2.19 (d, J = 13.8 Hz, 2 H), 2.02 (d, J = 13.8 Hz, 2 H), 0.90 (s, 18 H). $^{13}C\{^1H\}$ NMR ($CDCl_3$, 101 MHz): δ 198.7, 134.4, 134.3, 129.6, 127.0, 47.8, 46.8, 33.0, 31.8, 31.1. HRMS (EI) m/z: $[M]^{+\bullet}$ calcd for $C_{24}H_{32}O_2$, 352.2397; found, 352.2368.

4.6. General Procedure for Oxidation of Tetrahydroquinones 30a−e. The corresponding tetrahydroquinone (2.95 mmol) was dissolved in 5% ethanolic KOH (65 mL) and a strong stream of oxygen was passed through the dark red solution for 45 min. After stirring the reaction mixture for 1 h at 65 °C in an oil bath, the solvent was removed under reduced pressure and the solid residue dissolved in CH_2Cl_2 (100 mL). The organic phase was washed with water (4 × 50 mL), dried over anhydrous Na_2SO_4 and evaporated. The residue was purified by flash chromatography (silica gel, *n*-hexane/CH_2Cl_2 2:1).

4.6.1. 2,3-Di-n-butyl-9,10-anthraquinone (31a). **29a** (1.46 g, 4.49 mmol) was used for this synthesis. Bright yellow solid; yield: 1.18 g (3.67 mmol, 82%). R_f (silica gel, *n*-hexane/CH_2Cl_2 2:1): 0.16. mp 99−102 °C. ^1H NMR ($CDCl_3$, 400 MHz): δ 8.28 (dd, J_1 = 5.6 Hz, J_2 = 3.3 Hz, 2 H), 8.06 (s, 2 H), 7.76 (dd, J_1 = 5.0, J_2 = 3.3 Hz, 2 H), 2.76 (t, J = 7.9 Hz, 4 H), 1.70−1.59 (m, 4 H), 1.45 (sext, J = 7.4 Hz, 4 H), 0.98 (t, J = 7.3 Hz, 6 H). $^{13}C\{^1H\}$ NMR ($CDCl_3$, 101 MHz): δ 183.5, 148.2, 134.0, 133.9, 131.5, 128.0, 127.2, 33.0, 32.8, 22.9, 14.1. HRMS (EI) m/z: $[M]^{+\bullet}$ calcd for $C_{22}H_{24}O_2$, 320.1771; found, 320.1783.

4.6.2. 2,3-Di-iso-butyl-9,10-anthraquinone (31b). Yellow oil; yield: 0.87 g (2.68 mmol, 90%). R_f (silica gel, *n*-hexane/CH_2Cl_2 2:1): 0.13. ^1H NMR ($CDCl_3$, 400 MHz): δ 8.29 (dd, J_1 = 5.8 Hz, J_2 = 3.3 Hz, 2 H), 8.05 (s, 2 H), 7.77 (dd, J_1 = 5.8 Hz, J_2 = 3.3 Hz, 2 H), 2.66 (d, J = 7.4 Hz, 4 H), 1.98 (sept, J = 6.7 Hz, 2 H), 0.97 (d, J = 6.7 Hz, 12 H). $^{13}C\{^1H\}$ NMR ($CDCl_3$, 101 MHz): δ 183.6, 147.5, 134.0, 133.9, 131.2, 128.8, 127.2, 42.2, 30.0, 22.7. HRMS (EI) m/z: $[M]^{+\bullet}$ calcd for $C_{22}H_{24}O_2$, 320.1771; found, 320.1753.

4.6.3. 2,3-Di-(3-cyclohexylpropyl)-9,10-anthraquinone (31c). **30c** (1.66 g, 3.60 mmol) was used for this synthesis. Bright yellow solid; yield: 1.53 g (3.34 mmol, 93%). R_f (silica gel, *n*-hexane/CH_2Cl_2 2:1): 0.28. mp 146−148 °C. ^1H NMR ($CDCl_3$, 400 MHz): δ 8.29 (dd, J_1 = 5.7 Hz, J_2 = 3.4 Hz, 2 H), 8.07 (s, 2 H), 7.77 (dd, J_1 = 5.8 Hz, J_2 = 3.3 Hz, 2 H), 2.73 (br t, J = 8.1 Hz, 4 H), 1.77−1.60 (m, 14 H), 1.35−1.14 (m, 12 H), 0.96−0.85 (m, 4 H). $^{13}C\{^1H\}$ NMR ($CDCl_3$, 101 MHz): δ 183.5, 148.3, 134.0, 133.9, 131.5, 128.0, 127.2, 37.7, 37.6, 33.5, 33.4, 28.3, 26.8, 26.5. HRMS (EI) m/z: $[M]^{+\bullet}$ calcd for $C_{32}H_{40}O_2$, 456.3023; found, 456.3009. Single crystals of this compound suitable for X-ray analysis were obtained by slow evaporation of the solvent from a solution in CH_2Cl_2. The material crystallizes in form of long needles.

4.6.4. 2,3-Di-(ethyl-2-(1-adamantyl))-9,10-anthraquinone (31d). For synthesis of compound **31d,** the Diels−Alder adduct **30d** (0.24 g, 0.45 mmol) and the oxidation product **30d-2H** (1.29 g, 2.4 mmol) were combined and subjected to the general procedure for oxidation. Orange solid; yield: 0.70 g (1.31 mmol, 46%). All analytical data is identical to the data obtained from the material isolated from the reaction of **28d** with excess 1-4-naphthoquinone (**29**). Single crystals of this compound suitable for X-ray analysis were obtained by slow evaporation of the solvent from a solution in CH_2Cl_2. The material crystallizes in form of needles.

4.6.5. 2,3-Di-neopentyl-9,10-anthraquinone (31e). **30e** (1.52 g, 4.31 mmol) was used for this synthesis. Light yellow solid; yield: 1.46 g (4.19 mmol, 97%). R_f (silica gel, *n*-hexane/CH_2Cl_2 1:1): 0.41. mp 140−143 °C. ^1H NMR ($CDCl_3$, 400 MHz): δ 8.30 (dd, J_1 = 5.8 Hz, J_2 = 3.3 Hz, 2 H), 8.05 (s, 2 H), 7.78 (dd, J_1 = 5.8 Hz, J_2 = 3.3 Hz, 2 H), 2.82 (s, 4 H), 0.94 (s, 18 H). $^{13}C\{^1H\}$ NMR ($CDCl_3$, 101 MHz): δ 183.7, 146.4, 134.1, 134.0, 130.6, 130.2, 127.2, 46.2, 33.5, 29.9. HRMS (EI) m/z: $[M]^{+\bullet}$ calcd for $C_{24}H_{28}O_2$, 348.2084; found, 348.2118.

4.7. Example Procedure for MPV Reduction of Anthraquinones 31a−e in Cyclohexanol. A suspension of Al shavings (1.15 g, 42.6 mmol, 12 equiv) prepared from Al foil roughened with sandpaper, CBr_4 (0.6 g, 1.8 mmol, 0.5 equiv) and $HgCl_2$ (0.1 g, 0.37 mmol, 0.1 equiv) in degassed cyclohexanol (28 mL) was heated cautiously to 80 °C in an oil bath until the mixture began to boil vigorously under evolvement of hydrogen gas. After most of the aluminum shavings dissolved and boiling had ceased, the resulting black mixture was heated to 160 °C for 1 h. The reaction mixture was allowed to cool to rt and the corresponding anthraquinone (3.55 mmol) was added all at once. After complete addition the reaction mixture was stirred at 140 °C in an oil bath overnight, allowed to cool to rt, and poured into 3 M aq HCl (200 mL) followed by stirring for 30 min at rt. The aqueous phase was extracted with toluene (3 × 150 mL) and washed with water (10 × 200 mL), the solvent was removed in vacuo. Water (120 mL) was added to the oily residue which was removed under reduced pressure. This step was repeated four more times. The crystalline mass which formed was dissolved in toluene (200 mL) and the solvent was washed with water (3 × 100 mL). The organic phase was dried over anhydrous Na_2SO_4 and evaporated to dryness. The crystalline, yellowish residue was purified by flash chromatography (silica gel, *n*-hexane) and dried in oil pump vacuum at 90 °C using an oil bath as heat source for 1 d.

4.7.1. 2,3-Di-n-butylanthracene (20). It was obtained as a colorless solid; yield: 0.66 g (2.3 mmol, 65%). R_f (silica gel, *n*-hexane): 0.43. All analytical data are identical with the data obtained from the Suzuki−Miyaura coupling reaction.

4.7.2. 2,3-Di-iso-butylanthracene (21). Quinone **30b** (0.87 g, 2.7 mmol) was used for this synthesis. The quinone was applied as a solution in dry toluene (10 mL) to the reaction mixture. Colorless solid; yield: 0.53 g (1.83 mmol, 67%). R_f (silica gel, *n*-hexane): 0.64. All analytical data are identical with the data obtained from the Suzuki−Miyaura coupling reaction.

4.7.3. 2,3-Di-(3-cyclohexylpropyl)anthracene (32). Quinone **31c** (1.30 g, 2.85 mmol) was used for this synthesis. Slightly green solid; yield: 0.99 g (2.32 mmol, 81%). R_f (silica gel, *n*-hexane): 0.38. mp 118−121 °C. ^1H NMR ($CDCl_3$, 400 MHz): δ 8.31 (s, 2 H), 7.97 (dd, J_1 = 6.5 Hz, J_2 = 3.2 Hz, 2 H), 7.76 (s, 2 H), 7.41 (dd, J_1 = 6.5 Hz, J_2 = 3.2 Hz, 2 H), 2.78 (br t, J = 7.9 Hz, 4 H), 1.82−1.65 (m, 14 H), 1.41−1.14 (m, 12 H), 1.01−0.87 (m, 4 H). $^{13}C\{^1H\}$ NMR ($CDCl_3$, 101 MHz): δ 139.8, 131.5, 131.1, 128.2, 126.6, 125.1, 124.9, 37.8, 37.7, 33.6, 33.5, 28.3, 26.9, 26.6. HRMS (EI) m/z: $[M]^{+\bullet}$ calcd for $C_{32}H_{42}$, 426.3281; found, 426.3271. UV/vis (*n*-hexane) λ_{max} (log ε): 314 (3.11), 328 (3.44), 344 (3.67), 361 (3.79), 380 (3.66).

4.7.4. 9-Oxa-1,2,3,4b,5,6,7,8,8a,9,10,10a-dodecahydrophenanthrene-10-spiro-1-cyclohexane (33). The compound was sublimed from **32** at 90 °C in an oil pump vacuum using an oil bath as heat source. Colorless crystalline solid; yield: 0.14 g (0.53 mmol, 0.2% based on the amount of cyclohexanol). mp 75−77 °C. ^1H NMR ($CDCl_3$, 400 MHz): δ 5.52−5.47 (m, 1 H), 3.64−3.58 (m, 1 H), 2.28−2.19 (m, 1 H), 1.97−1.76 (m, 7 H), 1.73−1.50 (m, 6 H), 1.47−1.19 (m, 10 H), 1.13−1.02 (m, 2 H). $^{13}C\{^1H\}$ NMR ($CDCl_3$, 101 MHz): δ 140.8, 121.7, 76.4, 65.6, 45.5, 42.6, 36.9, 31.7, 28.5, 26.5, 26.2, 26.1, 25.5, 24.6, 22.6, 21.7, 20.8, 20.4. HRMS (EI) m/z: $[M]^{+\bullet}$ calcd for $C_{18}H_{28}O$, 260.2135; found, 260.2128.

4.7.5. 2,3-Di-(ethyl-2-(1-adamantyl))anthracene (35). Quinone **31d** (0.7 g, 1.31 mmol) was used for this synthesis. Colorless solid; yield: 0.49 g (0.97 mmol, 74%). R_f (silica gel, *n*-hexane/DCM 4:1): 0.25. mp 278−279 °C. ^1H NMR ($CDCl_3$, 400 MHz): δ 8.29 (s, 2 H), 7.95 (dd, J_1 = 6.5 Hz, J_2 = 3.3 Hz, 2 H), 7.74 (s, 2 H), 7.40 (dd, J_1 = 6.5 Hz, J_2 = 3.2 Hz, 2 H), 2.79−2.71 (m, 4 H), 2.03 (br s, 6 H), 1.77 (d, J = 12.2 Hz, 6 H), 1.71 (d, J = 11.9 Hz, 6 H), 1.65 (d, J = 2.2 Hz, 12 H), 1.50−1.42 (m, 4 H). $^{13}C\{^1H\}$ NMR ($CDCl_3$, 101 MHz): δ 140.6, 131.5, 131.3, 128.2, 126.8, 125.0, 124.8, 46.8, 42.7, 37.5, 32.9, 29.0, 26.3. HRMS (EI) m/z: $[M]^{+\bullet}$ calcd for $C_{38}H_{46}$, 502.3594; found, 502.3576. UV/vis (*n*-hexane) λ_{max} (log ε): 315 (3.11), 329 (3.43), 344 (3.67), 362 (3.78), 381 (3.64).

4.7.6. 2,3-Di-neopentylanthracene (36). Anthraquinone **31e** (1.22 g, 3.49 mmol) was used for this synthesis. Colorless solid; yield: 0.76 g (2.18 mmol, 63%). R_f (silica gel, *n*-hexane): 0.39. mp 205−208 °C. ^1H NMR ($CDCl_3$, 400 MHz): δ 8.33 (s, 2 H), 7.97 (dd, J_1 = 6.6 Hz, J_2 = 3.3 Hz, 2 H), 7.74 (s, 2 H), 7.40 (dd, J_1 = 6.6 Hz, J_2 = 3.2 Hz, 2 H), 2.86 (s, 4 H), 0.95 (s, 18 H). $^{13}C\{^1H\}$ NMR ($CDCl_3$, 101 MHz): δ 137.7, 131.6, 130.7, 129.2, 128.2, 125.1, 124.9, 46.2, 33.4, 29.9. HRMS (EI) m/z: $[M]^{+\bullet}$ calcd for $C_{24}H_{30}$, 318.2342; found, 318.2333. UV/vis (*n*-hexane) λ_{max} (log ε): 316 (3.02), 331 (3.38), 347 (3.64), 364 (3.78), 384 (3.67).

DOI: 10.1021/acs.joc.9b01317
J. Org. Chem. 2019, 84, 10120−10135

4.8. General Procedure for the Dimerization of Anthracene Derivatives. The respective anthracene monomer was dissolved in an appropriate amount of toluene and the solution was degassed by bubbling Ar gas through the solution for 2 h followed by irradiation with a 500 W high-pressure Hg lamp (wavelength region 305−400 nm) for 16 h at rt under an atmosphere of Ar. The solvent was removed under reduced pressure and the colorless solid subjected to flash chromatography.

*4.8.1. Dimerization of 2-tert-Butylanthracene (**9**).* A solution of the monomer (0.5 g, 2.1 mmol) in degassed toluene (20 mL) was used. The solid which precipitated (compound **37a**) was removed by centrifugation and dried in an oil pump vacuum. The liquid phase was kept in a refrigerator for crystallization.

*4.8.2. 2,6′-Di-tert-butyl-dianthracene (**37a**).* The compound was obtained as a colorless solid; yield: 0.156 g (0.33 mmol, 31%). mp 232−236 °C. ^{1}H NMR ($CDCl_3$, 400 MHz): δ 6.92 (d, J = 1.9 Hz, 2 H), 6.90−6.70 (m, 12 H), 4.48 (s, 4 H), 1.15 (s, 18 H). $^{13}C\{^1H\}$ NMR ($CDCl_3$, 101 MHz): δ 148.4, 143.9, 143.8, 143.2, 140.5, 127.1, 127.0, 126.7, 125.4, 125.3, 124.6, 121.9, 54.2, 53.3, 34.3, 31.4. HRMS (ESI) m/z: $[M + Na]^+$ calcd for $C_{36}H_{36}Na$, 491.2709; found, 491.2714. Single crystals suitable for X-ray crystallography were obtained by diffusion of toluene into a saturated $CHCl_3$ solution of this compound in the cold. Thin, orthorhombic crystals were obtained within a night.

*4.8.3. 2,7′-Di-tert-butyl-dianthracene (**37b**).* The compound crystallizes from the mother liquor in form of large rods which were removed by filtration and dried in vacuo. These crystals were suitable for X-ray crystallography. Crystalline rods; yield: 60 mg (0.13 mmol, 12%). mp 235−238 °C. ^{1}H NMR ($CDCl_3$, 400 MHz): δ 6.93 (d, J = 1.8 Hz, 2 H), 6.89−6.85 (m, 4 H), 6.83−6.72 (m, 8 H), 4.49 (s, 2 H), 4.48 (2 H), 1.16 (s, 18 H). $^{13}C\{^1H\}$ NMR ($CDCl_3$, 101 MHz): δ 148.4, 143.9, 143.8, 143.1, 140.6, 127.2, 127.1, 126.7, 125.4, 125.3, 124.6, 121.9, 54.2, 53.4, 34.3, 31.4. HRMS (ESI) m/z: $[M + Na]^+$ calcd for $C_{36}H_{36}Na$, 491.2709; found, 491.2714.

*4.8.4. Dimerization of 2,6-Di-tert-butylanthracene (**11**).* A solution of the monomer (0.1 g, 0.34 mmol) in degassed toluene (25 mL) was used. The crude product was purified by flash chromatography (silica gel, n-hexane/CH_2Cl_2 2:1).

*4.8.5. 2,3′,6,7′-Tetra-tert-butyl-dianthracene (**38a**).* The compound was obtained as a colorless solid; yield: 96.5 mg (0.166 mmol, 98%). R_f (silica gel, n-hexane/CH_2Cl_2): 0.54. mp 219−221 °C. ^{1}H NMR ($CDCl_3$, 400 MHz): δ 6.85 (d, J = 1.7 Hz, 4 H), 6.79−6.71 (m, 8 H), 4.40 (s, 4 H), 1.14 (s, 36 H). $^{13}C\{^1H\}$ NMR ($CDCl_3$, 101 MHz): δ 148.0, 143.3, 140.7, 126.6, 124.6, 121.8, 53.8, 34.2, 31.4. HRMS (ESI) m/z: $[M + Na]^+$ calcd for $C_{44}H_{52}Na$, 603.3961; found, 603.3965. Single crystals suitable for X-ray crystallography were obtained by diffusion of toluene into a saturated $CHCl_3$ solution of this compound, which crystallizes in the form of colorless needles. The syn isomer (**38b**) is only detectable in trace amounts by HPLC by its mass peak.

*4.8.6. Dimerization of 2,3-Dimethylanthracene (**8**).* A solution of the monomer (0.2 g, 0.97 mmol) in degassed toluene (30 mL) was used. After flash chromatography (silica gel, n-hexane/CH_2Cl_2 2:1), a 1:1 mixture of both isomers, determined by NMR spectroscopy, was obtained. Colorless solid; yield: 0.19 g (0.46 mmol, 95%). R_f (silica gel, n-hexane/CH_2Cl_2): 0.32.

*4.8.7. 2,3,6′,7′-Tetramethyl-dianthracene (**39a**).* Single crystals of the anti isomer suitable for X-ray crystallography could be obtained by diffusion of toluene into a saturated $CHCl_3$ solution of the isomers. The compound crystallizes in the form of cubic crystals containing two molecules of $CHCl_3$ per unit cell which quickly turn opaque when removed from the mother liquor. Colorless cubic crystals, yield: 92.3 mg (0.22 mmol, 46%). mp 248−253 °C. ^{1}H NMR ($CDCl_3$, 400 MHz): δ 6.86 (dd, J_1 = 5.4 Hz, 4 H, J_2 = 3.3 Hz, 4 H), 6.76 (dd, J_1 = 5.5 Hz, J_2 = 3.2 Hz, 4 H), 6.66 (s, 4 H), 4.42 (s, 4 H), 2.00 (s, 12 H). $^{13}C\{^1H\}$ NMR ($CDCl_3$, 101 MHz): δ 144.2, 141.2, 133.1, 128.4, 126.9, 125.3, 53.3, 19.4. HRMS (ESI) m/z: $[M + Na]^+$ calcd for $C_{32}H_{28}Na$, 435.2083; found, 435.2076.

*4.8.8. 2,2′,3,3′-Tetramethyl-dianthracene (**39b**).* After several months of crystallization in the cold the syn isomer, containing a small amount of the anti isomer (**39a**) could be isolated from the mother liquor. Colorless solid; yield: 94.6 mg (0.23 mmol, 47%). mp 236−240 °C. ^{1}H NMR ($CDCl_3$, 400 MHz): δ 6.86 (dd, overlapping signals of anti and syn, 4 H), 6.76 (dd, overlapping signals of anti and syn, 4 H), 6.67 (s, 4 H), 4.42 (s, overlapping signals of anti and syn, 4 H) 2.03 (s, 12 H). $^{13}C\{^1H\}$ NMR ($CDCl_3$, 101 MHz): δ 144.3, 141.2, 133.0, 128.5, 127.0, 125.3, 53.4, 19.4. HRMS (ESI) m/z: $[M + Na]^+$ calcd for $C_{32}H_{28}Na$, 435.2083; found, 435.2088.

*4.8.9. Dimerization of 2,3-Di-n-butylanthracene (**20**).* A solution of the monomer (0.2 g, 0.69 mmol) in degassed toluene (20 mL) was used. The isomers were separated by flash chromatography (silica gel, n-hexane/CH_2Cl_2 10:1).

*4.8.10. 2,3,6′,7′-Tetra-n-butyl-dianthracene (**40a**).* The compound was obtained as a colorless solid; yield: 0.115 g (0.20 mmol, 51%). R_f (silica gel, n-hexane/CH_2Cl_2 10:1): 0.32. mp 151−154 °C. ^{1}H NMR ($CDCl_3$, 400 MHz): δ 6.85 (dd, J_1 = 5.3 Hz, J_2 = 3.3 Hz, 4 H), 6.73 (dd, J_1 = 5.4 Hz, J_2 = 3.2 Hz, 4 H), 6.64 (s, 4 H), 4.40 (s, 4 H), 2.45−2.27 (m, 8 H), 1.42−1.31 (m, 8 H), 1.30−1.19 (m, 8 H), 0.91 (t, J = 7.3 Hz, 12 H). $^{13}C\{^1H\}$ NMR ($CDCl_3$, 101 MHz): δ 144.1, 140.8, 137.2, 128.1, 127.0, 125.2, 53.5, 33.7, 32.0, 22.5, 14.2. HRMS (ESI) m/z: $[M + Na]^+$ calcd for $C_{44}H_{52}Na$, 603.3961; found, 603.3965. Single crystals suitable for X-ray crystallography could be obtained by slow evaporation of the solvent from a saturated solution of the dimer in n-hexane. The compound crystallizes in form of large colorless rods.

*4.8.11. 2,2′,3,3′-Tetra-n-butyl-dianthracene (**40b**).* Colorless oil which solidifies to give a colorless solid when thoroughly dried in an oil pump vacuum; yield: 84 mg (0.14 mmol, 37%). R_f (silica gel, n-hexane/CH_2Cl_2 10:1): 0.18. mp 119−122 °C. ^{1}H NMR ($CDCl_3$, 400 MHz): δ 6.89 (dd, J_1 = 5.4 Hz, J_2 = 3.3 Hz, 4 H), 6.79 (dd, J_1 = 5.4 Hz, J_2 = 3.3 Hz, 4 H), 6.65 (s, 4 H), 4.42 (s, 4 H), 2.43−2.28 (m, 8 H), 1.41−1.24 (m, 16 H), 0.92 (t, J = 7.1 Hz, 12 H). $^{13}C\{^1H\}$ NMR ($CDCl_3$, 101 MHz): δ 144.2, 140.9, 137.1, 128.1, 127.0, 125.4, 53.5, 33.9, 32.1, 22.8, 14.3. HRMS (ESI) m/z: $[M + Na]^+$ calcd for $C_{44}H_{52}Na$, 603.3961; found, 603.3964.

*4.8.12. Dimerization of 2,3-Di-iso-butylanthracene (**21**).* A solution of the monomer (0.25 g, 0.86 mmol) in degassed toluene (20 mL) was used. The isomers were separated by flash chromatography (silica gel, n-hexane/CH_2Cl_2 6:1).

*4.8.13. 2,3,6′,7′-Tetra-iso-butyl-dianthracene (**41a**).* The compound was obtained as a colorless solid; yield: 0.15 g (0.25 mmol, 59%). R_f (silica gel, n-hexane/CH_2Cl_2 6:1): 0.43. mp 207−208 °C. ^{1}H NMR ($CDCl_3$, 400 MHz): δ 6.86 (dd, J_1 = 5.4 Hz, J_2 = 3.2 Hz, 4 H), 6.73 (dd, J_1 = 5.4 Hz, J_2 = 3.2 Hz, 4 H), 6.63 (s, 4 H), 4.42 (s, 4 H), 2.29 (dd, J_1 = 13.7 Hz, J_2 = 7.3 Hz, 4 H), 2.18 (dd, J_1 = 13.7 Hz, J_2 = 7.3 Hz, 4 H), 1.66 (sept, J = 6.7 Hz, 4 H), 0.82 (d, J = 6.6 Hz, 12 H), 0.79 (d, J = 6.6 Hz, 12 H). $^{13}C\{^1H\}$ NMR ($CDCl_3$, 101 MHz): δ 144.1, 140.6, 136.6, 128.7, 127.1, 125.2, 53.5, 41.6, 30.1, 22.7. HRMS (ESI) m/z: $[M + Na]^+$ calcd for $C_{44}H_{52}Na$, 603.3961; found, 603.3963.

*4.8.14. 2,2′,3,3′-Tetra-iso-butyl-dianthracene (**41b**).* Colorless oil which solidifies to give a colorless solid when thoroughly dried in an oil pump vacuum; yield: 87 mg (0.15 mmol, 35%). R_f (silica gel, n-hexane/CH_2Cl_2 6:1): 0.24. mp 135−138 °C. ^{1}H NMR ($CDCl_3$, 400 MHz): δ 6.88 (dd, J_1 = 5.4 Hz, J_2 = 3.3 Hz, 4 H), 6.79 (dd, J_1 = 5.4 Hz, J_2 = 3.2 Hz, 4 H), 6.63 (s, 4 H), 4.43 (s, 4 H), 2.27−2.13 (two d; not resolved, J = 2.5 Hz, 8 H), 1.62 (sept, J = 6.7 Hz, 4 H), 0.78 (t, J = 6.9 Hz, 24 H). $^{13}C\{^1H\}$ NMR ($CDCl_3$, 101 MHz): δ 144.4, 140.7, 136.5, 128.9, 127.1, 125.3, 53.5, 41.8, 29.8, 22.8, 22.6. HRMS (ESI) m/z: $[M + Na]^+$ calcd for $C_{44}H_{52}Na$, 603.3961; found, 603.3958. Single crystals suitable for X-ray crystallography could be obtained by slow evaporation of the solvent from a solution of the dimer in n-hexane. The compound crystallizes in form of colorless rods.

*4.8.15. Dimerization of 2,3-Di-(3-cyclohexylpropyl)anthracene (**32**).* A solution of the monomer (0.3 g, 0.7 mmol) in degassed toluene (30 mL) was used. The isomers were separated by flash chromatography (silica gel, n-hexane/CH_2Cl_2 10:1).

*4.8.16. 2,3,6′,7′-Tetra-(3-cyclohexylpropyl)-dianthracene (**42a**).* The compound was obtained as colorless solid; yield: 0.145 g (0.17 mmol, 49%). R_f (silica gel, n-hexane/CH_2Cl_2 10:1): 0.48. mp 188−

DOI: 10.1021/acs.joc.9b01317
J. Org. Chem. 2019, 84, 10120−10135

190 °C. ^{1}H NMR ($CDCl_3$, 400 MHz): δ 6.85 (dd, J_1 = 5.4 Hz, J_2 = 3.2 Hz, 4 H), 6.74 (dd, J_1 = 5.4 Hz, J_2 = 3.2 Hz, 4 H), 6.63 (s, 4 H), 4.40 (s, 4 H), 2.41−2.24 (m, 8 H), 1.76−1.64 (m, 20 H), 1.43−1.32 (m, 8 H), 1.26−1.10 (m, 24 H), 0.93−0.82 (m, 8 H). $^{13}C\{^1H\}$ NMR ($CDCl_3$, 101 MHz): δ 144.1, 140.8, 137.2, 128.1, 127.0, 125.2, 53.5, 37.8, 37.4, 33.6, 33.5, 32.6, 28.7, 27.0, 26.7. HRMS (ESI) m/z: $[M + Na]^+$ calcd for $C_{64}H_{84}Na$, 875.6465; found, 875.6467.

*4.8.17. 2,2′,3,3′-Tetra-(3-cyclohexylpropyl)-dianthracene (**42b**).* Colorless oil which solidifies to give a transparent glassy solid when dried in an oil pump vacuum; yield: 0.120 g (0.14 mmol, 40%). R_f (silica gel, *n*-hexane/CH_2Cl_2 10:1): 0.31. mp 54−58 °C. ^{1}H NMR ($CDCl_3$, 400 MHz): δ 6.88 (dd, J_1 = 5.4 Hz, J_2 = 3.3 Hz, 4 H), 6.78 (dd, J_1 = 5.4 Hz, J_2 = 3.2 Hz, 4 H), 6.62 (s, 4 H), 4.41 (s, 4 H), 2.29 (dd, J_1 = 9.0 Hz, J_2 = 7.0 Hz, 8 H), 1.77−1.65 (m, 20 H), 1.39−1.30 (m, 8 H), 1.29−1.16 (m, 24 H), 0.94−0.84 (m, 8 H). $^{13}C\{^1H\}$ NMR ($CDCl_3$, 101 MHz): δ 144.1, 140.9, 137.2, 128.1, 127.0, 125.4, 53.5, 38.0, 37.7, 33.6, 33.5, 33.0, 29.3, 26.9, 26.6. HRMS (ESI) m/z: $[M + Na]^+$ calcd for $C_{64}H_{84}Na$, 875.6465; found, 875.6463.

*4.8.18. Dimerization of 2,3-Di-(ethyl-2-(1-adamantyl))-anthracene (**35**).* A solution of the monomer (0.2 g, 0.4 mmol) in degassed toluene (40 mL) was used. The insoluble material which formed during the reaction was collected by centrifugation, toluene (20 mL) was added and the solid was treated in an ultrasonic bath followed by centrifugation. This step was repeated one more time. The supernatants collected were combined and evaporated to dryness leaving a colorless solid.

*4.8.19. 2,3,6′,7′-Tetra-(ethyl-2-(1-adamantyl))-dianthracene (**43a**).* The compound was obtained as a colorless solid; yield: 0.123 g (0.122 mmol, 61%). mp 259−262 °C. ^{1}H NMR ($CDCl_3$, 400 MHz): δ 6.82 (dd, J_1 = 5.3 Hz, J_2 = 3.3 Hz, 4 H), 6.72 (dd, J_1 = 5.4 Hz, J_2 = 3.2 Hz, 4 H), 6.58 (s, 4 H), 4.36 (s, 4 H), 2.30−2.24 (m, 8 H), 1.97 (br s, 12 H), 1.72 (d, J = 12.0 Hz, 12 H), 1.65 (d, J = 11.9 Hz, 12 H), 1.52 (d, J = 1.9 Hz, 24 H), 1.08−1.02 (m, 8 H). $^{13}C\{^1H\}$ NMR ($CDCl_3$, 101 MHz): δ 144.0, 140.9, 137.8, 128.3, 127.1, 125.2, 53.5, 47.2, 42.6, 37.5, 32.7, 29.0, 25.5. MS (LDI) m/z (%): 502.3 $[M]^{+\bullet}$ of monomer. No high resolution ESI-MS spectra could be obtained due to insolubility of the compound. Anal. Calcd for $C_{76}H_{92}$: C, 90.78; H, 9.22. Found: C, 90.46; H, 9.29.

*4.8.20. 2,2′,3,3′-Tetra-(ethyl-2-(1-adamantyl))-dianthracene (**43b**).* The compound was obtained as a colorless solid; yield: 87 mg (0.086 mmol, 43%). mp 246−248 °C. ^{1}H NMR ($CDCl_3$, 400 MHz): δ 6.88 (dd, J_1 = 5.4 Hz, J_2 = 3.3 Hz, 4 H), 6.78 (dd, J_1 = 5.5 Hz, J_2 = 3.2 Hz, 4 H), 6.55 (s, 4 H), 4.38 (s, 4 H), 2.31−2.24 (m, 8 H), 1.99 (br s, 12 H), 1.75 (d, J = 12.1 Hz, 12 H), 1.66 (d, J = 11.9 Hz, 12 H), 1.57 (d, J = 1.7 Hz, 24 H), 1.11−1.06 (m, 8 H). $^{13}C\{^1H\}$ NMR ($CDCl_3$, 101 MHz): δ 143.9, 141.0, 137.7, 128.7, 127.1, 125.4, 53.5, 47.7, 42.8, 37.5, 32.9, 29.0, 26.0. HRMS (ESI) m/z: $[M + Na]^+$ calcd for $C_{76}H_{92}Na$, 1027.7091; found, 1027.7071.

*4.8.21. Dimerization of 2,3-Di-neopentylanthracene (**36**).* A solution of the monomer (0.2 g, 0.61 mmol) in degassed toluene (20 mL) was used. The solvent was removed under reduced pressure and the solid residue purified by flash chromatography (silica gel, *n*-hexane/CH_2Cl_2 10:1).

*4.8.22. 2,3,6′,7′-Tetra-neopentyl-dianthracene (**44a**).* The compound was obtained as a colorless solid; yield: 69 mg (0.11 mmol, 36%). R_f (silica gel, *n*-hexane/CH_2Cl_2 10:1): 0.66. mp 249−252 °C. ^{1}H NMR ($CDCl_3$, 400 MHz): δ 6.88 (dd, J_1 = 5.3 Hz, J_2 = 3.3 Hz, 4 H), 6.75 (dd, J_1 = 5.3 Hz, J_2 = 3.2 Hz, 4 H) 6.62 (s, 4 H), 2.39 (d, J = 13.7 Hz, 4 H), 2.35 (d, J = 13.6 Hz, 4 H), 0.75 (s, 36 H). $^{13}C\{^1H\}$ NMR ($CDCl_3$, 101 MHz): δ 144.3, 140.1, 135.4, 129.9, 127.2, 125.3, 53.5, 45.4, 33.1, 29.8. HRMS (ESI) m/z: $[M + K]^+$ calcd for $C_{48}H_{60}K$, 675.4327; found, 675.4324.

An additional fraction (colorless solid, 44.5 mg) which consisted of a mixture of **44a** and 2,3,6,7-tetra-neopentyl-dianthracene (**44b**) was isolated. This mixture contained 22% of **44b** (determined by NMR spectroscopy). This amounts to an overall yield of 0.016 mmol (5%) for **44b** compared to the amount of starting material used. R_f (silica gel, *n*-hexane/CH_2Cl_2 10:1): 0.33. ^{1}H NMR ($CDCl_3$, 400 MHz): δ 0.78 (s, 36 H), 4.46 (s, 4 H), 6.68 (s, 4 H), 6.79 (dd, J_1 = 5.4 Hz, J_2 = 3.2 Hz). The CH_2 signals of the neopentyl groups could not be resolved due to overlap with signals for anti dimer **44a**. HRMS (ESI) m/z: $[M + K]^+$ calcd for $C_{48}H_{60}K$, 675.4327; found, 675.4324.

4.9. Computational Methods. All density functional theory computations were performed with Gaussian 09.[83] Geometry optimizations were carried out using the B3LYP-D3 functional[84] and the def2TZVP basis set. Dipole moments of ground and excited states of anthracene monomers were calculated using the ωB97XD functional[85] and the 6-31G* basis set. The computations were performed on the bwHPC cluster JUSTUS.

■ ASSOCIATED CONTENT

Supporting Information

The Supporting Information is available free of charge on the ACS Publications website at DOI: 10.1021/acs.joc.9b01317.

^{1}H NMR and $^{13}C\{^1H\}$-NMR for all compounds, NOESY spectra for selected compounds (**41a**, **42a**, **43a**, and **44a**), and spectroscopic data for anthracene monomers in the form of absorption, excitation, and fluorescence spectra (PDF)

X-ray data for compound **31c** (CIF)

X-ray data for compound **31d** (CIF)

X-ray data for compound **33** (CIF)

X-ray data for compound **37a** (CIF)

X-ray data for compound **37b** (CIF)

X-ray data for compound **38** (CIF)

X-ray data for compound **39a** (CIF)

X-ray data for compound **40a** (CIF)

X-ray data for compound **41a** (CIF)

■ AUTHOR INFORMATION

Corresponding Author

*E-mail: holger.bettinger@uni-tuebingen.de.

ORCID

Andreas Schnepf: 0000-0002-7719-7476

Holger F. Bettinger: 0000-0001-5223-662X

Notes

The authors declare no competing financial interest.

■ ACKNOWLEDGMENTS

The authors thank the Deutsche Forschungsgemeinschaft (DFG) for supporting this work through the Priority Program SPP1807 “Control of London dispersion interactions in molecular chemistry” and grant no INST 40/467-1 FUGG. The authors gratefully acknowledge the help of Dr. Hartmut Schubert for performing the X-ray crystallographic analysis of compound **40a**. Special thanks go to the Karlsruhe Institute of Technology (KIT) for measuring time at the synchrotron radiation source ANKA and Dr. Gernot Buth for his support during the measurement. The authors acknowledge support by the state of Baden-Württemberg through bwHPC.

■ REFERENCES

(1) Fritzsche, J. Ueber die festen Kohlenwasserstoffe des Steinkohlentheers. *J. Prakt. Chem.* **1867**, *101*, 333−343.

(2) Hengstenberg, J.; Palacios, J. *Strukturber.* **1932**, *II*, 916.

(3) Ehrenberg, M. The crystal structure of di-para-anthracene. *Acta Crystallogr.* **1966**, *20*, 177−182.

(4) Choi, C. S.; Marinkas, P. L. Refinement of di-para-anthracene. *Acta Crystallogr., Sect. B: Struct. Crystallogr. Cryst. Chem.* **1980**, *36*, 2491−2493.

(5) Abboud, K. A.; Simonsen, S. H.; Roberts, R. M. Redetermination of the structure of bi(9,10-dihydro-9,10-anthracenediyl) at 198 K. *Acta Crystallogr., Sect. C: Cryst. Struct. Commun.* **1990**, *46*, 2494−2496.

DOI: 10.1021/acs.joc.9b01317
J. Org. Chem. 2019, 84, 10120−10135

(6) Bowen, E. J. Fluorescence quenching in solution and in the vapour state. *Trans. Faraday Soc.* **1954**, *50*, 97−102.
(7) Bowen, E. J.; Tanner, D. W. The photochemistry of anthracenes. Part 3.-Inter-relations between fluorescence quenching, dimerization, and photo-oxidation. *Trans. Faraday Soc.* **1955**, *51*, 475−481.
(8) Birks, J. B.; Aladekomo, J. B. The photo-dimerization and excimer fluorescence of 9-methyl anthracene. *Photochem. Photobiol.* **1963**, *2*, 415−418.
(9) Yang, N. C.; Shold, D. M.; Kim, B. Chemistry of exciplexes. 5. Photochemistry of anthracene in the presence and absence of dimethylaniline. *J. Am. Chem. Soc.* **1976**, *98*, 6587−6596.
(10) Bouas-Laurent, H.; Desvergne, J.-P.; Castellan, A.; Lapouyade, R. Photodimerization of anthracenes in fluid solutions: (part 2) mechanistic aspects of the photocycloaddition and of the photochemical and thermal cleavage. *Chem. Soc. Rev.* **2001**, *30*, 248−263.
(11) Musgrave, O. C. Oxidation of alkyl aryl ethers. *Chem. Rev.* **1969**, *69*, 499−531.
(12) Fudickar, W.; Linker, T. *Singlet Oxygen: Applications in Biosciences and Nanosciences*; The Royal Society of Chemistry, 2016; Vol. *1*, pp 431−446.
(13) Becker, H. D. Unimolecular photochemistry of anthracenes. *Chem. Rev.* **1993**, *93*, 145−172.
(14) Becker, H. D.; Langer, V. Photochemical dimerization modes of 9-methoxyanthracenes and 9-(2-hydroxy-2-propyl)anthracene. *J. Org. Chem.* **1993**, *58*, 4703−4708.
(15) Bouas-Laurent, H.; Desvergne, J.-P.; Castellan, A.; Lapouyade, R. Photodimerization of anthracenes in fluid solution: structural aspects. *Chem. Soc. Rev.* **2000**, *29*, 43−55.
(16) Lapouyade, R.; Desvergne, J.-P.; Bouas-Laurent, H. Réactivité photochimique de dérivés de l'anthracène substitués en péri: photodimérisation et photooxygénation. III. *Bull. Soc. Chim. Fr.* **1975**, *42*, 2137−2142.
(17) Bouas-Laurent, H.; Castellan, A.; Desvergne, J.-P. From anthracene photodimerization to jaw photochromic materials and photocrowns. *Pure Appl. Chem.* **1980**, *52*, 2633−2648.
(18) Guesten, H.; Mintas, M.; Klasinc, L. Deactivation of the fluorescent state of 9-tert-butylanthracene. 9-tert-Butyl-9,10(Dewar anthracene). *J. Am. Chem. Soc.* **1980**, *102*, 7936−7937.
(19) Dreeskamp, H.; Jahn, B.; Pabst, J. Thermoreversible Photo Valence Isomerization of 9-t-Butylanthracene to its 9,10-Dewar-Isomer. *Z. Naturforsch., A: Phys. Sci.* **1981**, *36*, 665−668.
(20) Lapouyade, R.; Bouas-Laurent, H. Synthèse et structure de dérivés anthracénique trisubstitués présentant un effet péri. *Bull. Soc. Chim. Fr.* **1967**, *34*, 1823−1827.
(21) Bouas-Laurent, H.; Lapouyade, R. Effet stérique et déplacement bathochrome du spectre d'absorption ultraviolette de dérivés anthracénique substitués en péri. *Bull. Soc. Chim. Fr.* **1969**, *36*, 4250−4258.
(22) Aikawa, H.; Takahira, Y.; Yamaguchi, M. Synthesis of 1,8-di(1-adamantyl)naphthalenes as single enantiomers stable at ambient temperatures. *Chem. Commun.* **2011**, *47*, 1479−1481.
(23) Wagner, J. P.; Schreiner, P. R. London Dispersion in Molecular Chemistry-Reconsidering Steric Effects. *Angew. Chem., Int. Ed.* **2015**, *54*, 12274−12296.
(24) Matta, C. F.; Hernández-Trujillo, J.; Tang, T.-H.; Bader, R. F. W. Hydrogen-Hydrogen Bonding: A Stabilizing Interaction in Molecules and Crystals. *Chem.—Eur. J.* **2003**, *9*, 1940−1951.
(25) Sharma, C.; Joy, J.; Nethaji, M.; Jemmis, E. D.; Awasthi, S. K. Synthetic, Crystallographic, and Computational Studies of Extensively Hydrogen Bonded Bilayers in Thermally Stable Adamantane Hydroperoxides. *Asian J. Org. Chem.* **2016**, *5*, 1398−1405.
(26) Strauss, M. A.; Wegner, H. A. Molecular Systems for the Quantification of London Dispersion Interactions. *Eur. J. Org. Chem.* **2019**, *2019*, 295−302.
(27) Bursch, M.; Caldeweyher, E.; Hansen, A.; Neugebauer, H.; Ehlert, S.; Grimme, S. Understanding and Quantifying London Dispersion Effects in Organometallic Complexes. *Acc. Chem. Res.* **2019**, *52*, 258−266.
(28) Pollice, R.; Bot, M.; Kobylianskii, I. J.; Shenderovich, I.; Chen, P. Attenuation of London Dispersion in Dichloromethane Solutions. *J. Am. Chem. Soc.* **2017**, *139*, 13126−13140.
(29) Helberg, J.; Marin-Luna, M.; Zipse, H. Chemoselectivity in Esterification Reactions—Size Matters after All. *Synthesis* **2017**, *49*, 3460−3470.
(30) Marin-Luna, M.; Patschinski, P.; Zipse, H. Substituent Effects in the Silylation of Secondary Alcohols: A Mechanistic Study. *Chem.—Eur. J.* **2018**, *24*, 15052−15058.
(31) Marin-Luna, M.; Pölloth, B.; Zott, F.; Zipse, H. Size-dependent rate acceleration in the silylation of secondary alcohols: the bigger the faster. *Chem. Sci.* **2018**, *9*, 6509−6515.
(32) Hopf, H.; Greiving, H.; Bouas-Laurent, H.; Desvergne, J.-P. 2,3-Di-n-undecylanthracene and 2,3-Di-n-decyloxyanthracene (DDOA)—on the Connecting Link between the Aromatic Substrate and the Aliphatic Chain in Self-Assembling Systems. *Eur. J. Org. Chem.* **2009**, *2009*, 1868−1870.
(33) Bailey, D.; Seifi, N.; Williams, V. E. Steric effects on [4+4]-photocycloaddition reactions between complementary anthracene derivatives. *Dyes Pigm.* **2011**, *89*, 313−318.
(34) Whitton, A. J.; Kumberger, O.; Müller, G.; Schmidbaur, H. Preparation and characterisation of 9,10-dihydroanthracene and tert-butyl-9,10-dihydroanthracene complexes with one or two tricarbonylchromium units; crystal structure of tricarbonyl (η1,2,3,4,4a,9a-9,10-dihydroanthracene)chromium. *Chem. Ber.* **1990**, *123*, 1931−1939.
(35) Akula, M. R. A convenient synthesis of 2,3-dibromoanthracene. *Org. Prep. Proced. Int.* **1990**, *22*, 102−104.
(36) Meerwein, H.; Borner, P.; Fuchs, O.; Sasse, H. J.; Schrodt, H.; Spille, J. Reaktionen mit Alkylkationen. *Chem. Ber.* **1956**, *89*, 2060−2079.
(37) Moss, R. J.; Rickborn, B. Improved synthesis of 1-ethoxy-1,3-dihydroisobenzofuran, a useful precursor to isobenzofuran. *J. Org. Chem.* **1982**, *47*, 5391−5393.
(38) Smith, J. G.; Dibble, P. W. 2-(Dimethoxymethyl)benzyl alcohol: a convenient isobenzofuran precursor. *J. Org. Chem.* **1983**, *48*, 5361−5362.
(39) Crump, S. L.; Rickborn, B. 1-Lithio- and 1,3-dilithioisobenzofuran: formation and reactions with electrophiles. *J. Org. Chem.* **1984**, *49*, 304−310.
(40) Crump, S. L.; Netka, J.; Rickborn, B. Preparation of isobenzofuran-aryne cycloadducts. *J. Org. Chem.* **1985**, *50*, 2746−2750.
(41) Naito, K.; Rickborn, B. Isobenzofuran: new approaches from 1,3-dihydro-1-methoxyisobenzofuran. *J. Org. Chem.* **1980**, *45*, 4061−4062.
(42) Warrener, R. N. Isolation of isobenzofuran, a stable but highly reactive molecule. *J. Am. Chem. Soc.* **1971**, *93*, 2346−2348.
(43) Miller, G. P.; Mack, J. Completely Regioselective, Highly Stereoselective Syntheses of cis-Bisfullerene[60] Adducts of 6,13-Disubstituted Pentacenes. *Org. Lett.* **2000**, *2*, 3979−3982.
(44) Lin, C.-T.; Chou, T.-C. Synthesis of 2,3-Dibromoanthracene. *Synthesis* **1988**, *1988*, 628−630.
(45) Bailey, D.; Williams, V. E. An efficient synthesis of substituted anthraquinones and naphthoquinones. *Tetrahedron Lett.* **2004**, *45*, 2511−2513.
(46) Bailey, D.; Williams, V. E. Wavelength-Dependent Selectivity in [4 + 4]-Cycloaddition Reactions. *J. Org. Chem.* **2006**, *71*, 5778−5780.
(47) Li, C.; Chen, T.; Li, B.; Xiao, G.; Tang, W. Efficient Synthesis of Sterically Hindered Arenes Bearing Acyclic Secondary Alkyl Groups by Suzuki-Miyaura Cross-Couplings. *Angew. Chem., Int. Ed.* **2015**, *54*, 3792−3796.
(48) Li, L.; Zhao, S.; Joshi-Pangu, A.; Diane, M.; Biscoe, M. R. Stereospecific Pd-Catalyzed Cross-Coupling Reactions of Secondary Alkylboron Nucleophiles and Aryl Chlorides. *J. Am. Chem. Soc.* **2014**, *136*, 14027−14030.
(49) Navarro, O.; Kaur, H.; Mahjoor, P.; Nolan, S. P. Cross-Coupling and Dehalogenation Reactions Catalyzed by (N-Heterocyclic carbene)Pd(allyl)Cl Complexes. *J. Org. Chem.* **2004**, *69*, 3173−3180.

DOI: 10.1021/acs.joc.9b01317
J. Org. Chem. 2019, 84, 10120−10135

(50) Allen, C. F. H.; Bell, A. 2,3-Dimethylanthraquinone. *Org. Synth.* **1942**, *22*, 37.
(51) Hinshaw, J. C. A Convenient Synthesis of 2, 3, 6, 7-Tetramethylanthracene. *Org. Prep. Proced. Int.* **1972**, *4*, 211−213.
(52) Gaylord, N. G.; Štěpán, V. Reduction of methylated anthraquinones to methylated anthracenes with aluminium tri-(cyclohexyl oxide). *Collect. Czech. Chem. Commun.* **1974**, *39*, 1700−1710.
(53) Bender, D.; Müllen, K. Novel Alkylanthracenes Synthesis, Reductive Alkylation, and Reductive Polymerization. *Chem. Ber.* **1988**, *121*, 1187−1197.
(54) Pozzo, J.-L.; Clavier, G. M.; Colomes, M.; Bouas-Laurent, H. Different synthetic routes towards efficient organogelators: 2,3-substituted anthracenes. *Tetrahedron* **1997**, *53*, 6377−6390.
(55) Bahl, J. J.; Bates, R. B.; Gordon, B. 2,3-Dimethylenebutadiene dianion; convenient procedure for allylic metalation of conjugated dienes. *J. Org. Chem.* **1979**, *44*, 2290−2291.
(56) Bates, R. B.; Gordon, B.; Highsmith, T. K.; White, J. J. Reactions of 2,3-dimethylenebutadiene dianion with electrophiles. Synthesis and conformations of 2,3-disubstituted-1,3-butadienes. *J. Org. Chem.* **1984**, *49*, 2981−2987.
(57) Hudiono, Y. C.; Miller, A. L.; Gibson, P. W.; LaFrate, A. L.; Noble, R. D.; Gin, D. L. A Highly Breathable Organic/Inorganic Barrier Material that Blocks the Passage of Mustard Agent Simulants. *Ind. Eng. Chem. Res.* **2012**, *51*, 7453−7456.
(58) Araki, S.; Ohmura, M.; Butsugan, Y. A Facile Synthesis of 2,3-Dialkyl-1,3-butadienes. *Synthesis* **1985**, *1985*, 963−964.
(59) Kleijn, H.; Westmijze, H.; Meijer, J.; Vermeer, P. A convenient synthesis of specifically substituted conjugated dienes via organocopper(I) induced SN2′ reactions. An attractive route to myrcene. *Recl. Trav. Chim. Pays-Bas* **1980**, *99*, 340−343.
(60) Durola, F.; Rebek, J. The Ouroborand: A Cavitand with a Coordination-Driven Switching Device. *Angew. Chem., Int. Ed.* **2010**, *49*, 3189−3191.
(61) Shahane, S.; Toupet, L.; Fischmeister, C.; Bruneau, C. Synthesis and Characterization of Sterically Enlarged Hoveyda-Type Olefin Metathesis Catalysts. *Eur. J. Inorg. Chem.* **2013**, *2013*, 54−60.
(62) Sämann, C.; Dhayalan, V.; Schreiner, P. R.; Knochel, P. Synthesis of Substituted Adamantylzinc Reagents Using a Mg-Insertion in the Presence of ZnCl2 and Further Functionalizations. *Org. Lett.* **2014**, *16*, 2418−2421.
(63) Fringuelli, F.; Girotti, R.; Pizzo, F.; Vaccaro, L. [AlCl3+ 2THF]: A New and Efficient Catalytic System for Diels−Alder Cycloaddition of α,β-Unsaturated Carbonyl Compounds under Solvent-Free Conditions. *Org. Lett.* **2006**, *8*, 2487−2489.
(64) Chauzov, V. A.; Parchinskii, V. Z. Synthesis of 9-Oxa-1,2,3,4b, 5,6,7,8,8a,9,10,10a-dodecahydrophenanthrenes. *Russ. J. Gen. Chem.* **1997**, *67*, 159.
(65) Iranpoor, N.; Kazemi, F. RuCl3 catalyses aldol condensations of aldehydes and ketones. *Tetrahedron* **1998**, *54*, 9475−9480.
(66) Deng, G.; Ren, T. Indium Trichloride Catalyzes Aldol-Condensations of Aldehydes and Ketones. *Synth. Commun.* **2003**, *33*, 2995−3001.
(67) Chiang, J. F.; Bauer, S. H. Molecular structure of cyclohexene. *J. Am. Chem. Soc.* **1969**, *91*, 1898−1901.
(68) Ma, J. C.; Dougherty, D. A. The Cation−π Interaction. *Chem. Rev.* **1997**, *97*, 1303−1324.
(69) Dougherty, D. A. The Cation−π Interaction. *Acc. Chem. Res.* **2013**, *46*, 885−893.
(70) Mirchi, A.; Sizochenko, N.; Dinadayalane, T.; Leszczynski, J. Binding of Alkali Metal Ions with 1,3,5-Tri(phenyl)benzene and 1,3,5-Tri(naphthyl)benzene: The Effect of Phenyl and Naphthyl Ring Substitution on Cation−π Interactions Revealed by DFT Study. *J. Phys. Chem. A* **2017**, *121*, 8927−8938.
(71) Eisenschitz, R.; London, F. Über das Verhältnis der van der Waalsschen Kräfte zu den homöopolaren Bindungskräften. *Z. Phys.* **1930**, *60*, 491−527.
(72) London, F. Zur Theorie und Systematik der Molekularkräfte. *Z. Phys.* **1930**, *63*, 245−279.
(73) London, F. Über einige Eigenschaften und Anwendungen der Molekularkräfte. *Z. Phys. Chem.* **1930**, *B11*, 222−251.
(74) Grimme, S.; Peyerimhoff, S. D.; Bouas-Laurent, H.; Desvergne, J.-P.; Becker, H.-D.; Sarge, S. M.; Dreeskamp, H. Calorimetric and quantum chemical studies of some photodimers of anthracenes. *Phys. Chem. Chem. Phys.* **1999**, *1*, 2457−2462.
(75) Seip, R.; Schultz, G.; Hargittai, I.; Szabó, Z. G. Electron Diffraction Study of the Toluene Molecular Geometry. *Z. Naturforsch., A: Phys. Sci.* **1977**, *32*, 1178.
(76) Sakai, T. Crystal and molecular structure of 1,3,5-tri-tert-butylbenzene. *Acta Crystallogr., Sect. B: Struct. Crystallogr. Cryst. Chem.* **1978**, *34*, 3649−3653.
(77) Taft, R. W. *Steric Effects in Organic Chemistry*, Newman, M. S., Ed.; John Wiley & Sons: London, 1956.
(78) Hancock, C. K.; Meyers, E. A.; Yager, B. J. Quantitative Separation of Hyperconjugation Effects from Steric Substituent Constants. *J. Am. Chem. Soc.* **1961**, *83*, 4211−4213.
(79) Unger, S. H.; Hansch, C. *Progress in Physical Organic Chemistry*; Taft, R. W., Ed.; John Wiley & Sons, Ltd, 1976; Vol. *12*, pp 91−118.
(80) MacPhee, J. A.; Panaye, A.; Dubois, J.-E. Steric effects—I: A critical examination of the taft steric parameter—Es. Definition of a revised, broader and homogeneous scale. Extension to highly congested alkyl groups. *Tetrahedron* **1978**, *34*, 3553−3562.
(81) Charton, M. Steric effects. I. Esterification and acid-catalyzed hydrolysis of esters. *J. Am. Chem. Soc.* **1975**, *97*, 1552−1556.
(82) Pinter, B.; Fievez, T.; Bickelhaupt, F. M.; Geerlings, P.; De Proft, F. On the origin of the steric effect. *Phys. Chem. Chem. Phys.* **2012**, *14*, 9846−9854.
(83) Frisch, M. J.; Trucks, G. W.; Schlegel, H. B.; Scuseria, G. E.; Robb, M. A.; Cheeseman, J. R.; Scalmani, G.; Barone, V.; Mennucci, B.; Petersson, G. A.; Nakatsuji, H.; Caricato, M.; Li, X.; Hratchian, H. P.; Izmaylov, A. F.; Bloino, J.; Zheng, G.; Sonnenberg, J. L.; Hada, M.; Ehara, M.; Toyota, K.; Fukuda, R.; Hasegawa, J.; Ishida, M.; Nakajima, T.; Honda, Y.; Kitao, O.; Nakai, H.; Vreven, T.; Montgomery, J. A., Jr.; Peralta, J. E.; Ogliaro, F.; Bearpark, M.; Heyd, J. J.; Brothers, E.; Kudin, K. N.; Staroverov, V. N.; Kobayashi, R.; Normand, J.; Raghavachari, K.; Rendell, A.; Burant, J. C.; Iyengar, S. S.; Tomasi, J.; Cossi, M.; Rega, N.; Millam, J. M.; Klene, M.; Knox, J. E.; Cross, J. B.; Bakken, V.; Adamo, C.; Jaramillo, J.; Gomperts, R.; Stratmann, R. E.; Yazyev, O.; Austin, A. J.; Cammi, R.; Pomelli, C.; Ochterski, J. W.; Martin, R. L.; Morokuma, K.; Zakrzewski, V. G.; Voth, G. A.; Salvador, P.; Dannenberg, J. J.; Dapprich, S.; Daniels, A. D.; Farkas, Ö.; Foresman, J. B.; Ortiz, J. V.; Cioslowski, J.; Fox, D. J. *Gaussian 09*, 2015.
(84) Grimme, S.; Antony, J.; Ehrlich, S.; Krieg, H. A consistent and accurate ab initio parametrization of density functional dispersion correction (DFT-D) for the 94 elements H-Pu. *J. Chem. Phys.* **2010**, *132*, 154104.
(85) Chai, J.-D.; Head-Gordon, M. Long-range corrected hybrid density functionals with damped atom-atom dispersion corrections. *Phys. Chem. Chem. Phys.* **2008**, *10*, 6615−6620.

DOI: 10.1021/acs.joc.9b01317
J. Org. Chem. 2019, 84, 10120−10135

Synthesis and photodimerization of 2- and 2,3-disubstituted anthracenes: influence of steric interaction and London dispersion on diastereoselectivity

Thomas Geiger,[a] Anne Haupt,[a] Cäcilia Maichle-Mössmer,[b] Claudio Schrenk,[b] Andreas Schnepf,[b] Holger F. Bettinger*[a]

[a] Institut für Organische Chemie, Eberhard-Karls-Universität Tübingen, Auf der Morgenstelle 18, 72076 Tübingen, Germany; Email: holger.bettinger@uni-tuebingen.de

[b] Institut für Anorganische Chemie, Eberhard-Karls-Universität Tübingen, Auf der Morgenstelle 18, 72076 Tübingen, Germany

Contents:

1. ^{1}H and ^{13}C{^{1}H} spectra S2
2. UV/Vis and fluorescence data for newly prepared anthracene derivatives S53
3. Crystal structure data S58
4. Selected bond lengths and angles for compound 33 S67
5. Cartesian coordinates S68
6. References S92

1. ^{1}H and $^{13}C\{^{1}H\}$ spectra

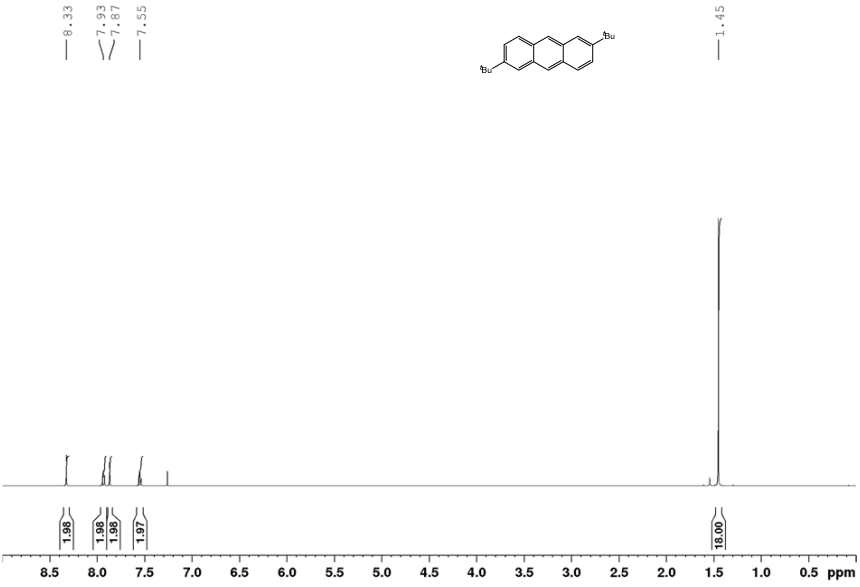

Figure S1. ^{1}H-NMR spectrum of **11** in $CDCl_3$

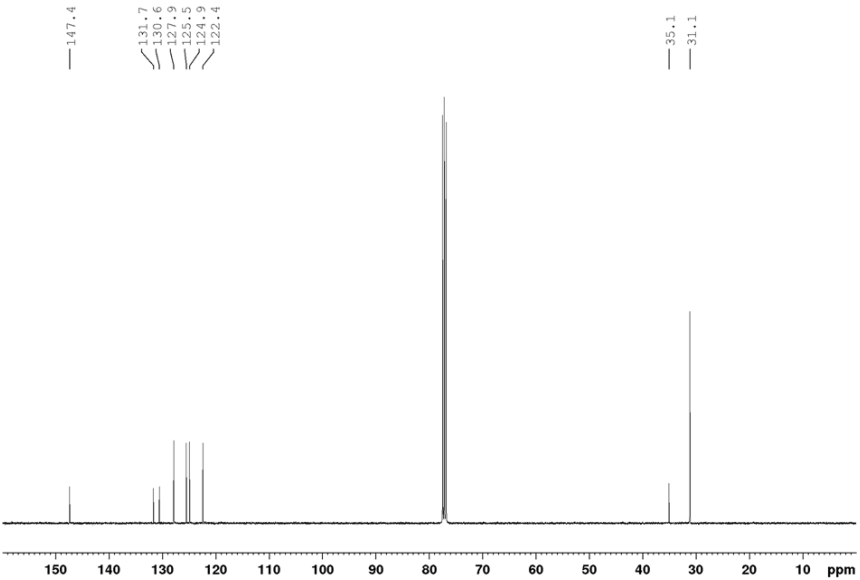

Figure S2. $^{13}C\{^{1}H\}$-NMR spectrum of **11** in $CDCl_3$

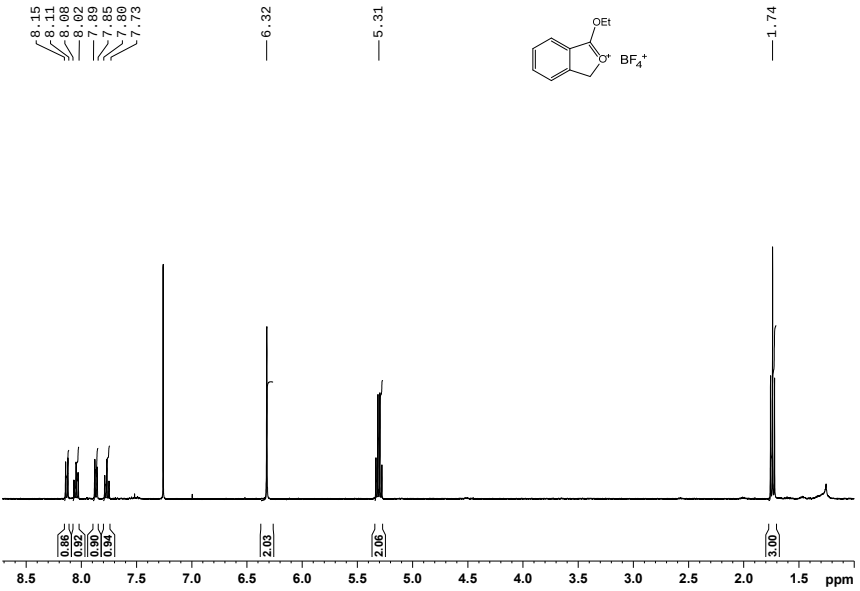

Figure S3. ^{1}H-NMR spectrum of **13** in $CDCl_3$

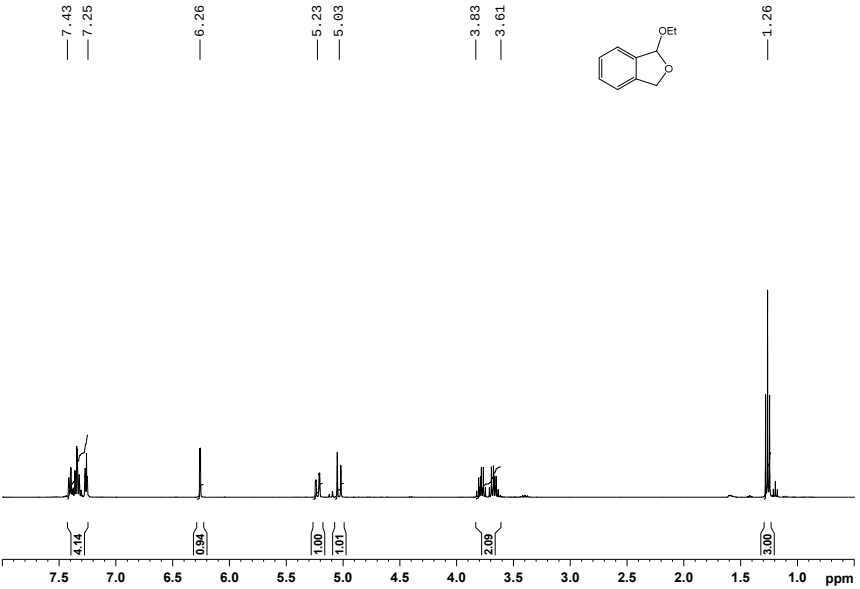

Figure S4. ^{1}H-NMR spectrum of **14** in $CDCl_3$

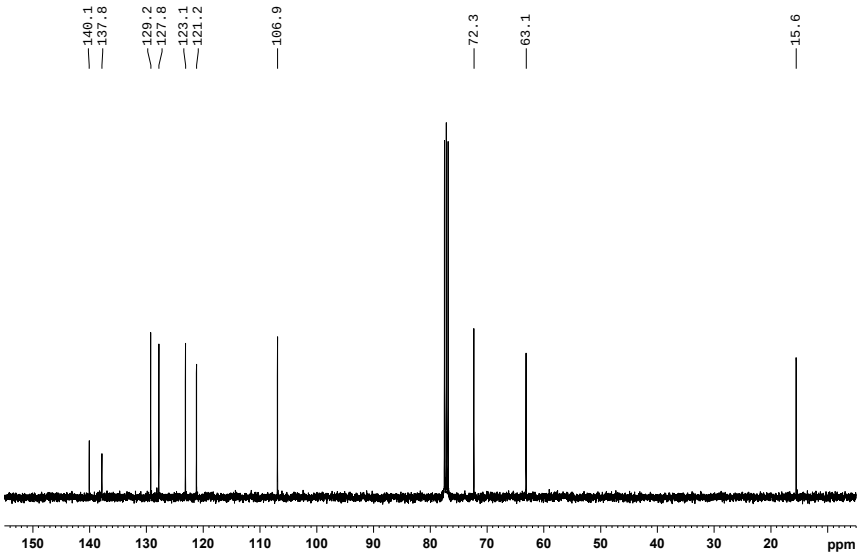

Figure S5. $^{13}C\{^{1}H\}$-NMR spectrum of **14** in $CDCl_3$

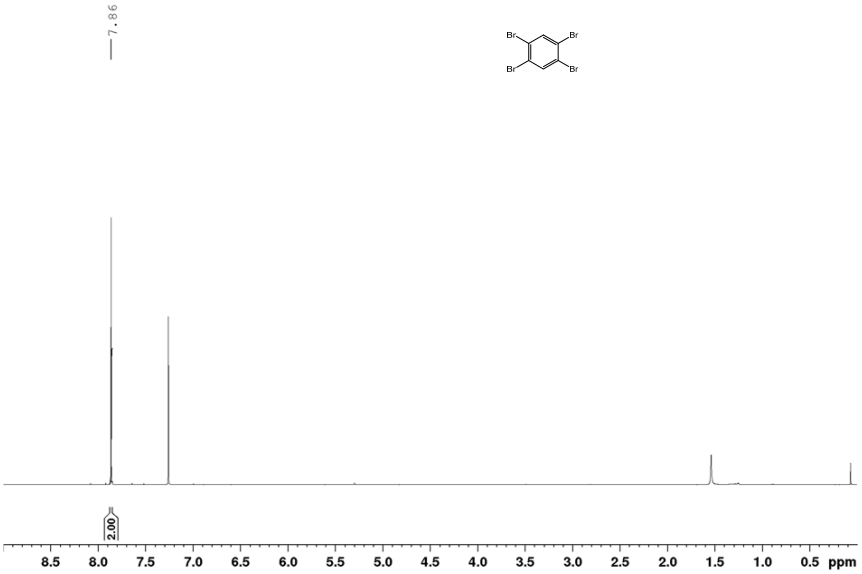

Figure S6. ^{1}H-NMR spectrum of **16** in $CDCl_3$

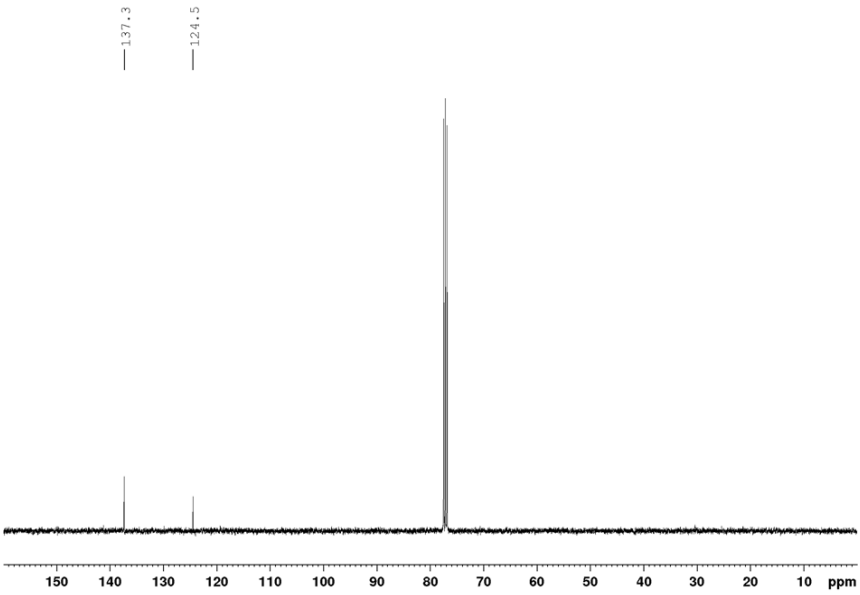

Figure S7. $^{13}C\{^{1}H\}$-NMR spectrum of **16** in $CDCl_3$

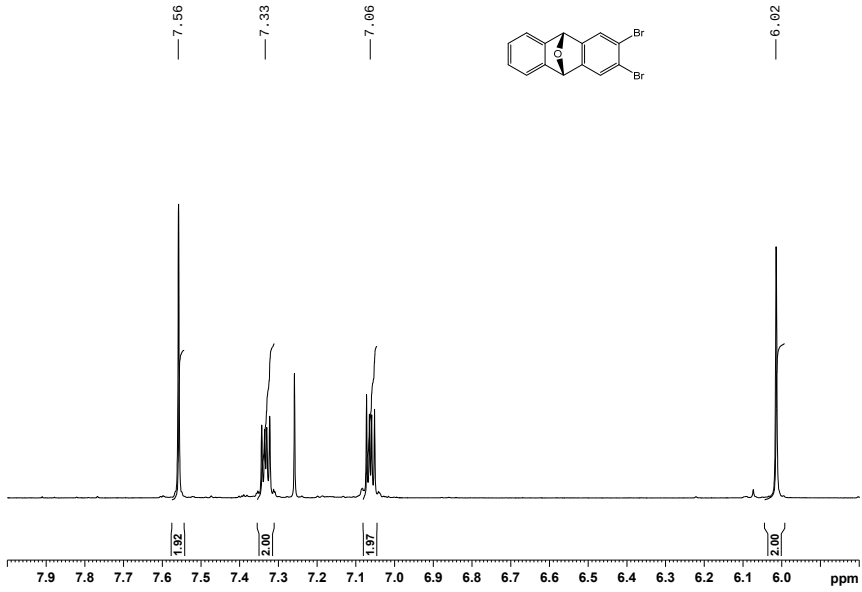

Figure S8. 1H-NMR spectrum of **17** in $CDCl_3$

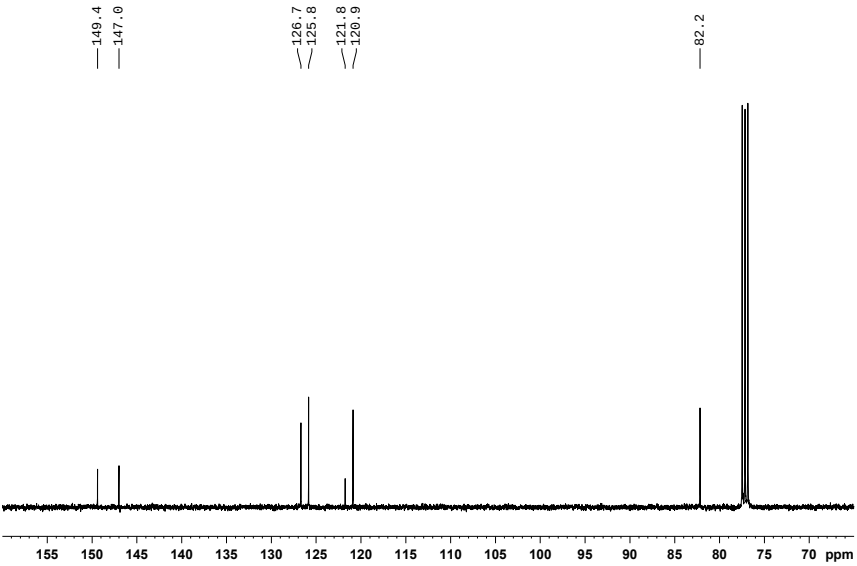

Figure S9. $^{13}C\{^{1}H\}$-NMR spectrum of **17** in $CDCl_3$

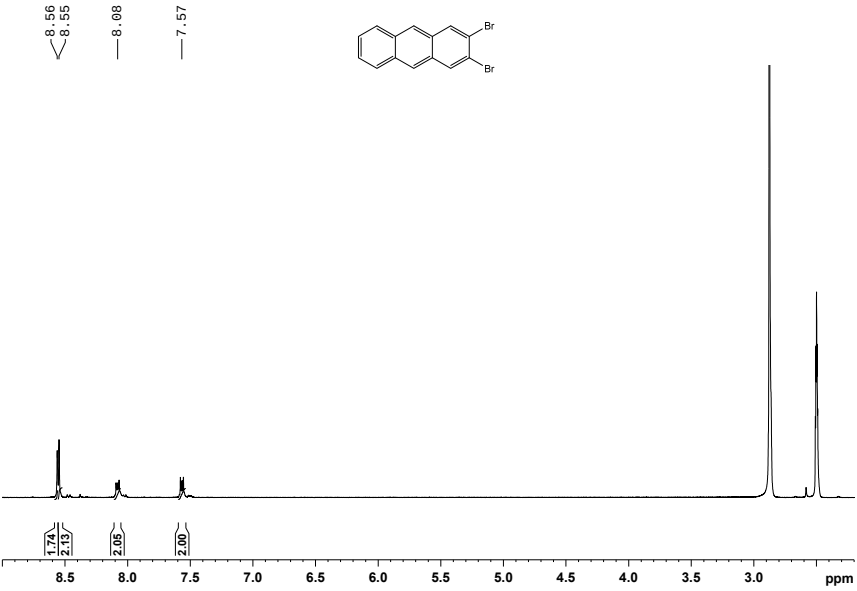

Figure S10. ^{1}H-NMR spectrum of **18** at 120 °C in DMSO-d_6

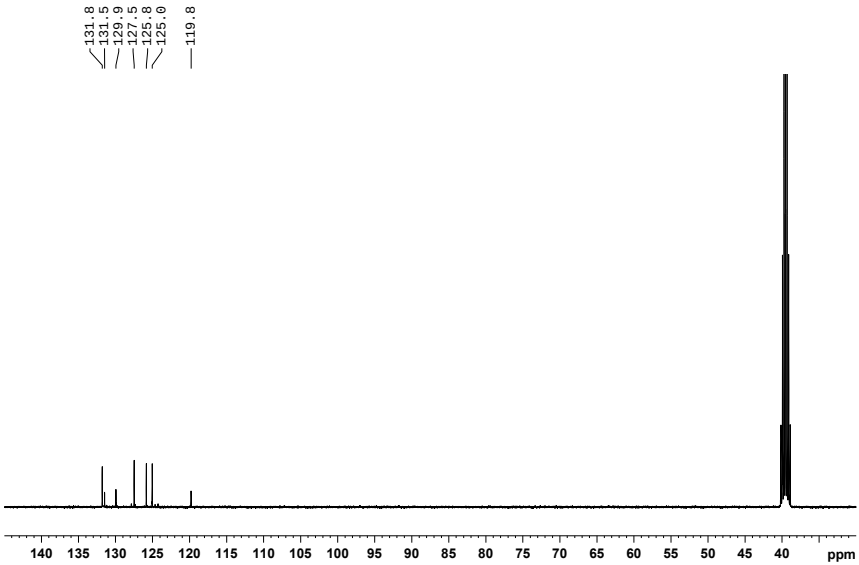

Figure S11. $^{13}C\{^{1}H\}$-NMR spectrum of **18** at 120 °C in DMSO-d_6

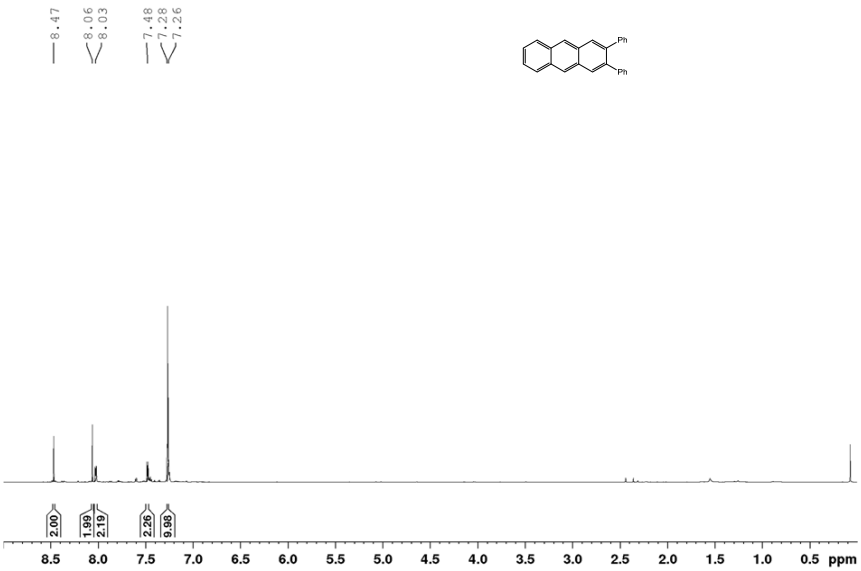

Figure S12. ^{1}H-NMR spectrum of **19** in $CDCl_3$

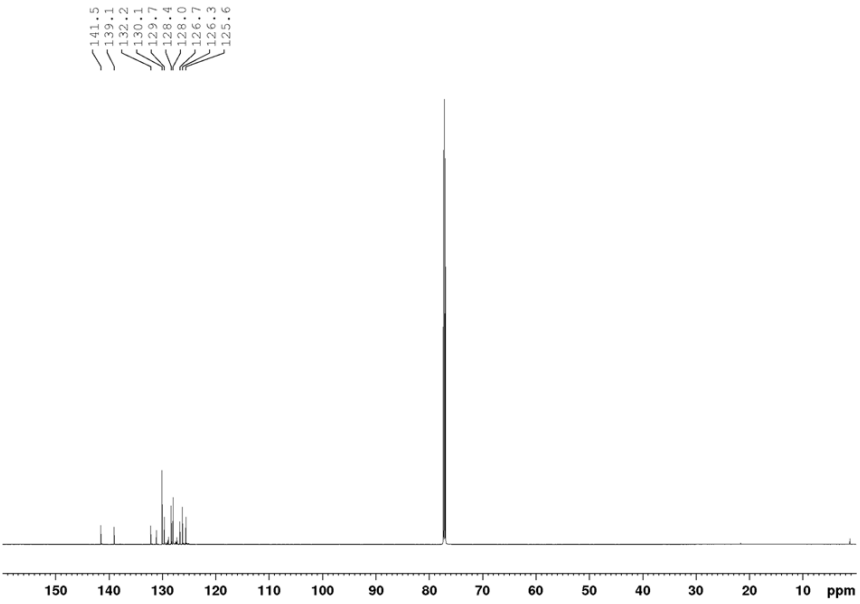

Figure S13. $^{13}C\{^{1}H\}$-NMR spectrum of **19** in $CDCl_3$

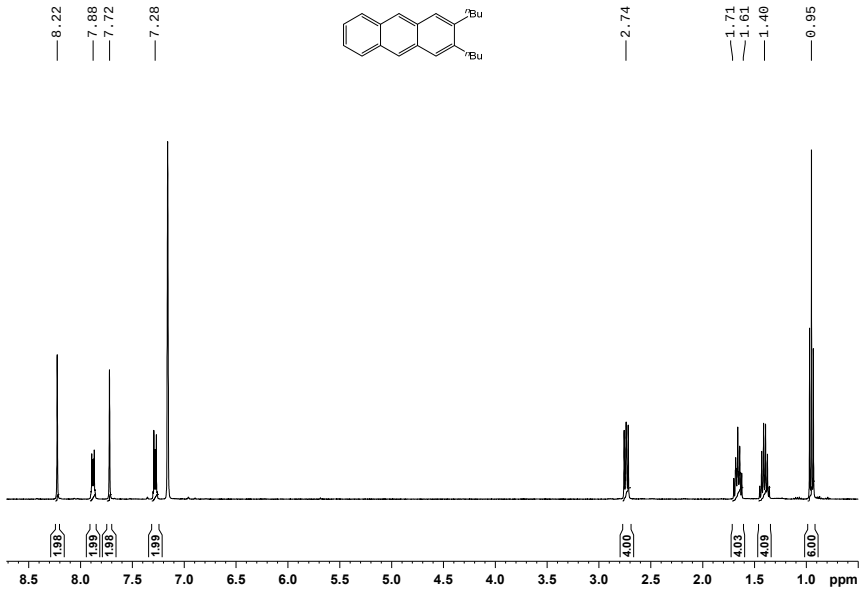

Figure S14. ^{1}H-NMR spectrum of **20** in C_6D_6

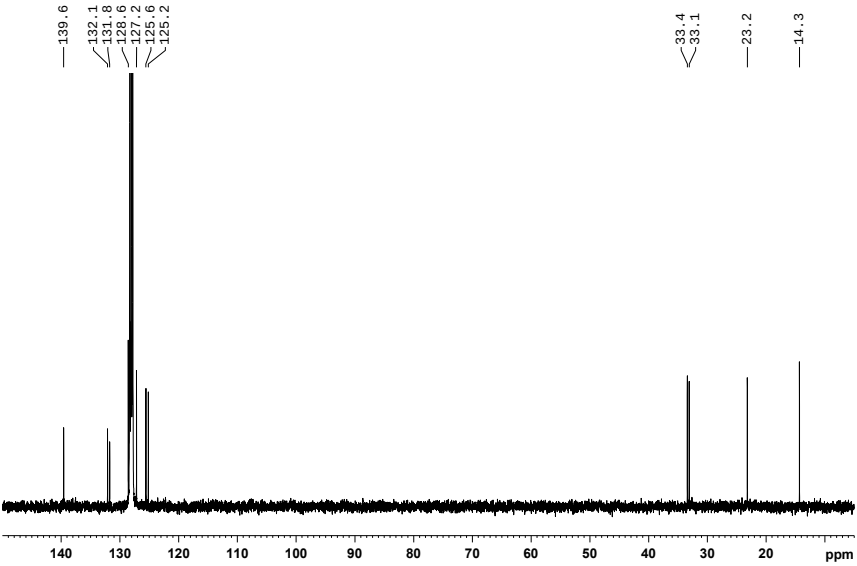

Figure S15. $^{13}C\{^{1}H\}$-NMR spectrum of **20** in C_6D_6

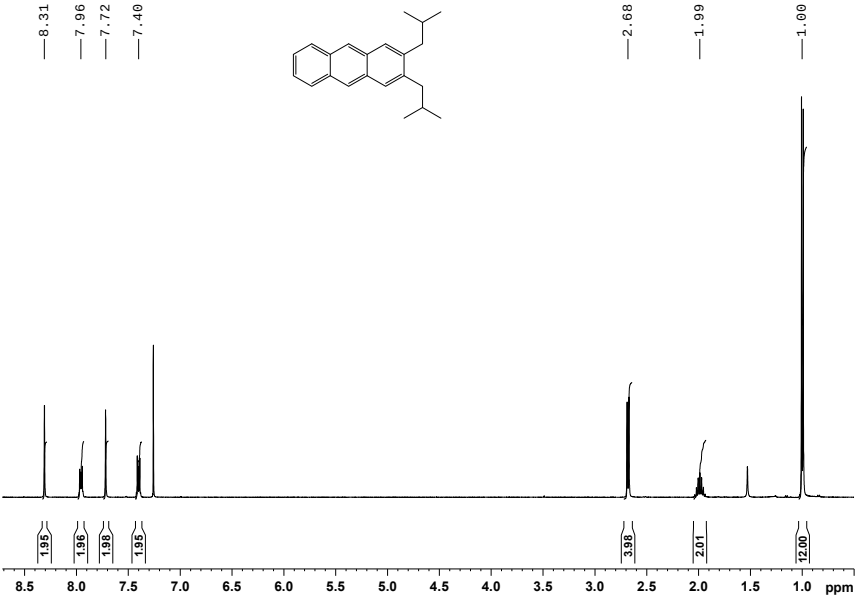

Figure S16. ^{1}H-NMR spectrum of **21** in $CDCl_3$

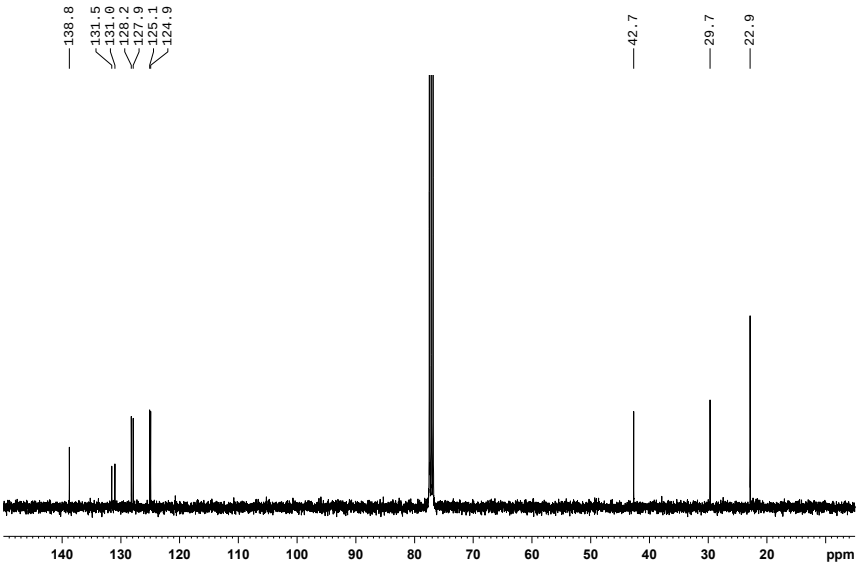

Figure S17. $^{13}C\{^{1}H\}$-NMR spectrum of **21** in $CDCl_3$

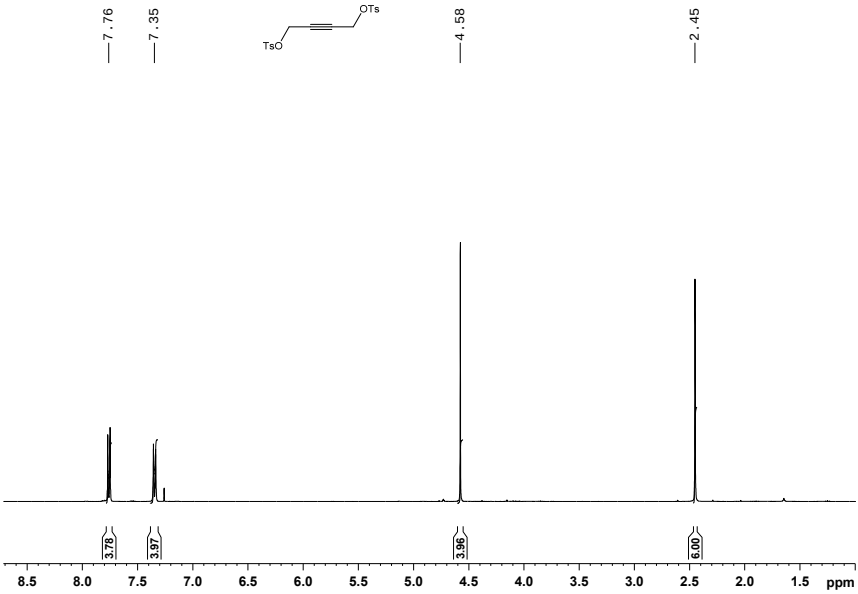

Figure S18. ^{1}H-NMR spectrum of **25** in $CDCl_3$

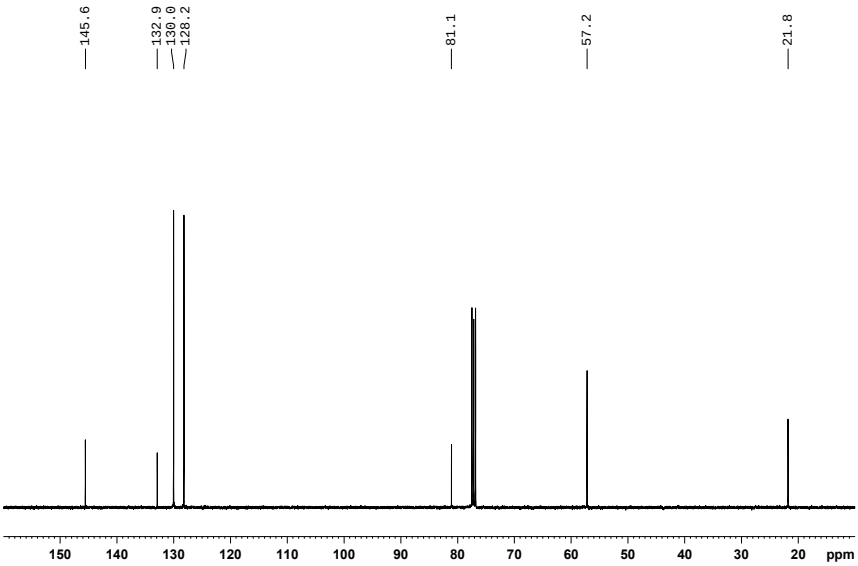

Figure S19. $^{13}C\{^{1}H\}$-NMR spectrum of **25** in $CDCl_3$

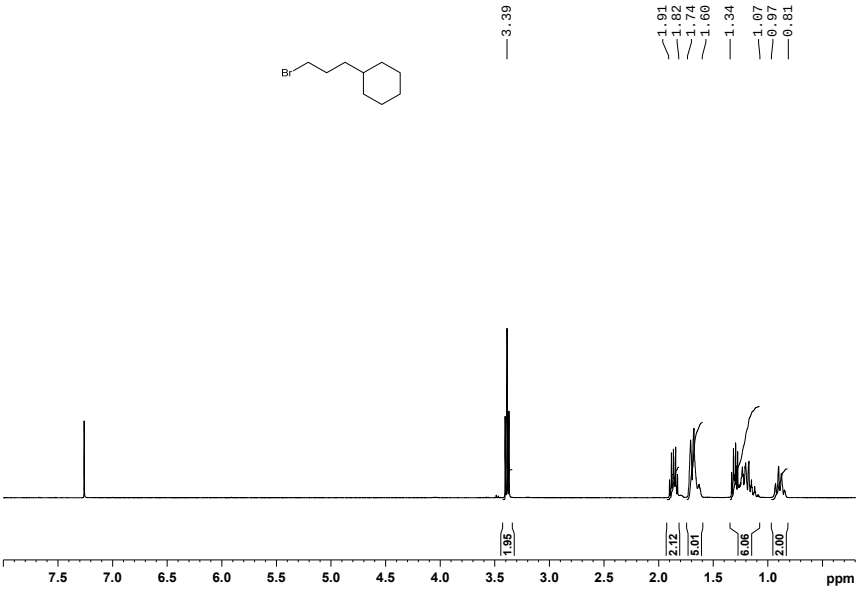

Figure S20. ^{1}H-NMR spectrum of **26** in $CDCl_3$

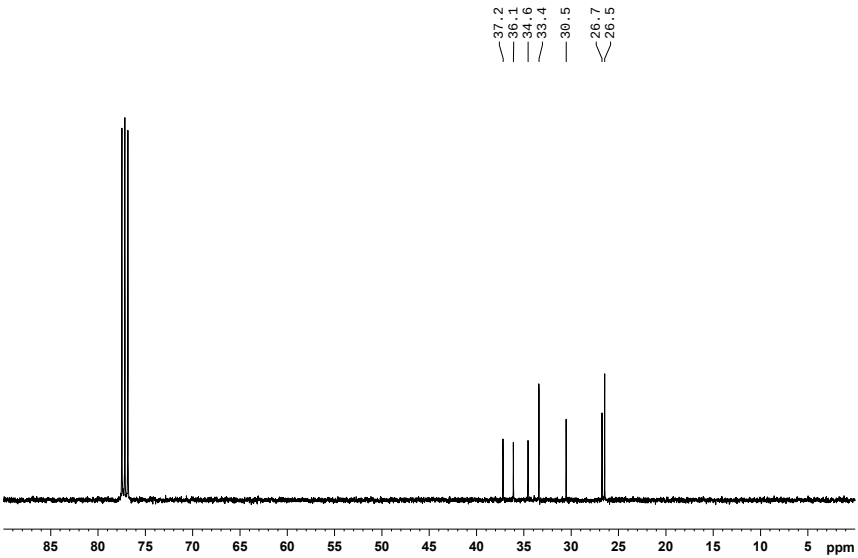

Figure S21. $^{13}C\{^{1}H\}$-NMR spectrum of **26** in $CDCl_3$

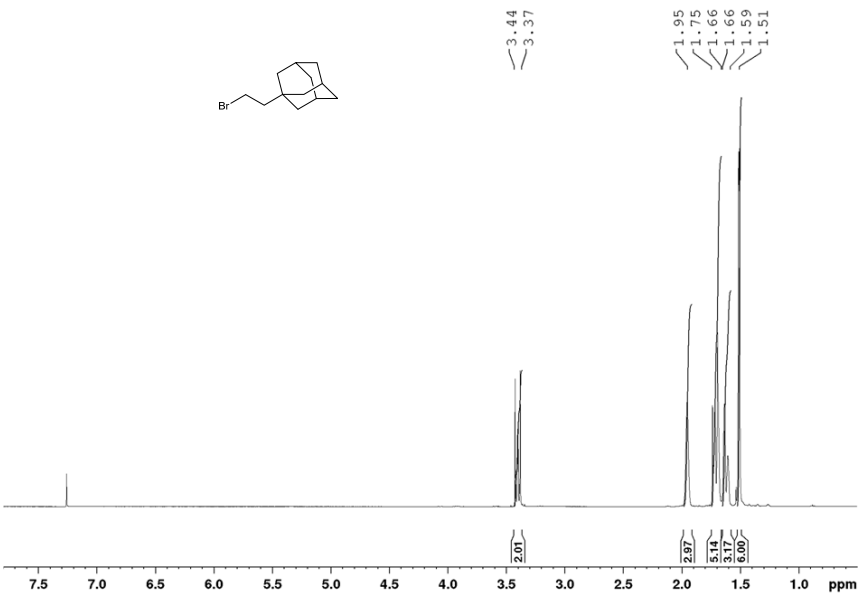

Figure S22. ^{1}H-NMR spectrum of **27** in $CDCl_3$

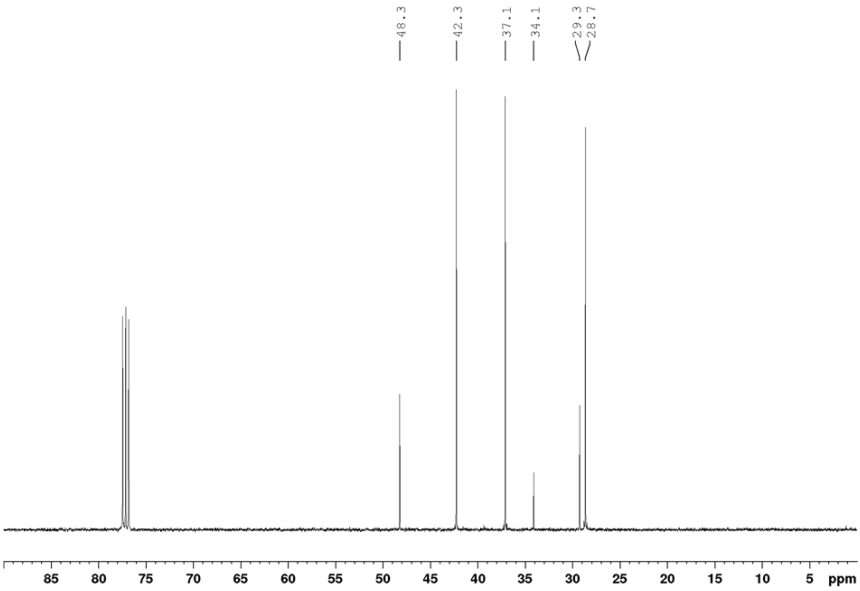

Figure S23. $^{13}C\{^{1}H\}$-NMR spectrum of **27** in $CDCl_3$

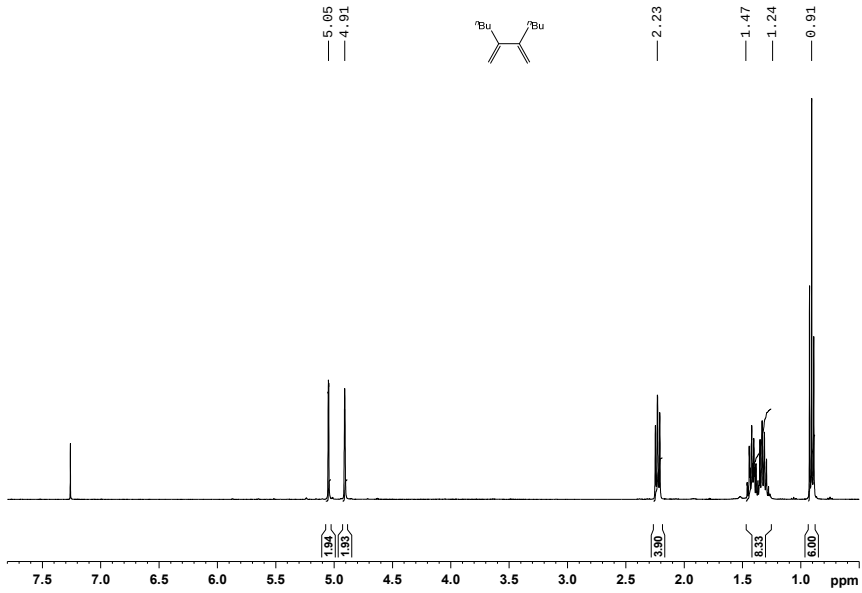

Figure S24. ^{1}H-NMR spectrum of **28a** in $CDCl_3$

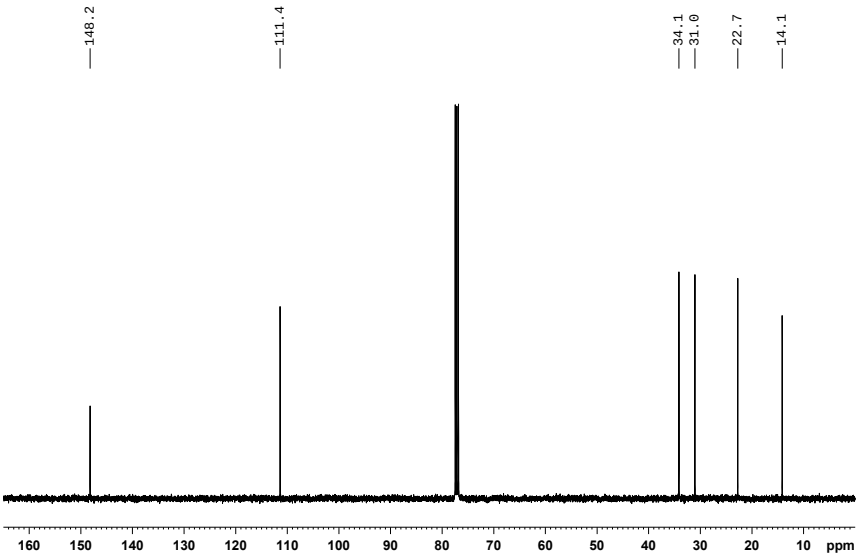

Figure S25. $^{13}C\{^{1}H\}$-NMR spectrum of **28a** in $CDCl_3$

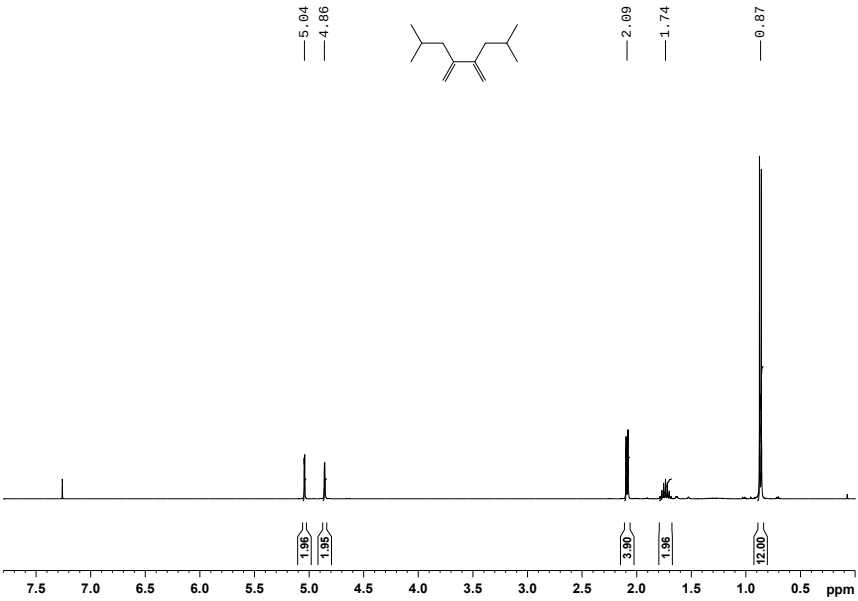

Figure S26. ^{1}H-NMR spectrum of **28b** in $CDCl_3$

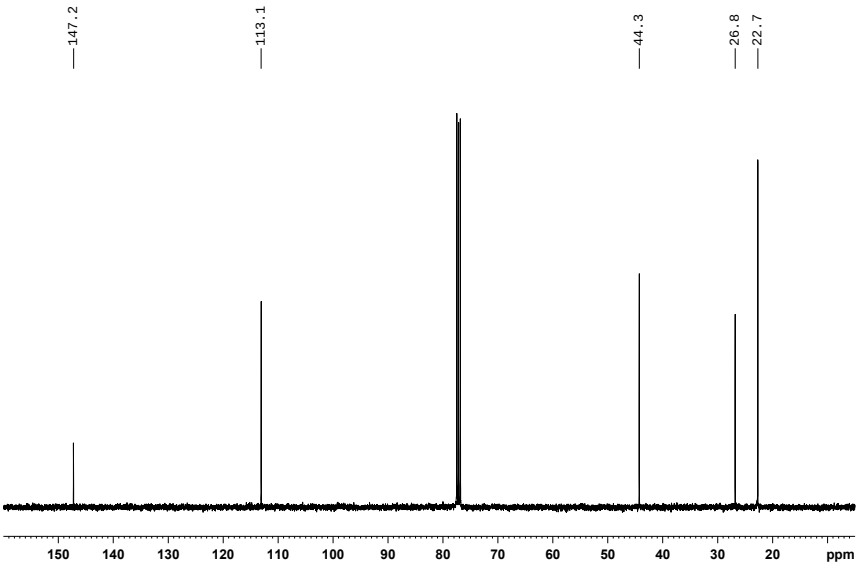

Figure S27. $^{13}C\{^{1}H\}$-NMR spectrum of **28b** in $CDCl_3$

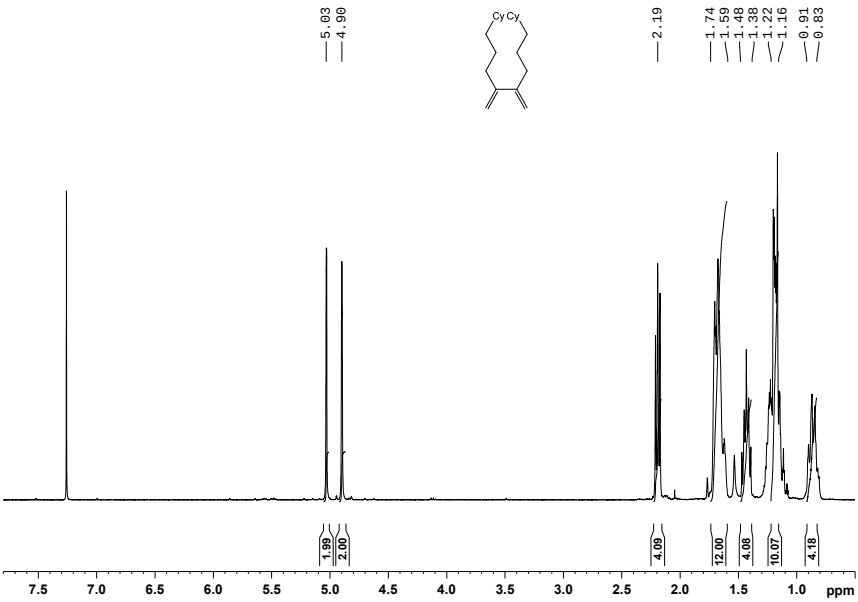

Figure S28. ^{1}H-NMR spectrum of **28c** in $CDCl_3$

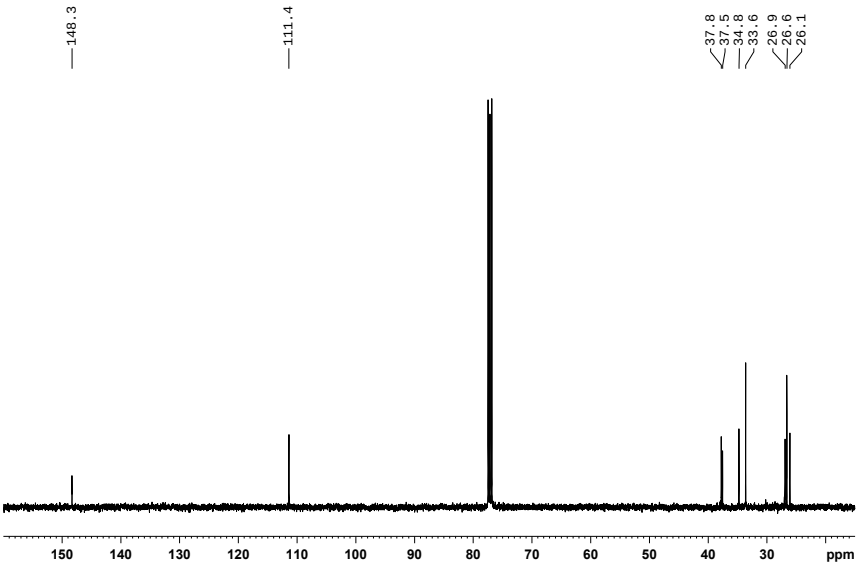

Figure S29. $^{13}C\{^{1}H\}$-NMR spectrum of **28c** in $CDCl_3$

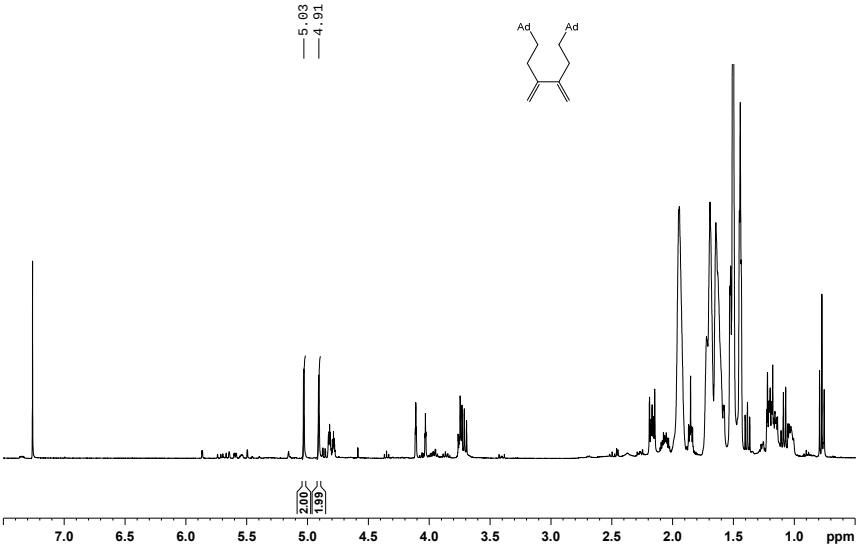

Figure S30. ^{1}H-NMR spectrum of **28d** in $CDCl_3$

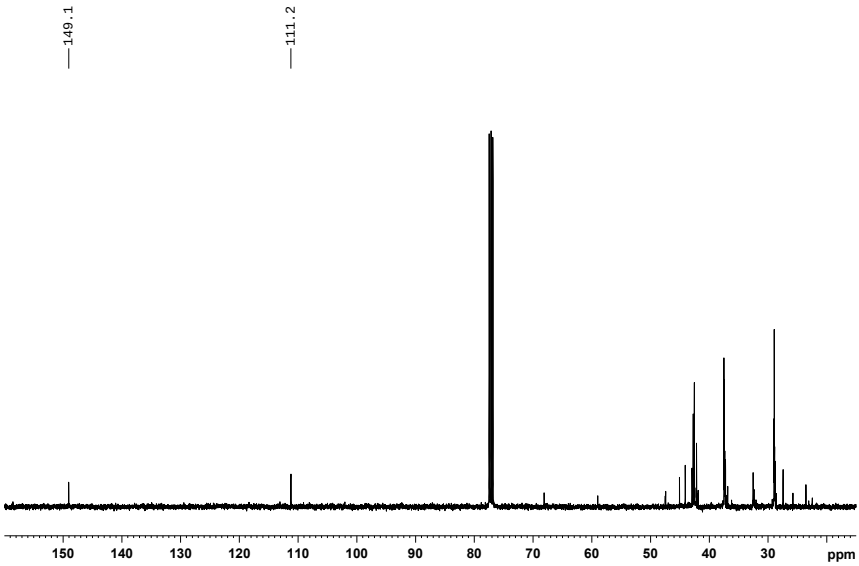

Figure S31. $^{13}C\{^{1}H\}$-NMR spectrum of **28d** in $CDCl_3$

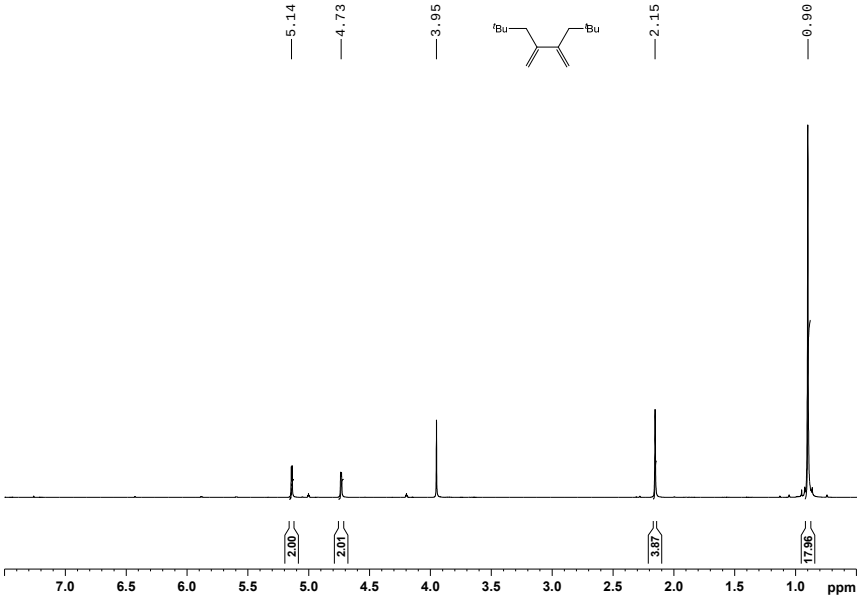

Figure S32. ^{1}H-NMR spectrum of **28e** in $CDCl_3$

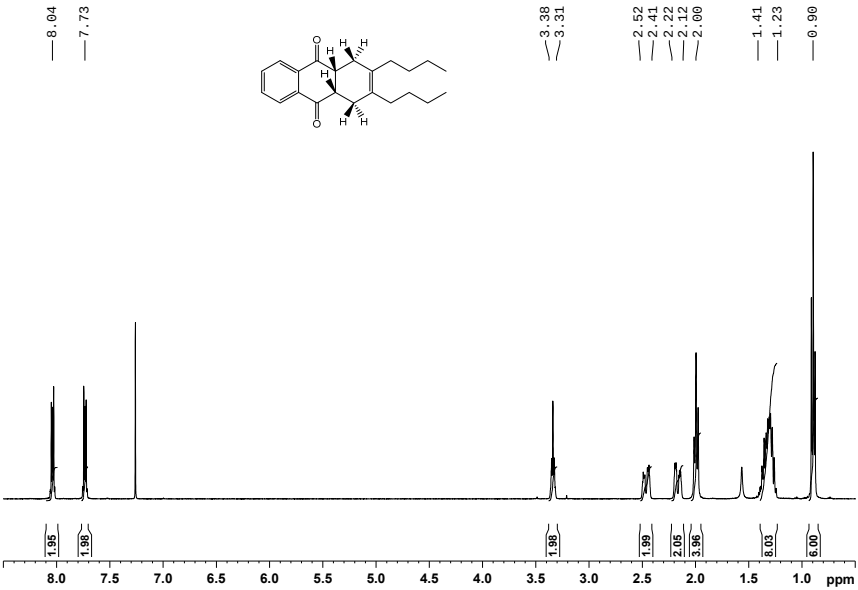

Figure S33. ^{1}H-NMR spectrum of **30a** in $CDCl_3$

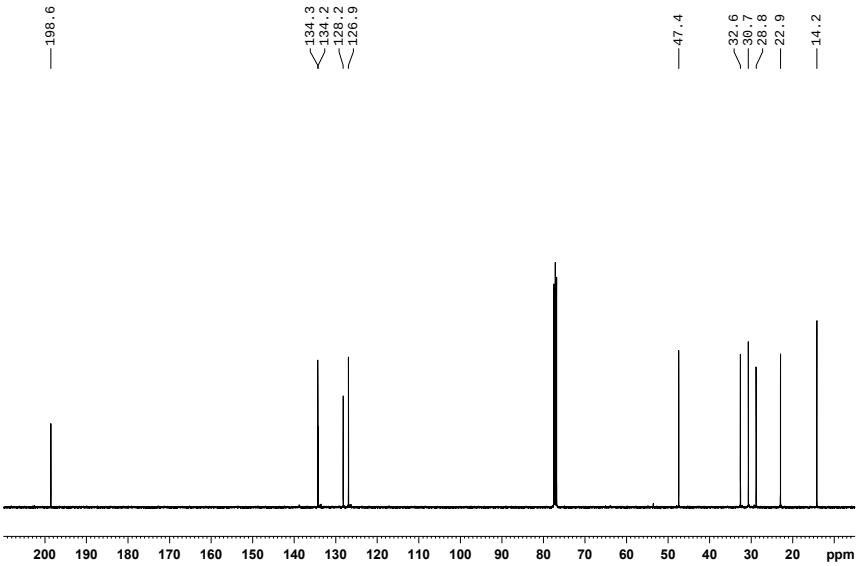

Figure S34. ^{13}C{^{1}H}-NMR spectrum of **30a** in $CDCl_3$

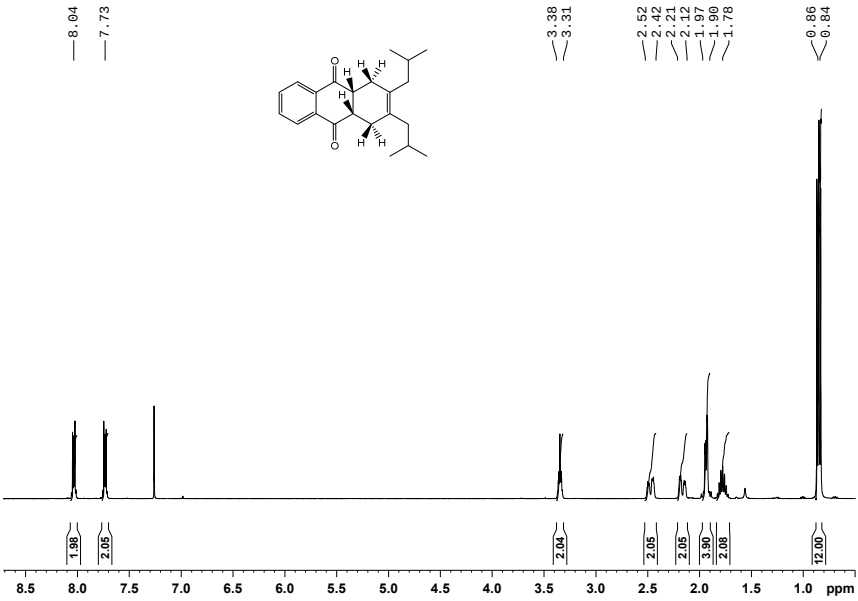

Figure S35. ^{1}H-NMR spectrum of **30b** in $CDCl_3$

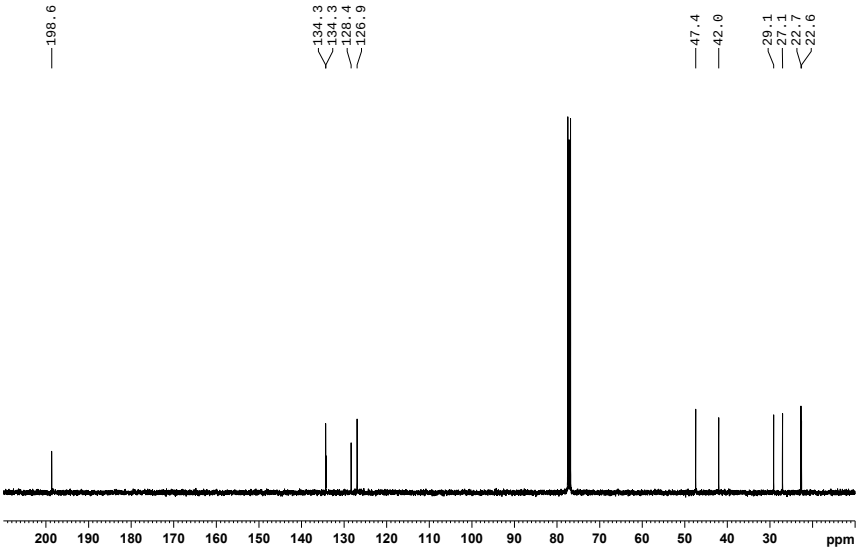

Figure S36. $^{13}C\{^{1}H\}$-NMR spectrum of **30b** in $CDCl_3$

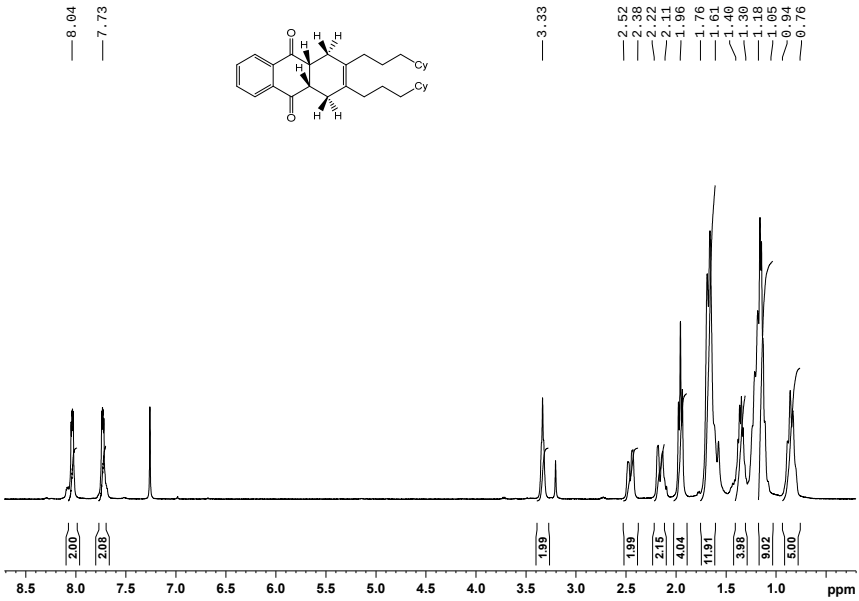

Figure S37. ^{1}H-NMR spectrum of **30c** in $CDCl_3$

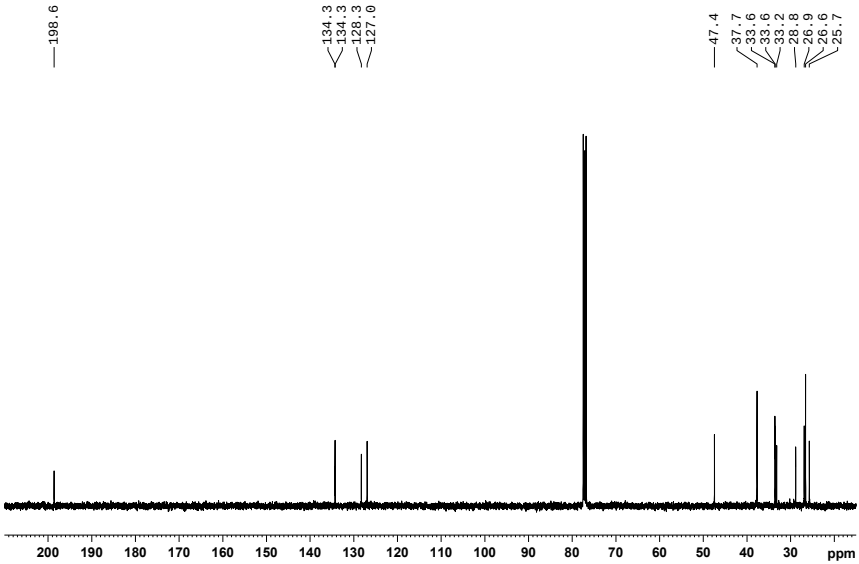

Figure S38. $^{13}C\{^{1}H\}$-NMR spectrum of **30c** in $CDCl_3$

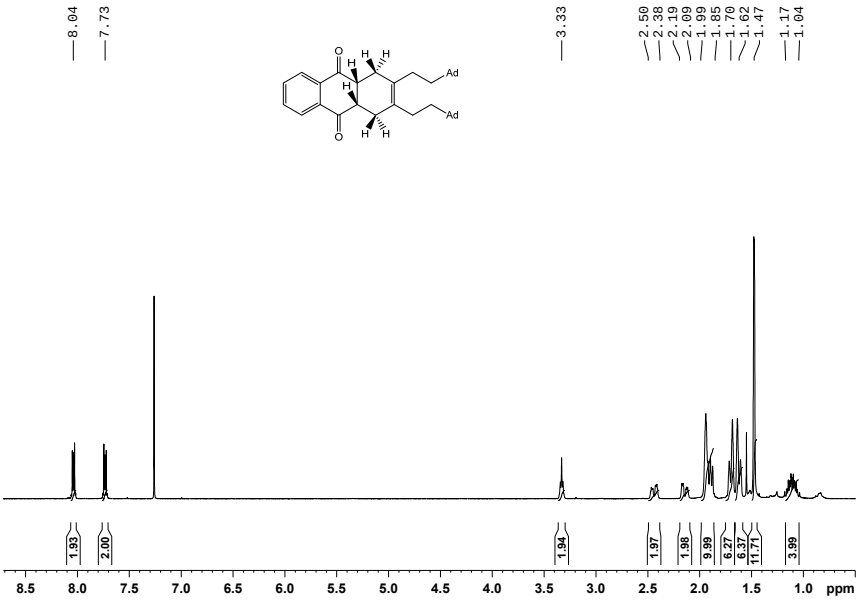

Figure S39. ^{1}H-spectrum of **30d** in $CDCl_3$

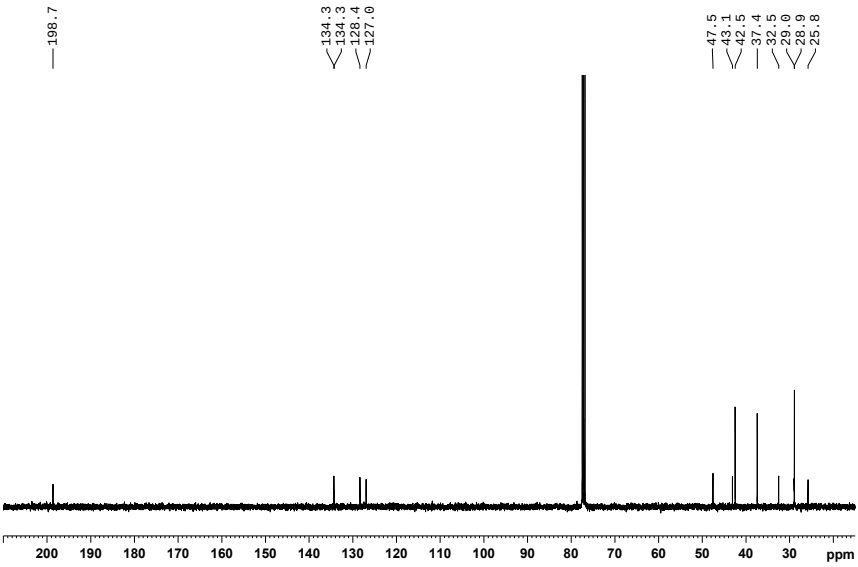

Figure S40. $^{13}C\{^{1}H\}$-spectrum of **30d** in $CDCl_3$

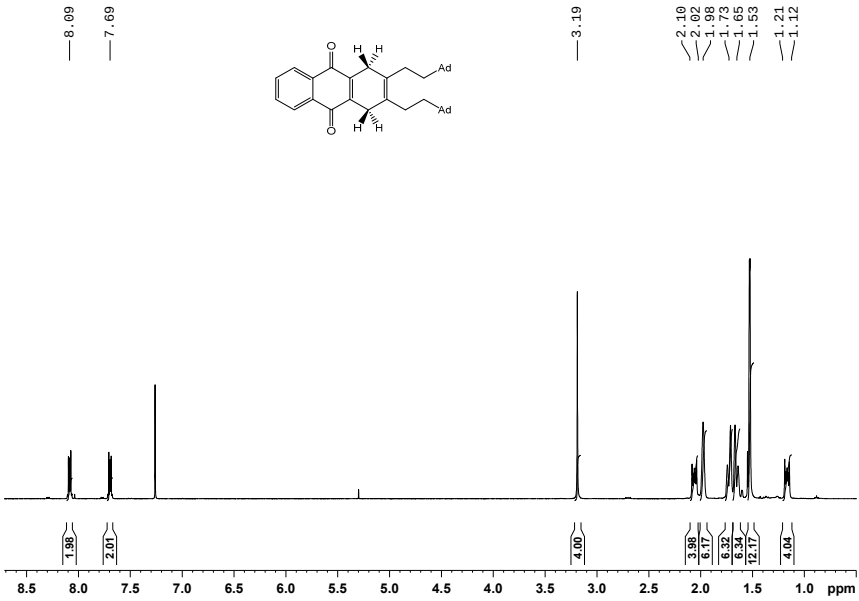

Figure S41. ^{1}H-spectrum of **30d-2H** in $CDCl_3$

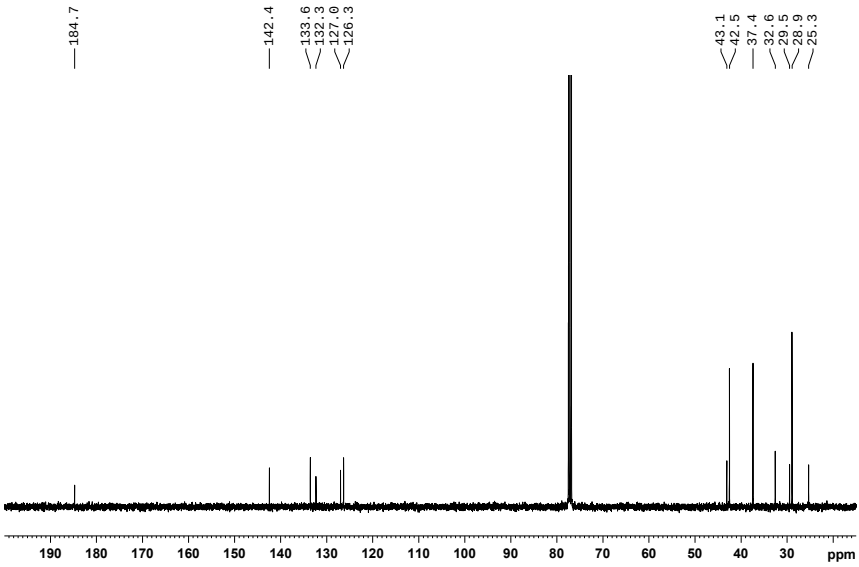

Figure S42. $^{13}C\{^{1}H\}$-spectrum of **30d-2H** in $CDCl_3$

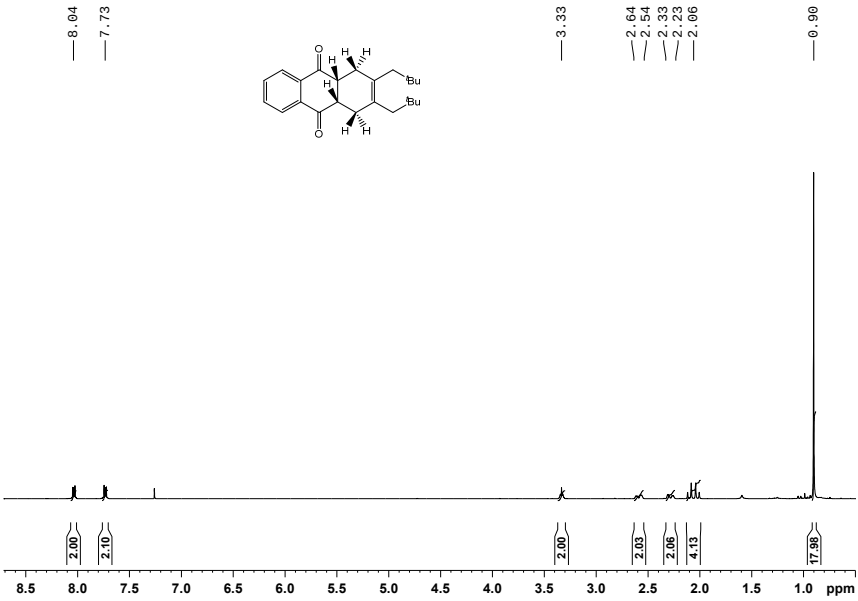

Figure S43. ^{1}H-NMR spectrum of **30e** in $CDCl_3$

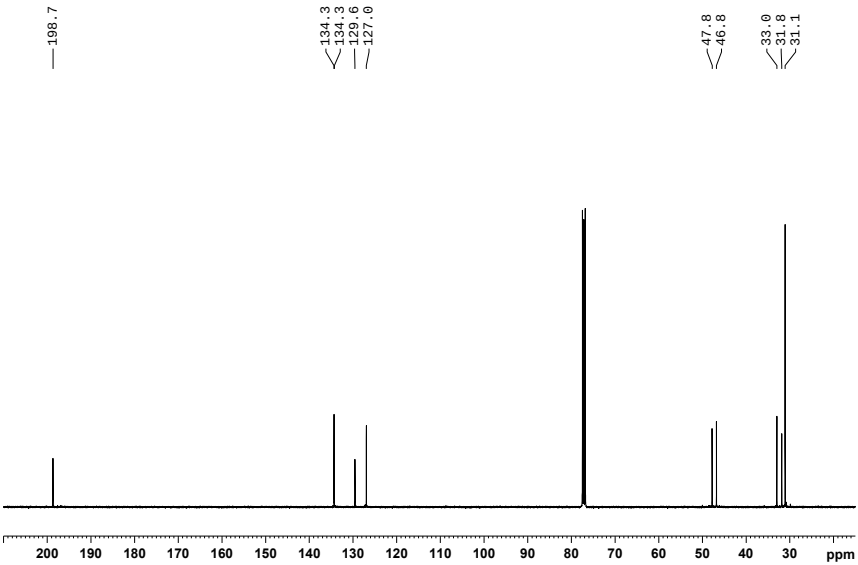

Figure S44. $^{13}C\{^{1}H\}$-NMR spectrum of **30e** in $CDCl_3$

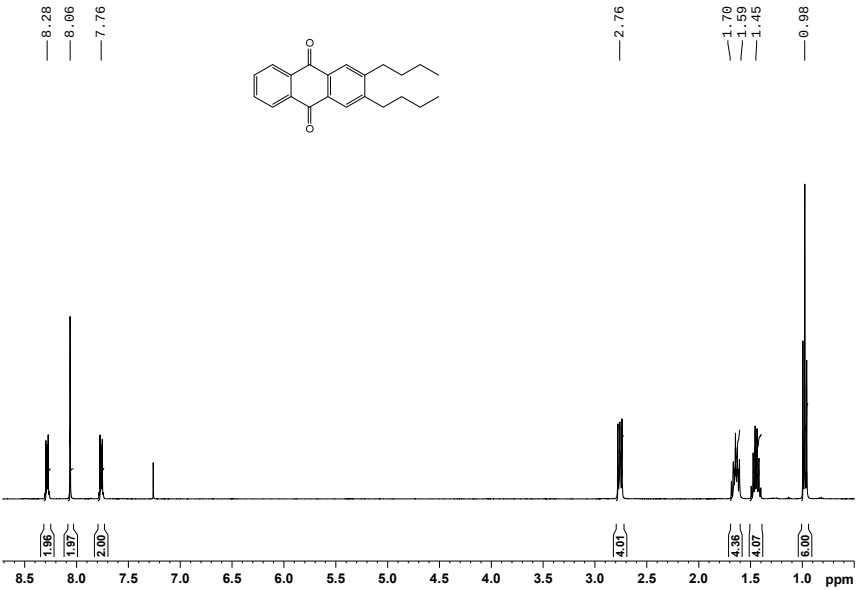

Figure S45. ^{1}H-NMR spectrum of **31a** in $CDCl_3$

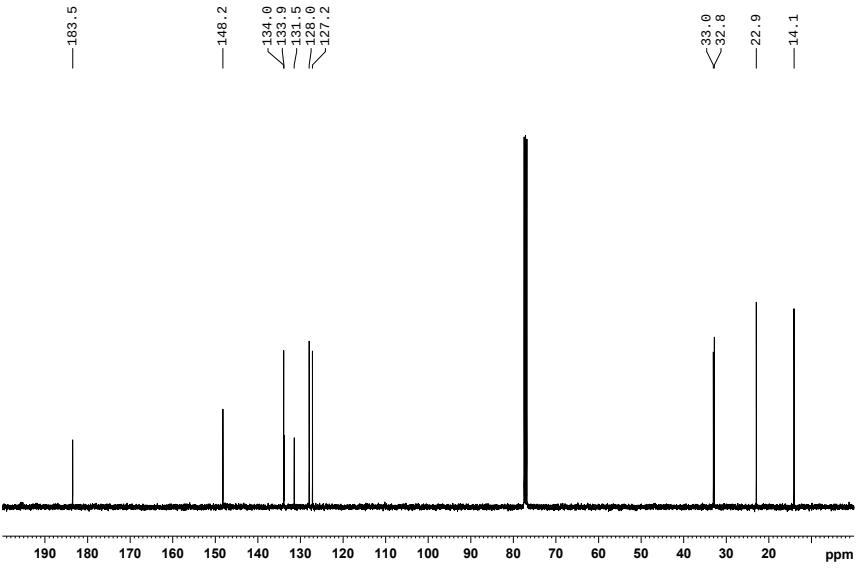

Figure S46. $^{13}C\{^{1}H\}$-NMR spectrum of **31a** in $CDCl_3$

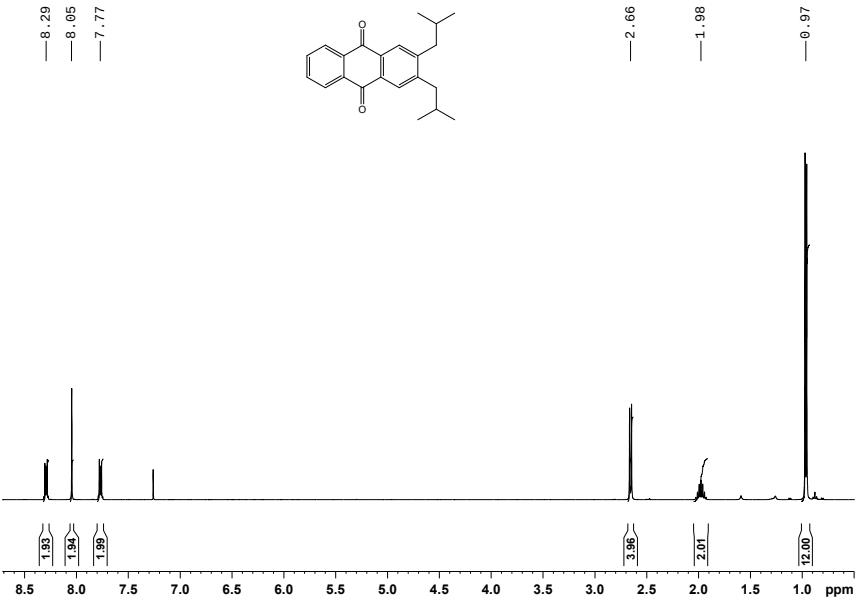

Figure S47. ^{1}H-NMR spectrum of **31b** in $CDCl_3$

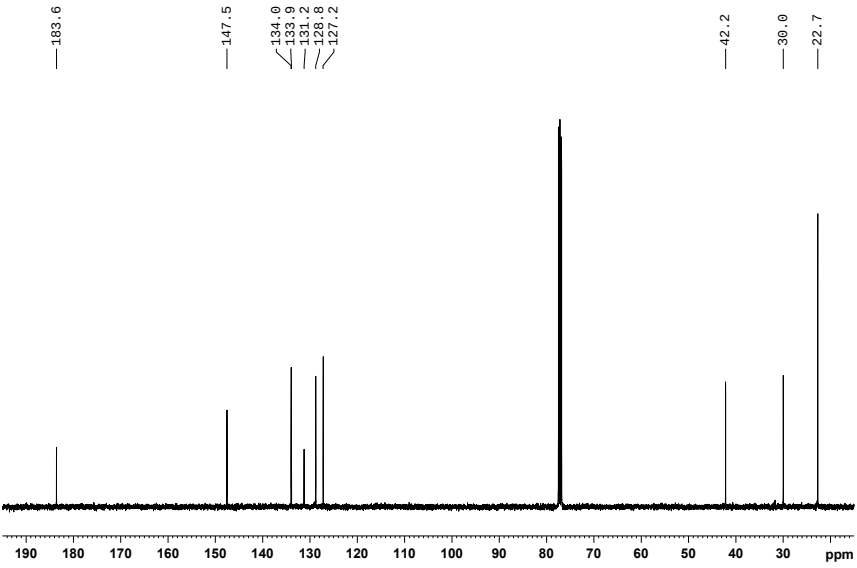

Figure S48. $^{13}C\{^{1}H\}$-NMR spectrum of **31b** in $CDCl_3$

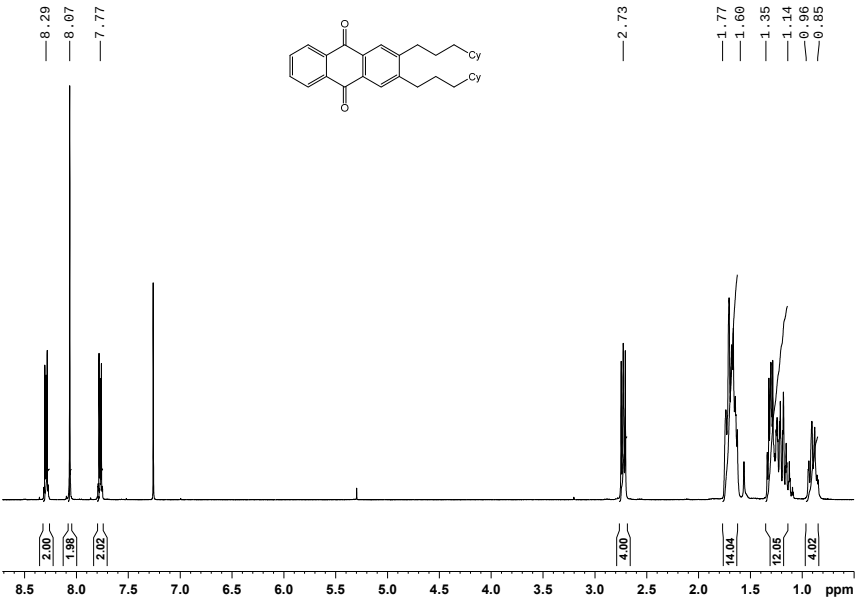

Figure S49. ^{1}H-NMR spectrum of **31c** in $CDCl_3$

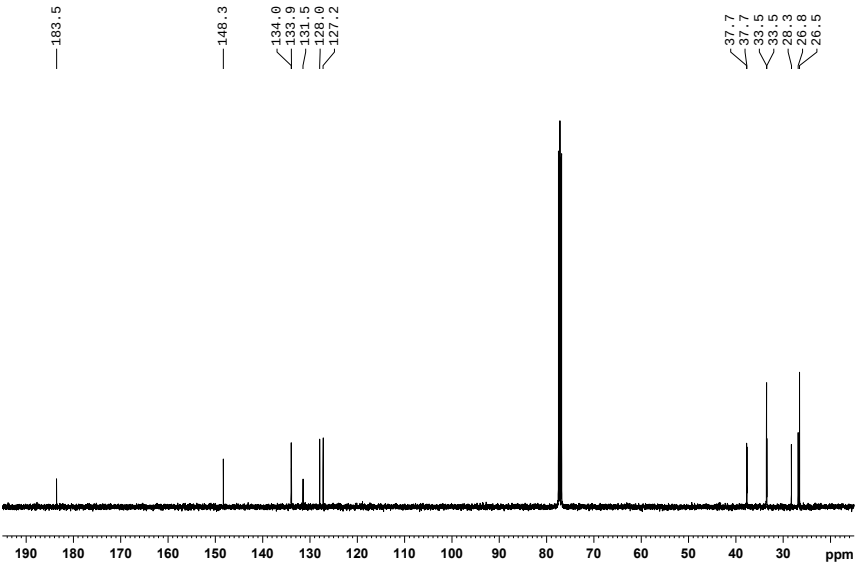

Figure S50. $^{13}C\{^{1}H\}$-NMR spectrum of **31c** in $CDCl_3$

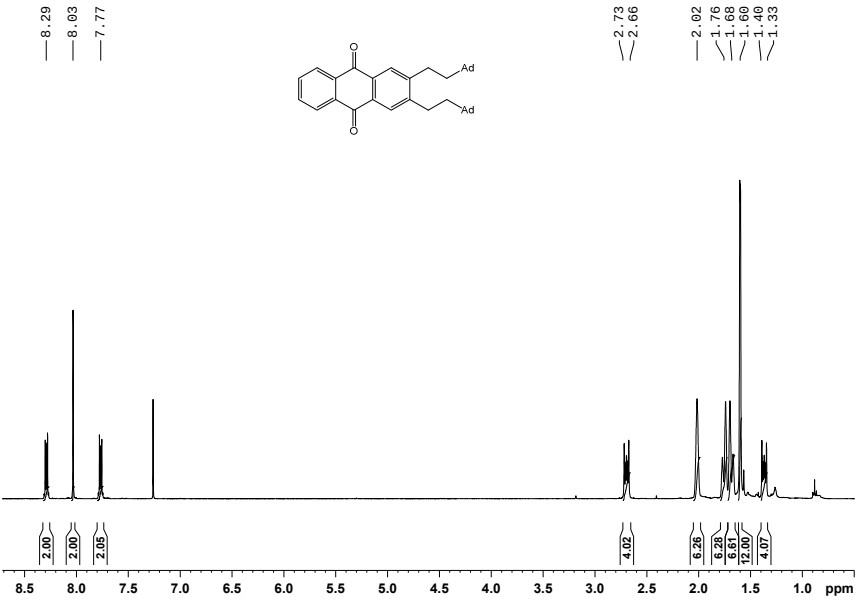

Figure S51. ^{1}H-spectrum of **31d** in $CDCl_3$

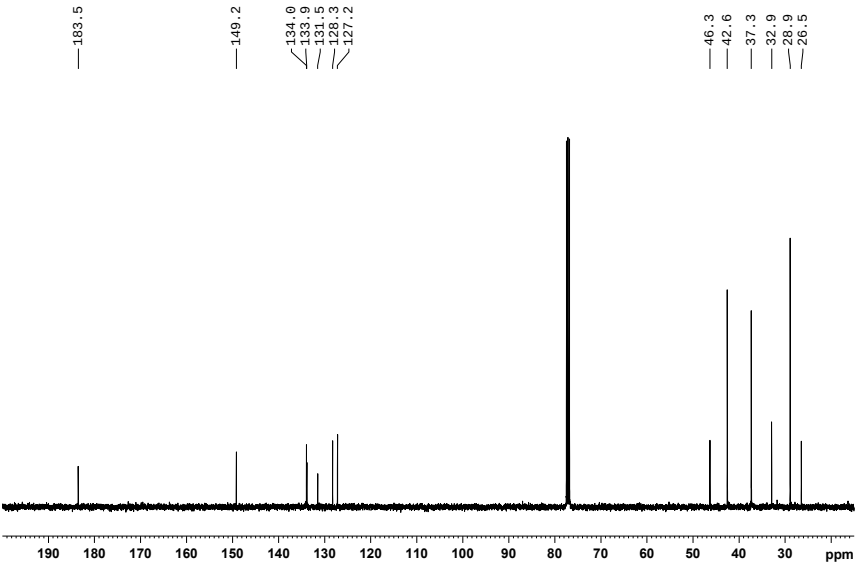

Figure S52. $^{13}C\{^{1}H\}$-spectrum of **31d** in $CDCl_3$

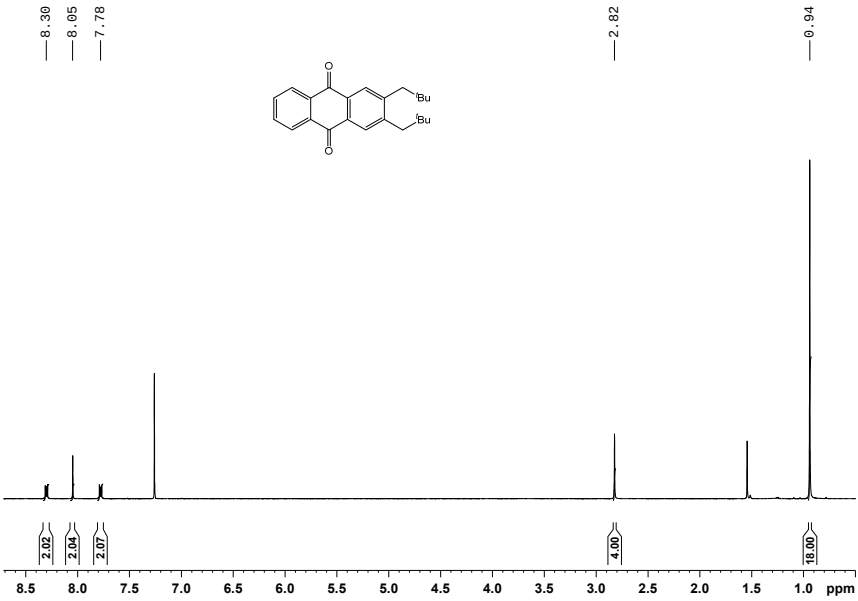

Figure S53. ^{1}H-NMR spectrum of **31e** in $CDCl_3$

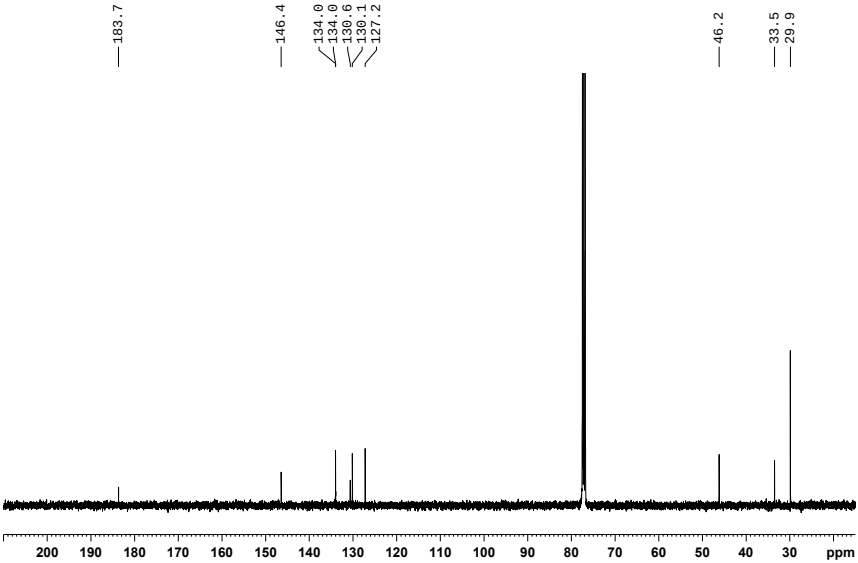

Figure S54. $^{13}C\{^{1}H\}$-NMR spectrum of **31e** in $CDCl_3$

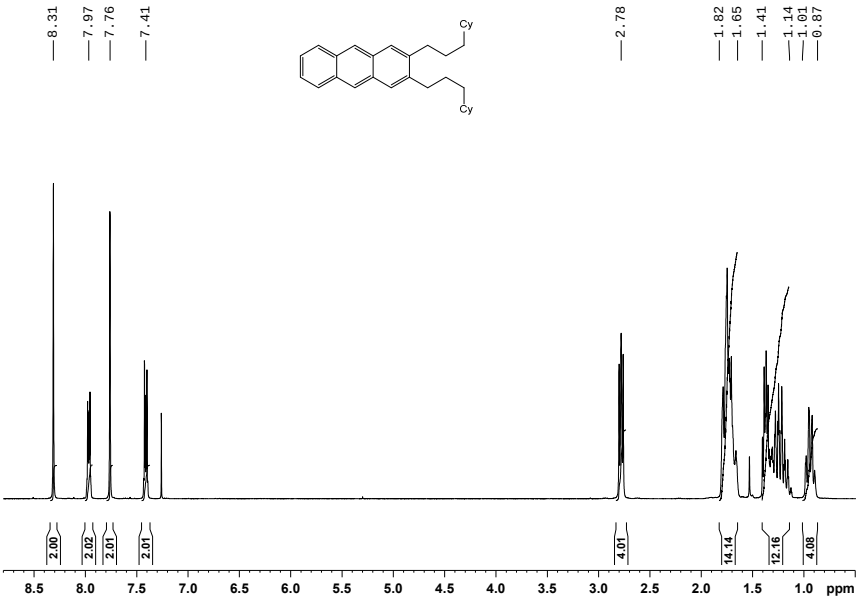

Figure S55. ^{1}H-NMR spectrum of **32** in $CDCl_3$

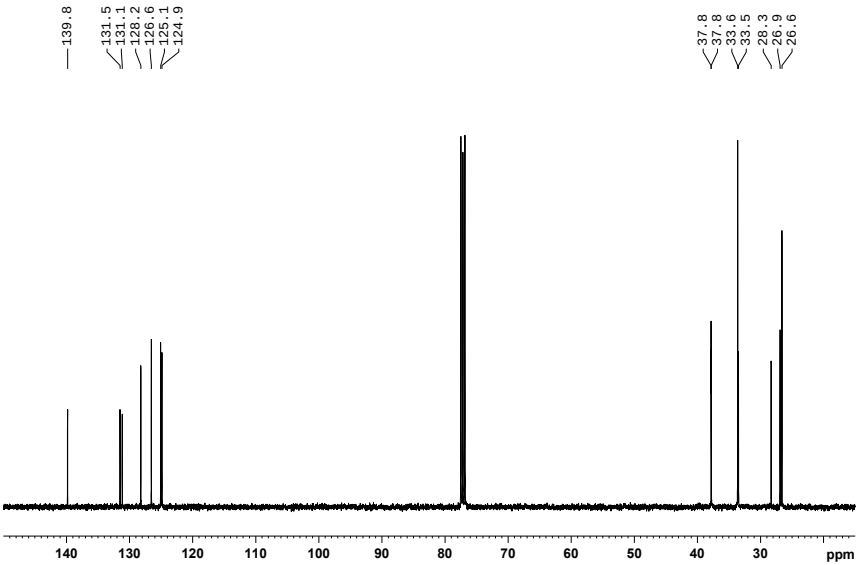

Figure S56. $^{13}C\{^{1}H\}$-NMR spectrum of **32** in $CDCl_3$

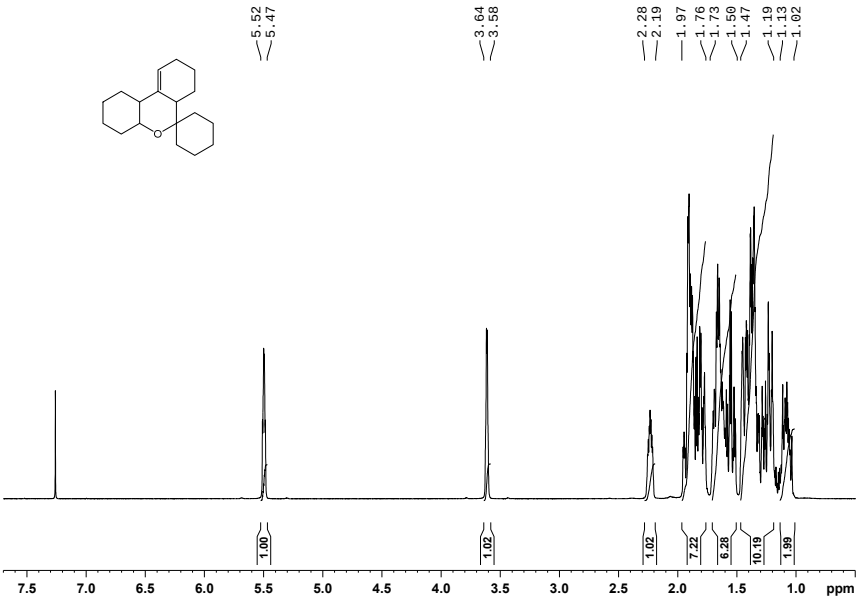

Figure S57. ^{1}H-NMR spectrum of **33** in $CDCl_3$

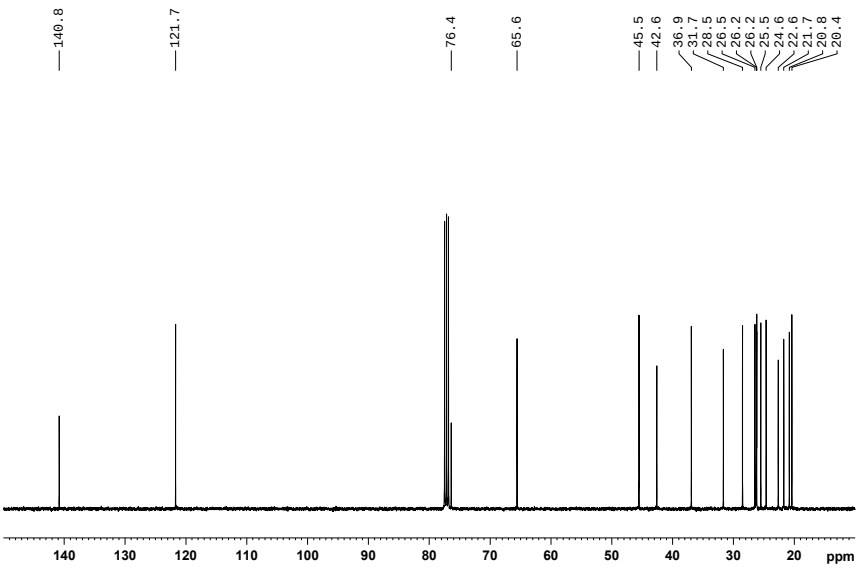

Figure S58. $^{13}C\{^{1}H\}$-NMR spectrum of **33** in $CDCl_3$

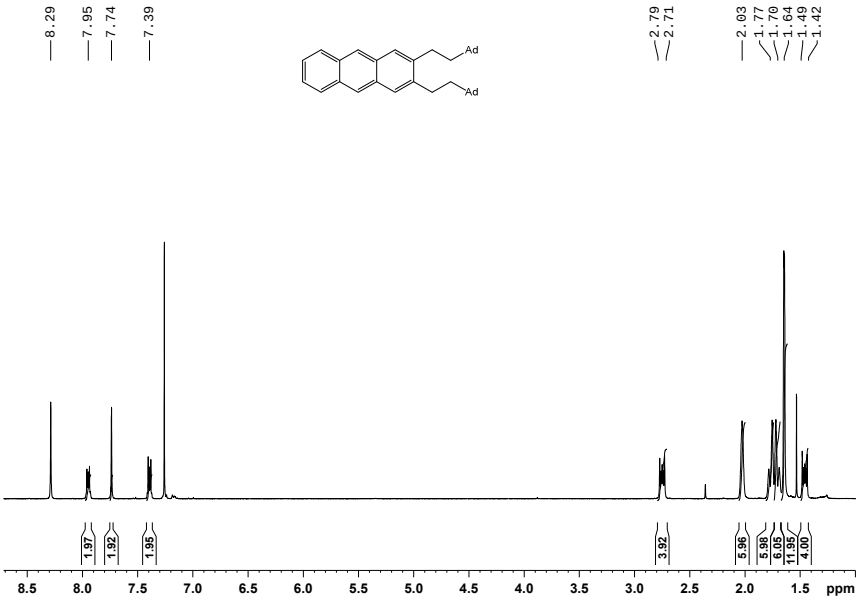

Figure S59. ^{1}H-NMR spectrum of **35** in $CDCl_3$

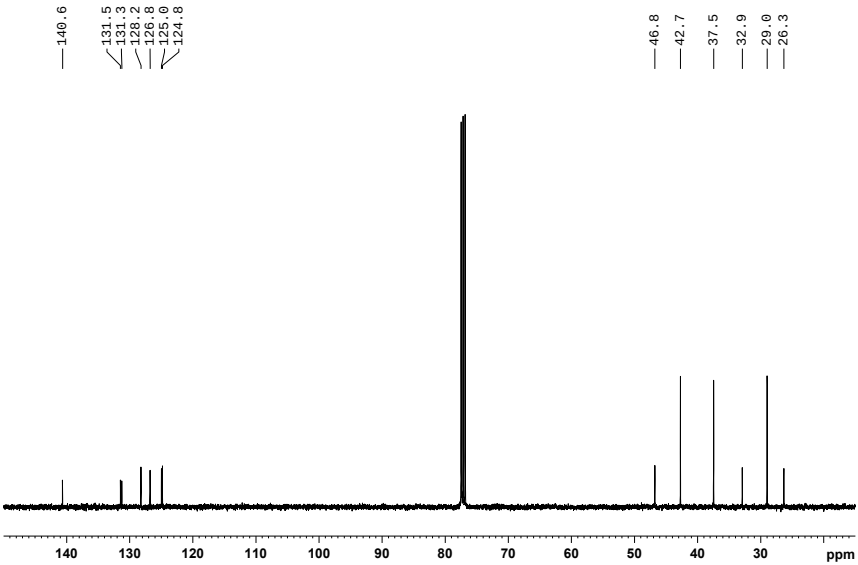

Figure S60. $^{13}C\{^{1}H\}$-NMR spectrum of **35** in $CDCl_3$

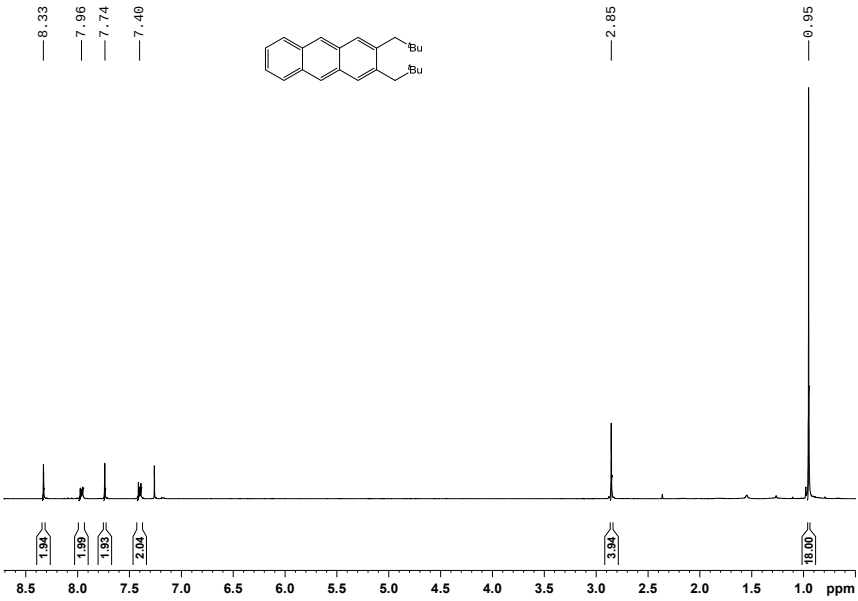

Figure S61. ^{1}H-NMR spectrum of **36** in $CDCl_3$

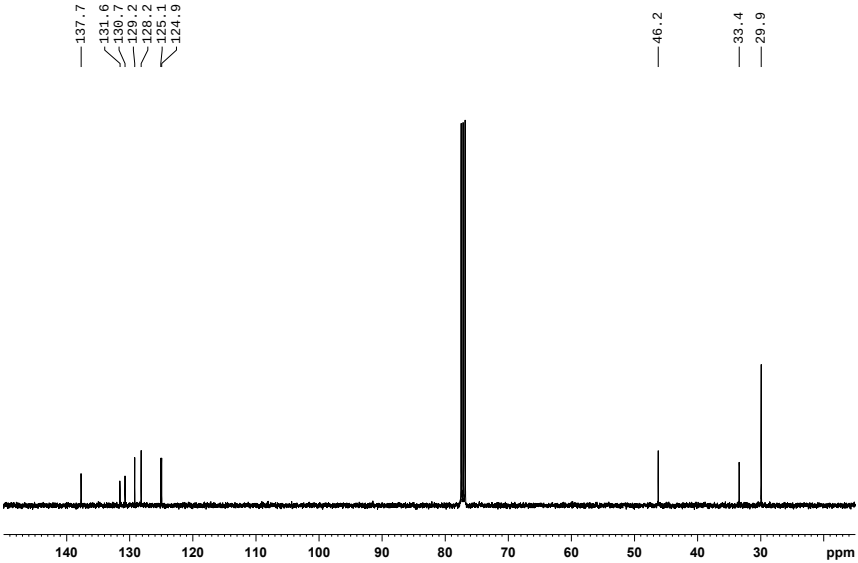

Figure S62. $^{13}C\{^{1}H\}$-NMR spectrum of **36** in $CDCl_3$

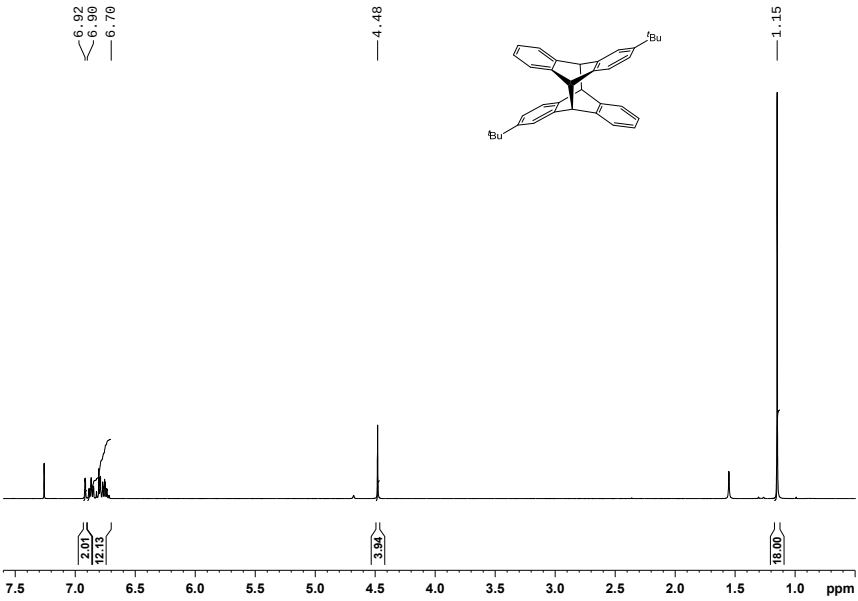

Figure S63. ^{1}H-NMR spectrum of **37a** in $CDCl_3$

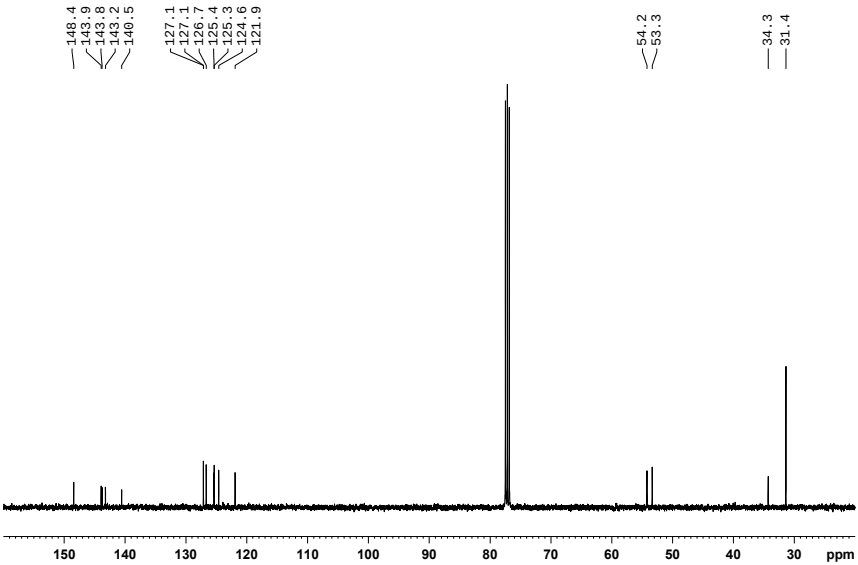

Figure S64. $^{13}C\{^{1}H\}$-NMR spectrum of **37a** in CDCl3

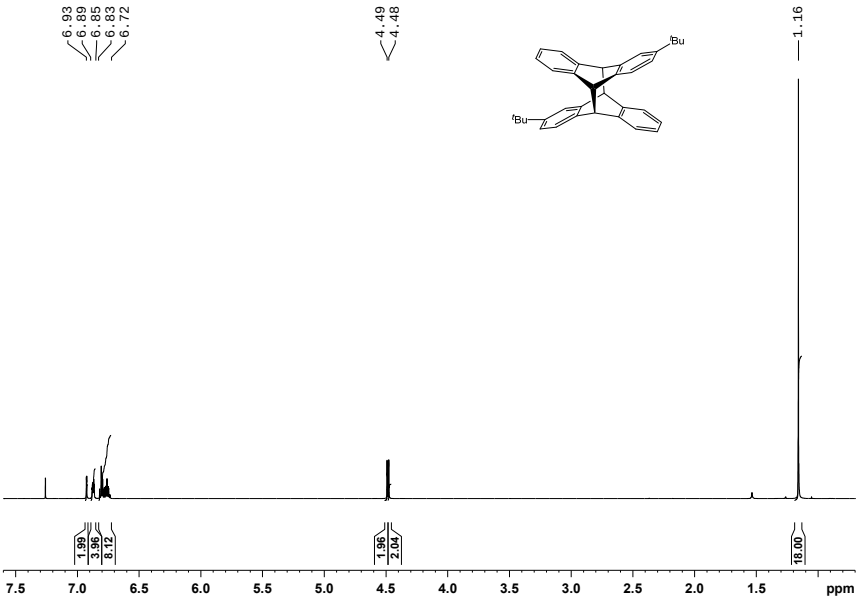

Figure S65. ^{1}H-NMR spectrum of **37b** in $CDCl_3$

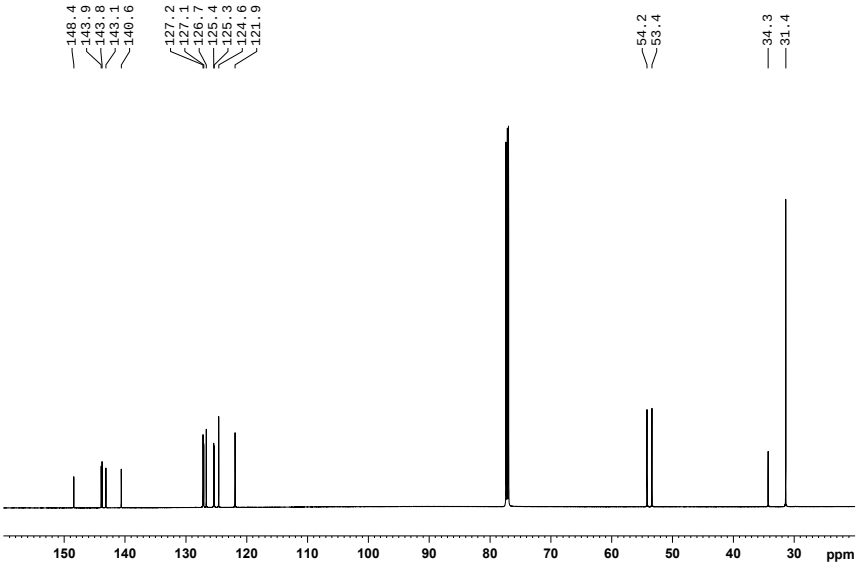

Figure S66. $^{13}C\{^{1}H\}$-NMR spectrum of **37b** in $CDCl_3$

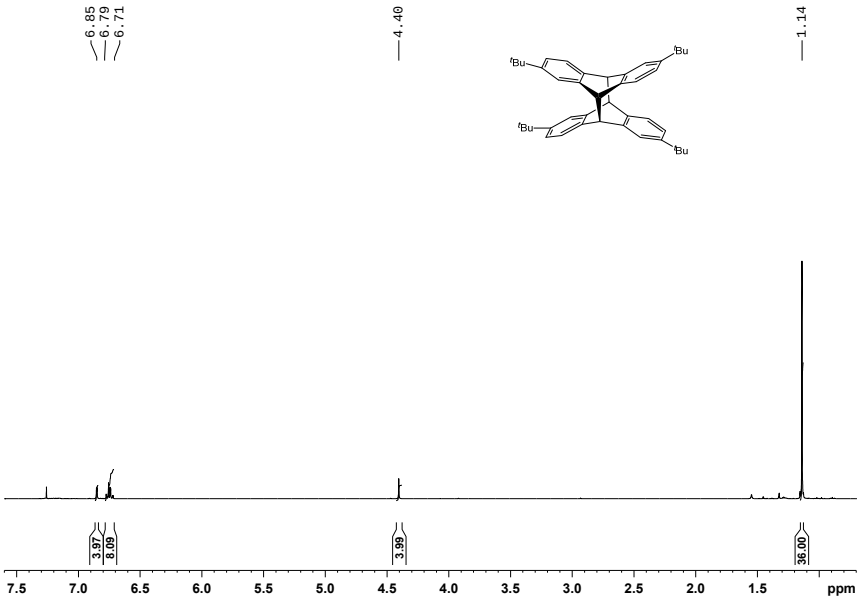

Figure S67. ^{1}H-NMR of **38a** in $CDCl_3$

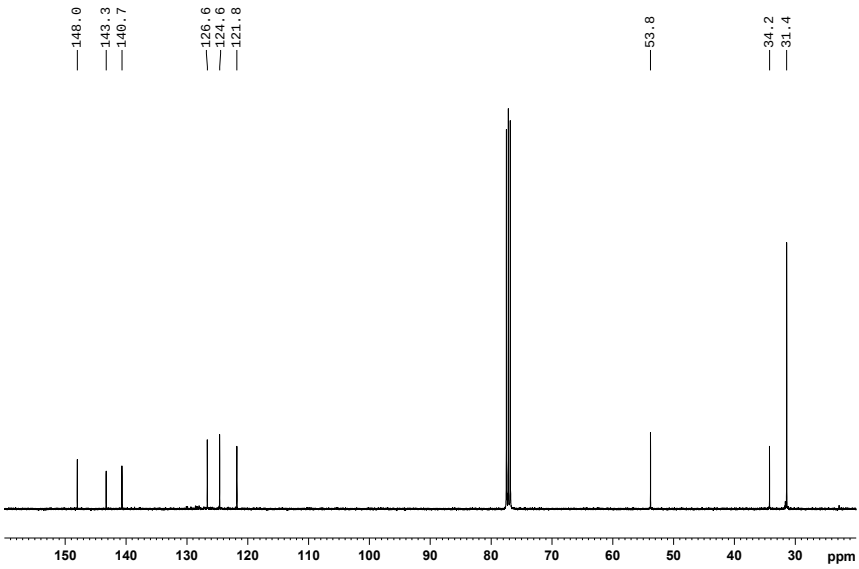

Figure S68. $^{13}C\{^{1}H\}$-NMR of **38a** in $CDCl_3$

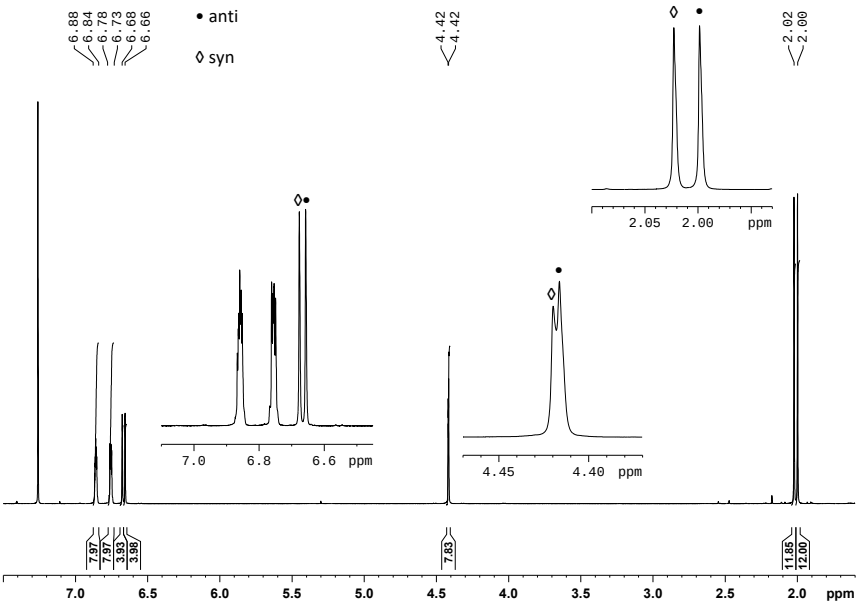

Figure S69. ^{1}H-NMR spectrum of the *anti*/*syn* mixture of **39a**/**b** in $CDCl_3$

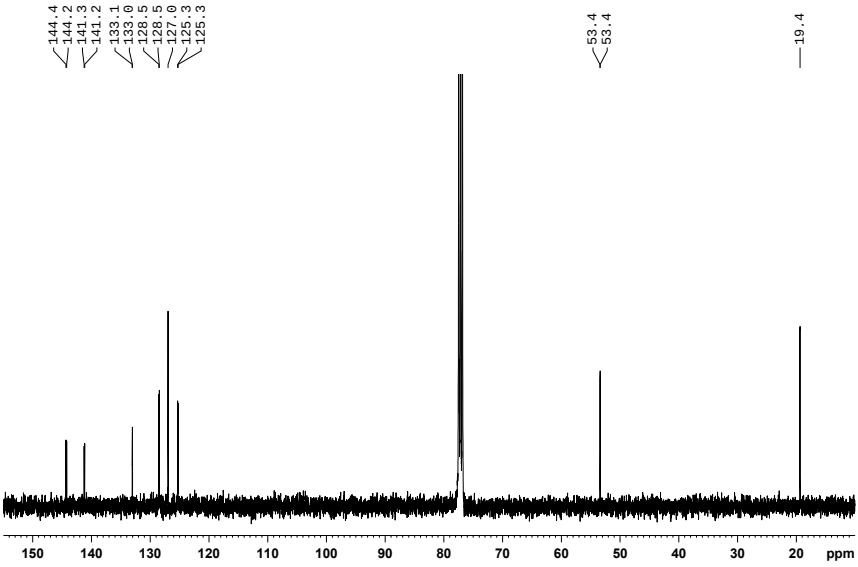

Figure S70. $^{13}C\{^{1}H\}$-NMR spectrum of the *anti*/*syn* mixture of **39a**/**b** in $CDCl_3$

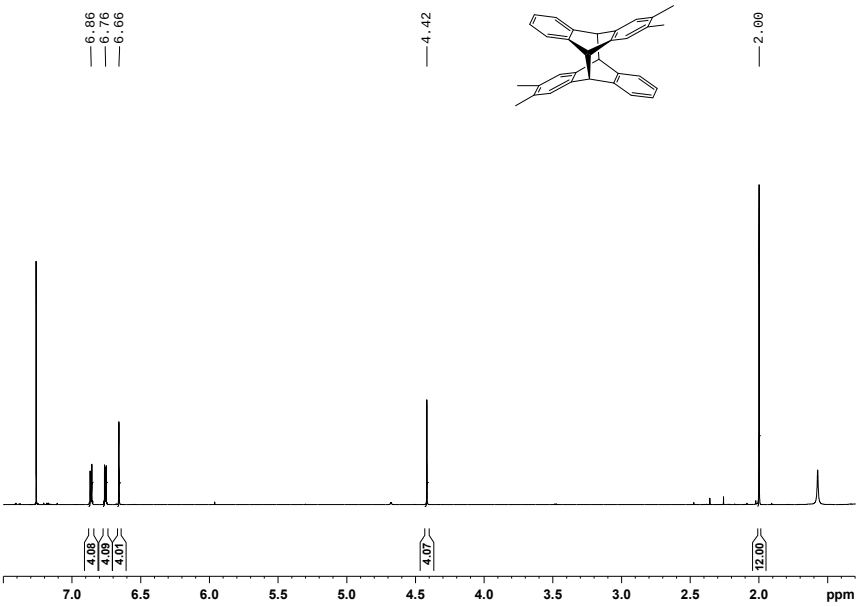

Figure S71. ^{1}H-NMR spectrum of **39a** in $CDCl_3$

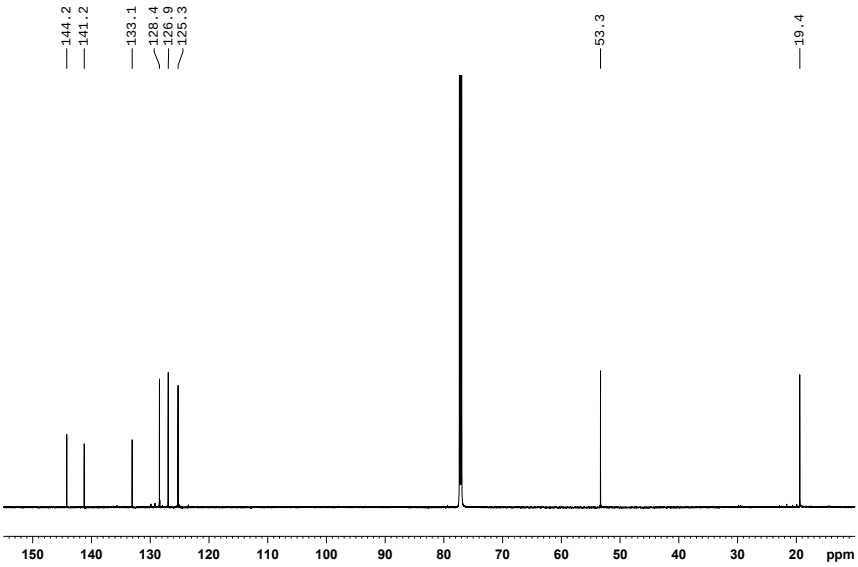

Figure S72. $^{13}C\{^{1}H\}$-NMR spectrum of **39a** in $CDCl_3$

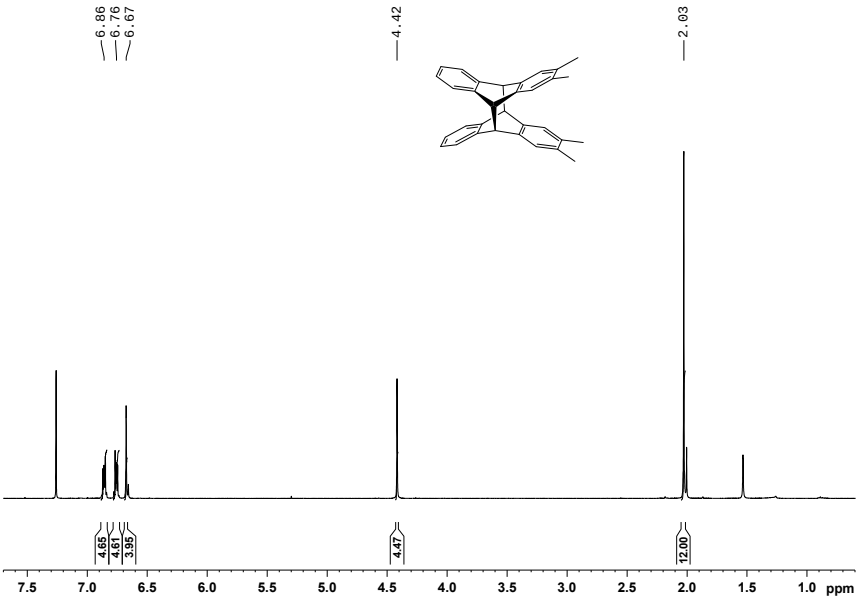

Figure S73. ^{1}H-NMR spectrum of **39b** in $CDCl_3$

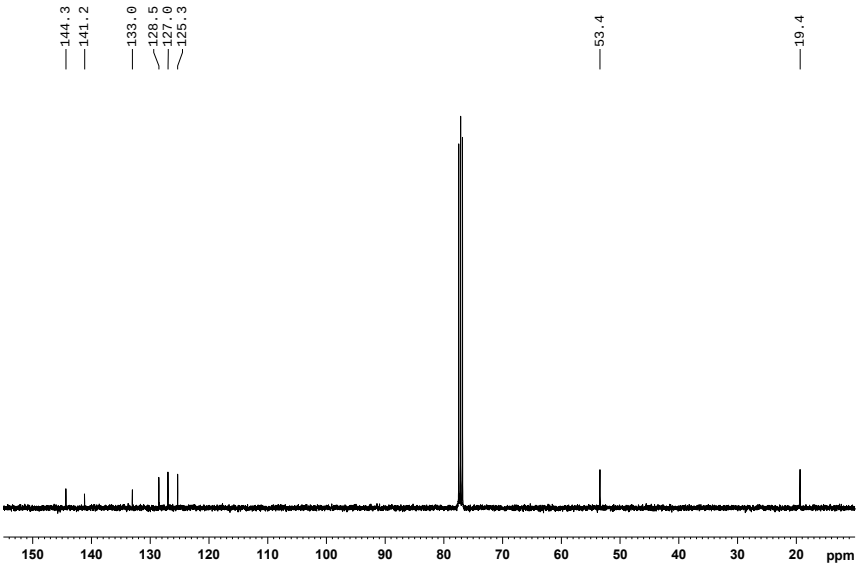

Figure S74. $^{13}C\{^{1}H\}$-NMR spectrum of **39b** in $CDCl_3$

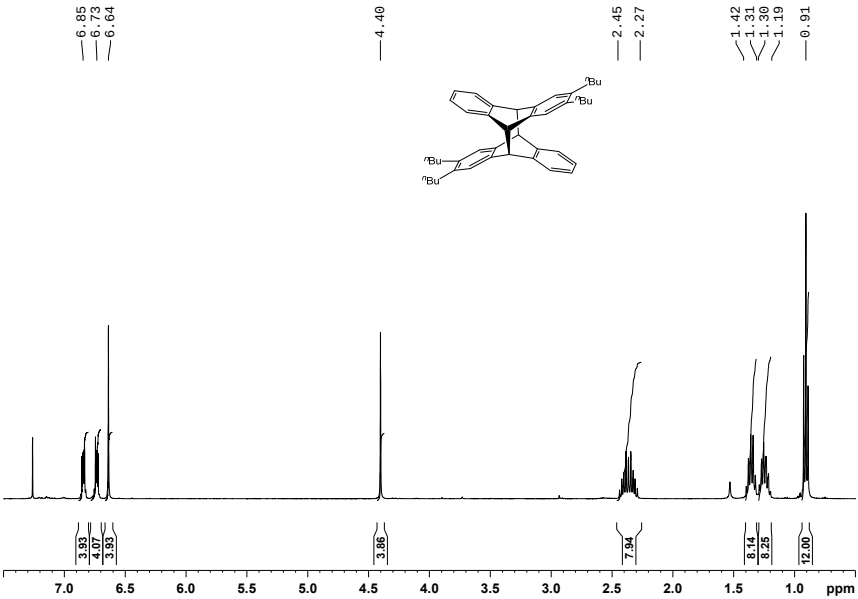

Figure S75. ^{1}H-NMR spectrum of **40a** in $CDCl_3$

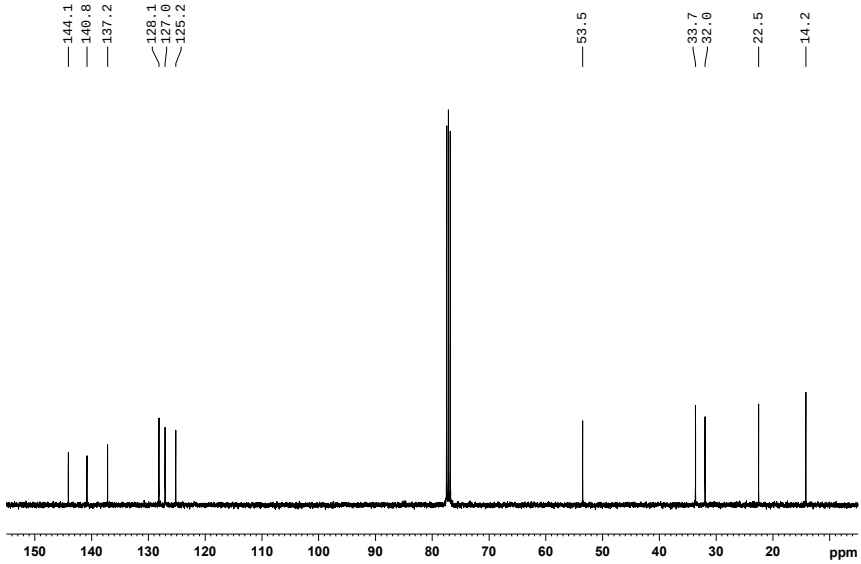

Figure S76. $^{13}C\{^{1}H\}$-NMR spectrum of **40a** in $CDCl_3$

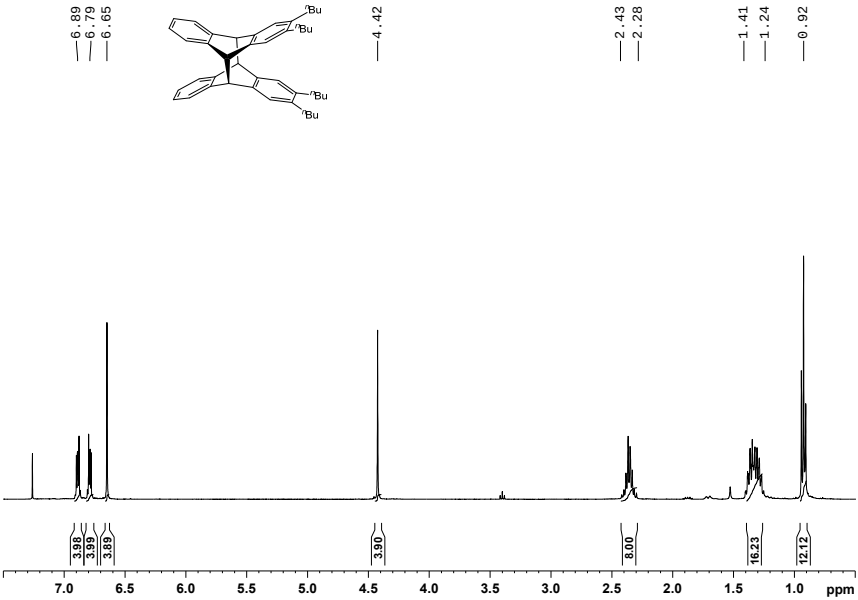

Figure S77. ^{1}H-NMR spectrum of **40b** in $CDCl_3$

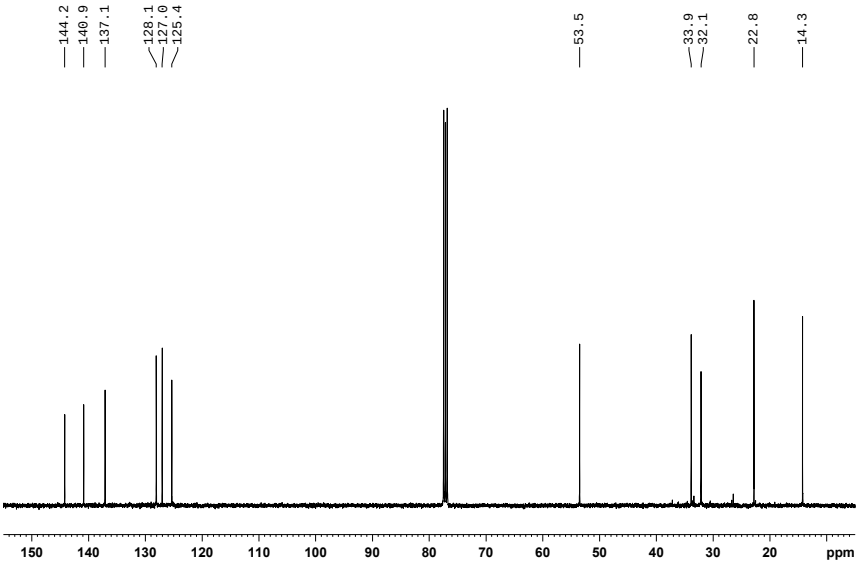

Figure S78. $^{13}C\{^{1}H\}$-NMR of **40b** in $CDCl_3$

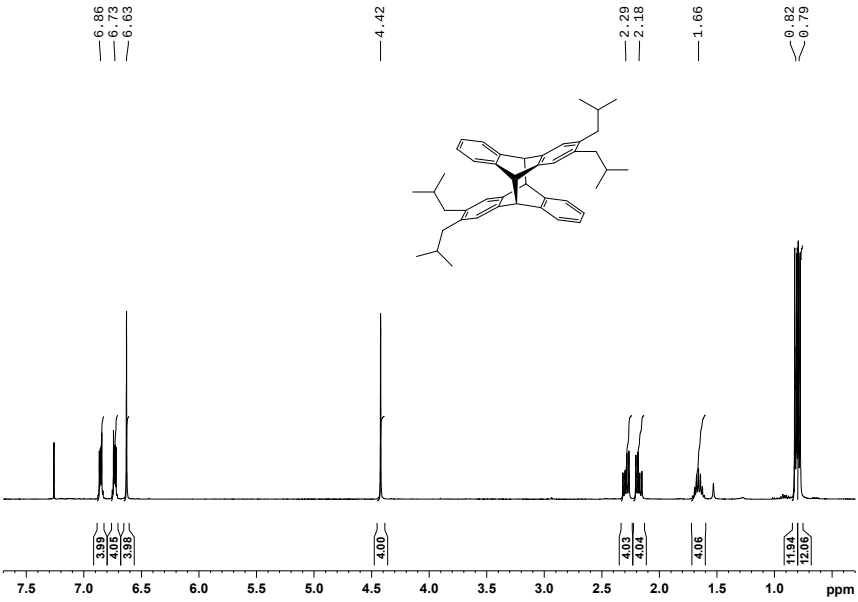

Figure S79. ^{1}H-NMR spectrum of **41a** in $CDCl_3$

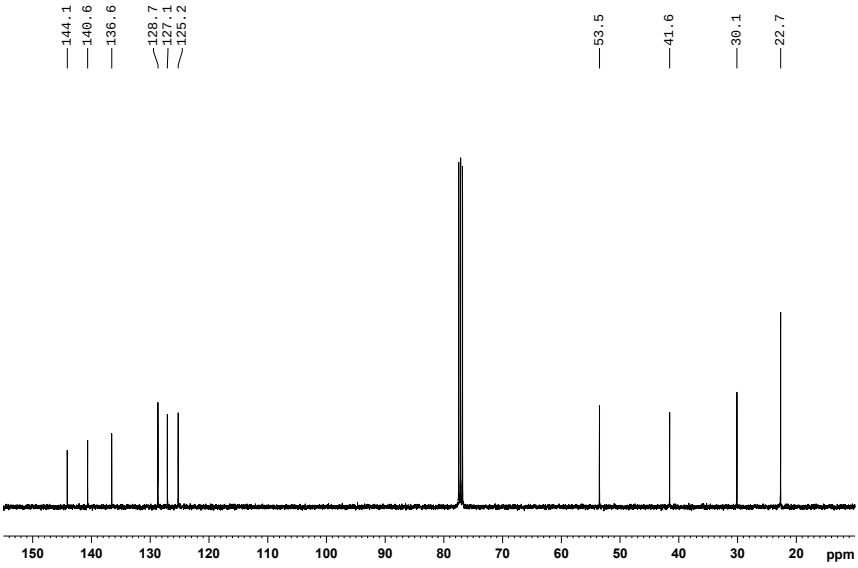

Figure S80. $^{13}C\{^{1}H\}$-NMR of **41a** in $CDCl_3$

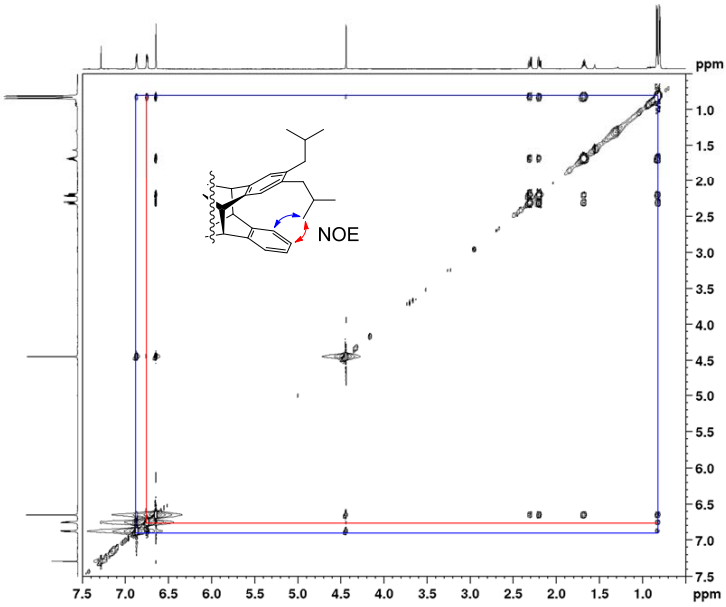

Figure S81. NOE spectrum of **41a** in $CDCl_3$

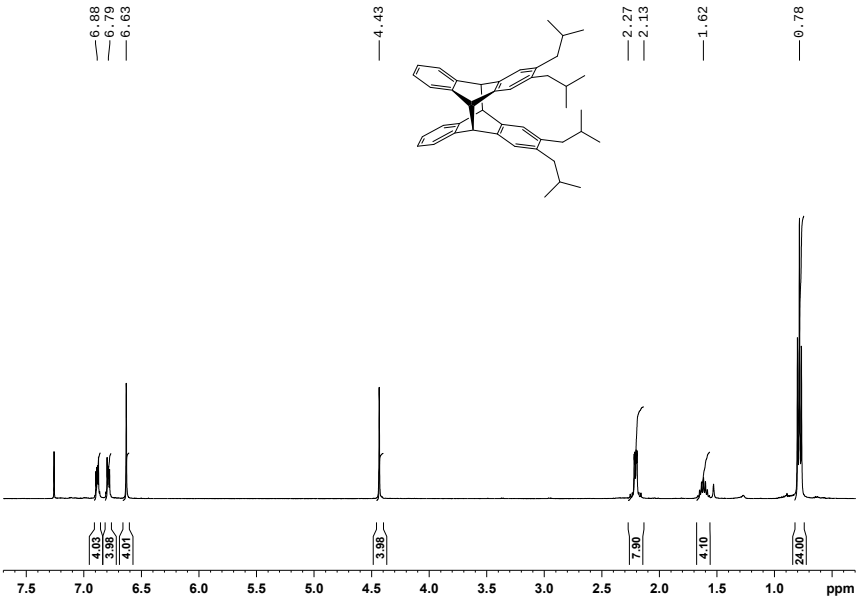

Figure S82. ^{1}H-NMR spectrum of **41b** in $CDCl_3$

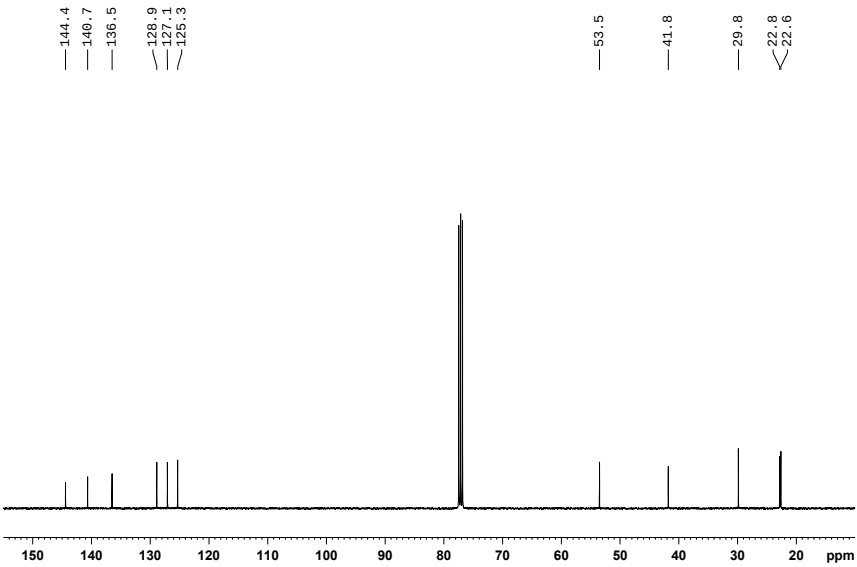

Figure S83. $^{13}C\{^{1}H\}$-NMR spectrum of **41b** in $CDCl_3$

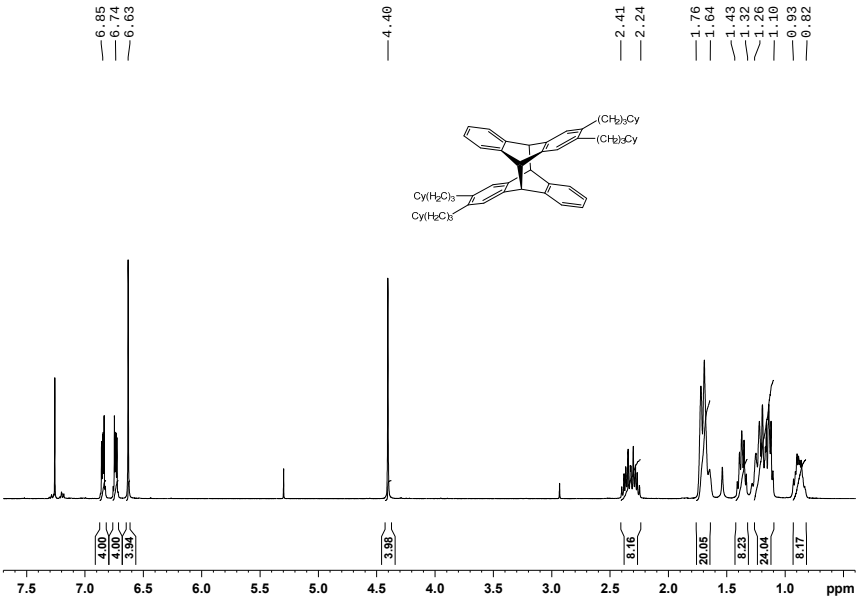

Figure S84. ^{1}H-NMR spectrum of **42a** in $CDCl_3$

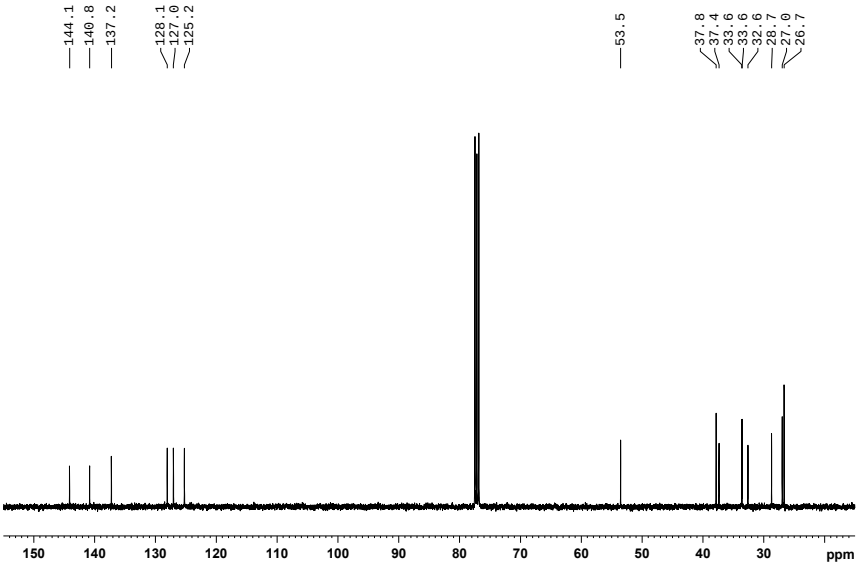

Figure S85. $^{13}C\{^{1}H\}$-NMR spectrum of **42a** in $CDCl_3$

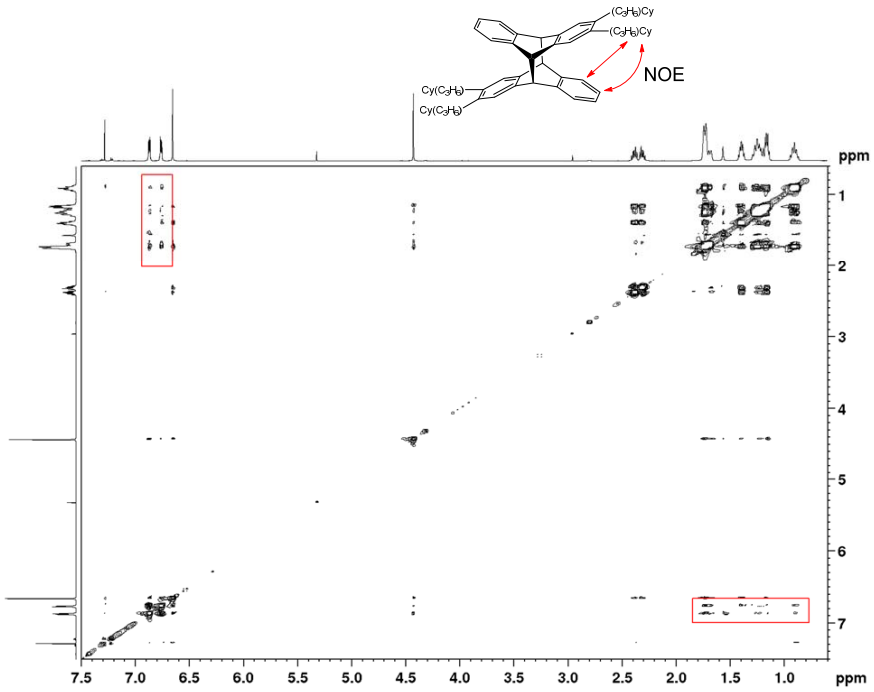

Figure S86. NOE spectrum of **42a** in $CDCl_3$

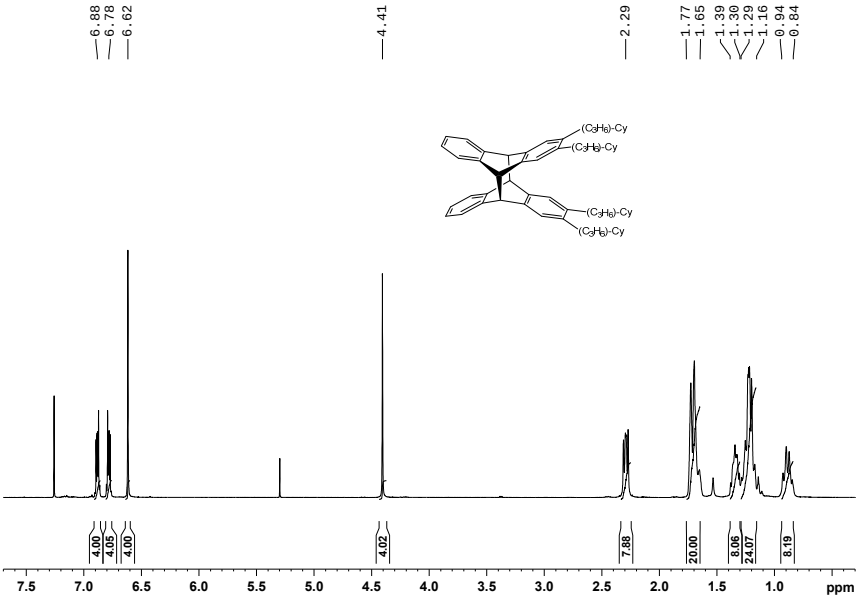

Figure S87. ^{1}H-NMR spectrum of **42b** in $CDCl_3$

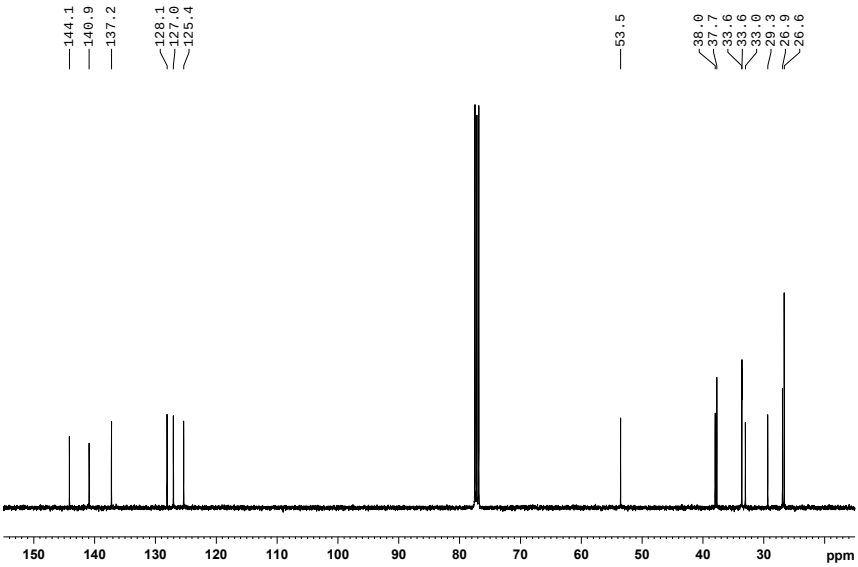

Figure S88. $^{13}C\{^{1}H\}$-NMR spectrum of **42b** in $CDCl_3$

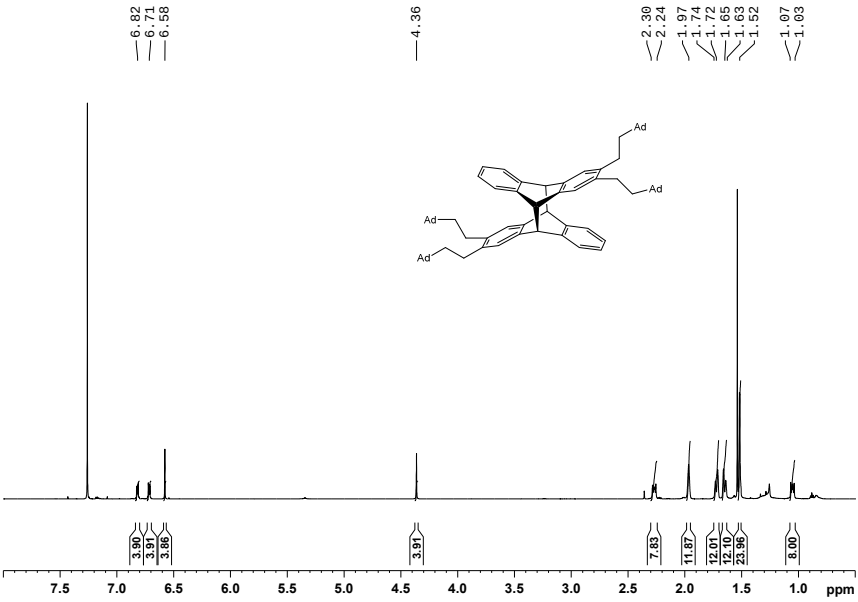

Figure S89. ^{1}H-NMR spectrum of **43a** in $CDCl_3$

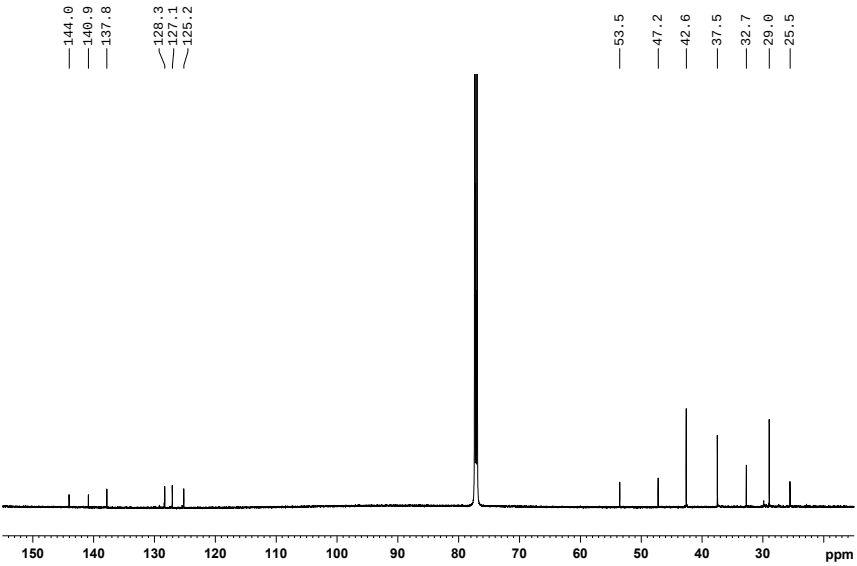

Figure S90. $^{13}C\{^{1}H\}$-NMR spectrum of **43a** in $CDCl_3$

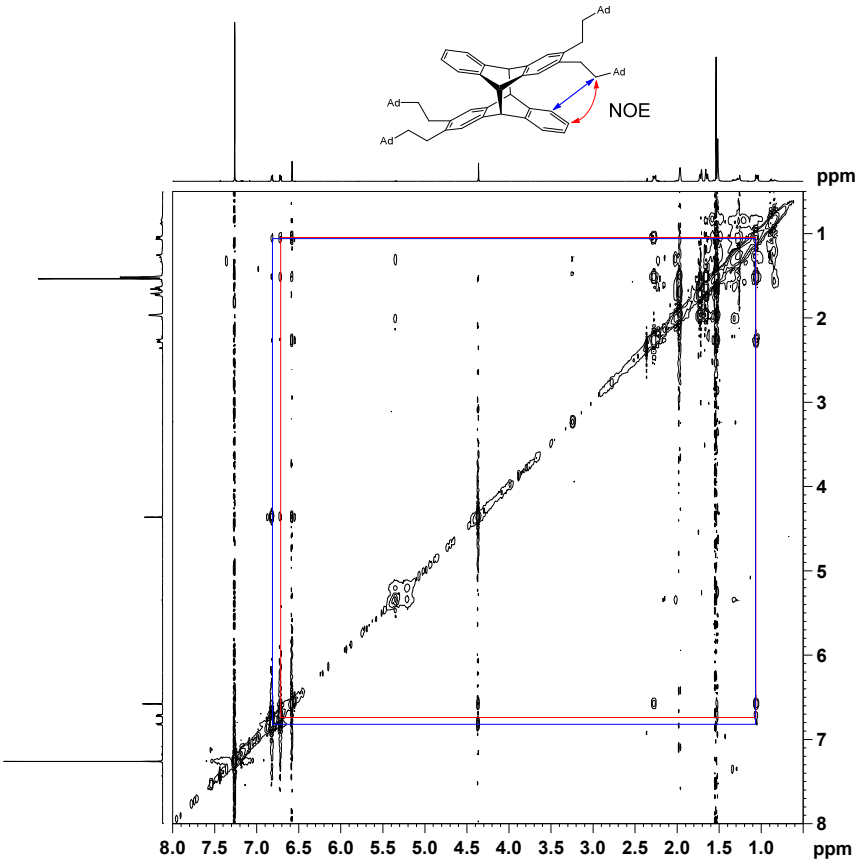

Figure S91. NOE spectrum of **43a** in $CDCl_3$

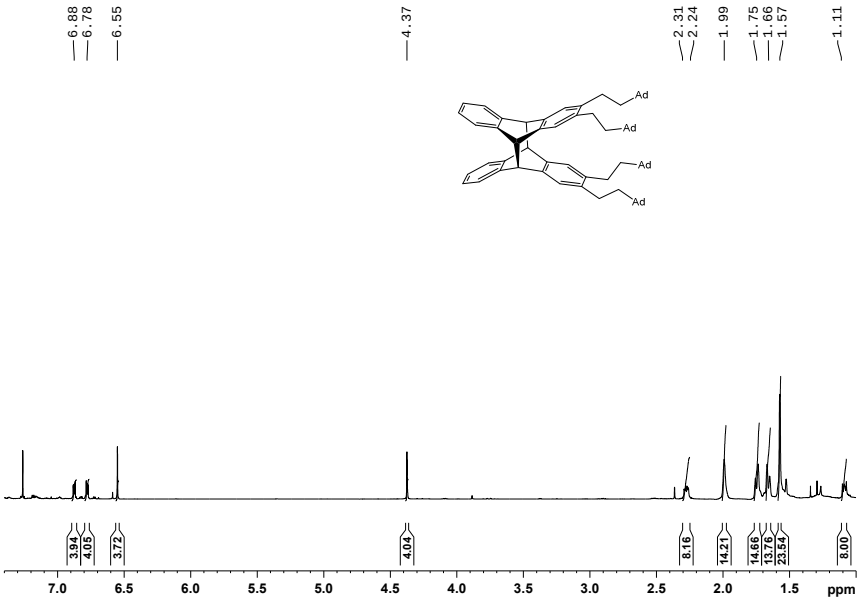

Figure S92. ^{1}H-NMR spectrum of **43b** in $CDCl_3$

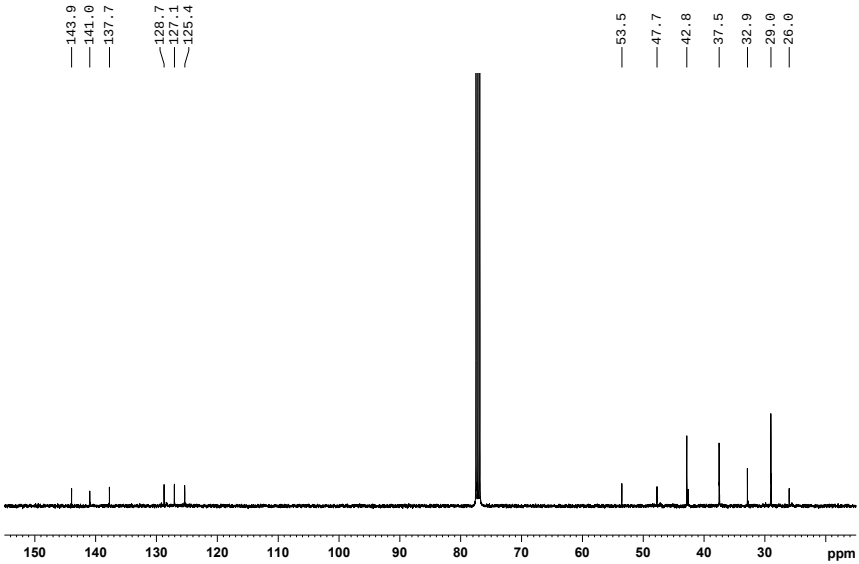

Figure S93. $^{13}C\{^{1}H\}$-spectrum of **43b** in $CDCl_3$

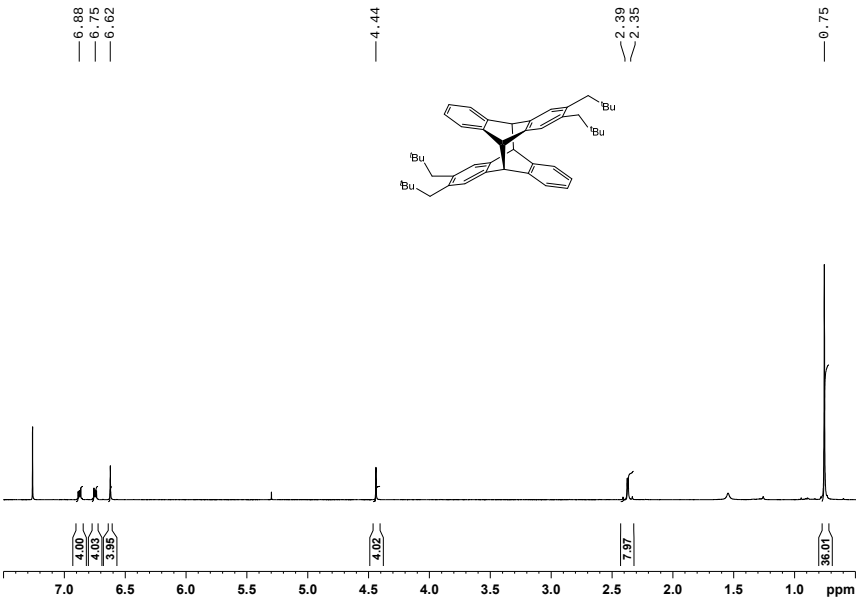

Figure S94. ^{1}H-NMR spectrum of **44a** in $CDCl_3$

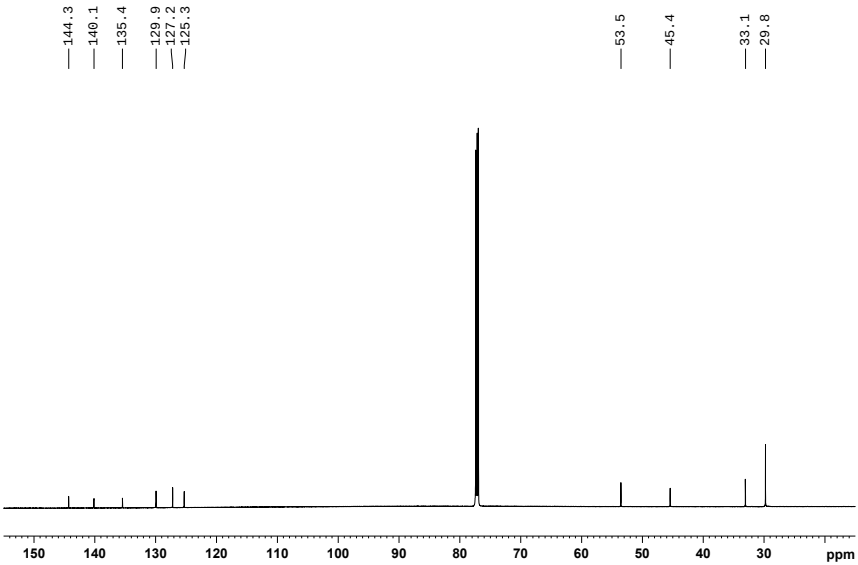

Figure S95. $^{13}C\{^{1}H\}$-NMR spectrum of **44a** in $CDCl_3$

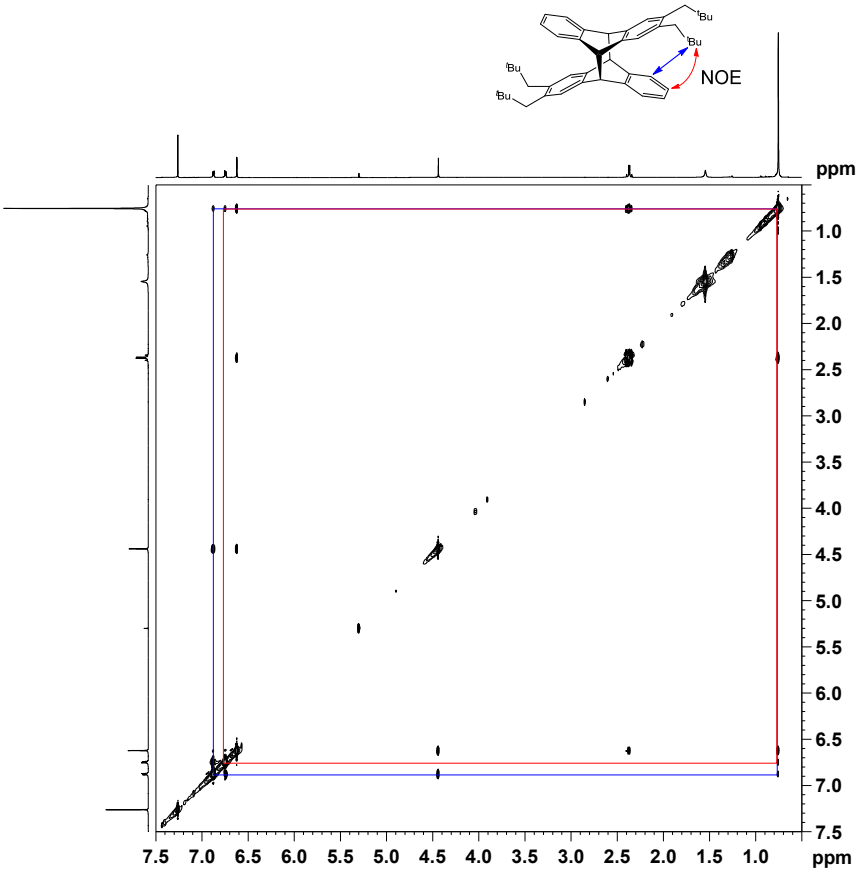

Figure S96. NOE spectrum of **44a** in $CDCl_3$

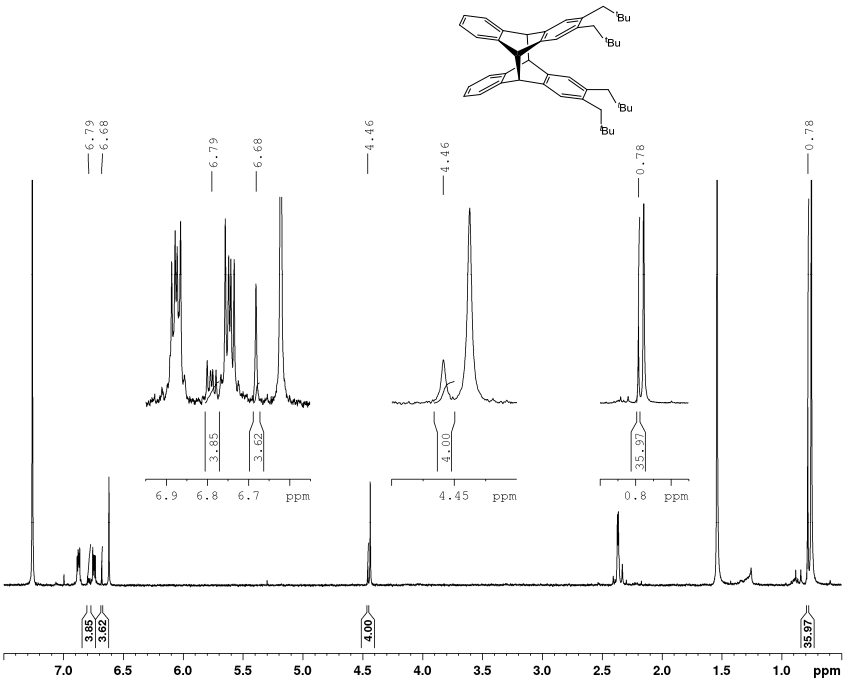

Figure S97. ^{1}H-NMR spectrum of **44b** in $CDCl_3$. The CH_2 signals of the neopentyl groups could not be resolved due to overlap with signals for dimer **44a**.

2. UV/Vis and fluorescence data for newly prepared anthracene derivatives

Absorption spectra were obtained using a PerkinElmer Lambda1050 UV/Vis/NIR spectrometer, fluorescence spectra were recorded on a Varian Cary Eclipse fluorescence spectrometer. In both cases solutions of the monomers in *n*-hexane were used, individual concentrations as well as excitation wavelengths are reported for the individual spectra. The fluorescence spectra were scaled down to match the highest absorption band in intensity.

2,3-Di-*n*-butyl-anthracene (20)

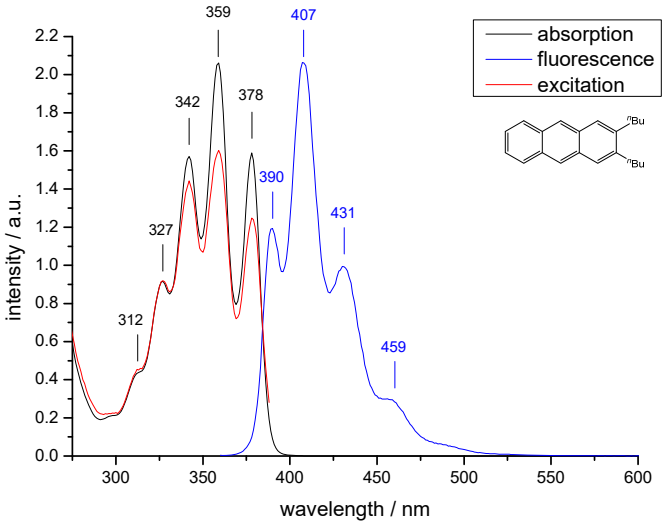

Figure S98. Absorption spectrum c = $3.7 \cdot 10^{-4}$ mol·L^{-1}, fluorescence spectrum: c = $3.1 \cdot 10^{-4}$ mol·L^{-1}, excitation wavelength: 359 nm

λ_{max} / nm	312	327	342	359	378
ε / L·mol^{-1}·cm^{-1}	1195.36±2.40	2509.84±11.61	4286.11±13.79	5632.55±6.28	4345.67±5.27

2,3-Di-*iso*-butyl-anthracene (21)

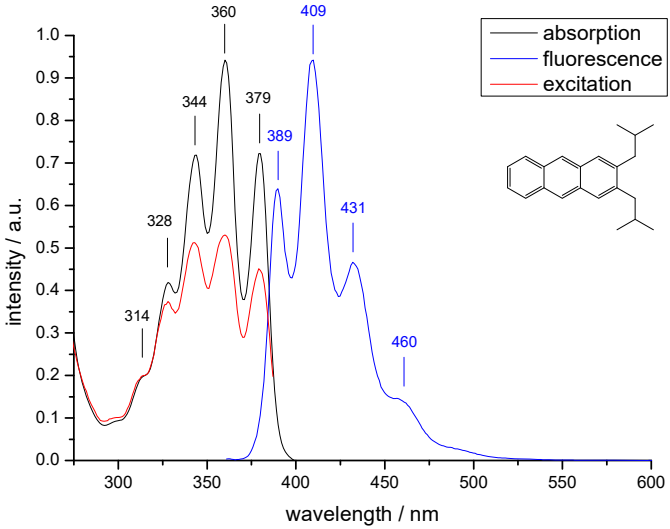

Figure S99. Absorption spectrum c = $8.3 \cdot 10^{-4}$ mol·L^{-1}, fluorescence spectrum: c = 9.2·10-5 mol·L^{-1}, excitation wavelength: 360 nm

λ_{max} / nm	314	328	344	360	379
ε / L·mol^{-1}·cm^{-1}	2410.06±11.75	5030.07±23.6	8506.54±30.97	10966.07±27.69	8526.11±33.64

2,3-Di-(3-cyclohexylpropyl)-anthracene (32)

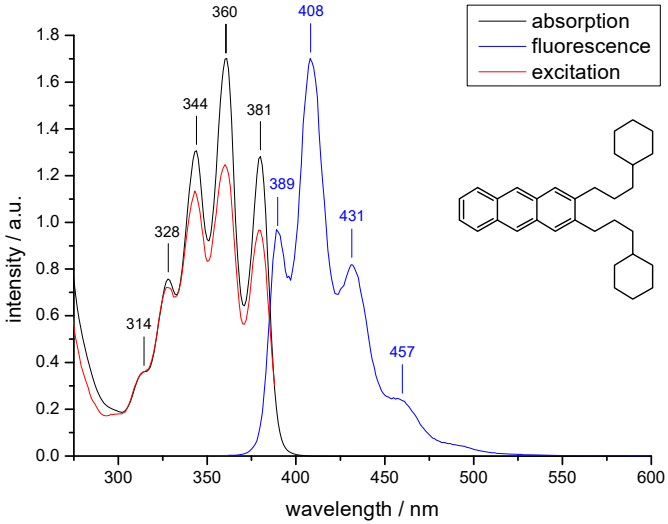

Figure S100. A solution (c = $2.8 \cdot 10^{-4}$ mol·L^{-1}) of **32** was used for both the absorption and fluorescence spectra, excitation wavelength: 361 nm

λ_{max} / nm	314	328	344	361	380
ε / L·mol^{-1}·cm^{-1}	1296.35±6.13	2725.76±9.47	4703.86±14.75	6132.11±19.15	4619.46±12.82

2,3-Di-(ethyl-2-(1-adamantyl))-anthracene (35)

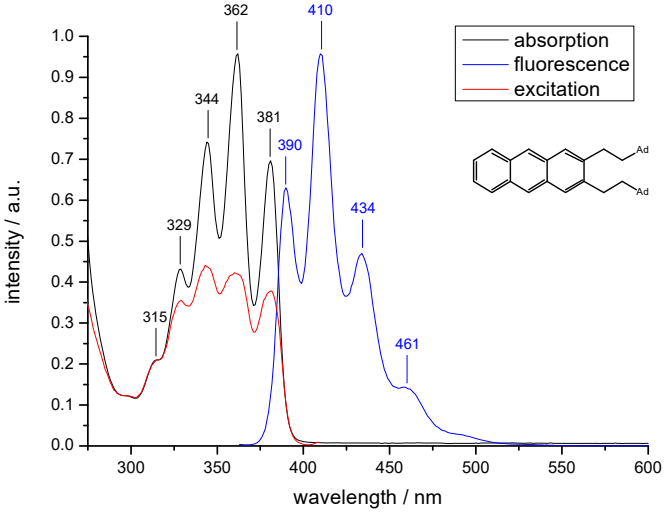

Figure S 101. A solution (c = $1.3 \cdot 10^{-4}$ mol·L^{-1}) of **35** was used for both the absorption and fluorescence spectra, excitation wavelength: 362 nm

λ_{max} / nm	315	329	344	362	381
ε / L·mol^{-1}·cm^{-1}	1570.01±22.98	3232.32±38.41	5558.19±60.55	7178.88±78.78	5185.50±60.42

2,3-Di-neopentyl-anthracene (36)

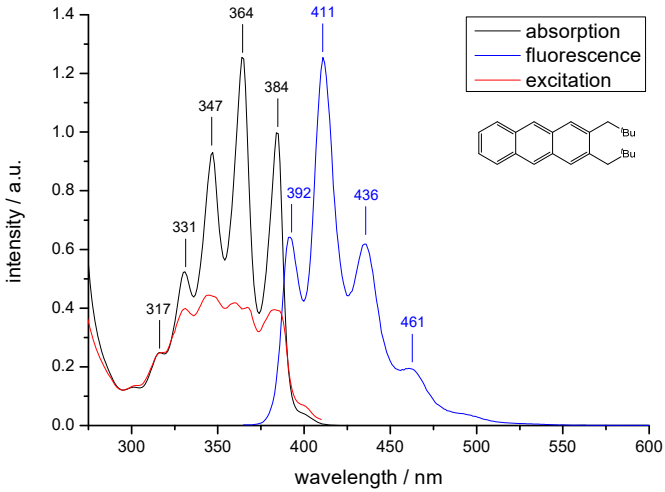

Figure S 102. A solution (c = $1.9 \cdot 10^{-4}$ mol·L^{-1}) of **36** was used for both the absorption and fluorescence spectra, excitation wavelength: 364 nm

λ_{max} / nm	316	331	347	364	384
ε / L·mol^{-1}·cm^{-1}	1050.16±22.98	2409.64±26.56	4395.77±45.53	5972.85±62.93	4722.92±48.88

3. Crystal structure data

Single crystals of the respective compounds were investigated on either a Bruker APEX II DUO instrument equipped with an IμS microfocus sealed tube, a Bruker Smart APEX II diffractometer with graphite monochromator or a Bruker Smart APEX diffractometer with synchrotron radiation source (λ = 0.8 Å). The data collection strategy was determined using COSMO[1] employing ω- and φ-scans. Raw data were processed using APEX[2,3] and SAINT,[4,5] corrections for absorption effects were applied using SADABS.[6] The structure was solved by direct methods and refined against all data by full-matrix least-squares methods on F^2 using SHELXTL[7] and Shelxle.[8]

2,3-Di-(3-cyclohexylpropyl)-9,10-anthraquinone (31c)

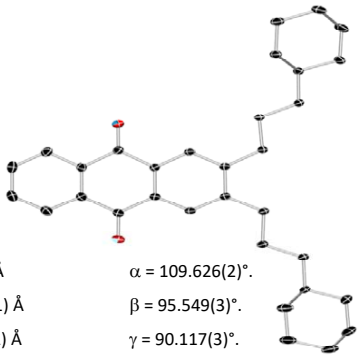

Empirical formula	C32 H40 O2	
Formula weight	456.64	
Temperature	100(2) K	
Wavelength	0.71073 Å	
Crystal system	Triclinic	
Space group	P -1	
Unit cell dimensions	a = 8.3688(7) Å	α = 109.626(2)°.
	b = 12.6818(11) Å	β = 95.549(3)°.
	c = 12.7859(11) Å	γ = 90.117(3)°.
Volume	1271.30(19) $Å^3$	
Z	2	
Density (calculated)	1.193 Mg/m^3	
Absorption coefficient	0.072 mm^{-1}	
F(000)	496	
Crystal size	0.278 x 0.136 x 0.064 mm^3	
Theta range for data collection	1.706 to 27.103°.	
Index ranges	-10<=h<=10, -16<=k<=16, -16<=l<=16	
Reflections collected	45809	
Independent reflections	5619 [R(int) = 0.0488]	
Completeness to theta = 25.242°	100.0 %	
Absorption correction	Numerical	
Max. and min. transmission	0.7458 and 0.6866	
Refinement method	Full-matrix least-squares on F^2	
Data / restraints / parameters	5619 / 0 / 307	
Goodness-of-fit on F^2	1.032	
Final R indices [I>2sigma(I)]	R1 = 0.0413, wR2 = 0.1081	
R indices (all data)	R1 = 0.0567, wR2 = 0.1187	

Extinction coefficient	n/a
Largest diff. peak and hole	0.325 and -0.210 e.Å^{-3}
CCDC	1915075

The ellipsoid probability was set to 50 %.

2,3-Di-(ethyl-2-(1-adamantyl))-9,10-anthraquinone (31d)

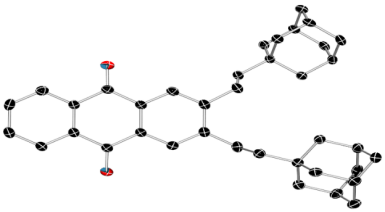

Empirical formula	C38 H44 O2	
Formula weight	532.73	
Temperature	100(2) K	
Wavelength	0.71073 Å	
Crystal system	Monoclinic	
Space group	$P2_1/n$	
Unit cell dimensions	a = 12.2567(12) Å	α = 90°.
	b = 17.8763(18) Å	β = 103.004(2)°.
	c = 13.3141(13) Å	γ = 90°.
Volume	2842.4(5) Å^3	
Z	4	
Density (calculated)	1.245 Mg/m^3	
Absorption coefficient	0.075 mm^{-1}	
F(000)	1152	
Crystal size	0.362 x 0.129 x 0.078 mm^3	
Theta range for data collection	2.051 to 25.682°.	
Index ranges	-14<=h<=14, -21<=k<=21, -16<=l<=16	
Reflections collected	45736	
Independent reflections	5393 [R(int) = 0.0672]	
Completeness to theta = 25.242°	99.9 %	
Absorption correction	Semi-empirical from equivalents	
Max. and min. transmission	0.7458 and 0.6653	
Refinement method	Full-matrix least-squares on F^2	
Data / restraints / parameters	5393 / 0 / 361	
Goodness-of-fit on F^2	1.025	
Final R indices [I>2sigma(I)]	R1 = 0.0430, wR2 = 0.1045	
R indices (all data)	R1 = 0.0602, wR2 = 0.1183	
Extinction coefficient	n/a	
Largest diff. peak and hole	0.221 and -0.223 e.Å^{-3}	
CCDC	1915079	

The ellipsoid probability was set to 50 %.

9-Oxa-1,2,3,4*b*,5,6,7,8,8*a*,9,10,10*a*-dodecahydrophenanthrene-10-spiro-1-cyclohexane (33)

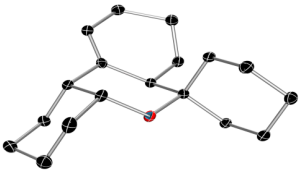

Empirical formula	C18 H28 O	
Formula weight	260.40	
Temperature	103(2) K	
Wavelength	0.71073 Å	
Crystal system	Triclinic	
Space group	P -1	
Unit cell dimensions	a = 8.4055(9) Å	α = 67.685(3)°.
	b = 9.6574(10) Å	β = 70.571(3)°.
	c = 10.6928(11) Å	γ = 66.514(3)°.
Volume	719.45(13) Å^3	
Z	2	
Density (calculated)	1.202 Mg/m^3	
Absorption coefficient	0.071 mm^{-1}	
F(000)	288	
Crystal size	0.273 x 0.131 x 0.047 mm^3	
Theta range for data collection	2.107 to 28.803°.	
Index ranges	-11<=h<=11, -13<=k<=13, -14<=l<=14	
Reflections collected	16335	
Independent reflections	3756 [R(int) = 0.0414]	
Completeness to theta = 25.242°	99.9 %	
Absorption correction	Semi-empirical from equivalents	
Max. and min. transmission	0.7458 and 0.6996	
Refinement method	Full-matrix least-squares on F^2	
Data / restraints / parameters	3756 / 0 / 172	
Goodness-of-fit on F^2	1.045	
Final R indices [I>2sigma(I)]	R1 = 0.0427, wR2 = 0.0998	
R indices (all data)	R1 = 0.0581, wR2 = 0.1095	
Extinction coefficient	n/a	
Largest diff. peak and hole	0.347 and -0.243 e.Å^{-3}	
CCDC	1915074	

The ellipsoid probability was set to 50 %.

***2,6'*-Di-*tert-butyl*-dianthracene (37a)**

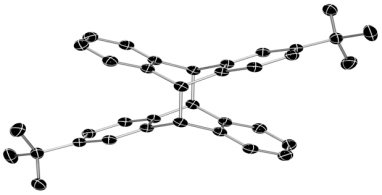

Empirical formula	C36 H36	
Formula weight	468.65	
Temperature/K	150	
Crystal system	Monoclinic	
Space group	$P2_1/c$	
Unit cell dimensions	a = 13.8935(15) Å	α = 90°
	b = 7.9659(9) Å	β = 93.3580(10) °
	c = 11.9709(13) Å	γ = 90°
Volume/Å^3	1322.6(3)	
Z	2	
ρ_{calc}g/cm^3	1.177	
μ/mm^{-1}	0.085	
F(000)	504.0	
Crystal size/mm^3	0.1 × 0.1 × 0.03	
Radiation	synchrotron (λ = 0.79942)	
2Θ range for data collection/°	6.608 to 59.79	
Index ranges	-17 ≤ h ≤ 17, -7 ≤ k ≤ 9, -14 ≤ l ≤ 14	
Reflections collected	6924	
Independent reflections	2569 [R_{int} = 0.0274, R_{sigma} = 0.0286]	
Data/restraints/parameters	2569/0/166	
Goodness-of-fit on F^2	1.068	
Final R indexes [I>=2σ (I)]	R_1 = 0.0407, wR_2 = 0.1015	
Final R indexes [all data]	R_1 = 0.0427, wR_2 = 0.1032	
Largest diff. peak/hole / e Å^{-3}	0.25/-0.16	
CCDC	1915073	

The ellipsoid probability was set to 50 %.

2,7'-Di-*tert-butyl*-dianthracene (37b)

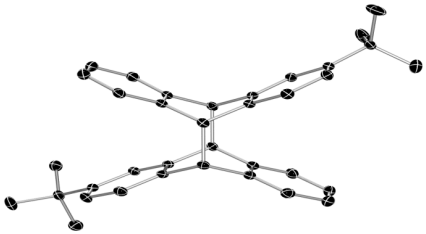

Empirical formula	C36 H36	
Formula weight	468.65	
Temperature	100(2) K	
Wavelength	0.71073 Å	
Crystal system	Monoclinic	
Space group	C 2	
Unit cell dimensions	a = 30.492(3) Å	α = 90°.
	b = 6.8073(8) Å	β = 90.618(2)°.
	c = 12.6172(14) Å	γ = 90°.
Volume	2618.8(5) Å^3	
Z	4	
Density (calculated)	1.189 Mg/m^3	
Absorption coefficient	0.067 mm^{-1}	
F(000)	1008	
Crystal size	0.425 x 0.106 x 0.074 mm^3	
Theta range for data collection	1.336 to 28.278°.	
Index ranges	-40<=h<=40, -9<=k<=9, -16<=l<=16	
Reflections collected	26214	
Independent reflections	6493 [R(int) = 0.0373]	
Completeness to theta = 25.242°	100.0 %	
Absorption correction	Numerical	
Max. and min. transmission	0.7445 and 0.6789	
Refinement method	Full-matrix least-squares on F^2	
Data / restraints / parameters	6493 / 1 / 331	
Goodness-of-fit on F^2	1.035	
Final R indices [I>2sigma(I)]	R1 = 0.0377, wR2 = 0.0933	
R indices (all data)	R1 = 0.0422, wR2 = 0.0968	
Absolute structure parameter	-1.2(10)	
Extinction coefficient	n/a	
Largest diff. peak and hole	0.308 and -0.237 e.Å^{-3}	
CCDC	1915078	

The ellipsoid probability was set to 50 %.

2,3',6,7'-Tetra-*tert*-butyl-dianthracene (38a)

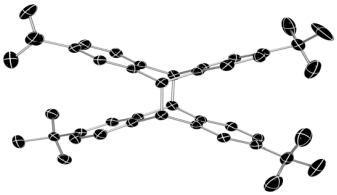

Empirical formula	C44 H52	
Formula weight	580.85	
Temperature	152(2) K	
Wavelength	1.54178 Å	
Crystal system	Orthorhombic	
Space group	P 21 21 2	
Unit cell dimensions	a = 18.9017(16) Å	α = 90°.
	b = 26.689(3) Å	β = 90°.
	c = 6.9776(6) Å	γ = 90°.
Volume	3520.0(5) Å^3	
Z	4	
Density (calculated)	1.096 Mg/m^3	
Absorption coefficient	0.453 mm^{-1}	
F(000)	1264	
Crystal size	0.336 x 0.126 x 0.074 mm^3	
Theta range for data collection	2.865 to 66.890°.	
Index ranges	-22<=h<=22, -31<=k<=31, -8<=l<=8	
Reflections collected	38920	
Independent reflections	6218 [R(int) = 0.0923]	
Completeness to theta = 66.890°	99.6 %	
Absorption correction	Semi-empirical from equivalents	
Max. and min. transmission	0.7528 and 0.6987	
Refinement method	Full-matrix least-squares on F^2	
Data / restraints / parameters	6218 / 0 / 424	
Goodness-of-fit on F^2	1.016	
Final R indices [I>2sigma(I)]	R1 = 0.0347, wR2 = 0.0789	
R indices (all data)	R1 = 0.0598, wR2 = 0.0829	
Absolute structure parameter	0.5(12)	
Extinction coefficient	n/a	
Largest diff. peak and hole	0.133 and -0.177 e.Å^{-3}	
CCDC	1915076	

The ellipsoid probability was set to 50 %.

2,3,6′,7′-Tetramethyl-dianthracene (39a)

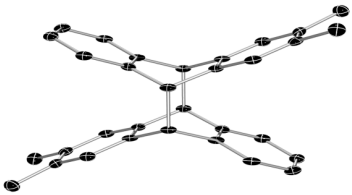

Empirical formula	C32 H28	
Formula weight	412.58	
Temperature	152(2) K	
Crystal system	Monoclinic	
Space group	P -1	
Unit cell dimensions	a = 8.3036(12) Å	α = 83.627(7)°
	b = 8.4034(12) Å	β = 87.534(7)°
	c = 11.0420(17) Å	γ = 87.470(6)°
Volume/Å^3	764.422	

Due to a poor R-value no further structural information is given. The ellipsoid probability was set to 50 %.

2,3,6',7'-Tetra-*n*-butyl-dianthracene (40a)

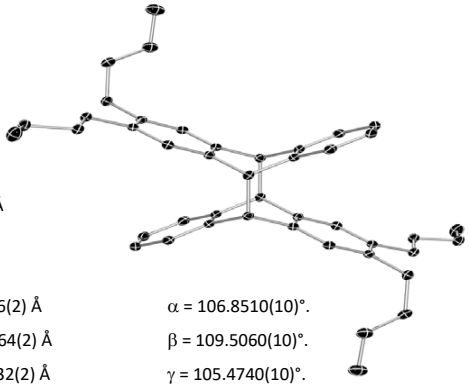

Empirical formula	C44 H52	
Formula weight	580.86	
Temperature	100(2) K	
Wavelength	0.71073 Å	
Crystal system	Triclinic	
Space group	P -1	
Unit cell dimensions	a = 9.7346(2) Å	α = 106.8510(10)°.
	b = 10.0564(2) Å	β = 109.5060(10)°.
	c = 10.2632(2) Å	γ = 105.4740(10)°.
Volume	829.51(3) Å^3	
Z	1	
Density (calculated)	1.163 Mg/m^3	
Absorption coefficient	0.065 mm^{-1}	
F(000)	316	
Crystal size	0.1 x 0.1 x 0.1 mm^3	
Theta range for data collection	2.312 to 27.054°.	
Index ranges	-12<=h<=12, -12<=k<=12, -13<=l<=12	
Reflections collected	22418	
Independent reflections	3631 [R(int) = 0.0138]	
Completeness to theta = 25.242°	99.9 %	
Absorption correction	Semi-empirical from equivalents	
Max. and min. transmission	0.7455 and 0.7177	
Refinement method	Full-matrix least-squares on F^2	
Data / restraints / parameters	3631 / 0 / 201	
Goodness-of-fit on F^2	1.008	
Final R indices [I>2sigma(I)]	R1 = 0.0380, wR2 = 0.1053	
R indices (all data)	R1 = 0.0412, wR2 = 0.1088	
Extinction coefficient	n/a	
Largest diff. peak and hole	0.363 and -0.192 e.Å^{-3}	
CCDC	1915080	

The ellipsoid probability was set to 50 %.

2,2',3,3'-Tetra-*iso*-butyl-dianthracene (41b)

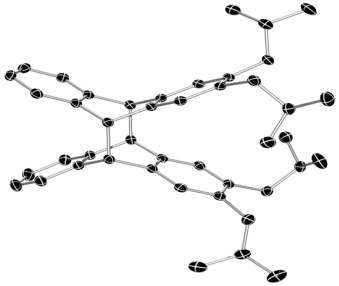

Empirical formula	C44 H52	
Formula weight	580.85	
Temperature	100(2) K	
Wavelength	0.71073 Å	
Crystal system	Triclinic	
Space group	P -1	
Unit cell dimensions	a = 13.0562(4) Å	α = 82.2500(10)°.
	b = 14.1031(4) Å	β = 74.0370(10)°.
	c = 22.1469(6) Å	γ = 62.8200(10)°.
Volume	3487.58(18) Å^3	
Z	4	
Density (calculated)	1.106 Mg/m^3	
Absorption coefficient	0.062 mm^{-1}	
F(000)	1264	
Crystal size	0.358 x 0.181 x 0.094 mm^3	
Theta range for data collection	1.821 to 27.103°.	
Index ranges	-16<=h<=16, -18<=k<=18, -28<=l<=28	
Reflections collected	87232	
Independent reflections	15369 [R(int) = 0.0394]	
Completeness to theta = 25.242°	99.9 %	
Absorption correction	Semi-empirical from equivalents	
Max. and min. transmission	0.7458 and 0.7039	
Refinement method	Full-matrix least-squares on F^2	
Data / restraints / parameters	15369 / 0 / 809	
Goodness-of-fit on F^2	1.023	
Final R indices [I>2sigma(I)]	R1 = 0.0415, wR2 = 0.0993	
R indices (all data)	R1 = 0.0565, wR2 = 0.1100	
Extinction coefficient	n/a	
Largest diff. peak and hole	0.294 and -0.223 e.Å^{-3}	
CCDC	1915077	

The ellipsoid probability was set to 50 %.

4. Selected bond lengths and angles for compound 33

Table S1. Comparison of experimental and calculated (B3LYP/def2TZVP) bond lengths and angles for compound **33** (left) and cyclohexene (right). Numbering on the ring containing the double bond is adjusted to match the numbering in cyclohexene. Hydrogen atoms are omitted for clarity, the ellipsoid probability was set to 50 %.

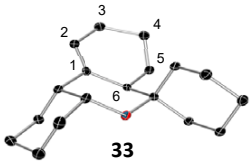

33

	r (C-C) / Å				∠ (C-C-C) / °		
	33	calcd.	cyclohexene		**33**	calcd.	cyclohexene
C1-C2	1.335(2)	1.387	1.335	C6-C1-C2	123.6(1)	120.9	123.5
C2-C3	1.501(2)	1.496	1.504	C1-C2-C3	124.4(1)	123.4	123.5
C3-C4	1.526(2)	1.527	1.515	C2-C3-C4	110.8(1)	111.2	112
C4-C5	1.529(2)	1.529	1.550	C3-C4-C5	110.9(1)	110.3	111
C5-C6	1.546(2)	1.510	1.515	C4-C5-C6	114.6(1)	112.6	111
C6-C1	1.515(2)	1.400	1.504	C5-C6-C1	112.0(1)	118.8	112

5. Cartesian coordinates

B3LYP/def2TZVP			
33			
E(SCF) = -777.64872911			
C	15.013653000	-8.659661000	-0.582093000
C	14.708960000	-9.977516000	0.135152000
C	13.877028000	-8.338952000	-1.571433000
C	14.443704000	-11.129899000	-0.840949000
C	13.579582000	-9.482192000	-2.545163000
C	13.293135000	-10.782947000	-1.791200000
C	16.427459000	-8.702522000	-1.155827000
C	17.385685000	-9.496756000	-0.514724000
O	15.699673000	-10.254524000	1.116286000
C	17.086169000	-10.302934000	0.733699000
C	16.768843000	-7.911819000	-2.242685000
C	18.137362000	-7.889498000	-2.846572000
C	18.815082000	-9.443708000	-0.998809000
C	18.916387000	-9.155232000	-2.497022000
H	13.800018000	-9.837878000	0.729620000
H	12.976091000	-8.140016000	-0.980174000
H	14.082023000	-7.414262000	-2.113135000
H	15.340227000	-11.335390000	-1.430250000
H	14.217684000	-12.033102000	-0.269083000
H	12.729272000	-9.215530000	-3.178676000
H	14.433654000	-9.630269000	-3.213291000
H	13.127105000	-11.604152000	-2.493092000
H	12.365438000	-10.672834000	-1.217320000
H	16.025961000	-7.260273000	-2.682049000
H	18.067718000	-7.765392000	-3.931793000
H	18.689216000	-7.007805000	-2.486948000
H	19.351295000	-8.654723000	-0.451567000
H	19.342194000	-10.369642000	-0.766456000
H	18.500489000	-10.000404000	-3.053637000
H	19.963641000	-9.059625000	-2.793333000
C	17.848324000	-9.699015000	1.942220000
C	17.634671000	-10.491129000	3.235061000
C	18.013589000	-11.963340000	3.062215000
C	17.496020000	-11.796172000	0.589966000
C	17.268831000	-12.588545000	1.880584000
H	17.523776000	-8.663705000	2.068569000
H	18.915812000	-9.677313000	1.704657000
H	18.224900000	-10.038948000	4.037238000
H	16.585904000	-10.415725000	3.531923000
H	19.094380000	-12.043185000	2.892137000
H	17.801745000	-12.518664000	3.979907000
H	16.942549000	-12.245820000	-0.235084000
H	18.554858000	-11.853723000	0.326670000

H	17.593743000	-13.622158000	1.731671000
H	16.199065000	-12.620419000	2.100956000
H	15.007587000	-7.879684000	0.187836000

B3LYP-D3/def2TZVP

2

E(SCF) = -1079.46918356

C	1.766546000	-0.531580000	0.701451000
C	1.766494000	-0.531804000	-0.699035000
C	2.690363000	-1.304327000	1.389608000
C	2.690217000	-1.304824000	-1.387014000
C	3.614669000	-2.081343000	0.695635000
C	3.614589000	-2.081612000	-0.692863000
C	0.735060000	0.338366000	1.386504000
C	0.745258000	1.687943000	0.701098000
C	0.735089000	0.338038000	-1.384567000
C	0.745446000	1.687841000	-0.699586000
C	0.757370000	2.892376000	1.389238000
C	0.766009000	4.099595000	0.694779000
C	0.757849000	2.892116000	-1.387947000
C	0.766257000	4.099476000	-0.693690000
C	-0.745258000	-1.687943000	0.701098000
C	-0.745446000	-1.687841000	-0.699586000
C	-0.757370000	-2.892376000	1.389238000
C	-0.757849000	-2.892116000	-1.387947000
C	-0.766009000	-4.099595000	0.694779000
C	-0.766257000	-4.099476000	-0.693690000
C	-0.735060000	-0.338366000	1.386504000
C	-1.766546000	0.531580000	0.701451000
C	-0.735089000	-0.338038000	-1.384567000
C	-1.766494000	0.531804000	-0.699035000
C	-2.690363000	1.304327000	1.389608000
C	-3.614669000	2.081343000	0.695635000
C	-2.690217000	1.304824000	-1.387014000
C	-3.614589000	2.081612000	-0.692863000
H	2.690187000	-1.301930000	2.473537000
H	2.689926000	-1.302870000	-2.470945000
H	4.333896000	-2.680387000	1.239764000
H	4.333661000	-2.680970000	-1.236847000
H	1.010550000	0.465438000	2.433207000
H	1.011079000	0.464634000	-2.431203000
H	0.758911000	2.890900000	2.473143000
H	0.759735000	2.890415000	-2.471852000
H	-0.758911000	-2.890900000	2.473143000
H	-0.759735000	-2.890415000	-2.471852000
H	-1.010550000	-0.465438000	2.433207000
H	-1.011079000	-0.464634000	-2.431203000
H	-2.690187000	1.301930000	2.473537000
H	-4.333896000	2.680387000	1.239764000

H	-2.689926000	1.302870000	-2.470945000
H	-4.333661000	2.680970000	-1.236847000
H	0.775126000	5.035916000	1.238418000
H	0.775759000	5.035622000	-1.237628000
H	-0.775759000	-5.035622000	-1.237628000
H	-0.775126000	-5.035916000	1.238418000

37a

E(SCF) = -1394.12286731

C	1.643686000	-0.597861000	0.910966000
C	1.906570000	-0.270919000	-0.425651000
C	2.476547000	-1.482637000	1.580004000
C	3.001180000	-0.831788000	-1.067338000
C	3.571350000	-2.048083000	0.930722000
C	3.834335000	-1.721423000	-0.393032000
C	0.430205000	0.043230000	1.548185000
C	0.437154000	1.510381000	1.185503000
C	0.948323000	0.686424000	-1.100537000
C	0.693849000	1.836768000	-0.151351000
C	0.185321000	2.529702000	2.085514000
C	0.166790000	3.860200000	1.668260000
C	0.680395000	3.159686000	-0.554021000
C	0.405770000	4.203730000	0.339895000
C	-0.693849000	-1.836768000	0.151351000
C	-0.437154000	-1.510381000	-1.185503000
C	-0.680395000	-3.159686000	0.554021000
C	-0.185321000	-2.529702000	-2.085514000
C	-0.405770000	-4.203730000	-0.339895000
C	-0.166790000	-3.860200000	-1.668260000
C	-0.948323000	-0.686424000	1.100537000
C	-1.906570000	0.270919000	0.425651000
C	-0.430205000	-0.043230000	-1.548185000
C	-1.643686000	0.597861000	-0.910966000
C	-3.001180000	0.831788000	1.067338000
C	-3.834335000	1.721423000	0.393032000
C	-2.476547000	1.482637000	-1.580004000
C	-3.571350000	2.048083000	-0.930722000
C	-0.362776000	-5.647901000	0.173925000
C	0.362776000	5.647901000	-0.173925000
H	2.268336000	-1.737644000	2.612741000
H	3.204007000	-0.578943000	-2.101734000
H	4.216370000	-2.738146000	1.459948000
H	4.685985000	-2.155178000	-0.901822000
H	0.492482000	-0.061992000	2.631073000
H	1.402581000	1.066207000	-2.015442000
H	-0.012487000	2.293418000	3.124960000
H	0.874315000	3.380946000	-1.596677000
H	-0.874315000	-3.380946000	1.596677000
H	0.012487000	-2.293418000	-3.124960000

H	-1.402581000	-1.066207000	2.015442000
H	-0.492482000	0.061992000	-2.631073000
H	-3.204007000	0.578943000	2.101734000
H	-4.685985000	2.155178000	0.901822000
H	-2.268336000	1.737644000	-2.612741000
H	-4.216370000	2.738146000	-1.459948000
H	-0.042226000	4.623721000	2.403100000
H	0.042226000	-4.623721000	-2.403100000
C	0.034039000	6.654974000	0.937049000
H	0.783292000	6.639373000	1.730772000
H	0.012569000	7.664613000	0.522387000
H	-0.943146000	6.459491000	1.382614000
C	1.731700000	6.024943000	-0.774803000
H	2.004471000	5.370478000	-1.603570000
H	1.711542000	7.050519000	-1.151680000
H	2.517718000	5.953740000	-0.020425000
C	-0.725055000	5.763287000	-1.262223000
H	-0.515196000	5.114589000	-2.113261000
H	-1.701369000	5.481885000	-0.863030000
H	-0.785902000	6.790062000	-1.631469000
C	0.725055000	-5.763287000	1.262223000
H	1.701369000	-5.481885000	0.863030000
H	0.515196000	-5.114589000	2.113261000
H	0.785902000	-6.790062000	1.631469000
C	-1.731700000	-6.024943000	0.774803000
H	-2.517718000	-5.953740000	0.020425000
H	-1.711542000	-7.050519000	1.151680000
H	-2.004471000	-5.370478000	1.603570000
C	-0.034039000	-6.654974000	-0.937049000
H	-0.012569000	-7.664613000	-0.522387000
H	-0.783292000	-6.639373000	-1.730772000
H	0.943146000	-6.459491000	-1.382614000

37b

E(SCF) = -1394.12235631

C	-0.497375000	1.775112000	-0.258356000
C	-0.497451000	1.775618000	1.142446000
C	-1.266390000	2.701836000	-0.946843000
C	-1.266005000	2.703525000	1.829835000
C	-2.040819000	3.628947000	-0.253243000
C	-2.040296000	3.629947000	1.135243000
C	0.354640000	0.729380000	-0.944141000
C	1.702140000	0.702542000	-0.257314000
C	0.355378000	0.729871000	1.827993000
C	1.700504000	0.705967000	1.138145000
C	2.901613000	0.650377000	-0.954399000
C	4.131151000	0.593650000	-0.294523000
C	2.913842000	0.667449000	1.809063000
C	4.108826000	0.610062000	1.102954000

C	-1.702140000	-0.702528000	-0.257311000
C	-1.700504000	-0.705954000	1.138148000
C	-2.901613000	-0.650369000	-0.954396000
C	-2.913843000	-0.667454000	1.809066000
C	-4.131151000	-0.593646000	-0.294521000
C	-4.108828000	-0.610075000	1.102956000
C	-0.354640000	-0.729367000	-0.944138000
C	0.497376000	-1.775097000	-0.258350000
C	-0.355378000	-0.729852000	1.827995000
C	0.497451000	-1.775600000	1.142452000
C	1.266390000	-2.701825000	-0.946833000
C	2.040820000	-3.628933000	-0.253229000
C	1.266007000	-2.703502000	1.829844000
C	2.040298000	-3.629927000	1.135257000
H	-1.266431000	2.699154000	-2.030824000
H	-1.266513000	2.701772000	2.913774000
H	-2.638605000	4.349065000	-0.797734000
H	-2.638105000	4.350481000	1.679072000
H	0.487270000	1.002955000	-1.990665000
H	0.489629000	1.002919000	2.874445000
H	2.860566000	0.642210000	-2.034754000
H	2.930215000	0.671077000	2.893090000
H	-2.860565000	-0.642204000	-2.034751000
H	-2.930218000	-0.671094000	2.893093000
H	-0.487271000	-1.002946000	-1.990661000
H	-0.489627000	-1.002897000	2.874449000
H	1.266431000	-2.699147000	-2.030814000
H	2.638606000	-4.349052000	-0.797717000
H	1.266516000	-2.701744000	2.913784000
H	2.638108000	-4.350458000	1.679089000
C	5.468947000	0.498614000	-1.039525000
C	6.358711000	1.700087000	-0.662923000
C	6.178129000	-0.811129000	-0.637693000
C	5.290873000	0.496082000	-2.564344000
H	5.879607000	2.639578000	-0.945554000
H	6.556935000	1.735324000	0.408687000
H	7.320035000	1.637672000	-1.178997000
H	5.558409000	-1.676064000	-0.882028000
H	7.128533000	-0.906963000	-1.168582000
H	6.388176000	-0.843533000	0.431888000
H	6.267386000	0.429341000	-3.047717000
H	4.696846000	-0.356058000	-2.900309000
H	4.809914000	1.410724000	-2.916478000
H	5.037272000	0.572821000	1.658137000
C	-5.468948000	-0.498636000	-1.039523000
C	-5.290886000	-0.496318000	-2.564345000
C	-6.358768000	-1.700011000	-0.662750000
C	-6.178059000	0.811199000	-0.637861000
H	-4.696755000	0.355704000	-2.900422000
H	-4.810044000	-1.411066000	-2.916368000
H	-6.267393000	-0.429518000	-3.047719000
H	-6.556953000	-1.735112000	0.408872000

H	-7.320108000	-1.637600000	-1.178794000
H	-5.879731000	-2.639564000	-0.945289000
H	-7.128443000	0.907029000	-1.168787000
H	-6.388134000	0.843741000	0.431710000
H	-5.558278000	1.676066000	-0.882281000
H	-5.037276000	-0.572860000	1.658138000

38a

E(SCF) = -1708.77787212

C	-1.378773000	-1.209637000	-0.693152000
C	-1.355430000	-1.241398000	0.701920000
C	-1.835080000	-2.322432000	-1.383983000
C	-1.758545000	-2.386347000	1.377394000
C	-2.227704000	-3.464470000	-0.699348000
C	-2.182208000	-3.529172000	0.696169000
C	-0.814565000	0.018717000	-1.363553000
C	-1.355534000	1.243329000	-0.656342000
C	-0.814685000	-0.017646000	1.411127000
C	-1.378773000	1.212023000	0.743328000
C	-1.766183000	2.382747000	-1.325147000
C	-2.200050000	3.527954000	-0.643214000
C	-1.839495000	2.319755000	1.431152000
C	-2.242551000	3.465838000	0.747412000
C	1.355534000	-1.243329000	-0.656342000
C	1.378773000	-1.212023000	0.743328000
C	1.766183000	-2.382747000	-1.325147000
C	1.839495000	-2.319755000	1.431152000
C	2.200050000	-3.527954000	-0.643214000
C	2.242551000	-3.465838000	0.747412000
C	0.814565000	-0.018717000	-1.363553000
C	1.378773000	1.209637000	-0.693152000
C	0.814685000	0.017646000	1.411127000
C	1.355430000	1.241398000	0.701920000
C	1.835080000	2.322432000	-1.383983000
C	2.227704000	3.464470000	-0.699348000
C	1.758545000	2.386347000	1.377394000
C	2.182208000	3.529172000	0.696169000
C	2.566107000	-4.788366000	-1.436020000
H	-1.858637000	-2.310831000	-2.467852000
H	-1.707090000	-2.382858000	2.457378000
H	-2.557564000	-4.322857000	-1.270090000
H	-1.118516000	0.040961000	-2.409994000
H	-1.118311000	-0.041193000	2.457600000
H	-1.718944000	2.387781000	-2.407604000
H	-1.863486000	2.308303000	2.515076000
H	1.718944000	-2.387781000	-2.407604000
H	1.863486000	-2.308303000	2.515076000
H	1.118516000	-0.040961000	-2.409994000
H	1.118311000	0.041193000	2.457600000

H	1.858637000	2.310831000	-2.467852000
H	2.557564000	4.322857000	-1.270090000
H	1.707090000	2.382858000	2.457378000
H	2.579401000	-4.314384000	1.324690000
C	1.323505000	-5.264167000	-2.217773000
H	0.501468000	-5.487072000	-1.535486000
H	0.973987000	-4.506046000	-2.919543000
H	1.555210000	-6.167984000	-2.786799000
C	3.705573000	-4.471203000	-2.424529000
H	4.596818000	-4.133803000	-1.891753000
H	3.968137000	-5.361677000	-3.001126000
H	3.422574000	-3.689487000	-3.129962000
C	3.025216000	-5.938266000	-0.528194000
H	3.273920000	-6.809410000	-1.137340000
H	3.914360000	-5.670736000	0.046023000
H	2.241534000	-6.237216000	0.170450000
C	2.544274000	4.836956000	1.411279000
C	1.559510000	5.935997000	0.958954000
C	2.452224000	4.715457000	2.938998000
C	3.982661000	5.254459000	1.048695000
H	1.625652000	6.117551000	-0.114450000
H	0.531221000	5.647027000	1.185084000
H	1.774579000	6.876736000	1.472008000
H	3.132429000	3.953912000	3.325478000
H	2.724631000	5.667230000	3.399152000
H	1.439653000	4.469309000	3.264421000
H	4.241703000	6.193673000	1.543618000
H	4.697958000	4.492758000	1.365166000
H	4.102956000	5.399872000	-0.025166000
H	-2.579401000	4.314384000	1.324690000
C	-2.544274000	-4.836956000	1.411279000
C	-1.559510000	-5.935997000	0.958954000
C	-2.452224000	-4.715457000	2.938998000
C	-3.982661000	-5.254459000	1.048695000
H	-1.625652000	-6.117551000	-0.114450000
H	-0.531221000	-5.647027000	1.185084000
H	-1.774579000	-6.876736000	1.472008000
H	-3.132429000	-3.953912000	3.325478000
H	-2.724631000	-5.667230000	3.399152000
H	-1.439653000	-4.469309000	3.264421000
H	-4.241703000	-6.193673000	1.543618000
H	-4.697958000	-4.492758000	1.365166000
H	-4.102956000	-5.399872000	-0.025166000
C	-2.566107000	4.788366000	-1.436020000
C	-3.025216000	5.938266000	-0.528194000
C	-1.323505000	5.264167000	-2.217773000
C	-3.705573000	4.471203000	-2.424529000
H	-3.914360000	5.670736000	0.046023000
H	-2.241534000	6.237216000	0.170450000
H	-3.273920000	6.809410000	-1.137340000
H	-0.973987000	4.506046000	-2.919543000
H	-1.555210000	6.167984000	-2.786799000

H	-0.501468000	5.487072000	-1.535486000
H	-3.968137000	5.361677000	-3.001126000
H	-3.422574000	3.689487000	-3.129962000
H	-4.596818000	4.133803000	-1.891753000

40a

E(SCF) = -1708.77545166

C	-0.012285000	0.301786000	1.926795000
C	0.011982000	-1.060300000	1.598784000
C	-0.515951000	0.704383000	3.154995000
C	-0.467755000	-1.994267000	2.505216000
C	-1.000400000	-0.236198000	4.061052000
C	-0.976247000	-1.585791000	3.736013000
C	0.526815000	1.266721000	0.893215000
C	1.834328000	0.705555000	0.379991000
C	0.575209000	-1.431260000	0.243671000
C	1.857755000	-0.652803000	0.051500000
C	2.977686000	1.462966000	0.200534000
C	4.164004000	0.913972000	-0.299789000
C	3.025383000	-1.206392000	-0.440248000
C	4.189246000	-0.451344000	-0.620359000
C	-1.816610000	0.755045000	-0.111577000
C	-1.793480000	-0.603280000	-0.439789000
C	-2.984687000	1.309995000	0.378209000
C	-2.937679000	-1.360365000	-0.262003000
C	-4.148990000	0.555717000	0.555868000
C	-4.124085000	-0.810133000	0.235803000
C	-0.533840000	1.533134000	-0.303377000
C	0.029402000	1.161952000	-1.658477000
C	-0.485870000	-1.164845000	-0.952655000
C	0.053269000	-0.200147000	-1.986457000
C	0.509230000	2.095753000	-2.565031000
C	1.017418000	1.687095000	-3.795897000
C	0.556599000	-0.602934000	-3.214727000
C	1.041149000	0.337485000	-4.120903000
H	-0.534254000	1.758515000	3.407030000
H	-0.448607000	-3.047702000	2.250326000
H	-1.390927000	0.086330000	5.018086000
H	-1.348239000	-2.321440000	4.438062000
H	0.707047000	2.233733000	1.362416000
H	0.793958000	-2.498753000	0.224974000
H	2.952582000	2.520254000	0.444084000
H	3.040645000	-2.259785000	-0.701999000
H	-2.999509000	2.363493000	0.639457000
H	-2.912946000	-2.417701000	-0.505346000
H	-0.752370000	2.600675000	-0.284909000
H	-0.666296000	-2.131912000	-1.421663000
H	0.490393000	3.149206000	-2.310184000
H	1.389510000	2.422614000	-4.498030000

H	0.574542000	-1.657081000	-3.466726000
H	1.431450000	0.014822000	-5.077983000
C	-5.388715000	1.263358000	1.052141000
H	-6.131492000	0.540355000	1.384876000
H	-5.134134000	1.864285000	1.931595000
C	-6.009304000	2.192460000	-0.005438000
H	-6.155684000	1.634842000	-0.935571000
H	-5.288311000	2.979998000	-0.240908000
C	-7.336724000	2.824051000	0.424413000
H	-7.598337000	3.611971000	-0.288080000
H	-7.205390000	3.320018000	1.392418000
C	-8.496503000	1.829950000	0.509196000
H	-8.315201000	1.052209000	1.253570000
H	-9.427527000	2.331070000	0.781097000
H	-8.653665000	1.334253000	-0.452300000
C	-5.332512000	-1.704799000	0.389110000
H	-5.818450000	-1.524264000	1.352374000
H	-5.000952000	-2.746473000	0.413073000
C	-6.369697000	-1.543089000	-0.729956000
H	-6.690498000	-0.500262000	-0.781489000
H	-5.892650000	-1.760221000	-1.691402000
C	-7.597449000	-2.433261000	-0.547747000
H	-8.055029000	-2.217519000	0.423989000
H	-7.284495000	-3.482236000	-0.510050000
C	-8.634828000	-2.244165000	-1.652417000
H	-9.503911000	-2.887780000	-1.502054000
H	-8.987306000	-1.210033000	-1.683469000
H	-8.211756000	-2.477728000	-2.632694000
C	5.369208000	1.813083000	-0.451915000
H	5.862030000	1.632335000	-1.411458000
H	5.030814000	2.852487000	-0.481098000
C	6.399881000	1.664341000	0.675020000
H	6.760348000	0.632724000	0.705761000
H	5.903881000	1.839376000	1.635467000
C	7.591954000	2.608674000	0.530223000
H	8.072078000	2.435829000	-0.439219000
H	7.233975000	3.643659000	0.511011000
C	8.620181000	2.441883000	1.647082000
H	9.462777000	3.125021000	1.522461000
H	8.172744000	2.638410000	2.624655000
H	9.016385000	1.423366000	1.665422000
C	5.425043000	-1.161813000	-1.122738000
H	6.175828000	-0.445557000	-1.458675000
H	5.161996000	-1.759901000	-2.001538000
C	6.056068000	-2.088308000	-0.072321000
H	5.329542000	-2.855836000	0.212738000
H	6.258358000	-1.517439000	0.839093000
C	7.342501000	-2.754513000	-0.555384000
H	7.136006000	-3.316975000	-1.472413000
H	8.066016000	-1.979699000	-0.831787000
C	7.961013000	-3.682654000	0.487988000
H	8.880474000	-4.142916000	0.120618000

H	8.203711000	-3.136933000	1.403314000
H	7.270553000	-4.485902000	0.757406000

ωB97XD/6-31G*			
8 (S_0-state)			
E(SCF) = -617.95466834			
C	0.000000000	-0.713041000	-4.404913000
C	0.000000000	-1.403117000	-3.229486000
C	0.000000000	-0.717402000	-1.974382000
C	0.000000000	0.717402000	-1.974382000
C	0.000000000	1.403117000	-3.229486000
C	0.000000000	0.713041000	-4.404913000
C	0.000000000	-1.398567000	-0.754737000
C	0.000000000	1.398567000	-0.754737000
C	0.000000000	0.715794000	0.461824000
C	0.000000000	-0.715794000	0.461824000
C	0.000000000	-1.392704000	1.720402000
H	0.000000000	-2.480959000	1.715261000
C	0.000000000	-0.721938000	2.908794000
C	0.000000000	0.721938000	2.908794000
C	0.000000000	1.392704000	1.720402000
H	0.000000000	-2.486817000	-0.754159000
H	0.000000000	-1.245464000	-5.351383000
H	0.000000000	-2.490302000	-3.225945000
H	0.000000000	2.490302000	-3.225945000
H	0.000000000	1.245464000	-5.351383000
H	0.000000000	2.486817000	-0.754159000
H	0.000000000	2.480959000	1.715261000
C	0.000000000	1.470318000	4.216081000
H	-0.881045000	1.222846000	4.820583000
H	0.881045000	1.222846000	4.820583000
H	0.000000000	2.550958000	4.049885000
C	0.000000000	-1.470318000	4.216081000
H	0.881045000	-1.222846000	4.820583000
H	-0.881045000	-1.222846000	4.820583000
H	0.000000000	-2.550958000	4.049885000
8 (S_1-state)			
E(SCF) = -617.82855617			
C	0.000000000	-0.692466000	-4.447964000
C	0.000000000	-1.394933000	-3.229340000
C	0.000000000	-0.720379000	-2.001600000
C	0.000000000	0.720379000	-2.001600000
C	0.000000000	1.394933000	-3.229340000
C	0.000000000	0.692466000	-4.447964000
C	0.000000000	-1.396438000	-0.758474000

C	0.000000000	1.396438000	-0.758474000
C	0.000000000	0.718264000	0.480195000
C	0.000000000	-0.718264000	0.480195000
C	0.000000000	-1.382393000	1.712151000
H	0.000000000	-2.470622000	1.716655000
C	0.000000000	-0.698936000	2.944853000
C	0.000000000	0.698936000	2.944853000
C	0.000000000	1.382393000	1.712151000
H	0.000000000	-2.484764000	-0.757861000
H	0.000000000	-1.241595000	-5.384380000
H	0.000000000	-2.481986000	-3.233048000
H	0.000000000	2.481986000	-3.233048000
H	0.000000000	1.241595000	-5.384380000
H	0.000000000	2.484764000	-0.757861000
H	0.000000000	2.470622000	1.716655000
C	0.000000000	1.473510000	4.234831000
H	-0.880694000	1.237420000	4.845622000
H	0.880694000	1.237420000	4.845622000
H	0.000000000	2.551410000	4.051146000
C	0.000000000	-1.473510000	4.234831000
H	0.880694000	-1.237420000	4.845622000
H	-0.880694000	-1.237420000	4.845622000
H	0.000000000	-2.551410000	4.051146000

20 (S_0-state)

E(SCF) = -853.77154446

C	-3.541632000	-1.264993000	0.545819000
C	-2.182924000	-1.133687000	0.513125000
C	-1.538291000	0.117087000	0.261436000
C	-2.352522000	1.272608000	0.043197000
C	-3.770782000	1.111094000	0.088430000
C	-4.364131000	-0.095651000	0.322321000
C	-0.149556000	0.243623000	0.223108000
C	-1.742660000	2.501914000	-0.207445000
C	-0.352061000	2.630737000	-0.251141000
C	0.465084000	1.472718000	-0.028386000
C	1.887239000	1.617327000	-0.073812000
H	2.502536000	0.737731000	0.097974000
C	2.460715000	2.827980000	-0.325546000
C	1.648708000	3.978427000	-0.549476000
C	0.289387000	3.881936000	-0.512556000
H	0.469144000	-0.635465000	0.392311000
H	-1.543783000	-1.995415000	0.681862000
H	-4.391158000	1.990044000	-0.078993000
H	-2.362603000	3.380114000	-0.376464000
H	3.541891000	2.924878000	-0.357943000
H	2.122818000	4.934485000	-0.750342000
H	-0.331467000	4.757759000	-0.683672000

C	-5.871744000	-0.200880000	0.284435000
C	-6.398973000	-0.540528000	-1.118226000
H	-6.308464000	0.753318000	0.603041000
H	-6.229262000	-0.953184000	0.996936000
C	-7.909114000	-0.772145000	-1.146877000
H	-6.133012000	0.277268000	-1.801107000
H	-5.885804000	-1.432286000	-1.503202000
C	-8.436643000	-1.055952000	-2.552012000
H	-8.156466000	-1.612048000	-0.483586000
H	-8.419568000	0.107312000	-0.731590000
H	-9.517220000	-1.231791000	-2.546231000
H	-8.236759000	-0.212757000	-3.223073000
H	-7.955018000	-1.942300000	-2.980943000
C	-4.210447000	-2.595477000	0.827508000
C	-3.291767000	-3.809069000	0.952182000
H	-4.947377000	-2.798019000	0.038205000
H	-4.797601000	-2.506762000	1.753197000
C	-4.069993000	-5.105447000	1.181017000
H	-2.683532000	-3.908685000	0.042950000
H	-2.589158000	-3.662891000	1.783560000
C	-3.157904000	-6.323307000	1.314771000
H	-4.685449000	-5.005453000	2.085092000
H	-4.770180000	-5.259353000	0.349106000
H	-3.734390000	-7.239513000	1.478273000
H	-2.554552000	-6.462892000	0.410380000
H	-2.467727000	-6.206274000	2.158178000

20 (S_1-state)

E(SCF) = -853.64842470

C	-3.218360000	-1.571335000	-0.190699000
C	-1.846328000	-1.289109000	-0.370720000
C	-1.317657000	0.002365000	-0.277880000
C	-2.217134000	1.085876000	0.011887000
C	-3.571329000	0.789541000	0.197254000
C	-4.088786000	-0.521628000	0.110087000
C	0.052510000	0.288282000	-0.457624000
C	-1.696369000	2.394569000	0.098709000
C	-0.323085000	2.685579000	-0.083573000
C	0.578949000	1.599306000	-0.368737000
C	1.939705000	1.881194000	-0.546580000
H	2.623594000	1.063478000	-0.759380000
C	2.430076000	3.195206000	-0.453954000
C	1.562009000	4.240427000	-0.182044000
C	0.192027000	3.985607000	0.002045000
H	0.733654000	-0.532568000	-0.673617000
H	-1.171082000	-2.113427000	-0.594197000
H	-4.256977000	1.605085000	0.421246000
H	-2.378044000	3.214964000	0.314757000
H	3.489637000	3.383823000	-0.595770000

H	1.932903000	5.258113000	-0.110555000
H	-0.486290000	4.808021000	0.214572000
C	-5.572716000	-0.723432000	0.291481000
C	-6.350582000	-0.609491000	-1.028628000
H	-5.955133000	0.028121000	0.993857000
H	-5.779734000	-1.698165000	0.748428000
C	-7.852508000	-0.830127000	-0.852804000
H	-6.169079000	0.381564000	-1.466004000
H	-5.952575000	-1.336614000	-1.749349000
C	-8.626930000	-0.708565000	-2.163722000
H	-8.021562000	-1.823826000	-0.416017000
H	-8.241917000	-0.105434000	-0.125323000
H	-9.698353000	-0.874756000	-2.012259000
H	-8.500071000	0.287510000	-2.603135000
H	-8.273625000	-1.441744000	-2.897815000
C	-3.675440000	-3.006383000	-0.276697000
C	-3.617714000	-3.727466000	1.078826000
H	-3.039863000	-3.544534000	-0.991430000
H	-4.695610000	-3.066593000	-0.673415000
C	-4.096095000	-5.176731000	1.000339000
H	-2.586845000	-3.696161000	1.456661000
H	-4.225532000	-3.177195000	1.809795000
C	-4.030934000	-5.896135000	2.346156000
H	-5.127417000	-5.195308000	0.622413000
H	-3.489565000	-5.718463000	0.262303000
H	-4.382100000	-6.929833000	2.264568000
H	-3.004221000	-5.919143000	2.729137000
H	-4.651680000	-5.388327000	3.093199000

21 (S_0-state)

E(SCF) = -853.77594002

C	-5.921698000	-0.380349000	0.824656000
C	-4.759241000	-1.060778000	1.030766000
C	-3.501495000	-0.505741000	0.634170000
C	-3.486332000	0.787291000	0.010330000
C	-4.729396000	1.467884000	-0.186815000
C	-5.906520000	0.904918000	0.205894000
C	-2.295884000	-1.180560000	0.833062000
C	-2.266229000	1.340332000	-0.382009000
C	-1.061362000	0.663591000	-0.181452000
C	-1.076584000	-0.625515000	0.439195000
C	0.168175000	-1.294994000	0.625152000
H	0.152707000	-2.278596000	1.092032000
C	1.366280000	-0.756934000	0.240895000
C	1.382933000	0.549744000	-0.372865000
C	0.198702000	1.207357000	-0.567154000
H	-2.306636000	-2.161099000	1.304653000
H	-6.869665000	-0.813522000	1.129477000

H	-4.767542000	-2.040400000	1.501873000
H	-4.714534000	2.447174000	-0.658449000
H	-6.842878000	1.432697000	0.051367000
H	-2.253765000	2.320779000	-0.853750000
H	0.207535000	2.191284000	-1.033521000
C	2.662370000	1.256345000	-0.768819000
H	3.474585000	0.544565000	-0.946997000
H	2.495855000	1.768181000	-1.724711000
C	3.129999000	2.303207000	0.263950000
H	2.304016000	3.015916000	0.397877000
C	4.342988000	3.068135000	-0.268795000
H	4.666722000	3.837009000	0.441194000
H	5.188813000	2.388166000	-0.431630000
H	4.120328000	3.560004000	-1.222403000
C	3.436986000	1.678493000	1.626123000
H	2.576481000	1.128641000	2.021072000
H	4.281716000	0.981660000	1.553304000
H	3.707551000	2.450028000	2.355218000
C	2.615449000	-1.590519000	0.435216000
H	3.512389000	-0.964575000	0.477240000
H	2.551926000	-2.090908000	1.409383000
C	2.807421000	-2.670383000	-0.650249000
H	1.903862000	-3.296247000	-0.646297000
C	4.007147000	-3.556455000	-0.309964000
H	3.890291000	-4.031208000	0.670768000
H	4.136313000	-4.348121000	-1.056042000
H	4.931525000	-2.965392000	-0.288419000
C	2.955825000	-2.068392000	-2.048687000
H	2.102778000	-1.432446000	-2.306897000
H	3.866579000	-1.459740000	-2.115837000
H	3.029508000	-2.857149000	-2.805313000

21 (S_1-state)

E(SCF) = -853.65301888

C	-5.956551000	-0.371502000	0.796985000
C	-4.754900000	-1.074748000	0.981872000
C	-3.523144000	-0.518123000	0.613312000
C	-3.503284000	0.800461000	0.034670000
C	-4.716406000	1.479554000	-0.138730000
C	-5.937473000	0.897670000	0.239558000
C	-2.294679000	-1.200777000	0.784595000
C	-2.255768000	1.359086000	-0.334257000
C	-1.033955000	0.676669000	-0.160308000
C	-1.054138000	-0.641664000	0.414190000
C	0.163702000	-1.306967000	0.577440000
H	0.155870000	-2.303877000	1.015021000
C	1.410111000	-0.745542000	0.209860000
C	1.429590000	0.533839000	-0.349159000
C	0.202659000	1.219078000	-0.519428000

H	-2.309635000	-2.197690000	1.220655000
H	-6.896628000	-0.827621000	1.091172000
H	-4.773411000	-2.069578000	1.419409000
H	-4.705035000	2.474737000	-0.575710000
H	-6.862260000	1.447204000	0.094245000
H	-2.240470000	2.355953000	-0.770409000
H	0.224673000	2.215249000	-0.958199000
C	2.685699000	1.266059000	-0.753056000
H	3.518012000	0.573317000	-0.914271000
H	2.507206000	1.756817000	-1.719220000
C	3.121228000	2.342723000	0.264758000
H	2.267489000	3.018964000	0.414340000
C	4.288047000	3.159154000	-0.293347000
H	4.593493000	3.940935000	0.410615000
H	5.158740000	2.516522000	-0.475298000
H	4.023903000	3.641409000	-1.241183000
C	3.481416000	1.730039000	1.618993000
H	2.653241000	1.141193000	2.026222000
H	4.353269000	1.069656000	1.525276000
H	3.732886000	2.509786000	2.346093000
C	2.635363000	-1.601967000	0.415884000
H	3.547246000	-0.996494000	0.438154000
H	2.563972000	-2.080386000	1.401874000
C	2.795557000	-2.708242000	-0.649625000
H	1.866130000	-3.295327000	-0.657033000
C	3.949243000	-3.640737000	-0.276836000
H	3.791870000	-4.102140000	0.704528000
H	4.060523000	-4.443189000	-1.014216000
H	4.897088000	-3.089001000	-0.239854000
C	2.995910000	-2.123360000	-2.048500000
H	2.176235000	-1.452079000	-2.324113000
H	3.932714000	-1.553391000	-2.099006000
H	3.050653000	-2.918289000	-2.800169000

32 (S_0-state)

E(SCF) = -1244.40509121

C	-7.646798000	-0.764567000	1.077705000
C	-6.543776000	0.036161000	1.047354000
C	-5.311277000	-0.430807000	0.492110000
C	-5.255496000	-1.765081000	-0.032213000
C	-6.435240000	-2.572097000	0.017831000
C	-7.591993000	-2.089404000	0.553619000
C	-4.166569000	0.369373000	0.443050000
C	-4.056527000	-2.233864000	-0.574797000
C	-2.915584000	-1.432648000	-0.619741000
C	-2.971663000	-0.100083000	-0.103014000
C	-1.794819000	0.709142000	-0.176312000
H	-1.864889000	1.721884000	0.210062000
C	-0.624206000	0.253533000	-0.711871000

C	-0.562342000	-1.103363000	-1.210698000
C	-1.676856000	-1.889730000	-1.163066000
H	-4.210141000	1.382157000	0.838882000
H	-8.576118000	-0.396894000	1.502518000
H	-6.583145000	1.046402000	1.447032000
H	-6.389448000	-3.581367000	-0.383569000
H	-8.481254000	-2.712055000	0.584668000
H	-4.011798000	-3.245922000	-0.972206000
H	-1.629843000	-2.907833000	-1.546045000
C	0.731936000	-1.688317000	-1.728178000
C	1.599122000	-2.275236000	-0.603473000
H	1.310961000	-0.938619000	-2.279879000
H	0.502946000	-2.486086000	-2.445296000
C	2.898025000	-2.889547000	-1.125232000
H	1.831155000	-1.495350000	0.134551000
H	1.005052000	-3.028148000	-0.072462000
H	2.657095000	-3.749764000	-1.767858000
H	3.403293000	-2.158368000	-1.772490000
C	0.602377000	1.135625000	-0.825875000
C	0.500131000	2.537529000	-0.228196000
H	0.861960000	1.233651000	-1.890125000
H	1.459147000	0.624571000	-0.366739000
C	1.798449000	3.322774000	-0.422580000
H	-0.332770000	3.075064000	-0.696837000
H	0.270950000	2.468958000	0.844024000
H	2.638070000	2.714801000	-0.056070000
H	1.975048000	3.467762000	-1.498909000
C	1.847530000	4.685716000	0.276618000
C	3.235291000	5.322104000	0.113316000
C	0.763375000	5.651688000	-0.223428000
H	1.678547000	4.521718000	1.353408000
C	3.334000000	6.690295000	0.792276000
H	3.444413000	5.437708000	-0.961054000
H	4.002039000	4.644722000	0.510196000
C	0.859100000	7.023462000	0.451931000
H	0.874896000	5.772953000	-1.311898000
H	-0.233197000	5.227652000	-0.054804000
C	2.249041000	7.639915000	0.278346000
H	4.328323000	7.122456000	0.629985000
H	3.217269000	6.563772000	1.877978000
H	0.091028000	7.694849000	0.050520000
H	0.648749000	6.909345000	1.524939000
H	2.306737000	8.603623000	0.797523000
H	2.423161000	7.842663000	-0.788057000
C	3.882999000	-3.336684000	-0.038783000
C	3.286811000	-4.383671000	0.913219000
C	5.176888000	-3.871683000	-0.669029000
H	4.145700000	-2.451340000	0.563697000
C	4.298317000	-4.850877000	1.964326000
H	2.950386000	-5.248544000	0.320640000
H	2.398865000	-3.981426000	1.413694000
C	6.190564000	-4.334534000	0.380287000

H	4.923795000	-4.719069000	-1.324282000
H	5.621682000	-3.101923000	-1.312478000
C	5.580589000	-5.379490000	1.317864000
H	3.847692000	-5.619526000	2.602954000
H	4.549892000	-4.005241000	2.620446000
H	7.084296000	-4.737502000	-0.110218000
H	6.519002000	-3.467940000	0.971874000
H	6.304575000	-5.670016000	2.087947000
H	5.347479000	-6.287597000	0.743542000

32 (S_1-state)

E(SCF) = -1244.28228608

C	-7.977735000	1.146122000	0.355865000
C	-6.749142000	1.547111000	0.908701000
C	-5.539246000	0.995297000	0.467682000
C	-5.569814000	0.000292000	-0.573134000
C	-6.807788000	-0.380919000	-1.106821000
C	-8.007039000	0.188530000	-0.645104000
C	-4.285554000	1.375919000	1.003906000
C	-4.344509000	-0.552932000	-1.016012000
C	-3.096609000	-0.170219000	-0.479835000
C	-3.065948000	0.821511000	0.560546000
C	-1.823614000	1.189953000	1.087385000
H	-1.794084000	1.939115000	1.876628000
C	-0.605621000	0.631521000	0.641088000
C	-0.634433000	-0.320288000	-0.380059000
C	-1.881945000	-0.708964000	-0.915971000
H	-4.262753000	2.127738000	1.790286000
H	-8.899262000	1.590849000	0.718329000
H	-6.730198000	2.299238000	1.693128000
H	-6.833781000	-1.132190000	-1.891872000
H	-8.951679000	-0.126351000	-1.077382000
H	-4.366632000	-1.304506000	-1.802647000
H	-1.897579000	-1.458397000	-1.705418000
C	0.610541000	-0.997875000	-0.896028000
C	0.934655000	-2.287209000	-0.125251000
H	1.472374000	-0.322007000	-0.852527000
H	0.471614000	-1.246026000	-1.956111000
C	2.186725000	-2.983941000	-0.657277000
H	1.065478000	-2.051497000	0.939734000
H	0.066188000	-2.953993000	-0.186518000
H	2.034406000	-3.242187000	-1.716080000
H	3.022048000	-2.269127000	-0.636230000
C	0.683084000	1.136400000	1.240510000
C	1.254621000	2.332578000	0.462839000
H	1.434541000	0.339092000	1.278346000
H	0.506064000	1.438185000	2.280595000
C	2.582306000	2.826821000	1.036256000
H	1.376974000	2.042996000	-0.587790000

H	0.517413000	3.146814000	0.471101000
H	2.457472000	3.007561000	2.113546000
H	3.335506000	2.029420000	0.946374000
C	3.127378000	4.103760000	0.386196000
C	4.392306000	4.585996000	1.111386000
C	3.413398000	3.929808000	-1.112820000
H	2.361653000	4.889862000	0.490281000
C	4.971466000	5.858855000	0.488810000
H	5.148922000	3.787851000	1.069361000
H	4.171064000	4.751107000	2.173477000
C	3.996144000	5.199738000	-1.740093000
H	4.125476000	3.100021000	-1.241680000
H	2.499081000	3.646169000	-1.645994000
C	5.254073000	5.664678000	-1.002892000
H	5.886166000	6.153991000	1.016049000
H	4.253355000	6.681443000	0.615835000
H	4.215716000	5.027179000	-2.800169000
H	3.240776000	5.997388000	-1.701101000
H	5.634463000	6.593254000	-1.444312000
H	6.043516000	4.909085000	-1.124576000
C	2.602516000	-4.246699000	0.106801000
C	1.542842000	-5.356235000	0.033780000
C	3.949604000	-4.768640000	-0.414280000
H	2.734690000	-3.978241000	1.167530000
C	1.992578000	-6.635350000	0.746609000
H	1.342996000	-5.580689000	-1.025393000
H	0.597174000	-5.010349000	0.466091000
C	4.400582000	-6.044540000	0.301471000
H	3.852915000	-4.974434000	-1.491135000
H	4.713516000	-3.987276000	-0.313028000
C	3.333188000	-7.137273000	0.206111000
H	1.224373000	-7.410787000	0.644663000
H	2.093221000	-6.431438000	1.822154000
H	5.348477000	-6.398534000	-0.120568000
H	4.590555000	-5.818482000	1.360414000
H	3.653012000	-8.033415000	0.750526000
H	3.210705000	-7.431271000	-0.846088000

35 (S_0-state)

E(SCF) = -1475.43395497

C	-1.595976000	1.048139000	-0.789532000
C	-2.793035000	1.661575000	-0.556504000
C	-3.996317000	0.930240000	-0.317685000
C	-3.928549000	-0.499119000	-0.324960000
C	-2.665500000	-1.117529000	-0.576294000
C	-1.527120000	-0.397880000	-0.802883000
C	-5.220027000	1.555721000	-0.077620000
C	-5.088143000	-1.238221000	-0.088352000
C	-6.314605000	-0.615117000	0.154110000

C	-6.382718000	0.818200000	0.158895000
C	-7.644845000	1.443833000	0.406091000
H	-7.693892000	2.529915000	0.407629000
C	-8.763389000	0.699096000	0.635180000
C	-8.695271000	-0.725306000	0.632685000
C	-7.511174000	-1.359081000	0.400100000
H	-5.270663000	2.642799000	-0.072955000
H	-2.844985000	2.748823000	-0.542914000
H	-2.630068000	-2.204490000	-0.586276000
H	-5.035851000	-2.325213000	-0.092776000
H	-9.715803000	1.186695000	0.820659000
H	-9.596976000	-1.301387000	0.818072000
H	-7.455435000	-2.444816000	0.397160000
C	-0.214331000	-1.097732000	-1.096488000
H	-0.131174000	-1.252447000	-2.180941000
H	0.609529000	-0.429375000	-0.844779000
C	0.001514000	-2.436537000	-0.370032000
H	-0.501622000	-2.404099000	0.605678000
H	-0.475796000	-3.248472000	-0.935326000
C	-0.346867000	1.879885000	-0.976501000
H	0.240861000	1.480256000	-1.809448000
H	-0.630245000	2.898334000	-1.263362000
C	0.496802000	1.922226000	0.311298000
H	0.539613000	0.914744000	0.744897000
H	-0.043306000	2.530177000	1.050209000
C	1.477748000	-2.799850000	-0.129464000
C	2.102227000	-1.869468000	0.932568000
C	1.576588000	-4.244026000	0.405298000
C	2.309693000	-2.710838000	-1.425841000
H	1.527883000	-1.948718000	1.866336000
H	2.036975000	-0.823911000	0.613787000
C	3.571021000	-2.234329000	1.191072000
H	1.138991000	-4.938127000	-0.325975000
H	0.984397000	-4.334646000	1.326714000
C	3.039538000	-4.631404000	0.679210000
H	2.269379000	-1.693238000	-1.835605000
H	1.876216000	-3.377589000	-2.185029000
C	3.774275000	-3.092665000	-1.160789000
H	3.990264000	-1.543271000	1.933434000
C	3.643560000	-3.674871000	1.720237000
C	4.366465000	-2.129052000	-0.120131000
H	3.077813000	-5.659547000	1.058998000
C	3.843737000	-4.531727000	-0.626799000
H	4.342176000	-3.018470000	-2.096067000
H	3.096511000	-3.754373000	2.668794000
H	4.686529000	-3.951197000	1.923821000
H	4.333099000	-1.099773000	-0.502651000
H	5.422423000	-2.369274000	0.060477000
H	4.888942000	-4.816767000	-0.448578000
H	3.440899000	-5.229741000	-1.372630000
C	1.935449000	2.451904000	0.193237000
C	1.968680000	3.950339000	-0.169049000

C	2.620096000	2.267107000	1.564923000
C	2.759590000	1.686373000	-0.864219000
H	1.384227000	4.519594000	0.567438000
H	1.495128000	4.110611000	-1.147255000
C	3.417446000	4.467304000	-0.203965000
H	2.607161000	1.202125000	1.837656000
H	2.043800000	2.799750000	2.334313000
C	4.065751000	2.779720000	1.538745000
H	2.315996000	1.816777000	-1.859420000
H	2.741984000	0.610898000	-0.647249000
C	4.211860000	2.188017000	-0.894132000
H	3.416117000	5.533138000	-0.462616000
C	4.066830000	4.273074000	1.175402000
C	4.217160000	3.681776000	-1.256152000
H	4.522086000	2.638965000	2.526043000
C	4.857996000	1.990637000	0.485432000
H	4.773377000	1.622627000	-1.648115000
H	3.515785000	4.843894000	1.934433000
H	5.094690000	4.659021000	1.163964000
H	3.775997000	3.828500000	-2.251000000
H	5.248136000	4.056631000	-1.301859000
H	5.902330000	2.328799000	0.463340000
H	4.869541000	0.923385000	0.746420000

35 (S_1-state)

E(SCF) = -1475.30857902

C	-1.557520000	1.125083000	-0.569707000
C	-2.814302000	1.726798000	-0.357419000
C	-3.989797000	0.985776000	-0.191745000
C	-3.900331000	-0.446695000	-0.242245000
C	-2.643294000	-1.031712000	-0.437072000
C	-1.466055000	-0.272302000	-0.596293000
C	-5.254785000	1.580421000	0.006063000
C	-5.082381000	-1.204799000	-0.099162000
C	-6.353997000	-0.612831000	0.090165000
C	-6.442855000	0.823880000	0.146954000
C	-7.699168000	1.415069000	0.333495000
H	-7.770667000	2.498853000	0.378051000
C	-8.861549000	0.633524000	0.461143000
C	-8.776091000	-0.747765000	0.404701000
C	-7.527078000	-1.367180000	0.220712000
H	-5.321902000	2.665984000	0.045556000
H	-2.875483000	2.813379000	-0.332573000
H	-2.584154000	-2.116335000	-0.475197000
H	-5.014204000	-2.290195000	-0.141600000
H	-9.821853000	1.119357000	0.603137000
H	-9.668986000	-1.357617000	0.501018000
H	-7.462983000	-2.451408000	0.175572000
C	-0.132242000	-0.942370000	-0.837170000

H	0.092846000	-0.899483000	-1.912987000
H	0.645841000	-0.340702000	-0.362655000
C	0.007072000	-2.390891000	-0.353112000
H	-0.533012000	-2.518159000	0.594984000
H	-0.469564000	-3.068352000	-1.074721000
C	-0.341633000	1.996977000	-0.770729000
H	0.269019000	1.579233000	-1.578698000
H	-0.662503000	2.985233000	-1.118041000
C	0.512183000	2.160254000	0.504975000
H	0.518642000	1.216329000	1.066572000
H	0.017621000	2.890007000	1.160339000
C	1.463097000	-2.842672000	-0.131453000
C	2.045222000	-2.208282000	1.150841000
C	1.502724000	-4.374730000	0.048233000
C	2.367569000	-2.474804000	-1.326761000
H	1.418736000	-2.489487000	2.008927000
H	2.015368000	-1.113511000	1.087852000
C	3.489972000	-2.675391000	1.385357000
H	1.091234000	-4.858725000	-0.848525000
H	0.857160000	-4.661585000	0.890407000
C	2.938797000	-4.864953000	0.291442000
H	2.376006000	-1.388068000	-1.477576000
H	1.961442000	-2.922968000	-2.245000000
C	3.805992000	-2.958973000	-1.090587000
H	3.884198000	-2.197740000	2.290560000
C	3.502540000	-4.202327000	1.558353000
C	4.359646000	-2.289997000	0.177785000
H	2.934709000	-5.954523000	0.416342000
C	3.813684000	-4.485082000	-0.913615000
H	4.426904000	-2.683860000	-1.951908000
H	2.901239000	-4.486100000	2.432259000
H	4.526222000	-4.553991000	1.742583000
H	4.370760000	-1.198429000	0.051937000
H	5.397933000	-2.603580000	0.347709000
H	4.840431000	-4.843210000	-0.761968000
H	3.433260000	-4.969758000	-1.822474000
C	1.969872000	2.594567000	0.277300000
C	2.057117000	3.903731000	-0.532221000
C	2.642805000	2.823486000	1.647654000
C	2.774474000	1.505981000	-0.464265000
H	1.490185000	4.692400000	-0.017257000
H	1.594239000	3.768505000	-1.518675000
C	3.522134000	4.335320000	-0.709910000
H	2.586736000	1.898921000	2.239736000
H	2.089140000	3.593074000	2.203321000
C	4.108333000	3.252012000	1.478702000
H	2.330962000	1.297950000	-1.446731000
H	2.733338000	0.570096000	0.107702000
C	4.238621000	1.930153000	-0.647100000
H	3.558496000	5.267198000	-1.286944000
C	4.164473000	4.557037000	0.668400000
C	4.290558000	3.233987000	-1.458574000

H	4.557655000	3.411062000	2.466378000
C	4.878211000	2.151784000	0.731629000
H	4.778918000	1.138780000	-1.181982000
H	3.636306000	5.356156000	1.205322000
H	5.206428000	4.882178000	0.549478000
H	3.848942000	3.076083000	-2.451535000
H	5.333305000	3.540309000	-1.613385000
H	5.932178000	2.437091000	0.617557000
H	4.856806000	1.217113000	1.308550000

36 (S_0-state)

E(SCF) = -932.37477634

C	-0.333267000	6.144485000	0.713473000
C	-0.171981000	4.980906000	1.403514000
C	0.001286000	3.736523000	0.718336000
C	0.001286000	3.736523000	-0.718336000
C	-0.171981000	4.980906000	-1.403514000
C	-0.333267000	6.144485000	-0.713473000
C	0.171061000	2.530676000	1.399781000
C	0.171061000	2.530676000	-1.399781000
C	0.335164000	1.325172000	-0.713651000
C	0.335164000	1.325172000	0.713651000
C	0.533993000	0.082396000	1.378574000
H	0.623416000	0.111658000	2.459967000
C	0.661379000	-1.117518000	0.726892000
C	0.661379000	-1.117518000	-0.726892000
C	0.533993000	0.082396000	-1.378574000
H	0.173445000	2.529276000	2.488045000
H	-0.463485000	7.082368000	1.245101000
H	-0.171675000	4.977554000	2.490674000
H	-0.171675000	4.977554000	-2.490674000
H	-0.463485000	7.082368000	-1.245101000
H	0.173445000	2.529276000	-2.488045000
H	0.623416000	0.111658000	-2.459967000
C	0.937647000	-2.353994000	-1.570623000
C	-0.167231000	-2.883823000	-2.530855000
H	1.220149000	-3.192768000	-0.929505000
H	1.825406000	-2.144297000	-2.183030000
C	0.937647000	-2.353994000	1.570623000
C	-0.167231000	-2.883823000	2.530855000
H	1.825406000	-2.144297000	2.183030000
H	1.220149000	-3.192768000	0.929505000
C	-1.448983000	-3.216387000	1.763768000
H	-1.830061000	-2.339692000	1.229414000
H	-1.273730000	-4.012392000	1.033918000
H	-2.229935000	-3.561240000	2.451597000
C	0.383837000	-4.168184000	3.171260000
H	1.297177000	-3.965045000	3.743311000
H	-0.350824000	-4.606996000	3.856252000

H	0.623817000	-4.920056000	2.410087000
C	-0.508674000	-1.894711000	3.654594000
H	-1.165056000	-2.377708000	4.387864000
H	0.391892000	-1.559159000	4.183775000
H	-1.035922000	-1.014749000	3.275124000
C	-0.508674000	-1.894711000	-3.654594000
H	0.391892000	-1.559159000	-4.183775000
H	-1.165056000	-2.377708000	-4.387864000
H	-1.035922000	-1.014749000	-3.275124000
C	0.383837000	-4.168184000	-3.171260000
H	-0.350824000	-4.606996000	-3.856252000
H	1.297177000	-3.965045000	-3.743311000
H	0.623817000	-4.920056000	-2.410087000
C	-1.448983000	-3.216387000	-1.763768000
H	-1.273730000	-4.012392000	-1.033918000
H	-1.830061000	-2.339692000	-1.229414000
H	-2.229935000	-3.561240000	-2.451597000

36 (S_1-state)

E(SCF) = -932.25293572

C	-0.326015000	6.190503000	0.693442000
C	-0.163575000	4.985359000	1.394785000
C	-0.001633000	3.768061000	0.720237000
C	-0.001633000	3.768061000	-0.720237000
C	-0.163575000	4.985359000	-1.394785000
C	-0.326015000	6.190503000	-0.693442000
C	0.168874000	2.536108000	1.397669000
C	0.168874000	2.536108000	-1.397669000
C	0.322544000	1.311434000	-0.717571000
C	0.322544000	1.311434000	0.717571000
C	0.518978000	0.092600000	1.369347000
H	0.608343000	0.110147000	2.450715000
C	0.653759000	-1.153132000	0.702108000
C	0.653759000	-1.153132000	-0.702108000
C	0.518978000	0.092600000	-1.369347000
H	0.182969000	2.537098000	2.485959000
H	-0.450472000	7.119340000	1.241280000
H	-0.161458000	4.989075000	2.481875000
H	-0.161458000	4.989075000	-2.481875000
H	-0.450472000	7.119340000	-1.241280000
H	0.182969000	2.537098000	-2.485959000
H	0.608343000	0.110147000	-2.450715000
C	0.937473000	-2.363345000	-1.569426000
C	-0.165015000	-2.893202000	-2.534913000
H	1.238398000	-3.209087000	-0.945425000
H	1.815869000	-2.122472000	-2.186818000
C	0.937473000	-2.363345000	1.569426000
C	-0.165015000	-2.893202000	2.534913000
H	1.815869000	-2.122472000	2.186818000

H	1.238398000	-3.209087000	0.945425000
C	-1.428712000	-3.275189000	1.761418000
H	-1.829353000	-2.418139000	1.210141000
H	-1.222495000	-4.075931000	1.044802000
H	-2.205848000	-3.632610000	2.447137000
C	0.409418000	-4.146969000	3.213749000
H	1.310464000	-3.907144000	3.791115000
H	-0.322814000	-4.586276000	3.901033000
H	0.676482000	-4.911245000	2.474357000
C	-0.542975000	-1.883841000	3.628615000
H	-1.198864000	-2.362393000	4.365262000
H	0.342812000	-1.516466000	4.161592000
H	-1.082767000	-1.024226000	3.220297000
C	-0.542975000	-1.883841000	-3.628615000
H	0.342812000	-1.516466000	-4.161592000
H	-1.198864000	-2.362393000	-4.365262000
H	-1.082767000	-1.024226000	-3.220297000
C	0.409418000	-4.146969000	-3.213749000
H	-0.322814000	-4.586276000	-3.901033000
H	1.310464000	-3.907144000	-3.791115000
H	0.676482000	-4.911245000	-2.474357000
C	-1.428712000	-3.275189000	-1.761418000
H	-1.222495000	-4.075931000	-1.044802000
H	-1.829353000	-2.418139000	-1.210141000
H	-2.205848000	-3.632610000	-2.447137000

6. References

(1) COSMO v. 1.61, Bruker AXS Inc., Madison, WI, **2012**.

(2) APEX 3 v. 2017.3-0, Bruker AXS Inc., Madison, WI, **2017**.

(3) APEX v. 2012.10_0, Bruker AXS Inc., Madison, WI, **2012**.

(4) SAINT v. 8.38A, Bruker AXS Inc., Madison, WI, **2017**.

(5) SAINT v. 8.34A, Bruker AXS Inc., Madison, WI, **2013**.

(6) Krause, L.; Herbst-Irmer, R.; Sheldrick, G. M.; Stalke, D. Comparison of silver and molybdenum microfocus X-ray sources for single-crystal structure determination, *J. Appl. Cryst.* **2015**, *48*, 3-10.

(7) Sheldrick, G. SHELXT - Integrated space-group and crystal-structure determination, *Acta Cryst.* **2015**, *A71*, 3-8.

(8) Hübschle, C. B.; Sheldrick, G. M.; Dittrich, B. ShelXle: a Qt graphical user interface for SHELXL, *J. Appl. Cryst.* **2011**, *44*, 1281-1284.

JOC The Journal of Organic Chemistry
Cite This: J. Org. Chem. 2018, 83, 3149−3158
Article
pubs.acs.org/joc

Bridging the Gap between Pentacene and Perfluoropentacene: Synthesis and Characterization of 2,3,9,10-Tetrafluoropentacene in the Neutral, Cationic, and Dicationic States

Bin Shen,[†] Thomas Geiger,[†] Ralf Einholz,[†] Florian Reicherter,[†] Simon Schundelmeier,[†] Cäcilia Maichle-Mössmer,[‡] Bernd Speiser,[†] and Holger F. Bettinger*[,†]

[†]Institut für Organische Chemie and [‡]Institut für Anorganische Chemie, Univertsität Tübingen, Auf der Morgenstelle 18, 72076 Tübingen, Germany

Supporting Information

ABSTRACT: The thermal and photochemical syntheses of 2,3,9,10-tetrafluoropentacene (F4PEN) from 6,13-etheno bridged precursors were investigated computationally and experimentally. A computational study of the retro-Diels−Alder reaction to give 2,3,9,10-tetrasubstituted pentacenes and pyridazine revealed a linear correlation between barrier height and substituent constant (σ_p) indicative of an electronic effect that could diminish the yield of electron-poor 2,3,9,10-tetrasubstituted pentacenes in this reaction. The photochemical route from the corresponding bridged α-diketone yields F4PEN, which was characterized photophysically, electrochemically, and structurally. The compound crystallizes in a herringbone motif with quite short intermolecular F−F contacts that are, however, only very weakly bonding according to computations. The electrochemical and photophysical data show that the HOMO−LUMO gap of F4PEN is increased compared to that of PEN. This is due to an increase of the oxidation potential of F4PEN by 0.18 V in combination with an essentially unchanged reduction potential. The radical cation and dication of F4PEN could be generated in oxidizing solvents and characterized by optical spectroscopy and ESR or NMR, respectively. Both charged F4PEN species persist for days in solution.

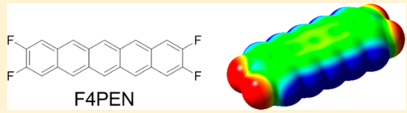

INTRODUCTION

Acenes, polycyclic aromatic compounds consisting of linearly fused benzene rings, have received significant attention as effective semiconductors in organic field-effect transistors (OFETs) because of their high charge carrier mobility.[1−5] The most important member of the acene family, pentacene (PEN), is a typical p channel semiconductor.[6] Introduction of inductively electron withdrawing fluorine atoms can modify the electronic structure to such an extent as to turn perfluoropentacene[7] (PFP) into an n channel semiconductor.[8,9] The availability of n channel interfaces is important for construction of complementary integrated circuits.

Besides providing a way to electronically modify an organic semiconductor, full or partial fluorination was recently introduced as a means for crystal engineering of rubrene (5,6,11,12-tetraphenyltetracene).[10,11] Partially fluorinated (hetero)acenes were shown to interact with fluorinated self-assembled monolayers, resulting in improved crystallinity and charge transport in OFETs.[12−14] In addition, partially fluorinated 6,13-di(triorganylsilylethynyl)-substituted pentacenes[15] were studied in the context of singlet fission,[16,17] and were employed in blends for investigation of charge-transfer processes that are relevant for photophysical applications.[18−23] The recent study by Leo and co-workers reveals that blends of organic semiconductors, phthalocyanines and partially fluorinated phthalocyanines, allow smooth tuning of the band gap over a wide energy range.[24,25] This finding also makes partially fluorinated pentacenes interesting objects of research. Other fluorinated acenes, e.g., octafluorodiphenylanthracene,[26] were investigated with respect to the tuning of the HOMO−LUMO gap.

Moreover, Toyoda et al.[27] argued, on the basis of a computational investigation of PEN, PFP, and partially fluorinated pentacenes, that the electron injection barrier at the PFP/Cu(111) interface might not be lower than at the PEN/Cu(111) interface. This is in contrast to expectations based on the electronic structure of individual molecules, due to similar energies of frontier orbitals on Cu(111) and a larger absorption distance for PFP.[28−30] Toyoda et al.[27] suggested, on the basis of density functional computations of a number of partially fluorinated pentacenes ($C_{22}F_nH_{14-n}$, n = 4, 8, 12) on Cu(111), that derivatives with eight or less fluorine atoms have lower barrier heights for carrier injection than PFP. Such compounds were thus claimed for efficient electron injection at copper electrodes in the patent literature.[31]

However, hexafluoro- and octafluoropentacenes are currently unknown and only the syntheses of two isomers (2,3,9,10 and 1,2,3,4) of tetrafluoropentacene have been disclosed.[32,33] 1,2,3,4-Tetrafluoropentacene, not considered computationally by Toyoda et al.,[27] has a pronounced tendency toward dimerization in solution, but it was found to be stable toward

Received: December 22, 2017
Published: February 27, 2018

DOI: 10.1021/acs.joc.7b03241
J. Org. Chem. 2018, 83, 3149−3158

dimerization in the solid state.[33] In OFET devices both p- and n-type charge transport was obtained.[33] Dimerization was not observed for 2,3,9,10-tetrafluoropentacene (F4PEN).[32] Thin films of F4PEN grown by vapor-phase deposition on gold single crystals were investigated by photoemission and X-ray absorption spectroscopies and by atomic force microscopy.[34,35] These investigations revealed the formation of nanoscaled crystalline phases with preferential orientation of these so-called nanorods and fractional charge transfer from the gold surface to the organic molecule.[34,35] Comparison of the electrostatic potential maps of PEN, F4PEN, and PFP reveals significant differences (Figure 1), but the consequences of these modified properties on the solid state and electronic structure have not been investigated.

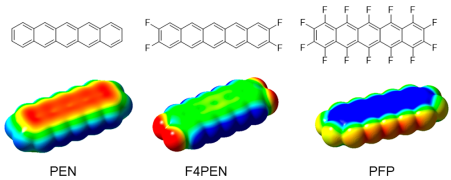

Figure 1. Pentacene (PEN), 2,3,9,10-tetrafluoropentacene (F4PEN), and perfluoropentacene (PFP), along with the computed (B3LYP/6-311+G**) electrostatic potential maps [−0.02 *e* (red) to +0.02 *e* (blue)].

Syntheses of both known tetrafluoropentacene isomers employ a protection group strategy that avoids the common problems associated with the low solubility and air sensitivity of pentacenes. While 1,2,3,4-tetrafluoropentacene was obtained by retro-cheletropic extrusion of CO from a bridged ketone,[33,36,37] we obtained F4PEN (**5c**) from a sequence of Diels–Alder (DA) and retro-DA reactions employing 2,3,9,10-tetrafluoro-6,13-dihydro-6,13-ethenopentacene (**1c**) and 3,6-disubstituted 1,2,4,5-tetrazines (**2**) (Scheme 1).[32,38,39] The yield, however, is rather low for the electron-poor tetrafluoro derivative.[32] It was significantly larger for parent pentacene and even more so for the electron-rich 2,3,9,10-tetrakis(benzyloxy)pentacene, hinting to the operation of an electronic effect in the reaction.[32]

This prompted us to investigate the thermal pentacene synthesis in more detail. Here, we explore the influences of substituents on the formation of 2,3,9,10-tetrasubstituted pentacenes **5** computationally, describe a photochemical synthesis of F4PEN, and analyze its crystal structure, electrochemical redox reactions, and the chemical generation and stability of its radical cation and dication.

RESULTS AND DISCUSSION

Computational Investigations. The generation of pentacenes **5** from 2,3,9,10-tetrasubstituted-6,13-dihydro-6,13-ethenopentacene precursors **1** with 3,6-disubstituted 1,2,4,5-tetrazines **2** involves one inverse-electron-demand Diels–Alder reaction[40−44] via **TS1** followed by two retro-Diels–Alder reactions via **TS2** and **TS3** (Scheme 1). In order to investigate possible electronic effects on reaction barriers, we have applied computational chemistry methods (M06-2X/6-31G*).

As the barrier for loss of nitrogen from **3** to **4** is very low or almost nonexistent,[45] we only studied the transition states of the first inverse-electron-demand DA reaction (**TS1**) and the third (**TS3**) step, i.e., the retro-DA reaction giving pentacenes **5** and pyridazines **6** (Scheme 1). The structure of **TS1** is characterized by carbon–carbon distances of the forming bonds of 2.224 Å (Figure 2a), which is typical for DA reactions of 1,2,4,5-tetrazines.[46] In **TS3**, the breaking bonds are stretched to 2.169 Å (Figure 2b). Although pentacene is well-known to act as a diene in Diels–Alder reactions[47] and the retro-Diels–Alder reaction was employed for obtaining pentacene for device applications,[48,49] little is known about the structure of the transition states.[50,51] Hence, comparison of **TS3** with transition state structures of related pentacene DA reactions is not possible.

It is well-know that tetrazines are electron-deficient dienes that quickly undergo inverse-electron-demand Diels–Alder reactions with alkenes or alkynes.[45,52−54] The observation that the energy barriers involving **TS1** are more than 20 kcal mol^{-1} lower than those of the retro-Diels–Alder reaction through **TS3** (Table 1), therefore, is in line with expectations and confirms that this last step is rate-determining in the reaction sequence. Hence, we focused our analysis on this final step.

Scheme 1. Stepwise Formation of Pentacenes 5 from Reaction of 6,13-Dihydro-6,13-ethenopentacenes 1 upon Reaction with 3,6-Disubstituted 1,2,4,5-Tetrazines 2

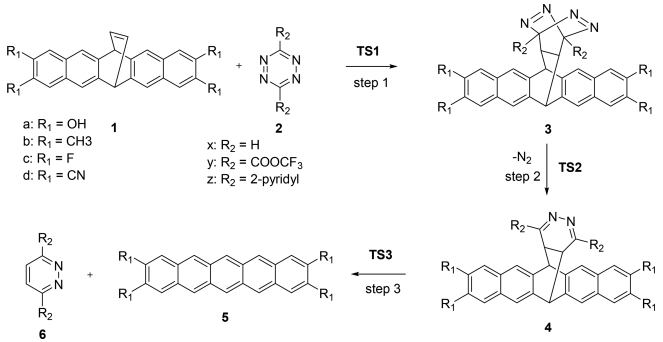

DOI: 10.1021/acs.joc.7b03241
J. Org. Chem. 2018, 83, 3149−3158

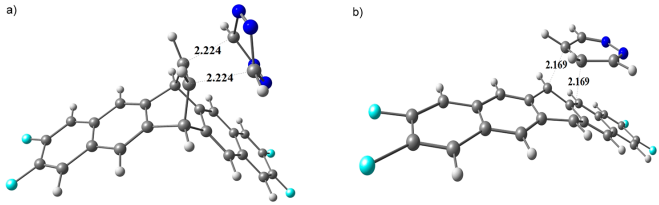

Figure 2. Structures of **TS1** (a) and **TS3** (b) as computed at the M06-2X/6-31G* level of theory.

Table 1. Energy Barriers Including Zero-Point Vibrational Energy Corrections (ΔE_0, kcal/mol) Involving TS1 and TS3 Calculated at the M06-2X/6-31G(d) Level of Theory[a]

	R_1 = OH	R_1 = CH_3	R_1 = F	R_1 = CN
ΔE_0(**TS1**)	11.0	11.4	11.8	13.1
ΔE_0(**TS3**)	35.4	35.9	36.1	36.3

[a]The substituent R_2 on tetrazine is H.

The reactivity of 1,2,4,5-tetrazines can be increased by introduction of electron-withdrawing groups at the 3,6-positions; hence, we have investigated the often-used 2-pyridyl (2-py) and trifluoromethylcarboxyl (CO_2CF_3) substituents. For all substituted pentacenes investigated, the barriers for retro-DA reactions via **TS3** are lowest with a CO_2CF_3 substituent and highest with parent tetrazine (Table 2). The differences range between 5 and 8 kcal mol^{-1}. Most interestingly, substituents on the pentacene backbone have a significant impact on the barrier heights (Table 2). These decrease in the series CN > F > CH_3 > OH, which is in line with the electron-withdrawing and electron-donating ability of these groups as expressed by the substituent constants, σ_p (0.660, 0.062, −0.170, −0.37, respectively).[55] For R_2 = CO_2CF_3, a linear correlation between σ_p and the computed barrier height (R^2 = 0.987) is obtained. In summary, electron-withdrawing groups on the 1,2,4,5-tetrazine and electron-donating groups on the pentacene backbone enhance the thermal extrusion of the pyridazine molecule. This is in good overall agreement to the observations we made experimentally.[32]

Table 2. Energy Barriers (ΔE_0, kcal mol^{-1}) Involving TS3 As Computed at the M06-2X/6-31G(d)+ZPVE Level of Theory

	ΔE_0(**TS3**)		
R_1	R_2 = H	R_2 = 2-pyridyl	R_2 = CO_2CF_3
OH	35.4	31.0	27.8
CH_3	35.9	31.7	28.8
F	36.1	32.1	29.7
CN	36.3	32.4	31.5

Reaction rates computed from Gibbs free energies of activation for CO_2CF_3-substituted 1,2,4,5-tetrazine (Table 3) show that the electron-donor substituent OH results in an almost 50-fold increase in rate compared to F and a more than 150-fold increase compared to CN.

Experimental Modifications. As the computations indicate that an increase in reaction time could improve the yields, the reactions were run for longer times. Disappointingly, the initially formed F4PEN reacted further, as seen by the disappearance of the blue color. Also, separating step 3 of the transformation from steps 1 and 2 by running the reaction at room temperature was not successful. Rather than the desired product **4**, we isolated its tautomer **7** in good yields, a finding that is not entirely unexpected (Scheme 2).[40] Compound **7** is prone to oxidation in solution, and after 7 days only the dehydrogenation product **8** can be detected.

Table 3. Free Energy of Activation ($\Delta G^{\ddagger}$, kcal/mol, T = 298.15 K) and the Reaction Rates (k, s^{-1}) Associated with TS3 Were Calculated at the M06-2X/6-31G(d) Level (R_2 = CO_2CF_3)

	R_1 = OH	R_1 = CH_3	R_1 = F	R_1 = CN
$\Delta G^{\ddagger}$	28.7	29.6	31.0	31.7
k (10^{-11})	567.4	124.2	11.7	3.6

Photochemical Synthesis of F4PEN. As the thermal route to F4PEN from **1c** could not significantly be improved, we have transformed **1c** into 2,3,9,10-tetrafluoro-6,13-dihydro-6,13-ethanopentacene-15,16-dione (**9**), as such α-diketones are well-known precursors to various acenes under photochemical conditions (Scheme 3).[56] Dihydroxylation with catalytic amounts of OsO_4 and *N*-methylmorpholine *N*-oxide (NMO) furnished the corresponding diol **10** in 89% yield following our previously reported procedures for closely related compounds.[57] The final oxidation step employed the Annelli protocol (NaOCl) that we have earlier found to be advantageous.[58] This step only proceeds with a yield of 40%, while the final photobisdecarbonylation again runs with high yield (90%). Overall, the three-step photochemical synthesis thus provides F4PEN in 32% from **1c**, an almost 3-fold increase over the reported procedure.[32] The photoirradiation ($\lambda \geq 395$ nm) of the α-diketone **9** can conveniently be run in DMSO solution at room temperature and results in precipitation of F4PEN in the form of a blue solid. Its spectral properties are identical to those of samples obtained previously by tetrazine-induced elimination.[32]

X-ray Structural Analysis. Crystals suitable for single-crystal X-ray crystallography were obtained by dissolving F4PEN (4−5 mg) in hot (200 °C) 1,2,4-trichlorobenzene (5 mL) in a long Schlenk tube and slowly cooling the solution in a tube furnace (1.2 °C/h). The compound crystallizes in the triclinic space group $P\bar{1}$ with two molecules in the unit cell. The intramolecular distances (C−C, 1.35−1.45 Å; CF, 1.34−1.35 Å) are similar to those of pentacene (PEN) and perfluoropentacene (PFP), respectively.[7,59]

Similar to PEN and PFP, F4PEN crystallizes in a herringbone motif (Figure 3a). The tilt angle of the F4PEN structure, 48.3° (Figure 3c), is smaller than it is in PEN (51.9°)[59] and PFP (91.2°).[7] There are fluorine−fluorine distances that are shorter than the sum of the van der Waals distance. The shortest of these, 2.85 Å, is between neighboring

DOI: 10.1021/acs.joc.7b03241
J. Org. Chem. 2018, 83, 3149−3158

Scheme 2. Reaction of 1c with dimethyl 1,2,4,5-tetrazine-3,6-dicarboxylate (at rt) Gives Tautomer 7 That Is Oxidized in Air to 8

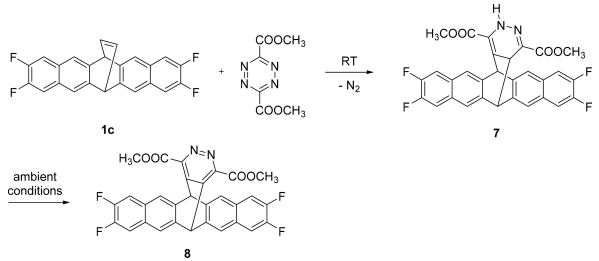

Scheme 3. Photochemical Synthesis of F4PEN (5c) Starting from 1c

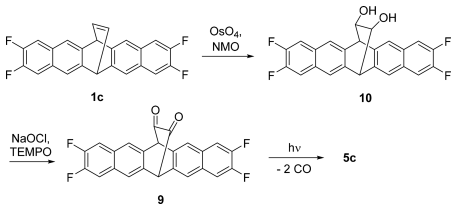

molecules that lie within the same plane (Figure 3b). Slightly longer ones, 2.87 and 2.95 Å, are additionally observed (not shown in Figure 3). The shortest fluorine−fluorine contacts are slightly shorter than the closest fluorine−fluorine intermolecular distances (2.92 Å) in PFP.[7]

As short intermolecular fluorine−fluorine distances are unusual, their origin has been discussed in the literature and most often is ascribed to crystal-packing effects.[60,61] The arrangement of the fluorine pairs in the structure of F4PEN (Figure 3b) is close to the type II arrangement that is assumed to be most favorable for significant fluorine−fluorine interactions and that is characterized by ideal CFF and FFC angles of 180° and 90°.[62] In F4PEN, the corresponding angles are 171° and 135°. In order to evaluate the strength of the bonding in the present case, the interaction energy of the dimer displayed in Figure 3b was computed using spin-component-scaled second-order Møller−Plesset perturbation theory (SCS-MP2) in conjunction with a large polarized triple-ζ basis set. This computation shows that the dimer is bound by less than 0.5 kcal mol^{-1}, indicating that the short distances are not a consequence of strong intermolecular fluorine−fluorine bonding.

Photophysical Properties. The optical spectrum (Figure 4) was measured using a saturated solution in degassed dichloromethane and is identical to the one published previously.[32] The p-band has its maximum at 561 nm with typical vibrational fine structure with intervals of roughly 1400 cm^{-1} (520, 485, and 455 nm). The α-band is detected at 422 nm and shows vibrational fine structure (roughly 1400 cm^{-1}, 398 nm). The additional weak and broad absorptions at 607 and 651 nm disappear in more diluted solutions, and no fluorescence is detected upon excitation into these bands. This shows that they are associated with formation of aggregates. The optical spectra of the solution did not show any change upon storage for 24 h under Ar in the dark, while in the presence of air the p-bands decrease after a few hours and the solution becomes colorless.

The fluorescence spectrum of F4PEN was not reported previously. It was obtained in dichloromethane solution at an excitation wavelength of 561 nm. As expected, a very small

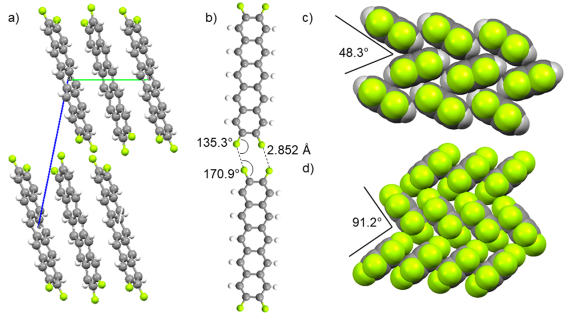

Figure 3. (a) Arrangement of F4PEN molecules in the solid-state structure viewed along the *a* axis. (b) Two adjacent molecules of F4PEN in the crystal with F···F contacts and angles. (c) Herring bone motif of F4PEN with tilt angle using a space-filling model. (d) Herring bone motif of PFP with tilt angle using a space-filling model. Data taken from Sakamoto et al.[7]

DOI: 10.1021/acs.joc.7b03241
J. Org. Chem. 2018, 83, 3149−3158

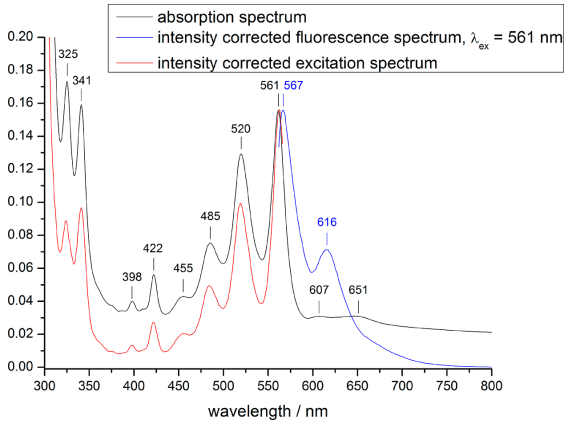

Figure 4. Absorption, emission (λ_{ex} = 561 nm), and excitation spectrum (λ_{em} = 567 nm) of F4PEN measured in dichloromethane.

Stokes shift of 6 nm (<200 cm^{-1}) is observed, and the emission band shows the typical fine structure of the acenes. The excitation spectrum was measured at an emission wavelength of 567 nm and is identical with the absorption spectrum.

Electrochemical Investigation. The solubility of F4PEN in most common aprotic organic electrolytes is insufficient for cyclic voltammetric experiments. Only in 1,2-dichlorobenzene could a satisfactory concentration be reached. Electrochemical oxidation and reduction of F4PEN were characterized in a 1,2-dichlorobenzene/0.08 M NBu_4PF_6 electrolyte at a concentration of about 0.4 mM in the entire accessible potential range. Two potential cycles were scanned from the rest potential of the solution (≈− 0.25 V; all potential values are reported versus an external ferrocene standard) to +0.648 V for oxidation and −2.052 V for reduction (Figure 5).

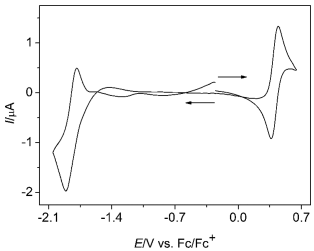

Figure 5. Cyclic voltammograms of F4PEN in 1,2-dichlorobenzene/0.08 M NBu_4PF_6 (saturated solution, c(F4PEN) ≈ 0.4 mM, ν = 1 V s^{-1}) at a Pt electrode; arrows indicate the initial scan direction for the two separately registered current/potential curves.

On the time scale of the experiments, the neutral starting compound is both oxidized and reduced in chemically reversible processes. The peak currents are proportional to the square root of the potential scan rate ν, indicating that the electroactive species is diffusing. The peak potential difference (ΔE_p) for the oxidation is ≈70 mV, close to the limit for electrochemical reversibility when considering a one-electron process. For reduction, at slow scan rates the same value is reached, however, ΔE_p increases at higher ν (quasi-reversibility). Still, again a one-electron transfer is assumed. Thus, the cyclic voltammograms prove the formation of radical ions $F4PEN^{\bullet+}$ and $F4PEN^{\bullet-}$ with a substantial lifetime at positive and negative potentials, respectively. We determine the formal potentials $E^0(F4PEN/F4PEN^{\bullet-})$ = −1.844 V and $E^0(F4PEN/F4PEN^{\bullet+})$ = +0.403 V as the midpoint potentials of the oxidation/reduction peak couples, respectively.

A second oxidation feature appears at ≈+ 1.0 V (not shown in Figure 5) very close to the positive limit of the potential window. The respective electrode process is chemically irreversible, and in the 1,2-dichlorobenzene electrolyte, the dication undergoes a chemical follow-up reaction. A more quantitative analysis of the voltammograms is precluded by the superimposition of the Faradaic current for the oxidation of F4PEN on the electrolyte discharge current. A second reduction is not found in the accessible potential window. Apart from this latter observation, the overall electrochemical reaction pattern of F4PEN is, however, similar to that of TIPS-pentacene.[63]

A rough estimate[64] of the HOMO−LUMO gap is derived from the E^0 values for oxidation and reduction as ≈2.25 eV, smaller than in the case of octafluorodiphenylanthracene[26] but larger than for TIPS-pentacene[65] and its 1-mono- and 1,11- or 1,8-difluorinated derivatives.[66] The HOMO−LUMO gap of F4PEN is also larger than that of parent pentacene (2.09 eV), while that of PFP is significantly smaller (1.92 eV, both values from differential pulse voltammetry, DPV).[7]

The reason for the increased HOMO−LUMO gap of F4PEN compared to that of PEN (both in 1,2-dichlorobenzene as electrolyte) is the pronounced shift of the oxidation potential from +0.22 to +0.40 V, while the reduction potential (−1.87 V for PEN) hardly experiences a shift (−1.844 V). Unfortunately, the two values for reduction are not directly comparable, because in the case of PEN a differential pulse voltammetry (DPV) peak potential is reported, while for F4PEN, we determined the formal potential. A correction requires knowledge of the DPV pulse height, which could not be

DOI: 10.1021/acs.joc.7b03241
J. Org. Chem. 2018, 83, 3149−3158

extracted from ref 7. With pulse heights usually in the range of 20 mV, the error is estimated to be in the range of 0.01 V. Keeping this in mind, we conclude that the four fluorine atoms of F4PEN make the pentacene core significantly more resistant toward oxidation but do not enhance its reducibility.

The increased HOMO−LUMO gap of F4PEN determined from the electrochemical analysis is in agreement with the optical absorption spectra (optical gaps of 2.15 eV for PEN and 2.21 eV for F4PEN), with our computations (B3LYP/6-311+G**) for the isolated molecules (2.19 eV for PEN and 2.23 eV for F4PEN), and earlier computational data reported for the molecule/Cu interface.[27]

Chemical Generation of the Radical Cation and Dication of F4PEN. Chemical oxidation of F4PEN can be achieved by dissolution in 2 M methanesulfonic acid (MSA) in nitrobenzene. This produces a pink solution. The ESR spectrum obtained from such a solution can be simulated reasonably well (see Figure 6 and Table 4). The two hydrogen

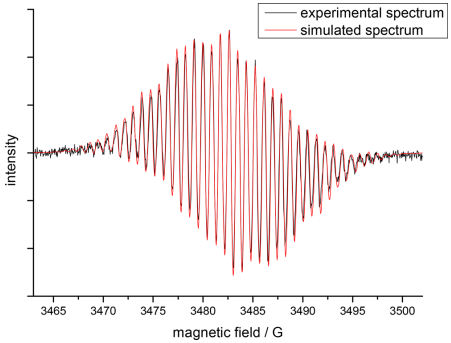

Figure 6. ESR spectrum of $F4PEN^{+\bullet}$ in 2 M methanesulfonic acid/nitrobenzene solution.

Table 4. Comparison of Simulated and Computed (B3LYP/EPR-III//B3LYP/6-311+G) Hyperfine Coupling Constants (in gauss) for $F4PEN^{\bullet+}$**

nuclei	simulated[a]	computed
H6/H13	5.294	5.115
H5/H7/H12/H14	3.530	3.792
H1/H4/H8/H11	1.592[b]	1.369
F2/F3/F8/F9	0.917[b]	1.142

[a]Simulation parameters: g factor = 2.00275; line width = 0.509; R^2 = 0.9925. [b]Tentative assignment based on the comparison with the computation.

atoms at the central ring have the largest hyperfine coupling constants (5.294 G) followed by those four at the adjacent rings (3.530 G). Similar coupling constants at the H6 (5.083 G) and H5 (3.554 G) positions were reported for parent pentacene.[67] The assignment is further supported by computations at the B3LYP/EPR-III//B3LYP/6-311+G** level of theory. The coupling constants of the four fluorine atoms are the smallest ones according to these computations. On the basis of the better agreement with the computation, the smaller hyperfine coupling constant is tentatively assigned to the fluorine atoms. Note that hyperfine coupling constants in fluorinated aromatics (computed at B3LYP/EPR-III) can show significant deviation from experiment[68] and that the assignment of the hyperfine coupling constants of H1 (given as 0.975 G) and H2 (0.757 G) in pentacene radical cation is considered uncertain.[67]

The electronic absorption spectrum of the radical cation $F4PEN^{\bullet+}$ was measured in 3 M MSA/nitrobenzene solution. It shows absorption maxima in the NIR (1112, 920, 817, 734 nm) and in the visible (437 nm) range (Figure 7b). This is

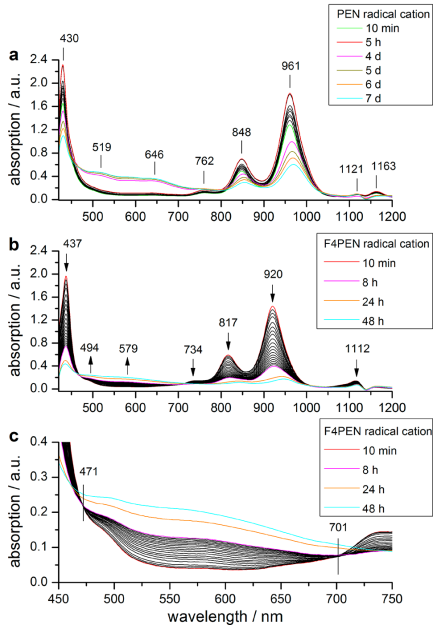

Figure 7. Absorption spectrum of $F4PEN^{\bullet+}$ obtained by dissolution of F4PEN in 3 M MSA/nitrobenzene and their temporal evolution indicating rather quick decomposition.

reminiscent of the absorption spectrum of the pentacene radical cation in cryogenic matrix[69−71] and in the same solvent mixture measured for comparison here (Figure 7a). While the pentacene radical cation bands (1163, 1121, 961, 848, 762, 430 nm) increase initially over a period of 5 h and slowly decrease during the next 7 days, the absorption peaks of $F4PEN^{\bullet+}$ quickly decrease in intensity within 8 h. This transformation of $F4PEN^{\bullet+}$ shows isosbestic points at 471 and 701 nm and goes along with growth of weak and very broad features with maxima at 494 and 594 nm. The decomposition product could not be identified. The investigation shows that the lifetime of the radical cation of pentacene is significantly larger than that of F4PEN. This observation is in agreement with the increased electron deficiency in F4PEN.

Dissolution of F4PEN in oleum results in a deep green solution of the dication. This is reminiscent of the behavior of PEN, which also dissolves in oleum as the dication with green

DOI: 10.1021/acs.joc.7b03241
J. Org. Chem. 2018, 83, 3149−3158

color.[72,73] The solution of the dication F4PEN^{2+} in oleum was subjected to NMR spectroscopy using an external D_2SO_4 standard for field locking and shimming, as the spectra directly diluted with D_2SO_4 showed rapid evolvement of side bands within minutes, presumably due to fast H/D exchange. Using the external standard, the spectra remained unchanged for a period longer than one month. The signals at 9.39, 9.10, and 8.28 ppm can be assigned to the hydrogen atoms at positions 6, 5, and 1, respectively, on the basis of integration, 2D NMR spectroscopy (NOESY, HSQC, and HMBC), and comparison with reported data for pentacene and heptacene dications.[73,74] For the hydrogen atoms at position 1, a H−F coupling with J = 7.0 Hz is observed. The ^{19}F NMR shows the expected single signal of F4PEN^{2+} (δ_F = −104.9 ppm). Due to a fwhm of 33 Hz of the ^{19}F signal, the H−F coupling could not be observed at room temperature (see Figure S17, Supporting Information). By heating the sample to 100 °C, the resolution could be increased and a splitting of the ^{19}F signal with J = 7 Hz was observed (see Figure S18, Supporting Information). The ^{13}C{^{1}H} and ^{13}C{^{19}F} NMR spectra display the expected number of signals, and HSQC and HMBC allow assignment of

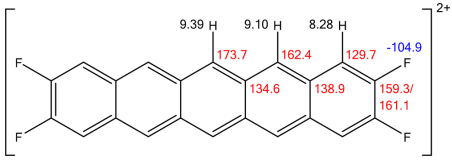

Figure 8. Assignment of the ^{1}H (black), ^{13}C (red), and ^{19}F (blue) NMR signals of F4PEN^{2+} in oleum.

these signals to the individual carbon atoms (Figure 8). The ^{19}F-coupled ^{13}C NMR spectrum shows C−F coupling for the carbon atoms in position 2 with $^1J_{CF}$ and $^2J_{CF}$ coupling constants of 284 and 15.7 Hz, respectively. Additional coupling between carbon atoms at position 1 with $^2J_{CF}$ = 13.9 Hz and $^3J_{CF}$ = 6.5 Hz is observed.

The influence of two positive charges on the ^{13}C chemical shifts was analyzed by Forsyth and Olah for a larger number of aromatic hydrocarbons, and a value of roughly 200 ppm/e was given.[74] Unfortunately, the very low solubility precludes measuring a ^{13}C NMR spectrum of F4PEN, and hence the consequence of a dipositive charge on δ_C cannot be evaluated. The δ_H and δ_F values undergo an average downfield shift of 0.60 and 30 ppm, respectively, using the data of neutral F4PEN obtained in TCE-d_2 (120 °C).[32]

The UV/vis spectrum of F4PEN^{2+} in oleum that was diluted with concentrated sulfuric acid is similar to that of PEN^{2+} (Figure 9). The signature of F4PEN^{2+} persists for days under ambient atmosphere.

The spectra are dominated by two strong features in the high-energy region (382 and 390 nm, respectively) and in the low-energy visible region (761 nm and roughly 710 nm). The intensities of the two features in the long-wavelength region differ, and the reason for this is not clear. The optical spectrum of the pentacene dication was first reported in 1970,[72] but it has not been analyzed in detail, to the best of our knowledge. For the pentacene dianion, however, a strong long-axis-polarized band at 735 nm and a weak short-axis-polarized band at 676 nm

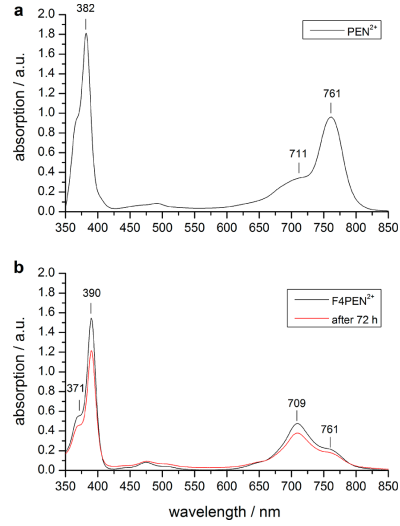

Figure 9. Absorption spectrum of dications obtained by dissolution of PEN (a) and F4PEN (b) in oleum diluted with H_2SO_4.

were assigned,[75] and on the basis of the pairing theorem, similar assignments may hold for the pentacene dication. A recent computational investigation at the TD-DFT level assigns the long-wavelength absorption of PEN^{2+} to the long-axis-polarized HOMO → LUMO excitation and the short-wavelength band to HOMO−1 → LUMO+1.[76] The computed transition energies differ by up to 0.5 eV from the measurements, possibly due to neglect of the polar environment.

CONCLUSIONS

The synthesis of a pentacene scaffold with four fluorine atoms at the termini is possible either by photobisdecarbonylation of a α-diketone precursor or by tetrazine-induced cycloreversion of a 6,13-dihydro-6,13-ethenopentacene. Although neither of these routes proceeds with high overall yields, both provide 2,3,9,10-tetrafluoropentacene (F4PEN) in pure form. This allows investigation of F4PEN in its neutral form and in its mono- and dicationic states and, hence, allows an in-depth analysis of the influence of four terminal fluorine atoms on the electronic, structural, and chemical properties.

The fluorination degree of the F4PEN molecule is intermediate between those of pentacene (PEN) and perfluoropentacene (PFP), but this is not reflected in the solid-state structure or in the electronic properties. All three compounds crystallize in a herringbone motif, but the tilt angle in the F4PEN structure is *smaller* than that in PEN and in PFP. Likewise, while the HOMO−LUMO gap derived from optical and electrochemical measurements of perfluoropentance is smaller than that of pentacene, partial fluorination at the 2,3,9,10 positions results in a *larger* gap. This is due to the increased oxidation potential and the almost unaffected reduction potential and, hence, shows that the four fluorine atoms primarily act by stabilizing the HOMO.

DOI: 10.1021/acs.joc.7b03241
J. Org. Chem. 2018, 83, 3149−3158

Despite the increased oxidation potential, both the radical cation and dication of F4PEN can be generated in oxidizing solvents. The optical spectrum of the radical cation resembles that of the pentacene radical cation, but as with the neutrals, the bands undergo a hypsochromic shift. The persistence of $F4PEN^{+\bullet}$ is significantly reduced compared to the parent ion, but it is sufficient for characterization by steady-state ESR spectroscopy. The dication in sulfuric acid is persistent under ambient conditions so that a full characterization by NMR spectroscopy is possible.

EXPERIMENTAL SECTION

General. ^{1}H NMR spectra were recorded on a Bruker Avance III HD 400 or a Bruker Avance III HDX 600 MHz instrument. Chemical shifts for ^{1}H NMR were reported as δ relative to the signal of $CHCl_3$ at 7.26 (s) ppm or relative to the signal of H_2SO_4 at 10.89 ppm, respectively. Chemical shifts for ^{13}C NMR were reported as δ relative to the signal of $CHCl_3$ at 77.16 ppm. The following abbreviations were used to describe splitting patterns: s = singlet, d = doublet, appt = apparent triplet, m = multiplet. The sample of $F4PEN^{2+}$ used for NMR spectroscopy (Bruker Avance III HDX 600 equipped with a 5 mm Progidy BBO-Cryo-Probe) was generated by dissolving neutral F4PEN in oleum and using an external D_2SO_4 standard for field locking and shimming.

Absorption spectra were measured on a PerkinElmer Lambda 1050 UV/vis/NIR spectrometer, and the fluorescence and excitation spectra of F4PEN were measured on a Agilent Cary Eclipse fluorescence spectrometer. ESR data was obtained using a Bruker ESP 300E (X-Band) spectrometer. High-resolution EI and ESI mass spectra were measured on a Finnigan MAT 95 mass spectrometer equipped with a sector field mass analyzer and a Bruker maXis 4G UHR-TOF mass spectrometer, respectively.

Unless otherwise stated, all chemicals were either used as received from their respective commercial suppliers or purified according to literature recommendation.[77] Solvents for flash column and thin layer chromatography, including dichloromethane, *n*-hexane, ethyl acetate, toluene, and methanol, were all of HPLC grade quality. 1,2,4-Trichlorobenzene was dried over 3 Å molecular sieves and degassed by the freeze−pump−thaw method. Dichloromethane used in the UV/vis and fluorescence experiments was taken from a MBRAUN SPS-800 solvent purification system and degassed by three consecutive freeze−pump−thaw cycles. Nitrobenzene (analytical grade) as well as methanesulfonic acid (99% extra pure) used for generating the radical cations of PEN and F4PEN were purchased from Acros Organics and used as received. Oleum (20−30% free SO_3) was purchased from Sigma-Aldrich and used as received. Thin layer chromatography was performed on fluorescence-indicator-marked precoated silica gel 60 plates and visualized by UV light (254 nm/366 nm). Flash column chromatography was performed on silica gel (0.040−0.063 mm). Compound **1c** was synthesized as described previously.[32]

Electrochemical Investigations. 1,2-Dichlorobenzene (Sigma-Aldrich; anhydrous) was used without purification. Acetonitrile was distilled successively over P_2O_5, CaH_2, and P_2O_5 again. NBu_4PF_6 was recrystallized four times from ethanol/water 3:1 and dried at ≈3 mbar and 105 °C for 1 week.

Electroanalytical experiments were performed in a full-glass, gastight three-electrode cell[78] under an argon atmosphere with an ECO-Autolab PGSTAT100 (Metrohm) with GPES-Software 4.9.007. As the working electrode, a Pt disk electrode tip (Metrohm part No. 6.1204.310; nominal diameter 3 mm) was used. The electrode was polished with alumina (0.3 μm; Buehler Micropolish) prior to experiments. The counter electrode consisted of a Pt wire with 1 mm diameter. A Haber−Luggin double reference electrode with a potential-determining Ag/Ag^+ redox system (0.01 M $AgClO_4$ in 0.1 M NBu_4PF_6 /CH_3CN)[79] was used as the potential standard. The *iR* drop was compensated by positive feedback under control of the GPES software. Cyclic voltammetric experiments were performed at scan rates between 0.1 and 2 V s^{-1}. The cyclic voltammetric data are background-corrected. Potentials are referenced to an external ferrocene (Fc) standard [$E^0(Fc/Fc^+)$ = +0.252 V vs the Ag/Ag^+ redox system].

*2,3,9,10-Tetrafluoro-6,13-dihydro-6,13-ethanopentacene-15,16-diol (**10**).* A solution of **1c** (407 mg, 1.08 mmol) dissolved in 80 mL of acetone was added to a solution of *N*-methylmorpholine *N*-oxide (585 mg, 5.00 mmol) and OsO_4 (1.35 mL, 2.5% in *t*BuOH) in 180 mL of acetone and 3 mL of water under argon. The mixture was stirred for 48 h at rt. The reaction was quenched by adding a solution of sodium dithionite (1.35 g) in 13 mL of water, and after 15 min of stirring, the mixture was filtered and the solid residue washed thoroughly with acetone. The filtrate was evaporated and the brown residue was dissolved in 200 mL of CH_2Cl_2 and 200 mL of water. The aqueous phase was separated and extracted with CH_2Cl_2. The combined organic phase was washed with brine and dried over $MgSO_4$, and then the solvent was removed. The brown residue was purified by column chromatography (silica, CH_2Cl_2/methanol = 100:1). The product was obtained as a white solid (394 mg, 0.96 mmol, 89%). ^{1}H NMR (DMSO-d_6, 400 MHz): δ 4.03 (s, 2H), 4.59 (s, 2H), 4.83 (s, 2H), 5.75 (s, 1H), 7.84 (s, 2H), 7.86−7.92 (m, 6H). ^{13}C{^{1}H} NMR (d_6-DMSO, 100 MHz): δ 50.8, 67.0, 113.4 (dd, J = 6.0, 26.0 Hz), 113.5 (dd, J = 6.0, 26.2 Hz), 122.5, 123.9, 128.9 (dd, J = 4.4, 12.0 Hz), 129.0 (dd, J = 4.4, 12.1 Hz), 138.1, 138.8, 148.5 (dd, J = 17.5, 246.1 Hz), 148.7 (dd, J = 17.6, 247.0 Hz). ^{19}F NMR (DMSO-d_6, 376 MHz): δ −139.3 (appt, J = 10.2 Hz), −138.6 (appt, J = 10.0 Hz). MS (FAB): m/z (%) 433 (10, M^+ + Na). HRMS (ESI): m/z [M + Na]$^+$ calcd for $C_{24}H_{14}F_4O_2$ 433.0822, found 433.0831. Mp: 149 °C.

*2,3,9,10-Tetrafluoro-6,13-dihydro-6,13-ethanopentacene-15,16-dione (**9**).* To a solution of **10** (50 mg, 0.12 mmol) dissolved in 30 mL of CH_2Cl_2 and 9 mL of water were added TEMPO (19 mg), KBr (75 mg), and $NaHCO_3$ (125 mg). Then a solution of NaOCl (0.40 mL, 5% active chlorine) diluted with 1.3 mL of water was added dropwise within 10 min at 0 °C. After stirring for another 5 min, the mixture was poured into 20 mL of water. The aqueous phase was separated and extracted with CH_2Cl_2. The combined organic phases were washed with brine and dried over $MgSO_4$, and then the solvent was removed on a rotary evaporator. The residue was purified by column chromatography (silica, CH_2Cl_2/*n*-hexane = 80:20). The product was obtained as a yellow solid (20 mg, 0.049 mmol, 40%). ^{1}H NMR ($CDCl_3$, 400 MHz): δ 5.29 (s, 2H), 7.59 (appt, J = 9.2, 4H), 7.89 (s, 4H). ^{13}C{^{1}H} NMR ($CDCl_3$, 100 MHz): δ 60.5, 114.0 (dd, J = 6.0, 12.0 Hz), 124.9, 130.6 (appt, J = 4.6), 132.4, 150.9 (dd, J = 16.0, 251.6 Hz), 184.4. ^{19}F NMR ($CDCl_3$, 376 MHz): δ −134.3 (appt, J = 9.2). MS (FAB): m/z (%) 407 (8, M^+ + H). HRMS (ESI): m/z [M + MeOH + Na]$^+$ calcd for $C_{24}H_{10}F_4O_2$ 461.0771, found 461.0775.

*2,3,9,10-Tetrafluoropentacene (F4PEN, **5c**).* The α-diketone precursor **9** (10 mg) was dissolved in 15 mL of dry DMSO in a Schlenk tube. The solution protected with argon was irradiated at $\lambda \geq$ 395 nm by using a high-pressure mercury lamp with a dichroic mirror (350−450 nm) and cutoff filters for wavelength selection. The solid pentacene was generated during 20−25 min of irradiation. Removal of the solvent by filtration and washing the solid with CH_2Cl_2 and *n*-hexane gave the product as a violet powder (9 mg, 90%) after drying under vacuum. Mp: 334 °C (dec).

*Compound **7**.* To a solution of **1c** (97.4 mg, 0.26 mmol) in 10 mL of $CHCl_3$ was added dimethyl 1,2,4,5-tetrazine-3,6-dicarboxylate (51.3 mg, 0.26 mmol) all at once. The mixture was stirred for 24 h at rt and the solvent removed under reduced pressure. The residue was purified by column chromatography (silica, gradient from CH_2Cl_2 to ethyl acetate/CH_2Cl_2 4:1). Compound **7** was obtained as a yellow solid (104.8 mg, 0.19 mmol, 74%). ^{1}H NMR ($CDCl_3$, 600 MHz): δ 8.43 (s, 1 H), 7.83 (s, 1 H), 7.79 (s, 1 H), 7.76 (s, 1 H), 7.64 (s, 1 H), 7.55−7.42 (m, 4 H), 6.39 (s, 1 H), 6.04 (d, J = 2.2 Hz, 1 H), 4.02 (s, 3 H), 3.83 (s, 3 H), 2.90 (d, J = 2.2 Hz, 1 H). ^{13}C{^{1}H} NMR ($CDCl_3$, 150 MHz): δ 163.5, 161.2, 151.5−150.7 (m), 149.5−149.2 (m), 149.1, 147.1, 140.9 (d, J = 2.3 Hz), 140.7 (d, J = 2.2 Hz), 138.1 (d, J = 2.3 Hz), 137.5 (d, J = 2.0 Hz), 130.0, 129.5−129.2 (m), 129.1 (d, J = 7.2 Hz), 124.5−124.4 (m), 124.1, 122.7 (d, J = 4.3 Hz), 122.4 (d, J = 4.3 Hz), 121.3 (d, J = 4.3 Hz), 113.9−113.4 (m), 52.9, 52.6, 46.1, 44.6, 41.8. ^{19}F NMR ($CDCl_3$, 565 MHz): δ −136.9 to −137.0 (m), −137.0

DOI: 10.1021/acs.joc.7b03241
J. Org. Chem. 2018, 83, 3149−3158

to −137.1 (m), −137.2 to −137.3 (m). HRMS (EI): m/z $[M]^{+\bullet}$ calcd for $C_{30}H_{18}N_2O_4F_4$ 546.1197, found 546.1211.

Oxidation product **8** was obtained after stirring at room temperature for 7 days. ^{1}H NMR ($CDCl_3$, 600 MHz): δ 7.92 (s, 4 H), 7.49 (appt, J = 9.0 Hz, 4 H), 6.91 (s, 2 H), 4.18 (s, 6 H). ^{13}C{^{1}H} NMR ($CDCl_3$, 151 MHz): δ 164.9, 151.4/149.7 (dd, J = 253.2 Hz, 17.4 Hz), 147.1 (d, J = 2.7 Hz), 138.4, 129.0 (appt, J = 4.5 Hz), 123.5, 113.8 (dd, J = 13.1 Hz, 4.9 Hz), 53.7, 47.7. ^{19}F NMR ($CDCl_3$, 565 MHz): δ −135.8 (appt, J = 8.2 Hz). HRMS (EI): m/z $[M]^{+\bullet}$ calcd for $C_{30}H_{16}N_2O_4F_4$ 544.1040, found 544.1028.

Computational Methods. All DFT computations were performed with Gaussian 09.[80] Geometry optimizations of all the minima and transition states were carried out at the M06-2X level of theory and the 6-31G(d) basis set,[81,82] which have been shown to give reliably energetics for cycloadditions.[83,84] The vibrational frequencies were computed at the same level to check whether each optimized structure is an energy minimum or a transition state and to evaluate its zero-point vibrational energy (ZPVE) and thermal corrections at 298 K, using the rigid rotor, harmonic oscillator model of an ideal gas. Intrinsic reaction coordinate (IRC)[85] calculations were carried out to verify the connectivity of each transition state with the corresponding product and reactant. The geometries of PEN, F4PEN, and F4PEN$^{\bullet+}$ radical were computed using the B3LYP[86,87] functional as implemented[88] in Gaussian 09 in conjunction with the 6-311+G** basis set. The hyperfine coupling constants of F4PEN$^{\bullet+}$ were computed using Barone's EPR-III basis set.[89]

Geometry optimizations of the F4PEN dimers were performed using spin-component-scaled[90,91] Møller−Plesset second-order perturbation theory (SCS-MP2) in conjunction with the resolution-of-the-identity (RI)[92] and frozen-core approximations. Dunning's[93] correlation consistent triple-ζ basis set (cc-pVTZ) and the recommended[94] RI fitting basis set were employed. All SCS-MP2 computations were performed with the TURBOMOLE program package.[95]

■ ASSOCIATED CONTENT

Supporting Information

The Supporting Information is available free of charge on the ACS Publications website at DOI: 10.1021/acs.joc.7b03241.

NMR spectra, X-ray crystallography details, absolute energies and Cartesian coordinates of computed stationary points (PDF)

Crystalllographic data for **5c** in CIF format (CIF)

Crystalllographic data for **11** in CIF format (CIF)

■ AUTHOR INFORMATION

Corresponding Author

*E-mail: holger.bettinger@uni-tuebingen.de.

ORCID

Bernd Speiser: 0000-0001-5111-8314

Holger F. Bettinger: 0000-0001-5223-662X

Notes

The authors declare no competing financial interest.

■ ACKNOWLEDGMENTS

Bin Shen thanks the China Scholarship Council for a fellowship. We thank the Karl and Anna Buck-Stiftung, Stuttgart, Germany, for a doctoral fellowship for S.S. We gratefully acknowledge assistance from Konstantin Doljabidian, Daniel Eppacher, Laura Schwarz, and Theresa Rieser. This work was funded in part by the Deutsche Forschungsgemeinschaft (DFG). The computations were performed on the bwHPC cluster Justus. The authors acknowledge support by the state of Baden-Württemberg through bwHPC and the DFG through grant no INST 40/467-1 FUGG.

■ REFERENCES

(1) Anthony, J. E. *Chem. Rev.* **2006**, *106*, 5028.

(2) Gundlach, D. J.; Royer, J. E.; Park, S. K.; Subramanian, S.; Jurchescu, O. D.; Hamadani, B. H.; Moad, A. J.; Kline, R. J.; Teague, L. C.; Kirillov, O.; Richter, C. A.; Kushmerick, J. G.; Richter, L. J.; Parkin, S. R.; Jackson, T. N.; Anthony, J. E. *Nat. Mater.* **2008**, *7*, 216.

(3) Anthony, J. E. *Angew. Chem., Int. Ed.* **2008**, *47*, 452.

(4) Watanabe, M.; Chen, K.-Y.; Chang, Y. J.; Chow, T. J. *Acc. Chem. Res.* **2013**, *46*, 1606.

(5) Payne, M. M.; Parkin, S. R.; Anthony, J. E.; Kuo, C.-C.; Jackson, T. N. *J. Am. Chem. Soc.* **2005**, *127*, 4986.

(6) Lee, S.; Koo, B.; Shin, J.; Lee, E.; Park, H.; Kim, H. *Appl. Phys. Lett.* **2006**, *88*, 162109.

(7) Sakamoto, Y.; Suzuki, T.; Kobayashi, M.; Gao, Y.; Fukai, Y.; Inoue, Y.; Sato, F.; Tokito, S. *J. Am. Chem. Soc.* **2004**, *126*, 8138.

(8) Sakamoto, Y.; Suzuki, T.; Kobayashi, M.; Gao, Y.; Inoue, Y.; Tokito, S. *Mol. Cryst. Liq. Cryst.* **2006**, *444*, 225.

(9) Inoue, Y.; Sakamoto, Y.; Suzuki, T.; Kobayashi, M.; Gao, Y.; Tokito, S. *Jpn. J. Appl. Phys.* **2005**, *44*, 3663.

(10) Ogden, W. A.; Ghosh, S.; Bruzek, M. J.; McGarry, K. A.; Balhorn, L.; Young, V.; Purvis, L. J.; Wegwerth, S. E.; Zhang, Z.; Serratore, N. A.; Cramer, C. J.; Gagliardi, L.; Douglas, C. J. *Cryst. Growth Des.* **2017**, *17*, 643.

(11) Sakamoto, Y.; Suzuki, T. *J. Org. Chem.* **2017**, *82*, 8111.

(12) Kim, C.-H.; Hlaing, H.; Payne, M. M.; Yager, K. G.; Bonnassieux, Y.; Horowitz, G.; Anthony, J. E.; Kymissis, I. *ChemPhysChem* **2014**, *15*, 2913.

(13) Kim, C.-H.; Hlaing, H.; Hong, J.-A.; Kim, J.-H.; Park, Y.; Payne, M. M.; Anthony, J. E.; Bonnassieux, Y.; Horowitz, G.; Kymissis, I. *Adv. Mater. Interfaces* **2015**, *2*, 1400384.

(14) Kim, C.-H.; Hlaing, H.; Payne, M. M.; Parkin, S. R.; Anthony, J. E.; Kymissis, I. *ChemPhysChem* **2015**, *16*, 1251.

(15) Swartz, C. R.; Parkin, S. R.; Bullock, J. E.; Anthony, J. E.; Mayer, A. C.; Malliaras, G. G. *Org. Lett.* **2005**, *7*, 3163.

(16) Pensack, R. D.; Ostroumov, E. E.; Tilley, A. J.; Mazza, S.; Grieco, C.; Thorley, K. J.; Asbury, J. B.; Seferos, D. S.; Anthony, J. E.; Scholes, G. D. *J. Phys. Chem. Lett.* **2016**, *7*, 2370.

(17) Pensack, R. D.; Tilley, A. J.; Parkin, S. R.; Lee, T. S.; Payne, M. M.; Gao, D.; Jahnke, A. A.; Oblinsky, D. G.; Li, P.-F.; Anthony, J. E.; Seferos, D. S.; Scholes, G. D. *J. Am. Chem. Soc.* **2015**, *137*, 6790.

(18) Grollman, R.; Quist, N.; Robertson, A.; Rath, J.; Purushothaman, B.; Haley, M. M.; Anthony, J. E.; Ostroverkhova, O. *J. Phys. Chem. C* **2017**, *121*, 12483.

(19) Sherman, J. B.; Moncino, K.; Baruah, T.; Wu, G.; Parkin, S. R.; Purushothaman, B.; Zope, R.; Anthony, J.; Chabinyc, M. L. *J. Phys. Chem. C* **2015**, *119*, 20823.

(20) Paudel, K.; Johnson, B.; Thieme, M.; Haley, M. M.; Payne, M. M.; Anthony, J. E.; Ostroverkhova, O. *Appl. Phys. Lett.* **2014**, *105*, 043301.

(21) Sherman, J. B.; Purushothaman, B.; Parkin, S. R.; Kim, C.; Collins, S.; Anthony, J.; Nguyen, T.-Q.; Chabinyc, M. L. *J. Mater. Chem. A* **2015**, *3*, 9989.

(22) Paudel, K.; Johnson, B.; Neunzert, A.; Thieme, M.; Purushothaman, B.; Payne, M. M.; Anthony, J. E.; Ostroverkhova, O. *J. Phys. Chem. C* **2013**, *117*, 24752.

(23) Kendrick, M. J.; Neunzert, A.; Payne, M. M.; Purushothaman, B.; Rose, B. D.; Anthony, J. E.; Haley, M. M.; Ostroverkhova, O. *J. Phys. Chem. C* **2012**, *116*, 18108.

(24) Schwarze, M.; Tress, W.; Beyer, B.; Gao, F.; Scholz, R.; Poelking, C.; Ortstein, K.; Günther, A. A.; Kasemann, D.; Andrienko, D.; Leo, K. *Science* **2016**, *352*, 1446.

(25) Ueno, N. *Science* **2016**, *352*, 1395.

(26) Tannaci, J. F.; Noji, M.; McBee, J.; Tilley, T. D. *J. Org. Chem.* **2007**, *72*, 5567.

(27) Toyoda, K.; Hamada, I.; Yanagisawa, S.; Morikawa, Y. *Org. Electron.* **2011**, *12*, 295.

(28) Koch, N.; Gerlach, A.; Duhm, S.; Glowatzki, H.; Heimel, G.; Vollmer, A.; Sakamoto, Y.; Suzuki, T.; Zegenhagen, J.; Rabe, J. P.; Schreiber, F. *J. Am. Chem. Soc.* **2008**, *130*, 7300.

DOI: 10.1021/acs.joc.7b03241
J. Org. Chem. 2018, 83, 3149−3158

(29) Toyoda, K.; Hamada, I.; Lee, K.; Yanagisawa, S.; Morikawa, Y. *J. Phys. Chem. C* **2011**, *115*, 5767.
(30) Koch, N.; Vollmer, A.; Duhm, S.; Sakamoto, Y.; Suzuki, T. *Adv. Mater.* **2007**, *19*, 112.
(31) Toyota, K. Organic field-effect transistors. Patent JP2011249715A, 2011.
(32) Bula, R. P.; Oppel, I. M.; Bettinger, H. F. *J. Org. Chem.* **2012**, *77*, 3538.
(33) Chien, C.-T.; Chiang, T.-C.; Watanabe, M.; Chao, T.-H.; Chang, Y. J.; Lin, Y.-D.; Lee, H.-K.; Liu, C.-Y.; Tu, C.-H.; Sun, C.-H.; Chow, T. J. *Tetrahedron Lett.* **2013**, *54*, 903.
(34) Savu, S.-A.; Biddau, G.; Pardini, L.; Bula, R.; Bettinger, H. F.; Draxl, C.; Chassé, T.; Casu, M. B. *J. Phys. Chem. C* **2015**, *119*, 12538.
(35) Savu, S.-A.; Sonström, A.; Bula, R.; Bettinger, H. F.; Chassé, T.; Casu, M. B. *ACS Appl. Mater. Interfaces* **2015**, *7*, 19774.
(36) Chuang, T.-H.; Hsieh, H.-H.; Chen, C.-K.; Wu, C.-C.; Lin, C.-C.; Chou, P.-T.; Chao, T.-H.; Chow, T. J. *Org. Lett.* **2008**, *10*, 2869.
(37) Chen, K.-Y.; Hsieh, H.-H.; Wu, C.-C.; Hwang, J.-J.; Chow, T. J. *Chem. Commun.* **2007**, 1065.
(38) Moursounidis, J.; Wege, D. *Tetrahedron Lett.* **1986**, *27*, 3045.
(39) Zhai, Y.; Ghiviriga, I.; Battiste, M. A.; Dolbier, W. R. *Synthesis* **2004**, *2004*, 2747.
(40) Sauer, J.; Heldmann, D. K.; Hetzenegger, J.; Krauthan, J.; Sichert, H.; Schuster, J. *Eur. J. Org. Chem.* **1998**, *1998*, 2885.
(41) Thalhammer, F.; Wallfahrer, U.; Sauer, J. *Tetrahedron Lett.* **1990**, *31*, 6851.
(42) Mayer, S.; Lang, K. *Synthesis* **2017**, *49*, 830.
(43) Devaraj, N. K. *Synlett* **2012**, *23*, 2147.
(44) Wu, H.; Devaraj, N. K. *Top. Curr. Chem.* **2016**, *374*, 3.
(45) Sadasivam, D. V.; Prasad, E.; Flowers, R. A.; Birney, D. M. *J. Phys. Chem. A* **2006**, *110*, 1288.
(46) Levandowski, B. J.; Hamlin, T. A.; Bickelhaupt, F. M.; Houk, K. N. *J. Org. Chem.* **2017**, *82*, 8668.
(47) Biermann, D.; Schmidt, W. *J. Am. Chem. Soc.* **1980**, *102*, 3163.
(48) Afzali, A.; Dimitrakopoulos, C. D.; Breen, T. L. *J. Am. Chem. Soc.* **2002**, *124*, 8812.
(49) Afzali, A.; Kagan, C. R.; Traub, G. P. *Synth. Met.* **2005**, *155*, 490.
(50) Schleyer, P. v. R.; Manoharan, M.; Jiao, H.; Stahl, F. *Org. Lett.* **2001**, *3*, 3643.
(51) Zade, S. S.; Bendikov, M. *J. Phys. Org. Chem.* **2012**, *25*, 452.
(52) Cioslowski, J.; Sauer, J.; Hetzenegger, J.; Karcher, T.; Hierstetter, T. *J. Am. Chem. Soc.* **1993**, *115*, 1353.
(53) Liu, F.; Liang, Y.; Houk, K. N. *J. Am. Chem. Soc.* **2014**, *136*, 11483.
(54) Yang, J.; Liang, Y.; Šečkutė, J.; Houk, K. N.; Devaraj, N. K. *Chem. - Eur. J.* **2014**, *20*, 3365.
(55) Hansch, C.; Leo, A.; Taft, R. W. *Chem. Rev.* **1991**, *91*, 165.
(56) Suzuki, M.; Aotake, T.; Yamaguchi, Y.; Noguchi, N.; Nakano, H.; Nakayama, K.-i.; Yamada, H. *J. Photochem. Photobiol., C* **2014**, *18*, 50.
(57) Tönshoff, C.; Bettinger, H. F. *Chem. - Eur. J.* **2012**, *18*, 1789.
(58) Tönshoff, C.; Bettinger, H. F. *Angew. Chem., Int. Ed.* **2010**, *49*, 4125.
(59) Mattheus, C. C.; Dros, A. B.; Baas, J.; Meetsma, A.; Boer, J. L. d.; Palstra, T. T. M. *Acta Crystallogr., Sect. C: Cryst. Struct. Commun.* **2001**, *57*, 939.
(60) Reichenbacher, K.; Suss, H. I.; Hulliger, J. *Chem. Soc. Rev.* **2005**, *34*, 22.
(61) Berger, R.; Resnati, G.; Metrangolo, P.; Weber, E.; Hulliger, J. *Chem. Soc. Rev.* **2011**, *40*, 3496.
(62) Ramasubbu, N.; Parthasarathy, R.; Murray-Rust, P. *J. Am. Chem. Soc.* **1986**, *108*, 4308.
(63) Schundelmeier, S.; Speiser, B.; Bettinger, H. F.; Einholz, R. *ChemPhysChem* **2017**, *18*, 2266.
(64) Holze, R. *Organometallics* **2014**, *33*, 5033.
(65) Hodgson, J.; Miller, G. P. *ECS Trans.* **2012**, *41*, 37.
(66) Wasikiewicz, J. M.; Abu-Sen, L.; Horn, A. B.; Koelewijn, J. M.; Parry, A. V. S.; Morrison, J. J.; Yeates, S. G. *J. Mater. Chem. C* **2016**, *4*, 7309.
(67) Bolton, J. R. *J. Chem. Phys.* **1967**, *46*, 408.
(68) Rakitin, A. R.; Yff, D.; Trapp, C. *J. Phys. Chem. A* **2003**, *107*, 6281.
(69) Halasinski, T. M.; Hudgins, D. M.; Salama, F.; Allamandola, L. J.; Bally, T. *J. Phys. Chem. A* **2000**, *104*, 7484.
(70) Mondal, R.; Tönshoff, C.; Khon, D.; Neckers, D. C.; Bettinger, H. F. *J. Am. Chem. Soc.* **2009**, *131*, 14281.
(71) Szczepanski, J.; Wehlburg, C.; Vala, M. *Chem. Phys. Lett.* **1995**, *232*, 221.
(72) Distler, D.; Hohlneicher, G. *Chem. Phys. Lett.* **1970**, *7*, 345.
(73) Einholz, R.; Bettinger, H. F. *Angew. Chem., Int. Ed.* **2013**, *52*, 9818.
(74) Forsyth, D. A.; Olah, G. A. *J. Am. Chem. Soc.* **1976**, *98*, 4086.
(75) Hoytink, G. J. *Chem. Phys. Lett.* **1974**, *26*, 318.
(76) Dominikowska, J.; Domagala, M.; Palusiak, M. *J. Chem. Phys.* **2014**, *140*, 044324.
(77) Armarego, W. L. F.; Chai, C. L. L. *Purification of Laboratory Chemicals, 6th ed.*; Elsevier Science Bv: Amsterdam, 2009.
(78) Dümmling, S.; Eichhorn, E.; Schneider, S.; Speiser, B.; Würde, M. *Curr. Sep.* **1996**, *15*, 53.
(79) Gollas, B.; Krauß, B.; Speiser, B.; Stahl, H. *Curr. Sep.* **1994**, *13*, 42.
(80) Frisch, M. J. T., G, W.; Schlegel, H. B.; Scuseria, G. E.; Robb, M. A.; Cheeseman, J. R.; Scalmani, G.; Barone, V.; Mennucci, B.; Petersson, G. A.; Nakatsuji, H.; Caricato, M.; Li, X.; Hratchian, H. P.; Izmaylov, A. F.; Bloino, J.; Zheng, G.; Sonnenberg, J. L.; Hada, M.; Ehara, M.; Toyota, K.; Fukuda, R.; Hasegawa, J.; Ishida, M.; Nakajima, T.; Honda, Y.; Kitao, O.; Nakai, H.; Vreven, T.; Montgomery, J. A., Jr.; Peralta, J. E.; Ogliaro, F.; Bearpark, M.; Heyd, J. J.; Brothers, E.; Kudin, K. N.; Staroverov, V. N.; Kobayashi, R.; Normand, J.; Raghavachari, K.; Rendell, A.; Burant, J. C.; Iyengar, S. S.; Tomasi, J.; Cossi, M.; Rega, N.; Millam, M. J.; Klene, M.; Knox, J. E.; Cross, J. B.; Bakken, V.; Adamo, C.; Jaramillo, J.; Gomperts, R.; Stratmann, R. E.; Yazyev, O.; Austin, A. J.; Cammi, R.; Pomelli, C.; Ochterski, J. W.; Martin, R. L.; Morokuma, K.; Zakrzewski, V. G.; Voth, G. A.; Salvador, P.; Dannenberg, J. J.; Dapprich, S.; Daniels, A. D.; Farkas, Ö.; Foresman, J. B.; Ortiz, J. V.; Cioslowski, J.; Fox, D. J. *Gaussian 09*, revision D.01; Gaussian, 2015.
(81) Zhao, Y.; Truhlar, D. *Theor. Chem. Acc.* **2008**, *120*, 215.
(82) Zhao, Y.; Truhlar, D. G. *Acc. Chem. Res.* **2008**, *41*, 157.
(83) Paton, R. S.; Mackey, J. L.; Kim, W. H.; Lee, J. H.; Danishefsky, S. J.; Houk, K. N. *J. Am. Chem. Soc.* **2010**, *132*, 9335.
(84) Lan, Y.; Zou, L.; Cao, Y.; Houk, K. N. *J. Phys. Chem. A* **2011**, *115*, 13906.
(85) Gonzalez, C.; Schlegel, H. B. *J. Phys. Chem.* **1990**, *94*, 5523.
(86) Becke, A. D. *J. Chem. Phys.* **1993**, *98*, 5648.
(87) Lee, C.; Yang, W.; Parr, R. G. *Phys. Rev. B: Condens. Matter Mater. Phys.* **1988**, *37*, 785.
(88) Stephens, P. J.; Devlin, F. J.; Chabalowski, C. F.; Frisch, M. J. *J. Phys. Chem.* **1994**, *98*, 11623.
(89) Barone, V. In *Recent Advances in Density Functional Methods*; Chong, D. P., Ed.; World Scientific, 1995; p 287.
(90) Grimme, S. *J. Chem. Phys.* **2003**, *118*, 9095.
(91) Grimme, S.; Goerigk, L.; Fink, R. F. *WIREs Comput. Mol. Sci.* **2012**, *2*, 886.
(92) Weigend, F.; Häser, M. *Theor. Chem. Acc.* **1997**, *97*, 331.
(93) Dunning, T. H. *J. Chem. Phys.* **1989**, *90*, 1007.
(94) Weigend, F.; Köhn, A.; Hättig, C. *J. Chem. Phys.* **2002**, *116*, 3175.
(95) *TURBOMOLE V7.0 2015*, a development of University of Karlsruhe and Forschungszentrum Karlsruhe GmbH, 1989−2007, TURBOMOLE GmbH, since 2007; available from http://www.turbomole.com.

DOI: 10.1021/acs.joc.7b03241
J. Org. Chem. 2018, 83, 3149−3158

Supporting Information

Bridging the Gap between Pentacene and Perfluoropentacene: Synthesis and Characterization of 2,3,9,10-Tetrafluoropentacene in the Neutral, Cationic and Dicationic State

Bin Shen,[a] Thomas Geiger,[a] Ralf Einholz,[a] Florian Reicherter,[a] Simon Schundelmeier,[a] Cäcilia Maichle-Mössmer,[b] Bernd Speiser,[a] Holger F. Bettinger*,[a]

[a] Institut für Organische Chemie, Auf der Morgenstelle 18, 72076 Tübingen, Germany

[b] Institut für Anorganische Chemie, Auf der Morgenstelle 18, 72076 Tübingen, Germany

E-Mail: holger.bettinger@uni-tuebingen.de

Table of Contents

1. NMR Spectra 2

2. X-Ray Crystallography 14

3. Cartesian Coordinates 18

4. References 45

1. NMR Spectra

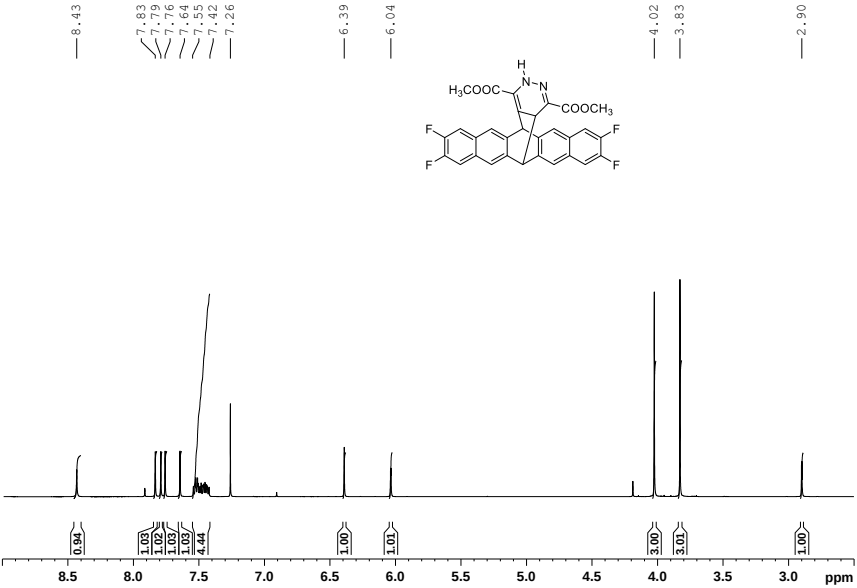

Figure S1. ^{1}H-NMR (600 MHz) spectrum of **7** in $CDCl_3$

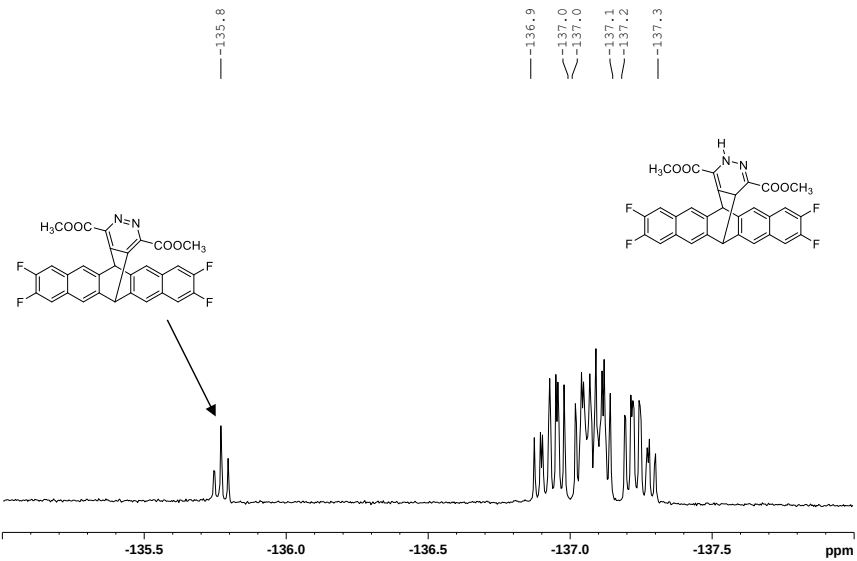

Figure S2. ^{19}F-NMR (565 MHz) spectrum of **7** in $CDCl_3$

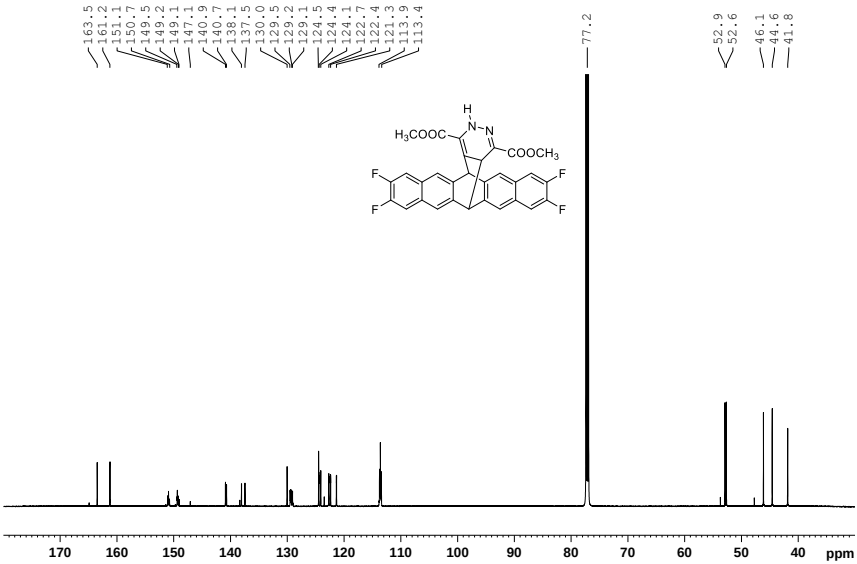

Figure S3. ^{13}C-NMR (151 MHz) spectrum of **7** in $CDCl_3$

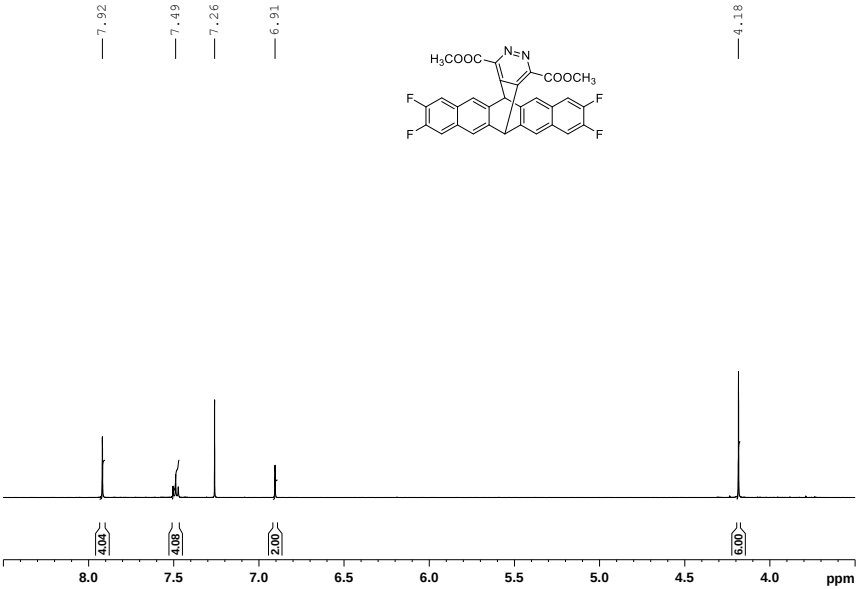

Figure S4. ^{1}H-NMR (600 MHz) spectrum of **8** in $CDCl_3$.

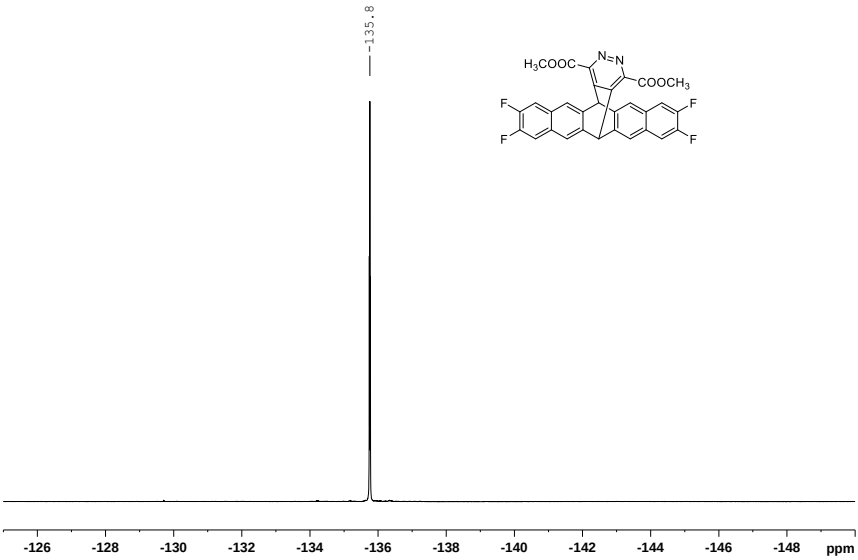

Figure S5. ^{19}F-NMR (545 MHz) spectrum of **8** in $CDCl_3$

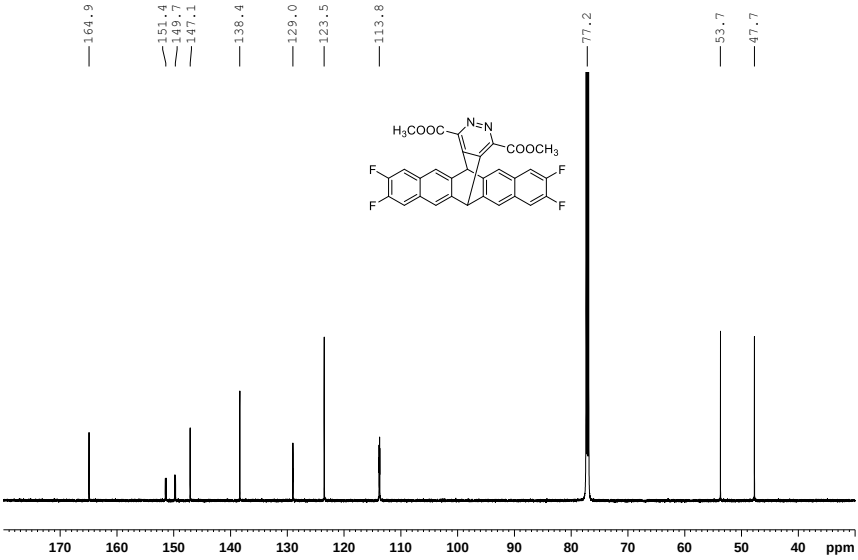

Figure S6. ^{13}C-NMR (151 MHz) spectrum of **8** in $CDCl_3$

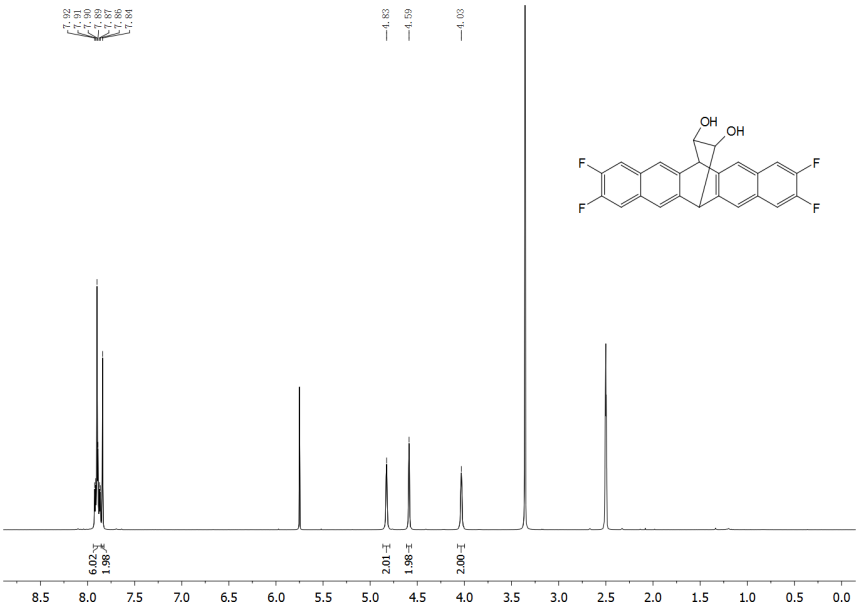

Figure S7. ^{1}H-NMR (400 MHz) spectrum of **10** in DMSO-d$_6$

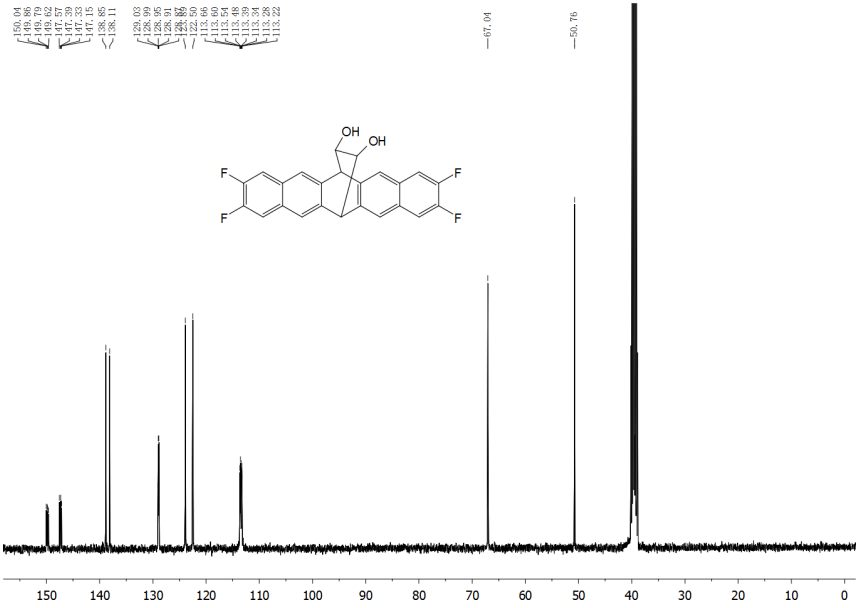

Figure S8. ^{13}C-NMR (100 MHz) spectrum of **10** in DMSO-d$_6$

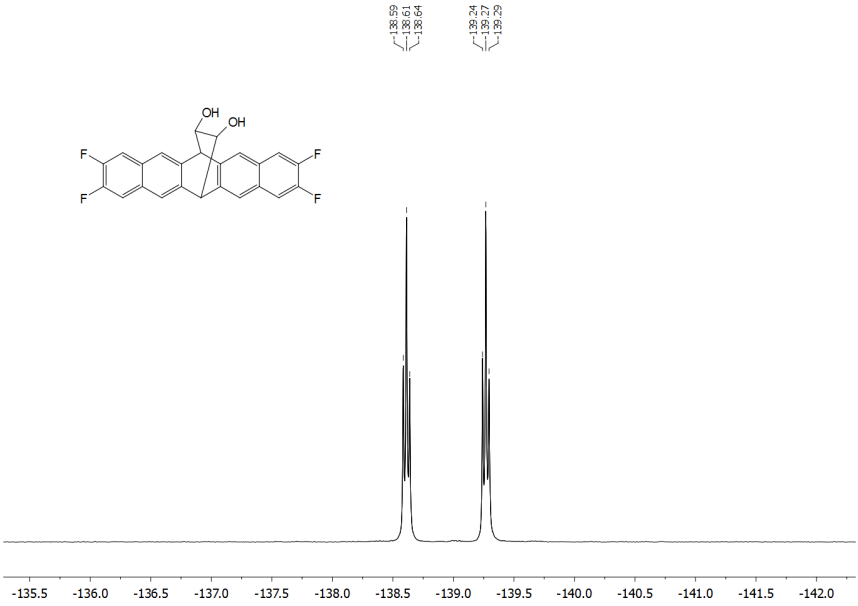

Figure S9. ^{19}F-NMR (376 MHz) spectrum of **10** in DMSO-d_6

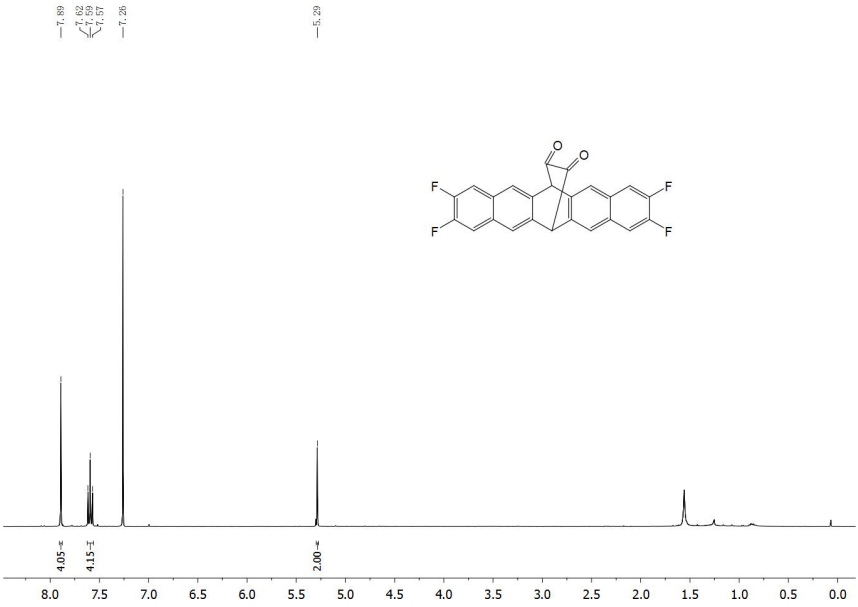

Figure S10. ^{1}H-NMR (400 MHz) spectrum of **9** in $CDCl_3$

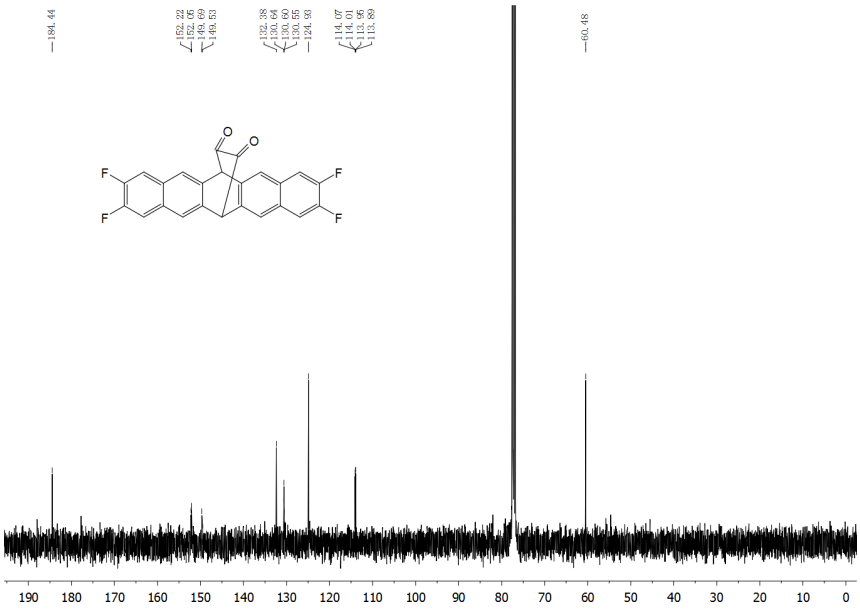

Figure S11. ^{13}C-NMR (100 MHz) spectrum of **9** in $CDCl_3$

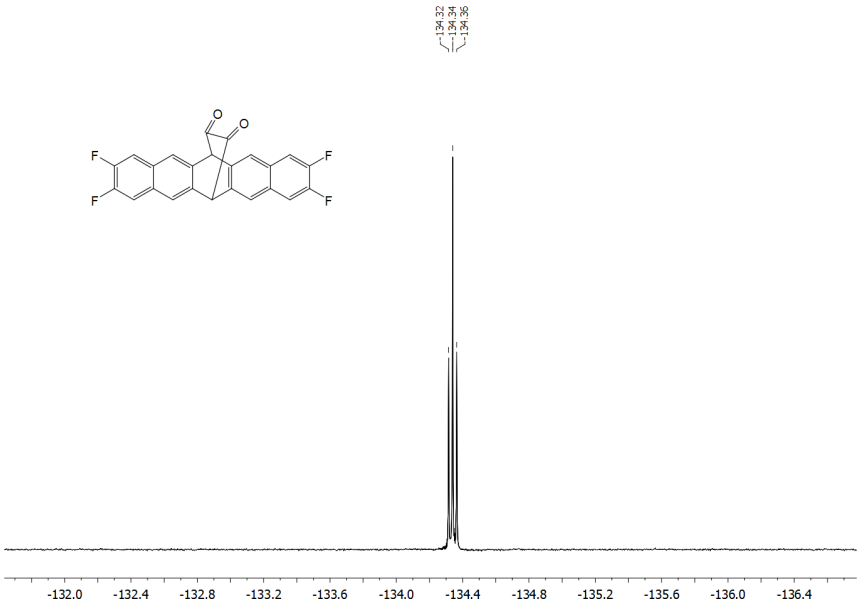

Figure S12. ^{19}F-NMR (376 MHz) spectrum of **9** in $CDCl_3$

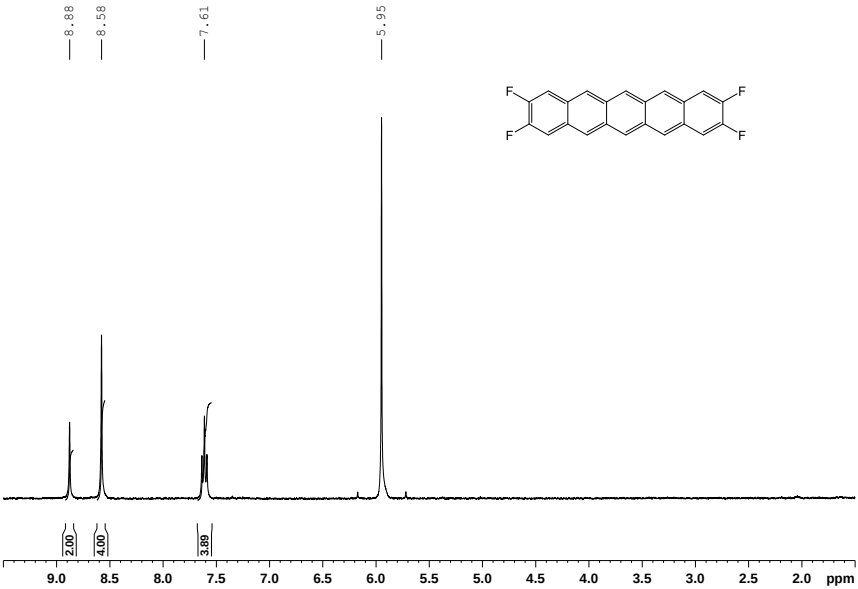

Figure S13. ^{1}H-NMR (400 MHz) spectrum of **5c** in TCE-d_2 at 120 °C

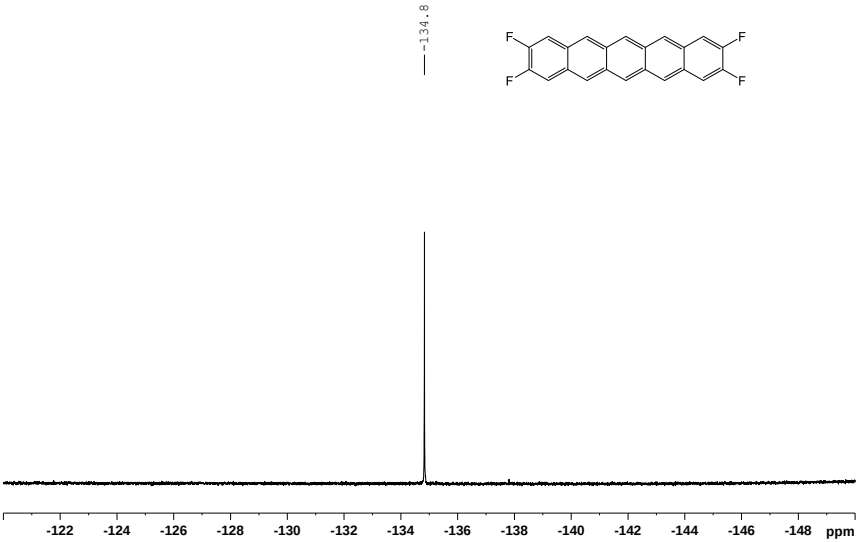

Figure S14. ^{19}F{^{1}H}-NMR (376 MHz) spectrum of **5c** in TCE-d_2 at 120 °C

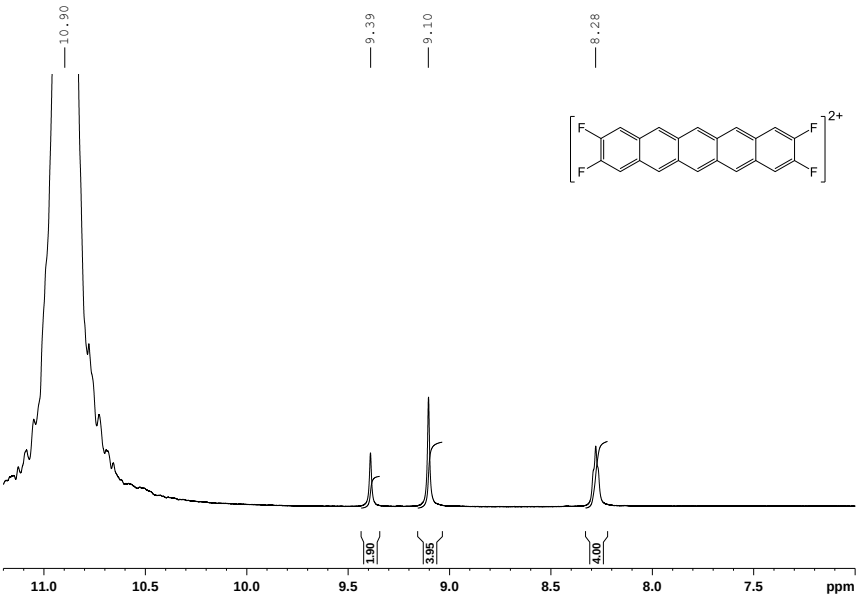

Figure S15. ^{1}H-NMR (600 MHz) spectrum of F4PEN^{2+} (**5c**$^{2+}$) in H_2SO_4, external D_2SO_4 standard

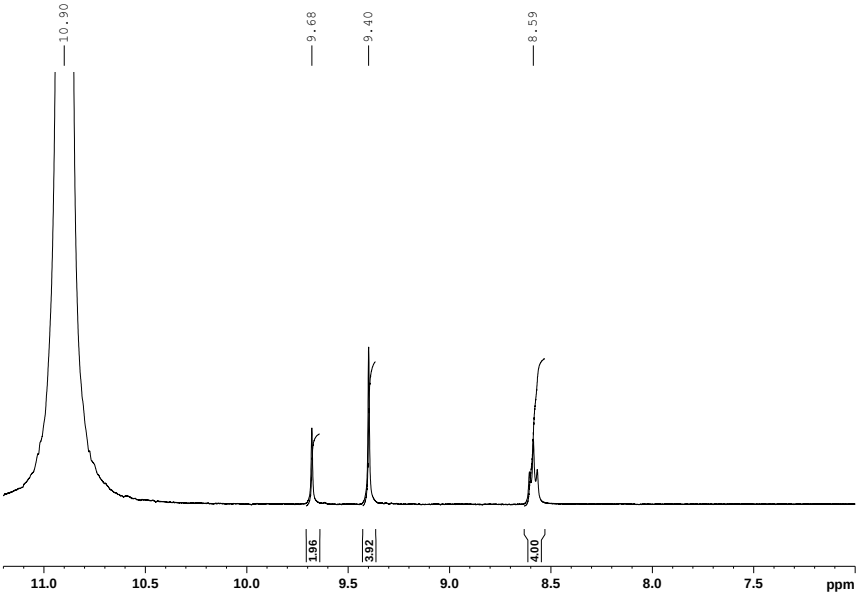

Figure S16. ^{1}H-NMR (400 MHz) spectrum of F4PEN^{2+} (**5c**$^{2+}$) in H_2SO_4 at 100 °C, external D_2SO_4 standard

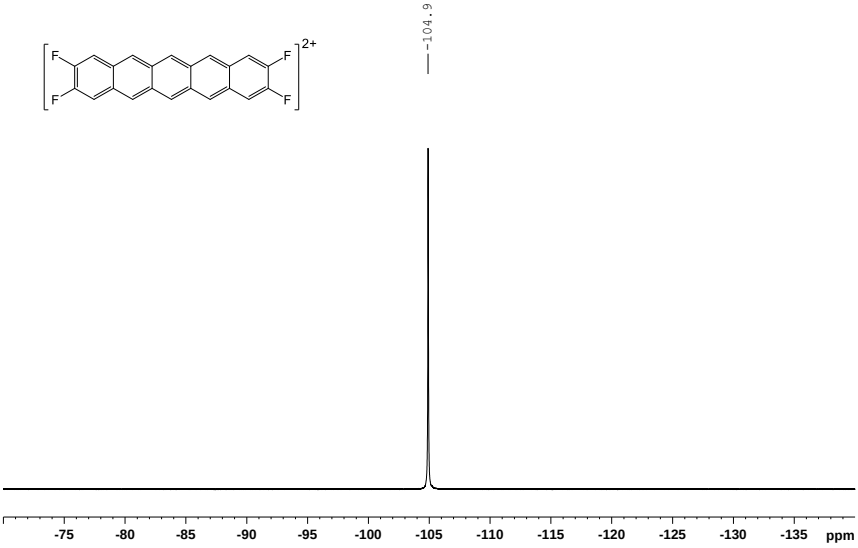

Figure S17. ^{19}F{^{1}H}-NMR (565 MHz) spectrum of F4PEN^{2+} (**5c**$^{2+}$) in H_2SO_4, external D_2SO_4 standard

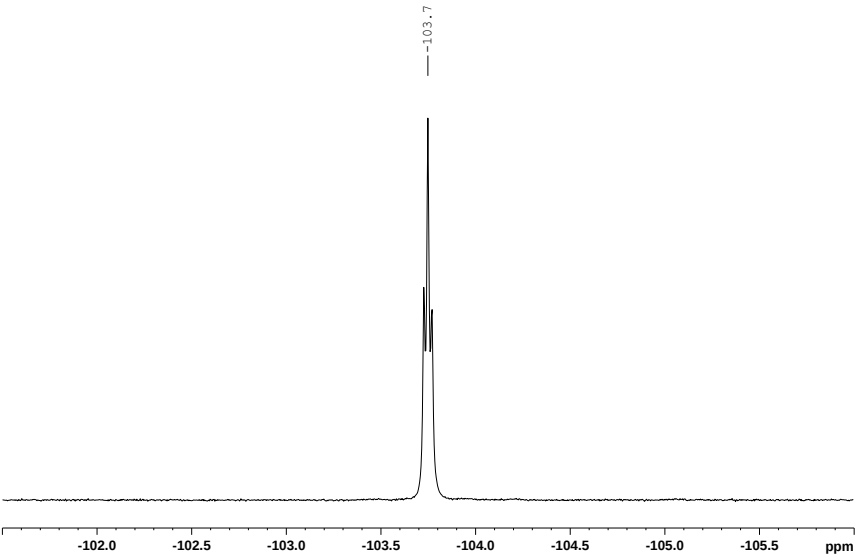

Figure S18. ^{19}F-NMR (376 MHz) spectrum of F4PEN^{2+} (5c^{2+}) in H_2SO_4 at 100 °C, external D_2SO_4 standard

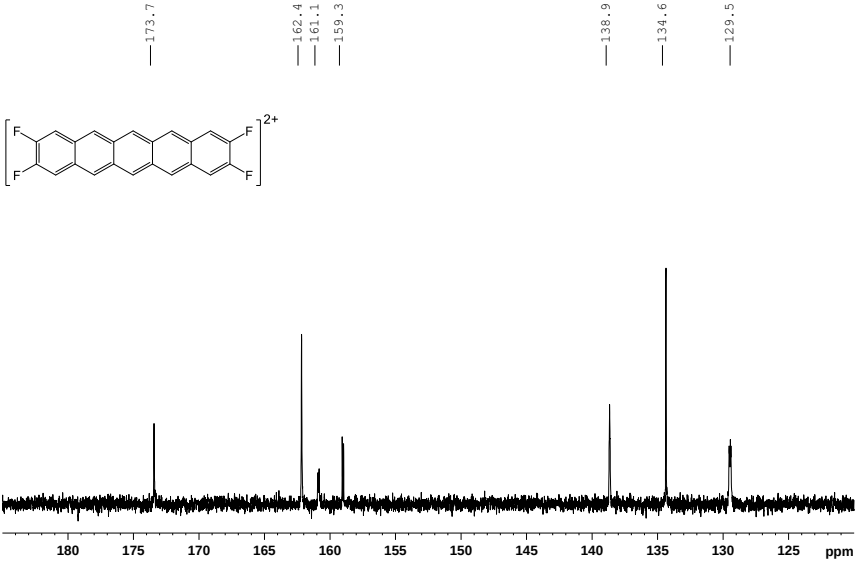

Figure S19. ^{13}C-NMR (151 MHz) spectrum of F4PEN^{2+} (**5c**$^{2+}$) in H_2SO_4, external D_2SO_4 standard

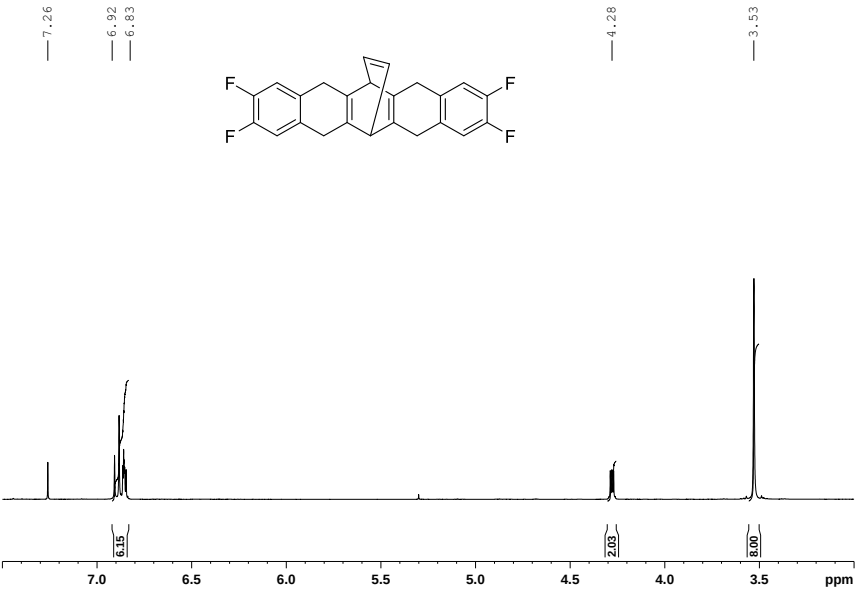

Figure S20. ^{1}H-NMR (400 MHz) spectrum of **11** in $CDCl_3$

Figure S21. ^{19}F-NMR (376 MHz) spectrum of **11** in $CDCl_3$

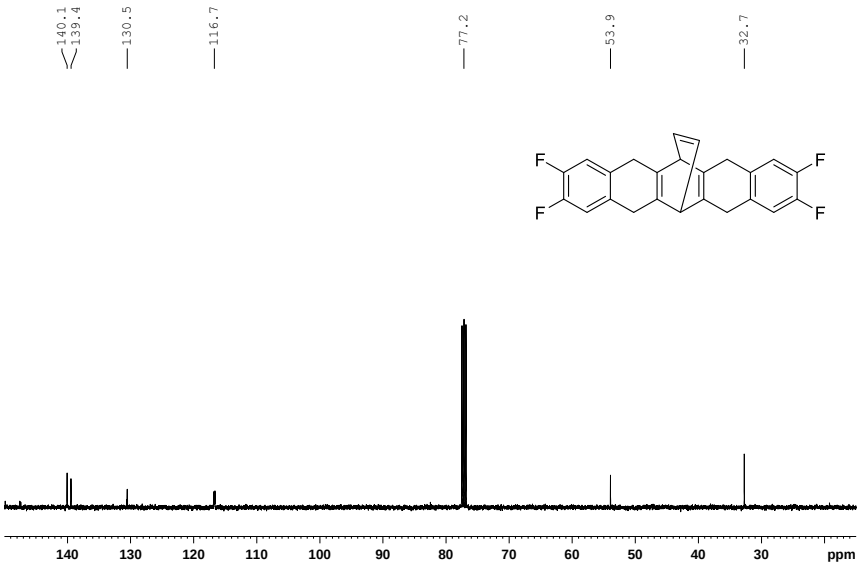

Figure S22. ^{13}C-NMR (101 MHz) spectrum of **11** in $CDCl_3$

2. X-ray crystallography

The synthesis of **1c** according to the published procedure,[1] involves dehydrogenation of tetrahydro derivative **11**. Crystals suitable for X-ray crystallography were obtained by slow evaporation of a solution in acetone.

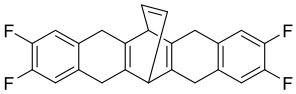

11

Single crystals were selected, coated with Parabar 10312 (previously known as Paratone N, Hampton Research) and fixed on a microloop. For F4PEN (**5c**) data were collected on a Bruker APEX DUO instrument equipped with an IμS microfocus sealed tube and QUAZAR optics for MoK_α radiation (λ = 0.71073 Å). Data for compound **11** were collected on a Bruker SMART APEX II instrument equipped with a fine focus sealed tube and curved graphite monochromator using MoK_α radiation (λ = 0.71073 Å). The data collection strategy was determined using COSMO[2] employing ϕ scans. Raw data were processed using APEX[3] and SAINT,[4] corrections for absorption effects were applied using SADABS.[5] The structures was solved by direct methods and refined against all data by full-matrix least-squares methods on F^2 using SHELXTL[6] and Shelxle.[7]

Table S1. Crystal data and structure refinement

	11	**5c**
Empirical formula	$C_{51}\,H_{38}\,F_8\,O$	$C_{22}\,H_{10}\,F_4$
Formula weight	818.81	350.30
Temperature	111(2) K	100(2) K
Wavelength	0.71073 Å	0.71073 Å
Crystal system	monoclinic	triclinic
Space group	P 2_1/n	P$\bar{1}$
Unit cell dimensions	a = 12.2856(4) Å	a = 6.7171(8) Å
	b = 23.0002(6) Å	b = 7.6452(9) Å
	c = 13.9552(4) Å	c = 14.3038(18) Å

	β= 101.088(2)°	α= 100.606(4) β= 94.579(4) γ = 98.384(4)°
Volume	3869.7(2) $Å^3$	709.98(15) $Å^3$
Z	4	2
Density (calculated)	1.405 Mg/m^3	1.639 Mg/m^3
Absorption coefficient	0.109 mm^{-1}	0.131 mm^{-1}
F(000)	1696	356
Crystal size	0.13 x 0.11 x 0.1 mm^3	0.218 x 0.158 x 0.050 mm^3
Reflections collected	43700	18671
Independent reflections	8500 [R(int) = 0.0292]	3132 [R(int) = 0.0347]
Absorption correction	Semi-empirical	numerical
Max. and min. trans.	0.7455 and 0.7055	0.9930 and 0.9720
Data / restraints / parameters	8500 / 0 / 543	3132 / 0 / 235
GOOF on F^2	0.934	1.100
Final R indices [I>2sigma(I)]	R_1 = 0.0470, wR_2 = 0.0968	R_1 = 0.0499, wR_2 = 0.1388
R indices (all data)	R_1 = 0.0670, wR_2 = 0.1074	R_1 = 0.0748, wR_2 = 0.1578

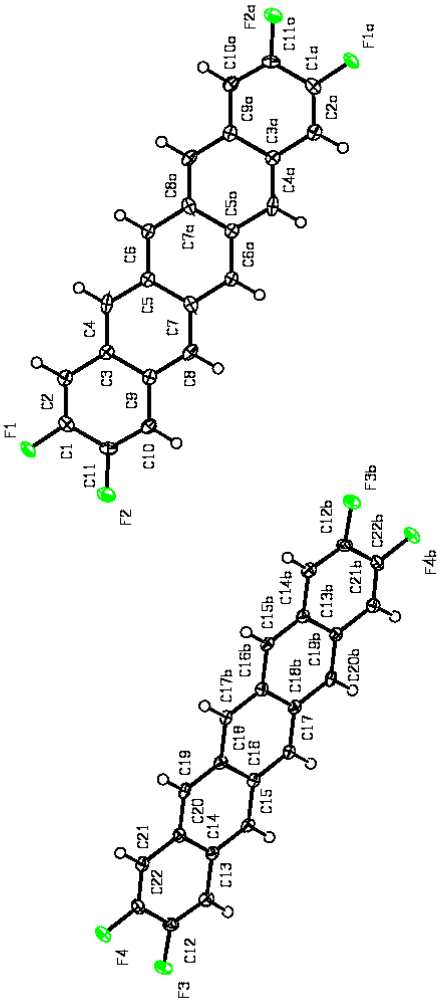

Figure S23. ORTEP view of **5c**. Atoms are represented by atomic displacement ellipsoids at the 50% level.

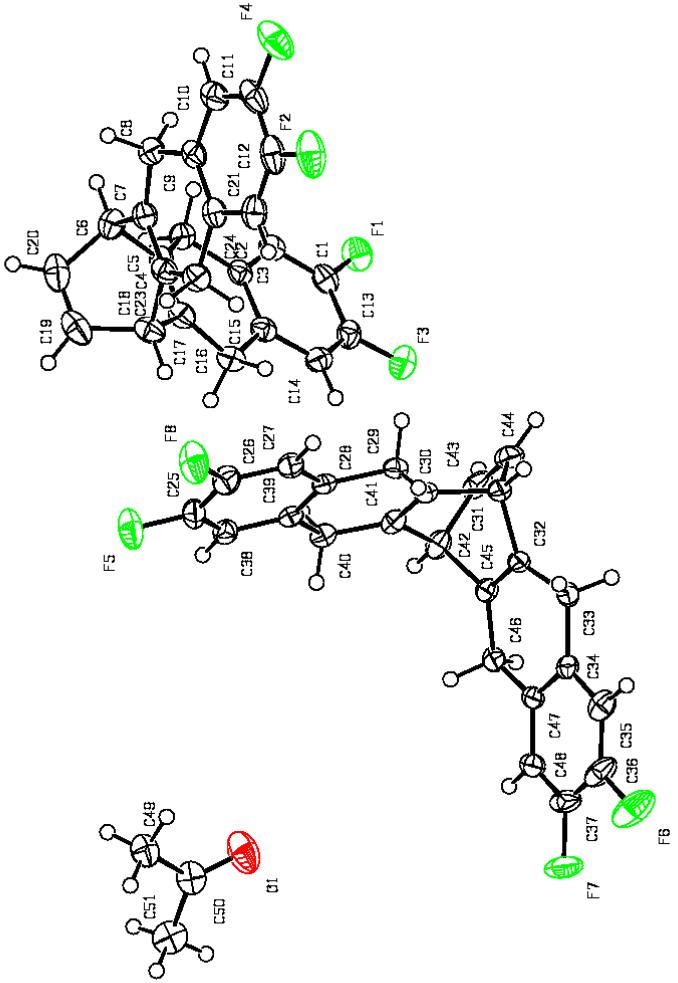

Figure S24. ORTEP view of **11**. Atoms are represented by atomic displacement ellipsoids at the 50% level.

3. Cartesian Coordinates

M062X/6-31G*, in Ångstrom								
1a				**1b**				
E(SCF) = -1224.59347669				E(SCF) = -1081.00691989				
C	-5.333396000	-1.303709000	0.691849000	C	-5.382006000	-1.274758000	0.714463000
C	-4.329366000	-0.692781000	1.390127000	C	-4.350388000	-0.664389000	1.386984000
C	-3.270101000	-0.042137000	0.704379000	C	-3.280389000	-0.028968000	0.709964000
C	-3.272959000	-0.038888000	-0.718288000	C	-3.280396000	-0.029034000	-0.709962000
C	-4.330055000	-0.680568000	-1.413537000	C	-4.350400000	-0.664521000	-1.386914000
C	-5.341521000	-1.301389000	-0.731563000	C	-5.382014000	-1.274824000	-0.714325000
H	-2.211046000	0.593309000	2.491499000	H	-2.215460000	0.602076000	2.496689000
H	-4.335101000	-0.702291000	2.478507000	H	-4.346821000	-0.662710000	2.475503000
C	-2.210337000	0.602008000	1.403388000	C	-2.213846000	0.607774000	1.408609000
C	-2.209725000	0.608546000	-1.410925000	C	-2.213867000	0.607648000	-1.408679000
H	-4.348882000	-0.688396000	-2.498973000	H	-4.346844000	-0.662943000	-2.475433000
C	-1.209869000	1.221926000	-0.713155000	C	-1.210980000	1.216830000	-0.712737000
C	-1.210305000	1.220435000	0.710100000	C	-1.210962000	1.216883000	0.712595000
H	-2.210129000	0.604762000	-2.498780000	H	-2.215492000	0.601851000	-2.496759000
C	1.209877000	1.221741000	0.713542000	C	1.210988000	1.216927000	0.712617000
C	2.209597000	0.607847000	1.411103000	C	2.213918000	0.607874000	1.408620000
C	3.272857000	-0.039249000	0.718273000	C	3.280447000	-0.028863000	0.709963000
C	3.270304000	-0.041499000	-0.704405000	C	3.280416000	-0.028970000	-0.709963000
C	2.210596000	0.602912000	-1.403197000	C	2.213861000	0.607667000	-1.408669000
C	1.210312000	1.220718000	-0.709674000	C	1.210962000	1.216823000	-0.712709000
H	4.348356000	-0.690077000	2.498757000	H	4.346951000	-0.662525000	2.475487000
H	2.209653000	0.603213000	2.498956000	H	2.215543000	0.602193000	2.496700000
C	4.329818000	-0.681455000	1.413318000	C	4.350470000	-0.664270000	1.386967000
C	4.329745000	-0.691681000	-1.390378000	C	4.350392000	-0.664508000	-1.386920000
H	2.211508000	0.595028000	-2.491318000	H	2.215453000	0.601849000	-2.496749000
C	5.333518000	-1.303200000	-0.692318000	C	5.381994000	-1.274844000	-0.714349000
C	5.341377000	-1.301850000	0.731139000	C	5.382048000	-1.274698000	0.714442000
H	4.335728000	-0.700329000	-2.478757000	H	4.346808000	-0.662947000	-2.475439000
C	0.001439000	1.946963000	-1.291223000	C	0.000002000	1.940915000	-1.291992000
C	-0.001437000	1.946537000	1.291897000	C	-0.000007000	1.941035000	1.291820000
C	-0.001094000	3.339138000	0.666566000	C	-0.000034000	3.333411000	0.665835000
C	0.001043000	3.339391000	-0.665329000	C	0.000021000	3.333346000	-0.666112000
H	-0.001988000	4.230701000	1.283785000	H	-0.000032000	4.225121000	1.282819000
H	0.001836000	4.231236000	-1.282168000	H	0.000024000	4.225000000	-1.283179000
H	0.002498000	1.955999000	-2.383172000	H	0.000023000	1.950171000	-2.383862000
H	-0.002499000	1.955507000	2.383842000	H	-0.000043000	1.950364000	2.383689000
O	6.354724000	-1.919069000	1.388127000	C	6.505517000	-1.939829000	1.465707000
H	6.950680000	-2.299754000	0.723356000	H	6.577011000	-3.005626000	1.219604000
O	6.397833000	-1.960431000	-1.251171000	H	7.474324000	-1.490188000	1.218875000
H	6.324704000	-1.939357000	-2.215112000	H	6.358708000	-1.852356000	2.544945000
O	-6.355011000	-1.918067000	-1.388828000	C	6.505346000	-1.940234000	-1.465563000
H	-6.951199000	-2.298663000	-0.724218000	H	7.474250000	-1.490808000	-1.218756000
O	-6.397525000	-1.961415000	1.250512000	H	6.576583000	-3.006036000	-1.219379000
H	-6.326193000	-1.937562000	2.214532000	H	6.358547000	-1.852830000	-2.544809000
				C	-6.505489000	-1.939881000	1.465716000
				H	-7.474303000	-1.490327000	1.218750000
				H	-6.576886000	-3.005713000	1.219726000
				H	-6.358773000	-1.852292000	2.544957000
				C	-6.505520000	-1.939985000	-1.465510000
				H	-6.577060000	-3.005755000	-1.219301000
				H	-7.474298000	-1.490263000	-1.218703000
				H	-6.358724000	-1.852635000	-2.544760000

1c

E(SCF) = -1320.62782963

C	-5.370308000	-1.271684000	0.706083000
C	-4.356196000	-0.685862000	1.405421000
C	-3.286045000	-0.063676000	0.711904000
C	-3.285961000	-0.063889000	-0.711840000
C	-4.355999000	-0.686311000	-1.405336000
C	-5.370214000	-1.271908000	-0.705970000
H	-2.217597000	0.562154000	2.496677000
H	-4.382966000	-0.699657000	2.490234000
C	-2.215447000	0.566911000	1.409132000
C	-2.215369000	0.566527000	-1.409215000
H	-4.382587000	-0.700442000	-2.490147000
C	-1.210640000	1.171239000	-0.712458000
C	-1.210720000	1.171339000	0.712185000
H	-2.217642000	0.561361000	-2.496768000
C	1.210669000	1.171305000	0.712347000
C	2.215382000	0.566788000	1.409156000
C	3.285982000	-0.063839000	0.711831000
C	3.285974000	-0.063968000	-0.711894000
C	2.215283000	0.566519000	-1.409231000
C	1.210677000	1.171140000	-0.712383000
H	4.382672000	-0.700053000	2.490205000
H	2.217814000	0.561914000	2.496711000
C	4.355994000	-0.686091000	1.405394000
C	4.356099000	-0.686156000	-1.405318000
H	2.217389000	0.561344000	-2.496776000
C	5.370336000	-1.271778000	-0.705902000
C	5.370249000	-1.271814000	0.706086000
H	4.382901000	-0.700132000	-2.490128000
C	0.000010000	1.894357000	-1.292451000
C	-0.000005000	1.894542000	1.292234000
C	0.000129000	3.287053000	0.665720000
C	0.000046000	3.286989000	-0.666073000
H	0.000136000	4.178104000	1.283330000
H	0.000094000	4.177973000	-1.283757000
H	0.000060000	1.903472000	-2.384109000
H	-0.000017000	1.903780000	2.383889000
F	6.396607000	-1.860488000	1.326446000
F	6.396814000	-1.860352000	-1.326154000
F	-6.396606000	-1.860704000	-1.326153000
F	-6.396794000	-1.860256000	1.326316000

1d

E(SCF) = -1292.66881802

C	-5.354762000	-1.076102000	0.713816000
C	-4.331007000	-0.463102000	1.399677000
C	-3.270960000	0.172590000	0.711764000
C	-3.270972000	0.172637000	-0.711745000
C	-4.331020000	-0.463014000	-1.399689000
C	-5.354771000	-1.076059000	-0.713862000
H	-2.209779000	0.803603000	2.499780000
H	-4.337806000	-0.467761000	2.485416000
C	-2.207567000	0.810207000	1.412602000
C	-2.207581000	0.810301000	-1.412539000
H	-4.337819000	-0.467611000	-2.485429000
C	-1.207995000	1.420834000	-0.713187000
C	-1.207986000	1.420798000	0.713302000
H	-2.209798000	0.803763000	-2.499718000
C	1.208040000	1.420879000	0.713249000
C	2.207622000	0.810327000	1.412573000
C	3.271002000	0.172646000	0.711748000
C	3.270981000	0.172626000	-0.711761000
C	2.207566000	0.810256000	-1.412575000
C	1.208004000	1.420835000	-0.713252000
H	4.337832000	-0.467695000	2.485407000
H	2.209881000	0.803787000	2.499751000
C	4.331027000	-0.463045000	1.399668000
C	4.331015000	-0.463036000	-1.399696000
H	2.209780000	0.803662000	-2.499752000
C	5.354773000	-1.076073000	-0.713849000
C	5.354775000	-1.076086000	0.713811000
H	4.337835000	-0.467659000	-2.485435000
C	-0.000016000	2.146602000	-1.293700000
C	0.000031000	2.146595000	1.293772000
C	-0.000025000	3.538508000	0.665830000
C	-0.000011000	3.538520000	-0.665724000
H	-0.000058000	4.428543000	1.284386000
H	-0.000036000	4.428576000	-1.284241000
H	-0.000078000	2.155238000	-2.384948000
H	0.000096000	2.155220000	2.385022000
C	6.418993000	-1.715502000	1.438441000
N	7.267280000	-2.225644000	2.036938000
C	6.419012000	-1.715435000	-1.438497000
N	7.267489000	-2.225290000	-2.036969000
C	-6.419001000	-1.715508000	1.438428000
N	-7.267463000	-2.225443000	2.036852000
C	-6.419022000	-1.715416000	-1.438494000
N	-7.267438000	-2.225389000	-2.036951000

2x

E(SCF) = -296.202948495

N	-0.657295000	-1.189766000	0.000195000
C	-1.260658000	-0.000259000	0.000086000
C	1.260658000	-0.000259000	-0.000086000
N	0.657295000	-1.189766000	0.000105000
H	-2.345305000	-0.000233000	0.000162000
H	2.345305000	-0.000233000	-0.000160000
N	0.656805000	1.190021000	-0.000195000
N	-0.656805000	1.190021000	-0.000105000

2y

E(SCF) = -1347.05398232

N	0.902376000	-1.014530000	-0.033262000
C	1.226923000	0.280376000	-0.024341000
C	-1.226922000	-0.280480000	-0.024363000
N	-0.374194000	-1.307539000	-0.031000000
N	-0.902343000	1.014502000	-0.033165000
N	0.374136000	1.307490000	-0.030883000
C	-2.689744000	-0.659581000	0.000272000
O	-3.086595000	-1.779908000	0.062726000
O	-3.467518000	0.454340000	-0.054089000

				C	-4.837221000	0.262338000	0.001287000
				F	-5.386189000	1.459732000	-0.049023000
				F	-5.186802000	-0.333620000	1.129649000
				F	-5.260479000	-0.458898000	-1.023185000
				C	2.689728000	0.659538000	0.000212000
				O	3.086533000	1.779885000	0.062619000
				O	3.467546000	-0.454351000	-0.054135000
				C	4.837238000	-0.262300000	0.001309000
				F	5.386256000	-1.459668000	-0.049064000
				F	5.186757000	0.333602000	1.129722000
				F	5.260505000	0.459015000	-1.023105000
2z							
E(SCF) = -790.201597226							
N	0.663452000	1.170592000	0.000173000				
C	1.280173000	-0.019442000	0.000102000				
C	-1.280196000	0.020158000	-0.000060000				
N	-0.642495000	1.199212000	0.000090000				
N	-0.663113000	-1.170239000	-0.000142000				
N	0.642091000	-1.198820000	-0.000060000				
C	-2.768730000	0.010201000	-0.000176000				
C	-3.455263000	-1.206765000	-0.000355000				
N	-3.376311000	1.199454000	-0.000091000				
C	-4.844713000	-1.176223000	-0.000451000				
H	-2.901897000	-2.137948000	-0.000413000				
C	-4.705503000	1.209574000	-0.000184000				
C	-5.488442000	0.055058000	-0.000365000				
H	-5.413123000	-2.100987000	-0.000589000				
H	-5.172828000	2.191784000	-0.000108000				
H	-6.570682000	0.127754000	-0.000434000				
C	2.768724000	-0.009884000	0.000185000				
C	3.455731000	1.206833000	0.000361000				
N	3.375872000	-1.199352000	0.000080000				
C	4.845139000	1.175712000	0.000431000				
H	2.902764000	2.138245000	0.000438000				
C	4.705095000	-1.210018000	0.000149000				
C	5.488441000	-0.055824000	0.000324000				
H	5.413920000	2.100248000	0.000566000				
H	5.171993000	-2.192427000	0.000057000				
H	6.570658000	-0.128871000	0.000373000				
TS1-ax				**TS1-bx**			
E(SCF) = -1520.78097299				E(SCF) = -1377.19431276			
C	4.721219000	-2.729186000	-0.728904000	C	4.713022000	-2.740999000	-0.715419000
C	3.782369000	-2.006525000	-1.412893000	C	3.777841000	-1.993135000	-1.388139000
C	2.808071000	-1.243585000	-0.718787000	C	2.804143000	-1.217841000	-0.710428000
C	2.810645000	-1.235219000	0.704889000	C	2.804130000	-1.218016000	0.710197000
C	3.794777000	-1.993315000	1.393051000	C	3.777824000	-1.993462000	1.387739000
C	4.721079000	-2.716473000	0.696108000	C	4.713017000	-2.741164000	0.714856000
H	1.831568000	-0.483728000	-2.499844000	H	1.839764000	-0.446370000	-2.496105000
H	3.797166000	-2.022353000	-2.498103000	H	3.776014000	-1.988707000	-2.476460000
C	1.825865000	-0.486885000	-1.412145000	C	1.830952000	-0.452285000	-1.408171000
C	1.832944000	-0.477121000	1.401030000	C	1.830914000	-0.452647000	1.408111000
H	3.806938000	-1.991098000	2.481200000	H	3.775985000	-1.989286000	2.476061000
C	0.901230000	0.240071000	0.704621000	C	0.907303000	0.272392000	0.710548000
C	0.899728000	0.235796000	-0.714199000	C	0.907330000	0.272584000	-0.710447000
H	1.845501000	-0.465358000	2.488926000	H	1.839692000	-0.447016000	2.496047000

C	-1.501865000	0.562947000	-0.716859000
C	-2.580010000	0.099197000	-1.412151000
C	-3.726625000	-0.384085000	-0.716541000
C	-3.724707000	-0.380853000	0.705795000
C	-2.580879000	0.103081000	1.403283000
C	-1.501385000	0.564754000	0.708323000
H	-4.886067000	-0.872122000	-2.495670000
H	-2.581842000	0.091760000	-2.499903000
C	-4.866681000	-0.861802000	-1.410333000
C	-4.870006000	-0.857810000	1.394081000
H	-2.583136000	0.098888000	2.491412000
C	-5.955189000	-1.313382000	0.697391000
C	-5.961309000	-1.318894000	-0.726049000
H	-4.878402000	-0.858817000	2.482356000
C	-0.194750000	1.108826000	1.290650000
C	-0.195010000	1.104621000	-1.300943000
N	2.786411000	2.498702000	-0.613794000
C	1.920968000	3.354249000	-1.222821000
C	-0.077835000	2.507362000	-0.697738000
C	-0.083410000	2.510821000	0.684418000
C	1.889007000	3.396346000	1.230930000
N	2.770884000	2.521602000	0.675136000
H	-0.489163000	3.342983000	-1.254094000
H	-0.509915000	3.344036000	1.232873000
H	-0.190886000	1.114283000	2.383341000
H	-0.192012000	1.107977000	-2.393433000
N	1.644468000	4.598935000	0.621422000
N	1.662436000	4.577316000	-0.661404000
H	1.854224000	3.290153000	-2.303430000
H	1.794991000	3.371266000	2.311083000
O	-7.054976000	-1.776914000	-1.381512000
H	-7.709734000	-2.046289000	-0.717511000
O	-7.108779000	-1.792235000	1.256707000
H	-7.041674000	-1.768617000	2.221158000
O	5.656809000	-3.459546000	-1.382963000
H	6.228708000	-3.875853000	-0.718447000
O	5.712309000	-3.477722000	1.254675000
H	5.681993000	-3.399285000	2.218070000

C	-1.493575000	0.593584000	-0.713641000
C	-2.568491000	0.124664000	-1.409326000
C	-3.709965000	-0.366989000	-0.709906000
C	-3.709991000	-0.367193000	0.709650000
C	-2.568543000	0.124256000	1.409253000
C	-1.493602000	0.593373000	0.713740000
H	-4.848567000	-0.856028000	-2.475939000
H	-2.570693000	0.117907000	-2.497365000
C	-4.852206000	-0.857328000	-1.387531000
C	-4.852257000	-0.857721000	1.387095000
H	-2.570783000	0.117186000	2.497290000
C	-5.953032000	-1.332662000	0.713923000
C	-5.953005000	-1.332460000	-0.714534000
H	-4.848657000	-0.856731000	2.475503000
C	-0.188582000	1.141079000	1.296309000
C	-0.188524000	1.141446000	-1.296007000
N	2.779777000	2.550320000	-0.644150000
C	1.904314000	3.414122000	-1.226650000
C	-0.078249000	2.543464000	-0.690761000
C	-0.078299000	2.543269000	0.691462000
C	1.904228000	3.413777000	1.227669000
N	2.779732000	2.550132000	0.644984000
H	-0.499705000	3.376653000	-1.243140000
H	-0.499785000	3.376330000	1.244012000
H	-0.185156000	1.145337000	2.388843000
H	-0.185055000	1.146015000	-2.388539000
N	1.650189000	4.626462000	0.642231000
N	1.650209000	4.626645000	-0.640868000
H	1.824146000	3.369453000	-2.307302000
H	1.823996000	3.368778000	2.308303000
C	-7.151371000	-1.850242000	-1.465516000
H	-7.355112000	-2.898896000	-1.220299000
H	-8.055428000	-1.283057000	-1.216039000
H	-6.996295000	-1.780367000	-2.544764000
C	-7.151430000	-1.850643000	1.464718000
H	-8.055440000	-1.283274000	1.215486000
H	-7.355272000	-2.899178000	1.219079000
H	-6.996328000	-1.781218000	2.543990000
C	5.733269000	-3.555730000	-1.466081000
H	6.754930000	-3.251774000	-1.211136000
H	5.648751000	-4.622184000	-1.226837000
H	5.606665000	-3.441056000	-2.545290000
C	5.733270000	-3.556050000	1.465341000
H	5.648664000	-4.622475000	1.225995000
H	6.754929000	-3.252135000	1.210331000
H	5.606776000	-3.441479000	2.544572000

TS1-cx

E(SCF) = -1616.81408949

C	4.667133000	-2.762102000	-0.706754000
C	3.754735000	-2.029472000	-1.406241000
C	2.788909000	-1.254835000	-0.712207000
C	2.788925000	-1.254785000	0.712196000
C	3.754777000	-2.029362000	1.406264000
C	4.667156000	-2.762043000	0.706807000
H	1.828252000	-0.478720000	-2.496105000
H	3.778897000	-2.047351000	-2.490918000
C	1.818563000	-0.485280000	-1.408700000
C	1.818591000	-0.485188000	1.408661000

TS1-dx

E(SCF) = -1588.85280900

C	-4.856805000	-2.350527000	0.714743000
C	-3.891572000	-1.651188000	1.400681000
C	-2.889332000	-0.926682000	0.712066000
C	-2.889440000	-0.926622000	-0.711707000
C	-3.891783000	-1.651075000	-1.400228000
C	-4.856912000	-2.350471000	-0.714201000
H	-1.897217000	-0.196150000	2.499138000
H	-3.899499000	-1.653960000	2.486296000
C	-1.886438000	-0.203596000	1.412090000
C	-1.886650000	-0.203479000	-1.411824000

H	3.778972000	-2.047150000	2.490941000
C	0.899886000	0.244574000	0.710153000
C	0.899875000	0.244528000	-0.710215000
H	1.828317000	-0.478546000	2.496065000
C	-1.495769000	0.585528000	-0.713404000
C	-2.572095000	0.121653000	-1.409802000
C	-3.715851000	-0.365468000	-0.711632000
C	-3.715848000	-0.365434000	0.711635000
C	-2.572088000	0.121718000	1.409780000
C	-1.495762000	0.585561000	0.713357000
H	-4.880201000	-0.864516000	-2.490245000
H	-2.574201000	0.113974000	-2.497332000
C	-4.852909000	-0.851457000	-1.405476000
C	-4.852904000	-0.851392000	1.405505000
H	-2.574190000	0.114086000	2.497310000
C	-5.929149000	-1.314789000	0.705987000
C	-5.929152000	-1.314822000	-0.705934000
H	-4.880194000	-0.864402000	2.490275000
C	-0.187433000	1.123443000	1.296391000
C	-0.187448000	1.123377000	-1.296473000
N	2.788028000	2.498169000	-0.644311000
C	1.922513000	3.371622000	-1.227373000
C	-0.062709000	2.525057000	-0.691470000
C	-0.062771000	2.525107000	0.691322000
C	1.922178000	3.372108000	1.227383000
N	2.787886000	2.498434000	0.644933000
H	-0.479250000	3.360425000	-1.244162000
H	-0.479510000	3.360400000	1.243977000
H	-0.184011000	1.127165000	2.388769000
H	-0.184056000	1.127049000	-2.388852000
N	1.681350000	4.588056000	0.640702000
N	1.681575000	4.587807000	-0.641285000
H	1.844176000	3.329487000	-2.308286000
H	1.843553000	3.330486000	2.308295000
F	-7.013395000	-1.784227000	-1.326669000
F	-7.013390000	-1.784166000	1.326748000
F	5.587504000	-3.504445000	1.326551000
F	5.587442000	-3.504575000	-1.326469000

H	-3.899873000	-1.653761000	-2.485842000
C	-0.939100000	0.485793000	-0.710972000
C	-0.938996000	0.485733000	0.711148000
H	-1.897600000	-0.195939000	-2.498869000
C	1.466064000	0.734993000	0.714376000
C	2.527390000	0.240757000	1.412918000
C	3.656704000	-0.273522000	0.711158000
C	3.656607000	-0.273471000	-0.711673000
C	2.527198000	0.240856000	-1.413245000
C	1.465965000	0.735044000	-0.714526000
H	4.790441000	-0.783993000	2.485090000
H	2.530877000	0.233988000	2.500126000
C	4.782550000	-0.780827000	1.399368000
C	4.782363000	-0.780724000	-1.400069000
H	2.530538000	0.234163000	-2.500453000
C	5.870707000	-1.270856000	-0.713918000
C	5.870802000	-1.270910000	0.713038000
H	4.790111000	-0.783809000	-2.485792000
C	0.180251000	1.322720000	-1.297340000
C	0.180432000	1.322622000	1.297413000
N	-2.725350000	2.810836000	0.644852000
C	-1.828325000	3.651337000	1.228254000
C	0.110050000	2.728637000	0.691865000
C	0.109982000	2.728694000	-0.691682000
C	-1.828322000	3.651653000	-1.227854000
N	-2.725347000	2.811002000	-0.644664000
H	0.566449000	3.542500000	1.244877000
H	0.566396000	3.542573000	-1.244656000
H	0.176838000	1.325813000	-2.389387000
H	0.177175000	1.325640000	2.389461000
N	-1.539479000	4.858391000	-0.639714000
N	-1.539491000	4.858231000	0.640422000
H	-1.754976000	3.609962000	2.309592000
H	-1.754980000	3.610556000	-2.309203000
C	7.003434000	-1.778119000	1.438584000
N	7.906148000	-2.180083000	2.039755000
C	7.003250000	-1.777998000	-1.439650000
N	7.905896000	-2.179900000	-2.040964000
C	-5.863055000	-3.078049000	1.439169000
N	-6.664410000	-3.658896000	2.037814000
C	-5.863266000	-3.077947000	-1.438529000
N	-6.664710000	-3.658760000	-2.037087000

TS1-ay

E(SCF) = -2571.65701000

C	-3.772813000	-0.835357000	4.130334000
C	-2.823889000	0.047812000	3.699556000
C	-2.011108000	-0.265839000	2.578212000
C	-2.201776000	-1.511661000	1.915913000
C	-3.193808000	-2.408558000	2.389829000
C	-3.966278000	-2.085087000	3.471723000
H	-0.897950000	1.598280000	2.595334000
H	-2.688360000	1.000959000	4.206207000
C	-1.022809000	0.636098000	2.105555000
C	-1.395911000	-1.827154000	0.789108000
H	-3.355637000	-3.360802000	1.894716000
C	-0.450388000	-0.938840000	0.356363000
C	-0.261550000	0.301422000	1.020192000
H	-1.561434000	-2.767967000	0.269713000

TS1-by

E(SCF) = -2428.06972869

C	-3.799172000	-0.869454000	4.130649000
C	-2.833107000	0.000537000	3.688091000
C	-2.021212000	-0.287594000	2.562839000
C	-2.217478000	-1.517270000	1.879084000
C	-3.219480000	-2.402733000	2.349207000
C	-3.999033000	-2.106671000	3.440449000
H	-0.899898000	1.573325000	2.607984000
H	-2.681211000	0.945668000	4.205229000
C	-1.028378000	0.619281000	2.103333000
C	-1.413616000	-1.824253000	0.747667000
H	-3.370391000	-3.341238000	1.819367000
C	-0.462710000	-0.935224000	0.330615000
C	-0.270037000	0.296435000	1.013456000
H	-1.583860000	-2.756514000	0.214125000

C	2.072860000	0.317450000	0.340143000
C	3.280320000	0.642887000	0.885653000
C	4.371919000	-0.267664000	0.795908000
C	4.181724000	-1.513949000	0.135845000
C	2.909790000	-1.823159000	-0.424690000
C	1.884650000	-0.927426000	-0.324955000
H	5.802764000	0.989352000	1.853924000
H	3.424937000	1.593264000	1.394311000
C	5.639819000	0.042903000	1.347993000
C	5.272444000	-2.417600000	0.050243000
H	2.768984000	-2.777730000	-0.927102000
C	6.483839000	-2.091554000	0.594843000
C	6.678748000	-0.844060000	1.254577000
H	5.136693000	-3.374166000	-0.450337000
C	0.456818000	-1.104094000	-0.849681000
C	0.801368000	1.166474000	0.370283000
N	-2.444537000	1.399959000	-0.616153000
C	-1.610436000	2.293748000	-1.215882000
C	0.440833000	1.318558000	-1.106895000
C	0.259463000	0.111303000	-1.758775000
C	-1.914076000	0.194221000	-2.420311000
N	-2.605125000	0.295279000	-1.251759000
H	0.788091000	2.190708000	-1.653849000
H	0.463712000	0.019220000	-2.822046000
H	0.312533000	-2.054117000	-1.369625000
H	0.941971000	2.125723000	0.874101000
N	-1.755723000	1.300111000	-3.213615000
N	-1.598751000	2.401903000	-2.581155000
C	-1.861788000	-1.127667000	-3.116909000
O	-1.387303000	-1.316832000	-4.194857000
O	-2.349212000	-2.112829000	-2.298805000
C	-2.208786000	-3.411791000	-2.725408000
F	-2.693781000	-4.179763000	-1.763103000
F	-0.927367000	-3.720532000	-2.909752000
F	-2.872434000	-3.641723000	-3.844156000
C	-1.217969000	3.464934000	-0.375507000
O	-1.420429000	3.567572000	0.795953000
O	-0.493605000	4.364644000	-1.115649000
C	0.092515000	5.401544000	-0.424458000
F	0.754659000	6.124296000	-1.308185000
F	0.947920000	4.940582000	0.484134000
F	-0.804652000	6.163344000	0.177333000
O	-4.917324000	-2.932495000	3.931161000
H	-5.350883000	-2.512293000	4.691304000
O	-4.611555000	-0.638763000	5.193015000
H	-4.452263000	0.233036000	5.580502000
O	7.892085000	-0.556183000	1.781262000
H	8.480414000	-1.308805000	1.609251000
O	7.598443000	-2.883101000	0.572305000
H	7.405122000	-3.714748000	0.118047000

TS1-cy

C	2.066130000	0.310261000	0.343780000
C	3.271148000	0.622214000	0.900720000
C	4.356682000	-0.295582000	0.801800000
C	4.167592000	-1.529170000	0.124181000
C	2.895657000	-1.826034000	-0.447888000
C	1.875627000	-0.926689000	-0.339737000
H	5.767121000	0.931610000	1.878059000
H	3.417664000	1.564577000	1.424075000
C	5.627169000	-0.015254000	1.360136000
C	5.258909000	-2.427262000	0.036034000
H	2.754078000	-2.773023000	-0.964203000
C	6.486229000	-2.140478000	0.585158000
C	6.675904000	-0.898953000	1.267031000
H	5.111150000	-3.372361000	-0.482861000
C	0.449098000	-1.088578000	-0.873575000
C	0.798838000	1.164789000	0.377776000
N	-2.437331000	1.429432000	-0.620233000
C	-1.595076000	2.324775000	-1.206428000
C	0.446419000	1.337320000	-1.099038000
C	0.262255000	0.139352000	-1.767553000
C	-1.907238000	0.241484000	-2.436305000
N	-2.602211000	0.333291000	-1.269109000
H	0.802918000	2.213900000	-1.632877000
H	0.471796000	0.059934000	-2.830813000
H	0.303063000	-2.031142000	-1.406362000
H	0.941646000	2.116710000	0.894643000
N	-1.739577000	1.355578000	-3.216158000
N	-1.578349000	2.448914000	-2.570401000
C	-1.860947000	-1.072333000	-3.148448000
O	-1.386091000	-1.251717000	-4.227804000
O	-2.355247000	-2.064727000	-2.342628000
C	-2.219964000	-3.359302000	-2.783328000
F	-2.709342000	-4.135479000	-1.829102000
F	-0.940351000	-3.672131000	-2.970252000
F	-2.884724000	-3.574698000	-3.904350000
C	-1.198681000	3.484013000	-0.350959000
O	-1.401058000	3.571994000	0.821424000
O	-0.469730000	4.389789000	-1.079502000
C	0.124558000	5.412557000	-0.374546000
F	0.790868000	6.142629000	-1.249320000
F	0.978198000	4.932438000	0.525986000
F	-0.765722000	6.172445000	0.239246000
C	-5.058941000	-3.066288000	3.913159000
H	-4.872749000	-3.392749000	4.942877000
H	-6.051868000	-2.602449000	3.899942000
H	-5.092515000	-3.954761000	3.278163000
C	-4.649175000	-0.533902000	5.327698000
H	-5.712579000	-0.497783000	5.064692000
H	-4.541047000	-1.285775000	6.117803000
H	-4.371124000	0.437108000	5.743910000
C	8.014343000	-0.572912000	1.875042000
H	8.305289000	-1.318525000	2.623824000
H	8.805185000	-0.557220000	1.116318000
H	7.994511000	0.404679000	2.362390000
C	7.626632000	-3.117957000	0.474933000
H	8.484788000	-2.673530000	-0.042086000
H	7.978636000	-3.434872000	1.463259000
H	7.324683000	-4.010375000	-0.078147000

TS1-dy

E(SCF) = -2667.68857203				E(SCF) = -2639.72503858			
C	-3.753531000	-0.794013000	4.147768000	C	4.157382000	1.332511000	3.515772000
C	-2.801302000	0.081502000	3.718347000	C	3.172118000	0.398442000	3.295434000
C	-1.997300000	-0.246701000	2.595494000	C	2.265099000	0.538286000	2.217200000
C	-2.196871000	-1.492476000	1.934480000	C	2.386173000	1.663870000	1.353998000
C	-3.197046000	-2.379868000	2.411381000	C	3.405567000	2.615295000	1.596447000
C	-3.952646000	-2.030545000	3.490827000	C	4.275639000	2.463836000	2.650168000
H	-0.874876000	1.612272000	2.600401000	H	1.171222000	-1.296800000	2.620361000
H	-2.673575000	1.026800000	4.235206000	H	3.092121000	-0.460993000	3.953899000
C	-1.004996000	0.649095000	2.115015000	C	1.246034000	-0.423735000	1.978276000
C	-1.397753000	-1.819855000	0.805916000	C	1.495866000	1.806929000	0.257379000
H	-3.373751000	-3.332756000	1.923295000	H	3.503806000	3.472289000	0.937029000
C	-0.450768000	-0.937538000	0.367410000	C	0.536283000	0.859178000	0.044564000
C	-0.253930000	0.305540000	1.026784000	C	0.402044000	-0.256197000	0.916425000
H	-1.572106000	-2.760524000	0.289673000	H	1.612191000	2.653515000	-0.413801000
C	2.073685000	0.311409000	0.333661000	C	-1.973056000	-0.349034000	0.408311000
C	3.282987000	0.635152000	0.873676000	C	-3.142115000	-0.556692000	1.079664000
C	4.368827000	-0.282699000	0.782618000	C	-4.233560000	0.340966000	0.888598000
C	4.173588000	-1.532650000	0.129472000	C	-4.087222000	1.444731000	0.002814000
C	2.896690000	-1.839138000	-0.425434000	C	-2.850929000	1.639356000	-0.677792000
C	1.878331000	-0.937391000	-0.325471000	C	-1.827713000	0.761429000	-0.477085000
H	5.816802000	0.970372000	1.831676000	H	-5.587539000	-0.684735000	2.234378000
H	3.433640000	1.586610000	1.378037000	H	-3.258693000	-1.397493000	1.758913000
C	5.640198000	0.024573000	1.329877000	C	-5.466106000	0.154741000	1.556579000
C	5.255082000	-2.446002000	0.042696000	C	-5.175596000	2.326950000	-0.187172000
H	2.751080000	-2.795467000	-0.922036000	H	-2.741465000	2.486023000	-1.350893000
C	6.464639000	-2.119542000	0.583745000	C	-6.368064000	2.130623000	0.471566000
C	6.658428000	-0.877966000	1.229447000	C	-6.516166000	1.023283000	1.359658000
H	5.135209000	-3.407059000	-0.446742000	H	-5.069950000	3.171124000	-0.861772000
C	0.448079000	-1.110408000	-0.843613000	C	-0.440680000	0.827915000	-1.113217000
C	0.806227000	1.165222000	0.365338000	C	-0.705809000	-1.203514000	0.492792000
N	-2.433188000	1.399715000	-0.608818000	N	2.421854000	-1.685493000	-0.649529000
C	-1.597751000	2.288269000	-1.215517000	C	1.536619000	-2.630317000	-1.074898000
C	0.436710000	1.312162000	-1.110942000	C	-0.448984000	-1.605814000	-0.962631000
C	0.248770000	0.101917000	-1.757531000	C	-0.301327000	-0.524820000	-1.817123000
C	-1.911481000	0.183909000	-2.408832000	C	1.797324000	-0.717251000	-2.565113000
N	-2.599629000	0.293049000	-1.238767000	N	2.558585000	-0.679539000	-1.436599000
H	0.791375000	2.178806000	-1.661904000	H	-0.865167000	-2.540070000	-1.329234000
H	0.456791000	0.002993000	-2.819431000	H	-0.586251000	-0.599533000	-2.862914000
H	0.298410000	-2.062505000	-1.357847000	H	-0.326800000	1.675647000	-1.792617000
H	0.952447000	2.125824000	0.864428000	H	-0.813751000	-2.061258000	1.159706000
N	-1.756474000	1.287200000	-3.208821000	N	1.584564000	-1.919305000	-3.195759000
N	-1.594677000	2.390572000	-2.582648000	N	1.450624000	-2.920264000	-2.414088000
C	-1.870223000	-1.141179000	-3.101389000	C	1.731198000	0.502449000	-3.431436000
O	-1.402064000	-1.336070000	-4.180588000	O	1.163726000	0.565469000	-4.477898000
O	-2.355949000	-2.120651000	-2.275301000	O	2.322762000	1.562646000	-2.799190000
C	-2.222242000	-3.423010000	-2.697256000	C	2.186802000	2.802385000	-3.383871000
F	-2.704742000	-4.183454000	-1.727221000	F	2.784169000	3.663034000	-2.575822000
F	-0.942370000	-3.735477000	-2.884607000	F	0.902707000	3.137812000	-3.487265000
F	-2.891770000	-3.655513000	-3.810462000	F	2.745880000	2.853455000	-4.575950000
C	-1.200043000	3.463345000	-0.381663000	C	1.171493000	-3.674706000	-0.067718000
O	-1.384838000	3.560614000	0.793222000	O	1.375914000	-3.586415000	1.105448000
O	-0.491746000	4.365373000	-1.131265000	O	0.463200000	-4.680424000	-0.661317000
C	0.105424000	5.402211000	-0.446329000	C	-0.152992000	-5.588378000	0.178401000
F	0.753220000	6.126220000	-1.338474000	F	-0.815194000	-6.428158000	-0.590834000
F	0.975559000	4.936023000	0.446078000	F	-1.011414000	-4.965379000	0.982266000
F	-0.782098000	6.160039000	0.172039000	F	0.721237000	-6.252915000	0.909359000
F	-4.905801000	-2.835624000	3.964299000	C	5.302706000	3.444001000	2.876177000
F	-4.531588000	-0.519655000	5.196445000	N	6.121179000	4.243606000	3.044924000
F	7.502092000	-2.955830000	0.523456000	C	5.066712000	1.164805000	4.616555000

F	7.865767000	-0.622642000	1.735138000	N	5.787868000	1.013438000	5.508060000
				C	-7.759571000	0.808233000	2.048305000
				N	-8.753129000	0.617884000	2.608861000
				C	-7.457633000	3.044520000	0.261110000
				N	-8.321006000	3.791929000	0.077845000

TS1-az				**TS1-bz**			
E(SCF) = -2014.79132675				E(SCF) = -1871.20374502			
C	3.861385000	-1.956467000	-3.560192000	C	3.853124000	-2.155616000	-3.488443000
C	3.010967000	-0.908179000	-3.350998000	C	2.999649000	-1.096876000	-3.297502000
C	2.105547000	-0.924309000	-2.256796000	C	2.105452000	-1.036724000	-2.199464000
C	2.101112000	-2.051474000	-1.386576000	C	2.100087000	-2.111552000	-1.269527000
C	2.992455000	-3.127807000	-1.635355000	C	2.985712000	-3.197717000	-1.484099000
C	3.857096000	-3.088415000	-2.694939000	C	3.845673000	-3.238695000	-2.554490000
H	1.244937000	1.030392000	-2.658111000	H	1.253663000	0.901076000	-2.698922000
H	3.026313000	-0.047235000	-4.016206000	H	3.004406000	-0.268447000	-4.003216000
C	1.215540000	0.154557000	-2.015446000	C	1.223969000	0.061346000	-2.009559000
C	1.211709000	-2.062650000	-0.278982000	C	1.220043000	-2.061983000	-0.154214000
H	3.001199000	-3.996358000	-0.983909000	H	2.977047000	-4.020674000	-0.771187000
C	0.377958000	-1.000193000	-0.062623000	C	0.391628000	-0.986557000	0.008555000
C	0.366602000	0.110413000	-0.945606000	C	0.381957000	0.076424000	-0.934734000
H	1.216925000	-2.912250000	0.400712000	H	1.225962000	-2.874780000	0.569703000
C	-1.971738000	0.501923000	-0.410895000	C	-1.957238000	0.489748000	-0.432332000
C	-3.119646000	0.843013000	-1.064784000	C	-3.100650000	0.788802000	-1.112660000
C	-4.314744000	0.097759000	-0.849961000	C	-4.293619000	0.050886000	-0.859647000
C	-4.289828000	-1.005113000	0.048355000	C	-4.275405000	-0.994818000	0.100566000
C	-3.075665000	-1.338228000	0.714617000	C	-3.062939000	-1.288725000	0.791740000
C	-1.949302000	-0.600400000	0.492370000	C	-1.937857000	-0.562592000	0.532249000
H	-5.561840000	1.272011000	-2.196172000	H	-5.515101000	1.132589000	-2.270928000
H	-3.138952000	1.683988000	-1.754477000	H	-3.118346000	1.588599000	-1.850324000
C	-5.524771000	0.433052000	-1.508161000	C	-5.506141000	0.330336000	-1.535123000
C	-5.483254000	-1.742900000	0.259898000	C	-5.472491000	-1.711486000	0.342819000
H	-3.061674000	-2.183651000	1.399376000	H	-3.052064000	-2.093666000	1.523862000
C	-6.635287000	-1.396435000	-0.390738000	C	-6.642179000	-1.427295000	-0.321894000
C	-6.664805000	-0.292955000	-1.289453000	C	-6.659216000	-0.376769000	-1.289773000
H	-5.474478000	-2.589532000	0.943691000	H	-5.455770000	-2.512201000	1.080105000
C	-0.566494000	-0.820630000	1.108239000	C	-0.557024000	-0.744747000	1.164983000
C	-0.612976000	1.191467000	-0.531186000	C	-0.599511000	1.176335000	-0.580684000
N	2.504106000	1.506376000	0.518494000	N	2.511326000	1.546323000	0.475696000
C	1.712975000	2.511834000	1.010674000	C	1.718120000	2.579050000	0.904186000
C	-0.295950000	1.598797000	0.909263000	C	-0.291821000	1.660964000	0.836861000
C	-0.240866000	0.519670000	1.778219000	C	-0.241082000	0.631056000	1.763653000
C	1.851520000	0.467237000	2.411314000	C	1.843132000	0.615709000	2.418655000
N	2.571618000	0.455616000	1.247325000	N	2.572479000	0.538736000	1.262728000
H	-0.644647000	2.566549000	1.255255000	H	-0.641835000	2.646331000	1.127454000
H	-0.479966000	0.626424000	2.831854000	H	-0.490524000	0.794830000	2.807486000
H	-0.539339000	-1.655786000	1.813032000	H	-0.531330000	-1.540487000	1.913999000
H	-0.622407000	2.036353000	-1.220526000	H	-0.607849000	1.982682000	-1.314733000
N	1.770915000	1.660893000	3.102319000	N	1.756889000	1.846048000	3.040607000
N	1.697351000	2.706168000	2.374698000	N	1.690035000	2.849092000	2.254748000
C	1.827454000	-0.796415000	3.196094000	C	1.813822000	-0.604661000	3.268976000
C	2.605461000	-1.887073000	2.800404000	C	2.591444000	-1.714863000	2.929810000
N	1.002587000	-0.821087000	4.247420000	N	0.985396000	-0.576981000	4.317231000
C	2.528752000	-3.052789000	3.553630000	C	2.509499000	-2.842683000	3.737633000
H	3.243312000	-1.800521000	1.927859000	H	3.231353000	-1.671549000	2.055777000
C	0.948217000	-1.943759000	4.961403000	C	0.926089000	-1.664172000	5.084025000
C	1.687970000	-3.085967000	4.660939000	C	1.664200000	-2.821049000	4.841907000
H	3.121526000	-3.920791000	3.281194000	H	3.100785000	-3.724188000	3.508572000
H	0.272860000	-1.932599000	5.814045000	H	0.246635000	-1.611118000	5.931826000

H	1.600422000	-3.973481000	5.278396000
C	1.520595000	3.715892000	0.156630000
C	1.334895000	4.972401000	0.739201000
N	1.516196000	3.513170000	-1.164945000
C	1.154897000	6.066863000	-0.097362000
H	1.348088000	5.068613000	1.818345000
C	1.345655000	4.574933000	-1.950861000
C	1.164043000	5.870915000	-1.474015000
H	1.015274000	7.058787000	0.321389000
H	1.350066000	4.378585000	-3.021123000
H	1.030660000	6.695317000	-2.166060000
O	-7.825809000	0.020876000	-1.914919000
H	-8.500026000	-0.616135000	-1.629128000
O	-7.838102000	-2.037979000	-0.262381000
H	-7.751160000	-2.777562000	0.354504000
O	4.716858000	-4.108844000	-2.937951000
H	5.238813000	-3.875597000	-3.722383000
O	4.776766000	-2.042419000	-4.575952000
H	4.762118000	-1.227947000	-5.097036000

H	1.570866000	-3.677585000	5.500857000
C	1.535385000	3.732004000	-0.019404000
C	1.364669000	5.023330000	0.485955000
N	1.526941000	3.449103000	-1.326102000
C	1.196567000	6.066807000	-0.416103000
H	1.379800000	5.184073000	1.557394000
C	1.367800000	4.462461000	-2.175514000
C	1.201982000	5.786966000	-1.778284000
H	1.069040000	7.084076000	-0.058748000
H	1.369296000	4.200927000	-3.231683000
H	1.077437000	6.569435000	-2.518903000
C	-7.931784000	-0.055724000	-2.028860000
H	-8.736506000	0.223769000	-1.339231000
H	-7.780777000	0.772654000	-2.725100000
H	-8.289287000	-0.918219000	-2.603260000
C	-7.898778000	-2.208453000	-0.040619000
H	-8.704024000	-1.556082000	0.316572000
H	-8.270100000	-2.707763000	-0.942962000
H	-7.722382000	-2.973195000	0.719472000
C	4.778247000	-4.404833000	-2.751043000
H	4.611035000	-4.893572000	-3.717758000
H	5.826944000	-4.086129000	-2.732910000
H	4.639877000	-5.153032000	-1.966687000
C	4.793337000	-2.186075000	-4.665040000
H	5.838218000	-2.254268000	-4.340966000
H	4.601652000	-3.051989000	-5.309486000
H	4.687291000	-1.283692000	-5.271793000

TS1-cz

E(SCF) = -2110.82525058

C	3.821366000	-1.913986000	-3.616831000
C	2.979147000	-0.866137000	-3.392230000
C	2.086525000	-0.898511000	-2.288688000
C	2.084801000	-2.034873000	-1.429051000
C	2.973852000	-3.109150000	-1.696533000
C	3.818650000	-3.041617000	-2.764526000
H	1.228766000	1.063820000	-2.658022000
H	3.005027000	-0.010158000	-4.058388000
C	1.200576000	0.180524000	-2.026501000
C	1.202934000	-2.061591000	-0.315409000
H	2.992318000	-3.987823000	-1.059713000
C	0.372792000	-1.001046000	-0.082762000
C	0.360658000	0.122512000	-0.951535000
H	1.211813000	-2.919122000	0.353728000
C	-1.971140000	0.512886000	-0.401748000
C	-3.118707000	0.866354000	-1.047813000
C	-4.313793000	0.119500000	-0.837110000
C	-4.291667000	-0.996976000	0.045928000
C	-3.074498000	-1.343242000	0.702831000
C	-1.949174000	-0.603964000	0.486030000
H	-5.570279000	1.313448000	-2.164151000
H	-3.138355000	1.716485000	-1.725730000
C	-5.525535000	0.467134000	-1.486362000
C	-5.482859000	-1.737025000	0.256713000
H	-3.061316000	-2.198241000	1.374720000
C	-6.631538000	-1.374803000	-0.385026000
C	-6.652969000	-0.267494000	-1.260892000
H	-5.495834000	-2.593184000	0.923330000
C	-0.565642000	-0.835581000	1.094700000

TS1-dz

E(SCF) = -2082.86690259

C	4.167382000	-2.516869000	-2.641325000
C	3.264776000	-1.484487000	-2.747592000
C	2.307015000	-1.243994000	-1.733204000
C	2.288442000	-2.088474000	-0.586063000
C	3.222065000	-3.148410000	-0.496220000
C	4.144386000	-3.367225000	-1.492731000
H	1.414293000	0.491801000	-2.692015000
H	3.289036000	-0.840327000	-3.620940000
C	1.374839000	-0.177644000	-1.837751000
C	1.349294000	-1.840006000	0.449531000
H	3.212056000	-3.797157000	0.374438000
C	0.476708000	-0.795281000	0.327347000
C	0.476589000	0.030529000	-0.830302000
H	1.352528000	-2.464926000	1.339409000
C	-1.890428000	0.454365000	-0.509562000
C	-3.016260000	0.553488000	-1.273208000
C	-4.193515000	-0.154163000	-0.892820000
C	-4.177573000	-0.961689000	0.279225000
C	-2.984478000	-1.050229000	1.052995000
C	-1.876315000	-0.355952000	0.666956000
H	-5.402953000	0.543328000	-2.548678000
H	-3.032130000	1.166381000	-2.170960000
C	-5.382716000	-0.070176000	-1.653193000
C	-5.350295000	-1.658228000	0.651542000
H	-2.975614000	-1.670071000	1.946009000
C	-6.499331000	-1.565115000	-0.100830000
C	-6.515861000	-0.755190000	-1.276060000
H	-5.345270000	-2.276429000	1.543984000
C	-0.521347000	-0.339269000	1.369098000

C	-0.612059000	1.201189000	-0.515886000
N	2.504428000	1.481198000	0.529156000
C	1.720873000	2.484851000	1.037765000
C	-0.286541000	1.586104000	0.929615000
C	-0.232961000	0.493851000	1.782998000
C	1.851400000	0.418889000	2.409013000
N	2.568190000	0.419713000	1.242830000
H	-0.633212000	2.549520000	1.289205000
H	-0.472575000	0.583438000	2.838077000
H	-0.538946000	-1.681290000	1.786451000
H	-0.620459000	2.055867000	-1.192532000
N	1.779938000	1.604212000	3.117352000
N	1.710660000	2.659432000	2.405489000
C	1.825389000	-0.853665000	3.180034000
C	2.616509000	-1.935127000	2.786252000
N	0.986832000	-0.892616000	4.219900000
C	2.539060000	-3.107145000	3.530099000
H	3.266964000	-1.836123000	1.924326000
C	0.931344000	-2.020812000	4.925109000
C	1.684203000	-3.154933000	4.625830000
H	3.142907000	-3.968378000	3.260608000
H	0.244758000	-2.021060000	5.768668000
H	1.596004000	-4.047506000	5.235733000
C	1.539460000	3.703267000	0.201348000
C	1.396973000	4.957103000	0.800472000
N	1.506248000	3.514003000	-1.121924000
C	1.231422000	6.064786000	-0.021999000
H	1.431895000	5.041904000	1.880104000
C	1.351455000	4.588183000	-1.894332000
C	1.212800000	5.883256000	-1.400317000
H	1.124748000	7.055580000	0.408766000
H	1.333714000	4.403640000	-2.966429000
H	1.091224000	6.718542000	-2.081353000
F	-7.810170000	0.031738000	-1.856426000
F	-7.770097000	-2.049915000	-0.208387000
F	4.671380000	-4.031859000	-3.043038000
F	4.676459000	-1.916323000	-4.643497000

C	-0.550719000	1.143600000	-0.765094000
N	2.493749000	1.834311000	0.284048000
C	1.660498000	2.911134000	0.448405000
C	-0.307534000	1.943042000	0.519500000
C	-0.263931000	1.145570000	1.655272000
C	1.771607000	1.327661000	2.360669000
N	2.547698000	1.023944000	1.274253000
H	-0.702762000	2.952469000	0.567482000
H	-0.566250000	1.519927000	2.628276000
H	-0.501639000	-0.948348000	2.275707000
H	-0.551651000	1.764727000	-1.660435000
N	1.633935000	2.664800000	2.694435000
N	1.574349000	3.468103000	1.708447000
C	1.746914000	0.332017000	3.467798000
C	2.630275000	-0.749143000	3.469176000
N	0.820603000	0.529941000	4.410863000
C	2.550870000	-1.657075000	4.519677000
H	3.354438000	-0.851273000	2.668680000
C	0.762725000	-0.346092000	5.412474000
C	1.602376000	-1.453764000	5.515549000
H	3.225645000	-2.506606000	4.562351000
H	0.002625000	-0.157595000	6.166921000
H	1.508442000	-2.135765000	6.353505000
C	1.492117000	3.832272000	-0.709550000
C	1.321162000	5.202610000	-0.504517000
N	1.497147000	3.264361000	-1.920552000
C	1.167563000	6.019806000	-1.618334000
H	1.325066000	5.598307000	0.504162000
C	1.353762000	4.064478000	-2.976318000
C	1.188689000	5.444433000	-2.883486000
H	1.040063000	7.091157000	-1.497811000
H	1.368261000	3.576635000	-3.948661000
H	1.078633000	6.043650000	-3.780739000
C	-7.710447000	-0.653642000	-2.069209000
N	-8.662824000	-0.561152000	-2.719208000
C	-7.675617000	-2.287431000	0.300618000
N	-8.611052000	-2.877305000	0.639805000
C	5.083722000	-4.448322000	-1.370450000
N	5.831548000	-5.323036000	-1.252912000
C	5.132009000	-2.734867000	-3.684504000
N	5.902083000	-2.897321000	-4.532283000

4ax

E(SCF) = -1411.41180578

C	-5.203853000	-2.036814000	0.698700000
C	-4.200405000	-1.424917000	1.394952000
C	-3.133180000	-0.789292000	0.705591000
C	-3.129427000	-0.802851000	-0.718021000
C	-4.186275000	-1.448457000	-1.411581000
C	-5.203998000	-2.053579000	-0.726624000
H	-2.085974000	-0.131109000	2.488103000
H	-4.212538000	-1.418943000	2.483057000
C	-2.075496000	-0.144431000	1.399998000
C	-2.064835000	-0.165502000	-1.411003000
H	-4.201155000	-1.466894000	-2.496784000
C	-1.053294000	0.439367000	-0.717013000
C	-1.057183000	0.449443000	0.706102000
H	-2.067858000	-0.167308000	-2.498974000
C	1.387058000	0.604463000	0.710172000

4bx

E(SCF) = -1267.82497739

C	-5.225844000	-2.033154000	0.715688000
C	-4.197678000	-1.420050000	1.388536000
C	-3.129552000	-0.780193000	0.710472000
C	-3.129551000	-0.780474000	-0.710144000
C	-4.197672000	-1.420607000	-1.387957000
C	-5.225837000	-2.033446000	-0.714867000
H	-2.075471000	-0.134458000	2.495288000
H	-4.194838000	-1.416418000	2.476846000
C	-2.068180000	-0.140034000	1.407105000
C	-2.068187000	-0.140578000	-1.407029000
H	-4.194826000	-1.417414000	-2.476269000
C	-1.054524000	0.458884000	-0.712717000
C	-1.054517000	0.459154000	0.712557000
H	-2.075486000	-0.135417000	-2.495214000
C	1.389172000	0.617531000	0.712808000

C	2.467277000	0.137818000	1.408106000	C	2.470048000	0.148569000	1.406924000
C	3.605597000	-0.363281000	0.719955000	C	3.604565000	-0.351296000	0.710397000
C	3.606663000	-0.365429000	-0.703774000	C	3.604559000	-0.351536000	-0.710348000
C	2.474314000	0.131074000	-1.402728000	C	2.470034000	0.148089000	-1.407035000
C	1.389895000	0.601466000	-0.713534000	C	1.389163000	0.617285000	-0.713067000
H	4.755177000	-0.863925000	2.503584000	H	4.740749000	-0.850628000	2.476689000
H	2.468869000	0.141435000	2.496109000	H	2.474571000	0.149008000	2.495178000
C	4.738295000	-0.857317000	1.418188000	C	4.744752000	-0.851639000	1.388289000
C	4.747207000	-0.864306000	-1.388241000	C	4.744741000	-0.852104000	-1.388082000
H	2.480646000	0.128804000	-2.491000000	H	2.474545000	0.148154000	-2.495289000
C	5.822740000	-1.332325000	-0.687534000	C	5.841389000	-1.332481000	-0.715118000
C	5.826144000	-1.332242000	0.737924000	C	5.841395000	-1.332241000	0.715478000
H	4.757333000	-0.870206000	-2.476439000	H	4.740730000	-0.851458000	-2.476481000
C	0.126038000	1.180950000	-1.305990000	C	0.124843000	1.201383000	-1.300179000
C	0.122240000	1.192023000	1.293257000	C	0.124867000	1.201852000	1.299733000
N	-2.146268000	3.884179000	0.712544000	N	-2.155693000	3.885820000	0.714813000
C	-1.170002000	3.352060000	1.328598000	C	-1.185292000	3.348493000	1.335491000
C	0.041266000	2.664152000	0.760393000	C	0.037257000	2.675632000	0.772639000
C	0.031256000	2.657246000	-0.785842000	C	0.037207000	2.675353000	-0.773605000
C	-1.203429000	3.313220000	-1.342799000	C	-1.185435000	3.347910000	-1.336619000
N	-2.169374000	3.853622000	-0.717830000	N	-2.155794000	3.885461000	-0.716071000
H	-1.230390000	3.399373000	2.418844000	H	-1.262931000	3.373857000	2.425355000
H	-1.298250000	3.316367000	-2.431631000	H	-1.263218000	3.372743000	-2.426485000
H	0.927003000	3.191833000	1.133041000	H	0.916013000	3.209019000	1.153694000
H	0.902377000	3.196802000	-1.175763000	H	0.915911000	3.208642000	-1.154918000
H	0.127829000	1.155726000	-2.400614000	H	0.124974000	1.180750000	-2.394847000
H	0.120868000	1.176040000	2.388067000	H	0.125016000	1.181609000	2.394408000
O	-6.216770000	-2.673022000	-1.379278000	C	-6.348762000	-2.700562000	-1.464671000
H	-6.830637000	-3.022957000	-0.713866000	H	-6.419131000	-3.765914000	-1.216634000
O	-6.275754000	-2.678614000	1.257089000	H	-7.317141000	-2.250571000	-1.217428000
H	-6.234304000	-2.609642000	2.220866000	H	-6.202764000	-2.614074000	-2.543988000
O	6.971100000	-1.829869000	-1.240799000	C	-6.348777000	-2.699962000	1.465750000
H	6.906178000	-1.812908000	-2.205595000	H	-7.317161000	-2.250121000	1.218253000
O	6.912982000	-1.803251000	1.395451000	H	-6.419099000	-3.765431000	1.218205000
H	7.564165000	-2.084287000	0.732757000	H	-6.202831000	-2.612969000	2.545034000
				C	7.038044000	-1.856084000	-1.464715000
				H	7.944182000	-1.292081000	-1.215494000
				H	7.237607000	-2.905179000	-1.218090000
				H	6.883726000	-1.786849000	-2.544105000
				C	7.038058000	-1.855587000	1.465240000
				H	7.237675000	-2.904739000	1.218902000
				H	7.944176000	-1.291610000	1.215885000
				H	6.883717000	-1.786066000	2.544608000

4cx				**4dx**			
E(SCF) = -1507.44446877				E(SCF) = -1479.48258462			
C	-5.185024000	-2.050036000	0.707357000	C	-5.249505000	-1.767489000	0.714882000
C	-4.181143000	-1.450060000	1.407216000	C	-4.221931000	-1.164038000	1.401039000
C	-3.119431000	-0.812461000	0.712428000	C	-3.154721000	-0.538910000	0.711925000
C	-3.119466000	-0.812669000	-0.712041000	C	-3.154740000	-0.539134000	-0.711689000
C	-4.181213000	-1.450471000	-1.406591000	C	-4.221970000	-1.164482000	-1.400575000
C	-5.185059000	-2.050244000	-0.706507000	C	-5.249525000	-1.767714000	-0.714196000
H	-2.067405000	-0.162824000	2.495299000	H	-2.095678000	0.093029000	2.498169000
H	-4.208486000	-1.462599000	2.491893000	H	-4.229414000	-1.166994000	2.486678000
C	-2.059428000	-0.169206000	1.407647000	C	-2.086905000	0.086873000	1.410852000
C	-2.059500000	-0.169611000	-1.407499000	C	-2.086944000	0.086429000	-1.410841000
H	-4.208609000	-1.463328000	-2.491264000	H	-4.229488000	-1.167780000	-2.486213000
C	-1.048644000	0.432963000	-0.712308000	C	-1.067158000	0.670913000	-0.713295000
C	-1.048606000	0.433167000	0.712232000	C	-1.067139000	0.671139000	0.713094000

H	-2.067534000	-0.163539000	-2.495152000
C	1.392051000	0.606750000	0.712473000
C	2.473523000	0.141158000	1.407402000
C	3.609415000	-0.356463000	0.712214000
C	3.609379000	-0.356653000	-0.712325000
C	2.473453000	0.140782000	-1.407590000
C	1.392014000	0.606559000	-0.712730000
H	4.770416000	-0.867674000	2.491321000
H	2.477946000	0.141136000	2.495139000
C	4.743395000	-0.854512000	1.406570000
C	4.743326000	-0.854887000	-1.406603000
H	2.477820000	0.140468000	-2.495327000
C	5.814212000	-1.326134000	-0.706933000
C	5.814247000	-1.325944000	0.706974000
H	4.770294000	-0.868339000	-2.491351000
C	0.125124000	1.183543000	-1.300561000
C	0.125197000	1.183902000	1.300215000
N	-2.182271000	3.838059000	0.714880000
C	-1.204003000	3.316549000	1.336345000
C	0.026100000	2.657061000	0.772710000
C	0.026034000	2.656848000	-0.773448000
C	-1.204154000	3.316114000	-1.337157000
N	-2.182368000	3.837795000	-0.715752000
H	-1.280482000	3.343855000	2.426127000
H	-1.280775000	3.343027000	-2.426939000
H	0.899925000	3.197702000	1.154460000
H	0.899807000	3.197410000	-1.155429000
H	0.125355000	1.162255000	-2.395003000
H	0.125487000	1.162910000	2.394663000
F	-6.202403000	-2.654830000	-1.323915000
F	-6.202341000	-2.654436000	1.324992000
F	6.896112000	-1.803749000	-1.325390000
F	6.896176000	-1.803396000	1.325505000

H	-2.095747000	0.092244000	-2.498160000
C	1.372862000	0.799342000	0.713397000
C	2.443835000	0.313372000	1.410719000
C	3.568710000	-0.203314000	0.711930000
C	3.568692000	-0.203549000	-0.711948000
C	2.443802000	0.312913000	-1.410880000
C	1.372845000	0.799111000	-0.713692000
H	4.700989000	-0.720978000	2.486371000
H	2.449187000	0.313247000	2.498120000
C	4.693665000	-0.717367000	1.400640000
C	4.693626000	-0.717837000	-1.400516000
H	2.449128000	0.312433000	-2.498281000
C	5.778520000	-1.211469000	-0.714367000
C	5.778542000	-1.211224000	0.714628000
H	4.700921000	-0.721818000	-2.486245000
C	0.118660000	1.401362000	-1.301858000
C	0.118690000	1.401778000	1.301400000
N	-2.150434000	4.078734000	0.714413000
C	-1.176575000	3.551980000	1.337586000
C	0.045373000	2.876555000	0.772478000
C	0.045356000	2.876309000	-0.773394000
C	-1.176610000	3.551540000	-1.338691000
N	-2.150459000	4.078486000	-0.715666000
H	-1.250402000	3.584780000	2.427145000
H	-1.250471000	3.583970000	-2.428259000
H	0.927489000	3.402214000	1.155254000
H	0.927466000	3.401842000	-1.156360000
H	0.118469000	1.379147000	-2.395821000
H	0.118521000	1.379906000	2.395369000
C	-6.318484000	-2.401041000	-1.437439000
N	-7.169119000	-2.909392000	-2.033961000
C	-6.318439000	-2.400599000	1.438351000
N	-7.169090000	-2.908690000	2.035070000
C	6.909679000	-1.723506000	-1.438862000
N	7.811464000	-2.129580000	-2.038662000
C	6.909729000	-1.722991000	1.439271000
N	7.811551000	-2.128836000	2.039171000

4ay

E(SCF) = -2462.28598492

C	4.038032000	-1.712264000	-3.851208000
C	3.319746000	-0.623411000	-3.438573000
C	2.299725000	-0.758070000	-2.461270000
C	2.022841000	-2.042386000	-1.911614000
C	2.784675000	-3.157091000	-2.351461000
C	3.762652000	-2.994736000	-3.291275000
H	1.772210000	1.345841000	-2.422524000
H	3.543542000	0.347207000	-3.869950000
C	1.550758000	0.363143000	-2.011102000
C	0.999584000	-2.179487000	-0.936666000
H	2.586217000	-4.139776000	-1.928863000
C	0.281405000	-1.084161000	-0.540762000
C	0.564809000	0.203235000	-1.075962000
H	0.803588000	-3.158437000	-0.502202000
C	-1.742854000	0.893640000	-0.601670000
C	-2.751142000	1.641770000	-1.145849000
C	-4.080875000	1.143674000	-1.159146000
C	-4.356942000	-0.132560000	-0.590152000
C	-3.290301000	-0.880349000	-0.022802000

4by

E(SCF) = -2318.69858960

C	4.110270000	-1.654891000	-3.819724000
C	3.379367000	-0.578082000	-3.381195000
C	2.339549000	-0.713713000	-2.427575000
C	2.050318000	-2.007620000	-1.916357000
C	2.815570000	-3.107084000	-2.379015000
C	3.820634000	-2.957235000	-3.302938000
H	1.817078000	1.393221000	-2.357956000
H	3.597933000	0.414376000	-3.770638000
C	1.587581000	0.402895000	-1.969141000
C	1.013059000	-2.162817000	-0.956096000
H	2.594827000	-4.094855000	-1.979571000
C	0.295577000	-1.073325000	-0.545907000
C	0.586782000	0.225682000	-1.054179000
H	0.806310000	-3.151548000	-0.550108000
C	-1.729615000	0.906663000	-0.603481000
C	-2.729693000	1.664410000	-1.147748000
C	-4.060746000	1.165358000	-1.184933000
C	-4.339993000	-0.118074000	-0.642178000
C	-3.282677000	-0.879856000	-0.074669000

C	-2.016740000	-0.379777000	-0.033033000
H	-4.950148000	2.864729000	-2.161824000
H	-2.546014000	2.621090000	-1.573121000
C	-5.150354000	1.888548000	-1.724679000
C	-5.686887000	-0.628305000	-0.601891000
H	-3.500579000	-1.854968000	0.412526000
C	-6.701151000	0.106867000	-1.151600000
C	-6.420107000	1.384126000	-1.720404000
H	-5.915325000	-1.599088000	-0.173186000
C	-0.787533000	-1.051863000	0.528443000
C	-0.291631000	1.294007000	-0.474679000
N	2.347599000	1.225068000	1.912315000
C	1.358633000	1.838608000	1.392556000
C	-0.012254000	1.309837000	1.073432000
C	-0.221659000	-0.110642000	1.660061000
C	1.082048000	-0.696036000	2.141948000
N	2.231359000	-0.150249000	2.203692000
H	-0.728343000	2.012244000	1.510597000
H	-0.936858000	-0.096205000	2.488813000
H	-1.010637000	-2.046730000	0.923536000
H	-0.094053000	2.277968000	-0.905811000
O	4.555711000	-3.992252000	-3.786649000
H	4.344292000	-4.829581000	-3.351077000
O	5.011846000	-1.595725000	-4.784018000
H	5.399385000	-2.474645000	-4.924625000
O	-7.973247000	-0.356026000	-1.165685000
H	-8.530533000	0.310662000	-1.598349000
O	-7.521395000	2.011658000	-2.233381000
H	-7.270966000	2.869566000	-2.603389000
C	1.090286000	-2.158316000	2.511889000
O	1.922069000	-2.966006000	2.248658000
O	-0.071786000	-2.449324000	3.208086000
C	-0.363877000	-3.776670000	3.413126000
F	-1.537119000	-3.822792000	4.021276000
F	0.539117000	-4.378486000	4.166852000
F	-0.456488000	-4.419427000	2.250895000
C	1.554673000	3.306069000	1.117435000
O	0.683839000	4.024322000	0.713304000
O	2.823248000	3.722476000	1.384553000
C	3.106640000	5.052134000	1.167558000
F	4.370492000	5.230525000	1.504649000
F	2.345102000	5.841880000	1.911473000
F	2.948455000	5.378990000	-0.107974000

C	-2.010195000	-0.378833000	-0.060386000
H	-4.912572000	2.894367000	-2.158020000
H	-2.520574000	2.651414000	-1.554988000
C	-5.129096000	1.911573000	-1.743695000
C	-5.673786000	-0.597058000	-0.683494000
H	-3.498656000	-1.862041000	0.341144000
C	-6.696702000	0.140478000	-1.226940000
C	-6.416057000	1.432729000	-1.773411000
H	-5.882466000	-1.580838000	-0.267325000
C	-0.788595000	-1.058235000	0.508319000
C	-0.280267000	1.305110000	-0.448112000
N	2.327210000	1.186703000	1.970139000
C	1.348907000	1.811333000	1.443744000
C	-0.021947000	1.295641000	1.103170000
C	-0.244868000	-0.133353000	1.663701000
C	1.045323000	-0.727706000	2.169294000
N	2.195967000	-0.188449000	2.257140000
H	-0.739649000	1.995124000	1.542468000
H	-0.978738000	-0.129971000	2.476039000
H	-1.016080000	-2.059502000	0.884648000
H	-0.077708000	2.296091000	-0.860348000
C	4.619266000	-4.144156000	-3.772717000
H	4.542171000	-4.273308000	-4.858357000
H	5.683753000	-4.026037000	-3.539976000
H	4.269864000	-5.063291000	-3.296776000
C	5.209964000	-1.478581000	-4.833214000
H	6.172715000	-1.825495000	-4.441460000
H	5.009589000	-2.054261000	-5.744174000
H	5.317894000	-0.428376000	-5.114305000
C	-8.104134000	-0.394555000	-1.251611000
H	-8.789227000	0.258976000	-0.699446000
H	-8.487445000	-0.466120000	-2.275810000
H	-8.152085000	-1.389469000	-0.802877000
C	-7.529439000	2.252345000	-2.370088000
H	-8.008306000	1.729012000	-3.205493000
H	-8.312995000	2.458522000	-1.631976000
H	-7.154573000	3.209000000	-2.741225000
C	1.036523000	-2.190447000	2.537968000
O	1.872379000	-3.001190000	2.299500000
O	-0.147133000	-2.476440000	3.199895000
C	1.560383000	3.278656000	1.179140000
O	0.697042000	4.008913000	0.780714000
O	2.833901000	3.679756000	1.447339000
C	3.130729000	5.007684000	1.238055000
C	-0.450072000	-3.802696000	3.396904000
F	4.397696000	5.170474000	1.571913000
F	2.972335000	5.344285000	-0.035082000
F	2.380336000	5.800838000	1.989289000
F	-0.516317000	-4.443887000	2.232477000
F	0.430678000	-4.408768000	4.172973000
F	-1.638544000	-3.843443000	3.975878000

4cy

E(SCF) = -2558.31694217

C	3.983363000	-1.721606000	-3.867111000
C	3.304350000	-0.619091000	-3.441116000
C	2.282133000	-0.754159000	-2.465303000
C	1.980280000	-2.046040000	-1.946192000
C	2.711861000	-3.170515000	-2.410151000

4dy

E(SCF) = -2530.35324048

C	4.415197000	-1.494719000	-3.374348000
C	3.549343000	-0.465205000	-3.088620000
C	2.520553000	-0.625697000	-2.129496000
C	2.387477000	-1.874282000	-1.458784000
C	3.291237000	-2.920558000	-1.761901000

C	3.687347000	-3.003320000	-3.347481000	C	4.284999000	-2.746144000	-2.696502000
H	1.797301000	1.359885000	-2.386116000	H	1.737023000	1.389685000	-2.330553000
H	3.555231000	0.352250000	-3.854612000	H	3.657068000	0.483860000	-3.604757000
C	1.557009000	0.374225000	-1.993574000	C	1.624634000	0.434817000	-1.822402000
C	0.956062000	-2.182182000	-0.969596000	C	1.357725000	-2.044412000	-0.493569000
H	2.508429000	-4.164113000	-2.024553000	H	3.199683000	-3.872280000	-1.247781000
C	0.263873000	-1.080210000	-0.550157000	C	0.501707000	-1.011387000	-0.230732000
C	0.569666000	0.213330000	-1.061737000	C	0.636842000	0.242493000	-0.897005000
H	0.739775000	-3.166543000	-0.559126000	H	1.274033000	-2.990021000	0.037847000
C	-1.725951000	0.931801000	-0.580872000	C	-1.751257000	0.661924000	-0.557260000
C	-2.719034000	1.704432000	-1.116319000	C	-2.821563000	1.204022000	-1.212399000
C	-4.057529000	1.225662000	-1.141743000	C	-4.072763000	0.529628000	-1.196861000
C	-4.351000000	-0.057019000	-0.594930000	C	-4.198380000	-0.700328000	-0.490254000
C	-3.299156000	-0.831741000	-0.035913000	C	-3.069775000	-1.235897000	0.188002000
C	-2.020170000	-0.348127000	-0.033605000	C	-1.876699000	-0.569018000	0.150541000
H	-4.916732000	2.981550000	-2.118962000	H	-5.115406000	1.996141000	-2.405598000
H	-2.499160000	2.687717000	-1.525534000	H	-2.731342000	2.148285000	-1.743728000
C	-5.109847000	2.000283000	-1.697605000	C	-5.202993000	1.057876000	-1.866255000
C	-5.687874000	-0.535182000	-0.621259000	C	-5.449329000	-1.363093000	-0.477279000
H	-3.525940000	-1.810099000	0.381797000	H	-3.169742000	-2.175537000	0.726126000
C	-6.672143000	0.235184000	-1.164896000	C	-6.536610000	-0.833892000	-1.132303000
C	-6.381777000	1.509867000	-1.704479000	C	-6.411057000	0.401252000	-1.840232000
H	-5.939389000	-1.509637000	-0.215301000	H	-5.552297000	-2.302523000	0.057306000
C	-0.803362000	-1.047696000	0.521106000	C	-0.592018000	-1.002706000	0.814583000
C	-0.269207000	1.307833000	-0.442161000	C	-0.373422000	1.268633000	-0.438601000
N	2.366753000	1.158089000	1.940211000	N	2.152993000	1.846618000	1.984133000
C	1.388702000	1.794789000	1.428617000	C	1.102266000	2.252073000	1.389443000
C	0.008251000	1.293027000	1.104846000	C	-0.162226000	1.488681000	1.102655000
C	-0.224767000	-0.133267000	1.667832000	C	-0.185742000	0.125354000	1.839116000
C	1.068960000	-0.746090000	2.144614000	C	1.181675000	-0.214954000	2.383809000
N	2.225911000	-0.218492000	2.215106000	N	2.234974000	0.499525000	2.395698000
H	-0.695383000	2.000791000	1.553532000	H	-0.990235000	2.119214000	1.440079000
H	-0.941931000	-0.120904000	2.494668000	H	-0.911241000	0.126643000	2.658919000
H	-1.043030000	-2.045206000	0.899306000	H	-0.696725000	-1.969040000	1.314910000
H	-0.056044000	2.295236000	-0.857288000	H	-0.291404000	2.217094000	-0.973060000
C	1.053678000	-2.213378000	2.493915000	C	5.188362000	-3.825448000	-2.989256000
O	1.875616000	-3.027830000	2.221926000	N	5.904233000	-4.705432000	-3.214624000
O	-0.117958000	-2.496399000	3.174966000	C	5.447388000	-1.307251000	-4.357391000
C	1.607214000	3.261904000	1.165592000	N	6.268895000	-1.139085000	-5.153928000
O	0.739704000	3.997122000	0.784757000	C	-7.796245000	-1.525783000	-1.098923000
O	2.887879000	3.650861000	1.406036000	N	-8.801480000	-2.096354000	-1.059020000
C	3.190368000	4.979696000	1.196524000	C	-7.543739000	0.962573000	-2.524782000
C	-0.425468000	-3.824145000	3.367284000	N	-8.443305000	1.431013000	-3.080708000
F	4.466564000	5.129056000	1.496449000	C	1.075553000	3.697069000	0.963611000
F	2.998845000	5.323528000	-0.069737000	O	0.115207000	4.208081000	0.457712000
F	2.466681000	5.771883000	1.973532000	O	2.245170000	4.337179000	1.211164000
F	-0.514259000	-4.454367000	2.198249000	C	2.322189000	5.668170000	0.846693000
F	0.465117000	-4.438880000	4.123176000	F	3.529711000	6.079805000	1.177010000
F	-1.604485000	-3.862291000	3.963872000	F	1.420613000	6.395709000	1.486710000
F	4.396339000	-4.034571000	-3.808083000	F	2.152165000	5.815278000	-0.459420000
F	4.947403000	-1.633666000	-4.784522000	C	1.396527000	-1.625485000	2.872019000
F	-7.395693000	2.209376000	-2.215760000	O	2.318308000	-2.334256000	2.622846000
F	-7.938589000	-0.180928000	-1.210652000	O	0.308615000	-2.004967000	3.633725000
				C	0.204129000	-3.341967000	3.955240000
				F	-0.914334000	-3.484544000	4.642032000
				F	1.221318000	-3.762544000	4.680246000
				F	0.125427000	-4.073910000	2.844814000

4az	**4bz**
E(SCF) = -1905.41451171	E(SCF) = -1761.82739336

C	4.495115000	-1.526018000	3.172851000	C	4.527779000	-1.816837000	3.024915000
C	3.593109000	-2.017908000	2.272817000	C	3.627454000	-2.194508000	2.059277000
C	2.561868000	-1.185508000	1.762549000	C	2.590394000	-1.334553000	1.618043000
C	2.488363000	0.166525000	2.201966000	C	2.490238000	-0.040120000	2.195403000
C	3.438982000	0.646032000	3.140826000	C	3.427685000	0.332500000	3.191058000
C	4.422389000	-0.175007000	3.620621000	C	4.423917000	-0.515337000	3.609277000
H	1.687103000	-2.695140000	0.471399000	H	1.749065000	-2.711874000	0.164905000
H	3.660831000	-3.050134000	1.935029000	H	3.705544000	-3.182504000	1.609526000
C	1.612197000	-1.668725000	0.824326000	C	1.656533000	-1.728407000	0.621117000
C	1.468040000	1.007404000	1.681223000	C	1.461748000	0.839903000	1.760720000
H	3.398685000	1.674060000	3.487151000	H	3.346007000	1.324597000	3.631283000
C	0.559174000	0.514492000	0.785032000	C	0.568611000	0.432843000	0.808988000
C	0.628307000	-0.840915000	0.357386000	C	0.664440000	-0.869087000	0.237392000
H	1.423539000	2.046473000	2.001236000	H	1.393923000	1.835509000	2.195061000
C	-1.772975000	-0.808060000	-0.147947000	C	-1.738579000	-0.831978000	-0.257112000
C	-2.871034000	-1.621862000	-0.079962000	C	-2.818626000	-1.671236000	-0.279899000
C	-4.096428000	-1.130024000	0.446099000	C	-4.049234000	-1.266795000	0.307040000
C	-4.163992000	0.220755000	0.891399000	C	-4.144284000	0.017113000	0.909242000
C	-3.011287000	1.045455000	0.798230000	C	-3.009017000	0.872983000	0.908663000
C	-1.842808000	0.541002000	0.296079000	C	-1.835786000	0.455591000	0.344089000
H	-5.215921000	-2.985911000	0.206973000	H	-5.116954000	-3.087285000	-0.146910000
H	-2.819071000	-2.654533000	-0.419020000	H	-2.747677000	-2.656087000	-0.737851000
C	-5.249483000	-1.953191000	0.539994000	C	-5.193589000	-2.104378000	0.314551000
C	-5.389722000	0.707270000	1.420705000	C	-5.377541000	0.402351000	1.493162000
H	-3.068475000	2.079560000	1.131753000	H	-3.086920000	1.859890000	1.360090000
C	-6.480883000	-0.110932000	1.500478000	C	-6.475294000	-0.422723000	1.492594000
C	-6.418355000	-1.463034000	1.054338000	C	-6.380907000	-1.713957000	0.883840000
H	-5.450959000	1.737853000	1.765102000	H	-5.445794000	1.385732000	1.954745000
C	-0.545854000	1.289918000	0.106847000	C	-0.559212000	1.252845000	0.228812000
C	-0.412944000	-1.179559000	-0.685482000	C	-0.372490000	-1.109079000	-0.837299000
N	2.248933000	0.262037000	-2.538025000	N	2.242590000	0.648238000	-2.506818000
C	1.264150000	-0.543927000	-2.429780000	C	1.303812000	-0.217589000	-2.474165000
C	-0.118441000	-0.225015000	-1.902325000	C	-0.098936000	-0.016383000	-1.937778000
C	-0.250775000	1.248981000	-1.437231000	C	-0.292573000	1.391073000	-1.313271000
C	0.975092000	2.062480000	-1.761410000	C	0.878362000	2.300667000	-1.575249000
N	2.076177000	1.627201000	-2.244647000	N	1.993989000	1.973168000	-2.108090000
H	-0.861449000	-0.436811000	-2.679745000	H	-0.822898000	-0.166160000	-2.747303000
H	-1.098369000	1.735628000	-1.927313000	H	-1.175734000	1.879967000	-1.733326000
H	-0.611933000	2.324029000	0.449239000	H	-0.646492000	2.239851000	0.685901000
H	-0.364572000	-2.227238000	-0.994019000	H	-0.302438000	-2.114026000	-1.261287000
O	5.335041000	0.273039000	4.517934000	C	5.405338000	-0.090131000	4.669415000
H	5.944141000	-0.457192000	4.712139000	H	5.367665000	-0.754891000	5.540219000
O	5.526843000	-2.236740000	3.726769000	H	6.434868000	-0.115380000	4.294037000
H	5.544193000	-3.129198000	3.355003000	H	5.195559000	0.926278000	5.011085000
O	-7.705490000	0.250936000	1.994801000	C	5.619555000	-2.753964000	3.470461000
H	-7.677479000	1.168350000	2.299554000	H	6.612676000	-2.328188000	3.285937000
O	-7.523975000	-2.241851000	1.150061000	H	5.556433000	-2.961689000	4.544949000
H	-8.232030000	-1.706844000	1.542930000	H	5.557309000	-3.706369000	2.938425000
C	0.911741000	3.535734000	-1.525585000	C	-7.770300000	0.017436000	2.123339000
C	2.079435000	4.306856000	-1.546054000	H	-8.585121000	0.043297000	1.390458000
N	-0.301908000	4.059150000	-1.313994000	H	-8.080950000	-0.667276000	2.920897000
C	1.971413000	5.674629000	-1.344293000	H	-7.673410000	1.016358000	2.555287000
H	3.029107000	3.816407000	-1.722613000	C	-7.579125000	-2.626324000	0.876038000
C	-0.388736000	5.376381000	-1.127404000	H	-7.909218000	-2.861465000	1.894520000
C	0.711124000	6.228124000	-1.132377000	H	-8.430746000	-2.163591000	0.364120000
H	2.857577000	6.301928000	-1.350712000	H	-7.351240000	-3.567303000	0.369736000
H	-1.389942000	5.769451000	-0.964710000	C	0.732319000	3.742723000	-1.215371000
H	0.579800000	7.292633000	-0.970447000	C	1.843982000	4.592714000	-1.233894000
C	1.545386000	-1.962733000	-2.817588000	N	-0.497684000	4.161834000	-0.895806000
C	0.613387000	-2.690012000	-3.565223000	C	1.659160000	5.929412000	-0.914352000

N	2.714296000	-2.479137000	-2.422244000	H	2.811306000	4.184698000	-1.501416000
C	0.917901000	-3.995643000	-3.932230000	C	-0.659000000	5.450539000	-0.594178000
H	-0.326243000	-2.236917000	-3.866091000	C	0.380449000	6.374807000	-0.587993000
C	2.988194000	-3.732922000	-2.775981000	H	2.500509000	6.615789000	-0.918435000
C	2.133350000	-4.535093000	-3.529785000	H	-1.672131000	5.757041000	-0.343498000
H	0.218261000	-4.578690000	-4.523449000	H	0.189680000	7.411403000	-0.331612000
H	3.945777000	-4.121061000	-2.434770000	C	1.670651000	-1.580801000	-2.973264000
H	2.415604000	-5.550232000	-3.787422000	C	0.778047000	-2.310657000	-3.765122000
				N	2.878126000	-2.043714000	-2.632544000
				C	1.164349000	-3.560968000	-4.234510000
				H	-0.195297000	-1.901134000	-4.018268000
				C	3.230724000	-3.245166000	-3.083230000
				C	2.419525000	-4.044603000	-3.887389000
				H	0.496574000	-4.144597000	-4.860969000
				H	4.217304000	-3.591554000	-2.782246000
				H	2.765974000	-5.015233000	-4.225413000

4cz				**4dz**			
E(SCF) = -2001.44841788				E(SCF) = -1973.48936943			
C	4.494108000	-1.598429000	3.127560000	C	-4.681322000	-1.539139000	-2.795713000
C	3.598245000	-2.073289000	2.216857000	C	-3.715697000	-2.006109000	-1.934934000
C	2.565262000	-1.227605000	1.734220000	C	-2.682443000	-1.158361000	-1.468176000
C	2.483966000	0.113279000	2.207600000	C	-2.654996000	0.199294000	-1.897292000
C	3.433215000	0.571751000	3.158848000	C	-3.657850000	0.662361000	-2.782437000
C	4.409620000	-0.269613000	3.602764000	C	-4.651013000	-0.177429000	-3.229285000
H	1.696619000	-2.705699000	0.403594000	H	-1.725390000	-2.660418000	-0.225119000
H	3.688109000	-3.095418000	1.863946000	H	-3.746408000	-3.040241000	-1.606028000
C	1.616010000	-1.690075000	0.783372000	C	-1.680729000	-1.634346000	-0.580081000
C	1.460822000	0.965892000	1.711341000	C	-1.629926000	1.061448000	-1.424333000
H	3.394250000	1.587761000	3.538074000	H	-3.642396000	1.696262000	-3.113590000
C	0.555773000	0.492440000	0.802288000	C	-0.671039000	0.574863000	-0.579800000
C	0.630910000	-0.852484000	0.339787000	C	-0.693458000	-0.787121000	-0.158961000
H	1.412336000	1.995551000	2.058978000	H	-1.623033000	2.103799000	-1.734430000
C	-1.768107000	-0.815146000	-0.166357000	C	1.725694000	-0.704844000	0.215590000
C	-2.860879000	-1.635987000	-0.122308000	C	2.832648000	-1.495181000	0.071706000
C	-4.087830000	-1.161211000	0.415943000	C	4.015397000	-0.956567000	-0.503212000
C	-4.164955000	0.176636000	0.899867000	C	4.035759000	0.407230000	-0.914559000
C	-3.014032000	1.008749000	0.831585000	C	2.871811000	1.205155000	-0.748599000
C	-1.844972000	0.521843000	0.315960000	C	1.743716000	0.657900000	-0.202611000
H	-5.207129000	-3.014935000	0.123150000	H	5.170481000	-2.785483000	-0.366357000
H	-2.804499000	-2.658225000	-0.490077000	H	2.822073000	-2.535567000	0.388214000
C	-5.237920000	-1.991630000	0.483151000	C	5.178822000	-1.744598000	-0.675400000
C	-5.391006000	0.648903000	1.439890000	C	5.220099000	0.937223000	-1.481213000
H	-3.077081000	2.032421000	1.193291000	H	2.890814000	2.246799000	-1.059611000
C	-6.474293000	-0.177217000	1.489507000	C	6.341533000	0.156857000	-1.638419000
C	-6.397506000	-1.504037000	1.007780000	C	6.320250000	-1.212077000	-1.227821000
H	-5.478496000	1.662375000	1.817884000	H	5.243248000	1.976112000	-1.796061000
C	-0.551901000	1.281685000	0.145290000	C	0.441352000	1.372426000	0.056481000
C	-0.407228000	-1.166574000	-0.713673000	C	0.407861000	-1.112358000	0.824579000
N	2.254387000	0.343871000	-2.506380000	N	-2.185692000	0.170133000	2.814413000
C	1.276720000	-0.473390000	-2.425360000	C	-1.150664000	-0.564473000	2.686587000
C	-0.113534000	-0.177727000	-1.903340000	C	0.171177000	-0.171970000	2.066922000
C	-0.259484000	1.282225000	-1.399603000	C	0.205763000	1.308326000	1.610305000
C	0.957133000	2.117476000	-1.706027000	C	-1.062246000	2.045280000	1.970176000
N	2.063776000	1.702155000	-2.193588000	N	-2.119398000	1.537933000	2.479568000
H	-0.848945000	-0.376925000	-2.691236000	H	0.977725000	-0.370736000	2.781605000
H	-1.113324000	1.772736000	-1.874689000	H	1.038965000	1.843557000	2.073480000
H	-0.622227000	2.306020000	0.514399000	H	0.466003000	2.410502000	-0.275777000
H	-0.354182000	-2.205082000	-1.050288000	H	0.397247000	-2.162618000	1.126918000

F	5.319023000	0.127115000	4.497090000
F	5.480576000	-2.364474000	3.601697000
F	-7.642056000	0.231716000	1.992168000
F	-7.497973000	-2.256526000	1.086296000
C	0.872882000	3.585807000	-1.447659000
C	2.024059000	4.379968000	-1.494041000
N	-0.343576000	4.081519000	-1.190895000
C	1.895289000	5.742693000	-1.270661000
H	2.977303000	3.911150000	-1.706776000
C	-0.450752000	5.394290000	-0.983276000
C	0.631725000	6.267669000	-1.011513000
H	2.768134000	6.387830000	-1.296922000
H	-1.453754000	5.764673000	-0.783276000
H	0.484606000	7.327118000	-0.831531000
C	1.575946000	-1.882829000	-2.832494000
C	0.678027000	-2.593471000	-3.634895000
N	2.727409000	-2.405311000	-2.396436000
C	1.001826000	-3.890497000	-4.016735000
H	-0.247573000	-2.133470000	-3.967672000
C	3.020304000	-3.650729000	-2.765426000
C	2.200223000	-4.436424000	-3.573731000
H	0.330741000	-4.462080000	-4.650633000
H	3.963046000	-4.044647000	-2.391801000
H	2.495978000	-5.444934000	-3.841661000

C	-5.652454000	0.319870000	-4.132770000
N	-6.446284000	0.739058000	-4.862278000
C	-5.715742000	-2.424289000	-3.256992000
N	-6.538055000	-3.152336000	-3.620121000
C	7.531288000	0.722552000	-2.213569000
N	8.480032000	1.194853000	-2.677044000
C	7.488069000	-2.035309000	-1.385460000
N	8.418059000	-2.713370000	-1.501462000
C	-1.093839000	3.519700000	1.734171000
C	-2.289913000	4.233715000	1.860142000
N	0.072393000	4.099903000	1.425703000
C	-2.262116000	5.606472000	1.661005000
H	-3.197580000	3.700367000	2.115523000
C	0.083268000	5.420692000	1.243027000
C	-1.051341000	6.219071000	1.348269000
H	-3.172194000	6.191961000	1.748837000
H	1.047951000	5.860588000	1.000533000
H	-0.983876000	7.289346000	1.186286000
C	-1.283415000	-1.985705000	3.137563000
C	-0.371667000	-2.510519000	4.057745000
N	-2.286775000	-2.699533000	2.617277000
C	-0.526095000	-3.827663000	4.474166000
H	0.425624000	-1.890893000	4.457261000
C	-2.417892000	-3.962653000	3.023455000
C	-1.572916000	-4.574377000	3.947019000
H	0.156384000	-4.259019000	5.199908000
H	-3.244438000	-4.516646000	2.583845000
H	-1.735572000	-5.606242000	4.238531000

TS3-ax

E(SCF) = -1411.35118974

C	-5.747481000	-1.200750000	0.759292000
C	-4.616191000	-0.882710000	1.443039000
C	-3.393843000	-0.644655000	0.742274000
C	-3.388860000	-0.748060000	-0.689059000
C	-4.596289000	-1.091816000	-1.368262000
C	-5.745674000	-1.312761000	-0.672728000
H	-2.225994000	-0.203399000	2.495506000
H	-4.632018000	-0.800408000	2.527679000
C	-2.213674000	-0.306573000	1.412435000
C	-2.201198000	-0.495095000	-1.384927000
H	-4.610579000	-1.172433000	-2.450364000
C	-1.021302000	-0.202404000	-0.709753000
C	-1.024158000	-0.113692000	0.716689000
H	-2.203664000	-0.537569000	-2.471840000
C	1.447681000	-0.006100000	0.710454000
C	2.648024000	-0.132513000	1.405360000
C	3.849822000	-0.370152000	0.731082000
C	3.853024000	-0.443446000	-0.703846000
C	2.648381000	-0.275380000	-1.395592000
C	1.448926000	-0.079705000	-0.716055000
H	5.094726000	-0.489171000	2.515884000
H	2.650307000	-0.063184000	2.491396000
C	5.086548000	-0.540084000	1.429082000
C	5.084996000	-0.681794000	-1.386886000
H	2.650273000	-0.318007000	-2.482658000
C	6.246602000	-0.836011000	-0.693952000
C	6.238200000	-0.762081000	0.741426000
H	5.105617000	-0.742497000	-2.470339000

TS3-bx

E(SCF) = -1267.76320415

C	-5.766153000	-1.255801000	0.721368000
C	-4.609595000	-0.979967000	1.393915000
C	-3.389135000	-0.686506000	0.715642000
C	-3.389142000	-0.686783000	-0.715314000
C	-4.609599000	-0.980532000	-1.393467000
C	-5.766153000	-1.256102000	-0.720807000
H	-2.214827000	-0.359089000	2.490874000
H	-4.605740000	-0.974936000	2.481989000
C	-2.206552000	-0.389420000	1.403275000
C	-2.206573000	-0.389936000	-1.403070000
H	-4.605743000	-0.975944000	-2.481543000
C	-1.022468000	-0.146430000	-0.715532000
C	-1.022452000	-0.146180000	0.715633000
H	-2.214860000	-0.360008000	-2.490680000
C	1.449151000	-0.031187000	0.715157000
C	2.648096000	-0.194746000	1.403633000
C	3.849745000	-0.400456000	0.716426000
C	3.849718000	-0.400731000	-0.716390000
C	2.648046000	-0.195261000	-1.403628000
C	1.449129000	-0.031438000	-0.715167000
H	5.084666000	-0.610333000	2.482142000
H	2.650941000	-0.181695000	2.491777000
C	5.089356000	-0.609034000	1.393895000
C	5.089297000	-0.609588000	-1.393832000
H	2.650850000	-0.182608000	-2.491777000
C	6.262166000	-0.804447000	-0.721506000
C	6.262198000	-0.804153000	0.721596000
H	5.084558000	-0.611320000	-2.482077000

C	0.194297000	0.187433000	-1.367417000
C	0.194501000	0.335958000	1.328994000
N	-2.162711000	3.007430000	0.580137000
C	-1.035573000	2.823618000	1.191428000
C	0.186250000	2.366111000	0.582426000
C	0.154532000	2.282735000	-0.848493000
C	-1.102836000	2.656943000	-1.444507000
N	-2.197930000	2.916652000	-0.803122000
H	-1.061271000	2.979380000	2.270163000
H	-1.187781000	2.673408000	-2.531120000
H	1.120660000	2.574703000	1.092013000
H	1.061378000	2.448096000	-1.420311000
H	0.190482000	0.211837000	-2.456819000
H	0.191548000	0.480452000	2.409189000
O	-6.899214000	-1.639845000	-1.300713000
H	-7.595031000	-1.720056000	-0.628812000
O	-6.970610000	-1.444187000	1.318975000
H	-6.929649000	-1.298692000	2.274357000
O	7.421789000	-1.058891000	-1.326774000
H	8.116915000	-1.138545000	-0.654066000
O	7.474063000	-0.935367000	1.297765000
H	7.412116000	-0.888248000	2.261992000

C	0.195154000	0.270231000	-1.352116000
C	0.195192000	0.270701000	1.352039000
N	-2.183286000	2.970274000	0.692676000
C	-1.071181000	2.753136000	1.320607000
C	0.169480000	2.342135000	0.715856000
C	0.169464000	2.341885000	-0.716639000
C	-1.071211000	2.752670000	-1.321507000
N	-2.183302000	2.970029000	-0.693627000
H	-1.126802000	2.839334000	2.405847000
H	-1.126855000	2.838491000	-2.406775000
H	1.090192000	2.528686000	1.257882000
H	1.090165000	2.528244000	-1.258749000
H	0.191914000	0.354806000	-2.438487000
H	0.191986000	0.355651000	2.438381000
C	-7.040711000	-1.554558000	-1.464568000
H	-7.428892000	-2.548133000	-1.212630000
H	-7.826239000	-0.831905000	-1.215558000
H	-6.879122000	-1.518113000	-2.544410000
C	-7.040703000	-1.553978000	1.465255000
H	-7.826394000	-0.831726000	1.215608000
H	-7.428613000	-2.547856000	1.214088000
H	-6.879214000	-1.516639000	2.545082000
C	7.553064000	-1.021033000	-1.465433000
H	8.293621000	-0.252802000	-1.214902000
H	8.001257000	-1.989527000	-1.215629000
H	7.389838000	-0.993254000	-2.545269000
C	7.553123000	-1.020457000	1.465556000
H	8.001103000	-1.989222000	1.216413000
H	8.293811000	-0.252553000	1.214409000
H	7.390003000	-0.991879000	2.545388000

TS3-cx

E(SCF) = -1507.38265930

C	-5.723548000	-1.265236000	0.712345000
C	-4.594847000	-0.994775000	1.413155000
C	-3.381534000	-0.701017000	0.717530000
C	-3.381538000	-0.700903000	-0.717594000
C	-4.594855000	-0.994547000	-1.413261000
C	-5.723553000	-1.265121000	-0.712489000
H	-2.207124000	-0.371985000	2.490470000
H	-4.624360000	-0.998362000	2.497548000
C	-2.198778000	-0.402431000	1.403392000
C	-2.198786000	-0.402212000	-1.403415000
H	-4.624373000	-0.997956000	-2.497654000
C	-1.016113000	-0.154993000	-0.715153000
C	-1.016109000	-0.155101000	0.715162000
H	-2.207138000	-0.371598000	-2.490488000
C	1.452816000	-0.025822000	0.714807000
C	2.651138000	-0.188495000	1.404034000
C	3.853263000	-0.394472000	0.718529000
C	3.853258000	-0.394395000	-0.718566000
C	2.651130000	-0.188336000	-1.404041000
C	1.452814000	-0.025737000	-0.714788000
H	5.114682000	-0.614609000	2.497829000
H	2.653679000	-0.176645000	2.491659000
C	5.085431000	-0.605970000	1.413293000
C	5.085420000	-0.605823000	-1.413363000
H	2.653664000	-0.176361000	-2.491665000
C	6.229740000	-0.800792000	-0.712866000

TS3-dx

E(SCF) = -1479.42035929

C	-5.762162000	-1.110071000	0.719889000
C	-4.610204000	-0.836125000	1.405424000
C	-3.396436000	-0.550113000	0.716335000
C	-3.396437000	-0.549997000	-0.716436000
C	-4.610209000	-0.835899000	-1.405566000
C	-5.762165000	-1.109956000	-0.720070000
H	-2.222818000	-0.230470000	2.493192000
H	-4.618205000	-0.835030000	2.490980000
C	-2.213576000	-0.260579000	1.406327000
C	-2.213577000	-0.260356000	-1.406384000
H	-4.618215000	-0.834632000	-2.491121000
C	-1.030699000	-0.020200000	-0.715957000
C	-1.030700000	-0.020310000	0.715938000
H	-2.222820000	-0.230074000	-2.493244000
C	1.437062000	0.093078000	0.715781000
C	2.631674000	-0.086895000	1.407161000
C	3.828595000	-0.308968000	0.717552000
C	3.828601000	-0.308832000	-0.717605000
C	2.631682000	-0.086643000	-1.407183000
C	1.437064000	0.093199000	-0.715779000
H	5.063792000	-0.540458000	2.491564000
H	2.635314000	-0.076031000	2.494575000
C	5.056357000	-0.535882000	1.405827000
C	5.056371000	-0.535606000	-1.405912000
H	2.635330000	-0.075584000	-2.494595000
C	6.221079000	-0.748095000	-0.720520000

C	6.229746000	-0.800863000	0.712766000
H	5.114663000	-0.614349000	-2.497901000
C	0.198145000	0.269151000	-1.352928000
C	0.198147000	0.268972000	1.352989000
N	-2.207929000	2.928614000	0.693277000
C	-1.092312000	2.733879000	1.322003000
C	0.154325000	2.341673000	0.716213000
C	0.154372000	2.341762000	-0.715896000
C	-1.092210000	2.734072000	-1.321730000
N	-2.207875000	2.928720000	-0.693065000
H	-1.148958000	2.821160000	2.406937000
H	-1.148765000	2.821516000	-2.406654000
H	1.072854000	2.538804000	1.258257000
H	1.072944000	2.538940000	-1.257851000
H	0.194385000	0.353544000	-2.439085000
H	0.194391000	0.353224000	2.439157000
F	7.399934000	-1.003338000	1.320102000
F	7.399922000	-1.003207000	-1.320232000
F	-6.878448000	-1.543366000	-1.319651000
F	-6.878440000	-1.543585000	1.319468000

C	6.221071000	-0.748242000	0.720406000
H	5.063819000	-0.539966000	-2.491649000
C	0.185586000	0.394579000	-1.355615000
C	0.185585000	0.394360000	1.355664000
N	-2.219706000	3.036533000	0.693406000
C	-1.103161000	2.855382000	1.323908000
C	0.146053000	2.472097000	0.715776000
C	0.146044000	2.472213000	-0.715393000
C	-1.103181000	2.855597000	-1.323442000
N	-2.219716000	3.036648000	-0.692893000
H	-1.159969000	2.944932000	2.408308000
H	-1.160007000	2.945324000	-2.407826000
H	1.064738000	2.668834000	1.257778000
H	1.064722000	2.669040000	-1.257375000
H	0.182237000	0.478724000	-2.441383000
H	0.182234000	0.478331000	2.441446000
C	-6.971129000	-1.401759000	-1.440301000
N	-7.933426000	-1.639504000	-2.036499000
C	-6.971124000	-1.401977000	1.440084000
N	-7.933414000	-1.639801000	2.036260000
C	7.444633000	-0.974118000	-1.439498000
N	8.420716000	-1.154985000	-2.033254000
C	7.444614000	-0.974420000	1.439354000
N	8.420686000	-1.155421000	2.033088000

TS3-ay

E(SCF) = -2462.23737970

C	5.334152000	0.421775000	2.071269000
C	4.416513000	-0.528324000	1.730336000
C	3.051251000	-0.169767000	1.558502000
C	2.667759000	1.199902000	1.737698000
C	3.653752000	2.161841000	2.106363000
C	4.954425000	1.790351000	2.272990000
H	2.398547000	-2.143029000	0.975478000
H	4.722391000	-1.558923000	1.565461000
C	2.086820000	-1.118300000	1.167603000
C	1.332750000	1.564013000	1.520184000
H	3.379368000	3.202713000	2.242388000
C	0.374330000	0.607542000	1.175179000
C	0.769921000	-0.753625000	0.975020000
H	1.040281000	2.607137000	1.620384000
C	-1.591370000	-1.396539000	0.566058000
C	-2.547701000	-2.388772000	0.450528000
C	-3.911757000	-2.111276000	0.657038000
C	-4.317565000	-0.764208000	0.942713000
C	-3.349379000	0.242578000	1.018767000
C	-1.998352000	-0.058917000	0.862371000
H	-4.615348000	-4.157147000	0.362470000
H	-2.246560000	-3.405038000	0.206471000
C	-4.900961000	-3.132506000	0.577426000
C	-5.706267000	-0.488477000	1.137181000
H	-3.652111000	1.271322000	1.205702000
C	-6.621500000	-1.490977000	1.052455000
C	-6.219888000	-2.840161000	0.767936000
H	-6.020282000	0.529884000	1.355065000
C	-0.974181000	0.941412000	0.869998000
C	-0.178948000	-1.577813000	0.234692000
N	2.001556000	0.546722000	-1.794018000
C	1.389165000	-0.598519000	-1.745990000

TS3-by

E(RM062X) = -2318.64851278

C	5.340694000	0.390787000	2.110507000
C	4.390215000	-0.535023000	1.770263000
C	3.028566000	-0.176241000	1.577219000
C	2.655707000	1.194502000	1.739212000
C	3.660839000	2.137521000	2.102034000
C	4.964416000	1.769156000	2.287420000
H	2.362874000	-2.147096000	0.996295000
H	4.674936000	-1.574317000	1.620594000
C	2.059126000	-1.118249000	1.180738000
C	1.326682000	1.576332000	1.513667000
H	3.369563000	3.178875000	2.219572000
C	0.360472000	0.626380000	1.174330000
C	0.746817000	-0.740281000	0.978670000
H	1.045604000	2.624208000	1.598046000
C	-1.620060000	-1.363775000	0.572066000
C	-2.583580000	-2.351655000	0.471672000
C	-3.942270000	-2.058752000	0.685994000
C	-4.339467000	-0.711452000	0.962274000
C	-3.364593000	0.292157000	1.022282000
C	-2.017294000	-0.019553000	0.858115000
H	-4.646729000	-4.086463000	0.421801000
H	-2.290049000	-3.372845000	0.237819000
C	-4.951018000	-3.062838000	0.630105000
C	-5.725265000	-0.437902000	1.164056000
H	-3.660392000	1.322937000	1.208312000
C	-6.674457000	-1.419268000	1.103867000
C	-6.273934000	-2.776093000	0.828693000
H	-6.020331000	0.588127000	1.373853000
C	-0.983631000	0.971954000	0.863172000
C	-0.210619000	-1.562415000	0.250990000
N	2.031305000	0.466433000	-1.792817000
C	1.369036000	-0.649940000	-1.755169000

C	-0.038879000	-0.817527000	-1.459098000
C	-0.749066000	0.450141000	-1.506522000
C	-0.000436000	1.629263000	-1.639957000
N	1.315481000	1.711218000	-1.695881000
H	-0.494053000	-1.647745000	-1.998878000
H	-1.821639000	0.475641000	-1.638793000
H	-1.280031000	1.985389000	0.945402000
H	0.131970000	-2.608321000	0.063977000
O	5.903625000	2.687776000	2.620189000
H	6.759856000	2.231236000	2.645853000
O	6.665375000	0.198442000	2.250539000
H	6.880355000	-0.721710000	2.040800000
O	-7.969141000	-1.354101000	1.218519000
H	-8.191610000	-0.430214000	1.400531000
O	-7.167631000	-3.798857000	0.693855000
H	-8.030972000	-3.387600000	0.862490000
C	-0.688403000	2.953299000	-1.507469000
O	-0.190022000	4.005883000	-1.262621000
O	-2.067884000	2.784096000	-1.623191000
C	-2.864005000	3.802280000	-1.182624000
F	-4.119510000	3.389254000	-1.291247000
F	-2.715061000	4.909883000	-1.887940000
F	-2.623788000	4.074856000	0.102549000
C	2.234730000	-1.815533000	-1.801208000
O	1.806418000	-2.938565000	-1.768070000
O	3.580418000	-1.531515000	-1.824792000
C	4.437382000	-2.575163000	-1.634027000
F	5.662483000	-2.072734000	-1.600868000
F	4.370462000	-3.477405000	-2.601064000
F	4.210479000	-3.190786000	-0.467365000

C	-0.064644000	-0.805714000	-1.469041000
C	-0.726477000	0.485621000	-1.512742000
C	0.077141000	1.632918000	-1.624688000
N	1.393640000	1.657929000	-1.672258000
H	-0.553816000	-1.627445000	-1.989975000
H	-1.795373000	0.559490000	-1.660446000
H	-1.280078000	2.018793000	0.935004000
H	0.091159000	-2.594993000	0.077790000
C	-0.553834000	2.976525000	-1.432918000
O	-0.040624000	3.945080000	-0.966062000
O	-1.898920000	2.928609000	-1.780250000
C	-2.698138000	3.945156000	-1.333000000
F	-3.933358000	3.668266000	-1.720061000
F	-2.349064000	5.122898000	-1.820971000
F	-2.678506000	4.010835000	0.001080000
C	2.161845000	-1.904412000	-1.819458000
O	1.682036000	-3.006139000	-1.775977000
O	3.514635000	-1.679071000	-1.864332000
C	4.329853000	-2.759051000	-1.670806000
F	5.574078000	-2.310636000	-1.664475000
F	4.205832000	-3.667426000	-2.627639000
F	4.088192000	-3.346853000	-0.495799000
C	6.778158000	-0.015220000	2.290889000
H	7.431166000	0.519739000	1.592093000
H	7.133577000	0.215933000	3.301552000
H	6.906113000	-1.086555000	2.121532000
C	6.009011000	2.787017000	2.659506000
H	6.494560000	2.534665000	3.609059000
H	6.797735000	2.843461000	1.900871000
H	5.565525000	3.780238000	2.759246000
C	-8.130036000	-1.103134000	1.321306000
H	-8.732953000	-1.382161000	0.449970000
H	-8.533805000	-1.653418000	2.178791000
H	-8.274671000	-0.036243000	1.505618000
C	-7.316069000	-3.860000000	0.764544000
H	-7.868070000	-3.937309000	1.708138000
H	-8.053668000	-3.659678000	-0.020870000
H	-6.858233000	-4.830414000	0.560005000

TS3-cy

E(SCF) = -2558.26546344

C	-5.310575000	0.373151000	-2.123028000
C	-4.404375000	-0.574943000	-1.768687000
C	-3.041744000	-0.205767000	-1.572738000
C	-2.655446000	1.164667000	-1.744140000
C	-3.641233000	2.126149000	-2.122356000
C	-4.926798000	1.732072000	-2.304767000
H	-2.390270000	-2.177106000	-0.987383000
H	-4.727956000	-1.600168000	-1.622368000
C	-2.081388000	-1.150219000	-1.170674000
C	-1.323919000	1.535771000	-1.514448000
H	-3.376091000	3.169627000	-2.254432000
C	-0.368361000	0.582813000	-1.160292000
C	-0.764657000	-0.778879000	-0.966125000
H	-1.035359000	2.580257000	-1.610632000
C	1.593290000	-1.421791000	-0.556403000
C	2.547903000	-2.420730000	-0.446605000
C	3.908480000	-2.141977000	-0.649907000
C	4.319781000	-0.794502000	-0.930092000

TS3-dy

E(SCF) = -2530.29886385

C	5.379757000	-0.003556000	-1.983174000
C	4.376306000	0.861850000	-1.638188000
C	3.047291000	0.393081000	-1.438376000
C	2.772810000	-1.004681000	-1.586651000
C	3.835040000	-1.882694000	-1.945296000
C	5.102703000	-1.406289000	-2.144979000
H	2.237588000	2.319197000	-0.896673000
H	4.593517000	1.916985000	-1.501813000
C	2.016003000	1.266631000	-1.059248000
C	1.475931000	-1.484364000	-1.353990000
H	3.634204000	-2.943680000	-2.056293000
C	0.447870000	-0.605036000	-1.020308000
C	0.730856000	0.789586000	-0.855266000
H	1.277681000	-2.551489000	-1.425110000
C	-1.676777000	1.247954000	-0.501626000
C	-2.709884000	2.174104000	-0.452141000
C	-4.034817000	1.775873000	-0.679837000
C	-4.328786000	0.392881000	-0.922032000

C	3.353799000	0.216337000	-0.998865000
C	2.003498000	-0.082750000	-0.840684000
H	4.617511000	-4.195159000	-0.363425000
H	2.242589000	-3.437965000	-0.212854000
C	4.898292000	-3.168385000	-0.573219000
C	5.708532000	-0.515800000	-1.123947000
H	3.661359000	1.243837000	-1.181794000
C	6.614374000	-1.521664000	-1.039510000
C	6.205981000	-2.858337000	-0.761804000
H	6.046203000	0.492722000	-1.338239000
C	0.976933000	0.919257000	-0.819629000
C	0.185496000	-1.610482000	-0.252352000
N	-2.009096000	0.562121000	1.784169000
C	-1.374652000	-0.569383000	1.761218000
C	0.052635000	-0.761498000	1.504485000
C	0.747492000	0.504962000	1.473619000
C	-0.024336000	1.682412000	1.617309000
N	-1.331573000	1.740093000	1.686804000
H	0.524974000	-1.592959000	2.022181000
H	1.816641000	0.551262000	1.627165000
H	1.284594000	1.962021000	-0.900193000
H	-0.129858000	-2.630365000	-0.038203000
C	0.640408000	3.020237000	1.473218000
O	0.116783000	4.058906000	1.223048000
O	2.018056000	2.874673000	1.588515000
C	2.798093000	3.912558000	1.151598000
F	4.058320000	3.521254000	1.263201000
F	2.622383000	5.012180000	1.860640000
F	2.551296000	4.179806000	-0.131981000
C	-2.203638000	-1.806088000	1.828264000
O	-1.747612000	-2.917444000	1.801808000
O	-3.545860000	-1.543140000	1.857432000
C	-4.392446000	-2.605732000	1.679254000
F	-5.621029000	-2.122455000	1.663561000
F	-4.290075000	-3.501198000	2.648365000
F	-4.161417000	-3.214305000	0.511979000
F	7.162331000	-3.783090000	-0.695395000
F	7.918779000	-1.309655000	-1.209333000
F	-6.594466000	0.075719000	-2.310269000
F	-5.882690000	2.591274000	-2.655790000

C	-3.288092000	-0.543143000	-0.926016000
C	-1.971761000	-0.130195000	-0.742573000
H	-4.891352000	3.763993000	-0.486618000
H	-2.492090000	3.220490000	-0.252422000
C	-5.105640000	2.715598000	-0.670094000
C	-5.681945000	0.004500000	-1.147637000
H	-3.508304000	-1.596880000	-1.083003000
C	-6.691340000	0.927897000	-1.132370000
C	-6.396603000	2.315857000	-0.886116000
H	-5.910937000	-1.039994000	-1.335614000
C	-0.866924000	-1.043604000	-0.658262000
C	-0.297819000	1.566744000	-0.201092000
N	2.070005000	-0.336070000	1.936562000
C	1.300011000	0.705639000	1.899043000
C	-0.131854000	0.712362000	1.631934000
C	-0.673546000	-0.620080000	1.560342000
C	0.243225000	-1.698780000	1.733229000
N	1.537618000	-1.592243000	1.836506000
H	-0.714545000	1.500631000	2.099352000
H	-1.726159000	-0.798953000	1.734860000
H	-1.087820000	-2.108809000	-0.725109000
H	-0.068278000	2.607767000	0.016584000
C	6.159245000	-2.307874000	-2.514661000
N	6.998951000	-3.043116000	-2.817940000
C	6.713915000	0.493725000	-2.181193000
N	7.779989000	0.913108000	-2.340239000
C	-8.047550000	0.511176000	-1.362562000
N	-9.133685000	0.160371000	-1.549698000
C	-7.459309000	3.283091000	-0.865378000
N	-8.303503000	4.073496000	-0.843302000
C	-0.251687000	-3.102886000	1.536254000
O	0.372200000	-4.014645000	1.092792000
O	-1.599324000	-3.173149000	1.841364000
C	-2.290893000	-4.272306000	1.389440000
F	-3.553235000	-4.100871000	1.739795000
F	-1.842154000	-5.398980000	1.905729000
F	-2.223808000	-4.344868000	0.058418000
C	1.973964000	2.039735000	1.957721000
O	1.383735000	3.083051000	1.882210000
O	3.330378000	1.938166000	2.033666000
C	4.055485000	3.092998000	1.852628000
F	5.328681000	2.761543000	1.916291000
F	3.790137000	4.000353000	2.775508000
F	3.807473000	3.618354000	0.649729000

TS3-az

E(SCF) = -1905.35901813

C	-5.252909000	-0.628726000	-2.378466000
C	-4.062847000	-1.265513000	-2.215400000
C	-2.912292000	-0.541155000	-1.775754000
C	-3.039470000	0.863847000	-1.516997000
C	-4.304578000	1.495975000	-1.706312000
C	-5.384464000	0.777929000	-2.123530000
H	-1.590294000	-2.241491000	-1.746945000
H	-3.977284000	-2.333236000	-2.404972000
C	-1.678916000	-1.170716000	-1.575919000
C	-1.925091000	1.576492000	-1.053476000
H	-4.419078000	2.557233000	-1.509367000
C	-0.699173000	0.948998000	-0.876351000

TS3-bz

E(SCF) = -1761.77035201

C	-5.273783000	-0.636796000	-2.413272000
C	-4.070620000	-1.255289000	-2.221556000
C	-2.916775000	-0.547784000	-1.770524000
C	-3.035275000	0.854947000	-1.516367000
C	-4.301596000	1.477104000	-1.724811000
C	-5.392923000	0.776434000	-2.156157000
H	-1.604647000	-2.257147000	-1.723418000
H	-3.976465000	-2.323211000	-2.407070000
C	-1.687866000	-1.185113000	-1.557321000
C	-1.922904000	1.568523000	-1.049400000
H	-4.387589000	2.543559000	-1.524937000
C	-0.699790000	0.936763000	-0.867775000

C	-0.565675000	-0.445822000	-1.156304000
H	-2.030807000	2.631814000	-0.809930000
C	1.890684000	-0.254292000	-0.869055000
C	3.161962000	-0.778333000	-1.089939000
C	4.302670000	0.027951000	-0.991277000
C	4.151496000	1.406179000	-0.616624000
C	2.872965000	1.916345000	-0.365637000
C	1.742017000	1.119016000	-0.507568000
H	5.745488000	-1.522251000	-1.534400000
H	3.273307000	-1.826509000	-1.361507000
C	5.611630000	-0.484587000	-1.245677000
C	5.321947000	2.220267000	-0.507618000
H	2.761464000	2.957225000	-0.069083000
C	6.550745000	1.692747000	-0.752583000
C	6.707392000	0.315396000	-1.129650000
H	5.217069000	3.265691000	-0.224935000
C	0.407306000	1.556488000	-0.184363000
C	0.692862000	-1.049898000	-0.825241000
N	-1.717352000	-1.608832000	1.663146000
C	-0.448601000	-1.884850000	1.532468000
C	0.562413000	-0.874585000	1.356053000
C	0.180497000	0.486267000	1.609805000
C	-1.228498000	0.652611000	1.893121000
N	-2.105791000	-0.307111000	1.820078000
H	1.598124000	-1.145577000	1.523143000
H	0.871061000	1.165197000	2.096779000
H	0.285661000	2.580891000	0.161163000
H	0.790642000	-2.121234000	-0.993866000
O	-6.593373000	1.360655000	-2.302390000
H	-7.219315000	0.671701000	-2.577863000
O	-6.419092000	-1.217261000	-2.784554000
H	-6.286894000	-2.170120000	-2.886093000
O	7.735733000	2.370135000	-0.676324000
H	7.575077000	3.287086000	-0.413294000
O	7.954499000	-0.156516000	-1.362858000
H	8.581017000	0.572687000	-1.228758000
C	-0.072160000	-3.332486000	1.499074000
C	1.212945000	-3.740556000	1.115499000
N	-1.013209000	-4.212622000	1.864546000
C	1.521972000	-5.096068000	1.114971000
H	1.964690000	-3.018411000	0.813965000
C	-0.704011000	-5.504211000	1.856235000
C	0.545258000	-6.006688000	1.493287000
H	2.512377000	-5.430478000	0.821075000
H	-1.498728000	-6.182044000	2.162577000
H	0.738068000	-7.073916000	1.510958000
C	-1.767761000	2.007666000	2.185909000
C	-3.150177000	2.221848000	2.253370000
N	-0.872024000	2.988696000	2.352350000
C	-3.608755000	3.505335000	2.505802000
H	-3.817165000	1.382198000	2.097968000
C	-1.330830000	4.215825000	2.605308000
C	-2.682454000	4.530294000	2.691033000
H	-4.674582000	3.706845000	2.557270000
H	-0.575681000	4.986941000	2.742045000
H	-2.996324000	5.548799000	2.893083000

C	-0.573980000	-0.462687000	-1.137271000
H	-2.024689000	2.625972000	-0.812188000
C	1.884244000	-0.280953000	-0.859410000
C	3.151727000	-0.813181000	-1.081051000
C	4.293329000	-0.006124000	-0.999046000
C	4.153793000	1.374531000	-0.644076000
C	2.878542000	1.894862000	-0.390276000
C	1.744493000	1.099387000	-0.513879000
H	5.706905000	-1.559737000	-1.523787000
H	3.257709000	-1.865527000	-1.339517000
C	5.604907000	-0.511194000	-1.250564000
C	5.332928000	2.174788000	-0.558134000
H	2.774146000	2.940239000	-0.107208000
C	6.577347000	1.665803000	-0.799530000
C	6.717863000	0.275525000	-1.157537000
H	5.221597000	3.223473000	-0.289416000
C	0.413521000	1.548093000	-0.192210000
C	0.682928000	-1.069789000	-0.804928000
N	-1.732288000	-1.570482000	1.702485000
C	-0.468744000	-1.867457000	1.566614000
C	0.556957000	-0.873903000	1.379069000
C	0.195693000	0.492858000	1.624625000
C	-1.207295000	0.683825000	1.915314000
N	-2.100082000	-0.262605000	1.853332000
H	1.589471000	-1.159100000	1.542170000
H	0.900888000	1.170408000	2.091750000
H	0.299157000	2.576316000	0.144143000
H	0.774208000	-2.143118000	-0.963834000
C	-6.718372000	1.460486000	-2.361173000
H	-7.064861000	1.361243000	-3.396298000
H	-7.495324000	1.025508000	-1.721941000
H	-6.647007000	2.525892000	-2.129534000
C	-6.475851000	-1.412883000	-2.882110000
H	-7.294244000	-1.359255000	-2.155004000
H	-6.863540000	-1.020284000	-3.829237000
H	-6.225452000	-2.465959000	-3.030098000
C	7.802245000	2.535389000	-0.699972000
H	8.508889000	2.149260000	0.043493000
H	8.338279000	2.581581000	-1.655038000
H	7.534167000	3.555158000	-0.414137000
C	8.088088000	-0.288009000	-1.424796000
H	8.584700000	0.239986000	-2.246832000
H	8.737645000	-0.193382000	-0.546986000
H	8.029956000	-1.346414000	-1.689486000
C	-1.722961000	2.048427000	2.206033000
C	-3.100938000	2.282392000	2.293930000
N	-0.811016000	3.017299000	2.354889000
C	-3.536952000	3.572991000	2.550640000
H	-3.781602000	1.451240000	2.152560000
C	-1.247993000	4.251563000	2.610851000
C	-2.593529000	4.585236000	2.717984000
H	-4.598811000	3.789613000	2.620857000
H	-0.480012000	5.012293000	2.733307000
H	-2.889371000	5.608433000	2.923512000
C	-0.116622000	-3.321369000	1.541930000
C	1.159881000	-3.754512000	1.157400000
N	-1.071814000	-4.182079000	1.916239000
C	1.444053000	-5.115530000	1.163595000
H	1.923921000	-3.048055000	0.849787000
C	-0.786640000	-5.479049000	1.913971000
C	0.452023000	-6.006170000	1.549480000

				H	2.427162000	-5.469726000	0.868311000
				H	-1.592878000	-6.140326000	2.226048000
				H	0.625174000	-7.076666000	1.571667000
TS3-cz				**TS3-dz**			
E(SCF) = -2001.39052065				E(SCF) = -1973.43382496			
C	-5.217259000	-0.646247000	-2.415509000	C	5.343909000	0.682625000	-2.068952000
C	-4.047662000	-1.301063000	-2.209324000	C	4.162118000	1.337488000	-1.848206000
C	-2.896828000	-0.577215000	-1.769164000	C	2.979407000	0.623343000	-1.503140000
C	-3.002153000	0.837423000	-1.553603000	C	3.041476000	-0.803085000	-1.381697000
C	-4.254722000	1.484582000	-1.783770000	C	4.283024000	-1.460280000	-1.615907000
C	-5.321271000	0.757773000	-2.201016000	C	5.404934000	-0.750624000	-1.949754000
H	-1.604835000	-2.297053000	-1.662885000	H	1.736700000	2.376176000	-1.281548000
H	-3.997788000	-2.372331000	-2.372744000	H	4.121904000	2.419144000	-1.930380000
C	-1.675954000	-1.219939000	-1.530064000	C	1.772190000	1.290229000	-1.257791000
C	-1.884308000	1.549541000	-1.100042000	C	1.896181000	-1.515577000	-1.002705000
H	-4.362483000	2.552618000	-1.625426000	H	4.337687000	-2.540782000	-1.522697000
C	-0.669182000	0.909196000	-0.895134000	C	0.695372000	-0.852192000	-0.785336000
C	-0.557331000	-0.498021000	-1.123541000	C	0.625246000	0.570072000	-0.935466000
H	-1.975337000	2.613333000	-0.890652000	H	1.954608000	-2.592078000	-0.858110000
C	1.897738000	-0.338823000	-0.826009000	C	-1.836467000	0.461003000	-0.702064000
C	3.159830000	-0.893627000	-1.020163000	C	-3.075833000	1.059834000	-0.907062000
C	4.310584000	-0.098087000	-0.964057000	C	-4.243123000	0.287886000	-0.939090000
C	4.184479000	1.300711000	-0.661782000	C	-4.161019000	-1.127565000	-0.718966000
C	2.913990000	1.842067000	-0.432912000	C	-2.914736000	-1.717638000	-0.476804000
C	1.772425000	1.053868000	-0.531998000	C	-1.753991000	-0.951244000	-0.486701000
H	5.738535000	-1.695678000	-1.428520000	H	-5.590585000	1.944495000	-1.344725000
H	3.255248000	-1.955654000	-1.237345000	H	-3.140078000	2.135013000	-1.057012000
C	5.612483000	-0.643652000	-1.194806000	C	-5.520565000	0.874070000	-1.176421000
C	5.363532000	2.107608000	-0.599180000	C	-5.359172000	-1.898811000	-0.747534000
H	2.819467000	2.897843000	-0.189762000	H	-2.854437000	-2.788079000	-0.295772000
C	6.577457000	1.546589000	-0.821611000	C	-6.573558000	-1.310349000	-0.974558000
C	6.702888000	0.159150000	-1.121777000	C	-6.656251000	0.111005000	-1.193426000
H	5.297166000	3.167053000	-0.374450000	H	-5.304321000	-2.970913000	-0.584405000
C	0.446644000	1.531343000	-0.236082000	C	-0.449851000	-1.481169000	-0.185586000
C	0.686940000	-1.111757000	-0.755827000	C	-0.609756000	1.198505000	-0.559861000
N	-1.794249000	-1.454949000	1.721284000	N	1.852878000	1.329927000	1.915347000
C	-0.543713000	-1.806935000	1.602253000	C	0.617000000	1.716534000	1.799954000
C	0.523741000	-0.856278000	1.410319000	C	-0.490518000	0.820949000	1.585938000
C	0.209643000	0.526845000	1.623055000	C	-0.226891000	-0.580314000	1.735718000
C	-1.184812000	0.780571000	1.900763000	C	1.160230000	-0.891322000	2.015320000
N	-2.112829000	-0.132141000	1.848670000	N	2.121117000	-0.013803000	2.006902000
H	1.542310000	-1.174627000	1.597026000	H	-1.491950000	1.203630000	1.755031000
H	0.939482000	1.194578000	2.065443000	H	-0.981299000	-1.250140000	2.131423000
H	0.343190000	2.570180000	0.068898000	H	-0.379887000	-2.537284000	0.063714000
H	0.766787000	-2.190441000	-0.880043000	H	-0.655443000	2.284820000	-0.612777000
C	-1.648064000	2.169641000	2.163073000	C	1.567200000	-2.308558000	2.223061000
C	-3.015020000	2.453482000	2.267661000	C	2.917791000	-2.645946000	2.361896000
N	-0.700102000	3.109033000	2.273374000	N	0.583009000	-3.215859000	2.249407000
C	-3.401713000	3.764891000	2.499196000	C	3.249577000	-3.981268000	2.539083000
H	-3.726940000	1.643537000	2.161590000	H	3.661944000	-1.858958000	2.325109000
C	-1.089399000	4.363628000	2.505627000	C	0.918362000	-4.494406000	2.430207000
C	-2.420965000	4.746569000	2.625936000	C	2.231097000	-4.930671000	2.578798000
H	-4.453954000	4.020003000	2.582406000	H	4.288075000	-4.278965000	2.647483000
H	-0.293916000	5.099923000	2.597982000	H	0.094681000	-5.204344000	2.454529000
H	-2.677471000	5.783980000	2.811645000	H	2.444550000	-5.984684000	2.719291000
C	-0.257624000	-3.275947000	1.588508000	C	0.367349000	3.188984000	1.786516000
C	1.020821000	-3.768893000	1.294375000	C	-0.471964000	3.763220000	2.742501000

N	-1.280204000	-4.091447000	1.875935000	N	0.964672000	3.895030000	0.819215000
C	1.235359000	-5.143015000	1.301796000	C	-0.678142000	5.137697000	2.710000000
H	1.842119000	-3.100593000	1.057534000	H	-0.930641000	3.142163000	3.505963000
C	-1.061409000	-5.400929000	1.876511000	C	0.753249000	5.211997000	0.799168000
C	0.173791000	-5.986188000	1.598124000	C	-0.049592000	5.882337000	1.718773000
H	2.219605000	-5.543930000	1.078753000	H	-1.312946000	5.617642000	3.448453000
H	-1.921177000	-6.023132000	2.117138000	H	1.252294000	5.759718000	0.003173000
H	0.291495000	-7.064186000	1.617248000	H	-0.176899000	6.957258000	1.652094000
F	7.703256000	2.261063000	-0.770987000	C	-7.766212000	-2.111759000	-0.991903000
F	7.935675000	-0.307777000	-1.327757000	N	-8.717099000	-2.770485000	-1.001295000
F	-6.509396000	1.322002000	-2.428810000	C	-7.931619000	0.730673000	-1.427292000
F	-6.317041000	-1.281071000	-2.826629000	N	-8.950821000	1.244989000	-1.614183000
				C	6.644220000	-1.442096000	-2.177622000
				N	7.631346000	-2.017894000	-2.357588000
				C	6.522539000	1.426916000	-2.417984000
				N	7.461579000	2.039983000	-2.702015000

Cartesian Coordinates optimized at the B3LYP/6-311+G** level of theory

```
   36
F4PEN, E(RB3LYP) =  -1244.05745637
 C      0.000000     6.087118    -0.714814
 C      0.000000     4.929395    -1.417079
 C      0.000000     3.671115    -0.727279
 C      0.000000     3.671115     0.727279
 C      0.000000     4.929395     1.417079
 C      0.000000     6.087118     0.714814
 C      0.000000     2.463516    -1.407330
 C      0.000000     1.224074    -0.726956
 C      0.000000     1.224074     0.726956
 C      0.000000     2.463516     1.407330
 C      0.000000     0.000000    -1.407324
 C      0.000000    -1.224074    -0.726956
 C      0.000000    -1.224074     0.726956
 C      0.000000     0.000000     1.407324
 C      0.000000    -2.463516    -1.407330
 C      0.000000    -3.671115    -0.727279
 C      0.000000    -3.671115     0.727279
 C      0.000000    -2.463516     1.407330
 C      0.000000    -4.929395    -1.417079
 C      0.000000    -6.087118    -0.714814
 C      0.000000    -6.087118     0.714814
 C      0.000000    -4.929395     1.417079
 H      0.000000    -4.961234    -2.499937
 H      0.000000    -4.961234     2.499937
 H      0.000000    -2.463643    -2.492624
 H      0.000000    -2.463643     2.492624
 H      0.000000     2.463643     2.492624
 H      0.000000     2.463643    -2.492624
 H      0.000000     4.961234     2.499937
 H      0.000000     4.961234    -2.499937
 F      0.000000     7.281167     1.334079
 F      0.000000     7.281167    -1.334079
 F      0.000000    -7.281167     1.334079
 F      0.000000    -7.281167    -1.334079
 H      0.000000     0.000000    -2.492855
 H      0.000000     0.000000     2.492855

   36
F4PEN radical cation, E(UB3LYP) =  -1243.81537191
 C      0.000000     6.085687     0.710641
 C      0.000000     4.915849     1.416444
 C      0.000000     3.675940     0.723181
 C      0.000000     3.675940    -0.723181
 C      0.000000     4.915849    -1.416444
 C      0.000000     6.085687    -0.710641
 C      0.000000     2.453665     1.408297
 C      0.000000     1.227256     0.725983
 C      0.000000     1.227256    -0.725983
```

```
 C     0.000000     2.453665    -1.408297
 C     0.000000     0.000000     1.409267
 C     0.000000    -1.227256     0.725983
 C     0.000000    -1.227256    -0.725983
 C     0.000000     0.000000    -1.409267
 C     0.000000    -2.453665     1.408297
 C     0.000000    -3.675940     0.723181
 C     0.000000    -3.675940    -0.723181
 C     0.000000    -2.453665    -1.408297
 C     0.000000    -4.915849     1.416444
 C     0.000000    -6.085687     0.710641
 C     0.000000    -6.085687    -0.710641
 C     0.000000    -4.915849    -1.416444
 H     0.000000    -4.949929     2.499049
 H     0.000000    -4.949929    -2.499049
 H     0.000000    -2.455861     2.493007
 H     0.000000    -2.455861    -2.493007
 H     0.000000     2.455861    -2.493007
 H     0.000000     2.455861     2.493007
 H     0.000000     4.949929    -2.499049
 H     0.000000     4.949929     2.499049
 F     0.000000     7.260124    -1.331236
 F     0.000000     7.260124     1.331236
 F     0.000000    -7.260124    -1.331236
 F     0.000000    -7.260124     1.331236
 H     0.000000     0.000000     2.494395
 H     0.000000     0.000000    -2.494395


   36
PEN, E(RB3LYP) =  -846.996875826
 C     0.000000     6.110138     0.715968
 C     0.000000     6.110138    -0.715968
 C     0.000000     4.936430     1.408864
 H     0.000000     4.936544    -2.493892
 C     0.000000     3.673717     0.726727
 H     0.000000     4.936544     2.493892
 C     0.000000     2.464847     1.406441
 C     0.000000     3.673717    -0.726727
 H     0.000000     2.465546    -2.492200
 C     0.000000     4.936430    -1.408864
 C     0.000000     1.224863     0.727504
 H     0.000000     2.465546     2.492200
 C     0.000000     0.000000     1.406953
 C     0.000000     1.224863    -0.727504
 C     0.000000     0.000000    -1.406953
 C     0.000000     2.464847    -1.406441
 C     0.000000    -1.224863     0.727504
 H     0.000000     0.000000     2.492615
 C     0.000000    -1.224863    -0.727504
 H     0.000000     0.000000    -2.492615
 C     0.000000    -2.464847    -1.406441
 C     0.000000    -2.464847     1.406441
 H     0.000000    -2.465546     2.492200
 C     0.000000    -3.673717     0.726727
 H     0.000000    -2.465546    -2.492200
 C     0.000000    -3.673717    -0.726727
 C     0.000000    -4.936430     1.408864
 C     0.000000    -4.936430    -1.408864
 H     0.000000    -4.936544     2.493892
 C     0.000000    -6.110138     0.715968
 H     0.000000    -4.936544    -2.493892
 C     0.000000    -6.110138    -0.715968
 H     0.000000    -7.055960     1.245891
 H     0.000000    -7.055960    -1.245891
 H     0.000000     7.055960     1.245891
 H     0.000000     7.055960    -1.245891


   36
PFP, E(RB3LYP) =  -2236.63246395
 C     0.000000     2.482231     1.392739
 C     0.000000     2.482231    -1.392739
 F     0.000000     2.487722     2.730492
 F     0.000000     2.487722    -2.730492
 C     0.000000     1.233771    -0.726665
 C     0.000000     1.233771     0.726665
 C     0.000000     0.000000     1.393801
```

```
C     0.000000     0.000000    -1.393801
F     0.000000     0.000000     2.730193
F     0.000000     0.000000    -2.730193
C     0.000000    -1.233771     0.726665
C     0.000000    -1.233771    -0.726665
C     0.000000    -2.482231    -1.392739
C     0.000000    -2.482231     1.392739
F     0.000000    -2.487722    -2.730492
F     0.000000    -2.487722     2.730492
C     0.000000    -3.700217    -0.728103
C     0.000000    -3.700217     0.728103
C     0.000000    -4.964225     1.405209
C     0.000000    -6.133841     0.711194
C     0.000000    -6.133841    -0.711194
C     0.000000    -4.964225    -1.405209
F     0.000000    -5.023545     2.740148
F     0.000000    -7.308125     1.340589
F     0.000000    -7.308125    -1.340589
F     0.000000    -5.023545    -2.740148
C     0.000000     3.700217     0.728103
C     0.000000     3.700217    -0.728103
C     0.000000     4.964225    -1.405209
C     0.000000     6.133841    -0.711194
C     0.000000     6.133841     0.711194
C     0.000000     4.964225     1.405209
F     0.000000     5.023545    -2.740148
F     0.000000     7.308125    -1.340589
F     0.000000     7.308125     1.340589
F     0.000000     5.023545     2.740148
```

Cartesian Coordinates optimized at the SCS-MP2/def2-TZVP level of theory

```
   36
F4PEN: MP2 energy =    -1241.3293055933 |dE/dxyz| =  0.000051
 C     6.081031    -0.715410     0.000000
 C     4.921308    -1.419527     0.000000
 C     3.667133    -0.723387     0.000000
 C     3.667133     0.723387     0.000000
 C     4.921308     1.419527     0.000000
 C     6.081031     0.715410     0.000000
 C     2.459264    -1.408717     0.000000
 C     1.222830    -0.724618     0.000000
 C     1.222830     0.724618     0.000000
 C     2.459264     1.408717     0.000000
 C     0.000000    -1.409842     0.000000
 C    -1.222830    -0.724618     0.000000
 C    -1.222830     0.724618     0.000000
 C     0.000000     1.409842     0.000000
 C    -2.459264    -1.408717     0.000000
 C    -3.667133    -0.723387     0.000000
 C    -3.667133     0.723387     0.000000
 C    -2.459264     1.408717     0.000000
 C    -4.921308    -1.419527     0.000000
 C    -6.081031    -0.715410     0.000000
 C    -6.081031     0.715410     0.000000
 C    -4.921308     1.419527     0.000000
 H    -4.951426    -2.503743     0.000000
 H    -4.951426     2.503743     0.000000
 H    -2.460840    -2.496134     0.000000
 H    -2.460840     2.496134     0.000000
 H     2.460840     2.496134     0.000000
 H     2.460840    -2.496134     0.000000
 H     4.951426     2.503743     0.000000
 H     4.951426    -2.503743     0.000000
 F     7.271130     1.328693     0.000000
 F     7.271130    -1.328693     0.000000
 F    -7.271130     1.328693     0.000000
 F    -7.271130    -1.328693     0.000000
 H     0.000000    -2.497580     0.000000
 H     0.000000     2.497580     0.000000
```

```
   72
F4PEN dimer: MP2 energy =    -2482.6590032978 |dE/dxyz| =  0.000011
 F    -1.420389    -0.755510     0.000000
 F    -1.576950     1.899031     0.000000
 C    -2.642090    -0.213336     0.000000
 C    -3.759581    -0.983587     0.000000
 H    -3.665425    -2.064159     0.000000
 C    -5.052495    -0.362931     0.000000
 C    -6.218080    -1.118083     0.000000
 H    -6.152343    -2.203532     0.000000
 C    -7.492698    -0.508140     0.000000
 C    -8.673088    -1.264157     0.000000
 H    -8.608964    -2.350026     0.000000
 C    -7.578176     0.938605     0.000000
 C    -6.384156     1.694261     0.000000
 H    -6.446598     2.779917     0.000000
 C    -5.137925     1.081351     0.000000
 C    -3.926902     1.849753     0.000000
 H    -3.960690     2.933890     0.000000
 C    -2.727170     1.215528     0.000000
 F   -16.093360     1.040955     0.000000
 F   -15.936664    -1.612100     0.000000
 C   -14.869060     0.498722     0.000000
 C   -13.752828     1.269950     0.000000
 H   -13.846852     2.350513     0.000000
 C   -12.459741     0.649059     0.000000
 C   -11.294331     1.404352     0.000000
 H   -11.360108     2.489805     0.000000
 C   -10.019681     0.794423     0.000000
 C    -8.839321     1.550462     0.000000
 H    -8.903465     2.636335     0.000000
 C    -9.934225    -0.652300     0.000000
 C   -11.128217    -1.408037     0.000000
 H   -11.065748    -2.493684     0.000000
 C   -12.374436    -0.795188     0.000000
 C   -13.585440    -1.563989     0.000000
 H   -13.551598    -2.648107     0.000000
 C   -14.784701    -0.929529     0.000000
 F    16.093360    -1.040955     0.000000
 F    15.936664     1.612100     0.000000
 C    14.869060    -0.498722     0.000000
 C    13.752828    -1.269950     0.000000
 H    13.846852    -2.350513     0.000000
 C    12.459741    -0.649059     0.000000
 C    11.294331    -1.404352     0.000000
 H    11.360108    -2.489805     0.000000
 C    10.019681    -0.794423     0.000000
 C     8.839321    -1.550462     0.000000
 H     8.903465    -2.636335     0.000000
 C     9.934225     0.652300     0.000000
 C    11.128217     1.408037     0.000000
 H    11.065748     2.493684     0.000000
 C    12.374436     0.795188     0.000000
 C    13.585440     1.563989     0.000000
 H    13.551598     2.648107     0.000000
 C    14.784701     0.929529     0.000000
 F     1.420389     0.755510     0.000000
 F     1.576950    -1.899031     0.000000
 C     2.642090     0.213336     0.000000
 C     3.759581     0.983587     0.000000
 H     3.665425     2.064159     0.000000
 C     5.052495     0.362931     0.000000
 C     6.218080     1.118083     0.000000
 H     6.152343     2.203532     0.000000
 C     7.492698     0.508140     0.000000
 C     8.673088     1.264157     0.000000
 H     8.608964     2.350026     0.000000
 C     7.578176    -0.938605     0.000000
 C     6.384156    -1.694261     0.000000
 H     6.446598    -2.779917     0.000000
 C     5.137925    -1.081351     0.000000
 C     3.926902    -1.849753     0.000000
 H     3.960690    -2.933890     0.000000
 C     2.727170    -1.215528     0.000000
```

4. References

1. Bula, R. P.; Oppel, I. M.; Bettinger, H. F. *J. Org. Chem.* **2012**, *77*, 3538.
2. COSMO v. 1.61, Bruker AXS Inc., Madison, WI, 2012.
3. APEX 3 V. 2016.5-0, Bruker AXS Inc., Madison, WI, 2016; APEX2 v. 2012.10_0, Bruker AXS Inc., Madison, WI, 2012.
4. SAINT v. 8.37A, Bruker AXS Inc., Madison, WI, 2015. SAINT v. 8.37A, Bruker AXS Inc., Madison, WI, 2015.
5. SADABS Krause, L., Herbst-Irmer, R., Sheldrick, G. M. & Stalke, D. (2015). J. Appl. Cryst. 48.
6. SHELXTL Acta Cryst. (2015), A71, 3-8, Shelxl Acta Cryst. (2015), C71, 3-8.
7. SHELXLE, C. B. Hübschle, G. M. Sheldrick, B. Dittrich, J. *Appl. Crystallogr.* **2011**, *44*, 1281-1284.

ChemPubSoc Europe

DOI: 10.1002/chem.201905843

CHEMISTRY A European Journal Full Paper

Organic Semiconductors

Modulating the Electronic and Solid-State Structure of Organic Semiconductors by Site-Specific Substitution: The Case of Tetrafluoropentacenes

Thomas Geiger,[a] Simon Schundelmeier,[a] Thorsten Hummel,[b] Markus Ströbele,[b] Wolfgang Leis,[b] Michael Seitz,[b] Clemens Zeiser,[c] Luca Moretti,[d] Margherita Maiuri,[d] Giulio Cerullo,[d] Katharina Broch,[c] Jörn Vahland,[e] Karl Leo,[e] Cäcilia Maichle-Mössmer,[b] Bernd Speiser,[a] and Holger F. Bettinger*[a]

Abstract: The properties as well as solid-state structures, singlet fission, and organic field-effect transistor (OFET) performance of three tetrafluoropentacenes (1,4,8,11: **10**, 1,4,9,10: **11**, 2,3,9,10: **12**) are compared herein. The novel compounds **10** and **11** were synthesized in high purity from the corresponding 6,13-etheno-bridged precursors by reaction with dimethyl 1,2,4,5-tetrazine-3,6-dicarboxylate at elevated temperatures. Although most of the molecular properties of the compounds are similar, their chemical reactivity and crystal structures differ considerably. Isomer **10** undergoes the orbital symmetry forbidden thermal [4+4] dimerization, whereas **11** and **12** are much less reactive. The isomers **11** and **12** crystallize in a herringbone motif, but **10** prefers π–π stacking. Although the energy of the first electric dipole-allowed optical transition varies only within 370 cm^{-1} (0.05 eV) for the neutral compounds, this amounts to roughly 1600 cm^{-1} (0.20 eV) for radical cations and 1300 cm^{-1} (0.16 eV) for dications. Transient spectroscopy of films of **11** and **12** reveals singlet-fission time constants (91 ± 11, 73 ± 3 fs, respectively) that are shorter than for pentacene (112 ± 9 fs). OFET devices constructed from **11** and **12** show close to ideal thin-film transistor (TFT) characteristics with electron mobilities of 2×10^{-3} and 6×10^{-2} $cm^2V^{-1}s^{-1}$, respectively.

Introduction

The world we know today has been shaped by the use of electronic devices in our everyday life. The need for miniaturization and adaption to new form factors, allowing for novel and lightweight devices, for example, consumer electronics with foldable displays as seen in the newest smartphone developments or flexible solar cells, cannot be met by silicon-based electronic components because they inherently lack flexibility. For such applications, devices based on organic semiconductors are highly advantageous, given that these can be manufactured using flexible substrate materials.[1,2]

To meet demands, material scientists are highly interested in finding new materials which can be incorporated into such systems, allowing for even better device performances.[3] Acenes, the group of polycyclic aromatic hydrocarbons (PAHs) consisting of linear annulated benzene rings with semiconductor properties and an almost linear correlation between the inverse of the number of rings and the HOMO–LUMO gap,[4] are interesting materials for such applications.[3,5,6] The most commonly used substance from this class of compounds is pentacene because of its good availability and higher stability in comparison with the higher homologues of the series. It has been shown that pentacene is a p-type semiconductor[7,8] with

[a] T. Geiger, S. Schundelmeier, Prof. Dr. B. Speiser, Prof. Dr. H. F. Bettinger
Institut für Organische Chemie, Universität Tübingen
Auf der Morgenstelle 18, 72076 Tübingen (Germany)
E-mail: holger.bettinger@uni-tuebingen.de

[b] T. Hummel, Dr. M. Ströbele, Dr. W. Leis, Prof. Dr. M. Seitz, Dr. C. Maichle-Mössmer
Institut für Anorganische Chemie, Universität Tübingen
Auf der Morgenstelle 18, 72076 Tübingen (Germany)

[c] C. Zeiser, Jun.-Prof. Dr. K. Broch
Institut für Angewandte Physik, Universität Tübingen
Auf der Morgenstelle 10, 72076 Tübingen (Germany)

[d] L. Moretti, Dr. M. Maiuri, Prof. Dr. G. Cerullo
IFN-CNR, Dipartimento di Fisica, Politecnico di Milano
Piazza Leonardo da Vinci 32, 20133 Milano (Italy)

[e] J. Vahland, Prof. Dr. K. Leo
Dresden Integrated Center for Applied Physics and Photonic Materials
Technische Universität Dresden
Nöthnitzer Strasse 61, 01187 Dresden (Germany)

Supporting information and the ORCID identification number(s) for the author(s) of this article can be found under: https://doi.org/10.1002/chem.201905843.

a hole mobility of up to 35 $cm^2V^{-1}s^{-1}$ in a single crystal at room temperature.[9] For some applications, an n-type semiconductor is desirable, and it could be shown that it is possible to convert the conduction mode of pentacene by introduction of electron-withdrawing groups like fluorine atoms or nitrile groups to the pentacene scaffold.[7,10–13] A very prominent example for the power of fluorine substitution is perfluoropentacene (PFP), in which the full exchange of all hydrogen atoms by fluorine atoms results in a change of charge-transport mechanism from p-type to n-type.[10,14] Since its first synthesis, many properties of PFP have been investigated very extensively.

In contrast, the influence of only partial fluorine substitution at the pentacene scaffold has received less attention. Groundbreaking work on partially fluorinated 6,13-bis(triisopropylsilylethynyl)pentacenes (TIPS-pentacenes) was performed by Anthony et al.[11,15–17] The partially fluorinated derivatives (1,2,3,4-tetrafluoro and 1,2,3,4,8,9,10,11-octafluoro) showed higher hole mobilities than TIPS-pentacene under identical deposition conditions.[11] Bao et al., in contrast, identified partially fluorinated tetracenothiophenes as ambipolar semiconductors with high performance.[18,19] More recently, further experimental evidence that the charge-carrier mobility can be modified by site-specific fluorination and changing the number of fluorine atoms on the pentacene backbone was provided by Wasikiewicz et al.[20] They reported the synthesis of a subgroup of soluble mono- and difluorinated TIPS-pentacenes and found that the 2,10-difluoro isomer reached the highest μ_{Mean} (average mobility) of all compounds they investigated.

In addition to these experimental investigations, there are a number of computational studies on partially fluorinated pentacenes without solubilizing side groups, and some very interesting predictions were made.[21–25] Toyoda et al.[21] were able to show by in silico investigations that the efficiency of electron injection on a Cu(111) surface can be related to the number of fluorine atoms and their respective position in the pentacene backbone. Although pentacene showed the highest efficiency, PFP showed a significantly lower efficiency. This was explained by a larger PFP/Cu(111) distance due to repulsive interactions of the fluorine 2p orbitals with the substrate,[22] as observed by an X-ray standing-wave investigation (2.34 vs. 2.98 Å for PEN and PFP, respectively, on Cu(111)).[26] Toyoda et al.[21] suggested that it could be possible to fabricate interfaces optimal for charge-carrier injection by using pentacenes with a number of fluorine atoms n_F less than or equal to eight. A systematic computational DFT study of symmetrical substituted fluoropentacenes ($n_F = 2$–14) by Lukeš et al.[23] came to the conclusion that charge-carrier mobility is lowest in PFP, whereas 1,4,8,11-tetrafluoropentacene should show the highest mobility of up to 7.30 $cm^2V^{-1}s^{-1}$ depending on the dimer configuration used for the calculations. Even though this value looks very promising, the authors cautioned that the relatively high LUMO energy would not be favorable for an n-type semiconductor. Given that charge-carrier mobility is not only affected by the HOMO and LUMO levels, but also relies on efficient through-space coupling between next neighbors, modification of the crystal packaging by fluorine substitution is an important factor.[27] The influence of partial fluorination on the packing motifs of a total of fifteen fluorinated rubrene derivatives was impressively shown by Ogden et al.[28]

Although interesting properties for partially fluorinated pentacenes were predicted, this compound class is quite rare and limited to 2-fluoro-, 1,2,3,4-tetrafluoro-, and 2,3,9,10-tetrafluoropentacene. Chow's group synthesized the former two derivatives by thermal decarbonylation from the bridged ketone (Scheme 1 a).[29,30] The 2-fluoro derivative was characterized as a p-channel semiconductor,[30] whereas 1,2,3,4-tetrafluoropentacene exhibits ambipolar charge-transport behavior depending on the electrode material used.[29] The Bettinger group obtained 2,3,9,10-tetrafluoropentacene either by thermal removal of a 6,13-etheno bridge using a 1,2,4,5-tetrazine derivative,[31] or by Strating–Zwanenburg reaction,[32] the photoinduced bis-decarbonylation of the 6,13-bridged α-diketone (Scheme 1 b).[33] The photochemical conversions usually give higher yields,[34] but losses of substance due to the additional two steps for preparation of the α-diketones have to be taken into account when comparing both methods.

For 2,3,9,10-tetrafluoropentacene, no OFET data are available, but its interfacial properties on metal surfaces were studied extensively.[35–37] The compound shows pronounced nanorod morphology on Au(110) and charge transfer from the surface, indicating that the chemical modification has impact on the morphology and electronic properties at the molecular and thin-film levels.[35,36] An X-ray standing-wave investigation could quantify the substantial molecular distortion that 2,3,9,10-tetrafluoropentacene is undergoing upon interaction with a Cu(111) surface on an atomic level.[37]

In this work, we describe the synthesis of two new isomers of peripherally substituted tetrafluoropentacenes with a 1,4,8,11- (for which computational predictions were made by Lukeš et al.)[23] and 1,4,9,10-substitution pattern (Scheme 1 c) using the 1,2,4,5-tetrazine-induced elimination of the 6,13-etheno bridge. We compare the chemical, electrochemical, and photophysical properties, including singlet-fission dynamics, as well as crystal-structure data and OFET device performance in the series of tetrafluoropentacenes.

Results and Discussion

Synthesis

The precursors used for thermal generation of the fluorinated pentacenes were synthesized by reaction of 5,6,7,8-tetramethylidenebicyclo[2.2.2]oct-2-ene (**1**)[38,39] with 3,6-difluoroaryne that was generated from 3,6-difluoro-2-(trimethylsilyl)phenyltriflate (**2**) and CsF (Scheme 2). Single crystals of compound **1** suitable for X-ray crystallography were obtained by slow evaporation of the solvent from a solution in *n*-hexane (for detailed structural information, see the Supporting Information).

The aryne precursor **2** was prepared using a synthesis published by Tsuchido et al.[40] starting from 2-bromo-3,6-difluorophenol in 26% yield (Scheme 3). Given that this consecutive reaction without isolation of the intermediate **3** leads only to

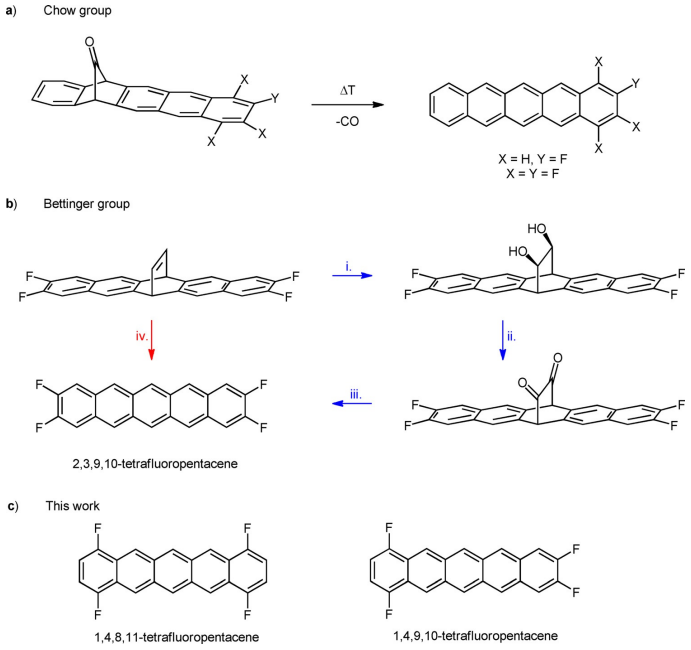

Scheme 1. Previously reported syntheses of partially fluorinated pentacenes by Chow et al. (**a**),[29,30] and Bettinger et al. (**b**; i. OsO_4 (cat.)/NMO, acetone/H_2O, ii. TEMPO/NaOCl, CH_2Cl_2, iii. *hν*, toluene, iv. *n*-pentylether, 180 °C, dimethyl 1,2,4,5-tetrazine-3,6-dicarboxylate, 1.5 min, then 0 °C),[31,33] and the novel tetrafluoropentacene derivatives synthesized and investigated here (**c**).

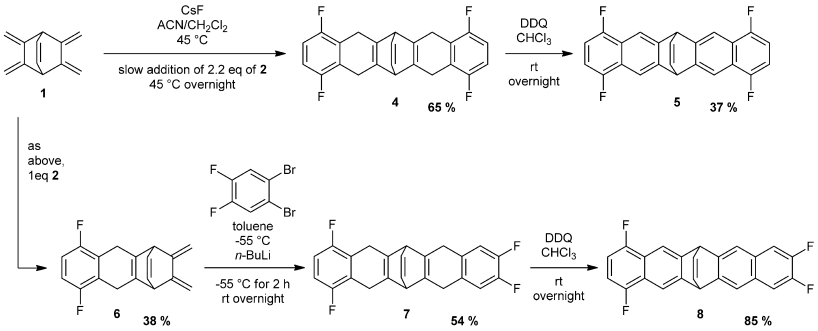

Scheme 2. Synthesis of the mono- (**6**) and bis-adducts (**4** and **7**) of compounds **1** and **2**. The monoadduct **6** is further reacted with 1,2-dibromo-4,5-difluorobenzene to give bis-adduct **7**. Subsequent oxidation with DDQ in $CHCl_3$ yields the corresponding ethenopentacenes **5** and **8**.

low yields of product with acceptable purity, we isolated compound **3** in 26% yield and applied a triflation strategy using Tf_2O and pyridine as the nucleophilic catalyst.[41,42] After reaction overnight, **2** was isolated in 85% yield. In comparison with the published synthesis[40] the two-step process gives an even lower yield (26% for the direct versus 22% through the two-step method), but the purity of the isolated product was increased significantly.

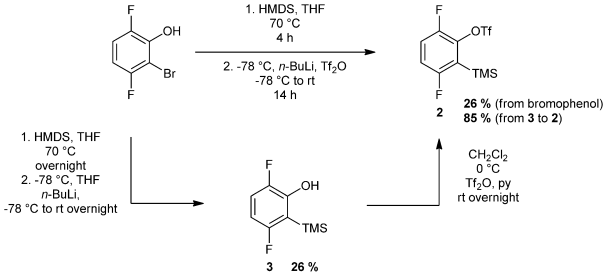

Scheme 3. Synthesis of *o*-TMS triflate (**2**) by one-pot reaction method[40] without isolation of *o*-TMS phenol (**3**) and the two step reaction with isolation of **3**.

Two equivalents of *o*-TMS triflate (**2**) were reacted with anhydrous CsF and **1** in a 1:1 (*v*/*v*) CH_3CN/CH_2Cl_2 mixture to give bis-adduct **4** (Scheme 2). This compound was subjected directly to 2,3-dichloro-5,6-dicyano-1,4-benzoquinone (DDQ) oxidation in $CHCl_3$ without further purification. Ethenopentacene **5** was isolated in 37% yield based on the amount of **1** used in the Diels–Alder reaction. For synthesis of the unsymmetrically substituted pentacene precursor, **1** was reacted with only 1 equiv of **2** under otherwise unchanged conditions giving monoadduct **6** in 38% yield. Using our published procedures[31,43] **6** was reacted with 1,2-dibromo-4,5-difluorobenzene giving adduct **7** in 54% yield. After DDQ oxidation, the ethenopentacene **8** was isolated in 85% yield. Single crystals of **5** and **8** suitable for X-ray crystallography were obtained by slow evaporation of a CH_2Cl_2 solution of the respective compounds.

The thermally induced Diels–Alder–retro-Diels–Alder sequence[31] was carried out between the tetrazine (**9**) prepared from ethyl diazoacetate over 5 steps,[44,45] and the respective ethenopentacenes (Scheme 4).

Compared with the previously published procedure,[31] we have introduced minor changes leading to increased yields and purities. Lowering the reaction temperature from 185 to 180 °C facilitated the addition of **9** to the reaction mixture because the only mildly boiling solvent does not hinder the addition of **9** significantly anymore. Additionally, the reactions were carried out multiple times (usually 5–8 times) consecutively in small batches and the reaction products were collected together in a fritted glass funnel under a stream of Ar. The reaction products were washed with degassed *n*-hexane, CH_2Cl_2, and ethyl acetate and dried under vacuum. The revised procedure increased the yield of 2,3,9,10-tetrafluoropentacene (**12**) to 36% compared with the original 12%.[31] 1,4,8,11- (**10**) and 1,4,9,10-tetrafluoropentacene (**11**) were prepared in 30 and 43% yield, accordingly. A computational investigation (M06-2X/6-31G* level of theory) of the reaction sequence (Scheme 4) reveals that the barriers do not strongly depend on the substitution pattern (see the Supporting Information for details). The solubility of **10** and **11** is high enough for measuring ^1H and ^{19}F NMR spectra in solution at room temperature. In contrast, no $^{13}C\{^1H\}$ NMR spectra could be obtained, even at 120 °C in $[D_2]$tetrachloroethane as done previously for NMR characterization of **12**. Although **12** is stable at this temperature for an extended period of time, and was indeed crystallized by slow cooling of a hot 1,2,4-trichlorobenzene solution,[33] isomer **10** underwent a reaction. After 3 h of heating to 120 °C, all pentacene ^1H NMR signals had completely disappeared (Figure 1) and a new set of three signals (integration ratio 8:8:4) had formed, indicative of a single reaction product with the same

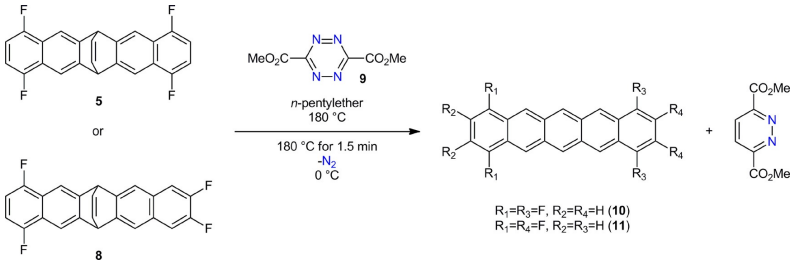

Scheme 4. Thermal synthesis of 1,4,8,11- (**10**) and 1,4,9,10-tetrafluoropentacene (**11**) from the reaction of ethenopentacenes **5** and **8** with dimethyl 1,2,4,5-tetrazine-3,6-dicarboxylate (**9**). Only the relevant reaction products are shown, the byproducts of the reaction have been discussed and characterized in previous publications.[31,33]

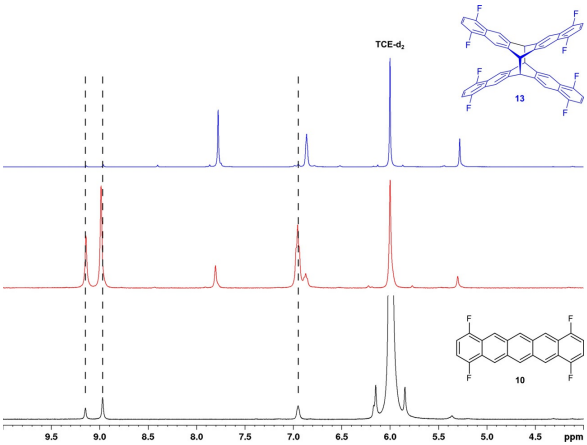

Figure 1. ^{1}H NMR (600 MHz, [D$_2$]tetrachloroethane) spectrum of **10** at rt (black), after 1 h at 120 °C (red, measured at 120 °C) and after 3 h at 120 °C (blue, measured at rt). The vertical dashed lines indicate the signals of **10**. Due to different temperatures at which the spectra were acquired and the fact that the spectra are scaled for better visual comparability the signal intensities are not directly quantitatively comparable.

symmetry. Correlation of chemical shifts with data for pentacene endoperoxide (PcEP),[46] an authentic sample of dianthracene prepared following our general method for preparation of substituted dianthracenes,[47] the thermal dimer of 1,2,3,4-tetrafluoropentacene,[29] and diheptacene[48] (see Supporting Information, Table S1) strongly indicates formation of the covalent dimer **13**.

Mass spectrometric investigation of **13** was precluded due to its instability under electron-impact (EI) conditions. Similar to the observations we have made investigating anthracene dimers,[47] only the mass of the monomer was detected, exhibiting the same fragmentation pattern as an authentic sample of the monomer. Given that the material is too insoluble, electrospray ionization (see the Supporting Information) could not be employed. For the same reason, no single crystals could be grown from solution for further structural elucidation, but a complete assignment of signals was possible using 2D NMR techniques (Figure 2).

Thermal dimerization reactions of pentacene derivatives bearing substituents on the terminal rings have been reported before.[29,49,50] Although orbital-symmetry forbidden according to the Woodward–Hoffmann rules, the thermal [4+4] cycloaddition reaction was rationalized by consideration of packing motifs in the crystal structure as well as by molecular dynamics calculations.[50] It was suggested that a π–π stacking arrangement in the crystal is able to facilitate the solid-state dimerization by pre-aligning the reaction partners.[50] A comparison of the crystal structures of **10**–**12** likewise shows different packing motifs (Figure 3). In comparison with **10**, compound **11** is thermally more stable, because heating for the same period of time at 120 °C shows a slower buildup of presumably dimer signals; the dimers of **11** were not isolated.

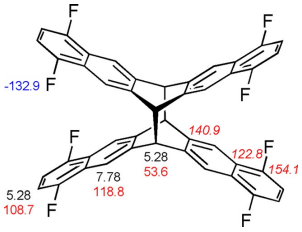

Figure 2. Full signal assignment based on 2D NMR for the thermal dimer **13** of 1,4,8,11-tetrafluoropentacene (**10**) generated by heating the monomer in [D$_2$]tetrachloroethane to 120 °C. ^{1}H (black), ^{13}C{^{1}H} (red), ^{19}F (blue). Shifts of quaternary carbon atoms are denoted in italics.

X-ray analysis

Due to the thermal dimerization, crystals of **10** and **11** were not grown from hot solutions as done for **12**, but by sublimation. The samples were fused into homemade two-chamber quartz ampoules (length = 14 cm, inner diameter = 0.7 cm, V = 6.2 cm^3) under vacuum. The ampoule was placed into a homemade tube furnace and heated to 80 °C with a heating and cooling rate of 2 °C min^{-1}. The powder was placed at one end of the ampoule exposed to 80 °C, whereas the other end was left at room temperature. After five days, single crystals of **10** and **11**, suitable for X-ray crystallography measurements were collected at the colder side of the ampoule (Table 1, for detailed crystallographic information see the Supporting Information). The carbon skeleton of **10** shows bond-length alternation between 1.33 and 1.44 Å (Figure 3a), the same range is also found in **11** (Figure 3d). The C–F bond lengths range be-

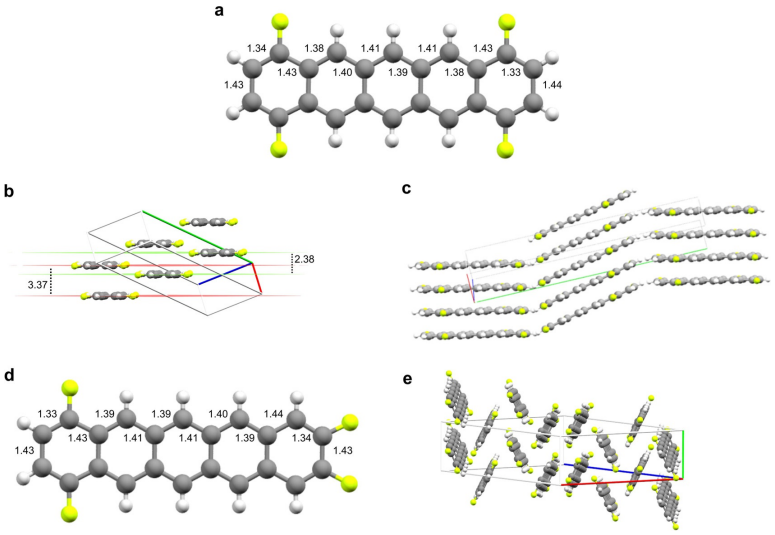

Figure 3. Molecular structure of **10** and **11** in the single crystal. Molecular structures with alternating C–C bond patterns (**a**/**d**), staircase motif found within the crystal of **10** (**b**) with intercolumn and interplanar distances, out of plane tilting (**c**) and the herringbone-like crystallization motif of **11** (**e**) are shown. Distances are given in Å.

tween 1.36 and 1.37 Å in **10**, whereas the C–F bond lengths in **11** are shorter (1.34–1.36 Å). These values are similar to the ones found in **12**[33] and PFP.[10] The closest intermolecular F–F contacts in the crystal packing of **10** have a distance of 3.34 Å. Although **12**,[33] pentacene, and PFP[10] crystallize in the typical herringbone pattern, **10** crystallizes in a staircase structure which is roughly oriented along the crystallographic *c* axis (Figure 3b). These molecular planes have an offset of 2.38 Å and the molecules in adjacent layers are shifted 6.4 Å sideways. This staircase motif is disrupted along the *b* axis by a 24.6° out-of-plane tilt of every second molecular column (Figure 3c). Inside individual molecular columns, the molecules have a vertical distance of 3.37 Å and show π–π stacking. In the crystal packing of **11**, which adopts the herringbone pattern, the closest intermolecular F–F contacts have a distance of 2.91 Å and are therefore significantly shorter than in the crystal packing of **10**. The interaction in this case involves the fluorine atoms in the 1,4-positions of a pentacene molecule and the fluorine atoms in the 9,10-positions of a neighboring pentacene molecule.

Absorption and photoluminescence spectroscopy in solution

The purple-colored solutions in degassed CH_2Cl_2 show the typical vibrational progression (1411 cm^{-1} for **10**; 1406 cm^{-1} for **11**) of the pentacene p-band (Figure 4). Absorption and emission spectra are roughly symmetrical with respect to the 0–0 transition. The excitation spectra contain every band present in the absorption spectra; hence the fluorescence spectra are independent of the excitation wavelength and show emission at 582/632 (**10**) and 579/624 nm (**11**). Overall, the position of the p-band experiences a bathochromic shift (0.02–0.03 eV) from **12** over **11** to **10**. The α bands follow the same trend, but the shift is smaller. The Stokes shift increases from 189 cm^{-1} in **12**[33] to 327 (**10**) and 334 cm^{-1} (**11**), respectively.

The triplet energies of **10**–**12** were measured at 77 K in CD_2Cl_2 and are similar for the three isomers (Table 1, Supporting Information Figures S35–37). Most importantly, the essential requirement for singlet fission, $E(S_1) \geq 2E(T_1)$, is fulfilled for each isomer.

Molecular electrochemistry

The electrochemical redox processes associated with **12** have already been described recently,[33] and are briefly summarized here. The radical cation and anion, as the one-electron oxidation and reduction products of **12**, are generated in a reversible or quasi-reversible electron transfer, respectively, at a Pt electrode in 1,2-dichlorobenzene. For scan rates *v* down to 0.1 Vs^{-1}, in cyclic voltammetry, follow-up reactions are absent (chemical reversibility) and the oxidation and reduction formal potentials of **12** are easily accessible. A second oxidation signal appears very close to the positive limit of the potential window and was not analyzed in detail.[33] The cyclic voltammograms of **10** and **11** (Figure 5), starting at the rest potential

Table 1. Overview over unit cell data, HOMO/LUMO levels (calculated at the B3LYP/6–311 + G** level of theory), formal oxidation and reduction potentials[a,b] from CV measurements and data for the S_1 and T_1 states obtained from optical spectroscopy in solution. Data for 1,2,3,4-tetrafluoropentacene is taken from Chien et al.,[29] for blank spaces no data is available.

	10	**11**	**12**	1,2,3,4-Tetrafluoropentacene[29]
Crystallography				
crystal system	monoclinic	monoclinic	triclinic	
space group	$P2_1$	$P2_1/n$	$P\bar{1}$	
unit cell dimensions	$a = 3.7815(2)$, $\alpha = 90^\circ$ $b = 27.642(2)$, $\beta = 93.428(5)^\circ$ $c = 6.9428(5)$ Å $\gamma = 90^\circ$	$a = 18.1971(11)$, $\alpha = 90^\circ$ $b = 5.9311(4)$, $\beta = 92.233(5)^\circ$ $c = 26.6590(16)$ Å $\gamma = 90^\circ$	$a = 6.7171(8)$, $\alpha = 100.606(4)^\circ$ $b = 7.6452(9)$, $\beta = 94.579(4)^\circ$ $c = 14.3038(18)$ Å $\gamma = 98.384(4)^\circ$	
Z	2	4	2	
Calculations				
LUMO [eV]	−3.21	−3.17	−3.13	−2.61[c]
HOMO [eV]	−5.39	−5.38	−5.36	−5.17[c]
LUMO–HOMO [eV]	2.18	2.21	2.23	2.56
Electrochemistry				
E^0_{ox} [V]	+0.539	+0.470	+0.402[d]	+0.46[e]
E^0_{red} [V]	−1.663	−1.739	−1.817[d]	−1.67[e]
ΔE^0 [V][f]	2.202	2.209	2.219	2.13
Optical spectroscopy				
S_1 state				
p band	462, 494, 531, 574	459, 490, 526, 568	455, 485, 520, 561	465, 497, 532, 574
α band [nm]	394, 426	400, 425	398, 422	
β band [nm]	328, 343	327, 344	325, 341	
S_1 lifetime [ns][g]	17.06 (98.6%), 65.76 (1.37%)	10.09 (98.5%), 55.49 (1.5%),	8.88 (57.3%), 16.4 (42.7%)	
T_1 state emission [nm][h]	1328	1336	1325	

[a] At Pt in 0.1 M nBu$_4$PF$_6$/1,2-dichlorobenzene as mid-point potential from oxidation and reduction peak potentials in cyclic voltammograms. [b] From chemically reversible cyclic voltammograms; maximum experimental range of scan rates: $0.02\,V\,s^{-1} \le v \le 5\,V\,s^{-1}$. [c] Calculated at the M06/6-31G* level of theory. [d] Values differ slightly from the previous measurement[33] and are based on additional data for conditions given in footnote [a]. [e] $^{ox}E_{1/2}$ and $^{red}E_{1/2}$ in 0.1 M nBu$_4$PF$_6$/CH$_2$Cl$_2$. [f] $\Delta E^0 = E^0_{ox} - E^0_{red}$. [g] Determined at 77 K in 2-Me-THF. Decay curves were fitted as biexponential decays, for more details see the Supporting Information. [h] T_1 lifetimes could not be determined at 77 K in CD_2Cl_2.

and spanning the positive and negative potential regions separately, show a similar general behavior. However, more quantitative analyses of the current potential curves indicate some subtle differences.

In the positive potential region (all potentials are reported versus an external ferrocene/ferrocenium standard), the re-reduction peak of tetrafluoropentacene **11** is considerably less intense as compared to the oxidation peak at smaller scan rates. This results in a peak current ratio I_p^{red}/I_p^{ox} (calculated according to Nicholson)[51] of less than unity. Only for the largest scan rate used ($v = 5\,V\,s^{-1}$), I_p^{red}/I_p^{ox} approaches unity, indicating that a follow-up reaction of the primary oxidation product occurs and is suppressed only at short time scales (large v).

The peak-potential separation ΔE_p at short time scales is around 70 mV, close to the so-called reversible value of 58 mV for a one-electron transfer reaction. We thus conclude that **11** is oxidized to a radical cation **11**$^{+\bullet}$. The observation that ΔE_p is slightly increasing with v for $1\,V\,s^{-1} \le v \le 5\,V\,s^{-1}$ indicates the beginning of quasi-reversibility (influence of electron-transfer kinetics). Nonetheless, the peak current is proportional to the square root of v, as expected for voltammograms of diffusing (rather than adsorbed) redox-active species. The formal potential E^0 for this oxidation step is calculated as the mid-point potential from the peak potentials in cyclic voltammograms at $v \ge 0.5\,V\,s^{-1}$ (Table 1). The reduction of **11** does not show any evidence of follow-up reactions. Instead, again, some degree of quasi-reversibility is indicated. The ΔE_p values ($\approx$80 mV) suggest formation of a radical anion **11**$^{-\bullet}$ through a one-electron reduction.

Most of these mechanistic features were also observed for compound **10**. The primary oxidation product undergoes a follow-up reaction that is somewhat slower than for **11**$^{+\bullet}$, as indicated by the peak–current ratio. The peak-potential difference is $\approx$70 mV with little increase for $v = 2\,V\,s^{-1}$ or higher (one-electron transfer to form **10**$^{+\bullet}$). The oxidation peak current increases proportionally to $v^{1/2}$, again showing the redox species to be diffusing rather than being adsorbed. In a similar way, the data are analyzed for the reduction process of **10**, and the analysis shows the chemically and electrochemically reversible formation of **10**$^{-\bullet}$ on the time scale of the experiments (E^0 data, see Table 1).

Apart from the determination of the E^0, for **10**, we support the assumption of a follow-up reaction of the radical cation by simulation of the cyclic voltammograms (Figure 6). We assume a first-order reaction of **10**$^{+\bullet}$ and use a single set of reaction parameters for the optimal fitting of voltammograms at different scan rates. Thus, a rate constant $k = 0.25\,s^{-1}$ for the follow-up reaction is estimated, corresponding to $t_{1/2} \approx 2.8$ s.

A further observation, which will not be discussed here in more detail, is the occurrence of a second, irreversible oxida-

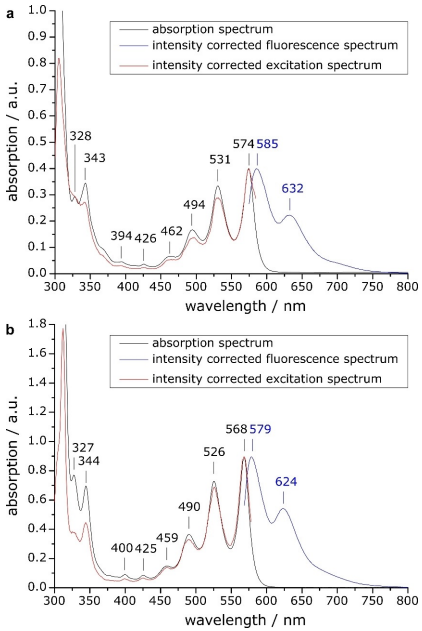

Figure 4. Absorption, fluorescence, and excitation spectra of **10** (**a**, $\lambda_{ex} = 574$ nm, excitation spectrum observed at $\lambda_{em} = 585$ nm) and **11** (**b**, $\lambda_{ex} = 568$ nm, excitation spectrum observed at $\lambda_{em} = 579$ nm) in CH_2Cl_2.

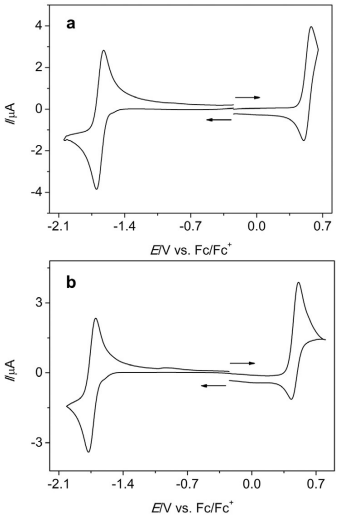

Figure 5. Cyclic voltammograms of **10** (**a**) and **11** (**b**) recorded in 0.1 M nBu$_4$PF$_6$/1,2-dichlorobenzene at a Pt disk electrode; **a.** $v = 0.2$ V s^{-1}, $c = 0.42$ mM, **b.** $v = 0.2$ V s^{-1}, $c = 0.38$ mM; the arrows indicate the initial scan directions.

tion peak for **10** above +0.9 V (Supporting Information, Figure S39). This is not present during the first potential cycle, but its intensity increases during subsequent voltammetric cycles. The signal disappears after polishing the electrode and reappears in the following potential cycles. Most likely, the first cycle on a freshly polished electrode leads to an irreversible modification of the Pt surface.

The formal redox potentials E^0 for oxidation and reduction of the tetrafluoropentacenes (Table 1) decrease to less positive or more negative values in the order **10**→**11**→**12**. The change of the substitution pattern results in an overall shift of approximately 140 mV. We refrain here from estimating orbital energies from the E^0 for reasons discussed in the Supporting Information. However, the difference of the formal potentials ΔE^0 is almost constant over the series with a change of only 17 mV for all compounds. Although these properties are not strictly comparable, the observation of similar values for the ΔE^0 of the compounds is in agreement with the behavior of the S_1 maxima obtained from the optical absorption spectra and the HOMO and LUMO energies and energy gaps computed at the B3LYP/6–311 + G** level of theory (Table 1).

The comparison with values for pentacene and 2,3,9,10-tetrafluoropentacene (**12**) shows a decrease in the energy gap from 2,3,9,10-tetrafluoropentacene (**12**) to **10** which is in agreement with the observed bathochromic shift of the p-bands. The decrease in energy gaps almost exclusively arises from the stabilization of the LUMO by up to 0.09 eV, whereas the HOMO energies throughout the series experience a stabilization of only 0.03 eV. The computed HOMO–LUMO energy gaps for **10** and pentacene differ by only 0.01 eV, the same difference is obtained when comparing the transitions of lowest energy (577 nm in pentacene versus 574 nm in **10**).

Acene radical cations

Radical cations of both pentacenes were generated by dissolving small samples in a 2 M solution of methanesulfonic acid (MSA) in nitrobenzene under ambient conditions.[33] The oxidation leads to bands in the NIR range (Figure 7). As observed previously for **12**$^{+\bullet}$,[33] the characteristic absorptions of **10**$^{+\bullet}$ and **11**$^{+\bullet}$ disappear within a few hours under buildup of new broad bands with two isosbestic points in each case (Supporting Information, Figures S40 and S41). A comparison of all three radical cation species shows that the energy strongly depends on the substitution pattern. Although **12**$^{+\bullet}$ absorbs at the shortest and **10**$^{+\bullet}$ at the longest wavelength, the difference between these transition energies amounts to 0.2 eV. For the band at 430 nm this effect is reversed, but is not as pronounced (Supporting Information, Table S3). Calculation of the excited-state energies at the UB3LYP/6–311 + G** level of theory agrees with the bathochromic shift in the series **12**$^{+\bullet}$ < **11**$^{+\bullet}$ < **10**$^{+\bullet}$, and deviates by 0.05 eV or less (Table S3).

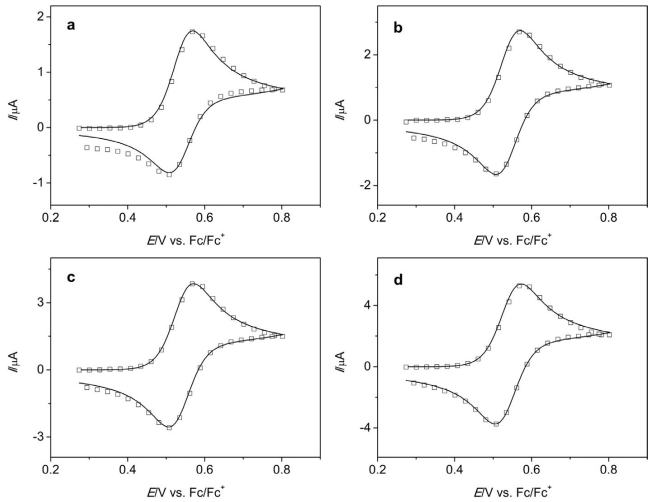

Figure 6. Experimental (symbols) and simulated (lines) cyclic voltammograms of **10** at Pt in 0.1 M nBu$_4$PF$_6$/1,2-dichlorobenzene; $c = 0.70$ mM, $v = 0.2$ (**a**), 0.5 (**b**) 1.0 (**c**), 2.0 V s^{-1} (**d**); parameters for simulation: temperature $T = 298$ K, electroactive area $A = 0.062$ cm^2, $E^0 = 0.539$ V, transfer coefficient $\alpha = 0.5$, electron-transfer rate constant $k_s = 0.05$ cm s^{-1}, diffusion coefficient $D = 1.5 \times 10^{-6}$ cm s^{-1}; to simulate an essentially irreversible chemical process, the equilibrium constant for the follow-up reaction was set to 10^{10}, with a rate constant $k = 0.25$ s^{-1}.

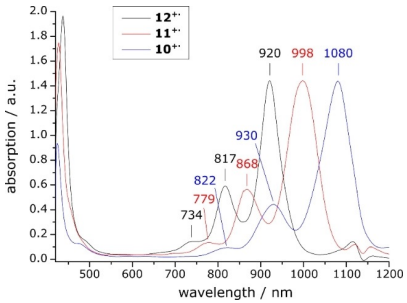

Figure 7. Comparison of the absorption spectra of the radical cations of **10**$^{+\cdot}$, **11**$^{+\cdot}$, and **12**$^{+\cdot}$ in 2 M MSA/nitrobenzene solution. The spectra of **10**$^{+\cdot}$ and **11**$^{+\cdot}$ are scaled in intensity for better comparability.

The radical cations in 2 M MSA/nitrobenzene were also investigated by EPR spectroscopy (Figure 8). Spectra simulation was performed starting from values obtained by computation of the hyperfine coupling constants using the UB3LYP functional and Barone's[52] EPR-III basis set. The simulation resulted in $a_{H_{6/13}} = 4.86$, $a_{H_{7/12/14}} = 3.16$, $a_{F_{1/4/8/11}} = 2.21$, and $a_{H_{2/3/9/10}} = 1.18$ G for **10**$^{+\cdot}$ (Table 2). Towards the periphery, the hyperfine couplings decrease, indicating that the electron is predominantly located at the central ring. The values found compare well with the ones already determined for **12**$^{+\cdot}$,[33] which shows that this symmetric substitution pattern does not influence the location of the electron. Simulation of the spectrum of **11**$^{+\cdot}$ resulted in $a_{H_{6/13}} = 4.34$, $a_{H_{7/12}} = 3.56$, $a_{H_{5/14}} = 2.65$, $a_{F_{1/14}} = 2.34$, $a_{H_{8/11}} = 1.49$, $a_{H_{2/3}} = 1.04$, and $a_{F_{9/10}} = 0.61$ G. In this case, the less symmetric fluorination pattern significantly influences the hyperfine coupling constants. Although the coupling constants decrease in both directions towards the periphery, the values for the 1,4-fluorinated naphthalene subsystem are slightly larger, showing that the electron is more strongly coupling to the protons and fluorine nuclei in this subunit. This is an indication that the electron is in closer spatial proximity to these coupling partners and therefore the probability density of the electron is shifted towards the 1,4-subsystem by the substitution. This is in agreement with the computed shapes of the HOMOs of **10**$^{+\cdot}$ and **11**$^{+\cdot}$ and also the spin densities (Supporting Information, Figures S45 and S46).

Acene dications

Solutions of the dications were prepared by dissolving samples of the corresponding pentacenes in oleum (20–30% free SO_3), yielding deeply colored solutions. These were used for acquisition of NMR spectra or, in diluted form, for the UV/Vis experiments. To prevent rapid H/D exchange, an external D_2SO_4 standard was used for the NMR experiments because spectra cannot be acquired in the deuterated solvent alone, as reported previously for **12**$^{2+}$.[33] The oxidation does not involve the evolution of H_2 or HD gas because no signals in the range expected for these species were found in the ^{1}H or ^{2}D spectra

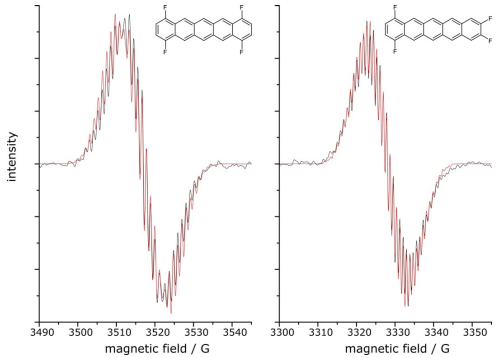

Figure 8. EPR spectra of $10^{+\cdot}$ (left) and $11^{+\cdot}$ (right) in 2 M MSA/nitrobenzene. Experimental spectrum in black, simulation in red.

changes in the proton spectra occur at positions attached to the fluorinated rings. Furthermore, starting from the carbon atoms of the innermost ring, every second carbon atoms experiences major deshielding in the dications. The carbon atoms adjacent to the fluorine atoms are additionally deshielded by the inductive effects of fluorine. We explain this chemical shift alternation by the predominant localization of the positive charges on these respective carbon atoms. Adjacent atoms are only deshielded to minor extent in this picture, which is indeed the case.

Transient-absorption spectroscopy of thin films of tetrafluoropentacenes

We also investigated the photophysics of thin films of **11** and **12** by transient-absorption (TA) spectroscopy given that partially fluorinated TIPS-pentacenes

Table 2. Comparison of the values for hyperfine coupling constants (in *G*) derived from EPR simulation and the values calculated at the UB3LYP/EPR-III level of theory.

	$10^{+\cdot}$			$11^{+\cdot}$	
	sim.	calcd		sim.	calcd
$H_{6/13}$	4.86	4.53	$H_{6/13}$	4.34	4.82
$H_{5/7/12/14}$	3.16	3.45	$H_{7/12}$	3.56[b]	3.59
$F_{1/4/8/11}$	2.21[a]	3.09	$H_{5/14}$	2.65[b]	3.64
$H_{2/3/9/10}$	1.18	1.07	$F_{1/4}$	2.34[a]	3.20
			$H_{8/11}$	1.49	1.31
			$H_{2/3}$	1.04	1.13
			$F_{9/10}$	0.61[a]	1.04

[a] Significant deviations for sim. and calcd hyperfine coupling constants for fluorine have been reported for other fluorinated acenes.[53] [b] Interchanging these values does not change the correlation (R^2) between simulation and experimental spectrum in a significant way.

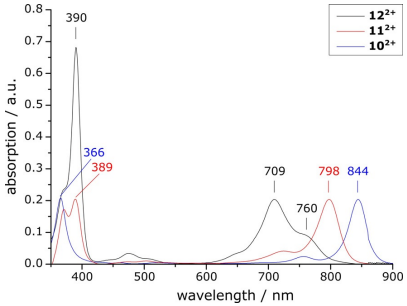

Figure 9. Comparison of the absorption spectra of 10^{2+}, 11^{2+}, and 12^{2+} in oleum. The spectra of 10^{2+} and 11^{2+} are scaled for better comparability. A distinct bathochromic shift of the absorption bands above 700 nm is visible.

when the reaction was performed in a sealed J-Young NMR tube.

The form of the absorption bands (Figure 9) of the newly prepared dications resemble the spectrum of the pentacene dication[33] rather than 12^{2+} which shows an inverted intensity profile of the bands above 700 nm. The reason for this behavior is unknown and 12^{2+} is the only compound in the sequence with an absorption spectrum that does not follow this general rule. The transitions of lowest energy were calculated at the B3LYP/6–311 + G** level of theory (Supporting Information, Table S3) and compare well with the experimentally obtained values, overestimating the energies by up to 0.25 eV.

Using 2D NMR techniques and spectra correlation, full signal assignment is possible for both dications (Figure 10). The ^{1}H, ^{19}F and $^{13}C\{^{1}H\}$ NMR spectra of 11^{2+} can be interpreted as an almost exact superposition of the spectra of 10^{2+} and 12^{2+}. This is also the case for all precursors and the neutral tetrafluoropentacenes themselves. Comparison with the chemical shifts of the neutral molecules shows that the greatest were shown to be relevant for singlet fission (SF).[54,55] This photophysical process converts an excited singlet state into two triplet states on neighboring molecules[56] and has received increasing attention due to its potential to boost solar cell efficiencies above the Shockley–Queisser limit.[57] It proceeds via a triplet pair state ^{1}(TT) in which the two molecules involved are already in their triplet state, but the overall character of the state is still a singlet.[58] Most importantly, the triplets are electronically coupled and spin-entangled.[59] A promising approach to optimize SF efficiencies for applications is chemical modification, which in turn often affects molecular arrangement.[60,61] Due to the coupled triplet-pair state, formation of which is a crucial step in the SF process, SF is highly sensitive to changes in molecular packing[60–66] and small modifications in the orbital overlap can be used to tune SF.[62]

Given that the molecular arrangement in thin films often differs from the single-crystal phase, we measured the structure of 80 nm thick films using X-ray reflectivity (Figure 11). Penta-

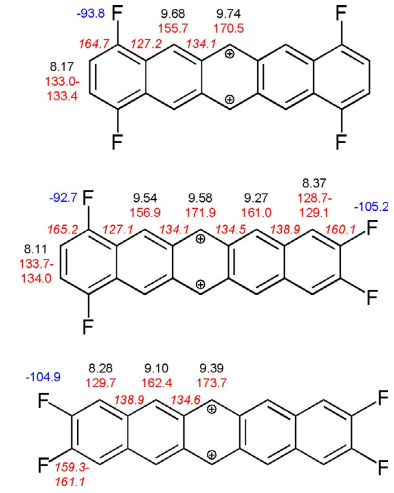

Figure 10. Signal assignment for $\mathbf{10}^{2+}$ (top), $\mathbf{11}^{2+}$ (middle), and $\mathbf{12}^{2+}$ (bottom)[33] measured in oleum with external D_2SO_4 standard. ^1H shifts (black), $^{13}C\{^1H\}$ shifts (red), ^{19}F shifts (blue). Chemical shifts in ppm, values for quaternary carbon atoms in italics. Assignment of the ^{19}F signals for $\mathbf{11}^{2+}$ is based on correlation with the spectra of the other two isomers.

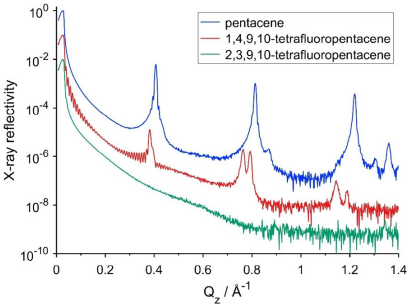

Figure 11. X-ray reflectivity scans of the thin films of pentacene, 1,4,9,10-tetrafluoropentacene (**11**) and 2,3,9,10-tetrafluoropentacene (**12**).

cene shows intense Bragg reflections as expected, because it grows in polycrystalline fashion on SiO_2.[67] The Bragg peak position indicates an out of plane lattice spacing of $d = 15.40$ Å, corresponding to the thin-film phase of pentacene.[67] As expected for film thickness above 40 nm, Bragg peaks of the bulk phase[68] ($d = 14.46$ Å) are observed at $q_z = 0.87$ and $q_z = 1.30$ Å^{-1}. The Bragg peak at $q_z = 1.36$ Å^{-1} is assigned to a small fraction of flat-lying molecules.

For the thin film of 1,4,9,10-tetrafluoropentacene (**11**) we observe pronounced Kiessig fringes, indicating a low roughness of the film, and two series of Bragg peaks, indicating the presence of two polymorphs with out-of-plane lattice spacings of $d = 16.46$ and $d = 15.85$ Å, respectively, in the film. We assign these polymorphs to a thin film ($d = 16.46$ Å) and a bulk phase ($d = 15.85$ Å) as observed for pentacene. Interestingly, 2,3,9,10-tetrafluoropentacene (**12**) does not exhibit Bragg peaks in the thin film, indicating an amorphous growth. The weak peak at $q_z = 1.35$ Å^{-1} might arise from a small fraction of crystalline domains within the film, where the molecules are flat lying.

The TA spectroscopy experiments were performed exciting the films (for the absorption spectra of the thin films see the Supporting Information, Figure S38) with 70 fs pulses at 620 nm and probing with a white light continuum covering the 430–780 nm wavelength range. The TA spectra of pentacene (Figure 12a) agree with previous reports.[69] The TA-spectra of **11** and **12** (Figure 12b/c) show features similar to pentacene, in particular regarding the photoinduced absorption (PA) bands below a probe wavelength of 500 nm and above a probe wavelength of 720 nm. The decay of the PA band <500 nm and the rise of the PA band >720 nm occur in parallel with time constants shorter than 200 fs, similar to pentacene. For compound **12** we reproducibly observe an additional spectral feature at 540 nm, which starts to build up after 200 fs.

A global analysis[70] of these measurements (Figure 13) reveals that there are three spectroscopically distinguishable species in **12**, whereas the TA-data for pentacene and **11** can be analyzed using only two species. Correspondingly, the data can be fitted with a 2-step (3-step) kinetic model, respectively, involving transitions between two species in pentacene and **11** and three species in **12**. The time constant of the transition from species 1 to 2 is 112 ± 9 (pentacene), 91 ± 11 (**11**) and 73 ± 3 fs (**12**). The population of the second species in pentacene and **11** remains constant on the 1 ns experimental observation window, whereas the second species in **12** decays to a third species with an intermediate time constant of 870 ± 140 fs.

The first and second species in pentacene have been assigned to singlets and triplets, respectively[69,71,72] and, therefore, the time constant of the transition from species 1 to 2 in pentacene corresponds to the singlet-fission time constant. For **11**, both, the PA signal at wavelengths below 500 nm and the PA signal at wavelengths above 720 nm have a spectral shape similar to the signals in pentacene, allowing us to assign them to the spectral features of singlets and triplets, respectively, and the conversion time to the SF time constant. In **12**, the first species can again be assigned to singlets. The spectroscopic signatures of the second and third species are very similar and both do not show pronounced intensity at short wavelengths below 500 nm, but a negative feature at wavelengths above 720 nm, which we assign to the characteristic triplet PA, similar to pentacene. Thus, the second and third species of **12** seem to be related to triplets. It is interesting that these two triplet signatures evolve into each other and do not arise independently in the TA data. Thus, it is unlikely that they are caused by exciton migration to low-lying sites within the film, but they have to have the same origin. We believe that the details of the SF process could provide a possible explanation for

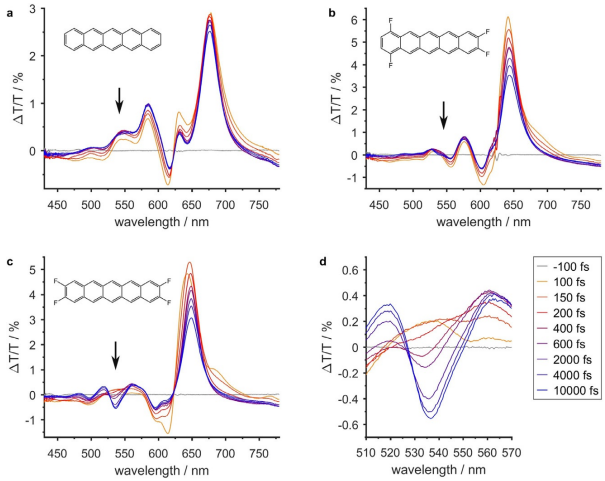

Figure 12. Transient absorption spectroscopy data of the three compounds pentacene (a), 1,4,9,10-tetrafluoropentacene (**11**, b) and 2,3,9,10-tetrafluoropentacene (**12**, c). d) Zoom into the wavelength region showing the ^{1}(TT)-signature of c.

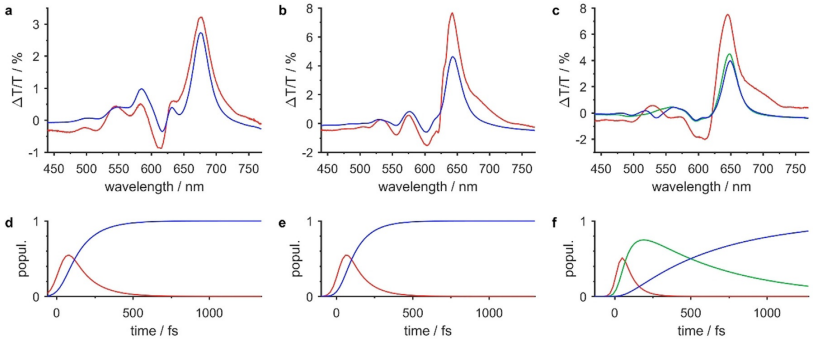

Figure 13. Global analysis of the TA spectroscopy data shown in Figure 12. a)–c) Resulting evolution associated spectra (EAS), d)–f) corresponding singlet and triplet population.

the presence of a third species. During a SF process two neighboring, spin-entangled triplet excitons are formed, which can be electronically coupled resulting in a multiexciton state ^{1}(TT).[58,59] This electronic coupling can be overcome by spatial separation of the triplets into T_1+T_1 via a spin-entangled, but electronically decoupled state ^{1}(T…T), as suggested recently.[58] Thus, the difference between the two triplet species observed in the TA data of **12** might be the electronic coupling. In this case, species 2 can be assigned to ^{1}(TT) and species 3 to ^{1}(T…T) or T_1+ T_1, given that these latter two cannot be distinguished in TA. The fact that ^{1}(TT) is observed as comparably long-lived species in **12** might be due to the lower long-range order in the thin film compared with **11**, reducing the delocalization of the ^{1}(TT) and increasing the dephasing time. Importantly, in both compounds **11** and **12**, SF proceeds faster than in pentacene and, surprisingly also in PFP.[63,73] This cannot be explained by energetics, because SF in **11** and **12** is less exothermic than in pentacene and, therefore, might be related to differences in the relative molecular arrangement.

Organic field-effect transistors

To evaluate the charge-carrier transport in the pentacene derivatives, OFETs were fabricated on a highly doped Si-wafer,

which simultaneously serves as a global gate electrode. The wafer was coated with 100 nm of SiO_2 and 40 nm of Cytop 809-M which both serve as gate insulator. The latter provides an almost ideal interface with a very low density of undesired interface states acting as trap states for charge carriers in the transistor channel. The organic semiconductor was evaporated on the prepared substrate with a nominal thickness of 30 nm. Source and drain electrodes were formed by evaporating Al through a shadow mask (contact thickness is 30 nm) yielding devices with channel widths of 1000 μm and channel lengths ranging from 50 to 200 μm. Aluminum has been chosen due to its low surface work function which is preferred for the injection of electrons into the semiconductor.

Electrical characteristics were obtained by Keithley SMUs 2400 and 2600A under nitrogen atmosphere. Devices are biased to form an electron channel, the obtained electron mobilities in the saturation regime are in the range of 2×10^{-3} $cm^2V^{-1}s^{-1}$ for 1,4,9,10-tetrafluoropentacene (**11**) and about 6×10^{-2} $cm^2V^{-1}s^{-1}$ for 2,3,9,10-tetrafluoropentacene (**12**) (Figure 14). For the 1,4,8,11 derivative (**10**) no lateral conductivity was observable. This is most likely due to strong island growth, which prohibits formation of a closed film at the channel interface. The devices show close to ideal TFT characteristics with only a slight hint of contact resistance which can be seen in the output characteristics (Figures S42/S43 in the Supporting Information). This effect however is already negligible at source-drain voltages over 1 V. From there on the channel governs the device characteristics.

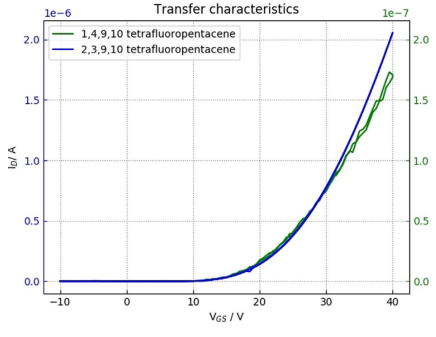

Figure 14. Transfer characteristics for 1,4,9,10-tetrafluoropentacene (**11**) and 2,3,9,10-tetrafluoropentacene (**12**). The depicted devices have a channel width of 1000 μm and channel lengths of 50 μm (2,3,9,10 tetrafluoropentacene) and 150 μm (1,4,9,10 tetrafluoropentacene), respectively. The drain-source bias is 20 V for each device. Note the difference of one order of magnitude in current between the two compounds.

Conclusions

We have performed a comprehensive comparative investigation of three tetrafluoropentacene isomers with two fluorine atoms on the terminal rings so that the dipole moment is either exactly zero or very small. We draw the following conclusions from our study:

1. The 1,2,4,5-tetrazine-induced elimination of the 6,13-etheno bridge is a good strategy for synthesis of partially fluorinated pentacenes that proceeds in good yields after minor modifications compared to our previous protocol[31] and allows easy isolation of the compounds in high purity.

2. Given that the fluorine atoms are on the two terminal rings, which have the smallest orbital coefficients in both HOMO and LUMO, it may be expected that the electronic properties are similar irrespective of the substitution patterns. We corroborated this expectation by investigation of the molecular properties using absorption and photoluminescence spectroscopy (S_0–S_1 and S_0–T_1 energy gaps), cyclic voltammetry (difference of formal potentials ΔE^0), and density functional theory (HOMO–LUMO energy gap) that all concur that the gaps are quite similar. The minor changes that are observed are due to the change of the LUMO energy, whereas the HOMO energy is hardly affected by the substitution pattern.

3. In contrast to the case of the neutral compounds, the optical gaps vary over a much larger energy range for the positively charged species, in particular for the radical cations. The EPR spectra indicate that the unpaired electron is mostly located at the central ring, and it appears that the distance of the fluorine atoms to the central ring has a significant impact on the energy of the excited state. The 1,4,8,11-isomer has the lowest energy absorption (at 1080 nm) whereas it is highest for the 2,3,9,10-isomer (920 nm). A similar trend is observed for the dications.

4. Although the molecular electronic properties of the neutral compounds are quite similar, their solid-state structures differ significantly. The 2,3,9,10- and 1,4,9,10-isomers share the herringbone packing motif with parent pentacene and perfluoropentacene, but with all four fluorine atoms at the *peri* positions (1,4,8,11-isomer, **10**) a π–π stacking motif is obtained instead. It is likely that the change in packing is due to unfavorable fluorine–π-interactions. Based on the characterization of Disiraju and Gavezzotti[74] the packing of **10** is that of the β motif due to the short axis of $a = 3.78$ Å.

5. The three isomers differ also in their chemical reactivity, because **10** readily undergoes a Woodward–Hoffmann forbidden [4+4] dimerization during NMR measurements at elevated temperatures. This is not the case for **12**, whereas **11** seems to be intermediate in reactivity so that its dimer could not be isolated. This increased reactivity does not appear to be due to decreased thermodynamic stability of **10**, because this is the most stable isomer among the series based on DFT computations (**11** and **12** are higher by 3 and 6 kcal mol^{-1}, respectively). It could however be associated with the high tendency of **10** to form noncovalent stacked dimers in the solid state that are also the immediate precursors to the transition state of thermal [4+4] dimerization according to computations reported for pentacene.[75] We feel that this difference in reactivity requires further detailed experimental and computational analysis that we plan to perform in due course.

6. Differences in crystal-structure packing may have an immediate impact on the properties of molecular films that are

of technological relevance. For example, pronounced island formation of **10** precludes its application in OFET devices, and hence the large charge-carrier mobility predicted based on computations[23] could not be experimentally confirmed. In contrast, isomers **11** and more so **12** show reasonably good n-channel semiconducting properties with charge carrier mobility up to 6×10^{-2} $cm^2V^{-1}s^{-1}$. Note that the crystal structure of **12** is most similar to that of parent pentacene.[33]

7. The two compounds crystallizing in the herringbone motif (**11**, **12**) still behave differently because films of **12** are amorphous. Nonetheless, both compounds undergo singlet fission, on a slightly shorter timescale as compared to pentacene. For **12** an additional species is observed in the TA-data, possibly a spin entangled, electronic decoupled state ^{1}(T…T).

We therefore believe that the variation of the fluorination degree and fluorination pattern of pentacene may provide a useful model for gaining detailed insight into forces that control crystallization and for studying the structure–property relationships of these organic semiconductors.

Acknowledgements

The authors are grateful to Dr. Christian Göb, Dr. Christian J. Schürmann, and Dr. Jakub Wojciechowski from Rigaku Europe SE for performing the single-crystal X-ray analysis of compounds **10** and **11**, and to Dominik Brzecki as well as Dr. Norbert Grzegorzek for help with the EPR measurements of compounds $\mathbf{10}^{+\bullet}$ and $\mathbf{11}^{+\bullet}$. The authors acknowledge support by the state of Baden-Württemberg through bwHPC and the German Research Foundation (DFG) through grant no INST 40/467-1 FUGG (JUSTUS cluster). This work was also funded in part by the DFG and the Fonds der Chemischen Industrie.

Conflict of interest

The authors declare no conflict of interest.

Keywords: acenes · organic field-effect transistors · organic semiconductors · singlet fission · synthesis

[1] H. T. Yi, M. M. Payne, J. E. Anthony, V. Podzorov, *Nat. Commun.* **2012**, *3*, 1259.
[2] M. Yi, J. Guo, W. Li, L. Xie, Q. Fan, W. Huang, *RSC Adv.* **2015**, *5*, 95273.
[3] C.-a. Di, F. Zhang, D. Zhu, *Adv. Mater.* **2013**, *25*, 313.
[4] K. N. Houk, P. S. Lee, M. Nendel, *J. Org. Chem.* **2001**, *66*, 5517.
[5] J. E. Anthony, *Chem. Rev.* **2006**, *106*, 5028.
[6] J. E. Anthony, *Angew. Chem. Int. Ed.* **2008**, *47*, 452; *Angew. Chem.* **2008**, *120*, 460.
[7] Y. Yamashita, *Sci. Technol. Adv. Mater.* **2009**, *10*, 024313.
[8] B. K. Kaushik, B. Kumar, S. Prajapati, P. Mittal, *Organic Thin-Film Transistor Applications: Materials to Circuits*, CRC, **2016**.
[9] O. D. Jurchescu, J. Baas, T. T. M. Palstra, *Appl. Phys. Lett.* **2004**, *84*, 3061.
[10] Y. Sakamoto, T. Suzuki, M. Kobayashi, Y. Gao, Y. Fukai, Y. Inoue, F. Sato, S. Tokito, *J. Am. Chem. Soc.* **2004**, *126*, 8138.
[11] C. R. Swartz, S. R. Parkin, J. E. Bullock, J. E. Anthony, A. C. Mayer, G. G. Malliaras, *Org. Lett.* **2005**, *7*, 3163.
[12] J. T. E. Quinn, J. Zhu, X. Li, J. Wang, Y. Li, *J. Mater. Chem. C* **2017**, *5*, 8654.
[13] A. Naibi Lakshminarayana, A. Ong, C. Chi, *J. Mater. Chem. C* **2018**, *6*, 3551.
[14] Y. Inoue, Y. Sakamoto, T. Suzuki, M. Kobayashi, Y. Gao, S. Tokito, *Jpn. J. Appl. Phys.* **2005**, *44*, 3663.
[15] O. D. Jurchescu, M. Feric, B. Hamadani, D. Mourey, S. Subramanian, B. Purushothaman, J. Anthony, T. Jackson, D. Gundlach, *ECS Trans.* **2008**, *16*, 283.
[16] J. B. Sherman, B. Purushothaman, S. R. Parkin, C. Kim, S. Collins, J. Anthony, T.-Q. Nguyen, M. L. Chabinyc, *J. Mater. Chem. A* **2015**, *3*, 9989.
[17] C.-H. Kim, H. Hlaing, M. M. Payne, S. R. Parkin, J. E. Anthony, I. Kymissis, *ChemPhysChem* **2015**, *16*, 1251.
[18] M. L. Tang, A. D. Reichardt, N. Miyaki, R. M. Stoltenberg, Z. Bao, *J. Am. Chem. Soc.* **2008**, *130*, 6064.
[19] M. L. Tang, A. D. Reichardt, P. Wei, Z. Bao, *J. Am. Chem. Soc.* **2009**, *131*, 5264.
[20] J. M. Wasikiewicz, L. Abu-Sen, A. B. Horn, J. M. Koelewijn, A. V. S. Parry, J. J. Morrison, S. G. Yeates, *J. Mater. Chem. C* **2016**, *4*, 7309.
[21] K. Toyoda, I. Hamada, S. Yanagisawa, Y. Morikawa, *Org. Electron.* **2011**, *12*, 295.
[22] K. Toyoda, I. Hamada, K. Lee, S. Yanagisawa, Y. Morikawa, *J. Phys. Chem. C* **2011**, *115*, 5767.
[23] V. Lukeš, D. Cagardová, M. Michalík, P. Poliak, *Synth. Met.* **2018**, *240*, 67.
[24] H.-Y. Chen, I. Chao, *ChemPhysChem* **2006**, *7*, 2003.
[25] B. Milián Medina, J. E. Anthony, J. Gierschner, *ChemPhysChem* **2008**, *9*, 1519.
[26] N. Koch, A. Gerlach, S. Duhm, H. Glowatzki, G. Heimel, A. Vollmer, Y. Sakamoto, T. Suzuki, J. Zegenhagen, J. P. Rabe, F. Schreiber, *J. Am. Chem. Soc.* **2008**, *130*, 7300.
[27] K. Reichenbächer, H. I. Süss, J. Hulliger, *Chem. Soc. Rev.* **2005**, *34*, 22.
[28] W. A. Ogden, S. Ghosh, M. J. Bruzek, K. A. McGarry, L. Balhorn, V. Young, L. J. Purvis, S. E. Wegwerth, Z. Zhang, N. A. Serratore, C. J. Cramer, L. Gagliardi, C. J. Douglas, *Cryst. Growth Des.* **2017**, *17*, 643.
[29] C.-T. Chien, T.-C. Chiang, M. Watanabe, T.-H. Chao, Y. J. Chang, Y.-D. Lin, H.-K. Lee, C.-Y. Liu, C.-H. Tu, C.-H. Sun, T. J. Chow, *Tetrahedron Lett.* **2013**, *54*, 903.
[30] C.-T. Chien, M. Watanabe, T. J. Chow, *Tetrahedron* **2015**, *71*, 1668.
[31] R. P. Bula, I. M. Oppel, H. F. Bettinger, *J. Org. Chem.* **2012**, *77*, 3538.
[32] J. Strating, B. Zwanenburg, A. Wagenaar, A. C. Udding, *Tetrahedron Lett.* **1969**, *10*, 125.
[33] B. Shen, T. Geiger, R. Einholz, F. Reicherter, S. Schundelmeier, C. Maichle-Mössmer, B. Speiser, H. F. Bettinger, *J. Org. Chem.* **2018**, *83*, 3149.
[34] M. Suzuki, T. Aotake, Y. Yamaguchi, N. Noguchi, H. Nakano, K.-i. Nakayama, H. Yamada, *J. Photochem. Photobiol. C* **2014**, *18*, 50.
[35] S.-A. Savu, G. Biddau, L. Pardini, R. Bula, H. F. Bettinger, C. Draxl, T. Chassé, M. B. Casu, *J. Phys. Chem. C* **2015**, *119*, 12538.
[36] S.-A. Savu, A. Sonström, R. Bula, H. F. Bettinger, T. Chassé, M. B. Casu, *ACS Appl. Mater. Interfaces* **2015**, *7*, 19774.
[37] A. Franco-Cañellas, Q. Wang, K. Broch, B. Shen, A. Gerlach, H. F. Bettinger, S. Duhm, F. Schreiber, *Phys. Rev. Materials* **2018**, *2*, 044002.
[38] R. Gabioud, P. Vogel, *Tetrahedron* **1980**, *36*, 149.
[39] R. Gabioud, P. Vogel, *Helv. Chim. Acta* **1983**, *66*, 1134.
[40] Y. Tsuchido, T. Ide, Y. Suzaki, K. Osakada, *Bull. Chem. Soc. Jpn.* **2015**, *88*, 821.
[41] H. Yoshio, S. Takaaki, K. Hiroshi, *Chem. Lett.* **1983**, *12*, 1211.
[42] J. M. Medina, J. L. Mackey, N. K. Garg, K. N. Houk, *J. Am. Chem. Soc.* **2014**, *136*, 15798.
[43] C. Tönshoff, H. F. Bettinger, *Chem. Eur. J.* **2012**, *18*, 1789.
[44] D. L. Boger, R. S. Coleman, J. S. Panek, F. X. Huber, J. Sauer, *J. Org. Chem.* **1985**, *50*, 5377.
[45] D. L. Boger, J. S. Panek, M. Patel, *Org. Synth.* **1992**, 79.
[46] D. Sparfel, F. Gobert, J. Rigaudy, *Tetrahedron* **1980**, *36*, 2225.
[47] T. Geiger, A. Haupt, C. Maichle-Mössmer, C. Schrenk, A. Schnepf, H. F. Bettinger, *J. Org. Chem.* **2019**, *84*, 10120.
[48] R. Einholz, T. Fang, R. Berger, P. Grüninger, A. Früh, T. Chassé, R. F. Fink, H. F. Bettinger, *J. Am. Chem. Soc.* **2017**, *139*, 4435.
[49] S. Li, Z. Li, K. Nakajima, K.-i. Kanno, T. Takahashi, *Chem. Asian J.* **2009**, *4*, 294.
[50] B. Pal, B.-C. Lin, M. V. C. dela Cerna, C.-P. Hsu, C.-H. Lin, *J. Org. Chem.* **2016**, *81*, 6223.
[51] R. S. Nicholson, *Anal. Chem.* **1966**, *38*, 1406.
[52] V. Barone, in *Recent Advances in Density Functional Methods* (Ed.: D. P. Chong), World Scientific, **1995**, pp. 287.
[53] A. R. Rakitin, D. Yff, C. Trapp, *J. Phys. Chem. A* **2003**, *107*, 6281.

[54] R. D. Pensack, A. J. Tilley, S. R. Parkin, T. S. Lee, M. M. Payne, D. Gao, A. A. Jahnke, D. G. Oblinsky, P.-F. Li, J. E. Anthony, D. S. Seferos, G. D. Scholes, *J. Am. Chem. Soc.* **2015**, *137*, 6790.
[55] R. D. Pensack, E. E. Ostroumov, A. J. Tilley, S. Mazza, C. Grieco, K. J. Thorley, J. B. Asbury, D. S. Seferos, J. E. Anthony, G. D. Scholes, *J. Phys. Chem. Lett.* **2016**, *7*, 2370.
[56] M. B. Smith, J. Michl, *Chem. Rev.* **2010**, *110*, 6891.
[57] M. K. Gish, N. A. Pace, G. Rumbles, J. C. Johnson, *J. Phys. Chem. C* **2019**, *123*, 3923.
[58] K. Miyata, F. S. Conrad-Burton, F. L. Geyer, X. Y. Zhu, *Chem. Rev.* **2019**, *119*, 4261.
[59] H. Kim, P. M. Zimmerman, *Phys. Chem. Chem. Phys.* **2018**, *20*, 30083.
[60] N. Alagna, J. Han, N. Wollscheid, J. L. Perez Lustres, J. Herz, S. Hahn, S. Koser, F. Paulus, U. H. F. Bunz, A. Dreuw, T. Buckup, M. Motzkus, *J. Am. Chem. Soc.* **2019**, *141*, 8834.
[61] L. Shen, X. Wang, H. Liu, X. Li, *Phys. Chem. Chem. Phys.* **2018**, *20*, 5795.
[62] I. Papadopoulos, J. Zirzlmeier, C. Hetzer, Y. J. Bae, M. D. Krzyaniak, M. R. Wasielewski, T. Clark, R. R. Tykwinski, D. M. Guldi, *J. Am. Chem. Soc.* **2019**, *141*, 6191.
[63] K. Kolata, T. Breuer, G. Witte, S. Chatterjee, *ACS Nano* **2014**, *8*, 7377.
[64] M. J. Y. Tayebjee, K. N. Schwarz, R. W. MacQueen, M. Dvořák, A. W. C. Lam, K. P. Ghiggino, D. R. McCamey, T. W. Schmidt, G. J. Conibeer, *J. Phys. Chem. C* **2016**, *120*, 157.
[65] L. Wang, Y. Olivier, O. V. Prezhdo, D. Beljonne, *J. Phys. Chem. Lett.* **2014**, *5*, 3345.
[66] N. Renaud, P. A. Sherratt, M. A. Ratner, *J. Phys. Chem. Lett.* **2013**, *4*, 1065.
[67] S. Schiefer, M. Huth, A. Dobrinevski, B. Nickel, *J. Am. Chem. Soc.* **2007**, *129*, 10316.
[68] R. B. Campbell, J. M. Robertson, J. Trotter, *Acta Crystallogr.* **1962**, *15*, 289.
[69] M. W. B. Wilson, A. Rao, J. Clark, R. S. S. Kumar, D. Brida, G. Cerullo, R. H. Friend, *J. Am. Chem. Soc.* **2011**, *133*, 11830.
[70] J. J. Snellenburg, S. Laptenok, R. Seger, K. M. Mullen, I. H. M. van Stokkum, *J. Stat. Software* **2012**, *49*, 1.
[71] C. Jundt, G. Klein, B. Sipp, J. Le Moigne, M. Joucla, A. A. Villaeys, *Chem. Phys. Lett.* **1995**, *241*, 84.
[72] W.-L. Chan, M. Ligges, A. Jailaubekov, L. Kaake, L. Miaja-Avila, X.-Y. Zhu, *Science* **2011**, *334*, 1541.
[73] V. O. Kim, K. Broch, V. Belova, Y. S. Chen, A. Gerlach, F. Schreiber, H. Tamura, R. G. D. Valle, G. D'Avino, I. Salzmann, D. Beljonne, A. Rao, R. Friend, *J. Chem. Phys.* **2019**, *151*, 164706.
[74] G. R. Desiraju, A. Gavezzotti, *Acta Crystallogr. Sect. B* **1989**, *45*, 473.
[75] S. S. Zade, N. Zamoshchik, A. R. Reddy, G. Fridman-Marueli, D. Sheberla, M. Bendikov, *J. Am. Chem. Soc.* **2011**, *133*, 10803.

Manuscript received: December 27, 2019
Accepted manuscript online: January 27, 2020
Version of record online: February 25, 2020

CHEMISTRY
A European Journal

Supporting Information

Modulating the Electronic and Solid-State Structure of Organic Semiconductors by Site-Specific Substitution: The Case of Tetrafluoropentacenes

Thomas Geiger,[a] Simon Schundelmeier,[a] Thorsten Hummel,[b] Markus Ströbele,[b] Wolfgang Leis,[b] Michael Seitz,[b] Clemens Zeiser,[c] Luca Moretti,[d] Margherita Maiuri,[d] Giulio Cerullo,[d] Katharina Broch,[c] Jörn Vahland,[e] Karl Leo,[e] Cäcilia Maichle-Mössmer,[b] Bernd Speiser,[a] and Holger F. Bettinger*[a]

chem_201905843_sm_miscellaneous_information.pdf

Contents:

1. General Information S3
2. Procedures S7
3. NMR S14
4. Luminescence data for tetrafluoropentacenes 10–12 at 77 K S32
5.Thin film absorption spectra S35
6. Molecular Electrochemistry S36
7. Additional data on the radical cations and dications of 10–12 ..... S38
8. OFET data S40
9. Crystallographic data S41
10. Computational details S46
11. Cartesian coordinates S50
12. References S68

1. General Information

Reagents were used as purchased from Acros Organics, Sigma-Aldrich, TCI Europe or fluorochem. Anhydrous solvents were either obtained from Acros Organics, or, in the cases of CH_2Cl_2, THF and toluene taken from a MBRAUN SPS 800 solvent purification system. *n*-pentylether, 2-MeTHF and CD_2Cl_2 were dried over 3 Å molecular sieves and degassed prior to use. Solvents were degassed by the freeze-pump-thaw method. MPLC chromatography was performed on an Interchim PuriFlash 430 system using pre-packed silica gel columns of appropriate lengths (particle size: 20 µm), solvent mixtures (HPLC grade) are reported in v/v ratios. NMR spectra were recorded on either a Bruker Avance III HD 400 MHz, Bruker Avance III HDX 400 MHz (high temperature spectra), Bruker Avance III HDX 600 MHz equipped with a 5 mm Prodigy BBO-Cryo-Probe, or Bruker Avance III HDX 700 MHz spectrometer equipped with a 5 mm Prodigy BBO-Cryo-Probe using $CDCl_3$ and TCE-d_2 as solvents. Spectra in H_2SO_4 were measured using an external D_2SO_4 standard for field locking and shimming. Low resolution EI data were obtained from an Agilent Technology MSD5977 (quadrupole mass analyzer), high resolution data were obtained using a Finnigan MAT 95 spectrometer (sector field mass analyzer). Melting points were recorded on a BÜCHI Melting-Point 540 and are reported uncorrected. Absorption spectra were measured on a PerkinElmer Lambda1050, the respective fluorescence and excitation spectra were obtained from an Agilent Cary Eclipse fluorescence spectrometer.

Low temperature luminescence spectra

Luminescence spectra at 77 K were recorded on a Horiba Fluorolog-3 DF spectrofluorimeter equipped with a 450 W Xe lamp for steady-state measurements. Emission was monitored at a 90 ° angle using a Hamamatsu R2658P PMT (UV/vis/NIR, 200 nm < λ_{em} < 1000 nm) or a Hamamatsu H10330-75 PMT (NIR, 900 nm < λ_{em} < 1700 nm) detector. Spectral selection was achieved by the double grating monochromator 320DFX for excitation (1200 grooves/nm,

blazed at 330 nm) and the single grating emission monochromators iHR550 for the visible path (1200 grooves/nm, blazed at 500 nm) or iHR320 for the NIR emission range (600 grooves/nm, blazed at 1000 nm). To avoid higher order excitation light, long pass filter plates were used when needed. For the lifetime measurements, excitation was performed in two different ways depending on the temperature and the corresponding magnitude of the lifetimes. For temperatures from 4–200 K, a pulsed Xe lamp (pulse width ~2 μs FWHM) using the excitation monochromator pathway was employed. For temperatures above 200 K, a pulsed LED (Horiba DeltaDiode-310, λ_{em} = 308±10 nm, pulse width ~1 ns FWHM, P_{avg} = 5 μW) was used instead. Lifetime data analysis (least square fitting, statistical parameters, etc.) was performed using the software package DAS from Horiba. Lifetimes were determined by tail-fitting the decay curves to biexponential functions. The solutions used were prepared in a glovebox by dissolving the fluoropentacenes **10**, **11** and **12** in 2-MeTHF or CD_2Cl_2 and further dilution until reaching an absorption < 2. These solutions were transferred into NMR tubes and were cooled by liquid N_2 during the measurements.

Cyclic voltammetry.

Purification of 1,2-dichlorobenzene and electrochemical experiments were performed in darkness under an argon atmosphere. The supporting electrolyte NBu_4PF_6 was recrystallized four times from ethanol/water 3:1 and dried at ≈ 1 mbar and 105 °C for one week. Acetonitrile for the reference electrode was purified by distillation over P_2O_5, CaH_2, and P_2O_5 again. 1,2-Dichlorobenzene (Sigma-Aldrich; anhydrous) was purified by passing through a column of basic alumina (activated at 200 °C/1 mbar for one week) prior to measurements. For the 1,2-dichlorobenzene electrolyte, a supporting electrolyte concentration of 0.1 M NBu_4PF_6 was created by stirring for more than 15 min to allow complete dissolution.

Electroanalytical experiments were performed in a full-glass, gas tight three-electrode cell[1, 2] with an ECO-Autolab PGSTAT100 (Metrohm) with GPES software 4.9.007. As the working

electrode, a Pt disk electrode tip (Metrohm part No. 6.1204.310; nominal diameter 3 mm) was used. The electrode was polished with alumina (0.3 µm; Buehler Micropolish) prior to experiments. The counter electrode consisted of a Pt wire with 1 mm diameter. A Haber-Luggin double reference electrode with a potential determining Ag/Ag^+ redox system (0.01 M $AgClO_4$ in 0.1 M NBu_4PF_6/CH_3CN)[3] was used as the potential standard. A glas frit with 0.1 M NBu_4PF_6/CH_3CN separated the reference system from the chlorinated solvent. The *IR* drop was compensated by positive feedback under control of the GPES software.

Cyclic voltammetric experiments were performed at scan rates between 0.02 and 5.0 Vs^{-1} using a potential step width of 1 mV. All discussed experimental data are background corrected and smoothed by the GPES FFT function. The potentials are referenced versus an external ferrocene standard ($E^0_{(Fc/Fc+)}$ vs. Ag/Ag^+ = +0.246 V). Cyclic voltammograms were numerically simulated with DigiSim 2.1 (BASi) with a potential step size of 0.5 mV, and under the assumptions of planar electrode geometry and semi-infinite diffusion. The "pre-equilibrium enabled for chemical equilibria only" option was set.

EPR

EPR data were obtained using a Bruker ESP 300E (X-Band) spectrometer, samples were prepared by dissolving the fluoropentacenes **10** and **11** in 2 M MSA/nitrobenzene and fused into thin walled EPR tubes. The isotropic EPR spectra were simulated using the WinSim software.[4]

X-ray reflectivity and singlet fission

Thin films were grown by organic molecular beam deposition on silicon with a native oxide layer and on borofloat glass substrates at a base pressure of 1 x 10^{-9} mbar. The total growth rate was 0.3–0.4 nm/min and the final film thickness was 90 nm. X-ray reflectivity was measured on a home diffractometer (3303TT, GE) in air using Cu Kα-radiation (λ = 1.5406 Å) and a 1 D detector (Meteor 1 D, XRD Eigenmann).

Ultrafast pump probe experiments were performed using a Ti-Sapphire chirp pulse amplified source, with 1mJ output energy, 1 kHz repetition rate, 800 nm central wavelength and 100 fs pulse duration. Excitation pulses at 620 nm were generated by non-collinear optical parametric amplification (NOPA) in β-Barium borate (BBO) crystal. Pump pulses were focused in a 350 μm diameter spot. Probing was achieved in the visible region (430–780 nm) by using white light generated (WLG) in a thin sapphire plate. Transient transmission spectra were collected by using a fast optical multichannel analyzer (OMA). The measured quantity is the normalized transmission change, $\Delta T/T$. Excitation energy has been kept at 70 nJ, in order to get around 75 $\mu J/cm^2$ excitation fluences. Measurements were performed at room temperature and under Nitrogen atmosphere.

2. Procedures

3,6-Difluoro-2-(trimethylsilyl)phenyltriflat (2). To a solution of 3.47 g (17.1 mmol) 3,6-difluoro-2-(trimethylsilyl)phenol (**3**) in CH_2Cl_2 (65 mL) 4.3 mL (25.65 mmol, 1.5 eq) Tf_2O were added dropwise over 30 min at 0 °C. After complete addition the mixture was stirred for 10 min at this temperature and 6.9 mL (85.5 mmol, 5 eq) pyridine were added dropwise over 1 h. The mixture was stirred for 10 min at 0 °C and at rt overnight. After pouring on sat. aq. $NaHCO_3$ (100 mL) followed by stirring for 10 min, the aqueous phase was extracted with *n*-hexane (3 x 100 mL). The organic phase was washed with sat. aq. $NaHCO_3$ (2 x 100 mL) and brine (100 mL), dried over Na_2SO_4 and removed under reduced pressure. The resulting oil was purified by flash chromatography (silica gel, *n*-hexane). Colorless oil; yield: 4.87 g (14.57 mmol, 85 %). R_f (silica gel, *n*-hexane): 0.44. ^{1}H NMR ($CDCl_3$, 400 MHz): δ = 7.21 (td, J_1 = 9.1 Hz, J_2 = 5.0 Hz, 1 H), 7.06–6.99 (m, 1 H), 0.45 (d, J = 1.8 Hz, 9 H). $^{13}C\{^1H\}$ NMR ($CDCl_3$, 101 MHz): δ = 162.2 (dd, J_1 = 241.5 Hz, J_2 = 2.6 Hz), 150.4 (dd, J_1 = 250.4 Hz, J_2 = 3.6 Hz), 124.4 (dd, J_1 = 35.9 Hz, J_2 = 3.7 Hz), 120.4, 118.9 (dd, J_1 = 21.7 Hz, J_2 = 10.7 Hz), 116.3 (dd, J_1 = 30.5 Hz, J_2 = 6.6 Hz), 0.3 (d, J = 3.7 Hz). ^{19}F NMR ($CDCl_3$, 376 MHz): δ = -72.4 (d, J = 19.4 Hz), -99.6–-99.7 (m), -130.5–130.7 (m). MS (EI): m/z (%) = 319.1 $[M\text{-}CH_3]^{+\cdot}$ (100), 186.1 (69), 77.1 (27). The spectra are in agreement with published data.[5]

3,6-Difluoro-2-(trimethylsilyl)phenol (3). To a solution of 10 g (47.85 mmol) 2-bromo-3,6-difluorophenol in THF (40 mL) 19.8 mL (95.7 mmol, 2 eq) HMDS were added and the mixture was stirred under reflux overnight in an oil bath. The solvent was removed in vacuo and the resulting oil was redissolved in THF (40 mL). After cooling to -78 °C, 20.8 mL (2.5 M in *n*-hexane, 52.1 mmol, 1.1 eq) *n*-BuLi were added dropwise. After complete addition the mixture was stirred for 1 h at this temperature and allowed to warm to rt overnight. Sat. aq. NH_4Cl (150 mL) and Et_2O (100 mL) were added and the aqueous phase was extracted with Et_2O

(3 x 100 mL). The organic phase was washed with water (3 x 150 mL) and brine (50 mL), dried over anhydrous Na_2SO_4 and evaporated. The remaining oil was purified by flash chromatography (silica gel, *n*-hexane). Colorless oil; yield: 3.47 g (17.15 mmol, 36 %). R_f (silica gel, *n*-hexane): 0.18. ^{1}H NMR ($CDCl_3$, 400 MHz): δ = 7.00 (td, J_1 = 9.4 Hz, J_2 = 5.1 Hz, 1 H), 6.48 (td, J_1 = 8.5 Hz, J_2 = 3.6 Hz, 1 H), 5.32 (dd, J_1 = 6.3 Hz, J_2 = 1.3 Hz, 1 H), 0.37 (d, J = 1.7 Hz, 9 H). ^{13}C{^{1}H} NMR ($CDCl_3$, 101 MHz): δ = 162.9 (dd, J_1 = 237.2 Hz, J_2 = 2.2 Hz), 148.2 (dd, J_1 = 16.8 Hz, J_2 = 15.0 Hz), 147.3 (dd, J_1 = 233.0 Hz, J_2 = 3.2 Hz), 116.6 (dd, J_1 = 20.9 Hz, J_2 = 11.3 Hz), 114.5 (d, J = 35.9 Hz), 106.9 (dd, J_1 = 30.8 Hz, J_2 = 6.2 Hz), 0.4 (d, J = 3.3 Hz). ^{19}F NMR ($CDCl_3$, 376 MHz,): δ = -103.4 – -103.5 (m), -147.4 – -147.5 (m). HRMS (EI): m/z $[M]^{+\cdot}$ calcd for $C_9H_{12}OF_2Si$: 202.06199; found: 202.05644. The data obtained is in agreement with literature data.[6]

1,4,8,11-Tetrafluoro-5,6,7,12,13,14-hexahydro-6,13-ethenopentacene (4). A solution of 1.18 g (7.53 mmol) 5,6,7,8-tetramethylidenebicyclo[2.2.2]oct-2-ene (**1**) and 2.52 g (16.58 mmol, 2.2 eq) anhydrous CsF in 100 mL of a 1:1 mixture of ACN and CH_2Cl_2 was heated to 45 °C using an oil bath as heat source. 3,6-Difluoro-2-(trimethylsilyl)phenyltriflate (**2**) (5.54 g, 16.58 mmol, 2.2 eq) was added dropwise and the resulting mixture was stirred at 45 °C overnight. After cooling to rt water (150 mL) was added. The aqueous phase was extracted with CH_2Cl_2 (3 x 100 mL) and the organic phase was washed with water (3 x 150 mL). After drying over Na_2SO_4 the solvent was removed leaving an orange solid which was used without further purification. Yield: 1.89 g (4.91 mmol, 65 %). ^{1}H NMR ($CDCl_3$, 400 MHz): δ = 6.87 (dd, J_1 = 4.0 Hz, J_2 = 3.1 Hz, 2 H), 6.80 (t, J = 6.5 Hz, 4 H), 4.38 (dd, J_1 = 3.9 Hz, J_2 = 3.1 Hz, 2 H), 3.54 (s, 8 H). ^{13}C{^{1}H} NMR ($CDCl_3$, 101 MHz): δ = 156.8 (dd, J_1 = 240.4 Hz, J_2 = 3.7 Hz), 139.4, 124.1 (dd, J_1 = 14.8 Hz, J_2 = 10.4 Hz), 112.8 (dd, J_1 = 19.7 Hz, J_2 = 14.0 Hz), 100.1, 54.1, 26.7 (t, J = 2.9 Hz). ^{19}F NMR ($CDCl_3$, 376 MHz,): δ

= -123.2 (t, J = 6.6 Hz). HRMS (EI): m/z $[M]^{+\cdot}$ calcd for $C_{24}H_{16}F_4$: 380.11826; found: 380.12077.

1,4,8,11-Tetrafluoro-6,13-dihydro-6,13-ethenopentacene (5). To a solution of 1.89 g (4.91 mmol) 1,4,8,11-tetrafluoro-5,6,7,12,13,14-hexahydro-6,13-ethenopentacene (**4**) in $CHCl_3$ (100 mL) 2.23 g (9.82 mmol, 2 eq) DDQ were added and the resulting mixture was stirred at rt overnight. The reaction mixture was diluted with $CHCl_3$ (100 mL) and the organic phase was washed with sat. aq. $NaHCO_3$ (5 x 100 mL) and water (3 x 100 mL). After drying over Na_2SO_4 and removing the solvent under reduced pressure the residue was purified by flash chromatography (silica gel, *n*-hexane/CH_2Cl_2 4:1). Light yellow solid; yield: 0.69 g (1.84 mmol, 37 %). R_f (silica gel, *n*-hexane/CH_2Cl_2 4:1): 0.47. Mp: 251–254 °C. ^{1}H NMR ($CDCl_3$, 400 MHz): δ = 7.97 (s, 4 H), 7.06 (dd, J_1 = 4.3 Hz, J_2 = 3.1 Hz, 2 H), 6.97 (dd, J_1 = 7.3 Hz, J_2 = 6.6 Hz, 4 H), 5.43 (dd, J_1 = 4.2 Hz, J_2 = 3.4 Hz, 2 H). ^{13}C{^{1}H} NMR ($CDCl_3$, 101 MHz): δ = 154.8 (dd, J_1 = 248.3 Hz, J_2 = 4.9 Hz), 143.3, 138.1, 122.7 (dd, J_1 = 13.3 Hz, J_2 = 10.2 Hz), 114.6 (t, J = 3.2 Hz), 109.0 (dd, J_1 = 18.3 Hz, J_2 = 13.2 Hz), 50.5. ^{19}F NMR ($CDCl_3$, 376 MHz): δ = -128.1 (t, J = 7.1 Hz). HRMS (EI): m/z $[M]^{+\cdot}$ calcd for $C_{24}H_{12}F_4$: 376.08511; found: 376.08696. Single crystals of the compound were obtained by slow evaporation of the solvent from a solution of the compound in CH_2Cl_2.

1,4-Difluoro-5,6,9,10-tetrahydro-6,9-dietheno-7,8-dimethyleneanthracene (6). A solution of 1.97 g (12.6 mmol) 5,6,7,8-tetramethylidenebicyclo[2.2.2]oct-2-ene (**1**) and 1.89 g (12.46 mmol, 0.98 eq) anhydrous CsF in 120 mL of a 1:1 mixture of ACN and CH_2Cl_2 was heated to 45 °C in an oil bath. 3,6-Difluoro-2-(trimethylsilyl)phenyltriflate (**2**) (4.13 g, 12.35 mmol, 0.98 eq) was added dropwise and the resulting mixture was stirred at 45 °C overnight. After cooling to rt water (100 mL) was added and the aqueous phase was extracted with CH_2Cl_2 (4 x 100 mL) and dried over Na_2SO_4. The solvent was removed in vacuo and the residue purified by flash chromatography (silica gel, *n*-hexane). Colorless, sticky gum; yield:

1.25 g (4.66 mmol, 38 %). R_f (silica gel, *n*-hexane): 0.21. ^{1}H NMR ($CDCl_3$, 400 MHz): δ = 6.81 (t, J = 6.6 Hz, 2 H), 6.50 (dd, J_1 = 4.4 Hz, J_2 = 3.2 Hz, 2 H), 5.10 (s, 2 H), 4.89 (s, 2 H), 4.00 (dd, J_1 = 4.3 Hz, J_2 = 3.4 Hz), 3.48 (s, 4 H). $^{13}C\{^1H\}$ NMR ($CDCl_3$, 101 MHz): δ = 156.8 (dd, J_1 = 241.4 Hz, J_2 = 3.9 Hz), 143.8, 133.8, 132.6, 123.9 (dd, J_1 = 14.7 Hz, J_2 = 10.3 Hz), 112.7 (dd, J_1 = 19.2 Hz, J_2 = 13.9 Hz), 102.1, 52.3, 25.4 (t, J = 2.9 Hz). ^{19}F NMR ($CDCl_3$, 376 MHz): δ = -123.2 (t, J = 6.6 Hz). HRMS (EI): m/z $[M]^{+\cdot}$ calcd for $C_{18}H_{14}F_2$: 268.10580; found: 268.11072.

1,4,9,10-Tetrafluoro-5,6,7,12,13,14-hexahydro-6,13-ethenopentacene (7). A solution of 0.98 g (3.66 mmol) 1,4-difluoro-5,6,9,10-tetrahydro-6,9-dietheno-7,8-dimethyleneanthracene (**6**) and 1.0 g (3.66 mmol, 1 eq) 1,2-dibromo-4,5-difluorobenzene in toluene (80 mL) was cooled to -55 °C. 2.4 mL *n*-BuLi (1.6 M in *n*-hexane, 3.84 mmol, 1.05 eq) diluted with *n*-hexane (7 mL) were added dropwise over 2 h. After complete addition the mixture was stirred for 2 h at this temperature and then allowed to warm to rt overnight. Methanol (13 mL) was added and the solvent was removed under reduced pressure. The residue was purified by flash chromatography (silica gel, *n*-hexane/CH_2Cl_2 10:1). Light yellow solid; yield: 0.75 g (1.98 mmol, 54 %). R_f (silica gel, *n*-hexane/CH_2Cl_2 10:1): 0.21. Mp: 177–180 °C. ^{1}H NMR ($CDCl_3$, 400 MHz): δ = 6.92–6.85 (m, 4 H), 6.80 (t, J = 6.6 Hz, 2 H), 4.33 (dd, J_1 = 4.1 Hz, J_2 = 3.0 Hz, 2 H), 3.54 (s, 4 H), 3.54/3.53 (two s, not resolved, 8 H). $^{13}C\{^1H\}$ NMR ($CDCl_3$, 101 MHz): δ = 156.8 (dd, J_1 = 241.2 Hz, J_2 = 3.6 Hz), 148.7 (dd, J_1 = 247.6 Hz, J_2 = 14.5 Hz), 140.0, 139.4, 139.0, 130.5 (t, J = 4.4 Hz), 124.1 (dd, J_1 = 14.8 Hz, J_2 = 10.6 Hz), 116.7 (dd, J_1 = 11.0 Hz, J_2 = 5.9 Hz), 112.8 (dd, J_1 = 19.7 Hz, J_2 = 14.1 Hz), 54.0, 32.7, 26.9 (t, J = 2.9 Hz). ^{19}F NMR ($CDCl_3$, 376 MHz): δ = -123.2 (t, J = 6.6 Hz), -141.8 (t, J = 9.6 Hz). HRMS (EI): m/z $[M]^{+\cdot}$ calcd for $C_{24}H_{16}F_4$: 380.11826; found: 380.11642.

1,4,9,10-Tetrafluoro-6,13-dihydro-6,13-ethenopentacene (8). To a solution of 0.74 g (1.94 mmol) 1,4,9,10-tetrafluoro-5,6,7,12,13,14-hexahydro-6,13-ethenopentacene (**7**) in $CHCl_3$ (60 mL) 0.88 g (3.88 mmol, 2 eq) DDQ were added in one portion and the resulting mixture was stirred overnight at rt. $CHCl_3$ (60 mL) was added and the organic phase was washed with sat. aq. $NaHCO_3$ (5 x 100 mL) and water (3 x 100 mL). After drying over Na_2SO_4 the solvent was removed under reduced pressure and the residue was purified by flash chromatography (silica gel, *n*-hexane/CH_2Cl_2 10:1). Colorless solid; yield: 0.62 g (1.65 mmol, 85 %). R_f (silica gel, *n*-hexane/CH_2Cl_2 10:1): 0.14. Mp: 212–214 °C. ^{1}H NMR ($CDCl_3$, 400 MHz): δ = 7.95 (s, 2 H), 7.66 (s, 2 H), 7.44 (t, J = 9.5 Hz, 2 H), 7.05 (dd, J_1 = 4.5 Hz, J_2 = 3.1 Hz, 2 H), 6.97 (dd, J_1 = 7.3 Hz, J_2 = 6.5 Hz, 2 H), 5.36 (dd, J_1 = 4.4 Hz, J_2 = 3.3 Hz, 2 H). ^{13}C{^{1}H} NMR ($CDCl_3$, 101 MHz): δ = 154.8 (dd, J_1 = 248.3 Hz, J_2 = 5.5 Hz), 150.0 (dd, J_1 = 250.9 Hz, J_2 = 17.7 Hz), 143.6, 142.3, 138.2, 128.4 (t, J = 4.4 Hz), 122.6 (dd, J_1 = 14.1 Hz, J_2 = 9.5 Hz), 121.0, 114.5 (t, J = 3.4 Hz), 113.5 (dd, J_1 = 13.1 Hz, J_2 = 4.5 Hz), 108.9 (dd, J_1 = 19.9 Hz, J_2 = 12.2 Hz), 50.2. ^{19}F NMR ($CDCl_3$, 376 MHz,): δ = -128.2 (t, J = 6.1 Hz), -137.9 (t, J = 10.2 Hz). HRMS (EI): m/z $[M]^{+\cdot}$ calcd for $C_{24}H_{12}F_4$: 376.08696; found: 376.08477.

General procedure for the thermal synthesis of fluorinated pentacenes. A suspension of 0.1 g (0.27 mmol) of the corresponding acene precursor in degassed *n*-pentylether was heated to 180 °C in the dark using an oil bath. To the resulting solution 52.7 mg (0.27 mmol, 1 eq) dimethyl-1,2,4,5-tetrazine-3,6-dicarboxylate were added quickly in one portion. After 1.5 min at 180 °C the reaction flask was submerged in an ice bath. The precipitate was collected in a fritted glass funnel (P4) and washed consecutively with *n*-hexane, CH_2Cl_2 and ethyl acetate. The product was dried at rt in diffusion pump vacuum for 3 d.

1,4,8,11-Tetrafluoropentacene (10). The thermal reaction was performed 6 consecutive times using a total of 0.69 g (1.84 mmol) precursor **5**. Purple solid; yield: 0.193 g (0.55 mmol, 30 %). ^{1}H NMR (TCE-d_2, 600 MHz): δ = 9.15 (s, 2 H), 8.97 (s, 4 H), 6.95 (br s, 4 H). ^{19}F NMR (TCE-d_2, 565 MHz): δ = -125.7 (br s). HRMS (EI): m/z $[M]^{+\cdot}$ calcd for $C_{22}H_{10}F_4$: 350.07131; found: 350.07189. Single crystals of this compound suitable for X-ray crystallography were grown by fusing a sample into a homemade silica ampule under vacuum and heating in a tube furnace. The part of the ampule containing the bulk material was heated to 80 °C while the other side of the ampule was kept at rt. After 5 days of heating single crystals were obtained.

1,4,9,10-Tetrafluoropentacene (11). The thermal reaction was performed 6 consecutive times using a total of 0.59 g (1.57 mmol) precursor **8**. Purple solid; yield: 0.237 g (0.68 mmol, 43 %). ^{1}H NMR (TCE-d_2, 600 MHz): δ = 9.04 (s, 2 H), 8.94 (s, 2 H), 8.66 (s, 2 H), 7.68 (t, J = 8.7 Hz, 2 H), 6.93 (br t, J = 6.5 Hz, 2 H). ^{19}F NMR (TCE-d_2, 565 MHz): δ = -125.9 (br t, J = 6.8 Hz), -131.8 (t, J = 9.0 Hz). HRMS (EI): m/z $[M]^{+\cdot}$ calcd for $C_{22}H_{10}F_4$: 350.07131; found: 350.06855.

1,4,8,11-Tetrafluoropentacene dimer (13). A sample of 1,4,8,11-tetrafluoropentacene (**10**) in TCE-d_2 was heated to 120 °C for 2 h. ^{1}H NMR (TCE-d_2, 700 MHz): δ = 7.78 (s, 8 H), 6.86 (br t, J = 5.9 Hz, 8 H), 5.28 (s, 4 H). ^{13}C{^{1}H} NMR (TCE-d_2, 176 MHz): δ = 154.1 (dd, J_1 = 250.8 Hz, J_2 = 4.3 Hz), 140.9, 122.8 (t, J = 10.4 Hz), 118.8, 108.7 (m), 53.6. ^{19}F NMR (TCE-d_2, 659 MHz): δ = -132.9 (br s). MS (EI): m/z (%) 350.1 $[M]^{+\cdot}$ (100) of monomer, 330 (6), 175 (19). No high resolution data could be obtained since the sample either monomerizes (EI) or is not soluble enough (ESI). MALDI measurements give the same result as the EI experiment.

General procedure for generation of the acene radical cations in solution. A few grains of the respective pentacene were dissolved in a 2 M solution of methanesulfonic acid (MSA) in nitrobenzene.

1,4,8,11-Tetrafluoropentacene$^{+\cdot}$ ($\mathbf{10}^{+\cdot}$). UV/Vis (2 M MSA/nitrobenzene): λ = 424, 822, 930, 1080.

1,4,9,10-Tetrafluoropentacene$^{+\cdot}$ ($\mathbf{11}^{+\cdot}$). UV/Vis (2 M MSA/nitrobenzene): λ = 427, 779, 867, 998.

General procedure for generation of the acene dications in solution. A few grains of the respective pentacenes were dissolved in oleum (20–30 % free SO_3). The NMR samples were measured using an external D_2SO_4 standard for field locking and shimming.

1,4,8,11-Tetrafluoropentacene^{2+} ($\mathbf{10}^{2+}$). ^{1}H NMR (H_2SO_4, 600 MHz): δ = 9.74 (s, 2 H), 9.68 (s, 4 H), 8.17 (s, 4 H). $^{13}C\{^1H\}$ NMR (H_2SO_4, 151 MHz): δ = 170.5, 164.7 (d, J = 287.8 Hz), 155.7 (d, J = 2.1 Hz), 134.1, 133.4–133.0 (m), 127.2 (d, J = 14.8 Hz). ^{19}F NMR (H_2SO_4, 565 MHz): δ = -93.8 (br s). UV/Vis (H_2SO_4): λ = 366, 756, 845.

1,4,9,10-Tetrafluoropentacene^{2+} ($\mathbf{11}^{2+}$). ^{1}H NMR (H_2SO_4, 600 MHz): δ = 9.58 (s, 2 H), 9.54 (s, 2 H), 9.27 (s, 2 H), 8.37 (br s, 2 H), 8.11 (br s, 2 H). $^{13}C\{^1H\}$ NMR (H_2SO_4, 151 MHz): δ = 171.9, 165.2 (d, J = 287.9 Hz), 161.0, 160.1 (dd, J_1 = 287.8 Hz, J_2 = 15.5 Hz), 156.9, 138.9, 134.5, 134.1, 134.0–133.7 (m), 129.1–128.7 (m), 127.1 (d, J = 15.9 Hz). ^{19}F NMR (H_2SO_4, 565 MHz): δ = -92.7 (br s), -105.2 (br s). UV/Vis (H_2SO_4): λ = 371, 389, 724, 798.

3. NMR

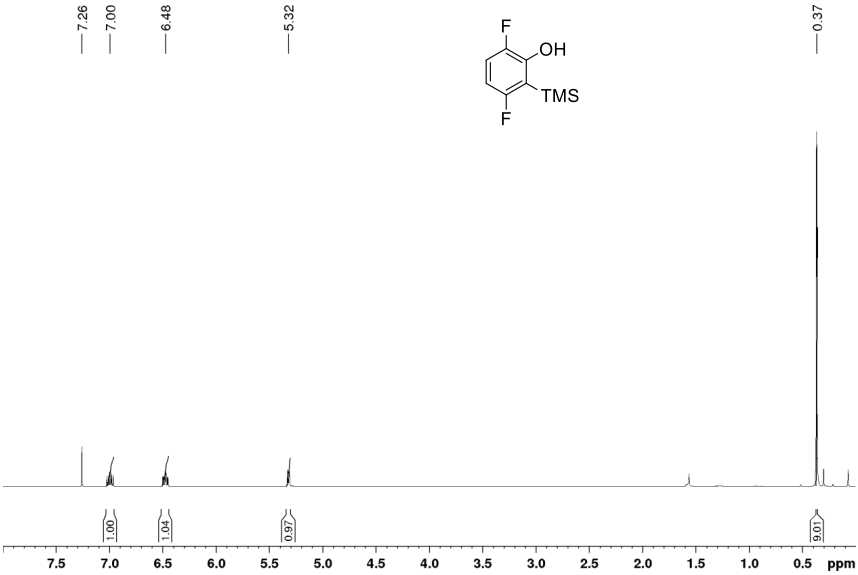

Figure S1. ^{1}H spectrum of **3** in $CDCl_3$

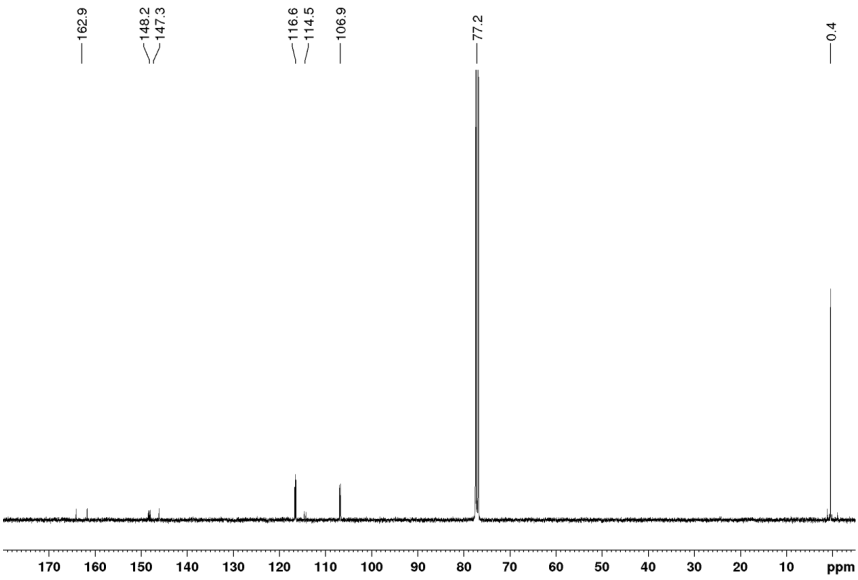

Figure S2. $^{13}C\{^{1}H\}$ spectrum of **3** in $CDCl_3$

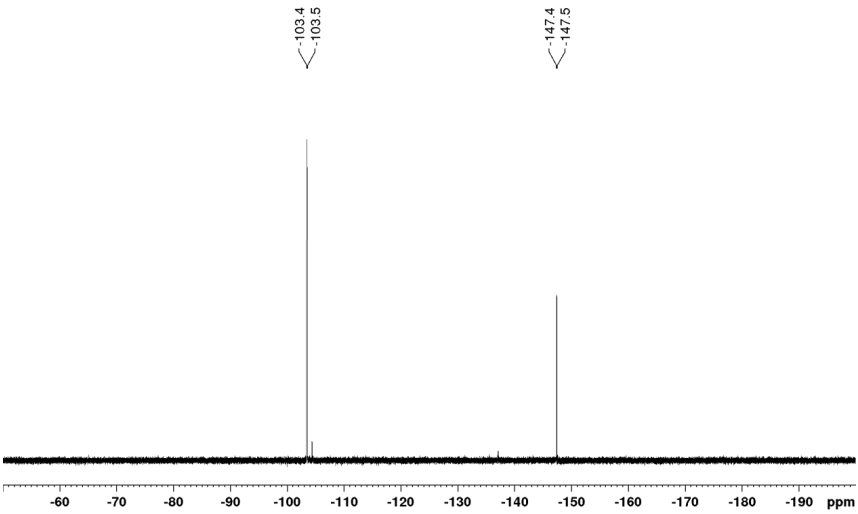

Figure S3. ^{19}F spectrum of **3** in $CDCl_3$

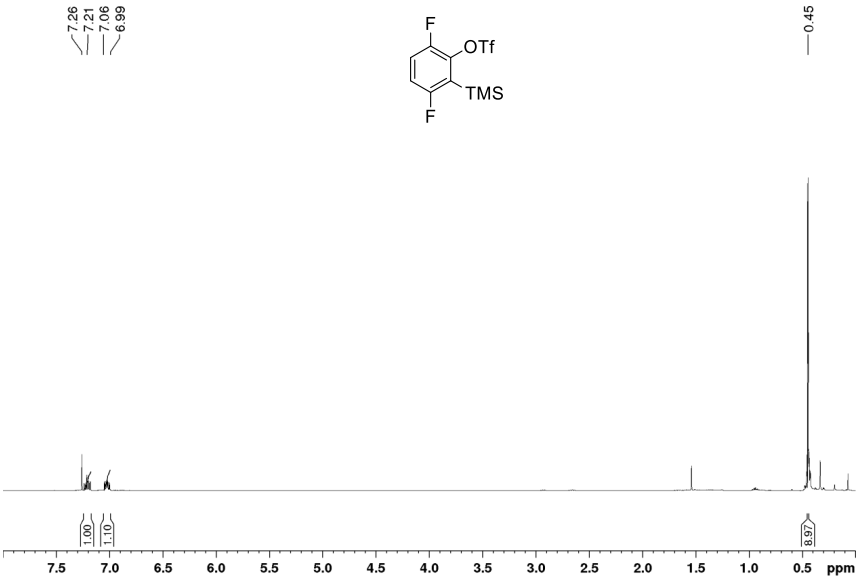

Figure S4. ^{1}H spectrum of **2** $CDCl_3$

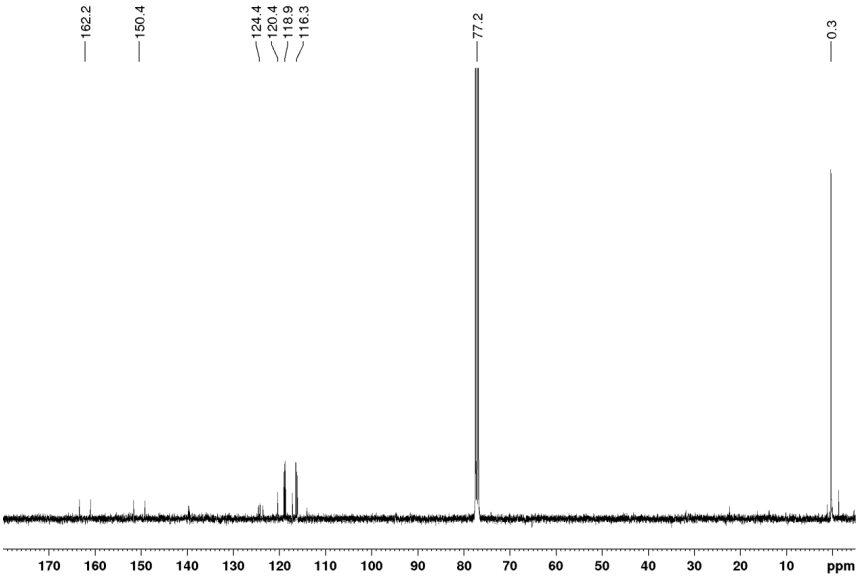

Figure S5. $^{13}C\{^{1}H\}$ spectrum of **2** in $CDCl_3$

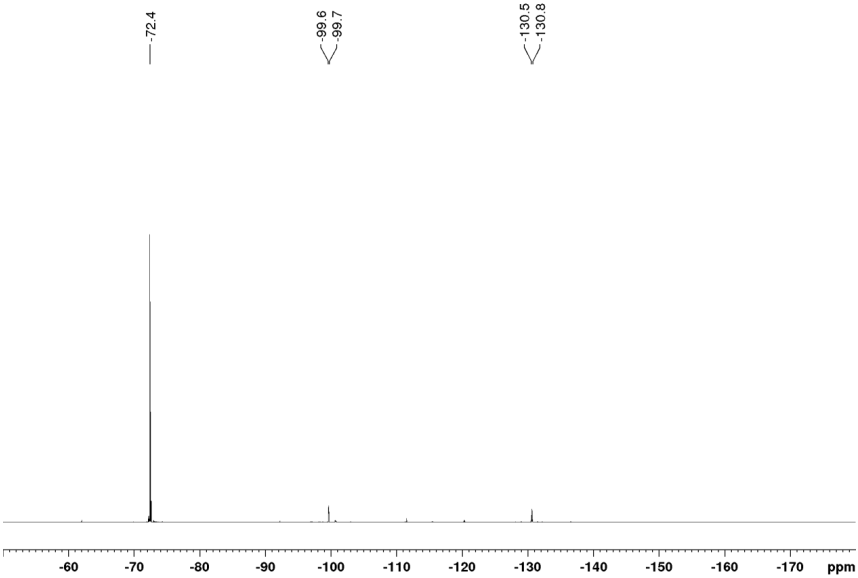

Figure S6. ^{19}F spectrum of **2** in $CDCl_3$

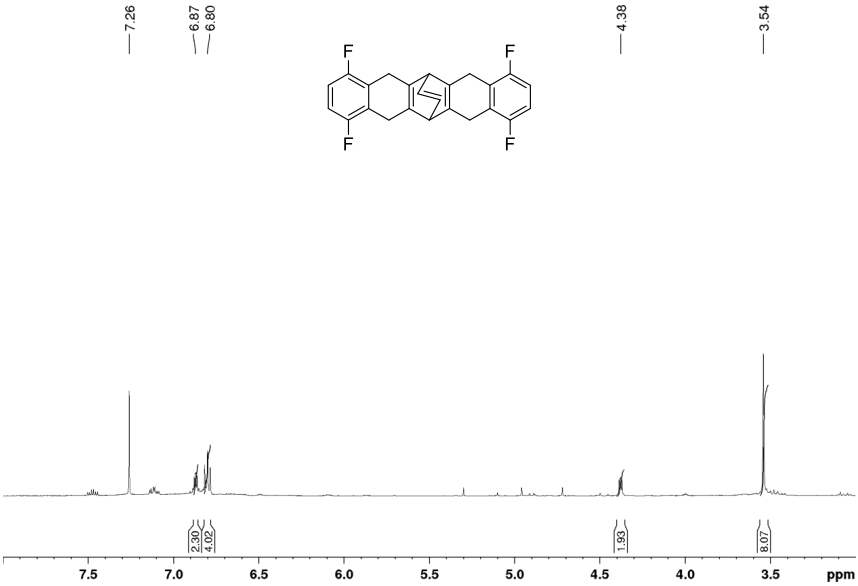

Figure S7. ^{1}H spectrum of **4** in $CDCl_3$

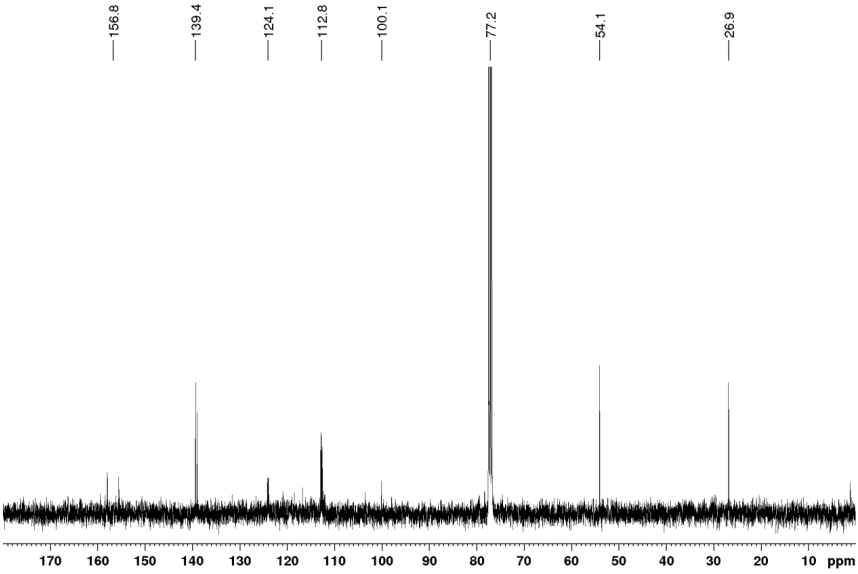

Figure S8. $^{13}C\{^{1}H\}$ spectrum of **4** in $CDCl_3$

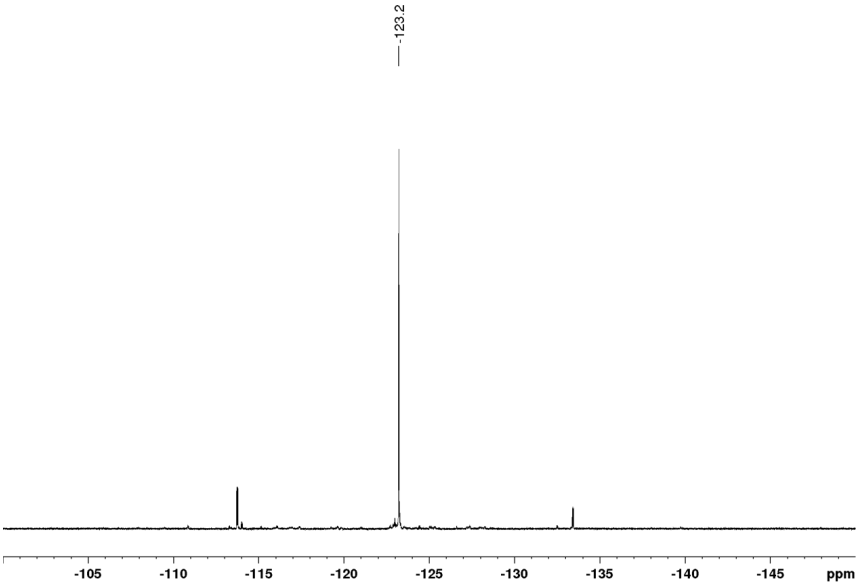

Figure S9. ^{19}F spectrum of **4** in $CDCl_3$

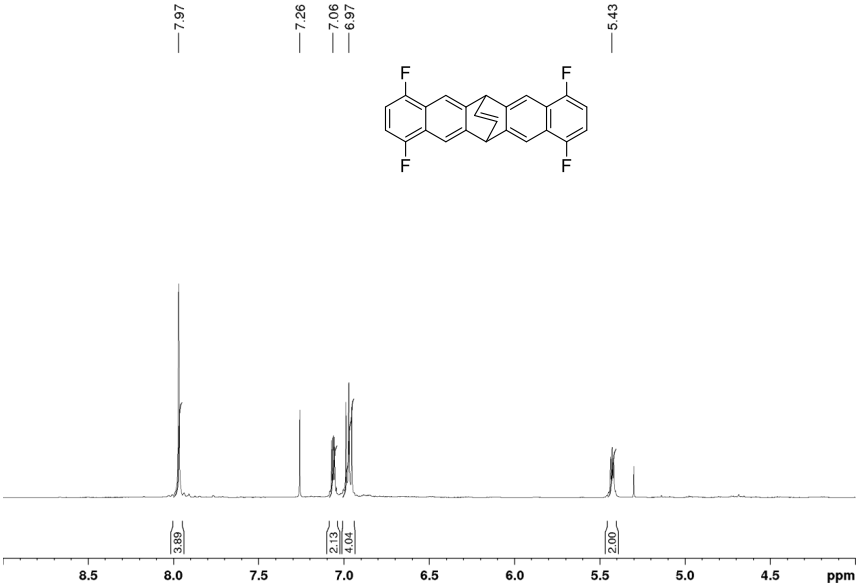

Figure S10. ^{1}H spectrum of **5** in $CDCl_3$

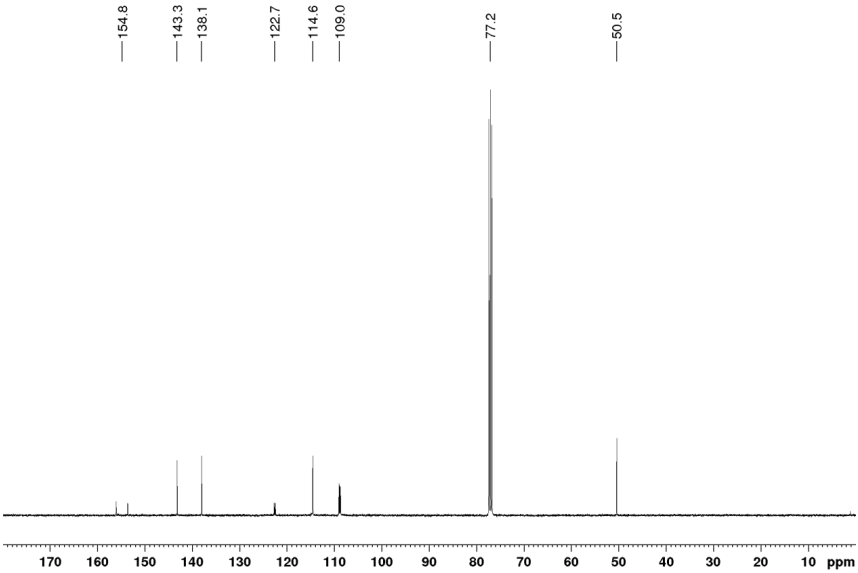

Figure S11. $^{13}C\{^{1}H\}$ spectrum of **5** in $CDCl_3$

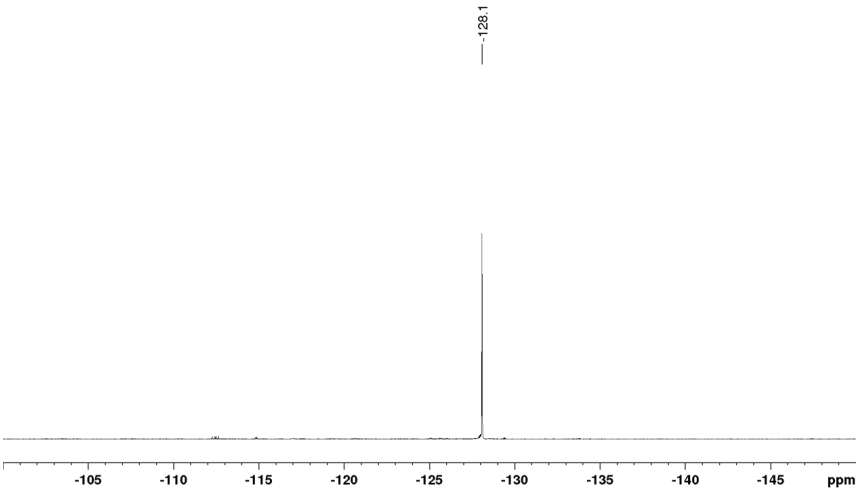

Figure S12. ^{19}F spectrum of **5** in $CDCl_3$

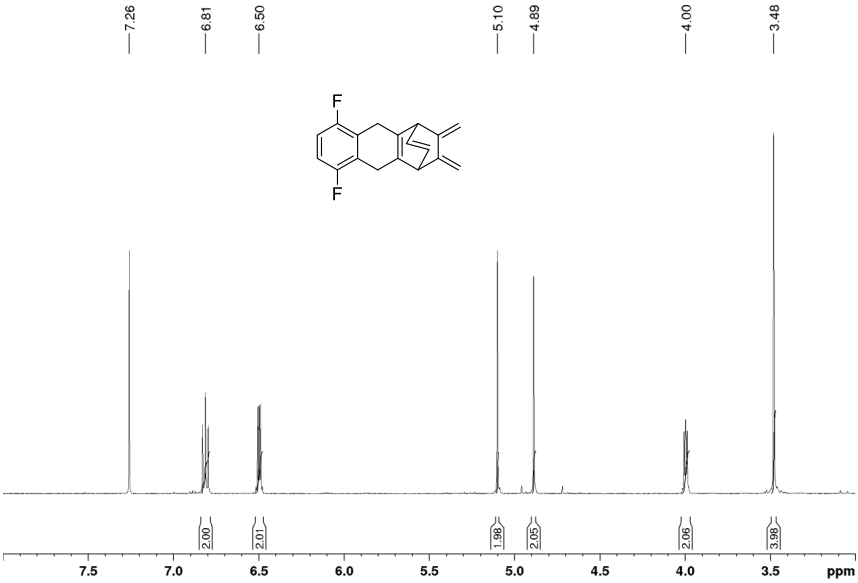

Figure S13. ^{1}H spectrum of **6** in $CDCl_3$

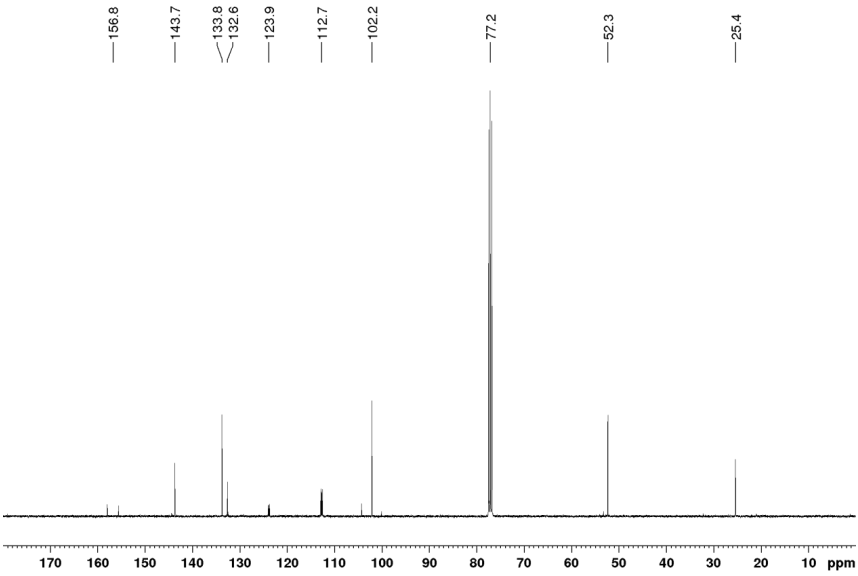

Figure S14. $^{13}C\{^{1}H\}$ spectrum of **6** in $CDCl_3$

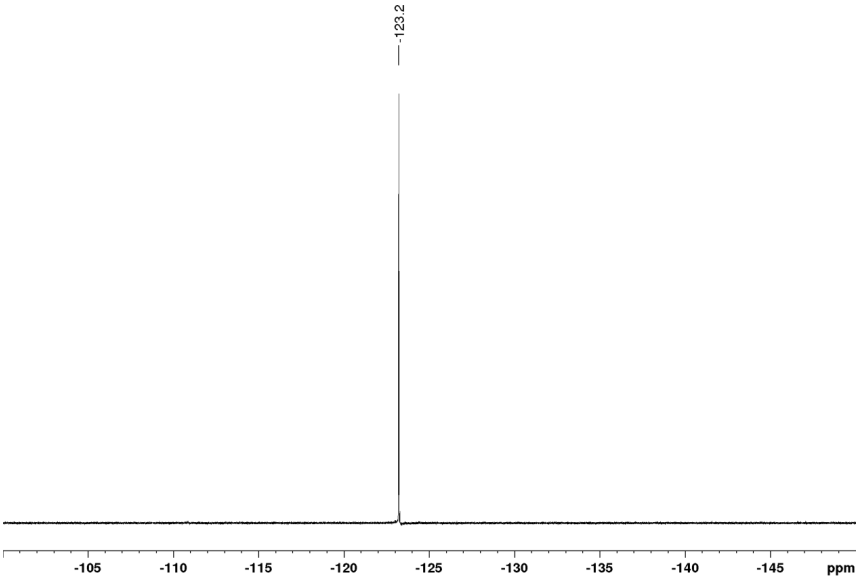

Figure S15. ^{19}F spectrum of **6** in $CDCl_3$

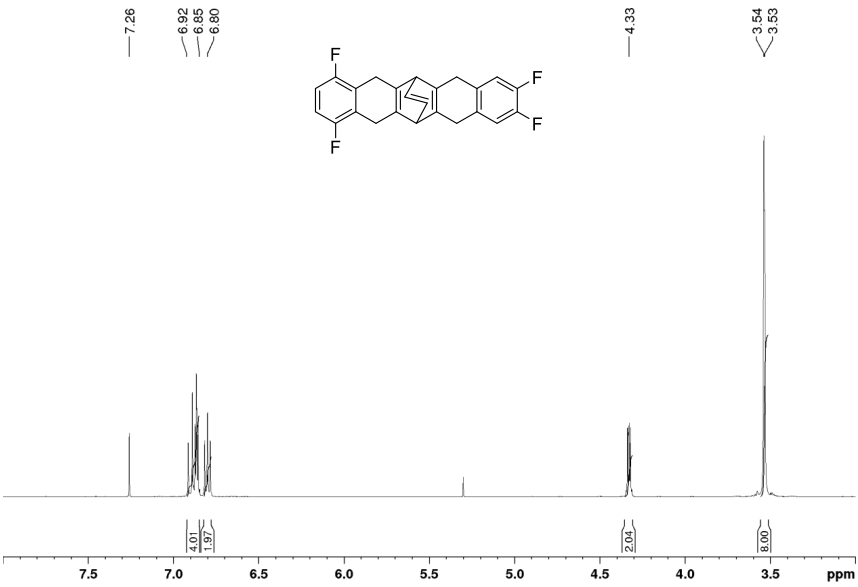

Figure S16. ^{1}H spectrum of **7** in $CDCl_3$

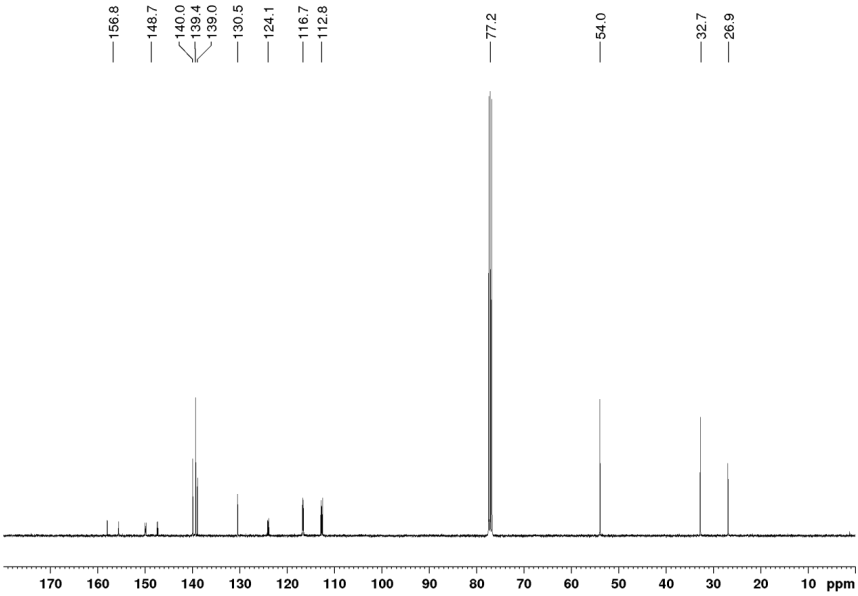

Figure S17. $^{13}C\{^{1}H\}$ spectrum of **7** in $CDCl_3$

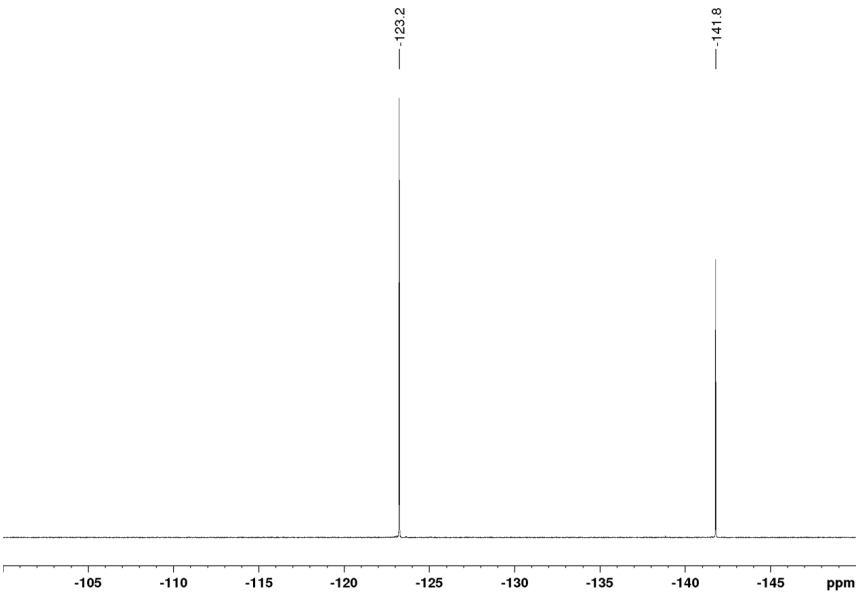

Figure S18. ^{19}F spectrum of **7** in $CDCl_3$

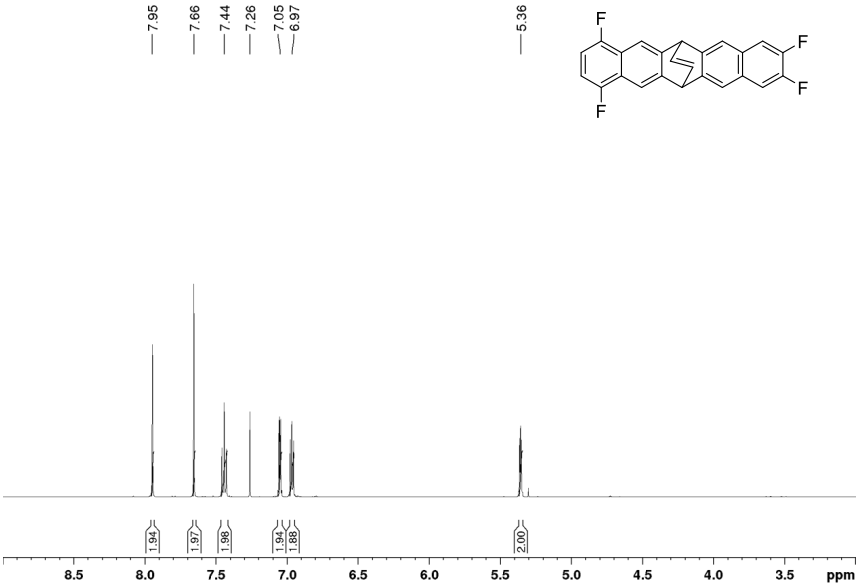

Figure S19. ^{1}H spectrum of **8** in $CDCl_3$

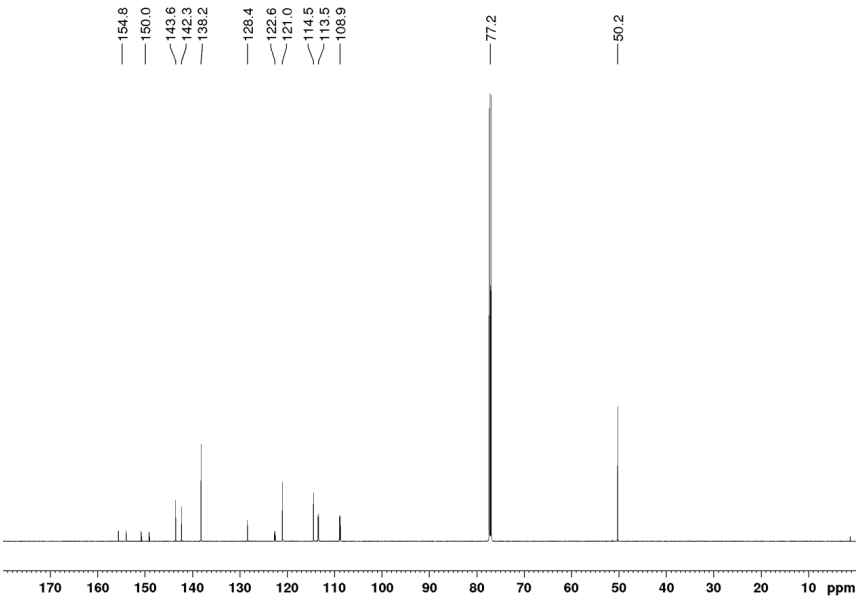

Figure S20. $^{13}C\{^{1}H\}$ spectrum of **8** in $CDCl_3$

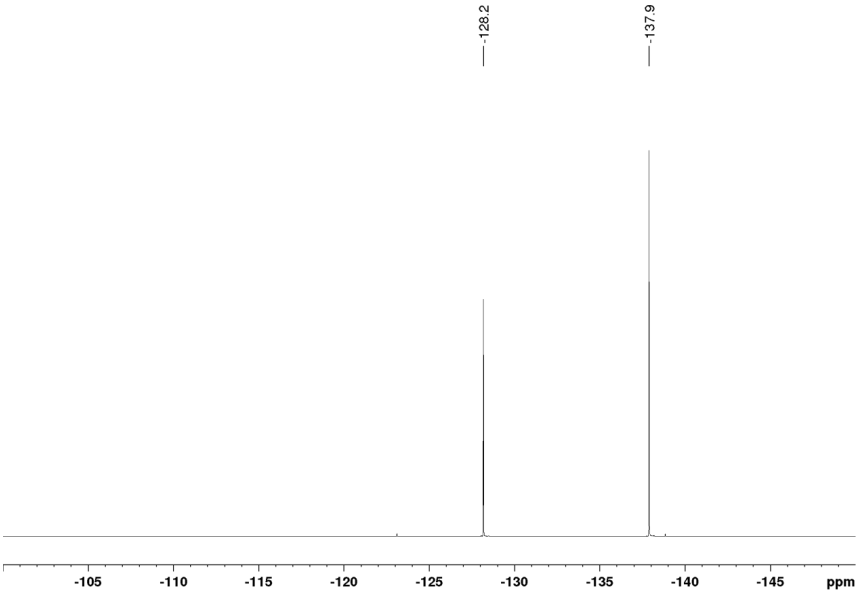

Figure S21. ^{19}F spectrum of **8** in $CDCl_3$

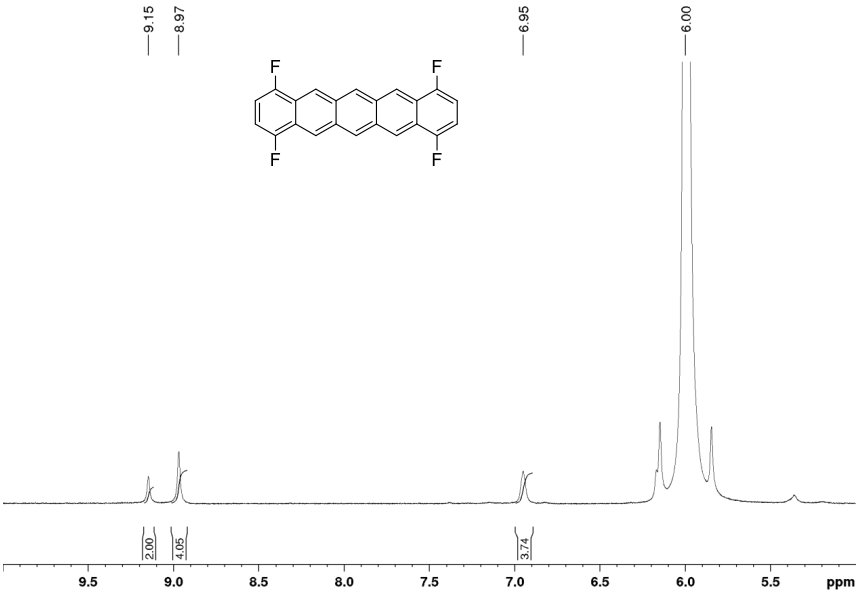

Figure S22. ^{1}H spectrum of **10** in TCE-d_2

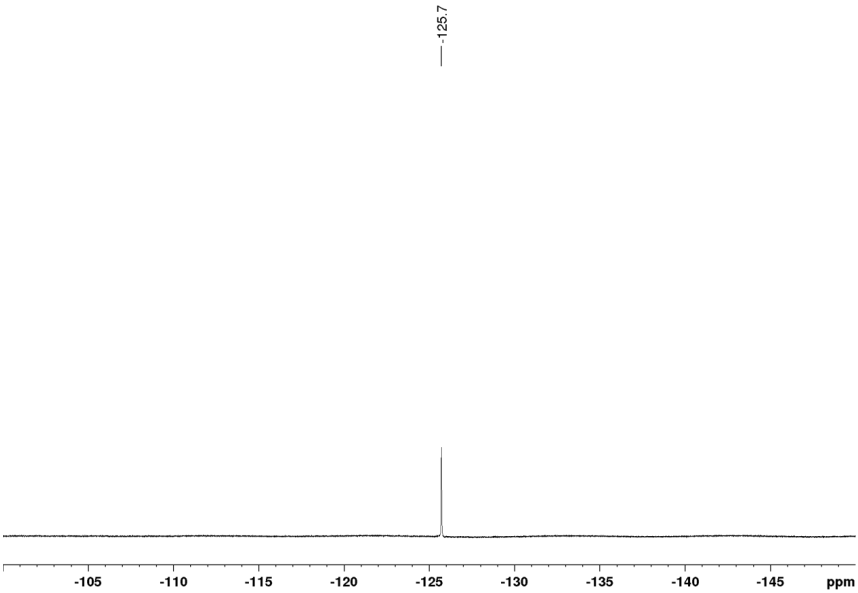

Figure S23. ^{19}F spectrum of **10** in TCE-d_2

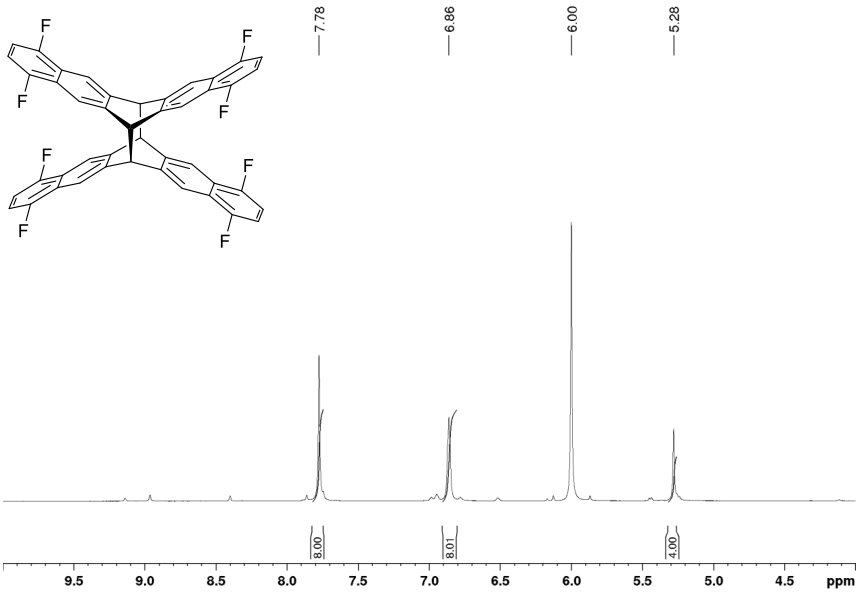

Figure S24. ^{1}H spectrum of **13** in TCE-d_2

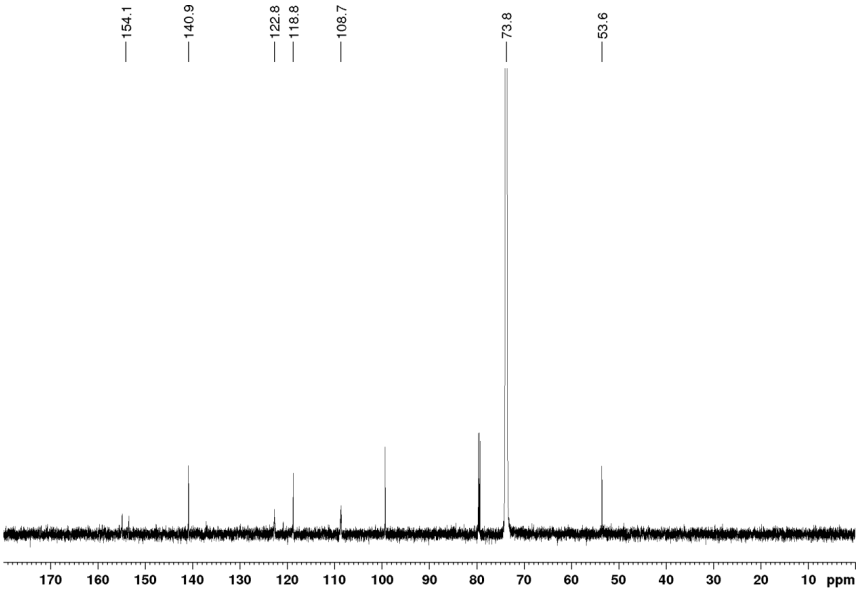

Figure S25. $^{13}C\{^{1}H\}$ spectrum of **13** in TCE-d_2

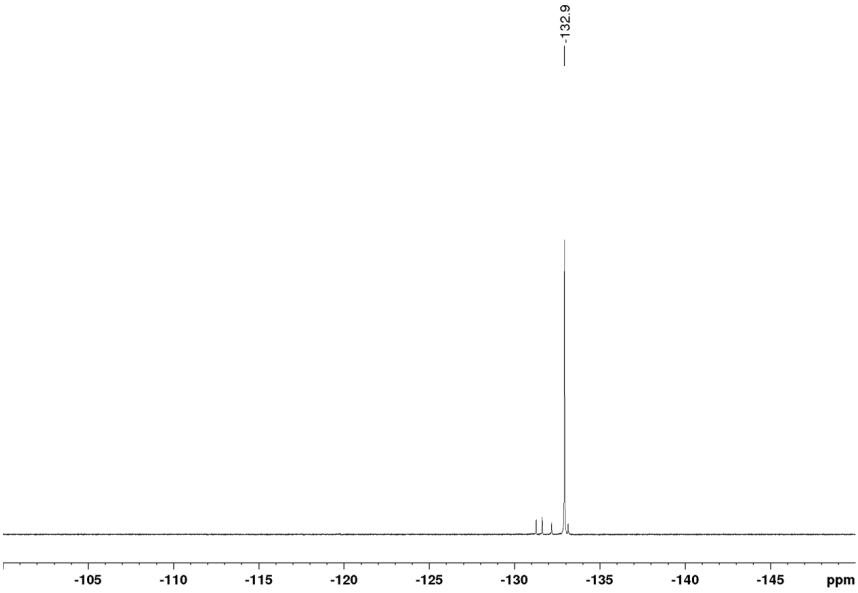

Figure S26. ^{19}F spectrum of **13** in TCE-d_2

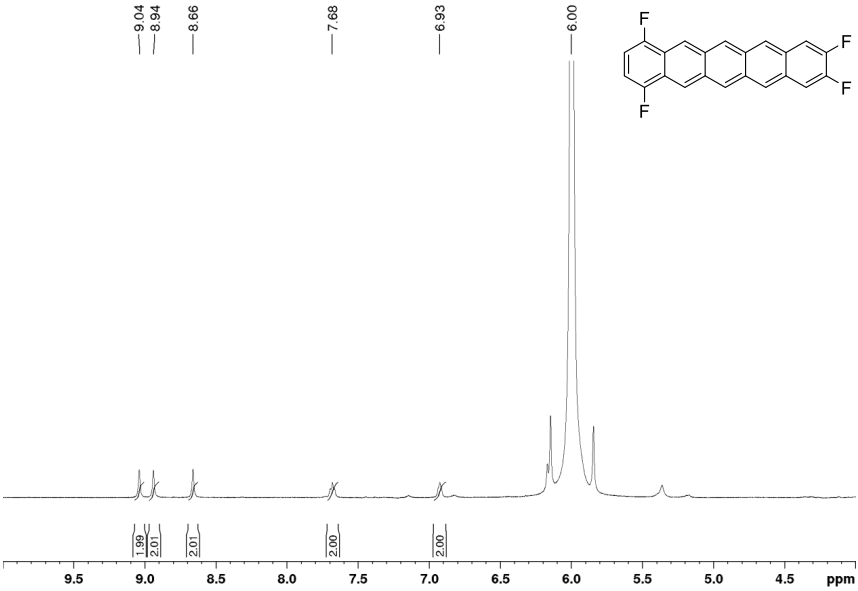

Figure S27. ^{1}H spectrum of **11** in TCE-d_2

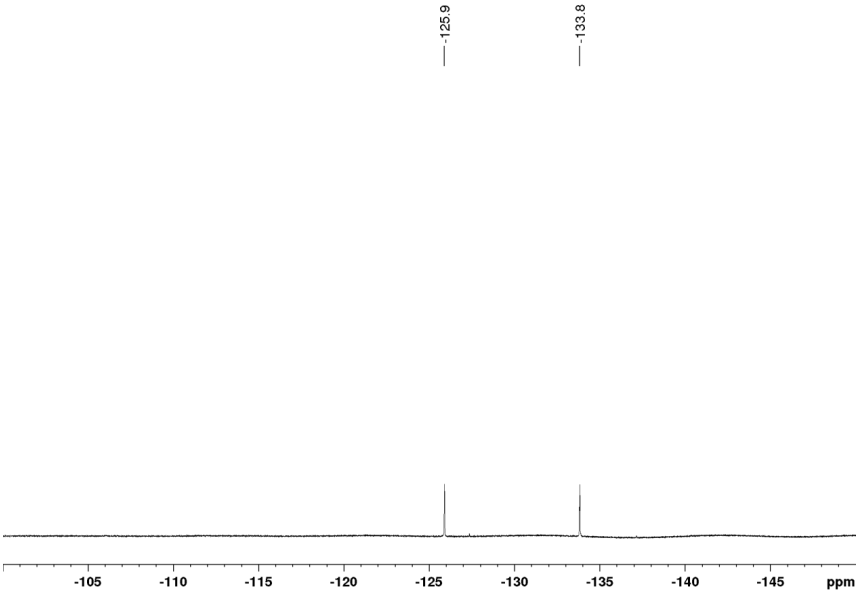

Figure S28. ^{19}F spectrum of **11** in TCE-d_2

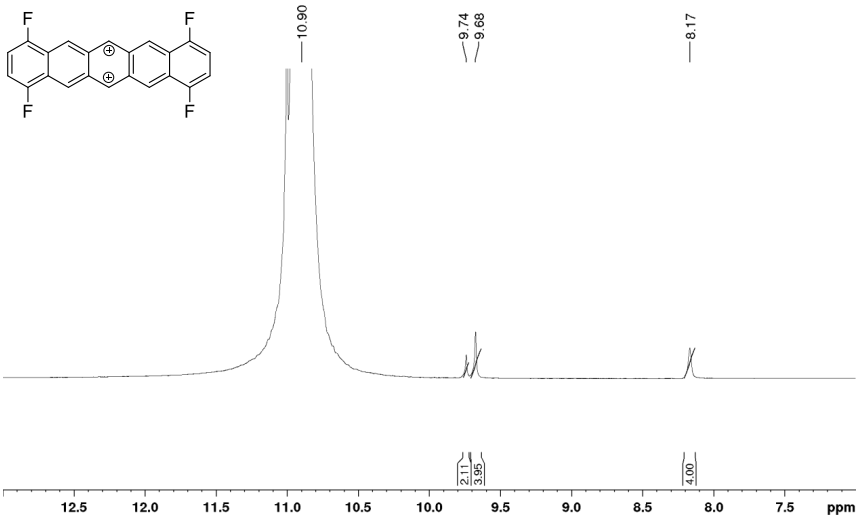

Figure S29. ^{1}H spectrum of $\mathbf{10}^{2+}$ in H_2SO_4, ext. D_2SO_4

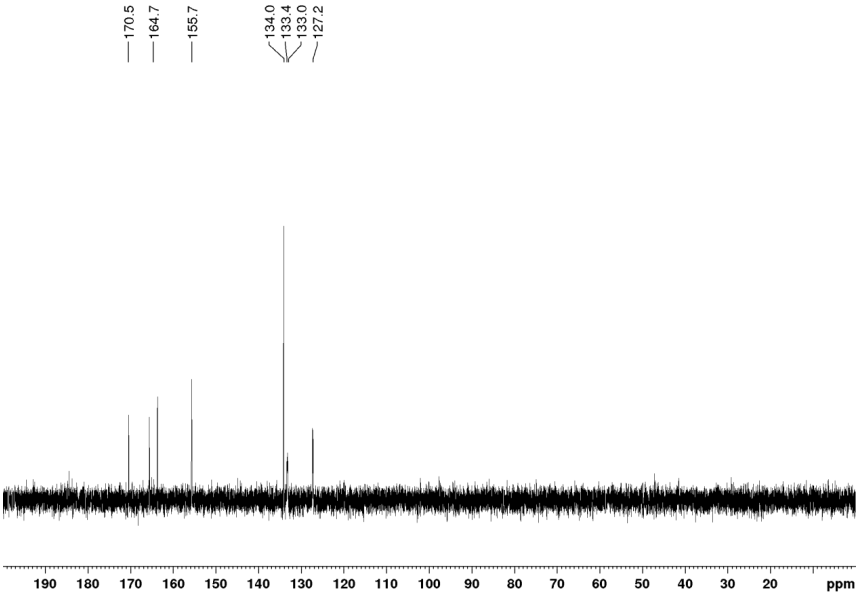

Figure S30. $13C\{^{1}H\}$ spectrum of $\mathbf{10}^{2+}$ in H_2SO_4, ext. D_2SO_4

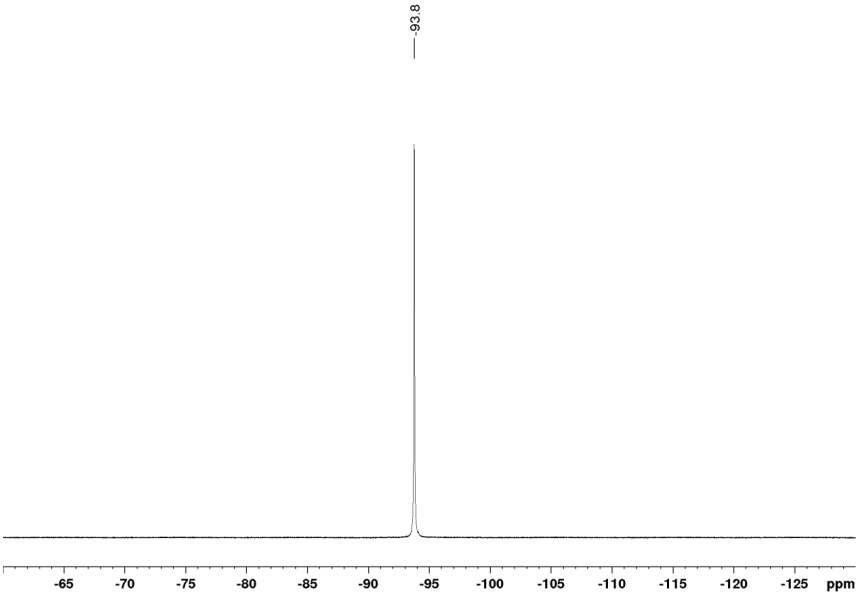

Figure S31. ^{19}F spectrum of $\mathbf{10}^{2+}$ in H_2SO_4, ext. D_2SO_4

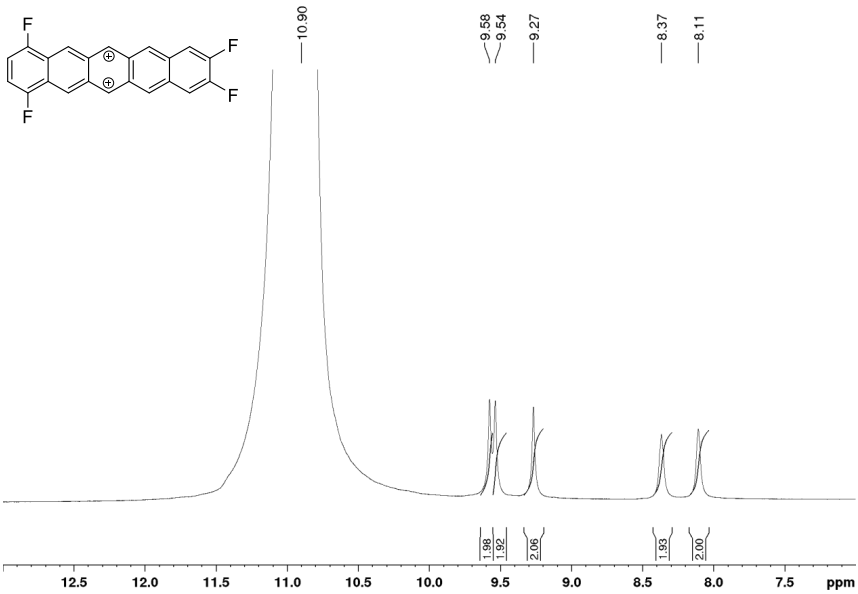

Figure S32. ^{1}H spectrum of $\mathbf{11}^{2+}$ in H_2SO_4, ext. D_2SO_4

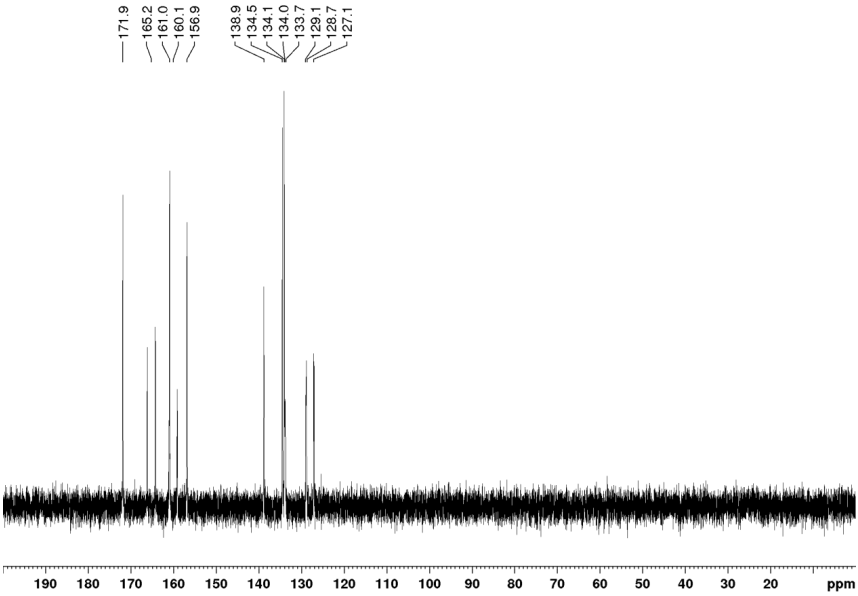

Figure S33. $^{13}C\{^{1}H\}$ spectrum of $\mathbf{11}^{2+}$ in H_2SO_4, ext. D_2SO_4

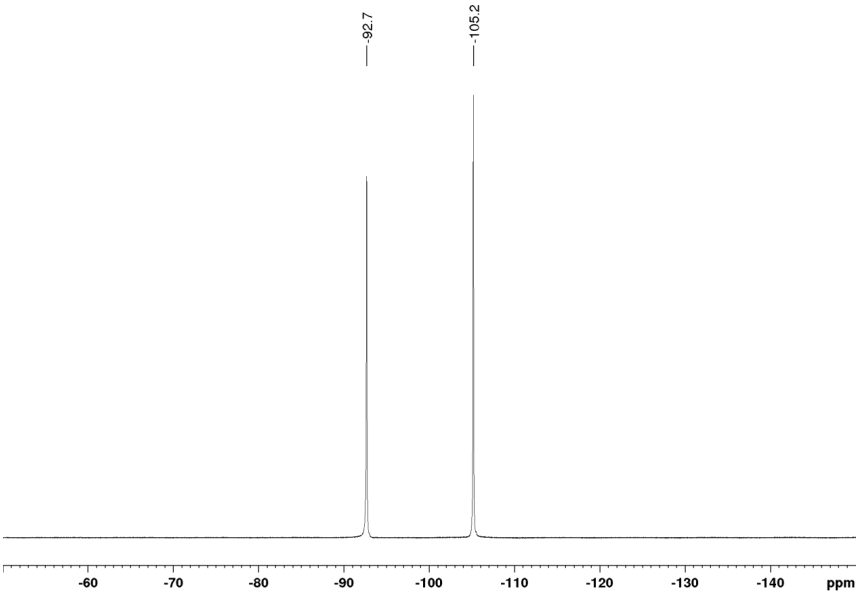

Figure S34. ^{19}F spectrum of $\mathbf{11}^{2+}$ in H_2SO_4, ext. D_2SO_4

Table S1. Comparison of available chemical shifts (in ppm) of bridgehead signals of different acene derivatives.

	δ	
	bridgehead protons	bridgehead carbons
13	5.30	53.6
PcEP[7]	6.28	–
dianthracene[a]	4.54	53.8
1,2,3,4-tetrafluoropentacene dimer[8]	5.00	–
diheptacene[9]	5.30	54.0

[a]Prepared by irradiation of anthracene in degassed toluene using the wavelength region from 305–400 nm.

4. Luminescence data for tetrafluoropentacenes 10–12 at 77 K

Spectra were measured as described in the General Information section. The emission bands at 950, 1056 and 1156 nm were assigned to emission from the NMR tubes used for the measurements. The bands at ~1320–1330 nm were assigned to the $T_1 \rightarrow S_0$ transitions of the tetrafluoropentacenes. The lifetimes of the T_1 states could not be determined due to low signal intensity.

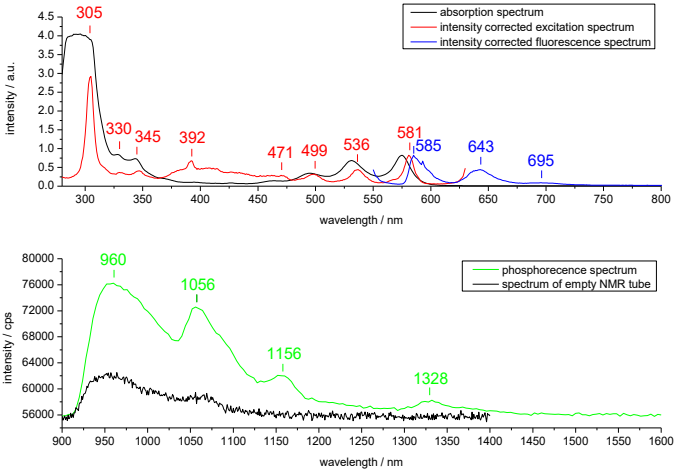

Figure S35. Absorption (at rt), excitation, fluorescence and phosphorescence spectra (at 77 K) of **10** in CD_2Cl_2. Excitation wavelength for the phosphorescence measurement λ_{ex} = 581 nm.

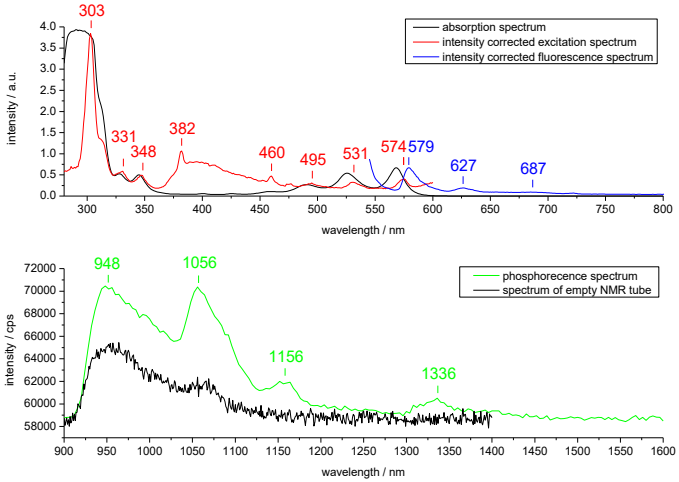

Figure S36. Absorption (at rt), excitation, fluorescence and phosphorescence spectra (at 77 K) of **11** in CD_2Cl_2. Excitation wavelength for the phosphorescence measurement λ_{ex} = 574 nm.

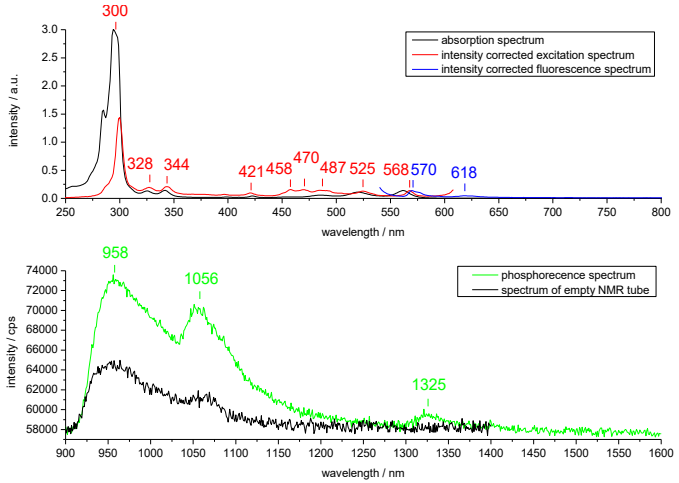

Figure S37. Absorption (at rt), excitation, fluorescence and phosphorescence spectra (at 77 K) of **12** in CD_2Cl_2. Excitation wavelength for the phosphorescence measurement λ_{ex} = 568 nm.

Table S2. Fluorescence lifetimes for tetrafluoropentacenes **10**, **11** and **12** determined in 2-MeTHF at 77 K. Data sets were fitted as biexponential decays, percentage values in parenthesis specify the individual contributions of the lifetimes found to the data fit.

	observed emission band / nm	lifetime / ns
10	585	17.06 (98.6 %), 65.76 (1.37 %)
11	579	10.09 (98.5 %), 55.49 (1.5 %),
12	570	8.88 (57.3 %), 16.4 (42.7 %)

5.Thin film absorption spectra

Thin films were grown by molecular beam deposition as described in the General Information section.

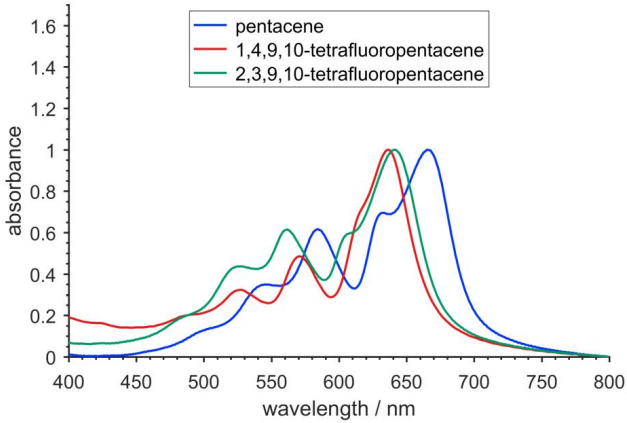

Figure S38. Thin film absorption spectra of pentacene as well as 1,4,9,10- (**11**) and 2,3,9,10-tetrafluoropentacene (**12**).

6. Molecular Electrochemistry

6.1 On the use of relations between formal redox potentials and orbital energies

Formal redox potentials E^0 are related to the relative stability of a redox couples' two components. They are always given relative to the potential of a reference system (in this paper, the ferrocene/ferrocenium couple), including possibly diffusion potentials. Moreover, they are determined for conditions where the redox active species are dissolved and solvated in an electrolyte. The solvent and possibly the ions of the supporting electrolyte will influence the E^0. Although often done in the literature, based on the above facts, here we refrain from using the E^0 values to estimate HOMO and LUMO energies (for a more detailed discussion of the fundamental differences between E^0 and orbital energies, see Cardona et al.[10] and Holze[11]). The estimation of the HOMO-LUMO gap from electrochemical data involves the calculation of the *difference* ΔE^0 of two formal redox potentials. This makes the above problems less severe, because some of the effects may cancel. Thus, even if the potentials under electrochemical solution conditions and their difference on one hand, and the calculated or experimental energy difference between the frontier orbitals on the other hand are fundamentally different quantities, a reasonable correlation is often found. This is also demonstrated by comparing the experimental data to the calculated HOMO and LUMO energies in the case of the tetrafluoropentacenes discussed in this work.

6.2 Demonstration of electrode modification during the first potential cycle on a polished electrode

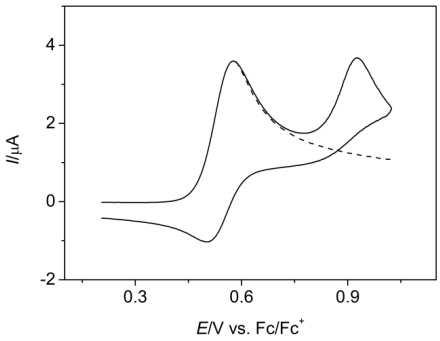

Figure S39. Third cycle in series of cyclic voltammograms of **10** in 1,2-dichloroben-zene/0.1 M NBu_4PF_6 recorded without polishing the Pt electrode surface; v = 0.2 Vs^{-1}, c = 0.59 mM. The broken line indicates the current fraction expected from the first (one-electron) oxidation peak at approximately +0.5 V, generated by simulation.

7. Additional data on the radical cations and dications of 10–12

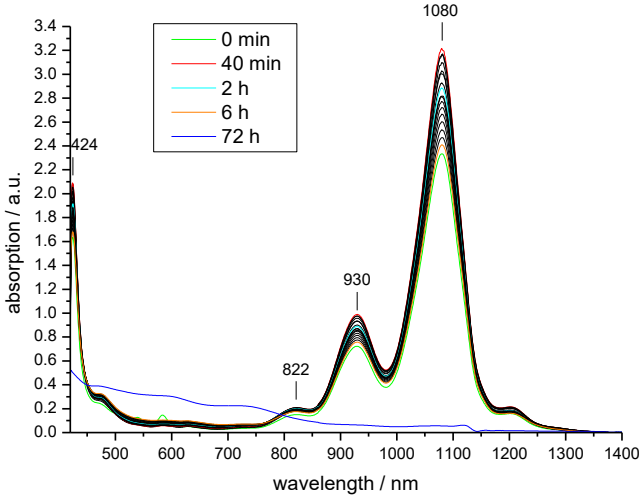

Figure S40. Time dependant UV-Vis spectra of $\mathbf{10}^{+\cdot}$ in 2 M MSA/nitrobenzene. A buildup of the radical cation signals over 40 min is visible.

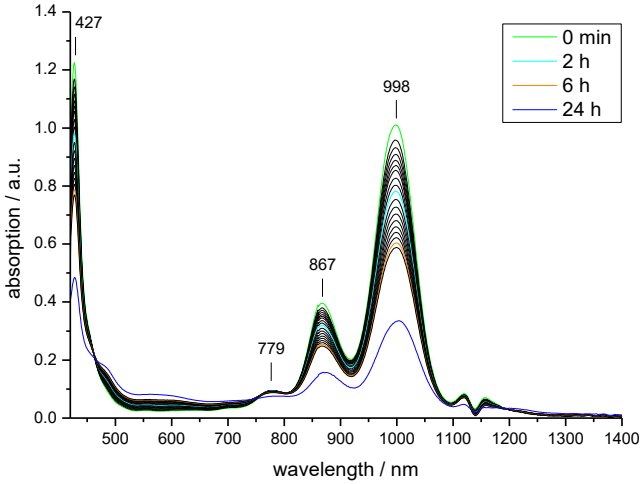

Figure S41. Time dependant UV-Vis spectra of $\mathbf{11}^{+\cdot}$ in 2 M MSA/nitrobenzene.

Table S3. Absorption wavelengths (in nm) of the radical cations in (2 M MSA/nitrobenzene) and the dications (in oleum) of tetrafluoropentacenes **10**–**12**. The transitions of lowest energy were calculated at the UB3LYP/6-311+G** level of theory for the radical cations and at the B3LYP/6-311+G** level of theory for the dications.

	absorption wavelength	calcd.
$\mathbf{12}^{+\cdot}$	437, 734, 817, 920	957
$\mathbf{11}^{+\cdot}$	427, 779, 868, 998	999
$\mathbf{10}^{+\cdot}$	424, 822, 930, 1080	1043
$\mathbf{12}^{2+}$	390, 709, 760	667[a]
$\mathbf{11}^{2+}$	389, 798	695[b]
$\mathbf{10}^{2+}$	366, 844	722

[a]The first transition (793 nm) was not considered as it shows an oscillator strength of 0. [b]The first transition (702 nm) was not considered as it shows an oscillator strength of only 0.0043.

8. OFET data

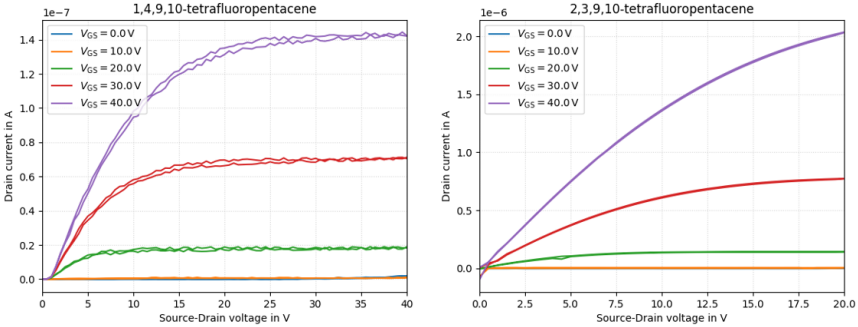

Figure S42. Output characteristics of devices fabricated from 1,4,9,10- (**11**) and 2,3,9,10-tetrafluoropentacene (**12**).

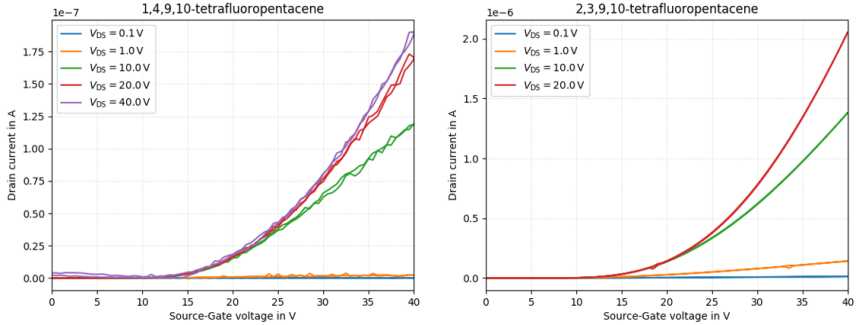

Figure S43. Transfer characteristics of devices fabricated from 1,4,9,10- (**11**) and 2,3,9,10-tetrafluoropentacene (**12**).

The device characteristics for the 1,4,9,10-tetrafluoropentacene (**11**) device were obtained for a device with a channel width of 1000 µm and a channel length of 150 µm. The 2,3,9,10-tetrafluoropentacene (**12**) device had the same channel width and a channel length of 50 µm.

9. Crystallographic data

Single crystals of the respective compounds were investigated on a Bruker APEX II DUO instrument equipped with a IμS microfocus sealed tube. Data for compounds **10** and **11** was collected on a Rigaku XtaLAB Synergy-S diffractometer with a PhotonJet (Cu) microfocus source. The data collection strategy for the measurements done with Bruker APEX II DUO was determined using COSMO[12] employing ω-scans. Raw data were processed using APEX[13] and SAINT,[14] corrections for absorption effects were applied using SADABS.[15] The structures were solved by direct methods and refined against all data by full-matrix least-squares methods on F^2 using SHELXTL[16] and Shelxle.[17] Hydrogen atoms were placed in calculated positions and refined with suitable AFIX, but are omitted for clarity.

5,6,7,8-Tetramethylidenebicyclo[2.2.2]oct-2-ene (1)

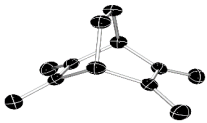

CCDC	1967865	
Empirical formula	C12 H12	
Formula weight	156.22 g·mol^{-1}	
Temperature	100(2) K	
Wavelength	0.71073 Å	
Crystal system	Orthorhombic	
Space group	*F mm2*	
Unit cell dimensions	a = 11.549(4) Å	α = 90°
	b = 13.427(5) Å	β = 90°
	c = 5.818(2) Å	γ = 90°
Volume	902.2(5) Å^3	
Z	4	
Density (calculated)	1.150 g/cm^3	
Absorption coefficient	0.065 mm^{-1}	
F(000)	336	
Crystal size	0.289 x 0.075 x 0.038 mm^3	
Theta range for data collection	3.034 to 28.340°	
Index ranges	$-15 \le h \le 15$, $-17 \le k \le 17$, $-7 \le l \le 7$	
Reflections collected	6036	
Independent reflections	610 [R_{int} = 0.0649]	
Completeness to theta = 25.242°	99.6 %	
Absorption correction	Semi-empirical from equivalents	
Refinement method	Full-matrix least-squares on F^2	
Data / restraints / parameters	610 / 1 / 31	
Goodness-of-fit on F^2	1.089	

Final R indices [I≥2σ(I)]	R_1 = 0.0373, wR_2 = 0.0904
R indices (all data)	R_1 = 0.0418, wR_2 = 0.0946
Absolute structure parameter	-10(1)
Largest diff. peak and hole	0.183 and -0.206 e·Å^{-3}

1,4,8,11-Tetrafluoro-6,13-dihydro-6,13-ethenopentacene (5)

CCDC	1967866	
Empirical formula	C24 H12 F4	
Formula weight	376.34 g·mol^{-1}	
Temperature	100(2) K	
Wavelength	0.71073 Å	
Crystal system	Monoclinic	
Space group	*C 2/c*	
Unit cell dimensions	*a* = 9.467(2) Å	α = 90°
	b = 12.605(2) Å	β = 104.736(2)°
	c = 14.064(3) Å	γ = 90°
Volume	1623.0(5) Å^3	
Z	4	
Density (calculated)	1.540 g/cm^3	
Absorption coefficient	0.121 mm^{-1}	
F(000)	768	
Crystal size	0.136 x 0.115 x 0.110 mm^3	
Theta range for data collection	2.750 to 26.394°	
Index ranges	-11 ≤ h ≤ 11, -15 ≤ k ≤ 15, -17 ≤ l ≤ 17	
Reflections collected	15840	
Independent reflections	1666 [R_{int} = 0.0546]	
Completeness to theta = 25.242°	99.9 %	
Absorption correction	Semi-empirical from equivalents	
Max. and min. transmission	0.7454 and 0.6627	
Refinement method	Full-matrix least-squares on F^2	
Data / restraints / parameters	1666 / 0 / 151	
Goodness-of-fit on F^2	1.064	
Final R indices [I≥2σ(I)]	R_1 = 0.0410, wR_2 = 0.1067	
R indices (all data)	R_1 = 0.0542, wR_2 = 0.1154	
Largest diff. peak and hole	0.261 and -0.188 e·Å^{-3}	

1,4,9,10-Tetrafluoro-6,13-dihydro-6,13-ethenopentacene (8)

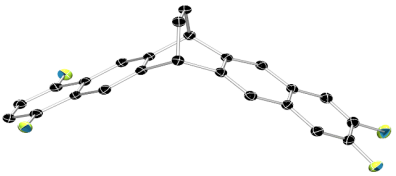

CCDC	1967867	
Empirical formula	C24 H12 F4	
Formula weight	376.34 g·mol^{-1}	
Temperature	100(2) K	
Wavelength	0.71073 Å	
Crystal system	Triclinic	
Space group	$P\bar{1}$	
Unit cell dimensions	a = 6.298(3) Å	α = 74.59(1)°
	b = 9.571(4) Å	β = 84.35(1)°
	c = 14.408(8) Å	γ = 74.064(5)°
Volume	804.7(6) Å^3	
Z	2	
Density (calculated)	1.553 g/cm^3	
Absorption coefficient	0.122 mm^{-1}	
F(000)	384	
Crystal size	0.424 x 0.219 x 0.168 mm^3	
Theta range for data collection	3.545 to 28.732°	
Index ranges	$-8 \le h \le 8$, $-12 \le k \le 12$, $-19 \le l \le 19$	
Reflections collected	20544	
Independent reflections	4155 [R_{int} = 0.0521]	
Completeness to theta = 25.242°	99.7 %	
Absorption correction	Numerical	
Max. and min. transmission	0.7458 and 0.5823	
Refinement method	Full-matrix least-squares on F^2	
Data / restraints / parameters	4155 / 0 / 301	
Goodness-of-fit on F^2	1.057	
Final R indices [I≥2σ(I)]	R_1 = 0.0424, wR_2 = 0.1163	
R indices (all data)	R_1 = 0.0503, wR_2 = 0.1246	
Largest diff. peak and hole	0.447 and -0.240 e·Å^{-3}	

1,4,8,11-Tetrafluoropentacene (10)

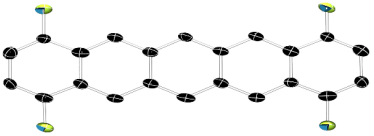

CCDC	1915510	
Empirical formula	C22 H10 F4	
Formula weight	350.30 g·mol^{-1}	
Temperature	100(2) K	
Wavelength	1.54184 Å	
Crystal system	Monoclinic	
Space group	*P* 2_1	
Unit cell dimensions	*a* = 3,7815(2) Å	α = 90°
	b = 27.642(2) Å	β = 93.428(5)°
	c = 6.9428(5) Å	γ = 90°
Volume	724.42(8) Å^3	
Z	2	
Density (calculated)	1.606 g/cm^3	
Absorption coefficient	1.098 mm^{-1}	
F(000)	356	
Crystal size	0.206 x 0.025 x 0.013 mm^3	
Theta range for data collection	3.198 to 66.583°	
Index ranges	$-4 \le h \le 4$, $-32 \le k \le 28$, $-8 \le l \le 7$	
Reflections collected	3868	
Independent reflections	2101 [R_{int} = 0.0313]	
Completeness to theta = 66.583°	98.6 %	
Absorption correction	Gaussian	
Max. and min. transmission	1.000 and 0.652	
Refinement method	Full-matrix least-squares on F^2	
Data / restraints / parameters	2101 / 1 / 235	
Goodness-of-fit on F^2	1.021	
Final R indices [I≥2σ(I)]	R_1 = 0.0618, wR_2 = 0.1609	
R indices (all data)	R_1 = 0.0734, wR_2 = 0.1695	
Absolute structure parameter	0.6(2)	
Largest diff. peak and hole	0.467 and -0.406 e·Å^{-3}	

1,4,8,11-Tetrafluoropentacene (11)

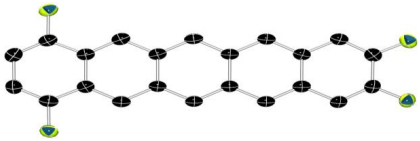

CCDC	1967949	
Empirical formula	C44 H20 F8	
Formula weight	700.60 g·mol^{-1}	
Temperature	100(2) K	
Wavelength	1.54184 Å	
Crystal system	monoclinic	
Space group	*P* $2_1/n$	
Unit cell dimensions	*a* = 18.197(1) Å	*α* = 90°
	b = 5.9311(4) Å	*β* = 92.233(5)°
	c = 26.659(2) Å	*γ* = 90°
Volume	2875.1(3) Å^3	
Z	4	
Density (calculated)	1.619 g/cm^3	
Absorption coefficient	1.106 mm^{-1}	
F(000)	1424.0	
Crystal size	0.258 × 0.026 × 0.002 mm^3	
Theta range for data collection	5.99 to 134.128°	
Index ranges	$-21 \le h \le 21$, $-7 \le k \le 7$, $-28 \le l \le 31$	
Reflections collected	44193	
Independent reflections	5093 [R_{int} = 0.1484, R_{sigma} = 0.0732]	
Data/restraints/parameters	5093 / 0 / 469	
Goodness-of-fit on F^2	1.018	
Final R indexes [I≥2σ(I)]	R_1 = 0.0702, wR_2 = 0.1751	
Final R indexes [all data]	R_1 = 0.1010, wR_2 = 0.1974	
Largest diff. peak and hole	0.53 and -0.34 e·Å^{-3}	

10. Computational details

All calculations were performed using Gaussian 09.[18] The transformation of **5** and **8** to the **10** and **11**, respectively, was investigated using the M06-2X[19] functional and the 6-31G* basis set by geometry optimizations of all relevant minima and transition states. Vibrational frequencies were calculated at the same level of theory to verify that the structure is an energy minimum or a transition state and to evaluate zero-point vibrational energies (ZVPE) as well as thermal corrections at 298 K.

In addition, the structures of acenes **10**–**12,** the radical cations $\mathbf{10}^{+\cdot}$–$\mathbf{12}^{+\cdot}$ and dications $\mathbf{10}^{2+}$–$\mathbf{12}^{2+}$ were also optimized using Becke's[20] three parameter hybrid functional in conjunction with the correlation functional of Lee, Yang, and Parr[21] (B3LYP) and the 6-311+G** basis set as implemented[22] in Gaussian 09. The lowest energy excited states of the radical cations and dications were computed at the geometry of the ground states using the time-dependent density functional theory (TD-DFT).[23] The TD-DFT computations employed the B3LYP functional and the 6-311+G** basis set.

Transition states for reactions with 1,2,4,5-tetrazine

Transition states for both syntheses are shown in Figure S44. For better comparability with the already published data[24] the reaction of the ethenopentacenes **5** and **8** with unsubstituted 1,2,4,5-tetrazine was studied computationally. The extrusion of N_2 from the initial Diels-Alder adducts[24, 25] was considered to be occurring without a barrier[26] and therefore is omitted in the presented data.

For the synthesis of **11** two reaction pathways leading to the same product (addition of the tetrazine from either the 1,4- or 9,10-difluorosubstituted side) have to be considered. Both pathways were investigated, but since the initial addition from the 1,4-side is 0.2 kcal·mol^{-1} lower in energy, only this pathway was used for energetic comparison with the other syntheses

(Table S4). The calculations show no significant difference between the obtained activation energies with maximum differences of 0.1 kcal·mol^{-1} for TS1 and 0.3 kcal·mol^{-1} for TS3 overall.

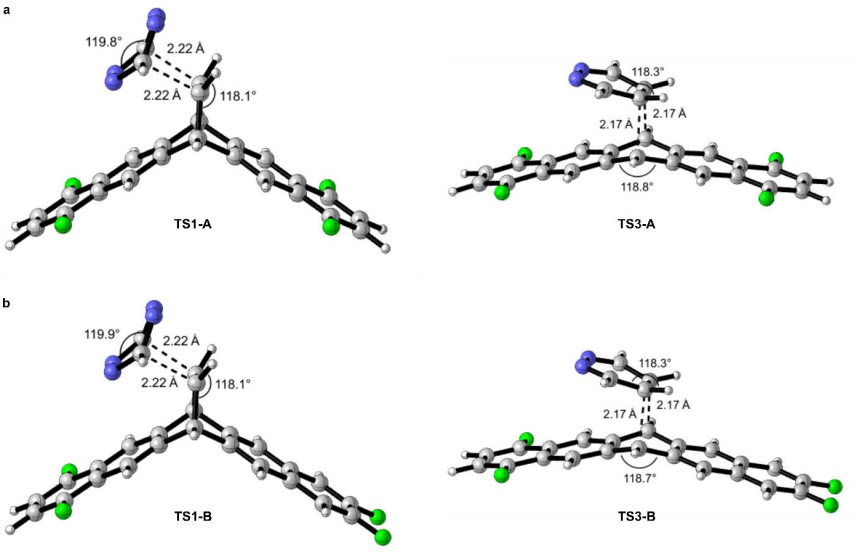

Figure S44. Transition states for the initial Diels-Alder reaction (left) and retro-Diels-Alder reactions (right) calculated on the M06-2X/6-31G* level of theory. Intermolecular distances (in Å) of the reaction sites and values for selected dihedral angles are given. For **11** (b) only the transition state of the addition of the tetrazine from the 1,4-difluorosubstituted side is shown since it is lower in energy.

Table S4. Energy barriers including Zero-Point Vibrational Energy corrections (ΔE_0, in kcal·mol^{-1}) for transition states of the Diels-Alder-retro-Diels-Alder sequences of ethenopentacenes **5** and **8** with unsubstituted 1,2,4,5-tetrazine. Values for the same reaction sequences with the precursor of 2,3,9,10-tetrafluoropentacene (**12**)[24] are given for comparison. Calculations were performed at the M06-2X/6-31G* level of theory.

	10	**11**	**12**
ΔE_0(TS1)	11.8	11.9	11.8
ΔE_0(TS3)	36.4	36.4	36.1

Orbital plots and spin density

Structures of radical cationic species **10**$^{+\cdot}$ and **11**$^{+\cdot}$ were optimized at the UB3LYP/6-311+G** level of theory. The HOMOs of both compounds were rendered using a contour value of 0.045 facilitating comparability while simultaneously showing that the HOMO of **11**$^{+\cdot}$ is not symmetric due to the substitution.

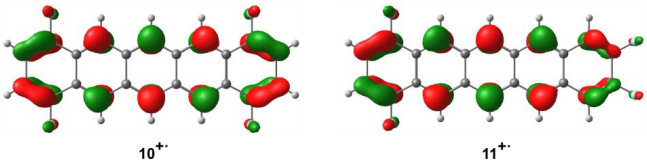

Figure S45. Orbital plots of **10**$^{+\cdot}$ and **11**$^{+\cdot}$.

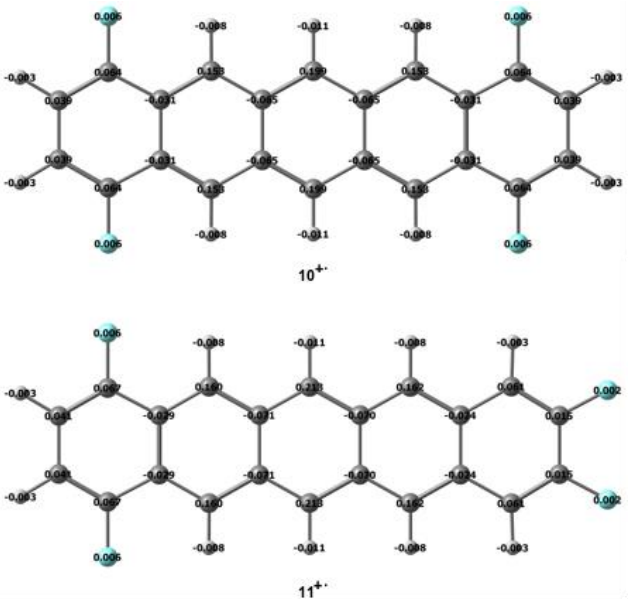

Figure S46. Calculated spin densities of **10**$^{+\cdot}$ and **11**$^{+\cdot}$.

11. Cartesian coordinates

M06-2X/6-31G*			
9			
E(SCF) = -296.202949016			
N	0.000000000	1.190230000	0.657039000
C	0.000000000	0.000000000	1.260279000
C	0.000000000	0.000000000	-1.260279000
N	0.000000000	1.190230000	-0.657039000
H	0.000000000	0.000000000	2.344928000
H	0.000000000	0.000000000	-2.344928000
N	0.000000000	-1.190230000	-0.657039000
N	0.000000000	-1.190230000	0.657039000

M06-2X/6-31G*			
5			
E(SCF) = -1320.64245817			
C	-5.362142000	-0.706841000	-1.509085000
C	-4.339040000	-1.372776000	-0.896025000
C	-3.266993000	-0.709866000	-0.253787000
C	-3.266991000	0.709867000	-0.253789000
C	-4.339038000	1.372778000	-0.896028000
C	-5.362141000	0.706845000	-1.509086000
H	-2.214054000	-2.501588000	0.370707000
F	-4.326664000	-2.717036000	-0.887451000
C	-2.207642000	-1.416286000	0.381121000
C	-2.207638000	1.416286000	0.381115000
F	-4.326659000	2.717038000	-0.887457000
C	-1.209628000	0.713022000	0.990233000
C	-1.209630000	-0.713023000	0.990237000
H	-2.214048000	2.501589000	0.370701000
C	1.209628000	-0.713023000	0.990233000
C	2.207638000	-1.416287000	0.381115000
C	3.266991000	-0.709867000	-0.253790000
C	3.266993000	0.709866000	-0.253786000
C	2.207641000	1.416285000	0.381122000
C	1.209630000	0.713022000	0.990237000
F	4.326660000	-2.717037000	-0.887459000
H	2.214048000	-2.501589000	0.370699000
C	4.339037000	-1.372777000	-0.896030000
C	4.339040000	1.372776000	-0.896024000
H	2.214054000	2.501588000	0.370710000

C	5.362142000	0.706843000	-1.509085000
C	5.362141000	-0.706843000	-1.509088000
F	4.326665000	2.717037000	-0.887448000
C	-0.000001000	1.292478000	1.715207000
C	0.000000000	-1.292480000	1.715206000
C	0.000006000	-0.665852000	3.107401000
C	-0.000005000	0.665848000	3.107401000
H	0.000010000	-1.283983000	3.998017000
H	-0.000009000	1.283978000	3.998018000
H	-0.000001000	2.383906000	1.723578000
H	0.000001000	-2.383908000	1.723577000
H	-6.156547000	1.267987000	-1.986958000
H	-6.156550000	-1.267983000	-1.986955000
H	6.156549000	1.267986000	-1.986954000
H	6.156547000	-1.267985000	-1.986959000

M06-2X/6-31G*			
8			
E(SCF) = -1320.63521865			
C	-5.426729000	-1.762263000	0.708848000
C	-4.448516000	-1.079044000	1.374069000
C	-3.421927000	-0.367190000	0.710329000
C	-3.421905000	-0.368911000	-0.709471000
C	-4.448465000	-1.082400000	-1.371506000
C	-5.426696000	-1.764004000	-0.704651000
H	-2.411876000	0.328022000	2.501092000
F	-4.437226000	-1.068055000	2.718468000
C	-2.406454000	0.336942000	1.415735000
C	-2.406417000	0.333527000	-1.416550000
F	-4.437121000	-1.074713000	-2.715927000
C	-1.449908000	1.007172000	-0.714317000
C	-1.449918000	1.008877000	0.711906000
H	-2.411807000	0.321992000	-2.501881000
C	0.964385000	1.155658000	0.710878000
C	2.001353000	0.608980000	1.408490000
C	3.104933000	0.037624000	0.711834000
C	3.104914000	0.035894000	-0.711923000
C	2.001330000	0.605585000	-1.409942000
C	0.964381000	1.153968000	-0.713636000
H	2.003272000	0.604195000	2.496039000
C	4.205923000	-0.526712000	1.406035000
C	4.205880000	-0.530144000	-1.404771000
H	2.003231000	0.598168000	-2.497476000
C	5.248791000	-1.062474000	-0.704775000
C	5.248813000	-1.060753000	0.707312000

C	-0.286901000	1.803989000	-1.294661000
C	-0.286898000	1.807042000	1.290365000
C	-0.371122000	3.196113000	0.662082000
C	-0.371126000	3.194542000	-0.669645000
H	-0.422202000	4.086263000	1.278908000
H	-0.422206000	4.083233000	-1.288574000
H	-0.288077000	1.811325000	-2.386204000
H	-0.288075000	1.816954000	2.381887000
H	-6.187338000	-2.294510000	-1.265290000
H	-6.187403000	-2.291370000	1.270764000
H	4.232872000	-0.545125000	-2.489501000
H	4.232947000	-0.539040000	2.490798000
F	6.302719000	-1.600923000	-1.324502000
F	6.302776000	-1.597665000	1.328320000

M06-2X/6-31G*			
TS1-A			
E(SCF) = -1616.82855526			
C	4.579543000	-3.077774000	-0.707165000
C	3.666513000	-2.311965000	-1.373796000
C	2.709593000	-1.508262000	-0.710035000
C	2.709591000	-1.508223000	0.710128000
C	3.666508000	-2.311891000	1.373935000
C	4.579541000	-3.077736000	0.707348000
H	1.782907000	-0.714223000	-2.500883000
F	3.652278000	-2.303704000	-2.717436000
C	1.766600000	-0.717092000	-1.415662000
C	1.766596000	-0.717013000	1.415709000
F	3.652269000	-2.303560000	2.717574000
C	0.872596000	0.037695000	0.710953000
C	0.872598000	0.037654000	-0.710949000
H	1.782903000	-0.714083000	2.500930000
C	-1.508596000	0.467382000	-0.714176000
C	-2.597460000	0.043290000	-1.416847000
C	-3.751475000	-0.399194000	-0.709622000
C	-3.751479000	-0.399154000	0.709628000
C	-2.597467000	0.043369000	1.416834000
C	-1.508600000	0.467422000	0.714146000
F	-4.902557000	-0.840276000	-2.716712000
H	-2.605840000	0.032726000	-2.502172000
C	-4.916804000	-0.846456000	-1.373181000
C	-4.916812000	-0.846379000	1.373205000
H	-2.605854000	0.032866000	2.502159000
C	-6.030133000	-1.275335000	0.706377000
C	-6.030129000	-1.275375000	-0.706335000

F	-4.902573000	-0.840123000	2.716736000
C	-0.181696000	0.956202000	1.296575000
C	-0.181691000	0.956128000	-1.296626000
N	2.843224000	2.217204000	-0.644605000
C	2.010883000	3.122352000	-1.227665000
C	-0.002559000	2.352630000	-0.691552000
C	-0.002567000	2.352671000	0.691421000
C	2.010861000	3.122469000	1.227509000
N	2.843213000	2.217266000	0.644551000
H	-0.387271000	3.202654000	-1.244898000
H	-0.387293000	3.202724000	1.244715000
H	-0.178224000	0.959024000	2.388702000
H	-0.178213000	0.958888000	-2.388753000
N	1.815654000	4.346786000	0.640768000
N	1.815667000	4.346725000	-0.641045000
H	1.931474000	3.083472000	-2.308626000
H	1.931433000	3.083694000	2.308472000
H	-6.895137000	-1.607445000	-1.268441000
H	-6.895144000	-1.607374000	1.268497000
H	5.290733000	-3.672124000	1.268833000
H	5.290739000	-3.672191000	-1.268617000

M06-2X/6-31G*			
TS1-A, product after loss of N_2			
E(SCF) = -1507.45870748			
C	-5.183096000	-2.272575000	0.707784000
C	-4.166102000	-1.652607000	1.374587000
C	-3.098018000	-1.002283000	0.710287000
C	-3.098047000	-1.002497000	-0.709858000
C	-4.166158000	-1.653021000	-1.373919000
C	-5.183125000	-2.272787000	-0.706888000
H	-2.058368000	-0.358716000	2.500356000
F	-4.150790000	-1.644919000	2.717750000
C	-2.045830000	-0.360031000	1.414869000
C	-2.045891000	-0.360451000	-1.414676000
F	-4.150900000	-1.645739000	-2.717085000
C	-1.039556000	0.242638000	-0.713117000
C	-1.039523000	0.242847000	0.713089000
H	-2.058479000	-0.359454000	-2.500162000
C	1.400837000	0.410527000	0.713358000
C	2.477183000	-0.058075000	1.414536000
C	3.605099000	-0.555896000	0.710051000
C	3.605064000	-0.556084000	-0.710105000
C	2.477115000	-0.058449000	-1.414668000
C	1.400802000	0.410340000	-0.713562000

F	4.734224000	-1.051212000	2.717327000
H	2.487887000	-0.061287000	2.500042000
C	4.749389000	-1.059964000	1.374066000
C	4.749323000	-1.060331000	-1.374040000
H	2.487766000	-0.061949000	-2.500173000
C	5.839812000	-1.540187000	-0.707312000
C	5.839847000	-1.539997000	0.707414000
F	4.734093000	-1.051940000	-2.717302000
C	0.135581000	0.991363000	-1.300626000
C	0.135652000	0.991721000	1.300331000
N	-2.163720000	3.652666000	0.714909000
C	-1.187530000	3.127806000	1.336846000
C	0.040685000	2.464923000	0.772640000
C	0.040601000	2.464710000	-0.773327000
C	-1.187736000	3.127329000	-1.337578000
N	-2.163854000	3.652366000	-0.715677000
H	-1.264082000	3.154768000	2.426540000
H	-1.264484000	3.153848000	-2.427269000
H	0.916128000	3.002648000	1.154698000
H	0.915968000	3.002380000	-1.155638000
H	0.135866000	0.969376000	-2.394771000
H	0.135995000	0.970029000	2.394482000
H	-5.975542000	-2.755400000	-1.266776000
H	-5.975490000	-2.755023000	1.267848000
H	6.689349000	-1.911901000	-1.268222000
H	6.689412000	-1.911556000	1.268383000

M06-2X/6-31G*			
TS3-A			
E(SCF) = -1507.39632626			
C	-5.729371000	-0.712120000	-1.404027000
C	-4.582691000	-1.379155000	-1.112829000
C	-3.360358000	-0.714933000	-0.803175000
C	-3.360343000	0.715279000	-0.802983000
C	-4.582662000	1.379609000	-1.112459000
C	-5.729357000	0.712675000	-1.403835000
H	-2.203717000	-2.495307000	-0.466146000
F	-4.561721000	-2.721593000	-1.108995000
C	-2.188170000	-1.410270000	-0.493446000
C	-2.188141000	1.410508000	-0.493060000
F	-4.561665000	2.722046000	-1.108259000
C	-1.011627000	0.715929000	-0.232456000
C	-1.011638000	-0.715785000	-0.232661000
H	-2.203669000	2.495538000	-0.465456000
C	1.456398000	-0.715547000	-0.078584000

C	2.652884000	-1.410996000	-0.231712000
C	3.849446000	-0.716067000	-0.425116000
C	3.849453000	0.716238000	-0.424847000
C	2.652899000	1.411109000	-0.231190000
C	1.456404000	0.715618000	-0.078323000
F	5.075304000	-2.721993000	-0.620281000
H	2.661969000	-2.496582000	-0.221737000
C	5.096365000	-1.379430000	-0.625153000
C	5.096379000	1.379662000	-0.624638000
H	2.661999000	2.496691000	-0.220817000
C	6.264361000	0.713025000	-0.811484000
C	6.264353000	-0.712734000	-0.811751000
F	5.075328000	2.722223000	-0.619268000
C	0.198799000	1.353961000	0.201707000
C	0.198793000	-1.353976000	0.201248000
N	-2.236310000	-0.693855000	2.834683000
C	-1.118921000	-1.323107000	2.652463000
C	0.132416000	-0.716078000	2.276712000
C	0.132282000	0.715340000	2.276946000
C	-1.119206000	1.321978000	2.652839000
N	-2.236460000	0.692425000	2.834864000
H	-1.176859000	-2.408023000	2.737337000
H	-1.177398000	2.406859000	2.738003000
H	1.048728000	-1.258785000	2.481959000
H	1.048474000	1.258152000	2.482459000
H	0.194177000	2.439930000	0.285339000
H	0.194158000	-2.439973000	0.284521000
H	7.182463000	-1.269107000	-0.959252000
H	7.182477000	1.269443000	-0.958779000
H	-6.630543000	1.269794000	-1.630904000
H	-6.630568000	-1.269164000	-1.631243000

M06-2X/6-31G*			
TS1-B			
E(SCF) = -1616.82153695			
C	4.576396000	-3.270646000	-0.707202000
C	3.700833000	-2.462180000	-1.373743000
C	2.784205000	-1.613009000	-0.709885000
C	2.784206000	-1.612969000	0.709980000
C	3.700834000	-2.462104000	1.373884000
C	4.576396000	-3.270607000	0.707388000
H	1.900523000	-0.772508000	-2.500688000
F	3.686678000	-2.453029000	-2.717469000
C	1.882486000	-0.775259000	-1.415484000
C	1.882487000	-0.775179000	1.415532000

F	3.686680000	-2.452878000	2.717609000
C	1.027754000	0.024092000	0.711118000
C	1.027754000	0.024051000	-0.711114000
H	1.900525000	-0.772366000	2.500736000
C	-1.326511000	0.590836000	-0.713304000
C	-2.442674000	0.233615000	-1.409812000
C	-3.628973000	-0.137785000	-0.711614000
C	-3.628975000	-0.137741000	0.711618000
C	-2.442679000	0.233700000	1.409797000
C	-1.326513000	0.590878000	0.713272000
H	-2.445197000	0.225856000	-2.497313000
C	-4.809923000	-0.504488000	-1.405628000
C	-4.809929000	-0.504400000	1.405649000
H	-2.445206000	0.226006000	2.497299000
C	-5.928915000	-0.851718000	0.706104000
C	-5.928912000	-0.851762000	-0.706067000
C	0.026346000	1.000228000	1.296563000
C	0.026348000	1.000153000	-1.296616000
N	3.120453000	2.094230000	-0.644631000
C	2.339272000	3.043532000	-1.227767000
C	0.286266000	2.384254000	-0.691575000
C	0.286264000	2.384294000	0.691441000
C	2.339264000	3.043612000	1.227601000
N	3.120449000	2.094272000	0.644532000
H	-0.049503000	3.254871000	-1.244667000
H	-0.049509000	3.254943000	1.244481000
H	0.030875000	1.003148000	2.388767000
H	0.030879000	1.003010000	-2.388820000
N	2.209205000	4.276410000	0.640748000
N	2.209209000	4.276368000	-0.640996000
H	2.258592000	3.009588000	-2.308813000
H	2.258578000	3.009741000	2.308649000
H	5.258117000	-3.898282000	1.269235000
H	5.258117000	-3.898352000	-1.269015000
H	-4.838448000	-0.513543000	2.490353000
H	-4.838438000	-0.513699000	-2.490332000
F	-7.058003000	-1.199658000	1.327098000
F	-7.057997000	-1.199742000	-1.327044000

M06-2X/6-31G*			
TS1-B, product after loss of N_2			
E(SCF) = -1507.45156076			
C	-5.142176000	-2.581322000	0.707692000
C	-4.181122000	-1.877327000	1.374462000
C	-3.171529000	-1.139984000	0.710377000

C	-3.171534000	-1.140204000	-0.709984000
C	-4.181132000	-1.877749000	-1.373836000
C	-5.142181000	-2.581538000	-0.706844000
H	-2.189221000	-0.411860000	2.500241000
F	-4.167506000	-1.868299000	2.717883000
C	-2.176397000	-0.412543000	1.414705000
C	-2.176412000	-0.412975000	-1.414544000
F	-4.167525000	-1.869130000	-2.717261000
C	-1.223022000	0.271138000	-0.713102000
C	-1.223012000	0.271353000	0.713044000
H	-2.189250000	-0.412623000	-2.500081000
C	1.195785000	0.628959000	0.712513000
C	2.306170000	0.238013000	1.407558000
C	3.473306000	-0.181491000	0.712211000
C	3.473282000	-0.181691000	-0.712286000
C	2.306128000	0.237630000	-1.407714000
C	1.195765000	0.628772000	-0.712742000
H	2.309968000	0.236292000	2.495277000
C	4.637778000	-0.603133000	1.406755000
C	4.637729000	-0.603538000	-1.406749000
H	2.309894000	0.235612000	-2.495432000
C	5.737426000	-1.002598000	-0.706959000
C	5.737453000	-1.002390000	0.707042000
C	-0.110427000	1.110323000	-1.300475000
C	-0.110386000	1.110681000	1.300154000
N	-2.615077000	3.576730000	0.714922000
C	-1.598760000	3.134215000	1.336709000
C	-0.321467000	2.571601000	0.772698000
C	-0.321553000	2.571381000	-0.773410000
C	-1.598986000	3.133674000	-1.337431000
N	-2.615223000	3.576380000	-0.715652000
H	-1.676686000	3.156343000	2.426438000
H	-1.677128000	3.155283000	-2.427156000
H	0.508797000	3.176836000	1.154575000
H	0.508609000	3.176581000	-1.155565000
H	-0.108989000	1.088354000	-2.394735000
H	-0.108915000	1.089010000	2.394421000
H	-5.891769000	-3.127720000	-1.267291000
H	-5.891758000	-3.127338000	1.268309000
H	4.665650000	-0.615313000	-2.491441000
H	4.665738000	-0.614591000	2.491450000
F	6.849310000	-1.405497000	-1.325434000
F	6.849365000	-1.405094000	1.325594000

M06-2X/6-31G*			
TS3-B			
E(SCF) = -1507.38940799			
C	-5.869169000	-0.711208000	-1.506216000
C	-4.729004000	-1.378282000	-1.190308000
C	-3.514005000	-0.714338000	-0.852904000
C	-3.513998000	0.715701000	-0.851880000
C	-4.728996000	1.380135000	-1.188325000
C	-5.869166000	0.713519000	-1.505190000
H	-2.365256000	-2.494904000	-0.490840000
F	-4.708054000	-2.720858000	-1.187146000
C	-2.348818000	-1.409836000	-0.517378000
C	-2.348799000	1.410705000	-0.515363000
F	-4.708039000	2.722706000	-1.183232000
C	-1.178526000	0.716076000	-0.228919000
C	-1.178536000	-0.715631000	-0.229941000
H	-2.365225000	2.495734000	-0.487267000
C	1.285444000	-0.714755000	-0.024392000
C	2.488454000	-1.404080000	-0.150181000
C	3.696050000	-0.718402000	-0.318271000
C	3.696068000	0.718917000	-0.317106000
C	2.488483000	1.404355000	-0.147964000
C	1.285452000	0.714861000	-0.023292000
H	2.490434000	-2.491684000	-0.139317000
C	4.934354000	-1.413122000	-0.491367000
C	4.934400000	1.413879000	-0.489037000
H	2.490488000	2.491942000	-0.135391000
C	6.084083000	0.713402000	-0.648690000
C	6.084057000	-0.712423000	-0.649889000
C	0.022812000	1.353286000	0.232017000
C	0.022803000	-1.353542000	0.230012000
N	-2.471040000	-0.695489000	2.813795000
C	-1.350161000	-1.324466000	2.652914000
C	-0.091533000	-0.717488000	2.302642000
C	-0.091677000	0.714080000	2.303728000
C	-1.350468000	1.320234000	2.654846000
N	-2.471200000	0.690750000	2.814807000
H	-1.409880000	-2.409490000	2.735787000
H	-1.410462000	2.405121000	2.739299000
H	0.820294000	-1.260093000	2.527173000
H	0.820016000	1.256549000	2.529125000
H	0.015673000	2.439325000	0.316312000
H	0.015645000	-2.439707000	0.312673000
H	-6.765080000	1.271059000	-1.751238000
H	-6.765086000	-1.268400000	-1.753044000
H	4.963924000	2.498414000	-0.495521000

H	4.963839000	-2.497646000	-0.499652000
F	7.260226000	1.320470000	-0.812881000
F	7.260170000	-1.319264000	-0.815139000

B3LYP/6-311+G**			
10			
E(SCF) = -1244.06719485			
C	0.000000000	6.114469000	0.715277000
C	0.000000000	4.934848000	1.382248000
C	0.000000000	3.662888000	0.726258000
C	0.000000000	3.662888000	-0.726258000
C	0.000000000	4.934848000	-1.382248000
C	0.000000000	6.114469000	-0.715277000
C	0.000000000	2.460311000	1.412317000
C	0.000000000	1.223481000	0.727081000
C	0.000000000	1.223481000	-0.727081000
C	0.000000000	2.460311000	-1.412317000
C	0.000000000	0.000000000	1.408115000
C	0.000000000	-1.223481000	0.727081000
C	0.000000000	-1.223481000	-0.727081000
C	0.000000000	0.000000000	-1.408115000
C	0.000000000	-2.460311000	1.412317000
C	0.000000000	-3.662888000	0.726258000
C	0.000000000	-3.662888000	-0.726258000
C	0.000000000	-2.460311000	-1.412317000
C	0.000000000	-4.934848000	1.382248000
C	0.000000000	-6.114469000	0.715277000
C	0.000000000	-6.114469000	-0.715277000
C	0.000000000	-4.934848000	-1.382248000
F	0.000000000	-4.928605000	2.737152000
F	0.000000000	-4.928605000	-2.737152000
H	0.000000000	-2.465653000	2.495359000
H	0.000000000	-2.465653000	-2.495359000
H	0.000000000	2.465653000	-2.495359000
H	0.000000000	2.465653000	2.495359000
F	0.000000000	4.928605000	-2.737152000
F	0.000000000	4.928605000	2.737152000
H	0.000000000	7.046448000	-1.265298000
H	0.000000000	7.046448000	1.265298000
H	0.000000000	-7.046448000	-1.265298000
H	0.000000000	-7.046448000	1.265298000
H	0.000000000	0.000000000	2.493191000
H	0.000000000	0.000000000	-2.493191000

B3LYP/6-311+G**
11

E(SCF) = -1244.06246293

C	0.000000000	0.715476000	-6.328929000
C	0.000000000	1.381671000	-5.148849000
C	0.000000000	0.726403000	-3.876677000
C	0.000000000	-0.726403000	-3.876677000
C	0.000000000	-1.381671000	-5.148849000
C	0.000000000	-0.715476000	-6.328929000
C	0.000000000	1.412218000	-2.673968000
C	0.000000000	0.727036000	-1.437007000
C	0.000000000	-0.727036000	-1.437007000
C	0.000000000	-1.412218000	-2.673968000
C	0.000000000	1.407782000	-0.213167000
C	0.000000000	0.726973000	1.010470000
C	0.000000000	-0.726973000	1.010470000
C	0.000000000	-1.407782000	-0.213167000
C	0.000000000	1.407575000	2.249810000
C	0.000000000	0.727314000	3.457096000
C	0.000000000	-0.727314000	3.457096000
C	0.000000000	-1.407575000	2.249810000
C	0.000000000	1.417264000	4.715347000
C	0.000000000	0.714860000	5.872733000
C	0.000000000	-0.714860000	5.872733000
C	0.000000000	-1.417264000	4.715347000
H	0.000000000	2.492756000	2.249763000
H	0.000000000	-2.492756000	2.249763000
H	0.000000000	-2.495401000	-2.679390000
H	0.000000000	2.495401000	-2.679390000
F	0.000000000	-2.737553000	-5.142444000
F	0.000000000	2.737553000	-5.142444000
H	0.000000000	-1.265689000	-7.260848000
H	0.000000000	1.265689000	-7.260848000
H	0.000000000	2.493103000	-0.213989000
H	0.000000000	-2.493103000	-0.213989000
H	0.000000000	-2.500062000	4.747139000
H	0.000000000	2.500062000	4.747139000
F	0.000000000	-1.333789000	7.066958000
F	0.000000000	1.333789000	7.066958000

B3LYP/6-311+G**
12

E(SCF) = -1244.05755645

C	0.000000000	6.086901000	0.714858000
C	0.000000000	6.086901000	-0.714858000
C	0.000000000	4.929275000	-1.417006000
C	0.000000000	3.671117000	-0.727216000
C	0.000000000	3.671117000	0.727216000
C	0.000000000	4.929275000	1.417006000
C	0.000000000	2.463460000	-1.407160000
C	0.000000000	1.224079000	-0.726982000
C	0.000000000	1.224079000	0.726982000
C	0.000000000	2.463460000	1.407160000
C	0.000000000	0.000000000	-1.407201000
C	0.000000000	-1.224079000	-0.726982000
C	0.000000000	-1.224079000	0.726982000
C	0.000000000	0.000000000	1.407201000
C	0.000000000	-2.463460000	-1.407160000
C	0.000000000	-3.671117000	-0.727216000
C	0.000000000	-3.671117000	0.727216000
C	0.000000000	-2.463460000	1.407160000
C	0.000000000	-4.929275000	-1.417006000
C	0.000000000	-6.086901000	-0.714858000
C	0.000000000	-6.086901000	0.714858000
C	0.000000000	-4.929275000	1.417006000
H	0.000000000	4.960987000	-2.499771000
H	0.000000000	4.960987000	2.499771000
H	0.000000000	2.463768000	-2.492354000
H	0.000000000	2.463768000	2.492354000
H	0.000000000	0.000000000	-2.492631000
H	0.000000000	0.000000000	2.492631000
H	0.000000000	-2.463768000	-2.492354000
H	0.000000000	-2.463768000	2.492354000
H	0.000000000	-4.960987000	-2.499771000
H	0.000000000	-4.960987000	2.499771000
F	0.000000000	7.281030000	1.333729000
F	0.000000000	7.281030000	-1.333729000
F	0.000000000	-7.281030000	1.333729000
F	0.000000000	-7.281030000	-1.333729000

UB3LYP/6-311+G**			
10$^{+\cdot}$			
E(SCF) = -1243.82406316			
C	0.000000000	6.112050000	0.706359000
C	0.000000000	4.921165000	1.383786000
C	0.000000000	3.665600000	0.722906000
C	0.000000000	3.665600000	-0.722906000
C	0.000000000	4.921165000	-1.383786000
C	0.000000000	6.112050000	-0.706359000
C	0.000000000	2.450687000	1.414037000
C	0.000000000	1.226064000	0.726503000
C	0.000000000	1.226064000	-0.726503000
C	0.000000000	2.450687000	-1.414037000
C	0.000000000	0.000000000	1.410904000
C	0.000000000	-1.226064000	0.726503000
C	0.000000000	-1.226064000	-0.726503000
C	0.000000000	0.000000000	-1.410904000
C	0.000000000	-2.450687000	1.414037000
C	0.000000000	-3.665600000	0.722906000
C	0.000000000	-3.665600000	-0.722906000
C	0.000000000	-2.450687000	-1.414037000
C	0.000000000	-4.921165000	1.383786000
C	0.000000000	-6.112050000	0.706359000
C	0.000000000	-6.112050000	-0.706359000
C	0.000000000	-4.921165000	-1.383786000
F	0.000000000	-4.919881000	2.724498000
F	0.000000000	-4.919881000	-2.724498000
H	0.000000000	-2.458058000	2.497322000
H	0.000000000	-2.458058000	-2.497322000
H	0.000000000	2.458058000	-2.497322000
H	0.000000000	2.458058000	2.497322000
F	0.000000000	4.919881000	-2.724498000
F	0.000000000	4.919881000	2.724498000
H	0.000000000	7.043155000	-1.258533000
H	0.000000000	7.043155000	1.258533000
H	0.000000000	-7.043155000	-1.258533000
H	0.000000000	-7.043155000	1.258533000
H	0.000000000	0.000000000	2.495781000
H	0.000000000	0.000000000	-2.495781000

UB3LYP/6-311+G**			
11$^{+\cdot}$			
E(SCF) = -1243.81981047			
C	0.000000000	0.705962000	-6.325425000
C	0.000000000	1.383354000	-5.133759000
C	0.000000000	0.722520000	-3.878967000
C	0.000000000	-0.722520000	-3.878967000
C	0.000000000	-1.383354000	-5.133759000
C	0.000000000	-0.705962000	-6.325425000
C	0.000000000	1.413576000	-2.662822000
C	0.000000000	0.726235000	-1.439021000
C	0.000000000	-0.726235000	-1.439021000
C	0.000000000	-1.413576000	-2.662822000
C	0.000000000	1.410203000	-0.211802000
C	0.000000000	0.726154000	1.014175000
C	0.000000000	-0.726154000	1.014175000
C	0.000000000	-1.410203000	-0.211802000
C	0.000000000	1.408798000	2.241324000
C	0.000000000	0.723554000	3.462300000
C	0.000000000	-0.723554000	3.462300000
C	0.000000000	-1.408798000	2.241324000
C	0.000000000	1.417136000	4.702830000
C	0.000000000	0.711181000	5.871792000
C	0.000000000	-0.711181000	5.871792000
C	0.000000000	-1.417136000	4.702830000
H	0.000000000	2.493430000	2.242918000
H	0.000000000	-2.493430000	2.242918000
H	0.000000000	-2.496896000	-2.670274000
H	0.000000000	2.496896000	-2.670274000
F	0.000000000	-2.724106000	-5.132933000
F	0.000000000	2.724106000	-5.132933000
H	0.000000000	-1.258415000	-7.256366000
H	0.000000000	1.258415000	-7.256366000
H	0.000000000	2.495177000	-0.212607000
H	0.000000000	-2.495177000	-0.212607000
H	0.000000000	-2.499693000	4.736060000
H	0.000000000	2.499693000	4.736060000
F	0.000000000	-1.330321000	7.046627000
F	0.000000000	1.330321000	7.046627000

UB3LYP/6-311+G**			
12$^{+\cdot}$			
E(SCF) = -1243.81537191			
C	0.000000000	6.085688000	0.710641000
C	0.000000000	6.085688000	-0.710641000
C	0.000000000	4.915848000	-1.416443000
C	0.000000000	3.675941000	-0.723181000
C	0.000000000	3.675941000	0.723181000
C	0.000000000	4.915848000	1.416443000
C	0.000000000	2.453665000	-1.408297000
C	0.000000000	1.227256000	-0.725982000
C	0.000000000	1.227256000	0.725982000
C	0.000000000	2.453665000	1.408297000
C	0.000000000	0.000000000	-1.409267000
C	0.000000000	-1.227256000	-0.725982000
C	0.000000000	-1.227256000	0.725982000
C	0.000000000	0.000000000	1.409267000
C	0.000000000	-2.453665000	-1.408297000
C	0.000000000	-3.675941000	-0.723181000
C	0.000000000	-3.675941000	0.723181000
C	0.000000000	-2.453665000	1.408297000
C	0.000000000	-4.915848000	-1.416443000
C	0.000000000	-6.085688000	-0.710641000
C	0.000000000	-6.085688000	0.710641000
C	0.000000000	-4.915848000	1.416443000
H	0.000000000	4.949929000	-2.499049000
H	0.000000000	4.949929000	2.499049000
H	0.000000000	2.455861000	-2.493007000
H	0.000000000	2.455861000	2.493007000
H	0.000000000	0.000000000	-2.494395000
H	0.000000000	0.000000000	2.494395000
H	0.000000000	-2.455861000	-2.493007000
H	0.000000000	-2.455861000	2.493007000
H	0.000000000	-4.949929000	-2.499049000
H	0.000000000	-4.949929000	2.499049000
F	0.000000000	7.260124000	1.331237000
F	0.000000000	7.260124000	-1.331237000
F	0.000000000	-7.260124000	1.331237000
F	0.000000000	-7.260124000	-1.331237000

B3LYP/6-311+G**			
10^{2+}			
E(SCF) = -1243.44680687			
C	0.000000000	6.119472000	0.697525000
C	0.000000000	4.911988000	1.386372000
C	0.000000000	3.666745000	0.722494000
C	0.000000000	3.666745000	-0.722494000
C	0.000000000	4.911988000	-1.386372000
C	0.000000000	6.119472000	-0.697525000
C	0.000000000	2.445407000	1.416563000
C	0.000000000	1.225735000	0.726566000
C	0.000000000	1.225735000	-0.726566000
C	0.000000000	2.445407000	-1.416563000
C	0.000000000	0.000000000	1.414122000
C	0.000000000	-1.225735000	0.726566000
C	0.000000000	-1.225735000	-0.726566000
C	0.000000000	0.000000000	-1.414122000
C	0.000000000	-2.445407000	1.416563000
C	0.000000000	-3.666745000	0.722494000
C	0.000000000	-3.666745000	-0.722494000
C	0.000000000	-2.445407000	-1.416563000
C	0.000000000	-4.911988000	1.386372000
C	0.000000000	-6.119472000	0.697525000
C	0.000000000	-6.119472000	-0.697525000
C	0.000000000	-4.911988000	-1.386372000
F	0.000000000	-4.922747000	2.709833000
F	0.000000000	-4.922747000	-2.709833000
H	0.000000000	-2.453634000	2.500874000
H	0.000000000	-2.453634000	-2.500874000
H	0.000000000	2.453634000	-2.500874000
H	0.000000000	2.453634000	2.500874000
F	0.000000000	4.922747000	-2.709833000
F	0.000000000	4.922747000	2.709833000
H	0.000000000	7.048956000	-1.254754000
H	0.000000000	7.048956000	1.254754000
H	0.000000000	-7.048956000	-1.254754000
H	0.000000000	-7.048956000	1.254754000
H	0.000000000	0.000000000	2.499559000
H	0.000000000	0.000000000	-2.499559000

B3LYP/6-311+G**			
11^{2+}			
E(SCF) = -1243.44119337			
C	0.000000000	0.696519000	-6.332189000
C	0.000000000	1.385883000	-5.122557000
C	0.000000000	0.721987000	-3.879008000
C	0.000000000	-0.721987000	-3.879008000
C	0.000000000	-1.385883000	-5.122557000
C	0.000000000	-0.696519000	-6.332189000
C	0.000000000	1.415760000	-2.655515000
C	0.000000000	0.726267000	-1.437534000
C	0.000000000	-0.726267000	-1.437534000
C	0.000000000	-1.415760000	-2.655515000
C	0.000000000	1.413084000	-0.209649000
C	0.000000000	0.726273000	1.014898000
C	0.000000000	-0.726273000	1.014898000
C	0.000000000	-1.413084000	-0.209649000
C	0.000000000	1.411320000	2.237834000
C	0.000000000	0.723216000	3.466275000
C	0.000000000	-0.723216000	3.466275000
C	0.000000000	-1.411320000	2.237834000
C	0.000000000	1.417556000	4.694706000
C	0.000000000	0.708290000	5.878695000
C	0.000000000	-0.708290000	5.878695000
C	0.000000000	-1.417556000	4.694706000
H	0.000000000	2.496447000	2.240975000
H	0.000000000	-2.496447000	2.240975000
H	0.000000000	-2.500243000	-2.664125000
H	0.000000000	2.500243000	-2.664125000
F	0.000000000	-2.708842000	-5.135048000
F	0.000000000	2.708842000	-5.135048000
H	0.000000000	-1.255583000	-7.260653000
H	0.000000000	1.255583000	-7.260653000
H	0.000000000	2.498699000	-0.210347000
H	0.000000000	-2.498699000	-0.210347000
H	0.000000000	-2.500764000	4.733141000
H	0.000000000	2.500764000	4.733141000
F	0.000000000	-1.331222000	7.034150000
F	0.000000000	1.331222000	7.034150000

B3LYP/6-311+G**			
12^{2+}			
E(SCF) = -1243.43522595			
C	0.000000000	6.091433000	0.707486000
C	0.000000000	6.091433000	-0.707486000
C	0.000000000	4.905732000	-1.416808000
C	0.000000000	3.678663000	-0.722455000
C	0.000000000	3.678663000	0.722455000
C	0.000000000	4.905732000	1.416808000
C	0.000000000	2.448082000	-1.410642000
C	0.000000000	1.226823000	-0.725529000
C	0.000000000	1.226823000	0.725529000
C	0.000000000	2.448082000	1.410642000
C	0.000000000	0.000000000	-1.411869000
C	0.000000000	-1.226823000	-0.725529000
C	0.000000000	-1.226823000	0.725529000
C	0.000000000	0.000000000	1.411869000
C	0.000000000	-2.448082000	-1.410642000
C	0.000000000	-3.678663000	-0.722455000
C	0.000000000	-3.678663000	0.722455000
C	0.000000000	-2.448082000	1.410642000
C	0.000000000	-4.905732000	-1.416808000
C	0.000000000	-6.091433000	-0.707486000
C	0.000000000	-6.091433000	0.707486000
C	0.000000000	-4.905732000	1.416808000
H	0.000000000	4.944349000	-2.500072000
H	0.000000000	4.944349000	2.500072000
H	0.000000000	2.451334000	-2.495859000
H	0.000000000	2.451334000	2.495859000
H	0.000000000	0.000000000	-2.497590000
H	0.000000000	0.000000000	2.497590000
H	0.000000000	-2.451334000	-2.495859000
H	0.000000000	-2.451334000	2.495859000
H	0.000000000	-4.944349000	-2.500072000
H	0.000000000	-4.944349000	2.500072000
F	0.000000000	7.245718000	1.332105000
F	0.000000000	7.245718000	-1.332105000
F	0.000000000	-7.245718000	1.332105000
F	0.000000000	-7.245718000	-1.332105000

12. References

(1) Dümmling, S.; Eichhorn, E.; Schneider, S.; Speiser, B.; Würde, M. Recycling of the supporting electrolyte tetra (n-butyl) ammonium hexafluorophosphate from used electrolyte solutions, *Curr. Sep.* **1996**, *15*, 53-56.

(2) Schundelmeier, S.; Speiser, B.; Bettinger, H. F.; Einholz, R. (Electro)chemical Oxidation of 6,13-Bis[tri(isopropyl)silylethynyl]pentacene to its Radical Cation and Dication, *ChemPhysChem* **2017**, *18*, 2266-2278.

(3) Gollas, B.; Krauß, B.; Speiser, B.; Stahl, H. Design of a single-unit Haber-Luggin capillary/dual reference-electrode system, *Curr. Sep.* **1994**, *13*, 42-44.

(4) Duling, D. R. Simulation of Multiple Isotropic Spin-Trap EPR Spectra, *J. Magn. Reson. B* **1994**, *104*, 105-110.

(5) Tsuchido, Y.; Ide, T.; Suzaki, Y.; Osakada, K. 1,4-Selective Diels–Alder Reaction of 9,10-Diethynylanthracene with 3,6-Difluorobenzyne, *Bull. Chem. Soc. Jpn.* **2015**, *88*, 821-823.

(6) Luliński, S.; Serwatowski, J.; Zaczek, A. Long-Range Effects in the Metalation/Boronation of Functionalized 1,4-Dihalobenzenes, *Eur. J. Org. Chem.* **2006**, *2006*, 5167-5173.

(7) Sparfel, D.; Gobert, F.; Rigaudy, J. Transformations thermiques des photooxydes méso des acénes—VI: Cas des photooxydes de pentacenes, *Tetrahedron* **1980**, *36*, 2225-2235.

(8) Chien, C.-T.; Chiang, T.-C.; Watanabe, M.; Chao, T.-H.; Chang, Y. J.; Lin, Y.-D.; Lee, H.-K.; Liu, C.-Y.; Tu, C.-H.; Sun, C.-H.; Chow, T. J. The synthesis and ambipolar charge transport properties of 1,2,3,4-tetrafluoropentacene, *Tetrahedron Lett.* **2013**, *54*, 903-906.

(9) Einholz, R.; Fang, T.; Berger, R.; Grüninger, P.; Früh, A.; Chassé, T.; Fink, R. F.; Bettinger, H. F. Heptacene: Characterization in Solution, in the Solid State, and in Films, *J. Am. Chem. Soc.* **2017**, *139*, 4435-4442.

(10) Cardona, C. M.; Li, W.; Kaifer, A. E.; Stockdale, D.; Bazan, G. C. Electrochemical Considerations for Determining Absolute Frontier Orbital Energy Levels of Conjugated Polymers for Solar Cell Applications, *Adv.Mater.* **2011**, *23*, 2367-2371.

(11) Holze, R. Optical and Electrochemical Band Gaps in Mono-, Oligo-, and Polymeric Systems: A Critical Reassessment, *Organometallics* **2014**, *33*, 5033-5042.

(12) COSMO v. 1.61, Bruker AXS Inc., Madison, WI, **2012**.

(13) APEX 3 v. 2017.3-0, Bruker AXS Inc., Madison, Wi, **2017**.

(14) SAINT v. 8.38A, Bruker AXS Inc., Madison, Wi, **2017**.

(15) Krause, L.; Herbst-Irmer, R.; Sheldrick, G. M.; Stalke, D. Comparison of silver and molybdenum microfocus X-ray sources for single-crystal structure determination, *J. Appl. Cryst.* **2015**, *48*, 3-10.

(16) Sheldrick, G. SHELXT - Integrated space-group and crystal-structure determination, *Acta Cryst.* **2015**, *A71*, 3-8.

(17) Hübschle, C. B.; Sheldrick, G. M.; Dittrich, B. ShelXle: a Qt graphical user interface for SHELXL, *J. Appl. Cryst.* **2011**, *44*, 1281-1284.

(18) Frisch, M. J.; Trucks, G. W.; Schlegel, H. B.; Scuseria, G. E.; Robb, M. A.; Cheeseman, J. R.; Scalmani, G.; Barone, V.; Mennucci, B.; Petersson, G. A.; Nakatsuji, H.; Caricato, M.; Li, X.; Hratchian, H. P.; Izmaylov, A. F.; Bloino, J.; Zheng, G.; Sonnenberg, J. L.; Hada, M.; Ehara, M.; Toyota, K.; Fukuda, R.; Hasegawa, J.; Ishida, M.; Nakajima, T.; Honda, Y.; Kitao, O.; Nakai, H.; Vreven, T.; Montgomery, J. A., Jr.; Peralta, J. E.; Ogliaro, F.; Bearpark, M.; Heyd, J. J.; Brothers, E.; Kudin, K. N.; Staroverov, V. N.; Kobayashi, R.; Normand, J.; Raghavachari, K.; Rendell, A.; Burant, J. C.; Iyengar, S. S.; Tomasi, J.; Cossi, M.; Rega, N.; Millam, J. M.; Klene, M.; Knox, J. E.; Cross, J. B.; Bakken, V.; Adamo, C.; Jaramillo, J.; Gomperts, R.; Stratmann, R. E.; Yazyev, O.; Austin, A. J.; Cammi, R.; Pomelli, C.; Ochterski, J. W.; Martin, R. L.; Morokuma, K.; Zakrzewski, V. G.; Voth, G. A.; Salvador, P.; Dannenberg, J. J.; Dapprich, S.; Daniels, A. D.; Farkas, Ö.; Foresman, J. B.; Ortiz, J. V.; Cioslowski, J.; Fox, D. J., *Gaussian 09,* **2015**.

(19) Zhao, Y.; Truhlar, D. G. The M06 suite of density functionals for main group thermochemistry, thermochemical kinetics, noncovalent interactions, excited states, and transition elements: two new functionals and systematic testing of four M06-class functionals and 12 other functionals, *Theor. Chem. Acc.* **2008**, *120*, 215-241.

(20) Becke, A. D. Density-functional thermochemistry. III. The role of exact exchange, *J. Chem. Phys.* **1993**, *98*, 5648-5652.

(21) Lee, C.; Yang, W.; Parr, R. G. Development of the Colle-Salvetti correlation-energy formula into a functional of the electron density, *Phys. Rev. B* **1988**, *37*, 785-789.

(22) Stephens, P. J.; Devlin, F. J.; Chabalowski, C. F.; Frisch, M. J. Ab Initio Calculation of Vibrational Absorption and Circular Dichroism Spectra Using Density Functional Force Fields, *J. Phys. Chem.* **1994**, *98*, 11623-11627.

(23) Stratmann, R. E.; Scuseria, G. E.; Frisch, M. J. An efficient implementation of time-dependent density-functional theory for the calculation of excitation energies of large molecules, *J. Chem. Phys.* **1998**, *109*, 8218-8224.

(24) Shen, B.; Geiger, T.; Einholz, R.; Reicherter, F.; Schundelmeier, S.; Maichle-Mössmer, C.; Speiser, B.; Bettinger, H. F. Bridging the Gap between Pentacene and Perfluoropentacene: Synthesis and Characterization of 2,3,9,10-Tetrafluoropentacene in the Neutral, Cationic, and Dicationic States, *J. Org. Chem.* **2018**, *83*, 3149-3158.

(25) Bula, R. P.; Oppel, I. M.; Bettinger, H. F. Thermal Generation of Pentacenes from Soluble 6,13-Dihydro-6,13-ethenopentacene Precursors by a Diels–Alder-retro-Diels–Alder Sequence with 3,6-Disubstituted Tetrazines, *J. Org. Chem.* **2012**, *77*, 3538-3542.

(26) Sadasivam, D. V.; Prasad, E.; Flowers, R. A.; Birney, D. M. Stopped-Flow Kinetics of Tetrazine Cycloadditions; Experimental and Computational Studies toward Sequential Transition States, *J. Phys. Chem. A* **2006**, *110*, 1288-1294.